



Alkaline magmatism

and the problems of mantle sources



**Щелочной магматизм и
проблемы мантийных
источников**

Irkutsk 2001

*Russian Academy of Sciences
Vinogradov Institute of Geochemistry
Siberian Branch
Russian Foundation of Basic Research*



Alkaline magmatism and the problems of mantle sources

**(Щелочной магматизм и проблемы мантийных
источников)**

PROCEEDING
of International Workshop
«Alkaline magmatism and
the problems of mantle
sources»

Edited by Dr. N.V. Vladykin

IRKUTSK

2001

The Organizing Committee:

academician: V.I. Kovalenko
L.N. Kogarko
N.L. Dobretsov
F.A. Letnikov
I.D. Rjabchikov

Corresponding member:

M.I. Kuzmin
I.V. Gordienko
Dr. N.V. Vladykin

Editor – in-chief N.V. Vladykin

20-30 august 2001

Irkutsk Russia

TABLE OF CONTENTS

1. Kogarko L.N. Alkaline magmatism in the history of the Earth	5
2. Vladykin N.V. The Aldan Province of K-alkaline rocks and carbonatites: problems of magmatism, genesis and deep sources	17
3. Kryvdik S.G. Alkaline magmatism of the Ukrainian shield	42
4. Perepelov A.B., Volynets O.N., Anoshin G.N., Puzankov Yu.M., Antipin V.S., Kablukov A.V. Western Kamchatka alkali-potassic basaltoid volcanism: geological and geochemical review	53
5. Morikiyo T., Miyazaki T., Kagami H., Vladykin N. V., Chernysheva E. A., Panina L.I., Podgornych N. M. Sr, Nd, C and O isotope characteristics of Siberian carbonatites	71
6. Sharygin V.V. Lamproites: a review of magmatic inclusions in minerals	88
7. Mitchell R.H. The classification of melilitite clan	120
8. Mahotkin I.L., Podkuiko Yu.A., Zhuravlev D.Z. Early paleozoic kimberlite-melnoite magmatism of the Pri-Polar Urals and the geodynamic formation model	157
9. Ashchepkov I.V., Vladykin N.V., Gerasimov P.A., Saprykin A.I., Khmelnikova O.S., Anoshin G.N. Petrology and mineralogy of disintegrated mantle inclusions of kimberlite-like diatremes from the Aldan shield (Chompolo field): mantle reconstructions	168
10. Nivin V.A., Ikorsky S.V., Kamensky I.L. Noble gas (He, Ar) isotope evidence for sources of devonian alkaline magmatism and ore formation related within the Kola province (NW Russia)	185
11. Miyazaki T., Kagami H., Mohan V.R., Shuto K., Morikiyo T. Evolution of South Indian enriched lithospheric mantle: evidence from the Yelagiri and evattur alkaline plutons in Tamil Nadu, South India	197
12. Ashchepkov I.V., Travin S.V., Andre L., Khmelnikova O.S. Cenozoic flood basalt volcanism, mantle xenoliths and melting regions in the lithospheric mantle of the Baikal rift and other regions of Central Asia	213
13. Asavin A.M. Geochemistry of the rare lithophile elements, Zr, Hf, Nb, Ta, Th, U, and variations in their ratios during fractionation of alkali-basalt series in oceanic islands	225
14. Gornova M.A., Solovjeva L.V., Glazunov O.M., Belozerova O.Yu. Formation of Precambrian lithosphere mantle - geochemical analysis of coarse-grained peridotites from kimberlites, Siberian craton	233
15. Kuzmin M.I., Yarmolyuk V.V., Kovalenko V.I., Ivanov V.G. Evolution of the central asian "hot" field in the phanerozoic and some problems of plume tectonics	252
16. Viladkar S.G. Carbonatites of India: an overview	267

Foreword

Alkaline rocks are unique formation on the Earth. They have been of particular interest for researchers. Large Nb, Ta, Zr, Y, TR, Cu, P deposits, gem stones of charoite, Cr-diospide, dianite are associated with alkaline rocks. The Australian lamproites are connected with diamonds. The complicated processes of their formation provoked multi-year scientific disputes, which are still the case. The new methods of investigations provided much information on the composition of alkaline rocks. The data on geochemistry of isotopes confirm the mantle sources of the substance of alkaline rocks. The new stage of the plume tectonics deepened the interest of scientists to the alkaline rocks from the viewpoint of plate tectonics. The deep-seated Earth's geodynamics can be interpreted using these data.

The given proceeding contains the invited reports of the International Workshop "Alkaline magmatism and the problems of the mantle source", held at the Institute of Geochemistry, SB RAS, Irkutsk city. The papers consider the features of the alkaline magmatism on the Earth's history. A detailed characteristics of the alkaline magmatism of different provinces of the world (Aldan, Ukraine shields, eastern Kamchatka, Kola Peninsula, Ural, India) is given in this proceedings. The classification of lamproite rocks and determination of PT-conditions of the crystallization of lamproites are provided using the data on the homogenization of melted inclusions. The papers consider the features of the genesis of kimberlites from the Urals and Siberia, alkaline basalts of the Baikal Rift and oceanic islands, Transbaikalia and Mongolia. The isotope characteristics of carbonatites of many Siberian massifs are presented. We hope that the similar meetings of scientists to discuss the genetic problems of the alkaline magmatism will be continued. The reports are translated into English by the authors.

The Chairman of the Organizing Committee
Dr. N. V. Vladykin

Alkaline magmatism in the history of the Earth

L. N. Kogarko

*Vernadskiy Institute of Geochemistry and Analytical Chemistry,
Russian Academy of Sciences, Moscow*

INTRODUCTION

The evolution of the Earth's magmatic regime is primarily controlled by processes of the global differentiation of the mantle, which is the largest shale of our planet.

On the one hand, the postaccretionary history of the Earth was generally related to recurrent episodes of mantle melting, which produced the continental and the oceanic crust. In the course of this process, the mantle should have continuously lost the so-called "basaltic," lower melting components (such as CaO, Al₂O₃, TiO₂ and rare lithophile elements) and become a strongly depleted source material, from which only highly mag-nesian melts depleted in rare elements could be derived later. However, no tendencies of this type occurred during the Earth's geologic evolution. To the contrary, more and more evidence suggests that primary mantle magmas (basalts and picrites) become progressively more enriched in Ti, LREEs, and incompatible elements with the passage of geologic time [Campbell and Griffiths, 1992].

Isotopic studies [Zindler and Hart, 1986] provide evidence for the existence of mantle reservoirs strongly enriched in trace elements; the occurrence of these reservoirs could not be explained within the guidelines of the model of continuous global mantle melting during the postaccretionary time. These facts and considerations caused the recent development of the idea of active crust-mantle interaction [Hoffmann, 1997], during which large-scale material exchange occurred and favorable conditions were created for the development of enriched reservoirs.

The continental crust growth, which was definitely controlled by the intensity of partial melting in the mantle, principally decelerated in Late Archean time [Fyfe, 1978], and the volume of the crust even began to decrease, a fact suggesting that the planet entered a stationary state, in which the amount of material ascending from the mantle became equal to the amount of rocks returning to it. According to Hargraves (1976), numerous facts suggest that the material building up continents and delivered to the oceanic crust in the form of basalt magmas is counterbalanced by the consumption of the oceanic crust and its erosion products in sub-duction zones. One of the most important geochemical implications of this process is the origin of REE-enriched blocks in the mantle. Evidently, the development of alkaline magmatism during the Earth's history, a process associated with extremely high concentrations of trace elements, was related to the generation of such zones in the mantle.

Synthesis of the extensive materials published earlier in the literature and our data [Wooley, 1987; Kogarko et al., 1995b; Kogarko, 1984] indicates that the first manifestations in the Earth's history of alkaline magmatism are dated at 2.5-2.7 Ga. At present about 1500 alkaline and carbonatite intrusive and volcanic complexes are known, but no rocks older than 2700 Ma were detected (Fig. 1). The only exceptions are the syenite and alkali basalt lavas of Archean age from Kirkland, Canada [Basu et al., 1984]. However, these data call for further studies to be verified.

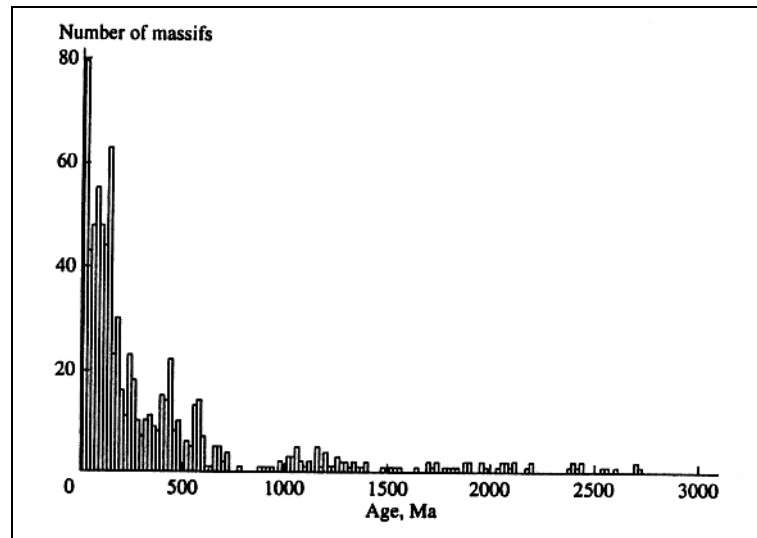


Fig. 1. Distribution of alkaline massifs over geological time

As can be seen in Fig. 1, the activity of alkaline magmatism increased continuously throughout the Earth's history. Moreover, according to Lazarenkov (1988), the thickness of the alkaline complexes also increased throughout geologic time. For example, the gross volume of young platiophonolite in Kenya is more than 50000 km³ [Logachev, 1977], i.e., much more than the integral thickness of alkaline rocks produced over other geologic epochs.

The appearance of alkaline rocks at the Archean-Proterozoic boundary coincided with a number of global geologic events. This time boundary was very important in the history of the Earth:

(1) Most scientists [Drummond and Defant, 1990] relate this boundary to a radical change in the geodynamic regime of our planet, when plume tectonics gave way to plate tectonics [Khain, 1994], although the role of mantle plumes remains very important up to the present. Nevertheless, many authors [Drummond, Defant, 1990; McCulluch, 1993] allow for subduction processes in the Archean, believing that the volumes of subducted material were then incomparably smaller than those sunk into the mantle over post-Archean time.

(2) This time boundary marked the origin of the Earth's oxygen atmosphere [Walker, 1977; Holland, 1984], which was produced mainly by the activity of living beings and hydrogen dissipation to outer space. The precursory atmosphere consisted of a CH₄-H₂ mixture [Rubey, 1955].

(3) The boundary between the Archean and Protero-zoic was the time of the most active continental crust growth. The effect of the oxygen-bearing atmosphere caused the origin of "oxidized" marine sediments such as jaspilite and carbonates and the oxidation of paleosoils [Holland, 1984; Cloud, 1968]. It is interesting to note that supergiant Archean sedimentary deposits of uraninite and pyrite (like the Witwatersrand deposit) or siderite (on Labrador) have no analogues among mineral deposits of post-Archean age, because the minerals composing these ores are unstable in oxygen atmosphere [Walker, 1977; Holland, 1984].

Global processes of plate tectonics at the Archean-Proterozoic boundary resulted in the subduction of the already significantly oxidized oceanic crust with a high content of volatiles (mainly H₂O and CO₂), which were then involved in mantle cycles. The active interaction between the crust and mantle facilitated not only an increase in the contents of volatiles in the mantle, which had lost these components in the course of high-temperature accretion during the early evolutionary stages of the Earth, but also resulted in the oxidation of the mantle atmosphere, which was most probably dominated by a methane-hydrogen mixture in pre-Proterozoic time [Arculus and Delano, 1980]. Let us examine these problems in more detail.

Active studies carried out during past years on the regime of mantle fluids revealed that mantle redox conditions are highly variable. In light of the data obtained by Haggerty and Tompkin (1983), the oxygen fugacity in the mantle material varies over an interval of 5-6 logarithmic units with respect to the quartz-fayalite-magnetite (QFM) buffer system. However, in spite of the significant diversity of redox conditions in the Earth's lithospheric and asthenospheric mantle, these variations show certain regularities.

Most scientists are inclined to believe that the oldest Archean lithospheric mantle, which was the source of diamond, was characterized by quite low f_{O_2} values. The point is that diamond, whose age is much older than the age of the host kimberlite [Richardson, 1986; Kramers, 1979; Ozima et al., 1983] and sometimes exceeds 3 Ga, occasionally bear inclusions of nickel-free iron [Sobolev et al., 1981], moissanite, magnesio-wuestite [Meyer, 1987], and methane [Giardini and Melton, 1975], a fact providing evidence that the atmosphere of the ancient Archean mantle was extremely reduced. These data are very consistent with materials on the V geochemistry of Archean tholeiites [Shervais, 1982]. These data indicate that the Ti/V ratio increases in the course of magmatic differentiation because of the fractionation of pyroxene, which becomes gradually enriched in reduced (trivalent) vanadium. Our recent studies led to a discovery of metallic copper-bearing iron-nickel alloys in the mantle, i.e., phases composing the Earth's core [Ryabchikov et al., 1994]. These minerals can be stable only under very low

oxygen fugacity, three logarithmic units lower than the wuestite-iron buffer [O'Neil, 1991]. These conditions seem to have occurred early in the Earth's geologic history at about 4.6 Ga, when the core was formed.

The experiments of Arculus and Delano (1980) on determining the redox conditions in mantle nodules by using electrochemical cells detected fairly low f_{O_2} values (close to the wuestite-iron buffer) of some xenoliths and megacrysts in basalts. At the same time, Bullhaus (1993) determined that most mantle peridotites are more oxidized (from two logarithmic units below the QFM buffer to values at this buffer). Even more oxidized conditions were determined in mantle rocks strongly recycled by metasomatic processes (up to two logarithmic units above the QFM buffer. Fig. 2).

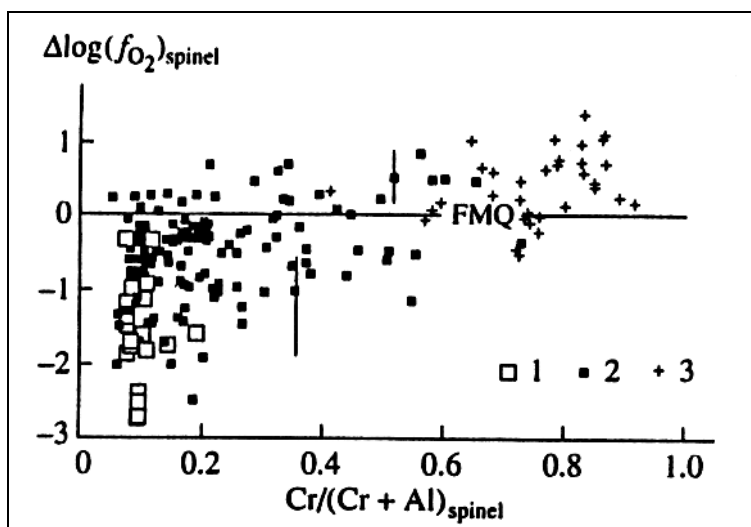


Fig. 2. Variations of oxygen fugacity in mantle xenoliths (Bullhaus, 1993).

(1) Primitive xenolith; (2) weakly metasomatized xenoliths; (3) strongly metasomatized xenoliths.

The most oxidized magmatic associations are island-arc andesites and basalts (three logarithmic units above the QFM buffer. Figs. 3, 4), whose genesis is closely related to the subduction of the oceanic crust, and alkaline rocks of oceanic islands (two logarithmic units above the QFM buffer. Fig. 4; [Bullhaus, 1993]). Kogarko et al., (1995b) demonstrated that the highly alkaline lavas of Trinidad Island are also strongly oxidized (their f_{O_2} is higher than the QFM buffer by three logarithmic units). Studies of the oxidation degree of modern volcanic gases [Holland, 1984] revealed that their H_2O and CO/CO_2 ratios are 0.01 and 0.03, respectively, a fact that unambiguously testifies to the high oxygen fugacity during modern magma generation in the mantle. All these data further accentuate the unequal redox conditions in the mantle and provide evidence for the existence of relics of more ancient reduced mantle in the relatively oxidized mantle material. This, in turn, points to global oxidation processes that operated in the Earth's mantle throughout geologic history.

In my opinion, the most important process of mantle oxidation is the descent of the oxidized lithosphere to the mantle, a process that continues from Late

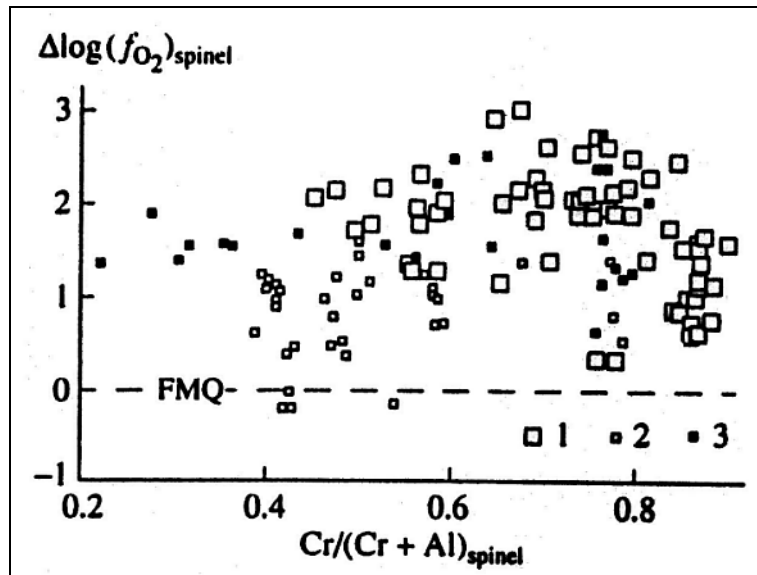


Fig. 3. Variations of oxygen fugacity in basalts (Bullhaus 1993).
 (1) Island-arc basalts; (2) back-arc basalts; (3) cumulative nodules in island-arc basalts.

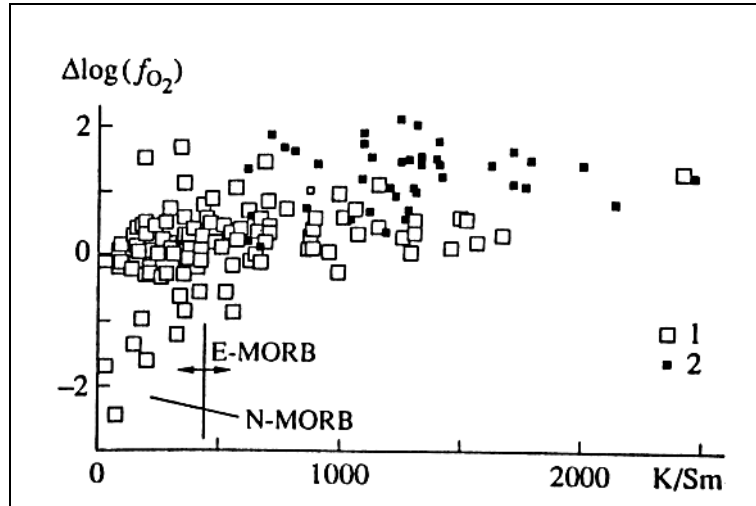


Fig. 4. Variations of oxygen fugacity in basalts of oceanic islands and mid-ocean ridges (Bullhaus, 1993).
 (1) Basalts of mid-ocean ridges; (2) basalts of oceanic islands.

Archean time. Our calculations, which were based on the assumption that approximately 20 km³ of basaltic material is erupted annually on mid-oceanic ridges, allowed us to estimate the overall water amount that has been added to the mantle for the last 2.5 g.y. In the calculations, we took the total length of mid-

oceanic ridges to be approximately 65000 km, the average spreading rate to be 5 mm per year, and the thickness of the oceanic crust to be about 7 km. It is interesting to note that in examining the problem of oceanic crust recycling, Hofmann (1997) assumed that the annual addition of material to the mantle is 20 km³. Provided that the water content of the altered oceanic crust is 2-3% [De Vore, 1983], the annual water inflow into the mantle would be approximately 10¹⁴ mol, which is one order of magnitude higher than the value cited by Kasting et al. [1993]. At a constant subduction velocity of plates, the total mass of water added to the mantle for 2.5 g.y. will be 2.5 x 10²³ g-mol. Taking the mass of the Earth's mantle to be equal 4.2 x 10²⁴ kg (i.e., 70% of the total Earth's mass) and the average iron content to be 8%, the overall amount of bivalent iron in the mantle (in equilibrium with fluid corresponding to the wuestite-iron buffer system) can be estimated at 4.7 x 10²⁴ g/mol.

Iron oxidizes in the mantle by the reaction



during which hydrogen can be released to the fluid and escape to the Earth's atmosphere or even outer space [Holland, 1984], causing an increase in f_{O_2} in the atmosphere.

Calculations indicate that the above-cited water amount (2.3 x 10²³ g/mol) is sufficient to oxidize 1/10 of the overall iron content in the mantle by reaction (1) and to increase f_{O_2} , of the mantle to the quartz-fayalite-magnetite buffer, i.e., to a value currently accepted by most geochemists [Bullhaus, 1993].

According to De Vore (1983), one-third of the subduction-related water is lost to the atmosphere as a consequence of island-arc volcanism. Sobolev and Shoussidon (1996) believe that no more than 60% of the water can be involved in mantle cycles.

Although our calculations cited above are semi-quantitative, they definitely point to the feasibility of mantle oxidation by subduction-related water.

According to the data of several researchers [Kasting et al., 1993; Ringwood, 1990], the inflow of carbon dioxide into the mantle caused by the subduction of oceanic crust bearing carbonate material is approximately 6 x 10¹² g/mol per year, i.e., much less than the addition of water. In this connection, it is interesting to note that, according to our calculations, carbonatites (which contain 20% carbon) account for no more than 6-27% of alkaline associations. Relations of carbonatites to the recycling of the oceanic crust is confirmed by the very wide spread in the δC^{13} values of different carbonatite complexes [Bell, 1989]. Our analysis indicates that potassic rocks are younger than the sodic ones and appeared at the time boundary of 1.5 Ga in the Earth's history. Conceivably, it was the time when the notably potassium-enriched oceanic crust started to descend to the mantle much more actively [Brown, Masset, 1981].

The degassing of subducted material and release of oxidized fluid (water and carbon dioxide) could lead to melting in thin films in accordance with the mechanism "described by Green et al. (1987) and Ringwood (1990).

Conceivably, it was water- and carbon dioxide-rich melts with low melting degrees that were able to transport vast concentrations of incompatible trace elements and alkalis [Ringwood, 1990; Wendland, Harrison, 1979] and were the principal agents of mantle metasomatism. The experimental works of Ryabchikov (1988) indicate that aqueous fluid under high pressures can contain up to a few ten percent of silicates enriched in alkalis.

Earlier, Ryabchikov (1988) and Kogarko et al. (1988) demonstrated that metasomatic processes play a decisive part in the genesis of alkaline magmas. It is only the metasomatic supply of rare lithophile elements to zones of magma generation that can account for, on the one hand, the strong enrichment of alkaline magmas in rare lithophile elements and, on the other, their depletion in radiogenic isotopes. As an illustrative example, I would like to refer to our data [Kogarko et al., 1981, 1995b] on the isotopic characteristics of the world's largest alkaline complexes on the Kola Peninsula (the Khibina and the Lovozero Massif), to which supergiant rare-metal deposits are related. It was proved that the mantle protoliths of the alkaline rocks were strongly depleted in rare elements. In a mantle (SND-Ssr) correlation plot, the data points of the rocks and ores from the Khibina and Lovozero massifs fall within the depleted field. This paradox can be explained only by the very rapid supply of metasomatizing material, highly enriched with incompatible trace elements, to the mantle melting chamber. The process should have been too rapid for the radiogenic isotopes (^{87}Sr and ^{143}Nd) to become enriched in the mantle protolith and modify its initial depleted Sr, Sm, and Nd isotopic ratios. Recent detailed studies of the mantle material from various regions [Meen et al., 1989; Menzies, Murthy, 1980] and our data [Kogarko, 1986] point to the significant role of metasomatic processes in the geochemical history of the mantle. The appearance of amphibole, phlogopite, apatite, primary carbonates, minerals of the lindsleyite-mathiasite group, and other phases able to concentrate rare elements could be caused only by metasomatic reactions in the mantle material, most probably in relation to melts with low degrees of melting. In this connection, it is interesting to mention the paper by Francis (1991) in which it was demonstrated that the partial melting of the strongly amphibolized and metasomatized mantle results in the generation of alkaline melts (Table 1). Highly alkaline glasses in metasomatized mantle xenoliths were also described by Edgar et al. (1989). Studies of intensely metasomatized and carbonized nodules from Montana-Clara Island, the Canaries, and Fernando de Noronha Island, Brazil, revealed glasses of alkali-oversaturated phonolite and trachyte composition in association with the primary carbonates. Hence, the generation of alkaline magmas during the partial melting of the metasomatized mantle now leaves little room for doubt.

The ideas of nonlinear geodynamics, which were successfully developed over the past few years by Pushcharovskii (1994), are in good agreement with our data on

the geochemical heterogeneity of mantle pro-toliths as a consequence of metasomatic processes.

The global oxidation of the mantle atmosphere in Early Proterozoic time gave rise to extensive mantle metasomatism, because it is the oxidized fluid phase ($\text{H}_2\text{O} + \tilde{\text{N}}\text{O}_2$) that is capable of transporting vast amounts of silicate material [Wendland, Harrison, 1979]. It is pertinent to reiterate that the reduced atmosphere is chemically inert and, thus, seems to have been hardly capable of transporting material under the Earth's mantle under these conditions. This conclusion is confirmed by the experimental works of Taylor and Green (1988), who proved that the reduced atmosphere ($\text{CH}_4 + \text{H}_2$ mixture) insignificantly affects the configuration of the basaltic solidus and liquidus. As is seen in Fig. 5, oxidized (H_2O) fluid decreases the solidus temperature of pyrolite by 300°C at 20 kbar, whereas the decrease caused by the reduced fluid ($\text{CH}_4 + \text{H}_2$ mixture) is only 100°C .

There are other concepts concerning the causes of fluid oxidation in the mantle throughout geologic time. For example, some scientists [Mao, Bell, 1977; Galimov, 1995; etc.] consider the mechanism of FeO dissolution in the Earth's core (Fe disproportionation) to be among the most important for the enrichment of Fe^{3+} and O in the mantle. Other researchers [Ringwood, 1997; Wanke, 1981; Newsom, 1990; O'Neil, 1991] believe that the Earth's accretion

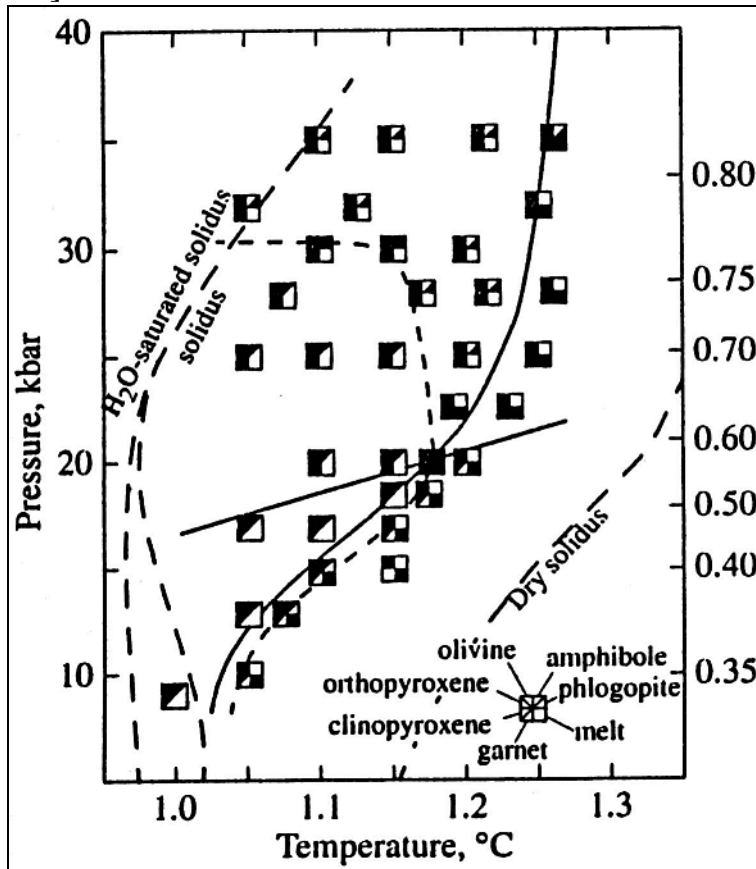


Fig. 5. Pyrolite solidus in the presence of water (QFM buffer) and $\text{CH}_4\text{-H}_2$ mixture (IW buffer) (Taylor, Green, 1988).

could be heterogeneous, and the partly oxidized material rich in volatiles (primarily water) produced hydrogen when coming in contact with the strongly reduced core. The loss of this hydrogen to the atmosphere and outer space should have resulted in the continuous oxidation of the mantle fluid and the Earth's atmosphere. Based on the calculated compositions of the Earth, its mantle, and

Table 1.

Composition (wt %) of glasses in mantle xenoliths

Locality	Fernando de Noronha Island, Atlantic Ocean	Montana-Clara Island, Atlantic Ocean	Nunivak Island, Alaska		
Rock	Wehrlitized and carbonized spinel lherzolite		Amphibole pyroxenite	Amphibole vein	Spinel lherzolite
SiO₂	57.47	6.38	49.02	48.33	52.55
TiO₂	1.02	0.7	1.69	3.26	2.78
Al₂O₃	25.42	16.0	18.69	19.93	18.97
FeO	1.56	2.0	8.99	6.52	3.85
Fe₂O₃	-	-	1.76	1.28	0.76
MnO	0.00	-	0.18	0.17	0.10
Cr₂O₃	0.00	0.06	0.02	0.03	0.04
NiO	0.65	-	-	-	-
MgO	0.00	2.5	2.65	2.35	2.85
CaO	0.97	3.8	5.12	8.91	8.03
Na₂O	9.04	6.4	6.74	5.16	3.79
K₂O	3.87	3.8	2.47	2.84	3.04
P₂O₅	-	-	2.36	1.87	2.27
Total	100.0	41.64	97.22	100.65_	99.03_

core, Allegre et al. (1995) arrived at the conclusion that silicon (which accounts for 7.3% of the core by mass) is transferred from the lower mantle to the core, and oxygen is simultaneously released to the mantle in amounts of about 8.3% of the core mass.

Analysis of the materials presented above indicates that the oxidation of the mantle fluid was most probably controlled by several factors operating in the history of the Earth. However, I think that it was the crust-mantle interaction that played the decisive role in the mantle oxidation.

It follows that the oxidation of the Earth's atmosphere and, later, at the Archean-Proterozoic boundary of its mantle as a consequence of changes of the geodynamic regime of the planet and the rapid activation of crust-mantle interaction resulted in global metasomatic transportation of material and the development of zones enriched in trace elements in the subcrustal source areas of alkaline magmatism. The simultaneous development of the oxidation of the atmosphere and the first appearance of alkaline rocks could not be accidental and definitely points out fundamental relationships between these processes.

ACKNOWLEDGMENTS

The study was supported by the Ministry of Mineral Sources and Technology, project no. 12MO-(00), RFBR 00-15-98497,

REFERENCES

1. Allegre, C.J., Poirier, J.P., Humler, E., and Hofmann, A.W., The Chemical Composition of the Earth, *Earth Planet. Sci. Lett.*, 1995, vol. 134, pp. 515-526.
2. Arculus, R.J. and Delano, J.W., Implications for the Primitive Atmosphere of the Oxidation State of Earth's Upper Mantle, *Nature*, 1980, vol. 288, pp. 72-74.
3. Basu, A.R., Goodwin, A.M., and Tatsumoto, M., Sm-Nd Study of Archean Alkaline Rocks From the Superior Province of the Canadian Shield, *Earth Planet. Sci. Lett.*, 1984, vol. 70, pp. 40-46.
4. Bell, K., Carbonatite Genesis and Evolution, London: Unwin Hyman, 1989.
5. Brown G.N. and Mussett A.E., *The Inaccessible Earth*, London: Alien and Unwin, 1981. Translated under the title *Nedostupnaya Zemlya*, Moscow: Mir, 1984.
6. Bullhaus, C, Redox States of Lithospheric and Asthenospheric Upper Mantle, *Contrib. Mineral. Petrol.*, 1993, vol. 114, pp. 331-348.
7. Campbell, J.H. and Griffiths, R.W., The Changing Nature of the Mantle Hotspots Through Time: Implications for the Chemical Evolution of the Mantle, *J. Geol.*, 1992, vol. 92, pp. 497-523.
8. Cloud, P.E., Atmospheric and Hydrospheric Evolution on the Primitive Earth, *Science*, 1968, vol. 160, pp. 729-736.
9. PC Vore, G.M., Relations Between Subduction, Slab Heating, Slab Dehydration and Continental Growth, *Lithos*, 1983, vol. 16, no. 4, pp. 255-264.
10. Drummond, M.S. and Defant, M.J., A Model for Trondhjemite-Tonalite-Dacite Geneses and Crustal Growth Via Slab Melting: Archean Modern Comparisons, *J. Geo-Phys. Res.*, 1990, vol. 95, no. 13, pp. 21503-21522.
11. Edgar, A.D., Lloyd, F.E., Forsyth, D.M., and Barnett, R.L., Origin of Glass in Upper Mantle Xenoliths From the Quaternary Volcanics of Gees, West Eifel, Germany, *Contrib. Mineral. Petrol.*, 1989, vol. 103, pp. 277-286.
12. Francis, D., Some Implications of Xenolith Glasses for the Mantle Sources of Alkaline Mafic Magmas, *Contrib. Mineral. Petrol.*, 1991, vol. 108, pp. 175-180.
13. Fyfe, W.S., The Evolution of the Earth's Crust: Modern Plate Tectonics to Ancient Hot Spot Tectonics, *Chem. Geol.*, 1978, vol. 23, pp. 89-114.
14. Galimov, E.M., Problem of Moon Formation, *Osnovnye napravleniya geokhimii* (Main Problems of Geochemistry), Moscow: Nauka, 1995, pp. 8-43.
15. Giardini, A.A. and Melton, C.E., The Nature of Cloud-like Inclusions in Two Arkansas Diamonds, *Am. Mineral.*, 1975, vol. 60, pp. 931-933.
16. Green, D.H., Falloon, T.J., and Taylor, W.R., Mantle-Derived Magmas—Roles of Variable Source Peridotite and Variable C-H-O Fluid Compositions, *Magmatic Processes/Physico-chemical Principles*, Mysen, B., Ed., Geochem. Soc. Publ., 1987, no. 1, pp. 158-172.
17. Haggerty, S. and Tompkin, S., Redox State of Earth's Upper Mantle from Kimberlitic Ilmenites, *Nature*, 1983, vol. 303, pp. 295-300.

18. Hargraves, R.B., Precambrian Geologic History, *Science*, 1976, vol. 193, pp. 363-371.
19. Hofmann, A.W., Mantle Geochemistry: The Message From Oceanic Volcanism, *Nature*, 1997, vol. 385, pp. 219-229.
20. Holland, H., *The Chemical Evolution of the Atmosphere and Ocean*, Princeton: Univ. Press, 1984.
21. Kasting, J.F., Egger, D.H., and Raeburn, S.P., Mantle Redox Evolution and the Oxidation State of the Archean Atmosphere, *Geoi*, 1993, vol. 101, no. 2, pp. 245-257.
22. Khain, V.E., *Osnovnye problemy sovremennoi geologii* (Main Problems of Modern Geology), Moscow: Nauka, 1994.
23. Kogarko, L.N., Heterogeneity of the Earth's Upper Mantle and Alkaline Magmatism, *Doklady 27-i sessii MGK. Geokhimiya i kosmikhimiya* (Proc. 27th IGC, Geochemistry and Cosmochemistry), Moscow: Nauka, 1984, pp. 157-164.
24. Kogarko, L.N., Heterogeneity of the Upper Mantle and Ocean Island Magmatism, *Okeanicheskiy magmatizm* (Oceanic Magmatism), Moscow: Nauka, 1986, pp. 73-80.
25. Kogarko, L.N., Henderson, I., and Pacheco, A.H., Primary Ca-Rich Carbonatite Magma and Carbonate-Silicate-Sul-fide Liquid Immiscibility in the Upper Mantle, *Contrib. Mineral. Petrol.*, 1995a, vol. 121, pp. 267-275.
26. Kogarko, L.N., Karpenko, S.F., Lyalikov, A.V., and Teptelev, M.P., Isotopic Criteria for the Genesis of Meimechite Magmatism, *Dokl. Akad. Nauk SSSR*, 1988, vol. 301, no. 4, pp. 939-942.
27. Kogarko, L.N., Kononova, V.A., Orlova, M., and Woolley, A., *Alkaline Rocks and Carbonatites of the World Part 2. Former USSR*, London: Chapman and Hall, 1995b.
28. Kogarko, L.N., Kramm, U., and Grauert, B., New Data on the Age and Genesis of the Alkaline Rocks of the Lovozero Massif (Rubidium and Strontium Isotopes), *Dokl. Akad. Nauk SSSR*, 1981, vol. 260, no. 4, pp. 1000-1005.
29. Kramers, S.D., Lead, Uranium, Strontium, Potassium and Rubidium in Inclusion-bearing Diamonds and Mantle-Derived Xenoliths From Southern Africa, *Earth Planet. Sci. Lett.*, 1979, vol. 42, pp. 58-70.
30. Lazarenko, V.G., *Formatsionnyi analiz shchelochnykh porod kontinentov i okeanov* (Analysis of Associations of Alkaline Rocks from Continents and Oceans), Leningrad: Nedra, 1988.
31. Logachev, N.A., *Vulkanogennyye i osadochnyye formatsii Hf-tovykh ion Vostochnoi Afriki* (Volcanic and Sedimentary Sequences of the Rift Zones of Eastern Africa), Moscow: Nauka, 1977.
32. Mao, H.K. and Bell, P.M., Disproportionation Equilibrium in Iron-bearing Systems at Pressures Above 100 Kbar with Applications to the Chemistry of the Earth's Mantle, *Energetics of Geological Processes*, New York: Springer, 1977, pp. 237-249.
33. McCulluch, M.T., The Role of Subducted Slabs in an Evolving Earth, *Earth Planet. Sci. Lett.*, 1993, vol. 115, pp. 89-100.
34. Meen, J.K., Ayers, J.C., and Fregeau, E.J., A Model of Mantle Metasomatism by Carbonated Alkaline Melts, *Trace-Element and Isotopic Compositions of Mantle Source Regions of Carbonatite and Other Continental Igneous Rocks*, London: Unwin Hyman, 1989, pp. 464-500.
35. Menzies, M.A. and Murthy, V.R., Nd and Sr Isotope Geochemistry of Hydrous Mantle Nodules and Their Host Alkali Basalts. Implication for Local Heterogeneities in Metasomatically Veined Mantle, *Earth Planet. Sci. Lett.*, 1980, vol. 46, pp. 323-334.
36. Meyer, H., Inclusions in Diamonds, *Mantle Xenoliths*, Nixon, R.H., Ed., Chichester: Wiley, 1987, pp. 501-522.
37. Newson, H.E., Accretion and Core Formation in the Earth: Evidence from Siderophile Elements, *Origin of the Earth*, Newson, H.E. and Jones, J.H., Eds., Oxford: Oxford Univ. Press, 1990, pp. 273-288.
38. O'Neill, H.S.C., The Origin of the Moon and the Early History of the Earth — a Chemical Model, *Geochim. Cosmochim. Acta*, 1991, vol. 55, no. 2, pp. 1159-1172.
39. Ozima, M., Zashu, S., and Nitoh, O., Primitive Helium in Diamonds, *Geochim. Cosmochim. Acta*, 1983, vol. 47, pp. 2217-2224.
40. Pushcharovskii, Yu.M., *Tektonika Atlantiki s elementami nelineinoy geodinamiki* (Tectonics of Atlantic with Elements of Nonlinear Geodynamics), Moscow: Nauka, 1994.
41. Richardson, S.H., Latter-Day Origin for Diamonds of Eclogitic Paragenesis, *Nature*, 1986, vol. 322, pp. 623-626.
42. Ringwood, A.E., Composition of the Core and Implications for Origin of the Earth, *Geochem. J.*, 1977, vol. 11, pp. 111-135.
43. Ringwood, A.E., Slab-Mantle Interactions. 3. Petrogenesis of Intraplate Magmas and Structure of the Upper Mantle, *Chem. Geol.*, 1990, vol. 82, pp. 187-207.
44. Rubey, W.W., Development of the Hydrosphere and Atmosphere, with Special Reference to Probable

- Composition of the Early Atmosphere, *Crust of the Earth*, Poldervaart, A., Ed., New York: Geol. Soc. America, 1955, pp. 631-650.
45. Ryabchikov, J.D., *Geokhimicheskaya evolyutsiya mantii Zemli* (Geochemical Evolution of the Earth's Mantle), Moscow: Nauka, 1988.
 46. Ryabchikov, I.D., Kogarko, L.N., Ntaflos, T, and Kurat, G., Metallic Phases in Mantle Xenoliths, *Dokl. Ross. Akad. Nauk*, 1994, vol. 338, no. 1, pp. 95-98.
 47. Shervais, J.W., Ti-V Plots and the Petrogenesis of Modern and Ophiolitic Lavas, *Earth Planet. Sci. Lett.*, 1982, vol. 59, pp. 101-118.
 48. Sobolev, A.V. and Chaussidon, O.N., H₂O Concentrations in Primary Melts From Suprasubduction Zones and Mid Ocean Ridges: Implications for H₂O Storage and Recycling in the Mantle, *Earth Planet. Sci. Lett.*, 1996, vol. 197, no. 1, pp. 45-55.
 49. Sobolev, N.V., Efimova, E.S., and Pospelova, L.M., Xenoliths of Diamond-bearing Peridotites in Kimberlites and Problems of Diamond Genesis, *Geol. Geofiz.*, 1981, no. 12, pp. 25-29.
 50. Taylor, W.R. and Green, D., Measurement of Reduced Peridotite C-O-H Solidus and Implications for Redox Melting of the Mantle, *Nature*, 1988, vol. 332, pp. 349-352.
 51. Walker, J.C., *Evolution of the Atmosphere*, New York: Mac-millan, 1977.
 52. Wanke, H., Constitution of Terrestrial Planets, *Philos. Trans. R. Soc. London*, 1981, vol. 303, pp. 287-302.
 53. Wendland, R.F. and Harrison, W.S., Rare Earth Partitioning Between Immiscible Carbonate and Silicate Liquids and CO₂ Vapor: Results and Implication for the Formation of Light Rare Earth-Enriched Rocks, *Contrib. Mineral. Petrol.*, 1979, vol. 69, pp. 409-419.
 54. Woolley, A., *Alkaline Rocks and Carbonatites of the World. Part 1. North and South America*, London: British Museum, 1987.
 55. Zindler, A. and Hart, S., Chemical Geodynamics, *Annu. Rev. Earth Planet. Sci. Lett.*, 1986, vol. 14, pp. 493-571.

The Aldan Province of K-alkaline rocks and carbonatites: problems of magmatism, genesis and deep sources

N.V. Vladykin

*Institute of Geochemistry SD RAS, Russia, Irkutsk-33, BOX 4019,
E-mail: vlad@igc.irk.ru*

New geological, petrochemical and geochemical data were used to develop the scheme of the magmatism for massifs of K-alkaline rocks of the Aldan province. A full set of differentiates of K-alkaline series, from K-alkaline-ultrabasic rocks through the basic and middle to acid alkaline granites is found for the Murun and Bilibin massifs. A common trend of compositions for rocks of the whole series is observed on petrochemical and geochemical diagrams of binary correlation of elements. The specific features of the K-alkaline Aldan complex are: 1) the occurrence of lamproitic rocks - intrusive analogs of lamproites during the differentiation; 2) alkaline granites are final differentiates of K-alkaline series; 3) separation of silicate-carbonate melt from the silicate magma on the last stages. When the silicate liquated melt is layered (stratified) the carbonatites (including the unique benstonite carbonatites and silicate charoite rocks) originate. The study of melted inclusions in minerals indicates the magmatic genesis of rocks in the range of the temperature from 1500 to 600 °C. The data on isotopic Pb, C, O, Sr, Nd geochemistry verifies the deep origin of their source from the enriched mantle EM-1. From the Pb isotope data in the galena the age of the substratum is estimated as 3.2 billion years. The origin of the magmatic source is related to the mantle plume.

INTRODUCTION

The Aldan K-alkaline province is located (Fig.1) in the north-eastern flank of the Mongol-Okhotsk area of the alkaline magmatism [Vladykin, 1997; Kalievyi, 1990; Petrologiya, 1967]. The alkaline massifs of this province are situated mainly in the northern periphery of the Aldan shield on the border with the Siberian Platform. The whole province can be divided into three regions: 1) Western-Aldan segment with Murun, Sakun and Khani massifs; 2) Central-Aldan segment with Inagli, Jakout, Rjabinovi, Tommot, Yllymakh and Khatastir, Kaila and Amga as well as the groups of small bodies and diatremes and the Bilibin massif in its eastern part; 3) the East-Aldan segment with the massifs Arbarastakh, Konder, Ingili and other smaller massifs. A new scheme of the magmatism for the alkaline massifs was developed using the data of petrologic-geochemical investigations of the last 20 years [Vladykin, 1997, 2000].

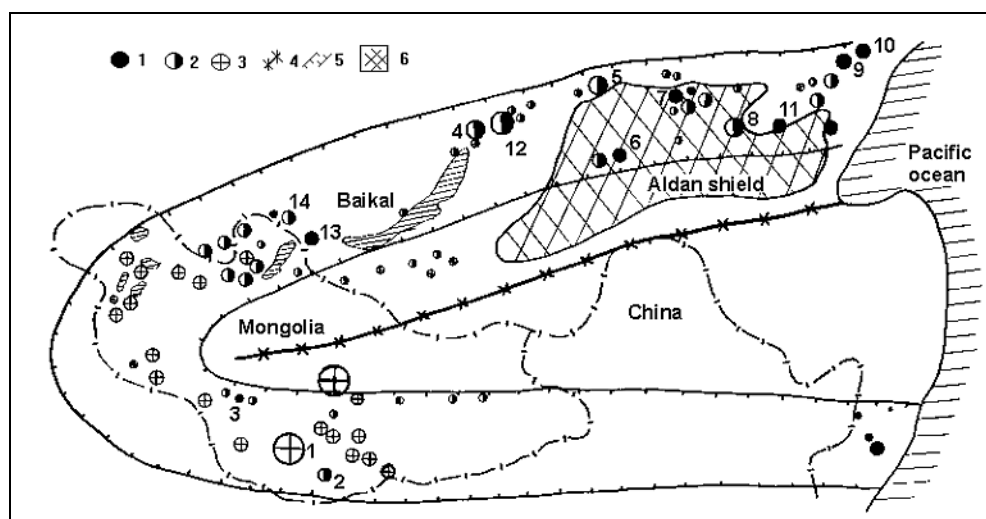


Fig. 1. The scheme of the alkaline magmatism area of the Mongol-Okhotsk belt.

Symbols: 1 - alkaline massifs with abundant ultrabasic rocks; 2 - alkaline massifs with scarce ultrabasic rocks; 3 - massifs of alkaline granites; 4 - Mongol-Okhotsk lineament; 5 - boundaries of the alkaline rocks area, 6 - Aldan shield.

Massifs: 1 - Khan-Bogdo, 2 -Lugingol, 3 - Mushugai, 4 - Burpala, 5 -Murun, 6 - Khani, 7 - Inagli, 8 - Bilibin, 9-Konder, 10-Ingili, 11-Arbarastakh, 12 - Synnyr, 13-Zhidoe, 14-Belay Zima.

THE SCHEME OF K-ALKALINE MAGMATISM OF THE ALDAN PROVINCE

The first specific feature of K-alkaline rocks of the Aldan province is:

Complexes of K-alkaline rocks from the Aldan shield form the most complete series of magmatic rocks. The main process, leading to the formation of the complete series are magmatic differentiation and lamination, resulting in the continuous series of rocks from the K-alkaline-ultrabasic through basic and middle rocks to acid alkaline granites.

The most complete series of rocks was found in the standard, the largest Murun and Bilibin massifs of the same age (120-145 Ma) of the Aldan province. The area of each massif is 150 km². These massifs were formed in different blocks of the Aldan shield, which were subjected to the tectonic movements of different intensity. The crystallization of the rocks from the Murun complex occurred simultaneously with the intensive tectonic movements in the western part of the Aldan shield, while the rocks of the Bilibin massif in the center of the shield solidified in a quite environment. As a result the Murun massif contains both the intrusive and volcanic rocks, which resulted from the 4 intrusion phases. The Bilibin massif involves only 2 intrusion phases and the second stage includes the gradual facies transitions from one rock to another. The difference in the massif formation implied an ore potential, which is more diverse for the Murun massif.

The geologic structure of the Murun massif is given in Fig. 2.

The early phase: 1) olivine-spinel rocks (occurred as xenoliths) with zones of the olivine-pyroxene-phlogopite-monticellite rocks, containing melilite; 2) laminated series of alkaline-ultrabasic rocks, containing Bt-pyroxenites, olivine lamproites, calcillite ijolites, leucite fergusites and sanidine shonkinites.

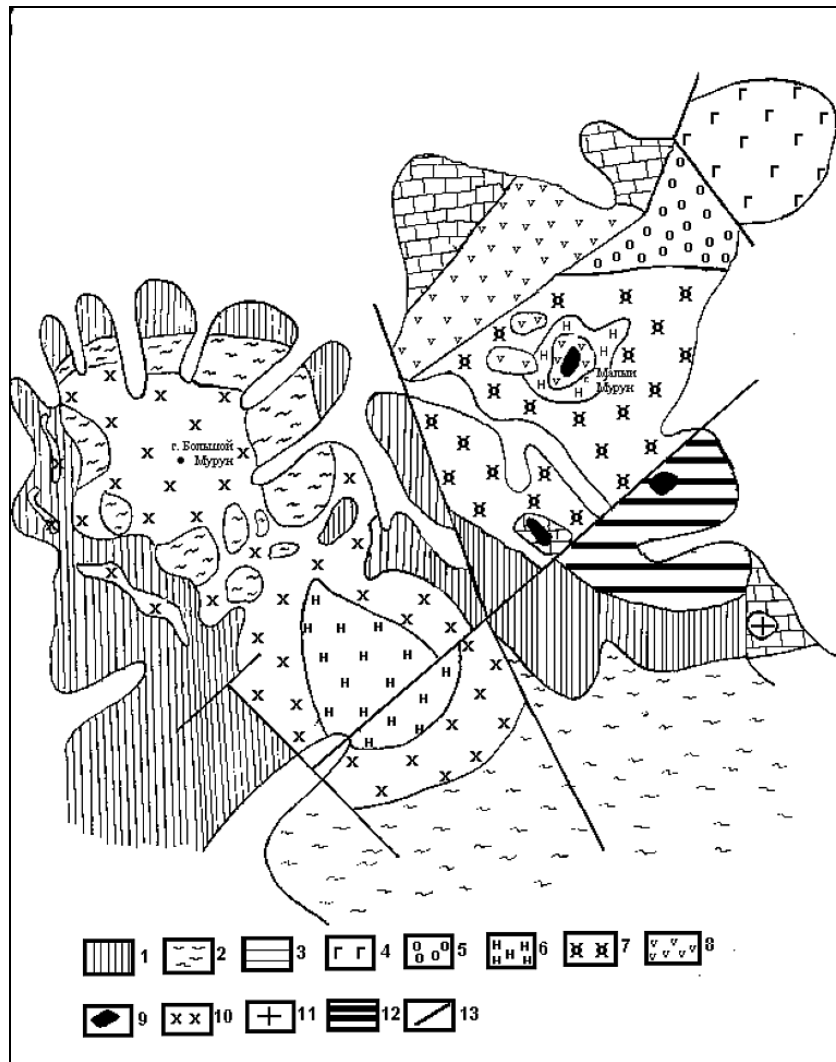


Fig. 2. Geological scheme of the Murun complex.

Host rocks: (1) Archean granite-gneiss, (2) Proterozoic quartz sandstone, (3) dolomite intrusive rocks, (4) layered series of Bt-pyroxenites, (5) pseudoleucite syenite, (6) nepheline syenite, (7) alkali feldspar syenite, (8) extrusive complex of leucite phonolites and leucite lamproites, (9) aegirine, (10) alkali feldspar and quartz syenites, (11) alkaline granite, (12) rocks of the charoite complex, (13) faults.

The main phase contains the layered series of different pseudoleucite, calcillite, potash feldspar syenites, crystallization of which is terminated by the quartz syenites, dikes and stocks of the alkaline granites.

The volcanic phase involves the layered flow of the leucite melaphonolites, leucites and leucitic lamproites, their tuff lavas, tuff breccias and veined rocks: leucitic tinguaites, richterite-sanidine lamproites, trachyte-porphyrries, syenite-porphyrries, eudialyte lujaurites.

The latest phase was crystallized from the residual melt-fluid and formed the laminated banded series of the silicate-carbonate rocks [Vladykin et al., 1983]. It contains the quartz-calcite pyroxene-microcline rocks, potash feldspar, pyroxene-potash feldspar rocks, calcite and “benstonite” carbonatites, charoite rocks and

rocks with the quartz-calcite structure. All rocks have the varieties, transitional in terms of the composition.

The fenites and calcite-richterite-tetraferriphlogopite rocks are found on the contact with the silicate-carbonate group rocks. The lamination in rocks of the Murun complex is horizontal (it is found in cores from numerous bore holes) and represents the alteration of rocks (layers of 1-5 m thick) of different mineral composition (leuco- and melanocratic) and fine-, average and coarse-grained structure. The blocks of the charoite rocks have the tilted and vertical lamination. The most significant lamination is observed in the near-contact parts of the massifs, which can be derived from the rate of magma chilling.

The geologic structure of the Bilibin massif is given on Fig. 3.

The early phase contains the layered series of rocks, involving the micaceous peridotites (with dunite xenoliths), biotite pyroxenites, olivine lamproites, leucite fergusonites and sanidine shonkinites. The thickness of some rock layers varies from 2 to 10 m.

The main phase is represented by the leucocratic series of rocks, which gradually alternate each other. The following rock series is found from the massif periphery to its center: pseudoleucite melano-, meso and leucosyenites, feldspar alkaline syenites, quartz syenites, amphibole alkaline granites and alkaline amphibole-biotites granites. The transition from one rock varieties to others is gradual, facies-like. It is evident in some cross-section from the contact to the massif center, which is possible owing to the significant (to 90%) outcrop of the massif at the height of 2500 m.

The magmatic stage in both massifs changes into the intensive hydrothermal stage. In the Murun massif these are zones of quartz alteration and sulfur alteration with Th, U, Au, Ag, Pb, Cu, Mo mineralization, scarns with galena and sphalerite, quartz veins with anatase and brookite. On the Bilibin massif they include the greisens with W, Mo, Au, Cu mineralization. The chemical composition of main rock varieties from these massifs and the concentration of rare elements are given in Tables 1 and 2.

PETROCHEMICAL AND GEOCHEMICAL FEATURES OF K-ALKALINE ROCKS

Petrochemical diagrams of binary and triple correlation dependencies of the petrogenic elements, compiled based on 500 silicate analyses of Murun massif rocks and 200 silicate analyses of the Bilibin massif rocks are given on Fig. 4 - 6. These diagrams show that the spectrum of the rock composition in standard massifs is wide. The classification alkalis-silica diagrams the rock compositions of these massifs overlap all fields of the composition points (from ultrabasic to

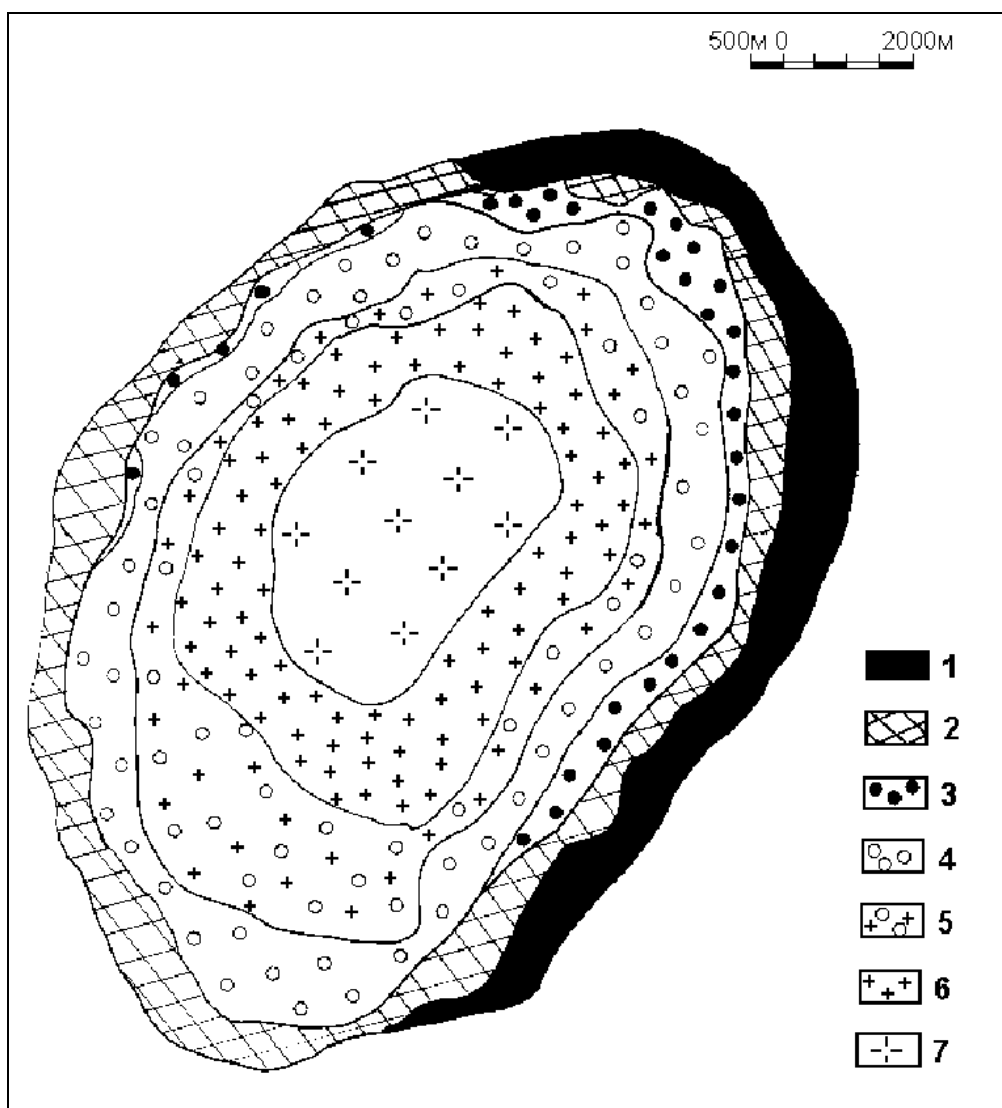


Fig. 3. Scheme of the geological structure of the Bilibin massif.

1- layered complex of K-ultrabasic-alkaline rocks; 2 - shonkinites and melanosyenites; 3- mesosyenites; 4 - alkaline leucosyenites; 5 - quartz syenites; 6 - alkaline granites; 7 - subalkaline amphibole-biotite granites.

granite composition) with the transitional varieties. These diagrams show the continuity of the composition change from early to late varieties, that is the indication of the common origin.

In our viewpoint one of the reasons of the intensive differentiation and magma layering in the Murun massif is their high K-alkalinity and high K-agpaite content when the K/Na ratio is 15-3. These two important features are observed in the mineral parageneses of rocks. The characteristic leucocratic paragenesis is the following: leucite, calcite and K-feldspar when the albite, nepheline and melanocratic paragenesis (mica, pyroxene, K-richterite and K-arfvedsonite) are not available. Like other alkaline massifs the rocks of the Murun massif are characterized by the similar behavior of sodium. It is accumulated from early to

Table 1. Chemical compositions of major types of rocks of Bilibinsky and Murun massifs (wt.%).

	1	2	3	4	5	6	7	8	9	10	11	12	13	14	15	16	17	18	19	20	21	22	23	24	25	26
SiO ₂	42.4	42.9	47.2	51.4	54.5	61.8	69.9	71.8	41.1	45.5	42.6	48.9	56.1	61.0	77.0	55.4	47.4	50.6	61.8	57.6	21.6	16.6	31.7	23.2	6.4	25.0
TiO ₂	1.1	1.4	0.3	0.6	1.0	0.5	0.2	0.2	1.4	1.1	0.8	1.1	0.5	0.8	0.6	1.0	1.3	1.3	0.3	0.3	0.5	0.3	1.0	0.3	0.1	1.1
Al ₂ O ₃	3.1	7.0	7.4	12.8	14.9	16.8	15.6	15.2	7.4	7.3	11.0	10.7	18.0	15.2	6.5	14.8	9.6	10.9	6.3	2.5	0.5	3.2	10.2	5.4	1.6	6.5
Fe ₂ O ₃	3.0	4.7	2.5	3.3	2.9	2.7	0.9	1.3	5.4	6.5	4.7	5.4	5.1	3.5	2.8	6.2	8.1	14.5	4.3	2.3	3.0	1.4	1.4	5.0	0.6	9.6
FeO	4.1	6.8	5.1	2.3	2.2	2.0	0.9	0.2	5.1	4.7	4.1	5.4	0.8	2.5	1.6	2.5	4.1	1.4	1.1	0.9	0.7	0.7	4.1	1.4	1.2	6.8
MnO	0.1	0.2	0.1	0.1	0.1	0.1	0.1	0.1	0.2	0.2	0.2	0.2	0.1	0.1	0.1	0.2	0.2	0.5	0.2	0.2	0.1	0.1	0.2	0.3	0.1	0.4
MgO	31.2	15.5	19.8	7.6	5.3	1.5	0.5	0.4	18.0	12.6	12.6	5.3	0.6	0.6	0.9	1.3	6.4	0.4	0.4	0.6	0.3	0.4	11.4	4.2	1.3	0.6
CaO	8.1	11.9	8.0	7.3	3.9	2.8	1.4	1.2	8.3	8.3	12.2	5.6	1.8	2.0	0.9	3.3	3.8	1.9	10.7	17.4	34.3	20.1	12.4	31.0	46.3	18.2
BaO	0.2	0.3	0.1	0.1	0.4	0.2	0.2	0.2	0.5	0.1	0.7	0.5	0.5	0.5	0.1	0.5	1.4	0.2	0.1	1.3	1.0	23.8	0.6	0.8	0.2	4.4
SrO	0.1	0.2	0.1	0.2	0.1	0.2	0.4	0.2	0.3	0.3	0.1	0.3	0.1	0.1	0.1	0.2	0.2	2.5	0.3	1.0	7.3	5.9	0.8	0.6	2.4	3.2
K ₂ O	2.5	5.4	6.1	11.7	11.6	6.6	5.4	4.8	7.4	7.1	7.7	10.5	15.5	12.4	5.8	10.7	8.9	4.6	5.8	7.3	0.9	3.1	7.7	2.5	1.2	3.9
Na ₂ O	0.7	0.9	0.8	0.6	1.4	4.6	4.6	4.6	0.5	1.4	0.5	1.2	0.6	1.0	2.0	0.9	3.2	9.7	2.3	3.4	1.8	0.5	1.4	0.9	1.6	0.2
P ₂ O ₅	1.2	2.0	1.2	1.1	0.7	0.2	0.1	0.1	1.8	1.9	0.7	1.7	0.01	0.03	0.2	0.3	1.9	0.01	0.03	0.1	0.4	0.3	0.2	1.2	0.1	0.2
H ₂ O	2.6	0.5	0.9	0.8	0.8	0.2	0.1	0.1	1.7	1.9	0.8	1.5	0.5	0.3	1.2	0.7	1.7	0.9	0.4	3.7	0.7	0.5	1.2	0.8	0.4	0.3
F	0.12	0.22	0.14	0.48	0.4	0.29	0.14	0.06	0.7	0.03	0.07	0.5	0.01	0.22	0.2	0.22	0.9	0.1	0.3	0.25	0.13	0.1	1.4	0.3	0.05	1.0
CO ₂	0.04	0.1	0.15	0.44	0.3	0.1	0.08	0.06	1.5	1.7	1.8	0.7	0.3	0.5	0.6	1.9	1.5	0.3	6.2	1.0	26.4	23.4	14.5	22.4	36.9	18.9

Note. Bilibin massifs: 1 - Bt-peridotite; 2 - Bt-pyroxenite; 3 - olivine lamproite; 4 - leucite shonkinite, 5 - leucite syenite; 6 - quartz syenite; 7 - alkaline granite; 8 - subalkaline granite.

Murun massifs: 9 - Bt-pyroxenite; 10 - olivine lamproite; 11 - K-ijolites; 12 - shonkinite; 13 - leucite syenite; 14 - alkaline syenite; 15 - alkaline granite; 16 - leucite phonolite; 17 - leucite lamproite, 18 - eudialyte lujaurite; 19 - silicate-carbonate rock; 20 - charoite rock; 21 - calcite carbonatite, 22-Ba-Sr-carbonatite, 23-24 -Py-Bt carbonatite; 25 - calcite carbonatite with Bt; 26 - Mgt-Bt-carbonatite.

Table 2. Composition Trace Elements in Rocks of the Bilibin and Murun massif (ppm).

	1	2	3	4	5	6	7	8	9	10	11	12	13	14	15	16	17	18	19	20	21	22	23	24	25	26
NN	2200	920	1200	310	140	43	24	9	260	500	120	76	3	3	7	20	78	3	12	40	3	5	3	1	3	1
Cr	1200	450	820	150	120	18	43	30	190	130	90	63	10	4	55	10	100	14	30	19	6	3	10	4	10	44
Ni	75	90	84	40	33	13	5	3	40	30	35	39	7	7	7	15	37	5	7	2	2	1	5	8	5	18
Co	27	280	50	37	120	82	39	21	500	290	190	300	90	120	990	410	390	660	1100	1000	380	100	240	210	250	740
V	13	86	46	51	24	9	4	19	20	18	16	20	4	4	2	7	22	2	1	2	2	1	1	1	1	1
Sc	1	2	1	1	1	3	2	2	7	8	5	6	6	4	7	5	6	15	51	12	14	27	1	1	2	1
Sn	3	1	3	1	2	26	45	32	220	12	20	11	10	11	150	140	8	1100	320	830	300	89	390	28	400	1040
Pb	40	100	46	17	3	60	50	39	160	200	87	210	95	60	37	100	320	550	80	54	30	28	270	112	54	190
Zn	11	14	15	7	85	30	11	24	200	70	130	300	12	48	12	82	220	50	49	170	10	170	58	15	80	270
Cu	1	3	5	8	10	8	11	12	70	20	10	16	10	20	50	10	50	160	60	48	21	10	100	80	330	430
Nb	24	91	45	19	50	250	160	110	285	200	440	390	290	110	160	360	490	4420	255	500	105	300	400	280	870	980
Zr	1	8	4	3	2	5	-	1	23	17	10	12	1	9	10	18	50	4	26	34	120	20	8	160	16	23
Y	64	586	280	332	171	322	217	141	222	170	150	292	20	126	100	160	376	264	250	883	1000	1100	160	4600	490	3640
TR																										

Note. Descriptions of samples as in Table 1.

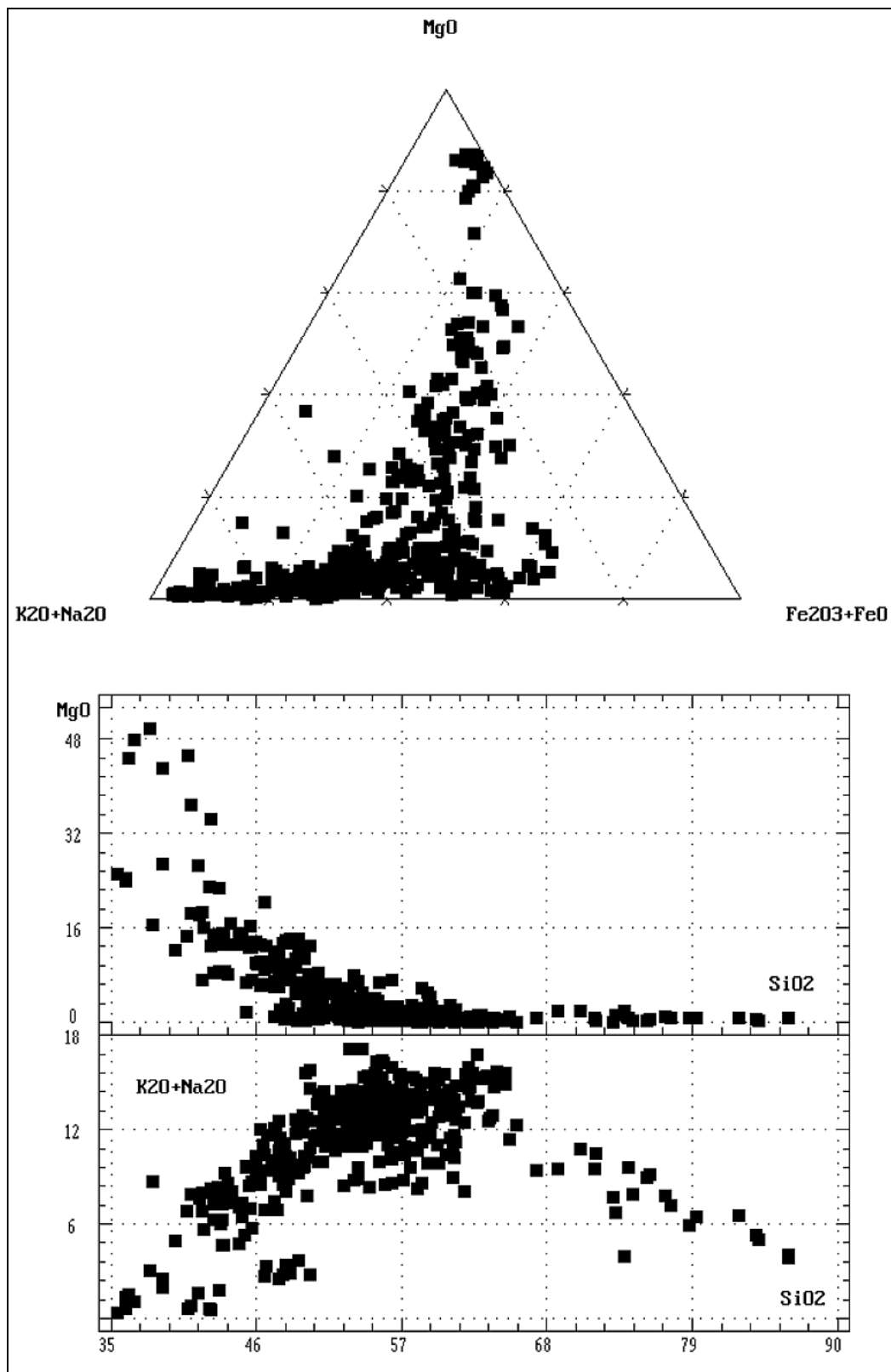
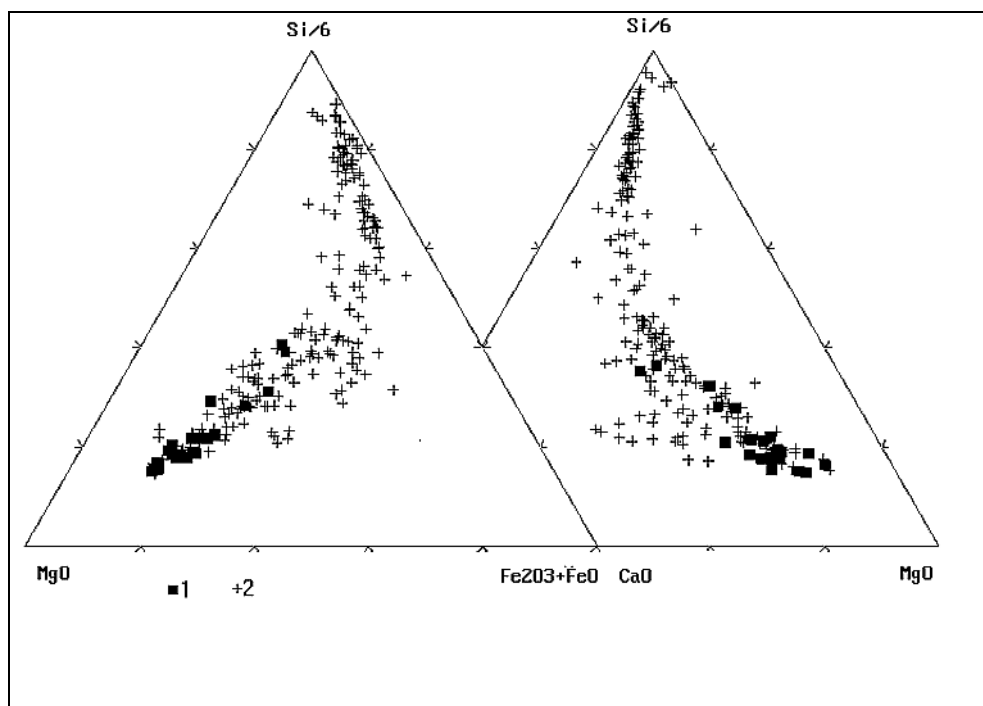


Fig. 4. Variations of some major element concentrations in silicate rocks of the Malyi Murun Massif.

late rocks (in the Murun massif it varies from 0.1 to 7-8 %), even in the latest rocks namely eudialyte lujaurites it is 5-6% K_2O and 7-8% of Na_2O . However, the leucocratic paragenesis remains potash (calcite + potash feldspar), while the sodium is spent for the formation of pyroxene (aegirine), the non-aluminum



*Fig. 5. Compositional variation of rocks from the Bilibin massif:
1-lamproites, 2-other alkali rocks of massif.*

minerals (K-richterite, K-arfvedsonite and tetraferriphlogopite are formed owing to K-agpaitic content. The late rocks even the eudialyte contains up to 3-4 % of K_2O . The specific indication of the K-agpaitic content is the accessory mineralization. The Zr-silicates of wadeite and deliite, Ti-silicates, K-batisite, davanites, tinaxite as well as the group of water alkaline silicates (charoite, fedorite, canasite, tokkaite, apophillite, mizerite etc.) are originated in the rocks.

As it is evident from the diagrams (Fig.7) the similar petrochemical features are common to other massifs of the Aldan alkaline rocks. Not the total genetic series of rocks is observed on the erosion shear. However, the direction of the magmatic evolution of the rocks is one and the same for all alkaline massifs of the Aldan province. A gradual increase of SiO_2 up to maximum values in the magmatic rocks during the differentiation is of interest (88%) (Murun and Yllymakh massifs). These granites contain quartz, aegirine and potash feldspar.

We have done the geochemical analysis to study the behavior of rare elements (Li, Rb, Cs, B, Be, F, Ba, Sr, Sn, Pb, Zn, Cu, Mo, Ag, Cr, Ni, Co, V, Sc, Zr, Hf, Nb, Ta, Y and TR group. The concentration of siderophile elements (Cr, Ni, Co, Sc) decreases and Ba, Sr, V, Be, Zn, F, Sn, Zr, Nb, TR, Y concentrations increase

from early to late rocks. Fig 8 and Fig 9 show the distribution of rare elements in the rocks from the Murun and Bilibin massifs, normalized from the Clarke in syenites (elements on the plot are located in terms of the ionic radius decrease). The Eu fractionation is found from the TR spectra data, that confirms their origin from the crystallization of the magmatic differentiation. The geochemical specialization of alkaline rocks of the Aldan shield is determined by the following features:

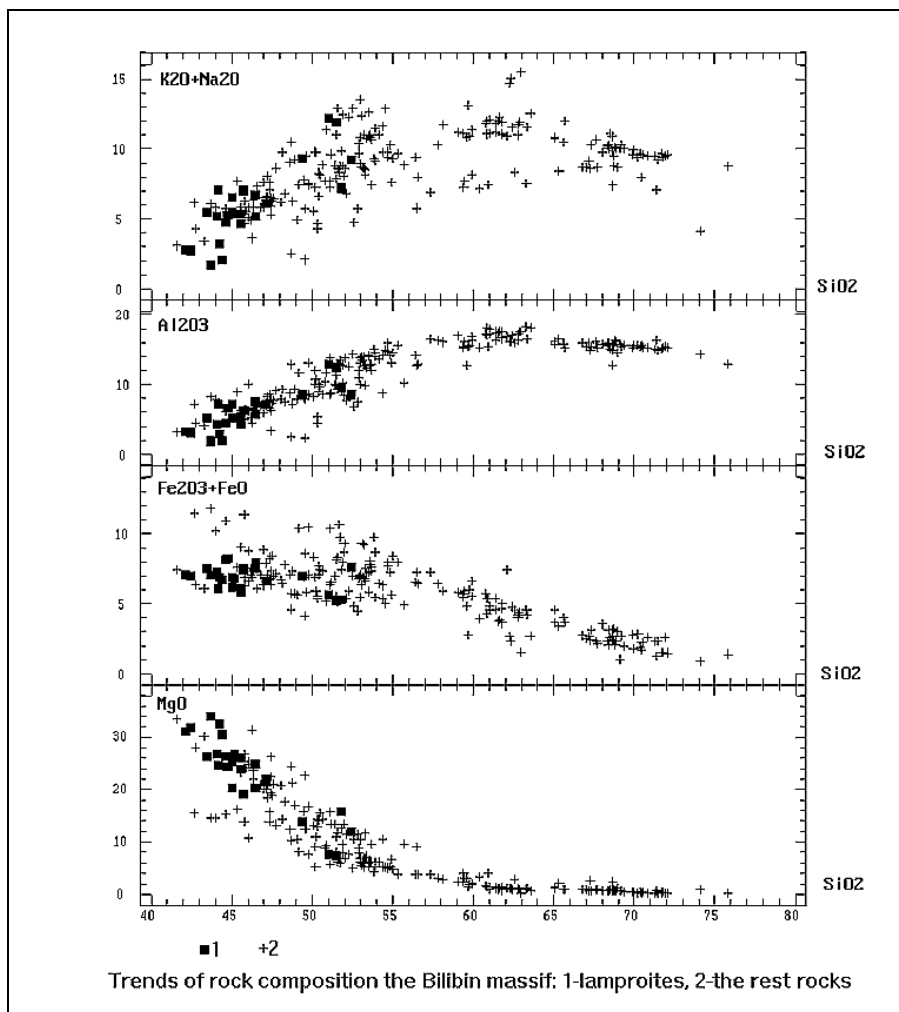


Fig. 6. Major element compositional variation of alkali rocks from the Bilibin massif:

1 - lamproites, 2 - other alkali rocks of massif.

1) high magnesia content from the early rocks and MgO decrease up to 0 in late rocks, the anomalously high potassium concentration, which varies from 4 to 16 % from early rocks to late ones and then it slightly decreases up to 10 % (if K/Na ratio is high);

2) anomalously high Ba and Sr concentrations, which in late rocks namely benstonite carbonatites form the ore concentrations (to 33% of Ba and 10 % of Sr);

3) high Cr and Ni concentrations in early rocks, which decrease in late rocks;

4) apgaitic character of Zr, Ti, Nb, TR behavior, which is evident in the accessory mineralization;

5) the saturation of magmas with volatile element, mainly in CO_2 , P_2O_5 , H_2), hydrocarbons, to lesser extent F;

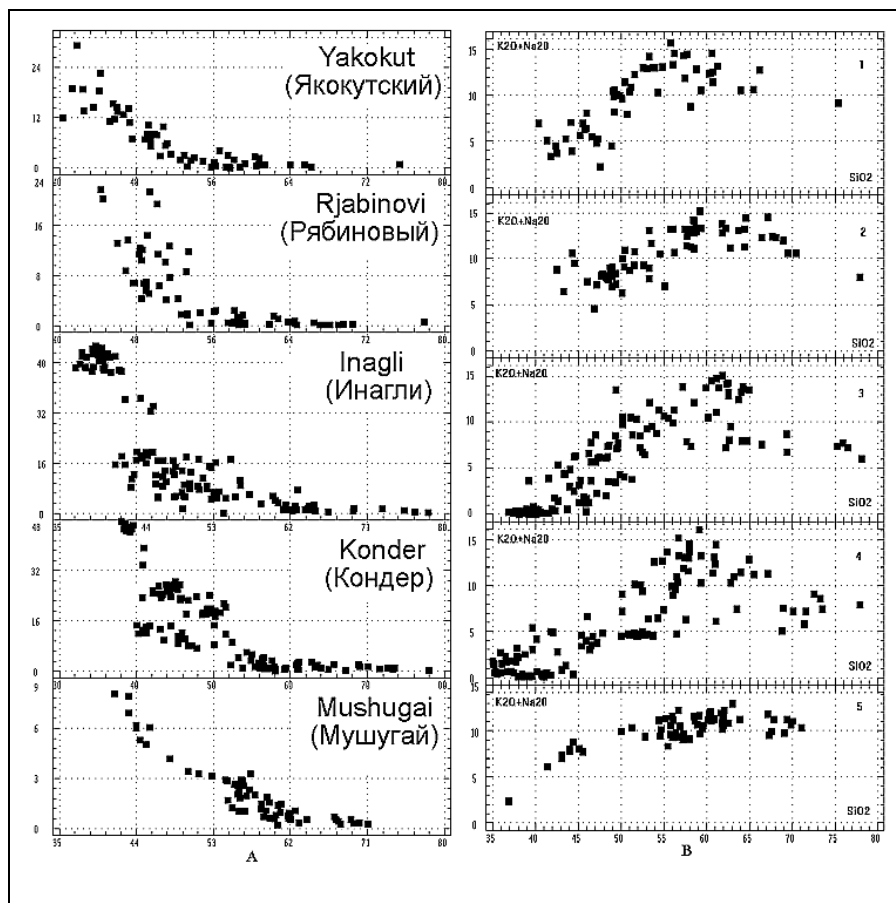


Fig.7. Variations of some major element concentrations in silicate rocks of the Aldan Shield Massifs.

6) the recovered pattern of the crystallization, which leads to the formation of numerous phases of native elements and intermetallides in the late silicate-carbonate complex.

THE ROCK OF THE LAMPROITIC SERIES IN MASSIFS OF K-ALKALINE COMPLEXES

Another characteristic feature of K-alkaline rocks of the Aldan province is the formation of the intrusive analogs of the lamproitic series during the differentiation. In terms of the mineral and chemical composition they do not differ from lamproites of other regions, though they have regional features. The trend of the composition of all rocks of separate massifs and their geochemical features indicate the genetic association between the lamproites and K-alkaline series of the Aldan.

14 occurrences of lamproites are found at present on the Aldan shield. Five of them were discovered by the author [Vladykin 1985, 1997₁]. The lamproites compose the sills, necks, eruptive breccias as well as dikes, stocks and layers in rocks of the layered alkaline complexes. They are observed in the Murun and

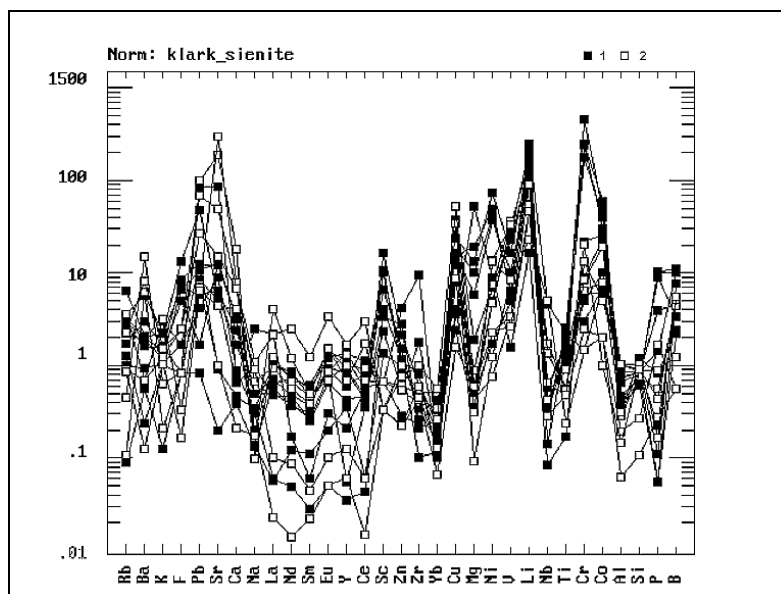


Fig. 8. REE distribution in the rocks of the Malyi Murun Massif, normalized to clark values in syenite. (1) Early silicate rocks. (2) silicate-carbonate rocks of the charoite complex.

Khani massifs and on the Molbo River in the Western part of the Aldan shield, in the Yakokut, Rjabinovy, Inagli, Yllymakh, Tommot, Yukhta massifs of the Central Aldan, Bilibin and Konder massifs of the Eastern Aldan. Some diatremes which are not related to the massifs of alkaline rocks are found in the northern part of the central Aldan. They include Kaila pipe and Khatastyr field. However, xenoliths of the alkaline rocks, the massifs of which were not exposed by erosion, are found in them. The rocks of the lamproitic Aldan series are Mesozoic [Makhotkin et al., 1989] and only Khani lamproites are Proterozoic, though they are located within the area of the alkaline rocks. The Aldan lamproites were described in detail earlier [Vladykin, 1997].

The rocks of the lamproitic Aldan series form both the eruptive breccias with the fine crystallized matrix and the rocks of subeffusive and intrusive outlook. In terms of the mineral composition the olivine, leucite and sanidine varieties are found. The varieties of the transitional composition are available between them.

In terms of the chemical and mineralogical composition the Aldan lamproites do not differ from the lamproites of other parts of the world (Tabl. 3), which is verified by the common trend of the composition on the plots of binary correlation of rock-forming elements. The gradual transitions from early olivine lamproites to less magnesia leucite and sanidine varieties are observed during the differentiation of the lamproitic magma. Moreover, the early olivine is replaced by K-richterite and tetraferriphlogopite while leucite is replaced by the K feld spar. The presence of these minerals (olivine and leucite) is found in the melted

Table 3.

Chemical Composition of Lamproites, Aldan Shield (mass. %).

N\N	1	2	3	4	5	6	7	8	9	10	11	12	13	14	15	16	17	18
SiO ₂	45.47	44.07	51.96	52.29	46.02	50.34	46.33	47.20	46.48	42.29	41.70	42.72	46.06	50.40	44.23	45.13	40.25	52.90
TiO ₂	1.07	1.05	2.02	6.56	0.84	0.80	1.34	1.25	1.23	0.69	0.54	0.82	.06	0.70	0.46	0.60	0.50	0.72
Al ₂ O ₃	7.25	6.26	7.40	7.30	7.29	8.20	9.40	8.65	8.52	5.57	3.14	5.08	8.65	10.19	4.50	6.33	5.36	13.39
Fe ₂ O ₃	6.45	6.03	1.49	8.90	4.90	3.70	8.20	8.00	8.26	5.85	4.83	6.42	3.84	4.33	11.00	5.33	5.51	5.00
FeO	4.67	4.50	2.80	1.80	3.30	4.40	4.00	2.24	3.00	4.30	6.82	6.92	4.50	3.86	0.00	4.74	4.83	2.59
MnO	0.20	0.15	0.25	0.09	0.11	0.09	0.17	0.13	0.11	0.15	0.26	0.27	0.15	0.13	0.17	0.16	0.16	0.13
MgO	12.59	16.78	4.80	1.56	10.08	7.00	6.30	6.04	7.86	27.66	32.76	16.06	13.20	10.87	22.52	17.64	21.19	6.60
CaO	8.28	9.89	2.90	1.42	8.03	6.00	3.72	5.76	4.55	6.16	3.10	10.10	8.37	7.75	9.11	10.42	7.27	5.24
BaO	0.11	0.11	2.33	5.29	0.29	2.36	1.42	2.21	1.25	0.32	0.29	0.29	0.34	0.30	0.12	0.24	0.38	0.31
SrO	0.27	0.20	0.23	0.09	0.22	0.76	0.22	0.82	0.58	0.03	0.03	0.32	0.17	0.19	0.07	0.11	0.17	0.10
K ₂ O	7.10	6.20	6.92	8.28	8.40	9.24	8.85	8.48	7.62	3.97	3.12	3.82	6.55	6.62	3.29	3.77	3.34	6.95
Na ₂ O	1.35	1.11	4.47	4.96	1.95	2.36	3.16	1.77	1.41	0.30	0.23	1.83	1.00	0.94	0.68	0.88	0.64	1.96
P ₂ O ₅	1.89	1.47	0.58	0.03	1.90	0.68	1.91	1.61	1.80	0.09	0.00	1.58	0.78	0.66	0.37	0.49	0.47	0.54
H ₂ O	1.87	1.13	0.97	0.94	2.80	1.40	2.63	2.94	5.51	1.98	2.04	1.41	2.46	1.79	2.16	1.76	2.58	2.28
CO ₂	1.69	0.44	0.22	0.10	3.00	3.10	1.50	2.25	1.16	0.22	0.50	2.74	2.80	1.20	1.20	2.07	6.99	0.97
F	0.30	0.12	0.30	0.21	1.20	1.00	1.25	0.15	0.40	0.20	0.36	0.18	0.15	0.08	0.10	0.10	0.14	0.10
Total	100.4	99.48	99.48	99.73	99.81	100.8	99.51	99.44	99.57	99.72	99.51	99.79	99.55	99.68	99.95	99.74	99.74	99.86

N\N	19	20	21	22	23	24	25	26	27	28	29	30	31	32	33	34	35	36
SiO ₂	52.56	45.87	45.59	50.73	48.76	42.46	48.96	44.03	44.66	42.66	45.83	48.22	50.16	42.43	51.04	46.46	44.03	45.70
TiO ₂	0.65	0.64	0.72	0.59	1.15	0.66	0.70	0.60	0.60	0.63	1.13	0.85	0.90	1.03	0.55	0.33	0.88	0.89
Al ₂ O ₃	12.81	8.35	7.73	10.61	12.40	7.90	12.16	6.21	6.80	8.15	9.47	9.88	12.40	3.12	12.89	7.49	7.50	8.03
Fe ₂ O ₃	5.54	7.50	5.32	4.33	5.23	5.13	4.03	5.70	6.25	5.68	3.77	6.48	4.82	3.00	3.33	2.45	8.85	9.52
FeO	1.34	1.98	4.47	3.13	5.50	6.20	4.34	5.90	4.80	4.10	8.17	5.21	5.03	4.03	2.33	5.10	1.08	0.54
MnO	0.11	0.13	0.15	0.13	0.15	0.15	0.13	0.18	0.18	0.12	0.19	0.17	0.16	0.11	0.06	0.14	0.10	0.11
MgO	5.12	12.44	15.40	11.72	6.71	10.86	6.32	19.66	17.52	15.65	7.71	8.27	7.70	31.89	7.62	20.43	22.72	20.50
CaO	6.24	6.99	9.93	6.05	8.27	10.52	8.54	8.78	9.23	13.50	12.19	9.44	9.30	7.96	7.30	8.01	1.90	1.98
BaO	0.31	0.69	0.28	0.19	0.22	0.40	0.17	0.22	0.28	0.20	0.27	0.24	0.19	0.16	0.12	0.08	0.02	0.02
SrO	0.12	0.14	0.17	0.13	0.13	0.15	0.11	0.11	0.10	0.07	0.10	0.07	0.13	0.09	0.18	0.13	0.03	0.03
K ₂ O	6.58	4.14	4.93	4.20	6.40	7.22	4.65	3.41	5.26	4.38	6.58	6.75	5.14	2.29	11.69	6.05	5.23	5.50
Na ₂ O	1.98	1.04	0.79	2.13	2.58	1.55	2.36	1.39	1.12	1.00	0.61	1.43	2.67	0.44	0.54	0.70	0.85	0.88
P ₂ O ₅	0.50	0.94	0.91	0.45	0.95	1.06	0.48	0.52	0.62	0.84	1.02	0.70	0.77	1.03	1.09	1.17	0.03	0.01
H ₂ O	5.63	5.27	1.60	4.25	1.74	1.70	0.47	2.47	1.86	2.70	0.17	0.58	0.90	1.98	0.41	0.43	7.05	6.32
CO ₂	0.38	3.64	1.91	1.20	0.06	4.16	6.27	0.50	0.40	0.34	2.00	0.93	0.02	0.04	0.15	0.44	0.22	0.11
F	0.20	0.07	0.07	0.07	0.70	0.15	0.10	0.20	0.10	0.20	0.70	0.42	0.08	0.16	0.48	0.14	0.06	0.12
Total	100.0	99.81	99.94	99.95	99.60	99.50	99.76	99.80	99.74	100.1	99.64	99.49	100.3	99.70	99.62	100.5	99.52	100.2

Note. Murun massif №1-7 Dike Molbo: N 8 — by contact part; N 9 — central part Khanl massif (Ukduska): N 10 — dike in adit; Ryablnovy massif: N12 — N 14. Yakokut massif: N 15 —N17 - Tabuk-Khalastyr field: N 18 — N 20. Pipe "Kalla": N 21 -N 22. M. YakhU: N 23 — N 24. R. Dzhekonda: N 25. Massif Inagli: N26 -N 28. Tommot massif: N 29 - N 30. Illymakh massif: N 31. Bilibln massif: N 32 -36.

inclusion in the pyroxenite impregnation. The crystallization temperature of lamproites from homogenization data of these inclusions is 1300-1000 °C [Panina, Vladykin, 1994].

The high K, Ba, Sr, Cr, Ni and low Zr and Nb contents are characteristic of the spectra of rare elements from the Aldan lamproites (Tabl.4). The latter are different from the Australian lamproites. The lamproite occurrences were found to relate genetically with the massifs of K-alkaline rocks (Fig.5,6). It is confirmed by the common trend of the lamproite compositions and the hosting K-alkaline massifs as well as the common evolution of rare elements and spectra of rare earths (Tabl.5). The studies of Nd, Sr, Pb isotope geochemistry in lamproites and alkaline massifs indicate their common origin [Vladykin, 1997], which is one of the genetic features of Aldan lamproites.

Table 4. Composition Trace Elements in Lamproites of the Aldan Shield (ppm).

NN	1	2	3	4	5	6	7	8	9	10	11	12	13	14	15	16	17	18
Cr	500	420	30	10	240	200	78	65	94	910	920	800	980	860	1100	1500	1400	600
Ni	130	370	21	12	130	150	100	100	100	1200	1300	220	500	440	870	360	640	120
Co	28	57	35	8	35	32	37	24	24	110	160	66	50	90	110	94	86	33
V	290	120	820	720	250	140	390	320	320	93	100	100	260	220	110	230	160	190
Sc	18	30	28	2	14	32	22	14	18	32	8	35	33	33	35	49	15	38
Cu	70	24	330	85	100	240	220	210	380	33	18	140	260	120	60	120	88	89
Pb	12	13	560	54	7,6	76	7,5	65	140	2	1	98	24	30	9	14	22	28
Sn	8	3	20	22	0,8	3	5,7	4,3	10	1	1,2	5,2	1,6	1,6	2	1,5	1,4	2
Zn	200	65	250	36	61	75	320	68	140	65	97	160	58	70	75	71	90	68
Zr	200	120	1095	4460	200	280	490	200	230	150	87	75	170	70	80	100	59	170
Nb	20	5	96	320	20	11	50	1	1	3	1	1	4	1	2	1	3	5
ZTR	170	105	125	160	180	160	376	160	174	53	25	100	110	120	242	120	150	90
Y	17	14	18	30	10	7	50	19	18	3,6	1	10	12	13	6	10	15	11
Li	92	30	30	50	37	80	90	30	20	4	3	14	20	13	11	24	96	46
Rb	250	150	120	90	210	160	280	120	150	180	100	80	190	180	115	122	164	190
Cs	4	2	2	5	1	7	2	3	5	5	1	1	6	4	5	5	7	1
B	40	2,2	65	20	2	10	11	9,3	21	5	8	10	18	24	19	25	18	24
Be	18	2,2	13	3	5,4	5	30	12	9	1	0,8	2,3	5,5	3,8	1,8	1,9	1,9	2
B	11	5	10	12	40	33	20	42	10	20	3,6	3,4	27	2	12	9,3	3,7	4,7
Be	2,3	3,1	2	2,3	3,7	5,5	3	2,7	1,2	1	2,5	2,8	2,5	0,8	1,2	1,6	1,4	1,3

End of Table 4.

NN	19	20	21	22	23	24	25	26	27	28	29	30	31	32	33	34	35	36
Cr	240	810	1100	680	370	610	260	1180	700	510	490	560	280	2400	1200	310	69	52
Ni	97	390	340	290	108	167	55	840	500	260	120	140	110	1300	820	150	94	84
Co	19	45	53	26	37	56	32	112	80	62	56	53	35	87	84	40	59	55
V	160	170	180	160	290	265	204	230	200	130	220	370	260	35	50	37	670	550
Sc	28	49	20	16	31	43	28	29	30	51	38	44	32	15	46	51	44	24
Cu	80	100	103	87	135	117	63	122	40	37	110	95	110	14	15	7	320	260
Pb	21	20	10	14	16	20	22	27	10	4,7	120	94	15	1,7	2,6	1	2	1
Sn	1,8	1,6	2	2	2,2	2,8	3	1,2	1,5	1,4	1	1	2,3	1,6	0,7	0,8	3,6	3,5
Zn	59	80	70	83	90	140	60	68	80	64	100	82	58	70	46	17	180	180
Zr	170	180	160	120	285	125	150	200	300	250	200	150	160	24	45	19	120	80
Nb	6	7	3	1	8	3	3	3	5	8	3	1	4	3	4	5	5	3
ZTR	140	120	115	110	190	110	100	140	160	125	220	214	103	90	167	176	158	140
Y	12	10	12	13	22	18	10	17	22	16	30	26	15	6	12	9	25	20
Li	40	30	70	16	18	76	26	4	5	8	19	52	20	1	5	8	44	70
Rb	188	140	176	110	170	200	112	70	64	78	210	120	180	70	280	456	60	70
Cs	3	3	8	2	2	4	3	1	1	1	5	2	1	1	5	8	1	1
B	11	5	10	12	40	33	20	42	10	20	3,6	3,4	27	2	12	9,3	3,7	4,7
Be	2,3	3,1	2	2,3	3,7	5,5	3	2,7	1,2	1	2,5	2,8	2,5	0,8	1,2	1,6	1,4	1,3

Note. The numbers and descriptions of samples as in Table 3. Analyzed by E. V. Smirnova, A. I. Kuznetsova, and L. N. Odareeva, Institute of Geochemistry, Irkutsk.

Table 5. Composition REE in Lamproites of the Aldan Shield (ppm).

NN	1	2	3	6	7	9	10	13	15	18	22	23	25	26	30	31	33	35
La	50	29	37	44	72	37	5.5	18	27	23	30	52	21	40	41	26	35	27
Ce	68	53	49	74	130	74	19	55	44	36	53	87	43	50	86	42	59	57
Nd	31	31	18	32	68	34	14	25	29	26	21	44	25	36	50	20	48	40
Sm	6.8	7.9	4.5	6.1	19	7	3.5	6.1	6.8	4.7	4.7	8.1	5.2	5	10	4.7	11	11
Eu	1.9	3.0	1.2	1.3	5.1	2.4	0.70	1.4	1.5	0.83	1	1.9	1.8	1.8	1.6	1.3	1.8	1.5
Gd	5.1	6.1	4.3	3.7	42	8.5	2.3	5.3	3.3	3.1	4.7	6.8	5	6.8	11	4.7	5	8.9
Dy	3.8	3.8	3.7	2.2	20	4.3	1	2.9	3.5	2.7	2.5	4.9	3.9	3.8	7	2.7	3.6	7
Ho	0.52	0.81	0.82	0.31	3	0.92	0.20	0.58	0.45	.54	0.60	1.1	0.68	0.62	1.2	0.56	0.55	1
Er	1.5	2.0	3.2	0.86	7	2.2	0.40	1.7	1.3	1	1.5	2.2	2	1.8	3.4	1.5	1.6	2.4
Yb	1.6	1.4	3.1	0.63	9	2	0.38	1.4	1.1	1.3	1.4	2.2	1.5	1.8	2.7	1.3	0.82	1.9
Lu	0.14	0.18	0.35	0.11	1	0.14	0.04	0.20	0.09	0.20	0.20	0.30	0.16	0.16	0.41	0.14	0.11	0.2

Note. Analyzed by E. V. Smirnova, Institute of Geochemistry, Irkutsk. The numbers and descriptions of samples as in Table 3.

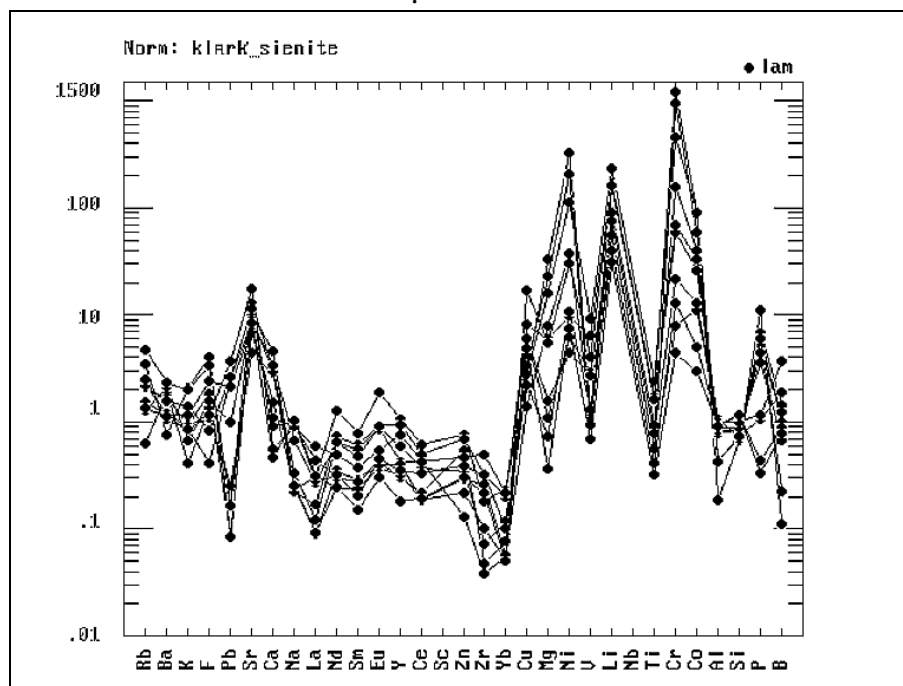


Fig. 9. REE distribution in the rocks of the Bilibin Massif, normalized to clark values in syenite

ALKALINE GRANITES - LATE DIFFERENTIATES OF K-ALKALINE COMPLEXES

The third characteristic feature of K-alkaline rocks of the Aldan province is: *one of the final magmatic differentiates of K-alkaline series of Aldan rocks are the agpaitic alkaline granites. In terms of the geochemical parameters these granites are different from the palingenic alkaline granites and rare-metal plumasitic granites in higher concentrations of siderophile elements (Cr, Ni, Co, Ba, Sr, Cu)*

and lower contents of lithophile (granitophile) elements (Li, Rb, Cs, Zn, Sn, F). The main fluid component of their differentiation is CO₂ instead of F.

As it was shown above (Fig. 4-6), the quartz syenites and alkaline granites are the final magmatic differentiates of the complete K-series of rocks in the reference sites. Depending on the intensity of the tectonic movements and fluid saturation of the residual magma during the differentiation and crystallization of massifs the fluid components separate in a different way. Under the calm tectonic setting and when the fluid accumulation is insignificant as it is found for the Bilibin massif, the alkaline and subalkaline granites originate under the gradual crystallization of the magma, forming the facies series: shonkinites → syenites → quartz syenites → alkaline granites → subalkaline granites. If the tectonic movements are intensive and the accumulation of CO₂ and H₂O is significant, the alkaline granites are separated as dikes, stocks and silicate-carbonate melt-fluid (charoite-carbonatite complex), the main silicate part of which contains mainly quartz, potash feldspar and pyroxene and corresponds to the alkaline granite. In addition to these two reference massifs the quartz syenites and alkaline granites are available almost in all alkaline massifs of the Aldan part of the area, though the volume of the outcrops is various in different massifs.

They are found in the Sakun, Khani and Murun massifs of the western Aldan; Yllymakh, Tommot, Inagli, Rjabinovi, Yukhta massifs of the central Aldan; Bilibin and Konder massifs of the Eastern Aldan.

The magnesia content decreases, silica contents, alkalinity (total alkalies) and apatitic content increase during the magmatic differentiation. When the apatitic coefficient (Ka) is more than 1, the alkaline granites are crystallized, if it is less than 1, the subalkaline granites originate. A zoning differentiation of the alkaline-granite residue is found for the Murun and Yllymakh massifs, which are marked by abundant alkaline granites. The concentration of alkalies and aluminum in the magmatic alkaline granite gradually decreases and the silica acid concentration increases to 88%. Two types of formations are the case among the granites, being the residue differentiates of the ultrabasic Aldan complex. The first types involve formations with almost equal K and Na ratios, while the second ones are marked by K predominance. The petrochemical diagrams of the binary and tertiary correlation of the petrogenic and some rare elements for all studied Aldan massifs are characterized by the common trends of rock composition from biotite pyroxenites to granites, which verifies the genetic belonging of the granite formations to these complexes (Fig. 3-7).

The analysis of spectra of rare earth elements of Aldan alkaline massifs also proves the unity of all rock series. The Eu fractionation is found. It is most evident in the granite rocks from the complex that indicates the granite origin as a result of the crystallization differentiation of complex rocks. Despite a wide spectrum of the rocks (from ultrabasic to granites) the differentiation of the rocks of the Bilibin massif was proceeded in a single stage with gradual transitions from one rock into another and took place within an short time span. It resulted in the absence of rare

earth elements accumulation; the concentrations of rare earth elements (REE) in granites (from early to late rocks) are similar to those in syenites and shonkinites. It can also explain the anomalous high MgO concentrations in granite micas (18%). In terms of the concentration of rare elements the granites being the derivatives of the ultraalkaline complexes are different from granites of the crustal origin. They possess the significant Cr, Ni, Co, V, Ba, Sr, Cu contents and low concentrations of lithophile elements (Li, Rb, Cs, Zn, Sn, F). Fluorine was initially low in the primary magma. The main volatile component in the rocks of the ultraalkaline complexes was CO₂. It's accumulation towards the end of the differentiation led to the separation of the silicate-carbonate melt. The silicate part of the melt is similar to syenites (Khani massif) or granites (Murun massif).

CARBONATITES OF K-ALKALINE COMPLEXES OF THE ALDAN AHIELD

The fourth characteristic feature of K-alkaline rocks of the Aldan province is: *another final differentiate of K-series of the Aldan province are carbonatites. As opposed to the carbonatites of Na-series they are characterized by ore mineralization (TR, Ba, Sr, F). In addition to the pure calcite carbonatites TR-apatite rocks, Ba-Sr "benstonite" carbonatites and non-typical dolomite and ankerite varieties originate. The carbonatite of K-series are separated from the silicate magma during the later period of differentiation within the syenite and alkaline granite crystallization.*

As to the Aldan province the carbonatites are more abundant in the Murun massif as well as in the Arbarastakh and Inagli massifs. They are scarce in the Khani, Rjabinovy and Bilibin massifs.

In terms of the chemical composition and volatile elements (fluid modifications) in the carbonatites and related rocks we divide these carbonatites into three types:

I. Silicate-carbonate with the fluid modifications such as CO₂, H₂O, H, F (Murun and Khani).

II. Phosphate-carbonate with the fluid modifications CO₂, P, F (Arbarastakh).

III. Carbonate with fluid modifications CO₂ (F, P) (Ingili, Rjabinovy, Bilibin).

The carbonatites of Aldan K-complexes are different from the classical carbonatites of Na-complexes (Kola Peninsula) in mineral parageneses and ore potential. One of the characteristic carbonatites from this group is the essentially calcite composition with the addition of the Ba- Sr benstonite carbonatites and the entire absence of the dolomite, ankerite and siderite carbonatites which are common for the sodium complexes.

We will consider the association of rocks from some massifs and the significance of carbonatites.

The Khani massif (Ukduska). The main phase involves the biotite pyroxenites with the apatite mineralization. The veined rocks contain shonkinites, melasyenites, leucosyenites, granites. The dikes of olivine lamproites are available

as well. The carbonatites are found in the bedrock outcrop as a vertical dike of 5 m thick, which cuts Bt-pyroxenites. The dike includes the layers of pyroxene-potash feldspar and carbonate compositions. The carbonatite contains calcite, apatite, pyroxene, Ti-garnet and accessory zircon, orthrite (?), monacite. Some dikes of the carbonatite of small thickness (0.3-1 m) are observed in the core from various boreholes in the biotite pyroxenites.

The Arbarastakh massif. The rock association involves pyroxenites, Bt-pyroxenites, biotite and carbonatite pyroxenites; dikes of ijolites, cancrinite syenites, tinguaites, pulaskites, syenite-porphyrries and alkaline picrites. The abundant ring dikes and a large ring dike of calcite-apatite-magnetite rocks occupies up to 20% of the massif area. Carbonatites are of calcite composition. In addition to the calcite the carbonatites contain alkaline amphibole, alkaline pyroxene, mica, khondrite, cancrinite, nepheline, albite, potash feldspar, apatite, magnetite. The accessory minerals involve pyrochlore, baddeleyite, zirconolite, betaphite, zirtolite, sphene, perovskite.

The Ingili massif. The massif is composed of the amphibole rocks with the sites of amphibole-pyroxenite rocks. The central part of the massif contains a big body of Bt-pyroxenites of 500 m thick. The dikes of ijolites, nepheline syenites, alkaline syenites and tinguaites are found as well. The carbonatites form the veined bodies of 30 m thick. The carbonatites contain calcite, mica, subalkaline amphibole, apatite, magnetite. The accessory minerals include zircon, sphene, pyrochlore, sulfides. Some dozens of small pipes of kimberlite-like rocks (ingilites) occur outside the massifs.

The carbonatite occurrences of the Murun massif

In terms of the mineral composition 6 varieties of carbonatites are revealed [Vladykin, 1997, 2000]:

1. ***Calcite carbonatites*** are the most widely spread variety of carbonatites. They are found on all sites of silicate-carbonate rocks occurrences, except for the "South", where only "benstonite" carbonatites are observed. The calcite carbonatites are found as elongated schlieren in silicate-carbonate rocks, veins, and horizontal bodies of 1-30 m thick and up to 1 km long. The carbonatites are composed of calcite, potash feldspar, pyroxene and scarce quartz. The secondary and accessory minerals are charoite, pectolite, tinaxite, sphene, torite, deliite, sulfides. All transitional compositions between calcite and charoite rocks are found.

2. ***"Benstonite" carbonatites***. The mineral benstonite is given in inverted commas, as at present it represents the pseudobenstonite (as pseudoleucite), decomposed into several carbonate phases [Vorob'ev et al., 1989]. The big body of carbonatites of this composition is located at the site "South". The thickness of the body is up to 30 m, the hosting potash feldspar-pyroxene rocks are cut by numerous carbonatite veinlets and are enriched in carbonatite. Carbonatites contain the "benstonite", pyroxene (50% of aegirine, 25 % of diopside, 25% of

gedenbergite), feldspar (microcline), K-richterite. The carbonatite body is divided into the leucocratic “benstonite”-potash feldspar and melanocratic pyroxene bands. The secondary and accessory minerals include quartz, charoite, sphene, wadeite, sulfides, rarely apatite. There are no transitions between calcite and “benstonite” carbonatites in this body.

3. **Calcite veins with quartz-benstonite core** and calcite-“benstonite” carbonatites of the stock-work zone. They form the veined body on the site “Original” of 2 m thick and 10 m long. The body contains the calcite, tinaxite, pyroxene, potash feldspar and quartz. The central part of the body involves the coarse-grained quartz with large “benstonite” crystals (up to 10 cm). The stockwork zone of the calcite-“benstonite” carbonatites is found in the core from the borehole N 107 of the “Andreevsky” site at the depth of 20-60 m. The alkaline syenites are cut by numerous veinlets of the leucocratic carbonatite. The veinlets are from 1 cm to 10 cm thick. The carbonatites contain the calcite, “benstonite”, potash feldspar. This carbonatite variety is widely distributed in the silicate-carbonate rock complex and cut the earliest calcite carbonatites.

4. **Carbonatite veins**, consisting of **quartz-calcite graphics**. Pyroxene, potash feldspar, richterite, sphene and abundant sulfides are observed among secondary minerals.

5. **Calcite carbonatites with iron mica and magnetite**. They occur in the core from the borehole N 107 in syenites as veinlets up to 20 cm thick. These veinlets contain the fine-grained calcite and larger impregnation of mica and magnetite. The fluorite is abundant (to 20%) in some veinlets.

6. **Pyroxene-phlogopite-calcite carbonatites** are found in the hosting rocks of the south exocontact of the massif in the cores from boreholes N 1026, N 1052. Carbonatites contain the layered calcite, making the trachyte-like texture of rocks, pyroxene, tetraferriphlogopite and quartz. The accessory minerals include apatite, brown zircon, ilmenite (geikelite). The carbonatite body of 20-30 m thick cuts the hosting gneiss. In the upper part the body is transferred into the eruptive breccias of rounded tetraferriphlogopite-microcline “xenoliths”, cemented by the calcite aggregate.

The geochemical specification of K-series carbonatites is marked by the increased and ore concentrations of Ba and Sr as well as the heightened concentrations of TR, Pb, Cu, V, P and in cases Nb, Co, Zn. The TR spectra of the Murun massif carbonatites are given on Fig. 10. Eu fractionation is typical of carbonatites that indicates the origin of residual magma.

K-series carbonatites as opposed to Na-series carbonatites are different from the silicate magma at the later stage of the crystallization of syenites and granites. It is confirmed by the drop-like separation of the carbonate in some syenites and granites from the Murun massif. The later separation of carbonatites from the silicate magma explains the accumulation of TR and Ba-Sr concentrations and not higher temperature Nb.

GENETIC FEATURES AND PROBLEM OF THE MANTLE SOURCES

In terms of the spectrum of rocks composition, geochemical and mineragenic specialization the studied K-alkaline series of the Aldan province rocks is similar to the lamproite series.

The main feature of the magmatism of alkaline rocks from the Aldan province are: 1). The formation of the complete spectrum of rocks (from K-alkaline-ultrabasic to alkaline granites with all transitional compositions) during the of the primary magma differentiation, 2) the occurrence of the lamproitic rocks in the massifs; 3) formation of the alkaline granites on the last stage of the magma differentiation; 4) separation of silicate-carbonate (melt-fluid) portion, which gives rise to different carbonatites of K-series and charoite rocks on the late magmatic stage. The carbonatite liquid separates in the studied K-series on the later stage of

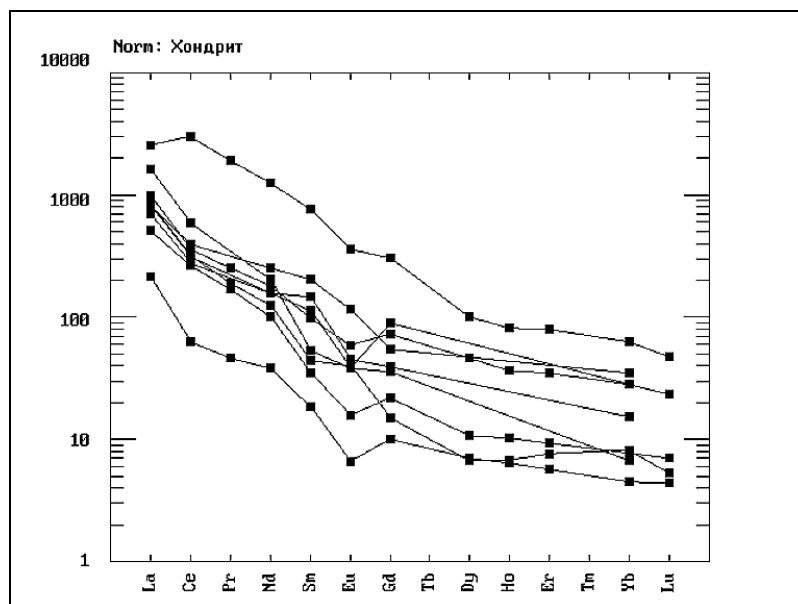


Fig. 10. Chondrite-normalized REE patterns in carbonatites.

magma differentiation as opposed to Na-series rocks, namely it is separated on the stage of crystallization of syenites and granites. It results in the geochemical specialization and ore potential of carbonatites of K-series: 1) high (to ore) concentrations of Ba and Sr; 2) TR is accumulated instead of Nb. The differentiation is prolonged in the K-series rocks. From the homogenization temperatures of melted inclusions it is estimated from 1500 to 700 °C. The above statements can be confirmed by the occurrence of the melted inclusions of 1) lamproitic composition, 2) separated from the silicate part the carbonatite saline melt [Panina et al., 1989, 2000].

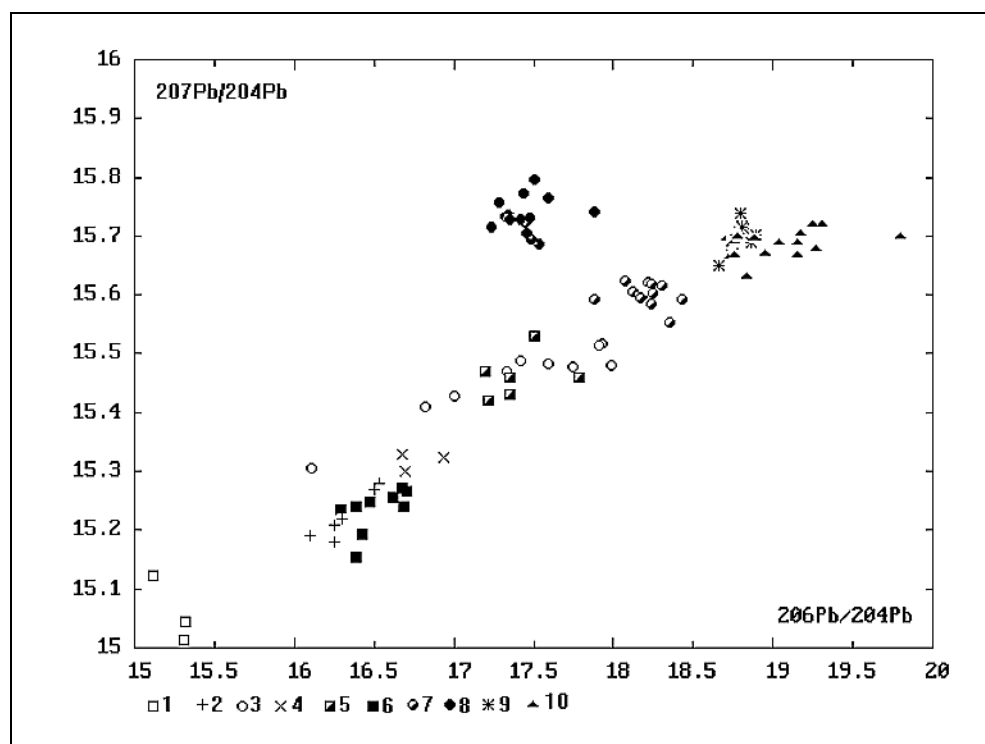


Fig. 11. Lead isotopic compositions in rocks of the Murun Massif and lamproites worldwide.

(/) Greenland, (2) Smoky Butte, (3) Montana, (4) Prairie Creek, (5) Leucite Hills, (6) Murun, (7) Australian alkaline basalts, (8) Australian lamproites, (9) Spain lamproites, (10) Italian alkaline rocks.

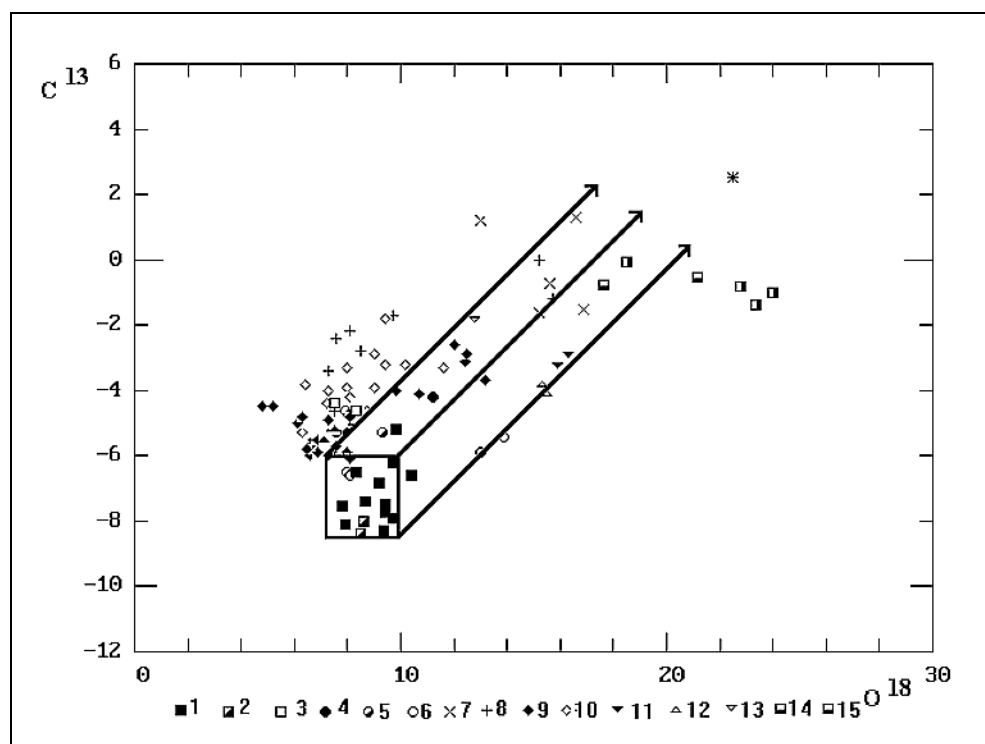


Fig. 12. Carbon and oxygen isotopic compositions in some carbonates.

Massifs: (1) Murun, (2) Khani, (3) Bilibin, (4) Koksharovki, (5) Arbarastakh, (6) Ingili, (7) Mushugai, (8) Kola Peninsula, (9) Belaya Zima, (10) Guli, (11) Darai-Pioz, (12) Tagna, (13) Burpala, (14) Seligdar, (15) Bayan-Khushu, (16) Lulingol.

The first data on Nd isotope composition and additional data on Sr, O, C, and Pb isotope composition on the K-alkaline rocks and associated carbonatites of the Aldan province have been for the first time obtained [Mitchell et al., 1994]. For comparison we use the available isotope data on the Mongol alkaline province and on carbonatites from alkaline massifs of the framing of the Siberian Platform as well as literature data on lamproites from the world [Mitchell, Bergman, 1991, Jaques et al., 1986].

The ratio of Pb isotopes in lamproites of the world is given on Fig.11. The isotope data of lamproites lie on the direct line, forming a common trend. Only the Australian lamproites are not involved in this trend. The Pb isotopic compositions of the Murun lamproites lie in the field of the North American lamproites, which are similar in terms of the geochemical indicators. The age of the mantle

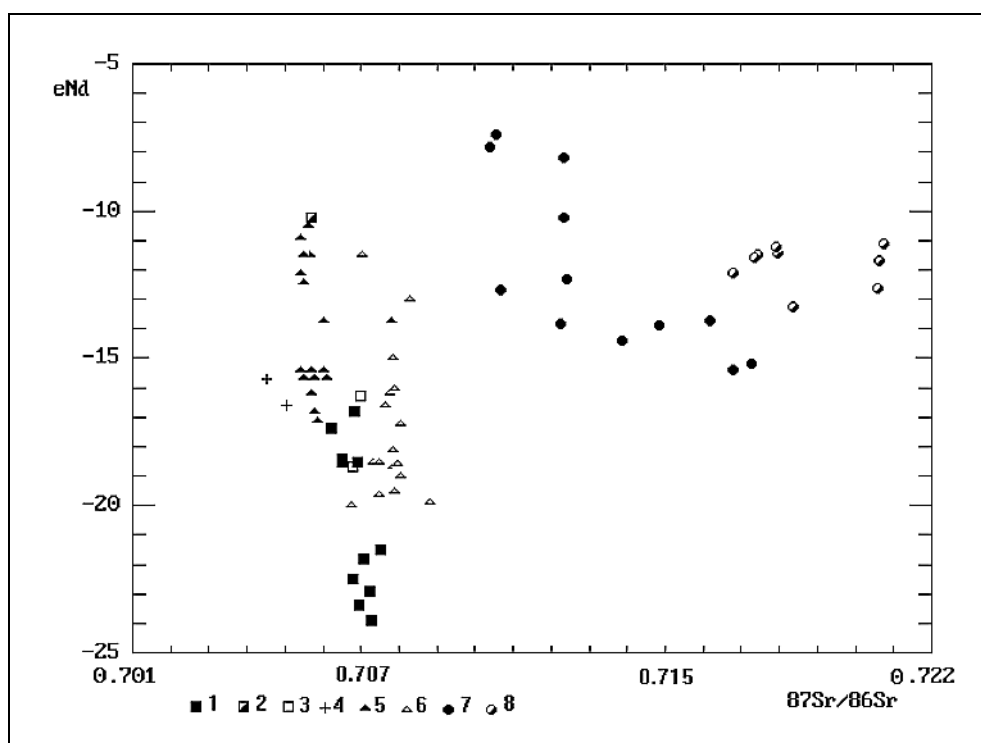


Fig. 13. Strontium and neodymium isotopic compositions in rocks of the Murun Massif and lamproites worldwide. (1) Murun, (2) Yakokut, (3) Bilibin, (4) Khani, (5) Leucite Hills, (6) Montana, (7) Australia, (8) Spain.

substratum is evaluated as 3.2 billion years. This figure is obtained from the calculation of analysis of Pb isotopes in the galena of the Murun massif rocks [Vladykin, 1997].

The ratio of carbon and oxygen isotopes in the Aldan carbonatites and carbonatites of Siberia and Mongolia are given on Fig. 12. The isotopes of carbonates of the Murun and Khani massifs lie in the mantle square (from Yavoy, 1986) and have the deepest origin. The isotope values of other carbonatites lie on the line of trends of the mantle differentiation.

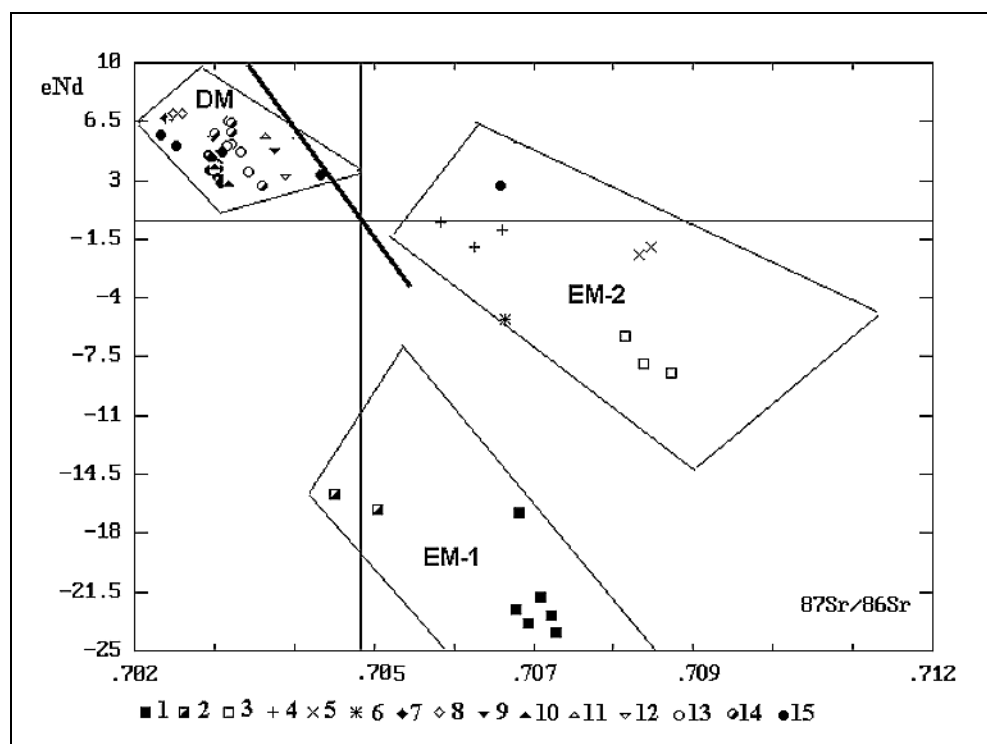


Fig. 14. Ratio of eNd and $87Sr/86Sr$ in carbonatites.

Massifs: 1 -Murun, 2 -Khani; 3 -Darai-Pioz; 4 -Mushugai; 5 - Luginol; 6 - Selegdar, 7 - Ingili; 8 - Arbarastakh, 9 - Mountain Lake; 10 -Zhidoi; 11 -Koksharovskiy; 12 - Kiiskiy, 13 - Guli, 14 - Kola massifs; 15 - Sayan massifs. DM - depleted mantle with the line of the mantle succession.

The greatest variety of isotope ratios in lamproites and carbonatites is found for Sr and Nd isotopes (Fig. 13, 14). The isotope ratio of studied alkaline rocks are divided into 3 fields, which correspond to three different mantles. The carbonatites of the Siberian platform framing (subduction zone) lie in the field of the depleted mantle (DM). The alkaline rocks and carbonatites of the Western and Central Aldan lie in the field of the enriched mantle (EM-1). The points of the isotope composition of North American lamproites lie there as well. The magmas of these massifs were melted from the deepest sites of the mantle on the boundary of the Aldan shield with the Siberian Platform and Canadian shield with the North American Platform. The points of isotope compositions from carbonatites of Mongolia, Transbaikalia, Tian-Shan and Baikal Region lie in the field of the enriched mantle EM-2 and overlap with the fields of the Australian, Spanish and Italian lamproites. These regions of the completed folding later adjoined the platforms. The plume processes are significant for these two last types .

The geochemistry of Nd, Sr, O, C, and Pb isotopes of alkaline rocks from the Aldan and Mongolian massifs indicates the deep origin and mantle sources of the substance of studied massifs.

The investigations were supported by the RFBR (grants 00-05-65288, 01-05-67243-Baikal).

REFERENCES

1. Jaques A.L., Lewis J.D. and Smith C.B. The kimberlite and lamproite of Western Australia, Perth, 1986.
2. Kalievyyi shchelochnoi magmatiztn Baikalo-Stanovoi riftogennoi sistemy (Potassic Alkaline Magmatism of the Baikal-Stanovoi Rift System), Novosibirsk: Nauka, 1990, p. 238.
3. Makhotkin, I.L., Vladykin, N.V., and Arakelyants, M.M., The Age of Lamproites of the Aldan Province, Dokl. Akad. Nauk SSSR, 1989, vol. 306, no. 3, pp. 703-707.
4. Mitchell, R.H., and Vladykin, N.V., Rare Earth Element-Bearing Tausonite and K-Ba-Titanites from the Little Murun Potassic Alkaline Complex, Yakutia, Russia, Mineral. Mag., 1993, vol. 57, pp. 651-664.
5. Mitchell, R.H., Smith, C.B., and Vladykin, N.V., Isotopic Composition of Strontium and Neodymium in Potassic Rocks of the Little Murun Complex, Aldan Shield, Siberia, Lithos, 1994, vol. 32, pp. 243-248.
6. Mitchell, R.H., and Bergman S.C. Petrology of lamproites. Plenum Publishing Corporation, New York 1991.
7. Petrologiya shchelochnogo vulkanicheskointruzivnogo kompleksa Aldanskogo shchita (Petrology of Alkaline Volcanic-Intrusive Complex of the Aldan Shield), Leningrad: Nedra, 1967.
8. Panina, L.I., Motorina, I.V., Sharygin, V.V., and Vladykin, N.V., Biotite Pyroxenites and Melilite-Monticellite-Olivine Rocks of the Malyi Murun Alkaline Massif, Yakutia, Geol. Geofiz., 1989, no. 12, pp. 41-51.
9. Panina, L.I., and Vladykin, N.V., Lamproitic Rocks of the Murun Massif and Their Genesis, Geol. Geofiz., 1994, vol. 35, no. 12, pp. 100-113.
10. Vladykin, N.V., Bogacheva, N.G., and Alekseev, Yu.A., New Data on Charoite and Charoite Rocks, in Mineralogiya i genezis tsvetnykh kamnei Vostochnoi Sibiri (Mineralogy and Genesis of Decorative Stones of Eastern Siberia), Novosibirsk: Nauka, 1983, pp. 41-57.
11. Vladykin, N.V., The First Finding of Lamproites in the USSR, Dokl. Akad. Nauk SSSR, 1985, vol. 280, no. 3, pp. 718-722.
12. Vladykin, N.V., Simonov, V.I., and Sokolov, V.S., Temperature of Mineral Formation in Charoite Rocks, in Termobarogeokhimiya mineraloobrazuyushchikh protsessov (Letuchie komponenty) (Thermo-barogeochemistry of Mineral-Forming Processes. Volatile Components), Novosibirsk: Nauka, 1994, issue 3, pp. 52-60.
13. Vladykin N.V. Bilibin massif - the layered highly differentiated complex of the Potassium-ultramafic alkaline rocks Dokl. Akad. Nauk SSSR, 1996, vol. 349, no. 6, pp. 792-794.
14. Vladykin, N.V., Petrology and Ore Potential of Potassic Alkaline Rocks of the Mongolia-Okhotsk Magmatic Province. Doctoral (Geol.-Mineral.) Dissertation, Irkutsk: Vinogradov Inst. Geokhim., Sib. Otd. Ross. Akad. Nauk, 1997.
15. Vladykin N.V. Geochemistry and genesis of lamproites of the Aldan Shield. Geol. Geofiz., 1997₁, v 38, N. 12, pp. 128-141.
16. Vladykin N.V. The Malyi Murun Volcano-Plutonic Complex: an Example of Differentiated Mantle Magmas of Lamproitic Type. Geochemistry International, v. 38 Suppl. 1. 2000.pp. S73-S83.
17. Vorob'ev, E.I., Konev, A.A., Malyshenok, Yu.V., and Piskunova, L.F., Subsolvus Transformations of Carbonatites in the Sr⁴⁴- Ba Carbonatites, Dokl. Akad. Nauk SSSR, 1989, vol. 304, no. 6, pp. 1449-1452.

Alkaline magmatism of the Ukrainian shield

S.G. Kryvdik

Institute of Geochemistry, Mineralogy and Ore Formation NAS of Ukraine

ABSTRACT

The Ukrainian shield is the unique and the richest province of the Proterozoic alkaline magmatism. There are known about 40 massifs and occurrences of alkaline rocks and carbonatites. They belong to two discrete age formations (complexes): alkaline-ultrabasic (2,0-2,1Ga) and gabbro-syenitic (1,7-1,8 Ga). There are also Paleozoic (Devonian) alkaline rocks in the Ukrainian shield, but their spreading is limited (only in marginal parts of this region). Some massifs of gabbro-syenitic formation are spatially and genetically related to anorthosite-rapakivi-granite plutons. Quite a few deposits and mineralizations of apatite, ilmenite and rare metals (TR, Y, Nb, Ta, Zr, Sr) are related to alkaline and carbonatitic complexes of the Ukrainian shield.

INTRODUCTION

The Ukrainian shield (US) is the unique and the richest province of the Proterozoic alkaline magmatism. There are known about 40 massifs and occurrences of alkaline, subalkaline rocks and carbonatites there (Fig. 1). It is interesting that US is rather passive in reference to Phanerozoic alkaline magmatism unlike to other similar Precambrian regions (Baltic, Canadian, Brazilian, African, Siberian shields and platforms). Even recently discovered kimberlites and lamproites in central part of this region are aged as Proterozoic. There are known some massifs of Paleozoic (Devonian) alkaline rocks in US, but their spreading is limited only by marginal parts of this region. Paleozoic and Mesozoic alkaline rocks (predominantly volcanic facies) spread wide in more young depression (Dnieper-Donetsk, Near Black Sea) surrounded US from North, East-North and South.

The Proterozoic alkaline and subalkaline rocks of US belong according to views [Kryvdik, Tkachuk, 1990], to two discrete age formations (complexes): alkaline-ultrabasic (2,0-2,1 Ga) and gabbro-syenitic (1,7-1,8 Ga). Recently the older (2,8 Ga) quartz syenites were found in this region [Artemenko, 1998].

ALKALINE-ULTRABASIC FORMATION

The alkaline-ultrabasic formation of US includes Chernigovka (Novo-Poltavka), Proskurovka, Antonovka and partly Mala-Tersa massif, Gorodnitsa intrusion as well as a number of bodies and veins of alkaline rocks and carbonatites

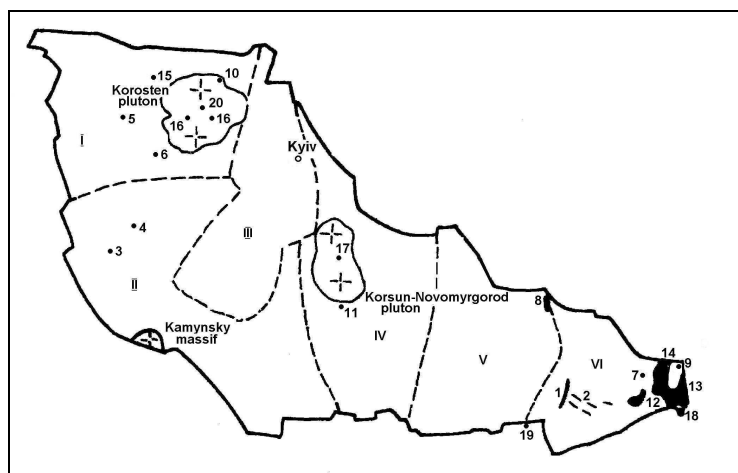


Fig. 1. Massifs and occurrences of carbonatites, alkaline and subalkaline rocks in the Ukrainian shield.

Ultrabasic-alkaline formation (complexes): 1 – Chernigovka (Novo-Poltavka), 2 – dikes of metajacupirangites, 3 – Proskurovka, 4 – Antonovka, 5 – Gorodnitsa intrusive body, 6 – fenites of Berezo-va Gat.

Gabbro-syenitic formation; 7 – Oktyabrsky, 8 – Mala Tersa, 9 – Pokrovo-Kyreyevo, 10 – Davydky, 11 – Velika Vyska, 12 – South Kalhyk, 13 – Yelanchyk, 14 – Kalmius, 15 – Yastrubetsky, 16, 17 – aegirine syenites of Korosten and Korsun-Novomyrhorod plutons, 18 – Prymorsky, 19 – Melitopol, 20 – Stremygorod apatite-ilmenite deposit.

Geological blocks of the Ukrainian shield: I - North-Western; II -Dniepr-Bug; III - Ros-Tikich; IV - Ingulo-Ingulets; V - Middle-Dniepr; VI - Azov.

in different area of this region (Fig. 1). Most of massifs of the alkaline-ultrabasic formation belong on their alkalinity type to potassic-sodium series. Only Kolarovka complex in Western Azov area represents potassium series. Potassium ultrabasites of this complex are considered as intrusive analog of low-titanium lamproite of Aldanian type [Razdorozhny et al., 1999]. Typical rocks of alkaline-ultrabasic formation are alkaline pyroxenites, jacupirangites, melteigites, ijolites, carbonatites, nepheline and alkaline syenites, including their quartz bearing varieties (nordmarkites). As a distinctive feature of massifs of this formation is an intensive fenitization of the country granitoids.

The massifs and occurrences of potassic-sodium series display very different geochemical peculiarities. Alkaline rocks and carbonatites of Near-Azov region have a district metallogenic specialisation on Nb, Zr, TR and P. Ultramafic members of this rock suite are enriched in Ti. Analogous alkaline rocks of Dniester-Bug region (Proskurovka and Antonovka massifs) are poor in these minor and rare elements (see Table 1). Alkaline-ultrabasic rocks (olivine jacupirangites and melteigites) of Gorodnitsa intrusive body (North-West region) show an another geochemical and petrological peculiarities. High contents of Cr (0,1-0,2%) and presence of chrome-spinels, including the high-chromian and magnesian varieties (to 62,6% Cr₂O₃ and 14,6% MgO), are characteristic for these rocks. The latter represent a little differentiated primitive mantle-derived melt like alkaline picrites - olivine melanephelinites.

Some features related to alkaline-ultrabasic formation manifest also alkaline rocks (fenites, alkaline and nepheline syenites) of Mala-Tersa massif (Middle Dnieper region). There are also gabbros (not characteristic rocks for the mentioned formation) as well as vein carbonatites and carbonatite-like rocks in this massif. It is some grounds to admit that in Mala-Tersa massif the rocks of two age different

Table 1.

The contents of minor and rare elements (ppm, TiO₂ in %) in some alkali rocks of US.

Massif, region	Rock	TiO ₂	Cr	Ni	Nb	Zr	TR	Ce	Y	Ba	Sr	Rb
Ultrabasic-alkaline formation												
Chernigovka	Alkali pyroxenites	5,63	370	90	205	460	400	213	41	305	1116	46
	Melteigites	0,24	226	20	820	173	3000	1500	27	470	8477	93
	Canadites	0,24	-	-	362	1811	200	100	10	960	1690	142
	Alkali pyroxenites	0,36	-	-	60	80	600	324	10	1590	2300	151
Western Azov belt of dikes	Metajacupirangites (hornblendites)	4,40	740	100	151	656	400	190	46	203	381	25
Proskurovka	Alkali pyroxenites	1,65	150	<30	8	130	300	180	28	250	1230	21
	Melteigites, ijolites	1,00	18	20	10	74	250	130	19	256	940	34
Antonovka	Alkali syenites	1,83	78	20	23	122	-	142	51	251	810	17
Gorodnitsa	Olivine jacupirangites	0,34	1023	374	7	46	-	50	20	85	507	22
Kirovograd-sky block	Kimberlite (lamproite)	3,50	1000	700	400	300	-	-	-	to 8000	-	-
Gabbro-syenitic formation												
Oktyabrsky	Gabbro	5,48	108	80	28	80	-	100	18	273	924	5
Mala Tersa	Gabbro	2,67	50	65	2	30	-	20	5	306	968	14
Davydky	Gabbro	5,63	<100	40	27	335	-	90	49	970	436	73
	Syenites	1,50	-	-	58	1058	-	174	160	1000	170	130
Velika Vyska	Syenites	0,67	-	-	144	2470	-	237	112	197	42	127
Yastrubetsky	Syenites	0,40	-	-	50-600	-6000	2000	60-1100	190-2670	13-1520	15-60	200-1285

formation are combined: early (2,05 Ga) alkaline-ultrabasic, and later (1,86 Ga) gabbro-syenitic [Zagnitko et al., 1993]. There are also carbonatites in Oktyabrsky gabbro-syenitic massif [Zagnitko, Matviychuk, 2001].

Among all other massifs of alkaline-ultrabasic formation of US most detailed is studied Chernigovka's one (Near-Azov area). Having all characteristic features of alkaline-ultrabasic formation this massif displays some phenomenal mineralogical, petrological and geochemical peculiarities.

Recently Chernigovka ultrabasic-alkaline massif belongs to one of the oldest (2,09 Ga by U-Pb data of zircon). Unlike to typical massif of this formation, which usually have round concentric-zonal forms, the Chernigovka massif is linear stretched. The associated with carbonatites alkaline silicate rocks - biotite-albite

nepheline syenites (canadites) and peralkaline pyroxenites (nephelineless jacupirangites) - are unaccustomed too. The mineral association olivine + dolomite +

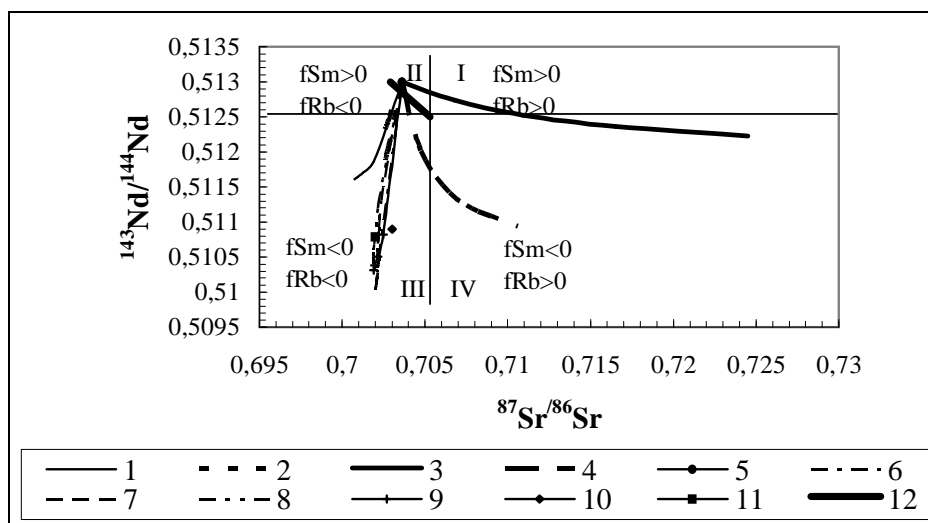


Fig. 2. Hyperbola of mixing for rocks of continental crust, continental tholeiitic basalts and carbonatites [Zagnitko, Matviychuk, 2001]

Carbonatites of massifs and occurrences: 1 – Chernigovka, 2 – Khlebodarovka (vein), 6 - Mt. Weld (Australia), 7 - Spanish River (N. America), 8 - Borden (*ibid.*), 9 - Cargill (*ibid.*). 3 – upper crust; 4 – low crust; 5 - continental tholeites. 10, 11 - subcalcian garnets from inclusions in diamond of Baltfouteen (Kimberli) and Finish. 12 - mantle sequence.

calcite is typical for Chernigovka carbonatites and very rare for other ones. As that olivine belong usually to iron-rich varieties, Fa_{20-65} , and even to Fa_{70} in melteigites.

In Chernigovka carbonatites Ce-fergusonite is the main ore Nb-mineral together with columbite and pyrochlore-hatchettolite. There are typical rare in nature amphiboles of intermediate composition both between edenite - katophorite and hastingsite - katophorite in alkaline rocks and carbonatites of this massif. Moreover, carbonatites of Chernigovka have some specific isotopic data: low $^{87}Sr/^{86}Sr$ (0,7013) at low ϵNd (+0,64) (Fig 2, Table 2, 3); proportional increase of $\delta^{18}O$ (from 5.0 to 17.5‰) in carbonates in parallel with decrease of FeO contents in these minerals and increase of magnetite amount in the rocks [Kryvdik et al., 1997]; those wide variation range of $\delta^{18}O$ have not any influence on «normal» isotopic composition of $\delta^{13}C$ in carbonates (from -3 to -9‰). At that we can note that modelling Sm-Nd age of Chernigovka carbonatites is valued in 2,4 Ga (the same one also by Pb-Pb isotopic ratio in calcite) while the U-Pb (zircon) and K-Ar age (amphiboles) of these rocks counts 2,0-2,1 Ga. We explain these and many other extraordinary peculiarities of Chernigovka carbonatites by abyssal condition during crystallization of carbonatitic melt in deep magmatic chamber (recent erosion cutting about 20 km). Other massifs of alkaline-ultrabasic formation of US are less eroded (to 3-5 km).

Table 2.

Izotopic composition of Sr, O and C in alkaline rocks and carbonatite of US.

Massif, intrusion	Rock	Mineral and rock	$^{87}\text{Sr}/^{86}\text{Sr}$	$\delta\text{C}^{13\&},\text{‰}$	$\delta\text{O}^{18},\text{‰}$	Source of information
Ultrabasic-alkaline formation						
Chernigovka	Carbonatite	calcite	0,7013	-3÷-9	5-13	[5, 11]
	"-	graphite	-	-9,5÷-12,1	-	[5]
	Nepheline-olivine	"-	-	-7,7	-	[5]
	Nepheline syenites (canadites)	rock	-	-	7,5	[5]
	Alkali syenites	"-	-	-	8,6	[3]
	Canadites	apatite	0,70346	-	-	[3]
	Carbonatite	"-	0,70245	-	-	[3]
	Alkali syenites (nordmarkites)	"-	0,70333	-	-	[3]
Apogranitic fenites	"-	0,70478	-	-	[3]	
Proskurovka	Melteigites	"-	0,70304	-	-	[3]
	Ijolites	"-	0,70324	-	-	[3]
	Apogranitic fenites	"-	0,70435	-	-	[3]
	Melteigites	calcite ingrained	-	-1,9	15	[3]
	Carbonate veins	calcite	-	0,2÷-1,3	11,9-16,8	[5]
	Apatite-calcitic	"-	-	1,6-1,7	11,6-11,8	[3]
Gorodnitsa	Melteigites	apatite	0,7035	-	-	[3]
Berezova Gat	Apogranitic fenites	calcite	-	-6,8÷-9,3	10,9-13,6	[3]
	The same	apatite	0,7029	-	-	[3]
	"-	"-	0,7036	-	-	[3]
Gabbro-syenitic formation						
Oktyabrsky	Alkali syenites	apatite	0,70288	-	-	[3]
	Pulaskites	"-	0,70333	-	-	[3]
	Vein foyaites	"-	0,70651	-	-	[3]
	Carbonatite	calcite	0,7024	-6.3	9.5	[12]
Mala Tersa	Alkali syenites	apatite	0,70511	-	-	[3]
	Fenites	"-	0,70397	-	-	[3]
	"-	"-	0,70497	-	-	[3]
Davydky	Gabbro	"-	0,70300	-	-	[3]
	"-	"-	0,70305	-	-	[3]
	Syenites	"-	0,70295	-	-	[3]
	"-	"-	0,70332	-	-	[3]
Yastrubetsky	Syenites	"-	0,73719	-	-	[3]
	"-	"-	0,75306	-	-	[3]
Velika Vyska	Syenites	"-	0,71536	-	-	[3]
	"-	"-	0,85593	-	-	[3]
Pokrovo-Kyreyevo	Ore pyroxenites	"-	0,70536	-	-	[3]
	Peridotites	rock	-	-	4,0	[3]
	Pyroxenites	"-	-	-	4,5-5,5	[2]
	Gabbro	"-	-	-	9,0-10,5	[2]
	Malignites	"-	-	-	6,5-8,0	[2]

GABBRO-SYENITIC FORMATION

Notwithstanding on above-mentioned interest to alkaline-ultrabasic rocks and related carbonatites, the overwhelming majority of alkaline massifs of US belong to gabbro-syenitic formation. In the latter two types of massifs (subformations) are distinguished:

Table 3.

Isotope systems in carbonatite of US [Zagnitko et al., 2000].

Massif	K-Ar Age		U-Pb	Pb-Pb	$^{87}\text{Sr}/^{86}\text{Sr}$	Sm-Nd		O	C	
	Mineral	Mica	Amphibole	Zircon		Calcite	Modelin g age	$\epsilon\text{Nd}(T)$	$\delta^{18}\text{O}, \text{‰}$	Carbo-nate
Chernigovka	1900-1750	2100-1950	2090	2400	0.7013	2400	+0.64	8.0±3	5.6±1.7	9.4±1.4
Khlebdarovka (dike)		1835			0.70258	2155	+1.7	9.1±2	7.1±1.1	
Oktyabrsky	1800-1600	1870-1750	1795		0.7024			9.5±1.5	6.3±1.2	
Petrovo-Gnutovo (dike)	1950			2000	0.7063			12.2±2.0	7.5±1.1	

The first with final nepheline syenites differentiates including their peralkaline varieties (Oktyabrsky, Mala Tera).

The second the development of witch was terminated by alkaline and subalkaline quartz syenites with iron-rich femic minerals such as fayalite, hedenbergite, aegirine, ferrohastingsite, taramite, riebeckite, annite (Davydki, South Kalchyk, Yastrubetske, Velika Viska etc.). Difference in residual melt of the two named type of massifs (subformations) caused, in our view, by different composition of initial parental basic magmas: nepheline- and quartz-normative for the first and second ones accordingly.

It is shown that in Oktyabrsky and Mala Tera massifs the agpaitic direction of evolution from carby gabbroides through alkaline syenites and foyaites to latter aegirine foyaites and peralkaline phonolites (with eudialite and astrophyllite) was realized [Kryvdik, Tkachuk, 1990]. As that each following differentiate of this series have been enriched by incompatible element (Zr, Nb, REE, Y). There are specific rocks as mariupolites in Oktyabrsky massif. Pyrochlore and britholite (often in high concentration) are characteristic for these rocks.

As into petrological, geochemical and metallogenic aspects, the massifs of second type (subformation) are very interesting. They are spatially and genetically related to anorthosite - rapakivi - granite plutons. These syenitic and gabbro-syenitic massifs (Davydki, Velika Viska, Yastrubetsky) practically are contemporary with rapakivi granites and are usually located on borderlands of these plutons or not far from them (Fig. 1). In our view, the South Kalchyk massif (Azov area) represents an abyssal gabbro-syenitic analog of anorthosite-rapakivi-granite plutons and demonstrates their deep-crust syenite differentiation trend (by the Fenner scheme). Beside syenites there are almost all typical for anorthosite - rapakivi - granite plutons rocks (gabbro-norite, ore gabbros and peridotites, plagioclasites, granites with ferrohastingsite, ferrohedenbergite and fayalite) in

South Kalchyk massif. The gabbroids of the latter massif are fairly similar to those rocks in Korosten and Korsun-Novomyrgorod plutons, as well as plagioclases (andesinites) of the first one are analogous to labradorites of the second ones.

A possibility of syenitic differentiation trend of anorthosite - rapakivi - granite plutons to the US we had confirmed on petrochemical calculation. It was shown [Kryvdik, Tkachuk, 1990] that fraction crystallization on Fenner scheme of parental basic magmas like leuconorite or labradorite porphyrite (Hogland Island) could have produced from 12 to 36% residual trachytic melt similar on composition to fayalite-hedenbergite syenites of US. Precipitated minerals (cumulates) have been represented by basic plagioclase, ferro-magnesian olivine, ortho- and clinopyroxenes, ilmenite and apatite.

If such parental basic magmas had crystallized on Bowen's scheme with precipitation of magnetite, residual melts would have a granitic composition (like rapakivi granites). As a realization of Fenner's fractional crystallization is more probable in abyssal conditions, it can rely on increase in volume of syenites and one decrease of granites by the deepening of erosion level of anorthosite-rapakivi-granite plutons. Erosion cutting of South Kalchyk massif is more than 10 km and the latter represents an abyssal gabbro-syenitic analog of such plutons. Other anorthosite-rapakivi-granite plutons (Korsun-Novomyrgorod and particularly Korosten) are less eroded, but they are followed by syenites too (Fig. 1).

Thus the Ukrainian shield belongs to unique Precambrian region with a district displayed syenitic differentiation trend of anorthosite - rapakivi - granite plutons.

These gabbro-syenitic and essentially syenitic massifs represent usually by layered intrusions with clear rhythmic and cryptic layering. Gabbroids of these massifs belong to subalkaline series and are always enriched in Ti and P but poor in Cr and Ni. The deposits of ilmenite and apatite are related to those gabbroids.

As it was mentioned above, syenites (usually quartzbearing) of these massifs are characterized by presence of high-ferruginous feric minerals (fayalite, hedenbergite, aegirine-hedenbergite, ferrohastingsite, taramite, annite) but by absence of primary magnetite. Evidently such rocks had originated under conditions of low oxygen fugacity. Final differentiates of layered syenitic intrusions are represented by aegirine and (or) riebeckite quartz varieties and granosyenites.

Moreover there are aegirine syenites of separate veined and indistinct layer forms among the rapakivi granitoids in Korosten and Korsun-Novomyrgorod plutons. Such rocks have maybe the same origin that the above mentioned aegirine syenites from layered intrusions, but they can also be as a residual melt by plagioclase fractionating of basic (anorthositic) magma.

The studied syenites are very enriched by such incompatible rare elements as Zr, REE and Y. They have moderate contents of Nb and their final differentiates are very depleted by Sr and Ba. In South Kalchyk and Yastrubetsky massifs there are rich zirconium and rare earth ore varieties of syenites (Table 4). In these rocks zircon, britholite and orthite become rock-forming minerals.

Table 4.

The chemical composition of some varieties of ore-bearing rare-metal syenite from the Azov and the Yastrubetsky deposits [Melnikov et al., 2000].

Component	The Azov deposit				The Yastrubetsky deposit			
	1	2	3	4	5	6	7	8
SiO ₂	46.70	48.04	44.98	60.81	57.50	47.20	59.50	56.60
TiO ₂	0.53	0.80	0.26	0.04	0.08	0.74	0.10	0.19
Al ₂ O ₃	11.73	12.20	16.51	20.21	16.67	13.80	16.75	15.50
Fe ₂ O ₃	7.70	4.47	4.40	1.44	0.42	2.00	1.45	2.29
FeO	10.00	8.95	8.29	0.86	2.73	11.70	1.94	4.52
MnO	0.30	0.35	0.37	0.05	0.08	0.17	0.07	0.16
MgO	0.42	1.02	0.99	0.62	0.48	0.98	0.43	0.55
CaO	3.05	3.96	2.56	0.70	1.92	4.80	1.23	2.57
Na ₂ O	3.80	3.94	2.60	5.10	5.96	4.24	6.04	5.51
K ₂ O	3.60	3.58	2.90	3.80	4.90	4.52	4.80	5.02
S	—	—	0.08	0.02	0.02	0.08	—	0.01
P ₂ O ₅	0.10	0.10	0.06	0.04	0.15	0.14	0.04	0.08
CO ₂	3.00	1.23	0.74	—	0.82	1.11	0.46	0.92
F	0.40	0.55	—	—	0.40	0.78	0.23	0.70
ZrO ₂	5.25	5.30	10.36	6.24	6.61	4.90	6.00	4.40
TR ₂ O ₃	1.80	4.52	2.51	0.14	—	—	0.15	0.27
H ₂ O	0.20	0.20	0.02	—	—	—	—	0.04
H ₂ O ⁺	0.40	0.60	1.33	0.22	0.98	2.87	0.59	0.86
Total	98.98	99.81	98.96	100.29	99.72	100.03	99.78	100.19

Note. 1, 6 — melanocratic; 2, 3, 8 — mezocratic; 4, 5, 7 — leucocratic layers.

Thus a very high ferruginosity of femic minerals and strong enrichment by incompatible rare elements (Zr, REE, Y) testify to a high fractionating degree of these syenites. A present of such syenites is a specific peculiarity of Proterozoic alkaline magmatism in US.

PALEOZOIC ALKALINE ROCKS

A spreading of Phanerozoic alkaline rocks in US is limited. They are only known in Azov part of this region. As it mentioned above, these rocks are widely spread in surrounded US depressions (especially in Dniepr-Donetsk avlacogene).

In Azov part of US the Devonian Pokrovo-Kyreyevo alkaline massif is known a long time ago. This massif consists of alkaline pyroxenites, peridotites, gabbros, malignites, juvites, epileucites etc. Malignites and juvites are very similar on their poikilitic texture to Khibinian rischorrites. These rocks belong to peralkaline (agpaitic) varieties and have a high concentration of some rare incompatible elements.

Recently in Azov part of US were discovered some other Paleozoic massifs of alkaline and subalkaline rocks (Zirka, Prymorsky, Mariypol, Berezhna ravine, Kyryllovka, Kychyksu). Some of these massifs have a new for Ukraine types of

alkaline rocks (essexites epileucite shonkinites and pyroxenites, two-feldspathoid syenites, sannaite-like lamprophyre). There are unusual titanian fassaitic pyroxenes and magnesian chrome–spinel in melanocratic rocks (pyroxenites, shonkinites, essexites) of these alkaline massifs. But on the contrary to alkaline rocks of Pokrovo-Kyreyevo massif the analogue rocks of these new occurrences are pure in incompatible element such as Nb, Zr, REE, Y etc. The cause of this difference in distribution of trace elements in Paleozoic alkaline rocks from Azov part of US is unknown for the present. We think that these differences in rare-element contents of alkaline rocks were formed under another geotectonic conditions.

The formation belonging of Paleozoic alkaline rocks in Azov part of US is discussed. Some investigators [Buturlinov, 1979] refer these rocks to different formation types (alkaline ultramafic and alkaline basic). We think that these massifs belong predominantly to alkaline basic (basaltic) formation and partly to alkaline-ultrabasic one. As it is mentioned above, alkaline ultrabasic volcanic and subvolcanic rocks are widely spread in Dnieper-Donetsk depression (beyond the borders of US).

GEOCHEMICAL PECULIARITIES OF ALKALINE ROCKS AS AN INDICATOR OF GEODYNAMIC CONDITIONS OF THEIR FORMATION

It was shown [Buturlinov, 1979] that massifs and occurrences of alkaline-ultrabasic formation are located in tectonic blocks of US with more crust (47-52 km) comparatively to those gabbro-syenitic (less 40 km). The granulite metamorphism is often present for the first type of blocks.

Alkaline rock and carbonatite intrusion of alkaline-ultrabasic formation mark probably the earliest Proterozoic (2,0-2,1 Ga) platform stage of US or its separate blocks. The later Proterozoic (1,7-1,8 Ga) tectono-magmatic activation epoch of this region resulted in alkaline and subalkaline rocks of gabbro-syenitic and anorthosite-rapakivi-granite formations. The Paleozoic and partly Mesozoic alkaline magmatism of US is connected as with the beginning of formation of a rifting depression surrounding US as well as with orogenic processes in neighbouring territories (Tethys, Scythian plate, Hercynian and Alpine Folding in Carpathians and Crimea).

The alkaline rocks of US formed in rifting (rupture) zones are usually enriched in Nb, Zr, REE. The early melanocratic varieties of alkaline rock series (alkaline pyroxenites, jacupirangites, melteigites, lamproites and kimberlites) are simultaneously enriched in Ti, Cr and Ni too. Such a picture we see in Chernigovka massif, dikes of metajacupirangites in the West Azov area, kimberlites and lamproites of Kirovograd (Table 2) [Tsymbal et al., 1999].

While the depletion of these rare and minor elements in alkaline rocks of Proskurovka Antonovka and partly Mala Tersa alkaline-ultrabasic massifs we explain by another geotectonic conditions of their formation. These massifs are probably located in a pressure zone. Maybe subduction occurrences took place here.

At least we have some evidences, based on $\delta^{18}\text{O}$ and $\delta^{13}\text{C}$ data, for contamination of mantle-derived magmas by crust material (Table 2) [Kryvdik, 2000].

On geochemical peculiarities two type of lamproite-like rocks are distinguished. The first one (pipe Mriya, Azov area) represent intrusive analog of lamproite which consist of olivine, phlogopite and amphibole. These rocks are poor in Ti, Nb, Zr, REE and approximate on their chemical composition to lamproite of Aldan shield [Vladykin, 1997]. The second type of lamproite-like rocks (the same Azov area) belong to dike faces and recently represents, in our view, epileucitic metalamproites (microcline-amphibole rocks). They have high concentration of Ti and Nb, and moderate contents of Zr, Ba, Cr. These metalamproites are similar on geochemical peculiarities to lamproite of West Australia.

Other massifs of alkaline rocks in US have a less distinct tectonic position and on geochemical peculiarities of their rocks occupy intermediate position between «rifting» and «subduction» formations. We do not know a cause of low contents of Nb in Ti-rich gabbroids and ilmenite ores of Korosten pluton and Stremygorod deposit. In general there is moderate or concentration of Nb in rich on Zr and REE syenites related to anorthosite-rapakivi-granite plutons. We think about a considerable admixture of crust material in these rocks. Such syenites pay attention to their high value of $^{87}\text{Sr}/^{86}\text{Sr}$ (0,715-0,859; Table 2). It is difficult to explain these date proceed only from crust mixing and assimilation. This phenomenon can take place by intensive increase of Rb and decrease (to almost full absent) of Sr during crystal fractionating of trachytic melts. Maybe the existence time of such melts was to long and sufficient for essential addition of radiogenic Sr.

Thus isotope geochemical peculiarities of alkaline rocks and carbonatites of US demonstrate as initial proportion of geep-derived and crust materials well as a degree of differentiation of alkaline melts.

The Ukrainian shield is a unique and richest province of Proterozoic alkaline, kimberlitic and carbonatitic magmatism.

REFERENCES

1. Artemenko G.V. Geochronology of Middle Dnieper-, Azov- and Kursk granite-greenstone regions: doctor's thesis. Kyiv, 1998. 32 p.
2. Buturlinov N.B. Magmatism of graben-like depressions in south part of east European platform in Phanerozoic eon: doctor's thesis. Kyiv, 1979. 460 p.
3. Kryvdik S.G. Alkaline magmatism of the Ukrainian shield: geochemical and petrogenetical aspects //Min. Journ. (Kyiv). 2000, N2/3. pp. 48-56.
4. Kryvdik S.G., Tkachuk V.I. Petrology of alkaline rocks of the Ukrainian shield. Kyiv: Nauk. Dumka. 1990. 408 p.
5. Kryvdik S.G., Zagnitko V.M., Lugova I.P. Isotope composition of minerals from carbonatites of Chernigovka massif (Azov arca) as an indicator of their formation conditions// Min. Journ. (Kyiv). 1997, N6. pp. 28-42.
6. Melnikov V.S., Kulchiska A.A., Kryvdik S.G., Gursky D.S., Strekozov S.N. The Azov Deposit - a new type of Rare-metal Objects of Ukraine// Min. Journ. (Kyiv). 2000, N5/6. pp. 39-79 (in English).

7. Razdorozhny V.F., Kryvdik S.G., Tsymbal S.N. Potassium ultrabasites from Western Azov area - intrusive analogies of Lamproites //Min. Journ. (Kyiv). 1999, N2/3. pp. 79-94.
8. Tsymbal S.N., Kryvdik S.G., Kyryanov N.N., Makivchuk O.F. Substantial composition of kimberlites from Kirovograd geoblock (Ukrainian shield)// Min. Journ. (Kyiv). 1999, N2/3. pp. 22-38.
9. Vladykin N.V. Petrology and orebearing potentiality of potassium alkaline complexes from Mongolia-Okhotsk area of magmatism: doctor's thesis. Irkutsk, 1997. 80 p.
10. Zagnitko V.M., Kryvdik S.G., Legkova G.V., Bartnitsky E.N. Geochronology, Petrology and Orebearing Potentiality of alkaline massifs of the Ukrainian shield// Isotope dating of endogene ore formations. Moscow: Nauka, 1993. pp. 27-38.
11. Zagnitko V.M., Matviychuk M.V. Evolution Sm-Nd and Rb-Sr systems in carbonate rocks of Azov area// Actual problems of Geology of Ukraine. Kyiv, 2001. pp. 12-13 (in Ukrainian).
12. Zagnitko V.M., Stepaniuk L.M., Parfenova A.Ya., Kryvdik S.G., Isotope geochemistry and Geochronology of Precambrian carbonate rocks of the Ukrainian shield //Thesis to I Russ. Conf. of Isotope geochronol., 15-17 nov., 2000. Moscow, pp. 142-144.

Western Kamchatka alkali-potassic basaltoid volcanism: geological and geochemical review

**A.B. Perepelov¹, O.N. Volynets², G.N. Anoshin³, Yu.M. Puzankov³,
V.S. Antipin¹, A.V. Kablukov¹**

¹ *Vinogradov Institute of Geochemistry, SB RAS, Irkutsk, Russia*

² *Institute of Volcanic Geology and Geochemistry, FEB RAS, Petropavlovsk-Kamchatsky, Russia*

³ *United Institute of Geology, Geophysics and Mineralogy, SB RAS, Novosibirsk, Russia*

INTRODUCTION

The actuality of the problem of origin alkali-potassic volcanic rock complexes in geodynamic settings of island-arc and active continental margins is defined by their specific substantial peculiarities and comparative rarity with regard to middle-potassic and high-potassic calc-alkaline rock series which are more typical for "ocean-continent" transition zones. These rocks are usually localised in back areas of island-arc systems or within multiple tectonic structures, like large-scale fault zones, local riftogenic structures or "hot fields", which have applied or transit character of evolution. The petrological aspect of the problem is determined by difficulties in reconstruction of alkali magmatism development in ocean-continent zones from the positions of simple models of island-arc or intraplate magmagenation. Most known provinces with alkali-potassic magmatism in island-arc and continental margin settings are Indonesian Archipelago [Stolz et al., 1988], Kamchatka [Volynets et al., 1987] (developed ensialic structures), Sierra-Nevada (West of U.S.A) [Van Kooten, 1980], Spain [Borley, 1967; Venturelli et al., 1984], Eolian arc [Keller, 1982] (modern and old active continental margins). Among noted provinces, alkali-potassic magmatic rocks of Kamchatka are the least studied. They are wide spread in the back area of this ripe island-arc system, significantly vary on composition and deposition forms. So, it is necessary to clear the place of this large magmatic stage in the evolution of Kamchatka structure as a whole. Data on Oligocene-Miocene-(Pliocene?) ages of alkali-potassic rock series from Western Kamchatka allow to connect this magmatism with one of large-scale tectonic reconstructions taken here the place in Neogene. During such stages of island-arc development there is a probability of subduction zones declining, riftogenic episodes and the start of forming a new island-arc systems. According with age, tectonic and structure position, the origin of Western Kamchatka alkali-potassic rock series may be considered in the genetic link with the so-called "postsubduction" geodynamic regim of magmatism. The postsubduction magmagenation suppose participation of processes inherent both as island-arc and intraplate settings in forming of melt composition.

Areal of Cenozoic alkali-potassic basaltoid volcanism in Western Kamchatka

is constrained by volcanic belt of Sredinny Rige on the East, by Okhotsky Sea on the West, by Sopochnaya river on the South, and by Palana river on the North. This areal extends in submeridional direction more then 500 km. The outcrops of igneous rocks cover here less then 10% of the area. Within Paleogene-Neogene sedimentary country rocks it is known more then 200 subvolcanic bodies of alkali rocks which are localized, in main, to Tigil anticline rise.

B.F. Dyakov (1939) was first who described alkali-potassic volcanites from Western Kamchatka; more full information about their geological position, age, petrographic and petrochemical peculiarities is shown by I.S.Guziev [Guziev, 1964; Guziev, 1966; Guziev, 1967; Guziev, 1971]. He differed three petrographic series of Western Kamchatka magmatic rocks: 1) trachydolerites-krinanites; 2) sanidine basaltoids; 3) andesite-basalts, trachyandesite-basalts and trachyandesites. Sanidine basaltoids series included absarokites, microshonkinites, selagites, banakites, shonkinites, also alkaline syenites and limburgites. Besides that, shoshonites were noted among the rocks of third, sub-alkaline series.

In 1982-2000, new data about composition, mineralogy and bedding forms of alkaline and sub-alkaline rocks of Western Kamchatka were obtained [Volynets et al., 1985; Volynets et al., 1990; Volynets, 1994; Perepelov et al., 1987; Perepelov, 1990; Volynets et al., 1990; Volynets, 1994; Perepelov et al., 2000]. It was determined that they belong, in main, to two series, shoshonite-latic and K-alkaline. Except of them, the group absarokite basaltoids was confirmed here.

Shoshonite-latic series is not a subject of this paper and not discussed here.

Analogues of absarokites are microshonkinites, full-crystallic varieties of magnesian K-basaltoids. The undetermined petrogenetic position of this group of rocks and similarity of their composition to trachybasalts make consider them together with volcanites of K-alkaline series.

The rocks of K-alkaline series were investigated in the region of rivers Khlebnaya, Napana and Amanina (Fig.1). In contradistinction to I.S. Gusiev nomenclature (1964, 1971), among the rocks of K-alkaline series we differ trachybasalts, melanocratic and leucocratic shonkinites, porphyric shonkinites, also properly shonkinites and syenites (Fig.2). Syenites, in their turn, are differed on syenites from small veins and syenites of apical parts of shonkinite subvolcanic bodies. They differs not only by conditions of bedding but in composition too. Besides, specific type of K-Na shonkinites is singled out. Trachybasalts, porphyric shonkinites and absarokites have an effusive appearance. Among absarokites we differ high-Mg ($MgO > 9$ mas.%) and middle-Mg ($7 < MgO < 9$ mas.%) types.

Classification diagrams (Fig.2) clearly show that the most of compositions of the rocks attribute to alkaline and sub-alkaline series. Some types of shonkinites, microshonkinites and trachybasalts also may be classified as subalkaline by presents alkaline components, Na_2O and K_2O .

Most rocks of K-alkaline series are basaltoids (including absarokites and microshonkinites): $SiO_2 = 46-50$ mas.%. The syenites are extended much more

sparsely and not occupy large volumes.

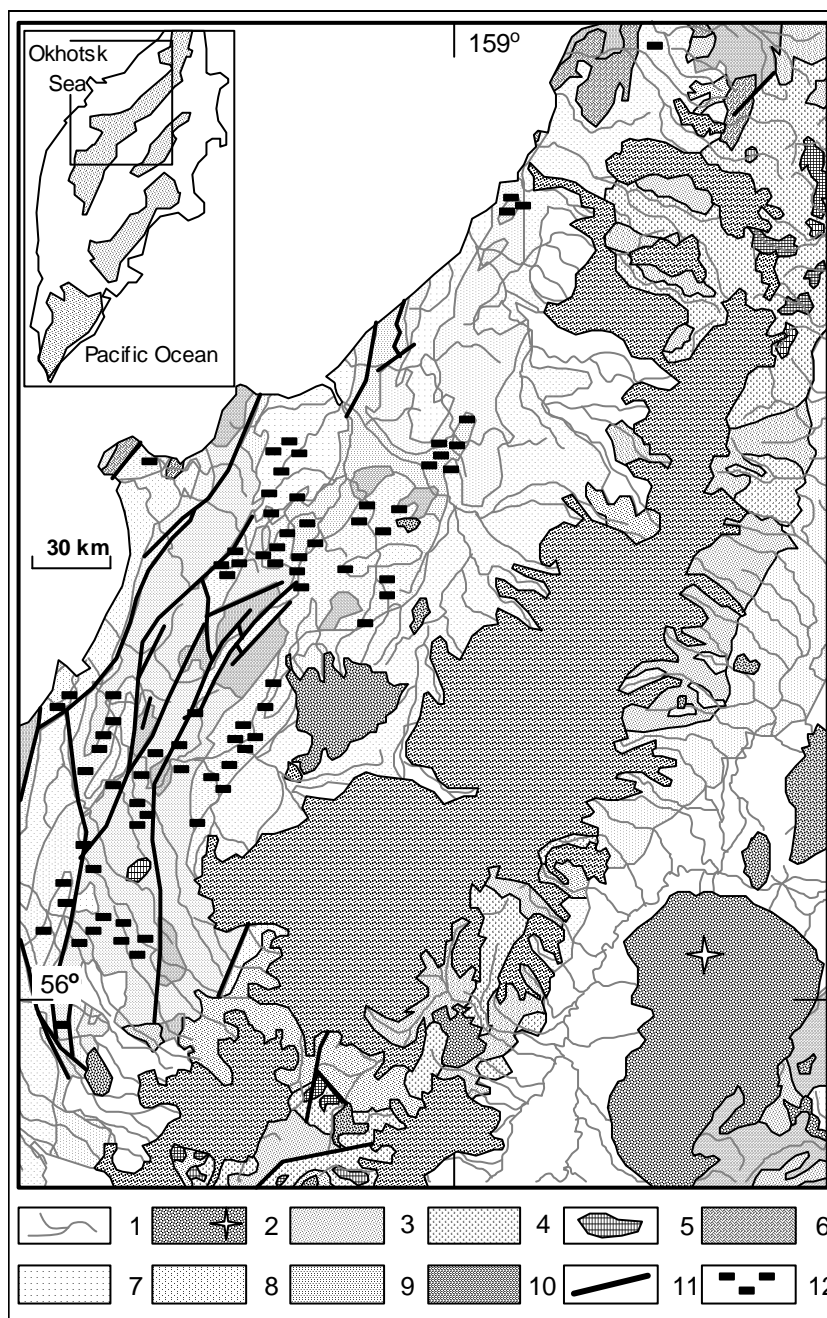


Fig.1. Geologic scheme of Centre- and Western-Kamchatka zones.

The scheme is compiled on the base of Government Geological Map of Kamchatka region with author's changes and additions. The position of the scheme in general structure of Kamchatka is shown in the cutting.

Conventional signs: 1 - river system and its recent deposits; 2 - Q_1-Q_4 volcanic deposits (special sign show the position of Klyuchevsky volcano); 3 - $N_1^3-N_2$ volcanic deposits; 4 - $Pg_3^3-N_1^2$ volcanic deposits; 5 - N_1 intrusions; 6 - Pg_2^{2-3} volcanic deposits; 7 - N_1 terrigenous-sedimental deposits; 8 - Pg_3-N_1 terrigenous-sedimental deposits; 9 - Pg_2 terrigenous-sedimental deposits; 10 - K_2 terrigenous-sedimental and metamorphic rocks; 11 - main faults; 12 - outcrops of subvolcanic bodies belonging to the K-alkaline and subalkaline rock series within Western-Kamchatka area.

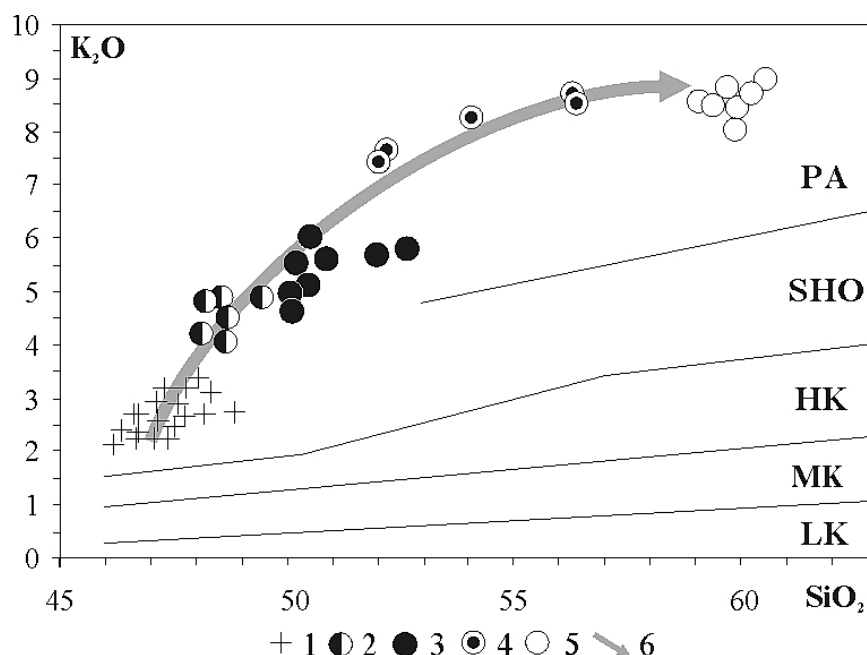


Fig. 2. $K_2O - SiO_2$ diagram of potassic alkaline basaltoids of Western Kamchatka

Rocks: 1- absarokites; 2- trachybasalts and porphyric shonkinites; 3- shonkinites; 4- syenites of massive zones; 5- syenites of veins. 6- evolution direction of rocks composition of potassic alkaline series.

Volcanic rocks serieses: LK - low-kalium series; MK - middle-kaluim series; HK - high-kalium series; SHO - shoshonitic series; PA - potassic-alkaline series.

AGE OF K-ALKALINE BASALTOIDS FROM WESTERN KAMCHATKA, THEIR STRUCTURAL POSITION AND GEOLOGICAL FORMS

Volcanic zone of Western Kamchatka is located on the back (relatively to volcanic belts of island-arc system of Kamchatka) side of Okhotomorskay plate. According to V.A. Legler model (1977), most of Late-Cenozoic magmatism is concerned here with the end of early island-arc activity in Oligocene-Miocene time. Quaternary volcanism is a result of magmatic processes in modern island-arc system. There are three stages distinguished in structure of this area: Upper Cretaceous (K_2), Paleogene - Middle Miocene ($Pg-N_1^2$), and Upper Miocene-Pliocene ($N_1^3-N_2$), and all stages are discordanted. (T.F. Moroz, 1965; L.I. Mohonina, 1968; G.P. Singaevsky, 1971). The fold basement for Tertiary volcanic-sedimentary layers is Upper Cretaceous metamorphic rocks formed in geosynclinal stage of Western Kamchatka development. Paleogene - Middle miocene stage is presented by sedimentary rocks of geoanticlinal stage, at the end of which Upper Miocene and Pliocene sedimentary rocks were formed. Among deposits of last stage tuffs and debris of alkaline basaltoids are found.

K-alkaline magmatic complexes of Western Kamchatka are near to Tigil rise and located in submerged parts of the fold basement and in borders of joint of Palansky and Bolsheretsky synclinories. The age of these complexes is estimated as Miocene - Upper Pliocene ($N_1^2-N_2$) [Guziev, 1964, 1966, 1971]. But older data on K/Ar dating gave their age 13-14,7 ma, i.e. a border between Low and Middle miocene (N_1) [Amirhanov et al, 1986]. New unpublished results of K/Ar and Ar/Ar dating (O.N. Volynets, 1998, oral poster) show more early age of K-alkaline rocks of Western Kamchatka - 42-21 ma. Paying attention the possibility of long time interval of studied rocks development, we suppose their age as Oligocene-Miocene (Pg_3-N_1).

The K-potassic alkaline rocks forms dykes, sills, intrusions, domes, lakkolites, sparse flows, also explosive pipes which consist of absarokite breccias and trachybasalts. Near subvolcanic bodies often are tuffobreccias showing that the magma had ways out on the surface. All kind of K-alkaline rocks, except of absarokites, has joint bedding with shonkinites. presented by a small veins both absarokites and trachybasalts, and among shonkinites too. In the apical parts of large shonkinite bodies, syenites forme massive zones. The most low horizons of differentiated bodies consist of melanocratic shonkinites, upper ones are presented by shonkinites and leucocratic shonkinites. The most upper parts of the bodies contain vein zones and zones of middle-grained, coarse-grained and pegmatoidal syenites. Effusive rocks forme, as a rool, their own subvolcanic bodies and dykes. K-Na shonkinites are found in the structures of separated subvolcanic complexes. The thickness of subvolcanic bodies vary from 15-20 to 60 m. The thickness of lakkolites and domes reaches to 1-1,5 km.

PETROGROPHY AND MINERALOGY OF K-ALKALINE ROCKS OF WESTERN KAMCHATKA

There are three groups of rocks were selected in K-alkaline series by mineralogical and structural characteristics: 1) absarokites and microshonkinites, 2) porphyric shonkinites and trachybasalts, 3) full-crystalline varieties of the rocks - shonkinites and syenites.

Absarokites contain to 10% phenocrysts of Ol^* and Cpx in their groundmass. Ore minerals are CrTiMgt, TiMgt, and sphinel in inclusions within olivines. Groundmass consists of of Pl, K-Na feldspar and ore mineral grains with small inclusions of chloritized glass, also with more rare and small grains of biotite and analcime. Trachybasalts differ from absarokites by larger quantity of Cpx among their phenocrysts, whereas Ol is spreaded much more sparsely. Porphyric sructure of some shonkinite is determined by large (to 3 mm) mica (and more rare Cpx)

* **shortened names of minerals, its minals and coefficients**: Ol- olivine, Pl- plagioclase, Cpx- clinopyroxene, Ilm- ilmenite, Bt- biotite, Amp- amphibole, TiMgt- titanmagnetite, CrTiMgt- crometitanmagnetite, Or- ortoclase minal, Fs- ferrosillite minal, Fo- forsterite minal, An- anorthite minal, f- iron coefficient.

phenocrysts in fine-grained ground mass. Groundmass of porphyric shonkinites

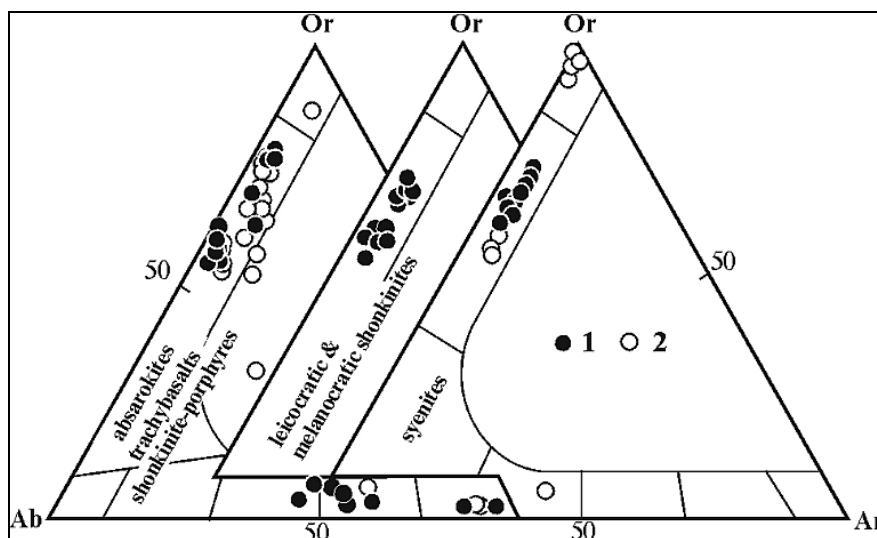


Fig. 3. Compositions of feldspars from potassic alkaline volcanic rocks of Western Kamchatka.

1. phenocrysts; 2. microlites.

consists of K-Na feldspar, in joints with small crystals of Cpx, Bt, TiMgt and Ilm.

Melanocratic and leucocratic shonkinites of differentiated bodies are connected between each other by gradual transitions in mineral composition and types of structures. Sometimes, leucocratic varieties of shonkinites are characterized by pegmatoid structures and have some similarity with syenites. The general mineral components of leucocratic shonkinites are K-Na feldspars, Bt, Cpx, small quantity of analcime and ore minerals (TiMgt, Ilm). Ol is very seldom in it. K-Na shonkinites have relic plagioclases in cores of K-Na feldspar grains and are enriched in analcime. Melanocratic shonkinites contain much of large grains of chloritized Bt and Ol. Cpx is presented here by subphenocrysts, the main component of ground mass is K-Na feldspar. Syenites of massive zones are leucocratic and consist of large crystals of K-Na feldspars, mica, Cpx and analcime. Vein syenites characterized aplitic structures. Both varieties of syenites contain rare small grains of Amp.

Thus, in differ to other high-K series of Kamchatka, the rocks of K-alkaline series are characterized by very various parageneses of main and accessory minerals. Except of feldspars, pyroxenes and olivines these rocks contain such specific for them minerals as phlogopite, spinel and analcime, while orthopyroxene is absent.

Among feldspars of K-alkaline rocks Na-sanidines predominate (Fig.3; Tab.1). Absarokites, microshonkinites and trachybasalts are characterized by two-feldspar mineral paragenesis. Bitovnite is presented in absarokites only as microlites; shonkinites contain this mineral both as microlites and subphenocrysts (An_{77,9-82,2}). With transition to trachybasalt rock composition Pl becomes more acid (labradore, andesine). Na-sanidines from full-crystalline rocks of alkaline series belong to

interval Or_{54,6-76,2}; syenites from massive zones and K-Na shonkinites contain small crystals of properly Kfs (Or_{93,9-99,5} and Or_{87,5}).

Table 1..

Representative microprobe analyses of feldspars from potassic alkaline rocks series of Western Kamchatka

Sample	KT-622		7038/1		7249	7214		7036/1			KT-633	1027
Phase	m	m	c	m	m	m	m	c	m	m	m	c
SiO ₂	47,07	61,10	47,89	64,40	64,49	52,72	64,55	56,46	62,07	62,82	63,61	65,79
TiO ₂	0,05	0,24	0,06	0,26	0,04	0,12	0,33	0,01	0,10	0,12	0,37	0,11
Al ₂ O ₃	33,36	19,79	33,74	19,70	19,60	28,96	18,86	27,18	21,59	20,64	20,05	19,19
FeO*	0,72	0,28	0,64	0,22	0,30	0,71	0,29	0,45	0,48	0,56	0,40	0,29
MnO	0,01	0,02	0,00	0,00	0,02	0,02	0,00	0,01	0,06	0,00	0,00	0,01
MgO	0,03	0,04	0,02	0,00	0,00	0,07	0,00	0,05	0,01	0,09	0,05	0,00
CaO	16,34	0,68	15,53	0,91	0,75	10,81	0,79	9,23	4,70	2,54	1,16	1,42
Na ₂ O	2,39	4,19	1,78	4,50	2,46	3,70	2,81	5,79	5,18	4,20	2,21	3,36
K ₂ O	0,12	9,96	0,12	9,43	13,18	1,48	10,81	0,24	5,27	9,35	12,01	11,11
Cr ₂ O ₃	0,00	0,00	0,00	0,04	0,01	0,00	0,02	0,04	0,05	0,03	0,00	0,03
Total	100,09	96,30	99,78	99,47	100,85	98,59	98,47	99,47	99,51	100,35	99,85	101,33
An	78,48	3,39	82,20	4,50	3,60	56,10	4,20	46,20	23,10	12,00	5,94	6,80
Ab	20,82	37,71	17,00	40,20	21,30	34,80	27,20	52,40	46,10	35,70	20,53	29,40
Or	0,70	58,90	0,80	55,30	75,10	9,20	68,70	1,40	30,80	52,30	73,53	63,80

Sample	1027	7038/6	KT-632	7047/1		1032	7382/1				AA-1023/2	
Phase	c	c	c	c	c	c	m	c	c	m	m	c
SiO ₂	64,35	60,02	64,18	63,88	53,60	63,12	57,94	65,66	65,28	66,29	66,63	66,23
TiO ₂	0,20	0,26	0,21	0,06	0,11	0,19	0,06	0,11	0,11	0,00	0,00	0,15
Al ₂ O ₃	19,01	20,16	19,72	19,69	28,66	18,87	25,59	19,38	18,75	18,84	19,00	19,40
FeO*	0,30	0,29	0,23	0,20	0,52	0,22	0,59	0,15	0,14	0,14	0,13	0,18
MnO	0,02	0,00	0,00	0,00	0,00	0,04	0,04	0,00	0,02	0,00	0,03	0,00
MgO	0,00	0,00	0,00	0,00	0,03	0,00	0,02	0,00	0,00	0,00	0,00	0,00
CaO	0,51	0,84	0,91	0,73	10,45	0,66	8,30	0,92	0,61	0,03	0,95	0,97
Na ₂ O	2,04	3,02	2,65	4,42	4,87	4,05	6,04	3,54	2,35	0,14	4,31	2,79
K ₂ O	13,60	9,45	12,05	10,19	0,87	10,19	0,86	11,56	13,03	12,47	10,40	12,28
Cr ₂ O ₃	0,03	0,00	0,01	0,00	0,04	0,06	0,00	0,00	0,05	0,00	0,00	0,01
Total	100,05	94,64	99,94	99,18	99,14	97,33	99,45	101,30	100,33	97,90	101,45	102,02
An	2,50	4,50	4,52	3,50	51,50	3,30	41,00	4,30	3,00	0,20	4,50	4,70
Ab	18,10	35,20	23,89	38,40	43,40	36,40	53,90	30,40	20,80	1,70	36,90	24,50
Or	79,40	60,30	71,59	58,10	5,10	60,30	5,10	65,30	76,20	98,10	58,60	70,80

Note. m - microlite; c - phenocryst. KT-622 - absarokite; 7038/1, 7249 - microshonkinite; 7214, 7036/1, KT-633 - trachybasalts; 1027 - porphyric shonkinite; 7038/6, KT-632 - leucocratic shonkinite; 7047/1 - leucocratic K-Na shonkinite; AA-1032 - melanocratic shonkinite; 7382/1 - massive syenites of differentiated body; AA-1023/2 - syenite from veins.

Pyroxenes from K-alkaline rocks correspond in composition to salites, diopsides, Mg-augites (Fig.4, Tab. 2). Salites usually predominate but in trachybasalts diopsides prevail. Clinopyroxenes are characterised by the tendency of Fs-mineral growth from core to ring zones of phenocrysts and further to microlites. The fassaite evolution direction of Cpx composition is tracked here, from diopsides and salites to Ti-fassaite. There is a difference in titanium concentration between pyroxenes from absarokites and shonkinites. There are separated trends of

increasing TiO_2 in Cpx from absarokites to trachybasalts and further to shonkinites and syenites.

Olivines from absarokites and microshonkinites has gorthonolitic compositions ($\text{Fo}_{61,5-78,6}$); in Ol phenocrysts from trachybasalts are found forsterites

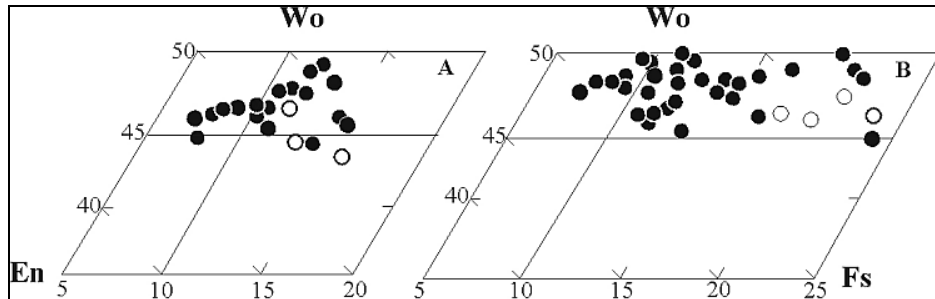


Fig. 4. Compositions of clinopyroxenes from potassic alkaline volcanic rocks of Western Kamchatka.

($\text{Fo}_{82,4-85,4}$) (Tab.2). In range from phenocrysts to microlites increasing MnO concentration and $\text{Fe}/(\text{Fe}+\text{Mg})$ in olivines take place.

Amphiboles from Western Kamchatka syenites correspond in compositions to ferroedinites and ferroedinite hornblend. Besides, riebecites and arfvedsonites present among amphiboles from syenites and leucocratic shonkinites (Tab. 3). The mica of K-alkaline rocks evolve from phlogopites to Mg- and Fe-biotites. Phlogopite present among phenocrysts in trachybasalts and porphyric shonkinites. In the ring zones of phenocrysts its composition becomes more magnesian (Tab. 3). The micas of trachybasalts and porphyric shonkinites have moderate TiO_2 concentration; Mg- and Fe-biotites from shonkinites and syenites are enriched in TiO_2 .

Composition zonality of trachybasalt micas is expressed by increasing of $\text{Fe}/(\text{Fe}+\text{Mg})$ and TiO_2 contents and decreasing of MgO and K_2O concentrations from cores to rings of phenocrysts, and further to microlites. In micas of shonkinites and syenites zonality is more complex. It is necessary to mark, the compositions of Mg-biotites of ring zones of phenocrysts from porphyric shonkinites and trachybasalts are the same as Bt from melanocratic shonkinites.

Except of TiMgt, CrTiMgt and Ilm, absarokites and trachybasalts contain some alumocromic spinels (46-60 mas.% Cr_2O_3) and pleonast (8-9 mas.% Cr_2O_3 and 54-55 mas.% Al_2O_3); microshonkinites bear some Cr-Al-Fe-spinels evolving to CrTiMgt compositions.

Analysis of mineral compositions show that shonkinites and syenites demonstrate common features of composition evolution of K-Na feldspars, Cpx, TiMgt; absarokites and microshonkinites form isolated group. It is found also, that compositions of minerals from porphyric, melanocratic and leucocratic shonkinites and syenites are similar.

GEOCHEMISTRY AND COMPOSITION EVOLUTION OF WESTERN KAMCHATKA K-ALKALINE ROCKS

General material peculiarities of Western Kamchatka K-alkaline rocks in comparison to high-K rocks of island-arc volcanic belts are: more high

Table 2.

Representative microprobe analyses of olivines and clinopyroxenes from potassic alkaline rocks series of Western Kamchatka.

Sample	KT-622	7029	7038/1		7214		KT-622		7038/1		AA-1030A	
Mineral	Ol	Ol	Ol	Ol	Ol	Ol	Cpx	Cpx	Cpx	Cpx	Cpx	Cpx
Phase	c	c	c	c	c	c	c	m	c	c	c	c
SiO ₂	38,47	38,58	36,96	38,35	39,07	38,25	49,67	47,08	49,00	52,61	53,31	53,28
TiO ₂	0,02	0,03	0,02	0,00	0,00	0,03	1,30	1,87	1,21	0,41	0,62	0,41
Al ₂ O ₃	0,00	0,01	0,00	0,00	0,00	0,00	4,29	6,77	4,39	1,75	1,52	0,86
FeO*	22,81	20,55	29,22	20,60	14,33	19,76	6,73	6,99	6,77	4,72	5,45	7,40
MnO	0,54	0,39	0,62	0,35	0,23	0,42	0,17	0,14	0,16	0,16	0,11	0,21
MgO	39,56	39,82	31,51	38,54	43,53	39,71	14,28	12,25	13,17	16,05	15,76	16,70
CaO	0,21	0,23	0,30	0,19	0,15	0,25	22,64	22,52	21,29	21,22	21,89	18,87
Na ₂ O	0,02	0,06	0,00	0,03	0,00	0,00	0,33	0,36	0,24	0,22	0,10	0,19
K ₂ O	0,00	0,00	0,00	0,00	0,01	0,03	0,00	0,01	0,04	0,00	0,00	0,02
Cr ₂ O ₃	0,00	0,04	0,00	0,02	0,06	0,00	0,35	0,45	0,65	0,60	0,29	0,19
Total	101,6 2	99,70	98,64	98,10	98,00	98,44	99,76	99,12	96,91	97,73	99,04	98,12
Fm	24,88	22,80	34,70	23,40	15,80	22,20	21,33	23,61	22,80	14,60	16,54	20,40
Wo							47,28	48,85	47,30	44,80	45,46	39,30
En (Fo)	75,12	77,20	65,30	76,60	84,20	77,80	41,48	39,07	40,70	47,10	45,53	48,40
Fs							11,24	12,08	12,00	8,10	9,01	12,30
Sample	KT-633		AA-1027		AA-1032		KT-632		7382/1			
Mineral	Cpx	Cpx	Cpx	Cpx	Cpx	Cpx	Cpx	Cpx	Cpx	Cpx	Cpx	Cpx
Phase	c	m	c	m	c	m	c	m	c	c	c	m
SiO ₂	51,99	50,21	52,14	50,01	50,92	51,11	47,87	48,29	50,52	50,74	51,99	48,84
TiO ₂	0,87	1,25	1,03	1,30	0,95	1,09	1,67	1,73	1,59	1,22	0,96	1,53
Al ₂ O ₃	2,20	3,13	2,23	3,11	3,14	2,54	4,74	4,09	3,35	2,81	2,19	3,55
FeO*	5,66	7,00	7,85	8,78	4,96	6,96	9,34	11,93	7,14	8,09	10,35	13,17
MnO	0,11	0,22	0,23	0,24	0,11	0,13	0,25	0,46	0,13	0,20	0,34	0,44
MgO	15,80	14,30	14,59	13,49	14,71	13,86	11,98	10,57	14,27	13,87	12,93	9,80
CaO	23,07	21,82	21,36	21,33	22,43	22,14	22,80	22,32	22,55	21,47	22,52	21,35
Na ₂ O	0,19	0,14	0,15	0,13	0,17	0,22	0,08	0,21	0,10	0,16	0,01	0,23
K ₂ O	0,00	0,09	0,01	0,11	0,02	0,06	0,00	0,11	0,00	0,01	0,08	0,01
Cr ₂ O ₃	0,23	0,00	0,01	0,01	0,72	0,00	0,00	0,02	0,18	0,00	0,00	0,00
Total	100,12	98,15	99,60	98,51	98,13	98,10	98,74	99,73	99,83	98,57	101,39	98,93
Fm	17,02	22,09	23,70	27,30	16,20	22,30	31,02	39,69	22,20	25,10	31,70	43,80
Wo	46,55	46,08	44,50	45,30	47,90	47,10	48,56	47,79	46,90	45,50	46,10	46,80
En	44,35	42,00	42,30	39,80	43,70	41,10	35,48	31,50	41,30	40,90	36,80	29,90
Fs	9,10	11,92	13,20	15,00	8,40	11,80	15,96	20,71	11,80	13,60	17,10	23,30

Note. Ol - olivine; Cpx - clinopyroxene; m - microlite; c - phenocryst. KT-632 - absarokite; 7029 - high-Mg absarokite; 7038/1 - microshonkinite; 7214 - trachybasalt; AA-1038 - microshonkinite; AA-1030A, KT-633 - trachybasalt; AA-1027 - porphyric shonkinite; AA-1032 -

melanocratic shonkinite; KT-632 - leucocratic shonkinite; 7382/1 - syenites of differentiated subvolcanic body.

Mg/Mg+Fe, contents of Ni, Co, Cr, and significant enrichment in incoherent elements such as P, K, Rb, Ba, Pb, Sn, Be, F, Zr, U, Th, REE (Tab. 4). Absarokites are the most magnesian (MgO to 11 mas.%) among rocks of K-alkaline series. They differ from trachybasalts by low contents of lithophile elements. These rocks form isolated group of compositions but they are connected with other rocks of the series by transitional varieties.

Trachybasalts, porphyric shonkinites and melanocratic shonkinites are the most titanic among K-alkaline basaltoids. Concentrations of TiO₂, K₂O and values

Table 3.

Representative microprobe analyses of amphiboles and micas from potassic alkaline rocks series of Western Kamchatka.

Sample	7382/8		7038/1	1030a	KT-633	7214	6982/7		AA-1027			
Mineral	Amp	Amp	Bt	Bt	Bt	Bt	Bt	Bt	Bt	Bt	Bt	Bt
Phase	m	m	m	c	m	m	c	c	c	c	c	c
SiO ₂	47,72	43,31	38,00	38,06	38,18	37,84	37,24	34,81	38,44	37,34	37,57	35,46
TiO ₂	1,22	1,13	6,71	4,90	4,08	6,04	3,66	8,28	4,53	8,01	8,26	9,59
Al ₂ O ₃	7,11	6,96	12,99	14,09	15,15	12,81	14,49	14,09	13,57	13,76	13,32	13,98
FeO*	23,91	23,46	13,59	9,08	6,88	9,30	6,70	12,78	7,93	11,79	13,39	13,25
MnO	0,88	0,96	0,11	0,09	0,05	0,17	0,07	0,12	0,06	0,08	0,11	0,10
MgO	6,85	7,75	13,91	17,76	19,36	17,29	18,74	12,36	18,88	13,36	12,10	10,80
CaO	10,59	10,24	0,07	0,11	0,00	0,10	0,02	0,03	0,01	0,04	0,02	0,00
Na ₂ O	2,02	1,86	0,70	0,45	0,61	0,58	0,40	0,31	0,32	0,43	0,41	0,32
K ₂ O	1,49	1,29	9,78	10,18	9,38	9,48	10,12	9,28	10,32	9,71	9,78	9,13
Cr ₂ O ₃	0,00	0,05	0,00	0,33	0,89	0,00	1,43	0,05	0,05	0,05	0,01	0,40
OH	1,89	1,91	4,04	4,08	4,13	4,03	4,02	3,88	4,07	4,02	4,01	3,92
Total	98,68	98,91	99,87	99,12	98,71	97,64	96,92	95,99	98,17	98,60	98,97	96,95
Fm	67,00	63,90	35,60	22,50	16,73	23,50	16,90	36,90	19,20	33,30	38,50	40,90

Sample	KT-632		7038/6	7047/3		7047/1		AA-1032		7382/1		1023/2
Mineral	Bt	Bt	Bt	Bt	Bt	Bt	Bt	Bt	Bt	Bt	Bt	Bt
Phase	c	c	c	c	c	c	c	c	c	c	c	c
SiO ₂	35,15	34,78	34,26	35,80	36,38	33,76	35,76	37,16	34,65	34,84	34,43	36,86
TiO ₂	9,29	9,87	10,65	8,05	7,98	10,21	9,24	7,58	7,85	9,23	9,38	7,15
Al ₂ O ₃	14,89	14,62	14,54	14,03	14,50	14,91	13,46	13,19	13,67	13,21	13,46	12,73
FeO*	11,24	15,19	14,04	16,72	12,80	13,19	18,35	10,84	12,42	17,40	16,25	16,66
MnO	0,04	0,18	0,17	0,19	0,09	0,12	0,24	0,10	0,08	0,22	0,19	0,14
MgO	13,49	10,14	11,10	11,12	13,73	11,70	9,13	14,38	13,14	9,74	10,93	11,33
CaO	0,01	0,06	0,00	0,00	0,00	0,01	0,04	0,01	0,00	0,00	0,00	0,00
Na ₂ O	0,42	0,48	0,52	0,73	0,72	0,69	0,84	0,57	0,76	0,38	0,51	0,66
K ₂ O	9,13	9,27	9,03	9,28	9,33	9,36	9,62	9,45	8,71	9,67	9,29	9,86
Cr ₂ O ₃	0,00	0,00	0,01	0,00	0,01	0,04	0,08	0,01	0,05	0,03	0,03	0,00
OH	3,99	3,95	3,95	3,97	4,04	3,94	3,96	3,98	3,86	3,89	3,90	3,94
Total	97,65	98,54	98,26	99,89	99,65	97,93	100,73	97,29	95,19	98,61	98,37	99,34
Fm	31,94	45,97	41,80	46,10	34,50	39,00	53,30	29,90	34,80	50,40	45,80	45,40

Note. Amp - amphibole; Bt - biotite; m - microlite; c - phenocryst. 7038/1 - microshonkinite; 1030a, KT-633, 7214, 6982/7, 6982/7 - trachybasalts; AA-1027 - porphyric shonkinite; KT-632, 7038/6 - leucocratic shonkinites; 7047/3 - melanocratic K-Na shonkinite; 7047/1 - leucocratic

K-Na shonkinite; AA-1032 - melanocratic shonkinite; 7382/1, 7382/8 - syenites of differentiated subvolcanic body; 1023/2 - syenite from veins.

Table 4.

Average compositions of potassium alkaline basaltoids from Western Kamchatka.

Rocks	MgA*	A	TB	TB	LSH	MSH	SH	PSH	S1	S2
n*	8	2	9	1	6	10	4	2	5	8
SiO ₂ , wt. %	47,26	49,26	49,88	50,31	50,65	48,64	51,80	52,38	55,55	59,33
TiO ₂	1,02	1,14	1,43	1,54	1,51	1,84	1,84	1,88	1,93	1,04
Al ₂ O ₃	14,66	14,41	14,21	13,71	15,88	14,12	13,78	13,85	15,67	17,72
Fe ₂ O ₃	2,99	3,38	3,85	4,53	3,82	3,52	4,78	4,31	3,48	1,89
FeO	5,13	5,08	4,25	2,87	3,45	4,06	2,47	3,23	2,62	1,3
MnO	0,15	0,14	0,20	0,10	0,13	0,12	0,13	0,11	0,08	0,06
MgO	10,47	8,08	7,02	7,08	5,78	9,44	6,63	5,46	3,36	1,35
CaO	6,96	6,63	6,44	5,90	3,82	5,11	4,28	6,47	3,13	2,40
Na ₂ O	2,74	3,21	2,43	1,94	3,22	2,16	1,57	1,92	2,45	3,61
K ₂ O	2,43	3,59	4,49	5,15	5,41	4,67	6,88	5,82	8,11	8,57
P ₂ O ₅	0,57	0,78	0,79	0,73	0,66	0,81	0,67	0,81	0,58	0,21
H ₂ O	5,63	3,60	4,50	5,77	5,38	5,52	4,98	3,39	2,64	2,28
Total	100,09	99,30	99,49	99,63	99,71	99,68	99,81	99,63	99,60	99,76
Rb, ppm	59	112	123	120	167	116	189	166	204	235
Ba	1110	1245	1540	1300	2080	1560	1530	1550	2230	1040
Sr	755	635	660	670	550	720	925	1215	1140	450
Pb	8,0	7,7	7,5	6,3	12,5	7,4	4,5	5,1	9,0	13,5
Co	37	35	29	22	20	31	19	25	16	10
Ni	260	150	87	120	53	224	89	42	34	11
Cr	550	375	173	160	148	229	118	110	93	20
V	230	245	300	330	230	270	350	390	290	155
Be	1,7	3,2	3,1	2,9	4,3	3,2	3,1	2,9	4,2	2,8
B	16	18	16	7,8	10,3	46	33	20	38	23
F	730	1200	1900	2500	1440	1250	2450	1950	2900	945
Ta	0,3	0,5	0,5	0,5		0,7	0,56	0,9	0,7	0,75
Nb	3,1	5,4	6,5	7,4	13,5	9,1		7,5	11,4	16,7
Zr	175	240	447	495	1120	527		494	621	836
Hf	4,0	7,8	11,5	11,4	25,0	14,6	13,9	11,6	15,9	21,3
La	17	25	35	36	41	44	36,7	51	42	55
Ce	39	43	96	95	135	97	81	110	94	130
Nd	23	25	46	49	54	50	44	57	46	50
Sm	4,8	6,4	8,2	7,1	10	11,2	8,4	10	7,1	8,3
Eu	1,3	1,5	1,6	2,2	2,5	3,2	1,96	2,0	2,0	2,0
Gd	5,0	5,9	6,7	6,5	5,4	8,2	4,5	8,8	6,3	8,3
Dy	4,3	4,0	4,4	3,2	3,2	4,6		3,2	3,8	7,4
Er		2,5	2,6	2,1	1,9	2,4		1,6	1,8	3,5
Yb	2,0	2,0	2,3	1,9	1,5	1,8	1,7	1,7	1,7	3,8
Lu	0,25	0,26	0,31	0,25	0,06	0,23	0,25	0,18	0,22	0,38
Y	19	21	22	14	19	22		19	13	30
Th	3,5	5,4	4,5	5,1	6,2	4,1	3,5	3,9	7,7	9,4
U	1,9	2,7	2,5	2,2	3,3	2,0	2,5	2,3	4,0	5,2

Note. MgA* - high-magnesium absarokite, A - absarokite, TB - trachybasalts, LSH - leucocratic shonkinite, MSH - melanocratic shonkinite, SH - shonkinite, PSH - porphyric shonkinite, S1 - syenite of differentiated subvolcanic body; S2 - syenite from veins. n* - number samples. Rock data: Perepelov A.B., Volynets O.N.

K_2O/Na_2O increase from trachybasalts to shonkinites, and go down to syenites (TiO_2 from 2 to 0,8 mas.%). Behaviour of Al_2O_3 is opposite (Fig. 5). Besides, concentrations of Fe, Mg, Ca, P, Co, Ni, Cr go down, Rb, Ba, Sr, Sn, Be, F, Zr, Nb, U, Th increase in this direction, that is usual for differentiated series. All rocks of K-alkaline series are significantly enriched in REE and characterised by high degree of their fractionation (La/Yb 8,5 - 17,5 for absarokites and microshonkinites, 10,4 - 34 for shonkinites and syenites) is characteristic to rocks of potassic alkaline series. Trachybasalts, K-Na shonkinites and syenites are the most enriched in REE ($TR+Y=$ 330, 318, 312 ppm). REE concentrations increase from absarokites to shonkinites. (Tab. 4, Fig. 6).

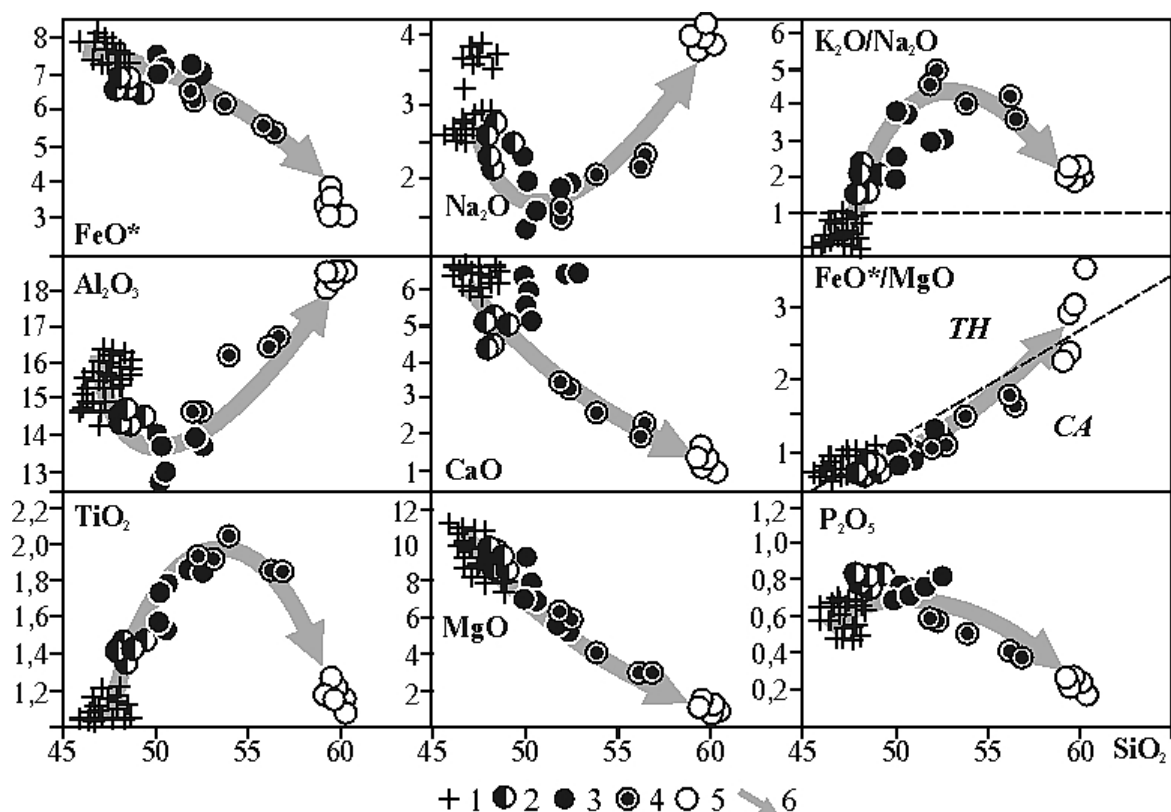


Fig. 5. Distribution of major elements in potassic alkaline rocks of Western Kamchatka.

Rocks: 1- absarokites; 2- trachybasalts and porphyritic shonkinites; 3- shonkinites; 4- syenites of massive zones; 5- syenites of veins. 6- evolution direction of rocks composition of potassic alkaline series. TH - tholeiitic series, CA - calc-alkaline series.

K-alkaline rocks of Western Kamchatka are also enriched in F (to 2600 ppm in shonkinites and to 3100 ppm in syenites) and Be (4,3 ppm in leucocratic shonkinites and 4,2 ppm in syenites). According to high TiO_2 contents in trachybasalts and shonkinites, these rocks, as much as syenites, are enriched in Zr and Hf (1120 and 25 ppm in leucocratic shonkinites, 1030 and 23,5 ppm in syenites). It is necessary to say, that the most significant contents of Nb, U and Th are in the K-Na shonkinites (38,2; 26,6; 6,0 ppm in average) and syenites (7,3;

11,7; 16,6 ppm in average).

THE QUESTIONS OF WESTERN KAMCHATKA K-ALKALINE ROCKS ORIGIN

Significant difference between K-alkaline rocks of Western Kamchatka and high-K island-arc series in material and mineral composition, as much as specific behaviour features of petrogenic and rare elements, show that their forming in conditions which can not be considered within the framework of simple models, like subduction or riftogenic magmatism.

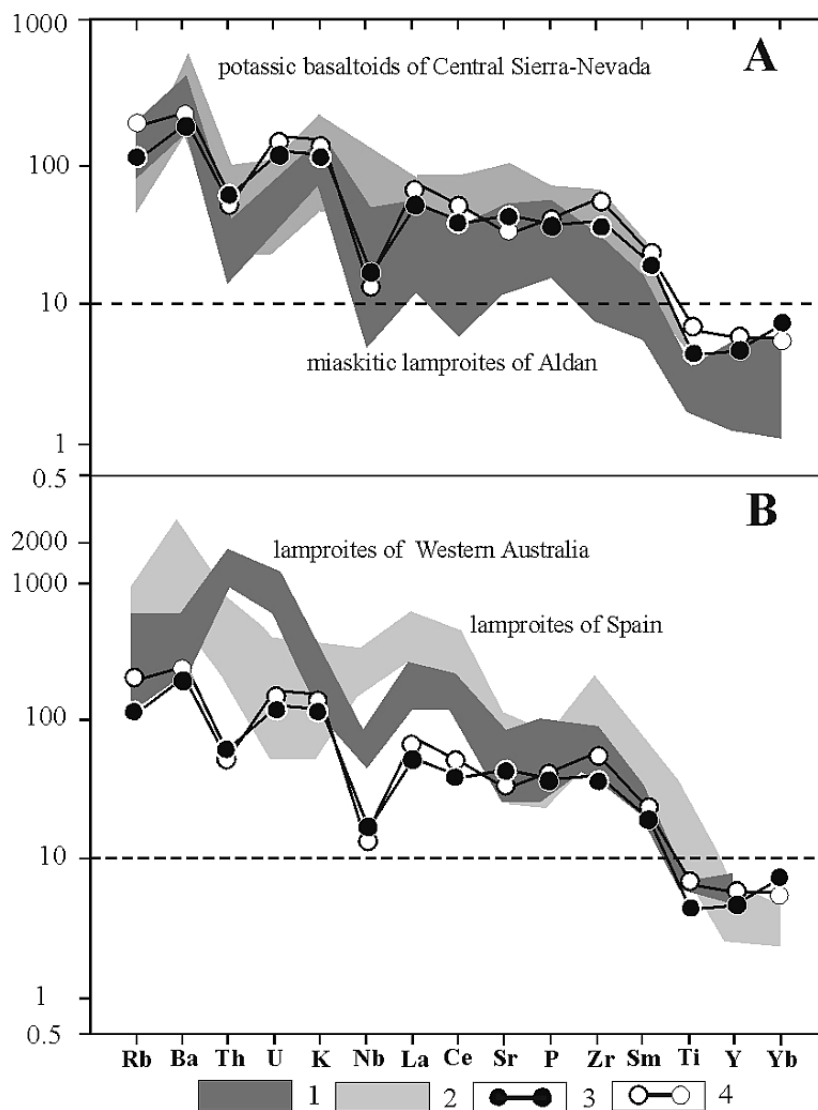


Fig. 6. Spidergram of distribution of gigromagmatophylic elements in basaltoids of potassic and lamproitic serieses (primordial mantle [Wood, 1979]).

A: 1- potassic basaltoids of Central Sierra-Nevada; 2- miaskitic lamproites of Aldan, Siberia; 3 - 4- potassic basaltoids of Western Kamchatka (3 - absarokites, 4 - trachybasalts).
 B: 1- lamproites of Western Australia; 2- lamproites of Spain.

Bedding conditions and character of subvolcanic rock complexes construction show the fact that processes of rocks forming taken place in near-surface cameras. It seems that source melts for K-alkaline rocks were closed in composition to absarokites, microshonkinites, trachybasalts and porphyric shonkinites. Emanation differentiation of absarokite magmas in some cases led to formation of syenitic shlires and veins within subvolcanic bodies of absarokites. As a result of intracamera differentiation of trachybasalt melts, multiple melanocratic and leucocratic shonkinite and syenite massives were formed. This process was connected with separation of melts at the emanation and crystal differentiation during short intervals of time. Melanocratic shonkinites are the result of cumulative fractionation of Ol, Cpx and TiMgt with separating of remaining melt of leucoshonkinite and syenite composition.

The questions of primary for K-alkaline series magmas origin are still under discussion. O.N. Volynets et al. (1987) are made comparison K-alkaline basaltoids with lamproites of orendite row. To proceed from high contents of K, Mg, lithophilic elements, the presence of high-Cr spinel and high Cr concentration in clinopyroxenes and phlogopites, they made conclusion about possible belonging of K-alkaline basaltoids to lamproites. But Bogatikov et al. (1991) suppose this conclusion to be not proved enough. High Al and moderate concentration of Ti, Ta, Nb in potassic basaltoids, side by side with the fact of their forming within island-arc system (probably, during the period of active subduction stopping), need making the model of primary K-alkaline magmas origin with provision of influence of processes attributive to island-arc conditions of magmagenation. In addition to all, "lamproitic" (more exactly, "mantle" or "intraplate") hypothesis haven't confirmation in this case, because of absence in K-alkaline rocks of xenogeneous high-pressure minerals (garnets of almandine-pyrope line, etc.). Available data about finds of these minerals are not trustworthy enough and must be checked. Though, recently in trachybasalts we found rare crystals of pyrope-almandine.

On the Onuma and Motya (1984) diagrams (Fig. 7) evolution lines of K-alkaline rocks compositions say about fractionation of primary K-alkaline melts at the different melting degrees of the same metasomatized mantle substratum. The highest melting degree determined the absarokite magma appearance, the lowest - magmas closed in composition to porphyric shonkinites. Displacement of evolutionary lines of K-alkaline rock compositions on diagram Fig. 7 to side of high values of Sr/Ca from the trend of chondrite mantle or garnet peridotite melting is probably determined by high degree of mantle substratum metasomatism. We suppose that in generation of K-alkaline magmas under Western Kamchatka metasomatized (in result of preceding stage of subduction zone development) and enriched in lithophilic components mantle substratum took part.

Like shoshonites and latites, the K-alkaline rock series are described in regions of some other island-arc systems and active continental margins. However,

it is well known, they are more usual in riftogenic structures of intracontinental. On the spider-diagram Fig. 6 potassic basaltoids of Western Kamchatka are shown in comparison with miaskite lamproites of Aldan (Siberia), lamproites from Australia and Spain, and potassic basaltoids of Sierra-Nevada (USA.). Concentration levels of main hydromagmatophilic elements (with the exception of Ti, Y, Yb) in studied rocks are more high than in island-arc volcanites. Distribution patterns underline the enrichment of K-alkaline rocks in lithophile elements. Character features of their patterns are the absence of Sr maxima and presence Th and Nb minima. Lamproites of Spain and Western Australia (Jaques et al., 1984; McDonough et al., 1985) are more enriched in hydromagmatophile elements than Western Kamchatka K-alkali basaltoids; their distribution graphs have more steep slopping (Fig. 6). Spanish and Australian lamproites has common features of their

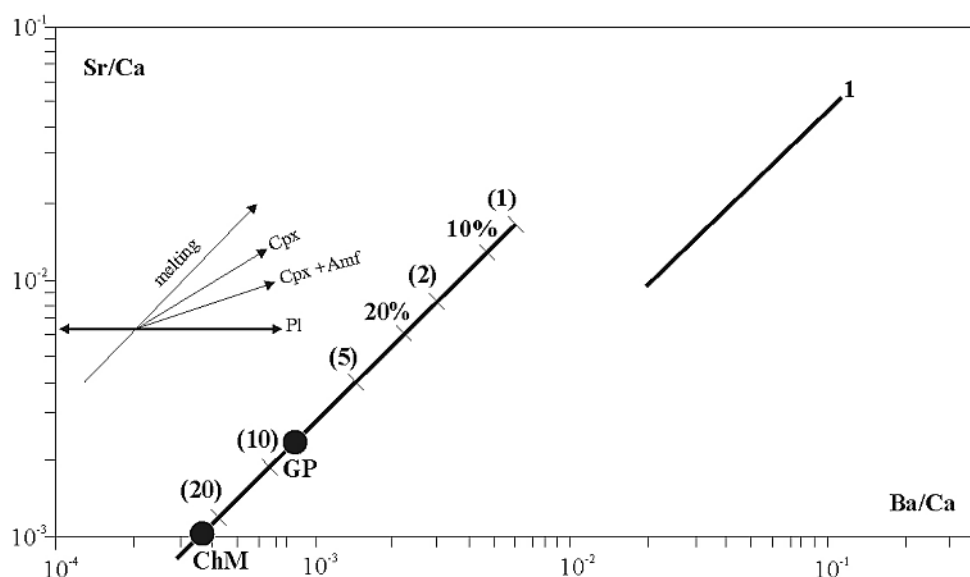


Fig. 7. Diagrams Sr/Ca-Ba/Ca [Onuma, Motya, 1984] for potassium alkaline rocks of Western Kamchatka.

GP - composition of garnet peridotite, ChM - composition of chondrite mantle.

1 - line of compositions K-alkaline rocks of Western Kamchatka.

spider-diagrams: La maxima, Sr and P minima. Similar peculiarities are characteristic for the most alkaline varieties of Kamchatka potassic basaltoids. Compositions of Spanish lamproites have Nb minimum too, but they are characterised by Th maxima on this diagram. And so, the typical lamproites of any geostructural settings are differed from Kamchatka potassic basaltoids by higher concentrations of hydromagmatophile elements. However, K-alkali basaltoids of Sierra-Nevada are very similar in composition with those of Kamchatka. The presence of Nb minimum on spider-diagrams of studied potassic basaltoids, like of basaltoids of Sierra-Nevada and of Spanish lamproites, brings them together with subalkaline basaltoids of active continental margins and island arcs which usually forms at postsubduction period.

The model of K-alkaline magmas of Western Kamchatka origin must be based on exact data on the geodynamic history of the region. At present, absence of sufficient isotopic age data for studied alkaline complexes make it difficult.

The areas of K-alkaline basaltoids are located within geological structure which placed between Palogene margin-continental volcanic belt, some fragments of which are fixed in western and north-western seasides of Kamchatka, and island-arc Oligocene-Quaternary volcanic belt of Sredinny Ridge. Analysis of geological materials and age data obtained allow to expect that the time of K-alkaline basaltoids forming is corresponding with the time between the stopping of Paleogene subduction and the beginning of modern island arc development. This interval may be approximately estimated in 10-15 m.a.

It seems probably that, as a result of lithosphere stretching in Western Kamchatka during Oligocene-Miocene time, the levels of magmagenation could moved to more deep mantle horizons. Source mantle substratum from which the potassic magmas could form was, probably, phlogopite gartzburgite. It is proposed that the K-subalkaline (absarokite) melts were formed first, at relatively low degrees of melting, and trachybasalte alkaline magmas - later, at the rising of melting degree. In this case absarokites and thachybasaltes age data are to be lie within short time interval (10-15 ma), and absarokites ages data are to be younger.

One of important questions on K-alkaline volcanism geodynamic position is the question is it attributive to the back side of Paleogene island-arc system of "west-east" direction or to back side of Oligocene-Miocene island arc in direction "east-west" belongs it? In first case, the decision is connected with proofs of existence of subduction zone in Paleogene time, from Okhotsky sea-side, i.e., with the geodynamic history of this sea basin and Okhotsky-Chukotsky active continental margin.

This study was supported by Russian Foundation for Basic Research, grant 01-05-64206.

REFERENCE

1. Amir khanov H.I., Batymurzaev A.T., Antipin V.S., Perepelov A.B. K-Ar age of the Kamchatka alkaline basaltoids // Doklady AS USSR. - 1986. - Vol. 207, p. 494-496 (in russian).
2. Bogatkov O.A., Tsvetkov A.A., Kovalenko V.I. Magmatic evolution of the island arcs // Pacific geology. - 1985. -N 6. - p. 32-48 (in russian).
3. Bogatkov O.A., Kononova V.A. The TR and rare elements as an indicator of genesis Aldan lamproites // Volcanology and seismology. - 1987. - N 1. - p. 15-29 (in russian).
4. Borley G.D. Potash-rich volcanic rocks from Southern Spain // Min. Mag. -1967. - Vol.36, N268. -P. 364-379.
5. Dyakov B.F. Geological setting and oil-gas prospects of the Western Kamchatka. - M. : Gosgeoltechizdat, 1955. - 255 p. (in russian).
6. Ewart A., Taylor S.R. Trace element geochemistry of the rhyolitic volcanic rocks central North Island, New Zealand. Phenocryst date // Contribs Mineral. Petrol.- 1969.- v. 22.- h. 127-146.

7. Gill J.B. Orogenic andesites and plate tectonics.- Berlin: Springer-Verlag, 1981.- 383p.
8. Guziev I.S. Alkaline petrographical province of Western Kamchatka (Tigil'sky area) // Problems of volcanism. : Materials to II Vsesouzn. volcanol. conference. - Petropavlovsk-Kamchatsky, 1964 (in russian).
9. Guziev I.S. Alkaline magmatism of the Tigil'sky area of Western Kamchatka // Volcanic and volcano-plutonic formations. - M. : Nauka, 1966. - p59-62 (in russian).
10. Guziev I.S. About chemical composition dependency of cenozoic rocks of Western Kamchatka from composition and width of cenozoic sediments // North-East magmatism of USSR: Tes. dokl. of First North-East petrographic conference . -Magadan, 1968. -p. 159 (in russian).
11. Guziev I.S. Neogene-quaternary alkaline basaltoids of Western Kamchatka // Petrology of the neogene-quaternary basaltoids of North-West Pacific belt. - M. : Nedra,1971. - p. 107-113 (in russian).
12. Jaques A.L., Lewis J.D. The diamond-bearing ultrapotassic (lamproitic) rocks of the west Kimberley region, Western Australia // Kimberlites and Related Rocks / Ed. by J. Kornprobst. - Amsterdam: Elsevier, 1984. -1984. -P. 225-254.
13. Keller J. Mediterranean island arcs // Andesites / Ed. R.S. Thorpe. - London: J. Welley & Sons, 1982. - P. 307-325.
14. Legler V.A. The cenozoic Kamchatka development from theory of tectonic lithosphere plates points of view. -M. : Izd. VINITI,1977. - p. 137-169 (in russian).
15. Magmatic rocks. Classification. Nomenclature. Petrography. -M. : Nauka, 1983. - Vol. 1, 2. - 1978 (in russian).
16. McDonough W.F., McCulloch M.T., Sun S.S. Isotopic and geochemical systematics in Tertiary-Recent basalts from southeastern Australia and implications for the evolution of the sub-continental lithosphere // Geochi. Cosmochim. Acta. -1985. -Vol.49, N 5. -P 2051-2067.
17. Onuma N., Motya M. Sr/Ca - Ba/Ca systematics of volcanic rocks from the central Andes, southern Peru, and its implication for Andean magmatism // Geochem. Journ. - 1984. - vol.18. -p. 251-262.
18. Peccerillo A., Taylor S.R. Geochemistry of Eocene calc-alkaline volcanic rocks from the Kastomonu area, Northern Turkey // Contribs Mineral. Petrol. -1976. -Vol. 58, N 1. - p .63-81.
19. Perepelov A., Antipin V.,Kablukov A. Geochemistry, mineralogy, an geodynamic framework of late cenozoic potassic alkaline basalts in Western Kamchatka. // CD-ROM Abstracts Volume, 31th International Geological Congress, Symp. 6.8, Rio de Janeiro, Brasil, 2000.
20. Stolz A. J., Varne R., Wheller G. E., Foden J. D., Abbot M. J. The geochemistry and perogenesis of K-rich alkaline volcanics from the Batu Tara volcano, eastern Sunda arc // Contribs Mineral.Petrol. - 1988. - Vol.98. - P. 374-389.
21. Van Kooten G.K. Mineralogy, petrology and geochemistry of an ultrapotassic basaltic suite, Central Sierra Nevada, California, U.S.A. // Journ. Petrol. - 1980. -Vol.21,N 4. -P. 651-684.
22. Venturelli G., Caperdi S. et al. The ultrapotassic rocks from southeastern Spain // Lithos. - 1984. -Vol.17, N 1. -P. 37-54.
23. Volynets O.N., Antipin V.S., Perepelov A.B., Anoshin G.N., Puzankov J.M. First geological and mineralogical data about late cenozoic potassic basaltoids of Western Kamchatka. - Doklady AS USSR, 1985, Vol. 284, N1, p. 205 - 208 (in russian).
24. Volynets O.N., Anoshin G.N., Puzankov J.M., Perepelov A.B., Antipin V.S. Potassic basaltoids of Western Kamchatka - the rocks of the lamproite series in island arc system // Geology and geophysic, 1987, N 11. p. 41-50 (in russian).
25. Volynets O.N., Flerov G.B. Segment of Kamchatka // Petrology and geochemistry of island arcs and back arcs seas. - M. : Nauka, 1987. - p.56-85 (in russian).

26. Volynets O.N., Antipin V.S., Perepelov A.B., Anoshin G.N. Geochemistry of volcanic series of island arc system in terms to geodynamic (Kamchatka). // *Geology and geophisic.* 1990. N 5. p. 3 - 13 (in russian).
27. Volynets O.N. Geochemical types, petrology and genesis of Late Cenozoic volcanic rocks from the Kurile-Kamchatka island-arc system, // *International Geological Review.* 1994. V.36. № 4. P. 373-40 (in russian).
28. Wood D.A. A variably viened suboceanic mantle-genetic significance for mid-ocean ridge basalts from geochemical evidance // *Journ. Geol.-* 1979.- Vol. 7, № 3.- p.499 -503.

SR, ND, C AND O ISOTOPE CHARACTERISTICS OF SIBERIAN CARBONATITES

T. Morikiyo¹, **T. Miyazaki**², **H. Kagami**²,
N.V. Vladykin³, **E.A. Chernysheva**³, **L.I. Panina**⁴, **N.M. Podgornych**⁴

¹ *Department of Geology, Shinshu University, Asahi, Matsumoto 390-8621, Japan*
T. Morikiyo: xmoriki@gipac.shinshu-u.ac.jp

² *Department of Geology, Niigata University, Igarashi, Niigata 950-2181, Japan*
T.Miyazaki:miyazaki@geows.ac.niigata-u.ac.jp; H. Kagami:kagami@gs.niigata-u.ac.jp

³ *Russian Academy of Sciences, Vinogradov Institute of Geochemistry, Irkutsk 66403, Russia*
N.V. Vladykin: vlad@igc.irk..ru

⁴ *United Institute of Geology, Geophysics and Mineralogy, Siberian Branch of the Russian
Academy of Sciences, Novosibirsk 630090, Russia*

Sr, Nd, C and O isotopic compositions of carbonatites from Siberia were measured in order to clarify the geochemical nature of subcontinental lithospheric mantle of the Siberia region. Carbonatite samples were collected from 16 alkaline rocks-carbonatite complexes occurring in various tectonic environments. Two different types of carbonatites were recognized from their ϵ Sr and ϵ Nd values. One (Group 1 carbonatites) includes the carbonatites which have positive ϵ Nd (2.7-7.0) and negative ϵ Sr (-20.2 - -4.5) values. Carbon and oxygen isotopic compositions of the carbonatites free from secondary alteration are similar to those of mantle CO₂. These facts indicate that Group 1 carbonatites were derived from the slightly depleted mantle source.

Another type (Carbonatites of Group 2) includes carbonatites having negative, low ϵ Nd and positive, high ϵ Sr values. The Malomuruskii and Khani bodies in the Western Aldan subprovince show this unusual isotopic character for carbonatites. The carbon and oxygen isotopic ratios for the carbonatites are plotted near mantle CO₂ field in the $\delta^{18}\text{O}$ versus $\delta^{13}\text{C}$ diagram.

The Malomuruskii and Khani bodies occur closely in space, but the age of emplacement is completely different. The facts lead to the view that carbonatite magma is not related to mantle plume derived from asthenosphere but originated in subcontinental lithosphere. It is inferred that subcontinental lithospheric mantle below the Siberian Craton consists essentially of slightly depleted mantle, except for the Western Aldan area.

INTRODUCTION

The view that carbonatite magmas were generated in the mantle region is now widely accepted. Carbonatites commonly show considerable enrichments in Sr and Nd. This means that carbonatitic magmas or the parental magma of carbonatites were generated through the partial melting of the large volume of mantle source. Therefore, the Sr and Nd isotopic ratios of carbonatites may reflect the mean isotopic ratios of Sr and Nd of the mantle source. The occurrences of carbonatites are virtually restricted in continental regions. The geochemical nature of subcontinental mantle, unlike that of oceanic mantle, has not been well understood. Thus, to study the Sr and Nd isotopic compositions of carbonatites is very promising to elucidate the geochemical nature of the mantle below continental regions [Bell and Blenkinsop, 1989].

The aims of this study are, firstly, to clarify the Sr, Nd, C and O isotopic characteristics of Siberian carbonatites overall, and secondary, to infer the geochemical nature of subcontinental mantle below the Siberian Craton, on the basis of Sr and Nd isotopic ratios of the carbonatites.

SAMPLES

The samples studied and the petrographic descriptions are given in Table 1. The ages of each carbonatite body used for the calculation of initial Sr and Nd isotopic ratios are also described in the table.

ANALYTICAL PROCEDURE

The details of Sr and Nd isotopic analysis have been given in Miyazaki and Shuto (1998). Initial Sr and Nd isotopic ratios were calculated from the measured $^{87}\text{Sr}/^{86}\text{Sr}$, $^{87}\text{Rb}/^{86}\text{Sr}$, $^{143}\text{Nd}/^{144}\text{Nd}$, $^{147}\text{Sm}/^{144}\text{Nd}$ ratios and ages for the bodies which were taken from literatures. Initial $\epsilon\text{Sr}(t)$ and $\epsilon\text{Nd}(t)$ values were also calculated. For the calculation of ϵ values, the following parameters for Bulk Earth were employed: $(^{87}\text{Sr}/^{86}\text{Sr})_{\text{pr}}=0.7045$, $^{87}\text{Rb}/^{86}\text{Sr}=0.0827$, $(^{143}\text{Nd}/^{144}\text{Nd})_{\text{pr}}=0.512638$, $^{147}\text{Sm}/^{144}\text{Nd}=0.1966$ [Goldstein et al., 1984, Depaolo, 1988].

The experimental procedure for carbon and oxygen isotope ratio determination follows that outlined by McCrea (1950). The oxygen isotope fractionation factor determined by Sharma and Clayton (1965), $\alpha_{\text{CO}_2\text{-CC}}=1.01025$, was used to calculate the $^{18}\text{O}/^{16}\text{O}$ ratio of calcite. The isotopic data are presented in terms of the δ notation relative to PDB for carbon and SMOW for oxygen. Analytical uncertainty is about $\pm 0.1\%$ for both $\delta^{13}\text{C}$ and $\delta^{18}\text{O}$.

Table 1.

Descriptions of the carbonatite samples studied and their carbon and oxygen isotopic compositions.

Sample	Rock type	Calcite		Dolomite	
		¹⁸ O (‰)	¹³ C (‰)	¹⁸ O (‰)	¹³ C (‰)
Maimecha-Kotui province.					
Guli (240Ma, Kogarko et al., 1988) The age 230Ma is used for the calculation of Sr/I and Nd/I.					
G1	Phl-Cal-carbonatite(1st stage)	6.3	-5.3		
G2	Ol-Dol-Cal-carbona-tite (2nd stage)	7.2	-4.4	7.3	-4.0
G3	Dol-carbonatite (3-4th stage)			6.4	-3.8
802/2	Dol-carbonatite			9.0	-2.9
803/2	Cal-carbonatite	8.1	-4.2		
823/2	Dol-Cal carbonatite	11.6	-3.3	10.2	-3.2
Essei (not dated) Age used for calculation: 230Ma.					
2000/8f	Dol-Cal-carbonatite	9.0	-3.9	9.4	-3.2
2014/14	Dol-Cal-carbonatite	8.0	-3.9	8.0	-3.3
2028/1	Cal-carbonatite	8.7	-4.6		
Enisei province					
Kiiskii (251Ma, Plyushin et al., 1990) Age used for calculation: 250Ma.					
K240	Cal-carbonatite	4.7	-3.5		
Srednetatarskii (660-675Ma, Sveshnikova, et al., 1976) Age used for calculation: 640Ma.					
162/35	Trem-Dol-carbona-tite			8.2	-5.0
1704/27	Sodic amph-Dol-carbonatite			7.4	-5.2
2371/10	Ol-Dol-Cal-carbona-tite	15.5	-4.1	15.3	-3.8
East Sayan province					
Bolshetagninskii (628Ma, Chernysheva, et al.,1992) Age used for calculation: 600Ma.					
BT1	altered carbonatite	12.0	-2.6		
BT2	altered carbonatite	12.4	-3.1		
BT3-4	carbonate-microcline rock	13.9	-3.9		
BT5	Hematitic carbona-tite (last stage)	13.2	-3.7		
TC8/11	Cal-carbonatite	12.5	-2.9		
Nizhnesayanskii (675-720Ma, Kononova, 1976, Chernysheva et al., 1992) Used age: 600Ma.					
HC1a	Cal-carbonatite(1st stage)	7.4	-5.9		
HC1b	Ol-Cal-carbonatite(1st stage)	6.6	-5.8		
HC1c	Phl-Cal-carbonatite(1st stage)	6.7	-5.5		
HC2a	Ol-Ap-Cal-carbonatite(2nd stage)	6.6	-6.0		
HC2b	Aeg-Cal-carbonatite(2nd stage)	6.9	-5.9		
HC6white	Ank-Cal-carbonatite(4th stage)	6.6	-5.7	6.1	-5.0
HC6gray	Ank-Cal-carbonatite(4th stage)	7.3	-4.9	6.3	-4.8
HC7	Cal-Ank-carbonatite w.cavities	10.7	-4.1	9.8	-4.0
Verhnesayanskii (660, 725Ma, Kononova, 1976) Age used for calculation: 600Ma.					
C1/1	Bio-Cal-carbonatite	6.8	-5.5		

End of Table 1.

Sample	Rock type	Calcite		Dolomite	
		¹⁸ O (‰)	¹³ C (‰)	¹⁸ O (‰)	¹³ C (‰)
CC86/7	Bio-Cal-carbonatite	7.6	-5.7		
CC113/3	Cal-carbonatite	6.9	-5.5		
Zhidoy (680Ma, Kononova, 1976). Age used for calculation: 600Ma.					
Zhd316/3	Cal-carbonatite	7.5	-5.2		
Zhd327	Cal-carbonatite	7.1	-5.5		
Baikal province					
Burpalinskii (325-327Ma, Arkhangelskaya, 1974) . Age used for calculation: 300Ma.					
Bur311/2 1	Qtz-Cal-carbonatite	12.8	-1.8		
Aldan alkali province					
Malomurunskii (130-138Ma, Orlova, 1990, Bogatikov et al., 1991) Used age: 145Ma.					
Mur143	Cal-carbonatite	7.9	-8.1		
Mur157	Benst-carbonatite	8.3	-6.5		
Mur136/5 2	Cal-Benst-carbonatite	9.4	-7.5		
Mur173	Cal-Charo-carbonatite	9.4	-7.7		
Mur137/5	Qtz-Cal-carbonatite	9.7	-7.9		
Mur1052/ 20	Cal-carbonatite	9.8	-5.2		
Mur186	Cal-carbonatite	10.4	-6.6	9.7	-6.2
Khani (1818-1870Ma, Bogatikov et al., 1991) Age used for calculation: 1835Ma.					
Khn205	Aeg-Cal-carbonatite	8.6	-8.0		
Khn206	Aeg-Cal-carbonatite	8.5	-8.4		
Seligidar (1844-2038Ma, Smirnov et al., 1975). Age used for calculation: 1950Ma					
Aslg50	Qtz-Ap-Dol-rock			22.5	2.5
Arbarastakh (690-720Ma, Glagolev and Korchagin, 1974) Age used for calculation: 675Ma.					
Arb273	Dol-Cal-carbonatite	7.6	-5.0	7.9	-4.6
Arb275	Phl-Cal-carbonatite	9.3	-5.3		
Ingili (648-704Ma, Orlova et al., 1986) Age used for calculation: 665Ma.					
Ing314	Bio-Cal-carbonatite	8.1	-6.6		
Ing309	Bio-Cal-carbonatite	8.0	-6.5		
Ing42/50	Fluo-Cal-carbonatite(later stage)	13.0	-5.9	13.9	-5.4
Sette-Daban Range/					
Ozernyi (280-350Ma, El'yanov and Moralev, 1961) Age used for calculation: 360Ma.					
Go1	Phl-Cal-Dol-carbonatite	8.5	-4.7	8.3	-4.4
Go2	Dol-carbonatite			17.8	-2.5
Primorye region					
Koksharovskii (135-145Ma, Rub and Levitsky, 1962) Age used for calculation: 165Ma.					
Ksh22	Cal carbonatite	11.2	-4.2		

Note. Abbreviation for minerals: Cal:calcite; Dol:dolomite; Ank:ankerite; Ol:olivine; Bio:biotite; Phl:phlogopite; Aeg:aegirine; Ap:apatite; Fluo:fluorite; Qtz:quartz; Trem:tremolite; Sodic amph:sodic amphibole; Charo:charoite; Benst:benstonite.

Concentrations of rare-earth elements of the carbonatites were determined by the instrumental neutron activation analysis at the Research Reactor Institute of

Kyoto University following the procedure described by Koyama and Matsushita (1980).

RESULTS

The results of carbon and oxygen isotopic analysis is presented in Table 1, and those of Sr and Nd analysis in Table 3. Rare-earth element analyses are given in Table 2.

Maimecha-Kotui province

Guli(Gulinskii) body.

Initial Sr and Nd isotopic compositions of the carbonatites from the Guli body are plotted in the upper left (depleted) quadrant in the ϵ Nd versus ϵ Sr diagram (Fig.5). With the exception of sample 823/2, carbon and oxygen isotopic ratios of the rocks fall within or near the inferred mantle CO₂ field (Fig.3). Chondrite-

Table 2.

Rare earth element analyses of the carbonatites from Siberia.

Complex	Sample	La (ppm)	Ce (ppm)	Nd* (ppm)	Sm* (ppm)	Eu (ppm)	Tb (ppm)	Yb (ppm)	Lu (ppm)
Maimecha-Kotui province									
Guli	G1	95.9	99.7	32.3	5.57	1.82	0.80	1.41	-
Essei	2014/14	63.9	105.0	48.9	7.68	2.08	0.97	0.99	-
Enisei province									
Kiiskii	K240	55.7	131.0	66.1	11.6	3.00	3.02	-	2.58
Srednetatarskii	1704/27	32.6	72.2	32.4	5.00	1.22	0.32	-	-
East Sayan province									
Bolshetagninskii	BT1	61.3	79.4	19.9	2.21	0.64	-	-	-
	BT5	97.9	118.0	41.2	6.36	1.95	0.92	0.89	0.14
Nizhnesayanskii	HC2a	296.0	803.0	320	49.2	12.0	8.85	4.46	0.82
Zhidoy	Zhd327	419	804	348	46.6	10.6	3.85	6.05	0.99
Baikal province									
Burpalinski	Bur311/2 1	17.6	32.2	14.6	4.10	3.59	0.93	2.62	0.34
Aldan alkali province									
Malomuruskii	Mur143	224	377.0	117	15.0	3.20	-	-	0.56
	Mur186	59.6	83.2	22.2	2.33	0.54	0.18	0.51	
Khani	Kh206	1190	2320	1060	146	30.1	12.2	2.47	0.97
Seligdar	Aslg50	470	-	403	49.7	9.21	-	-	0.35
Arbarastakh	Arb273	201	-	453	66.7	11.5	-	-	-
Ingili	Ing314	551	1190	522	74.2	17.9	6.67	5.67	0.95
Sette-Daban Range									
Ozernyi	Go1	192	360	150	19.4	4.51	1.46	0	0.34
Primorye region									
Koksharovskii	Ksh22	361	609	228	34.4	9.17	4.11	5.75	1.13

Note. (-)not detected. * Isotope dilution analysis.

Sr and Nd isotopic results for the carbonatites from Siberia.

Table 3.

Sample	Sm	Nd	$^{147}\text{Sm}/^{144}\text{Nd}$	$^{143}\text{Nd}/^{144}\text{Nd}$	$^{143}\text{Nd}/^{144}\text{Nd}$	Rb	Sr	$^{87}\text{Rb}/^{86}\text{Sr}$	$^{87}\text{Sr}/^{86}\text{Sr}$	$^{87}\text{Sr}/^{86}\text{Sr}$	Nd	Sr
	(ppm)	(ppm)	(atomic)	(measured)	(initial)	(ppm)	(ppm)	(atomic)	(measured)	(initial)		
Guli (230Ma)												
G1	5.57	32.3	0.1042	0.51274	0.51258	14.3	7370	0.0056	0.70309	0.70307	4.7	-16.4
G2	34.3	234	0.0889	0.51274	0.51261	0.62	4370	0.0004	0.70321	0.70321	5.2	-14.5
G3-4	12.0	80.8	0.0895	0.51273	0.51260	1.24	3720	0.0010	0.70316	0.70315	5.1	-15.2
Essei (230Ma)												
2000/8f	8.69	45.5	0.1155	0.51269	0.51252	2.80	2890	0.0028	0.70344	0.70343	3.5	-11.3
2014/14	7.68	48.9	0.0950	0.51272	0.51258	1.18	4190	0.0008	0.70334	0.70333	4.7	-12.7
Kiiskii (250Ma)												
K240	11.6	66.1	0.1062	0.51265	0.51248	10.6	928	0.0331	0.70400	0.70388	3.2	-4.5
Srednetatarskii (640Ma)												
162/35	93.5	552	0.1024	0.51250	0.51208	45.2	7220	0.0181	0.70268	0.70252	5.1	-17.4
1704/27	5.00	32.4	0.0943	0.51250	0.51211	1.38	6690	0.0006	0.70233	0.70233	5.7	-20.2
Bolshetagninskii (600Ma)												
BT1	2.21	19.9	0.0672	0.51230	0.51203	0.90	645	0.0040	0.70438	0.70434	3.3	7.8
BT34	2.31	25.6	0.0545	0.51227	0.51205	83.9	1550	0.1566	0.70439	0.70305	3.7	-10.6
BT5	6.36	41.2	0.0932	0.51237	0.51200	0.59	429	0.0040	0.70662	0.70658	2.7	39.7
Nizhnesayanskii (600Ma)												
HC1b	39.5	240	0.0995	0.51246	0.51207	22.0	4040	0.0157	0.70318	0.70305	4.0	-10.6
HC1c	16.4	130	0.0764	0.51235	0.51205	62.0	5800	0.0309	0.70321	0.70294	3.6	-12.1
HC2a	49.2	320	0.0930	0.51239	0.51203	1.46	6850	0.0006	0.70304	0.70304	3.2	-10.7
HC6w	37.5	307	0.0739	0.51230	0.51201	0.65	8690	0.0002	0.70308	0.70307	2.9	-10.2
HC6g	43.4	510	0.0515	0.51226	0.51205	0.45	11300	0.0001	0.70303	0.70303	3.7	-10.9
Verhnesayanskii (600Ma)												
C1/1	26.0	158	0.0994	0.51249	0.51209	8.28	6940	0.0035	0.70295	0.70292	4.5	-12.4
CC86/7	19.4	118	0.1001	0.51250	0.51211	152	1580	0.2783	0.70547	0.70309	4.7	-10.0
CC113/3	22.7	139	0.0985	0.51247	0.51209	13.9	5400	0.0074	0.70303	0.70297	4.3	-11.7
Zhidoy (600Ma)												
Zd316/3	57.4	393	0.0883	0.51241	0.51206	0.48	13600	0.0001	0.70300	0.70300	3.8	-11.2
Zhd327	46.6	348	0.0810	0.51233	0.51201	2.65	7770	0.0010	0.70318	0.70317	2.8	-8.8
Burpalinskii (300Ma)												
Br311/21	4.10	14.6	0.1694	0.51226	0.51193	1.37	3230	0.0012	0.70851	0.70851	-6.3	61.9
Malomurunskii (145Ma)												
Mur143	15.0	117	0.0777	0.51133	0.51125	15.7	41400	0.0011	0.70694	0.70694	-23.4	37.0
Mr36/52	25.2	199	0.0764	0.51141	0.51134	152	27200	0.0162	0.70711	0.70708	-21.8	39.0
Mur173	9.39	69.5	0.0817	0.51136	0.51128	55.5	23400	0.0069	0.70724	0.70722	-22.9	41.1
Mr137/5	2.84	18.3	0.0937	0.51139	0.51130	15.7	4730	0.0096	0.70680	0.70678	-22.5	34.8
Mr1052/2	4.62	46.2	0.0606	0.51165	0.51159	25.5	29600	0.0025	0.70681	0.70681	-16.8	35.2
Mur186	2.33	22.2	0.0635	0.51129	0.51123	50.1	8060	0.018	0.70731	0.70727	-23.9	41.7
Khani (1835Ma)												
Khn205	74.0	539	0.0831	0.51047	0.50946	126	4370	0.0837	0.70671	0.70450	-15.7	31.1
Khn206	146	1060	0.0834	0.51042	0.50942	16.1	4790	0.0097	0.70531	0.70506	-16.6	39.0
Seligdar (1950Ma)												
Aslg50	49.7	403	0.0745	0.51080	0.50985	1.69	149	0.0328	0.70756	0.70664	-5.3	63.6
Arbarastakh (675Ma)												
Arb273	66.7	453	0.0890	0.51252	0.51213	1.65	7980	0.0006	0.70250	0.70249	7.0	-17.2
Arb275	39.8	279	0.0860	0.51251	0.51212	28.5	3480	0.0237	0.70282	0.70260	7.0	-15.7
Ingili (665Ma)												
Ing314	74.2	522	0.0860	0.51250	0.51213	48.2	12200	0.0114	0.70257	0.70246	6.8	-17.8
Ing309	58.0	393	0.0893	0.51251	0.51212	44.1	6600	0.0193	0.70257	0.70239	6.7	-18.9
Ozernyi (360Ma)												
Go1	19.4	150	0.0778	0.51264	0.51246	34.2	3690	0.0268	0.70312	0.70298	5.5	-15.6

End of Table 3.

Sample	Sm	Nd	¹⁴⁷ Sm/ ¹⁴⁴ Nd	¹⁴³ Nd/ ¹⁴⁴ Nd	¹⁴³ Nd/ ¹⁴⁴ Nd	Rb	Sr	⁸⁷ Rb/ ⁸⁶ Sr	⁸⁷ Sr/ ⁸⁶ Sr	⁸⁷ Sr/ ⁸⁶ Sr	Nd	Sr
	(ppm)	(ppm)	(atomic)	(measured)	(initial)	(ppm)	(ppm)	(atomic)	(measured)	(initial)		
Go2	1250	16800	0.0450	0.51253	0.51242	0.56	1530	0.0011	0.70376	0.70376	4.8	-4.5
Koksharovskii (165Ma)												
Ksh22	34.4	228	0.0912	0.51281	0.51271	1.83	10300	0.0005	0.70363	0.70363	5.6	-9.6

normalized rare-earth element pattern for the Guli carbonatite is similar to that of common carbonatites from the world [for example, Nelson et al., 1988] (Fig.1). Calcite and dolomite in sample 823/2 show slightly higher $\delta^{18}\text{O}$ value than that of the mantle CO_2 . The sample contains numerous drusy cavities, which indicates the crystallization of the carbonate minerals at later stage

Essei body.

The Essei carbonatite has chemical and isotopic features generally similar to those of the Guli carbonatite (Figs. 1, 3, 5). However, the carbon and oxygen isotopic variation is smaller than that of the Guli carbonatite.

Enisei province

Kiiskii body.

The initial Sr and Nd isotopic compositions of the Kiiskii carbonatite fall in the slightly depleted field in the ϵNd versus ϵSr diagram. The $\delta^{18}\text{O}$ value for the calcite in the sample is 4.7‰, which is unusually low for carbonatites (Fig. 3, solid square). The chondrite-normalized REE pattern for the sample is also unusual (Fig.1, solid square). Kogarko et al. (1995) has described that all the rocks from the Kiiskii body were intensively altered.

Srednetatarskii (Tatarsk) body. Two samples (162/35, 1704/27) out of three have carbon and oxygen isotopic compositions similar to those of the mantle CO_2 (Fig. 3, open circle). Their initial Sr and Nd isotopic ratios are plotted in the depleted quadrant in the ϵNd versus ϵSr diagram (Fig. 5, open circle)). Another sample (237/10) show remarkable enrichment in ^{18}O in both calcite and dolomite. The C and O isotopic data are plotted in the intermediate position between the mantle CO_2 and marine limestone field (Fig. 3, open circle). Sr and Nd isotopic compositions for the sample, however, were not obtained.

East Sayan province

Bolshetagninskii (Tagna) body.

Five samples from the Bolshetagninskii body were isotopically analyzed. Most samples underwent intensive alteration and secondary minerals such as

hematite occur in the rocks. Carbon and oxygen isotopic ratios of the rocks deviate significantly from the range of mantle CO₂. They are plotted just intermediate position between the mantle CO₂ and marine limestone fields (Fig. 3, solid circle). εSr value for the rocks vary widely; it ranges from -10.6 to +39.7 (Fig.5, solid circle). Sample BT3-4 has Sr concentration of 1550ppm and it has the lowest εSr value of -10.6. Sample BT5, which is the latest carbonate vein in hematitic carbonatite, has the highest εSr value (+39.7) and the lowest Sr contents (429ppm). Sample BT1 has intermediate value both in εSr and Sr contents. Thus we can conclude that, for the carbonatites from the Bolshetagninskii body, εSr value increased with the decrease in whole-rock Sr contents.

Nizhnesayanskii (Belozima) body.

Except for one sample (HC-7), carbon and oxygen isotopic compositions of the carbonatites from the Nizhnesayanskii body are plotted within the mantle CO₂ field (Fig. 3, plus). The initial εSr and εNd values for the rocks are plotted in the depleted quadrant in the εNd versus εSr diagram (Fig.5, plus). The δ¹⁸O value of sample HC-7 is higher than any other sample from the body. HC-7 contains drusy cavities, which were produced by leaching. Thus, water-rock interaction must have occurred after the crystallization of the rock.

Verhnesayanskii (Sredneziminskii) body.

Three carbonatite samples from the Verhnesayanskii body were isotopically analyzed. Rare-earth element analysis was not made for the rocks. Carbon and

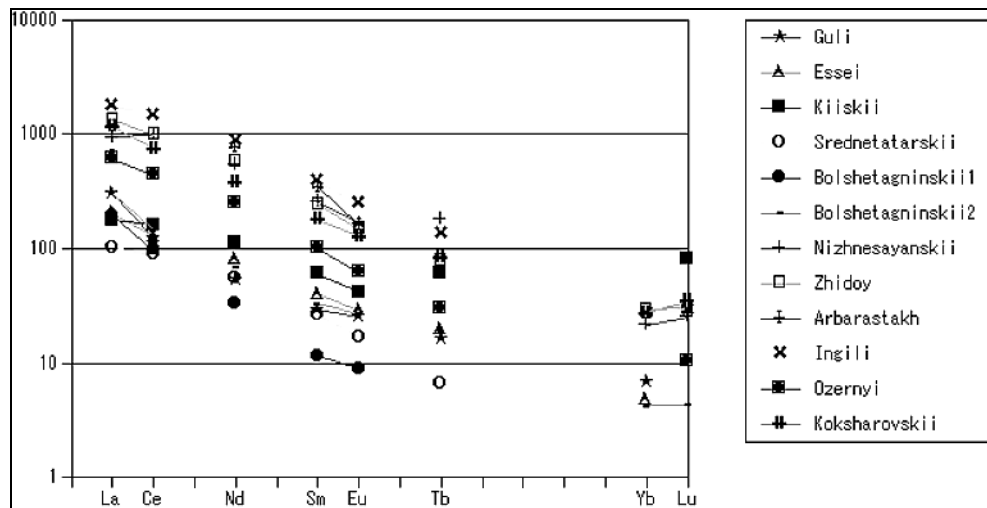


Fig. 1. Chondrite-normalized rare-earth patterns for the Group 1 carbonatites.
 (Footnote) Chondrite values are those of Taylor and Gorton (1977).

oxygen isotopic compositions for the samples are plotted within mantle CO₂ field (Fig.3, open plus). Initial Sr and Nd isotopic ratios for the rocks are plotted in the depleted quadrant in the εNd versus εSr diagram (Fig.5, open plus). These carbonatite samples show little variations in Sr, Nd, C and O isotopic compositions.

Zhidoy body.

Zhidoi carbonatite has the same isotopic features as the Verhnesayanskii carbonatite. Further isotopic data for the body have been presented in Morikiyo et al. (2000), where they have interpreted the large variation in Sr concentrations and εSr values seen in the Zhidoi carbonatites as being due to the results of carbonatite-carbonatite mixing.

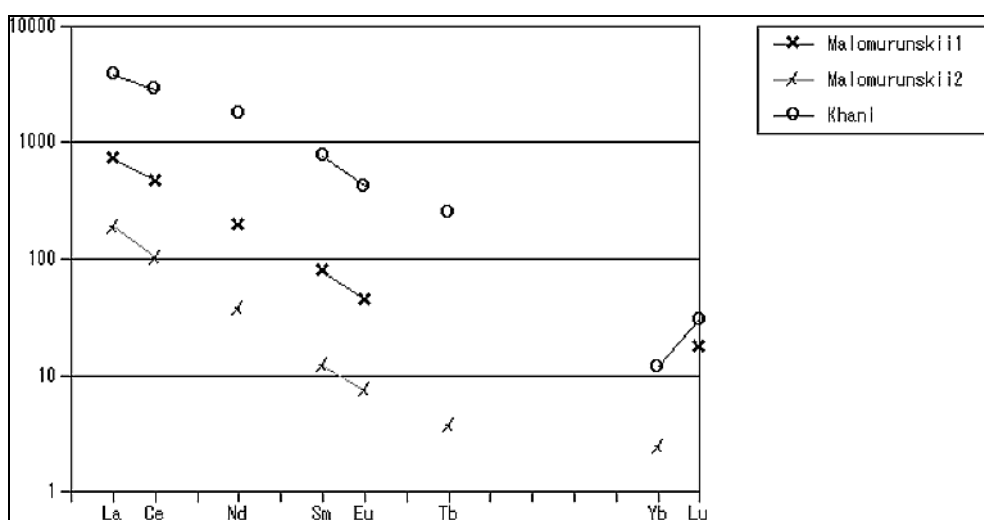


Fig. 2. Chondrite-normalized rare-earth patterns for the Group 2 carbonatites. (Footnote) Chondrite values are those of Taylor and Gorton (1977).

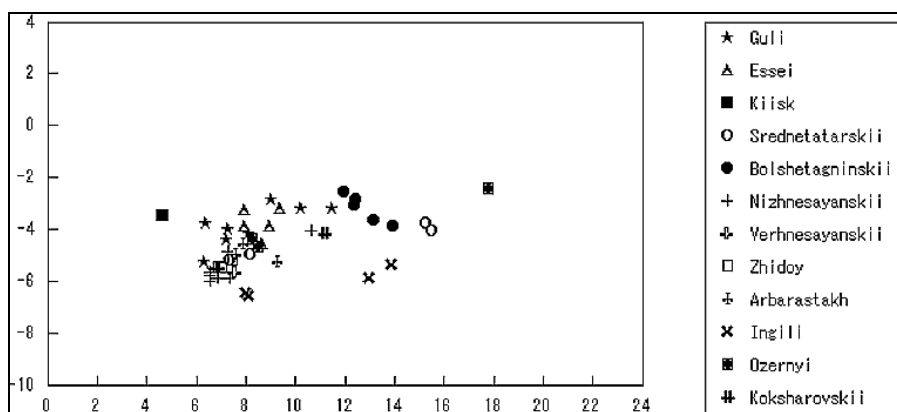


Fig. 3. Carbon and oxygen isotopic compositions for the Group 1 carbonatites. (Footnote) Abscissa: δ¹⁸O values (‰) relative to SMOW. Ordinate: δ¹³C values (‰) relative to PDB.

Baikal province

Burpalinskii (Burpala) body.

The carbonate rock from the Burpalinskii body has an ϵSr and ϵNd value of +61.9 and -6.3, respectively. The data fall in the lower right (enriched) quadrant of the ϵNd versus ϵSr diagram. But the data for the rock is not shown in the figures, because, as described later, there is a doubt about its origin. Carbon and oxygen isotopic ratios ($\delta^{13}\text{C} = -1.8\text{‰}$, $\delta^{18}\text{O} = 12.8\text{‰}$) plot in the intermediate position between the mantle CO_2 and marine limestone fields (also not shown either in Fig.3 or Fig.4). REE concentrations of the sample are remarkably low as compared with common carbonatites. The chondrite-normalized REE pattern for the sample is almost flat and it shows positive Eu anomaly.

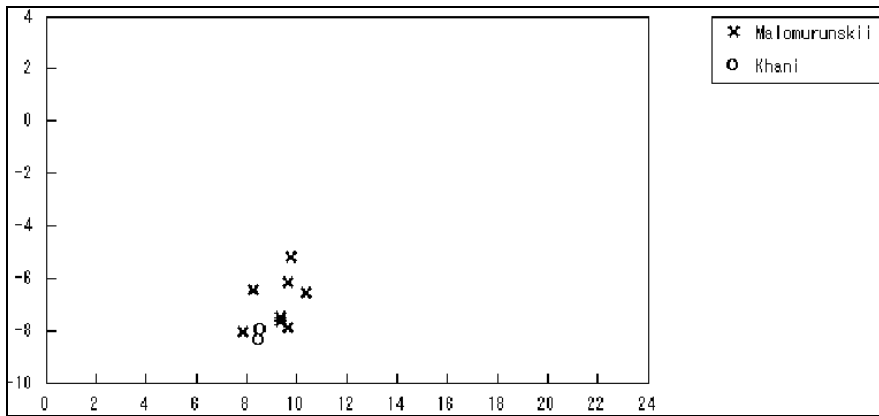


Fig. 4. Carbon and oxygen isotopic compositions for the Group 2 carbonatites.
(Footnote) Abscissa: $\delta^{18}\text{O}$ values (‰) relative to SMOW. Ordinate: $\delta^{13}\text{C}$ values (‰) relative to PDB. Inferred mantle CO_2 field was taken from Nelson et al. (1988).

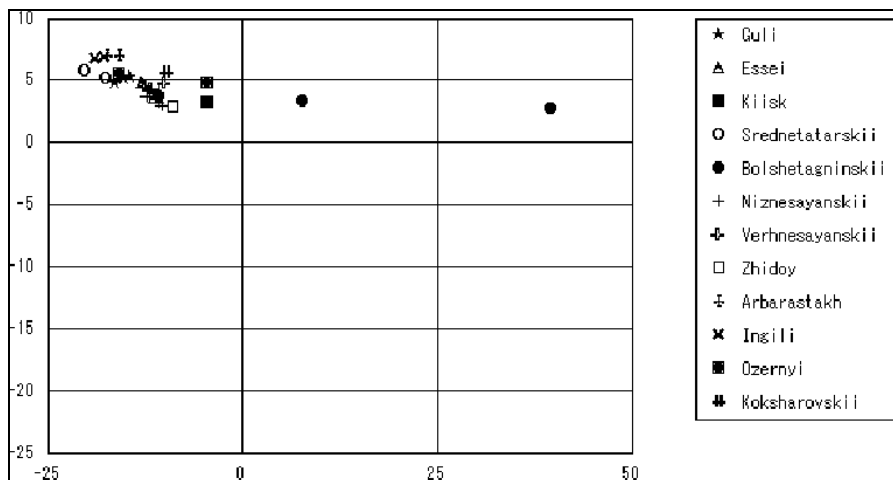


Fig. 5. Initial ϵNd versus ϵSr for the Group 1 carbonatites.
(Footnote) Abscissa: Initial $\epsilon\text{Sr}(t)$ values. Ordinate: Initial $\epsilon\text{Nd}(t)$ values.

Aldan alkali province

Malomurunskii (Murun) body.

The carbonatite samples from the Malomurunskii body are distinct, because they have negative, very low ϵNd values and positive, high ϵSr values (Fig. 6, heavy cross). The Sr and Nd isotopically enriched feature of the Malomurunskii carbonatites has already been reported by Mitchell et al. (1994). Carbon and oxygen isotopic ratios for the carbonatites (Fig. 4, heavy cross) are close to the range of mantle CO_2 , but the data points of the both Malomurunskii (heavy cross) and Khani (open circle) bodies are plotted at different position from those of other carbonatites from Siberia. It is noteworthy that the Malomurunskii and Khani carbonatites have lowest $\delta^{13}\text{C}$ values among the carbonatites from Siberia. Chondrite-normalized REE patterns of the carbonatites are not different from those of common carbonatites from the world (Fig. 2).

Khani body.

The Khani carbonatite has quite similar isotopic features to the Malomurunskii carbonatite in both radiogenic (Sr and Nd, Fig. 6) and stable (carbon and oxygen, Fig. 4) isotopes. However, the emplacement age of the two bodies is completely different. The age of the Khani body is 1818-1870Ma [Bogatikov et al., 1991], while that of the Malomurunskii body is 130-138Ma [Orlova, 1990; Bogatikov et al., 1991].

Seligdar.

The carbon and oxygen isotopic ratios ratios ($\delta^{13}\text{C}=2.5\text{‰}$, $\delta^{18}\text{O}=22.5\text{‰}$) for the sample from the Seligdar apatite ore field fall in the marine limestone field in the $\delta^{18}\text{O}$ versus $\delta^{13}\text{C}$ diagram. But the data are not shown in the figures of this paper. The dolomite, quartz and apatite grains in the sample carry many two phase

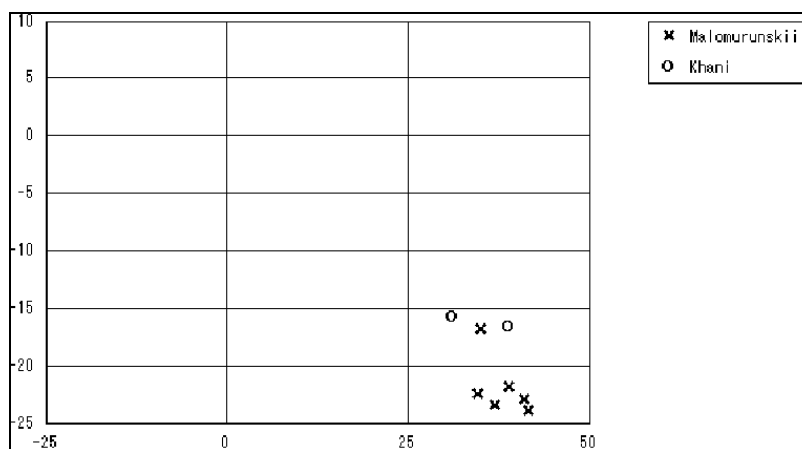


Fig. 6. Initial ϵNd versus ϵSr for the Group 2 carbonatites.

(Footnote) Absissa: Initial $\epsilon\text{Sr}(t)$ values. Ordinate: Initial $\epsilon\text{Nd}(t)$ values.

(vapor+liquid), aqueous fluid inclusions. Thus, it is conceivable that these minerals were precipitated from a hydrothermal solution. Although the REE concentrations as well as chondrite-normalized REE pattern of the sample are compatible with those of common carbonatites, we regard the rock as not carbonatite.

Arbarastakh body.

Carbon and oxygen isotopic compositions for the samples from the Arbarastakh body fall in the range of mantle CO₂ (Fig. 3, plus-like symbol). Initial Sr and Nd isotopic ratios are plotted in the depleted quadrant in the εNd versus εSr diagram (Fig. 5, plus-like symbol). The Arbarastakh carbonatites possess the highest εNd values (+7.0) among all the carbonatites from Siberia. The concentrations of light REE for sample Arb273 are similar to those of common carbonatites, but those of heavy REE were not obtained.

Ingili body.

Two samples (Ing309, 314) have Sr, Nd, C and O isotopic features similar to those of the Arbarastakh carbonatite (Figs. 3, 5, cross). Another sample, Ing42/50, shows remarkable enrichment in ¹⁸O in both calcite (δ¹⁸O=13.0‰) and dolomite (δ¹⁸O=13.9‰). The sample contains fluorite, which is indicative of later-stage crystallization.

Sette-Daban Range

Ozernyi (Gornoozerskii) body.

Two samples from the Ozernyi body were isotopically analyzed. One (sample Go1) has carbon and oxygen isotopic compositions close to those of mantle CO₂, and has positive εNd and negative εSr values (Figs. 3, 5, square with solid circle). Another sample (Go2) has much higher isotopic ratios in both carbon and oxygen. It is noteworthy that sample Go2 has also higher εSr value than sample Go1. Thus we may generalize that εSr value of the carbonatite increased with δ¹⁸O. Although the rise in εSr value from samples Go1 to Go2 is seen, the isotopic data of Go2 are still plotted in the depleted quadrant in the εNd versus εSr diagram (Fig. 5, square with solid circle).

Primorye region

Koksharovskii body.

The sample Ksh22 has relatively high δ¹⁸O (11.2‰, Fig. 3, sharp). But the initial Sr and Nd isotopic ratios fall in the slightly depleted field in the εNd versus εSr diagram (Fig. 5, sharp). Another carbonatite sample from the body, which is not

described in this paper, contains an yellowish-colored carbonate vein of probably hydrothermal origin. The $\delta^{18}\text{O}$ value for the vein is 20.1‰, which value is distinctly high for carbonatites [Morikiyo, in preparation]. It has been reported that the rocks in the body underwent various degrees of metasomatic alterations [Zalishchak, 1969].

DISCUSSION

1. Classification of the Siberian carbonatites according to isotopic features.

On the basis of Sr, Nd, C and O isotopic features of carbonatite samples, Siberian carbonatites are classified into four groups, 1a, 1b, 1c, and 2. As will be discussed below, we conclude that the differences between 1a, 1b, and 1c were caused by the secondary process and that group-1a, -1b, -1c carbonatites were derived from Sr and Nd isotopically similar mantle source. Thus, group-1a, -1b, -1c carbonatites are put together and are designated as Group 1 carbonatites.

A Carbonatites derived from slightly depleted mantle source (Group 1 carbonatites).

Group 1a carbonatites: Many carbonatites from Siberia have carbon and oxygen isotopic compositions similar to those of mantle CO_2 and have initial Sr and Nd isotopic ratios correspondent to those of the slightly depleted mantle. The carbonatite bodies showing the above isotopic features typically are the Essei, Nizhnesayanskii, Verhnesayanskii, Zhidoy, and Arbarastakh bodies. These carbonatite bodies are designated as Group 1a carbonatites. The Guli and Kiisk bodies may be included in this Group, although their carbon and oxygen isotopic ratios are slightly different from those of mantle CO_2 .

Since their carbon and oxygen isotopic ratios fall within or near the mantle CO_2 field, we can consider that the carbonatites did not undergo crustal contamination during their emplacement. Thus their initial Sr and Nd isotopic ratios must represent the geochemical nature of the source for the rocks. The source material for the Group 1a carbonatites is the slightly depleted mantle, which is similar to that for some ocean-island basalts.

Group 1b carbonatites: Three samples from the Ingili body are plotted at two different positions separately in the $\delta^{18}\text{O}$ versus $\delta^{13}\text{C}$ diagram. Two samples are plotted within the mantle CO_2 field, whereas another one is obviously outside the field. The latter has higher $\delta^{18}\text{O}$ value than the mantle CO_2 . The initial Sr and Nd isotopic ratios of the former samples fall in the same range as Group 1a carbonatites (i.e., slightly depleted mantle source field). The carbonatite bodies showing the similar isotopic features to the Ingili body are Srednetatarskii body and probably, Koksharovskii body. These bodies are designated as Group 1b carbonatites. The Ingili carbonatite having higher $\delta^{18}\text{O}$ value (Ing42/50) carries

fluorite. The carbonatite from the Koksharovskii body showing higher $\delta^{18}\text{O}$ value has yellowish secondary carbonate vein of hydrothermal origin [Morikiyo, in preparation]. Concerning to the Srednetatarskii body, the occurrence of widespread hydrothermal alteration has been described [Kogarko et al., 1995]. These facts make us to consider that the increase in $\delta^{18}\text{O}$ is due to the results of the crystallization of carbonatitic magma to hydrothermal stage, and that the primary Sr and Nd isotopic features for the bodies are similar to those of Group 1a carbonatites. Morikiyo et al. (1990) described the extreme ^{18}O enrichment in the Catalao I carbonatite in Brazil and concluded that the carbonates with extremely high $\delta^{18}\text{O}$ values were precipitated from low-temperature hydrothermal fluids.

Group 1c carbonatites: In the case of Ozernyi body, one of the two samples (Go2) has carbon and oxygen isotopic ratios close to those of marine limestone. Its ϵSr value is higher than that of the sample Go1 by 10. In the case of the Bolshetagninskii body, the variation of ϵSr value is very large, ranging from -10.6 to 39.7. The ϵSr value increases with the decrease of whole-rock Sr contents, as described before. The carbon and oxygen isotopic ratios for the rocks fall in the intermediate position between mantle CO_2 and marine limestone fields. The high ϵSr and high $\delta^{18}\text{O}$ values found in these bodies are interpreted as being due to the results of crustal contamination in carbonatitic magma. However, the detailed process of the contamination is not well understood.

Although the isotopic compositions of the Ozernyi and Bolshetagninskii bodies have been modified as the results of crustal contamination, we can still estimate the primary Sr and Nd isotopic signatures for the carbonatites from the variation trend of ϵSr and ϵNd values. It is concluded that the primary carbonatite magma for the Ozernyi and Bolshetagninskii bodies had Sr and Nd isotopic characters similar to those of the Group 1a carbonatites .

B. Carbonatites derived from the enriched mantle source (Group 2 carbonatites).

The carbonatites from the Malomurunskii and Khani bodies have negative, very low ϵNd and positive, high ϵSr values. The carbon and oxygen isotopic ratios for the rocks are almost similar to those of the mantle CO_2 . Since Sr and Nd concentrations of the carbonatites are remarkably high, it is not possible to ascribe these enriched isotopic features to the results of crustal contamination. Therefore, it is concluded that the Malomurunskii and the Khani carbonatite bodies were derived from the enriched mantle source. The same conclusion has already been described for the Malomurunskii body by Mitchell et al. (1994).

The carbonate rock from the Burpalinskii body also shows positive, high ϵSr value. However, the Sr and Nd isotopic ratios plot in the different position from

those of the Malomurunskii and the Khani bodies in the ϵNd versus ϵSr diagram. Furthermore, REE contents of the sample are low for carbonatites and the chondrite-normalized REE pattern is unusual. Since the number of sample studied is only one for the Burpalinskii body, it is not clear whether or not the chemical and isotopic features obtained in this study is intrinsic to the body. There is a possibility that the studied sample is not carbonatite.

2. The site of generation of the parental melts to carbonatite. Lithosphere versus asthenosphere.

As described above, most of the Siberian carbonatites (Group 1 carbonatites) were derived from the slightly depleted mantle. But it was found that the Malomurunskii and Khani bodies (Group 2 carbonatites) were derived from the enriched mantle source. Although both of them occur in the Western Aldan subprovince, their ages are completely different. The emplacement age is 130-138 Ma for Malomurunskii and 1818-1870 Ma for Khani bodies, respectively. If the above ages are true, then this leads to the conclusion that isotopically similar magmatism occurred at the particular area at different age. This fact does not support the view that carbonatite magma originated from a mantle plume from the asthenosphere. Instead, the fact favors the view that carbonatite magma was generated at the subcontinental lithospheric mantle. It is presumed that the unusual enriched mantle is quite locally distributed in the western Aldan subprovince, and that the site of generation of parental carbonatitic magma is subcontinental lithospheric mantle. In order to confirm this interpretation, it is necessary to re-determine the age of the Khani body and to obtain Sr and Nd isotopic data for the other alkaline bodies occurring in the Western Aldan subprovince, such as Molbo, Bolshemurunskii, Dogaldynskii, and Yuzhnosakunskii bodies.

CONCLUSION

1. The geochemical nature of the source materials for the Siberian carbonatites are, mostly the slightly depleted mantle similar to the source of some ocean-island basalts.
2. The unusual enriched mantle is locally distributed in the Western Aldan subprovince.
3. The site of carbonatite generation is considered to be subcontinental lithospheric mantle region.

The investigations were supported by the RFBR (grants 00-05-65288, 01-05-67243 - Baikal).

ACKNOWLEDGEMENTS

One of the authors, Morikiyo, wishes to express his appreciation to Dr. A. P. Berzina of the Institute of Geology and Geophysics, Siberian Branch of the Academy of Sciences, Russia, for her considerable assistance. The authors would like to thank Prof. Y. Miyake and Prof. M. Musashino for their help in neutron activation analysis.

REFERENCES

1. **Arkhangelskaya, V.V.** (1974) Rare-metal alkaline complexes of the southern margin of the Siberian platform. Nedra, Moscow, 128pp.
2. **Bell, K. and Blenkinsop, J.** (1989) Neodymium and strontium isotope geochemistry of carbonatites. In: Carbonatites (Bell, K. Ed.). Unwin Hyman, London, 278-300.
3. **Bell, K., Kjarsgaard, B.A. and Simonetti, A.** (1998) Carbonatites-Into the twenty first century. *Jour. Petrol.*, vol. 39, 1839-1845.
4. **Bogatikov, O.A., Ryabchikov, I.D. and Kononova, V.A.** (1991) Lamproite. Nauka, Moscow, 320pp.
5. **Butakova, E.L.** (1979) Regional distribution and tectonic relations of the alkaline rocks of Siberia. In: The Alkaline rocks (Sorensen, H. Ed.). John Wiley and Sons, London, 172-189.
6. **Chernysheva, E.A., Sandimirova, G.P., Pahol'chenko, U.A. and Kuznetsova, S.V.** (1992) Rb-Sr age and some specific features of the genesis of the Bolshetagninskii carbonatite complex (East Sayan). *Doklady of the USSR Academy of Sciences. Earth Sci. Sec.*, vol.323, 942-947.
7. **DePaolo, D.J.** (1988) Neodymium isotope geochemistry: Springer-Verlag, New York, 187pp.
8. **El'yanov, A.A. and Moralev, V.M.** (1961) New data on the age of the ultramafic and alkaline rocks of the Aldan Shield. *Doklady Akademii Nauk SSSR*, vol.141, 687-689.
9. **Glagolev, A.A. and Korchagin, A.M.** (1974) Alkaline-ultrabasic massifs. Arbarastakh and Inagli. Nauka, Moscow, 176pp.
10. **Goldstein, S.L., O'Nions, R.K. and Hamilton, P.J.** (1984) A Sm-Nd study of atmospheric dusts and particulates from major river system. *Earth and Planetary Sci. Lett.*, vol.70, 221-236.
11. **Kogarko, L.N., Karpenko, S.F., Lyalikov, A.V. and Tepteleev, M.P.** (1988) Isotopic criteria for the origin of melteigite magmatism (Polar Siberia). *Doklady Akademii Nauk SSSR*, vol.301, 939-942.
12. **Kononova, V.A.** (1976) The jacupirangite-urtite series of alkaline rocks. Nauka, Moscow, 214pp.
13. **Koyama, M. and Matsushita, R.** (1980) Use of neutron spectrum sensitive motions for instrumental neutron activation analysis. *Bull.Inst.Chem.Res.*, Kyoto Univ., vol.58, 235-243.
14. **McCrea, J.M.** (1950) On the isotopic chemistry of carbonates and a paleotemperature scale. *Jour. Chem. Phys.*, vol.18, 849-857.

15. **Mitchell, R.H., Smith, C.B. and Vladykin, N.V.** (1994) Isotopic composition of strontium and neodymium in potassic rocks of the Little Murun complex, Aldan Shield, Siberia. *Lithos*, vol.32, 243-248.
16. **Miyazaki, T. and Shuto, K.** (1998) Sr and Nd isotope ratios of twelve GSJ rock reference samples. *Geochem. Jour.*, vol. 32, 345-350.
17. **Morikiyo, T., Hirano, H. and Matsuhisa, Y.** (1990) Carbon and oxygen isotopic composition of the carbonates from the Jacupiranga and Catalao I carbonatite complexes, Brazil. *Bull. Geol. Surv. Jpn*, vol.41, 619-626.
18. **Morikiyo, T., Miyazaki, T., Kagami, H., Vladykin, N.V.** (1998) Sr, Nd, C and O isotope characteristics of Siberian carbonatites. *Chinese Sci. Bull., Supp.*, p.90.
19. **Morikiyo, T., Takano, K., Miyazaki, T., Kagami, H., Vladykin, N.V.** (2000) Sr, Nd, C and O isotopic compositions of carbonatite and peralkaline silicate rocks from the Zhidoy complex, Russia: evidence for binary mixing, liquid immiscibility and a heterogeneous depleted mantle source region. *Jour.Mineral.Petrol.Sci.*, vol.95, 162-172.
20. **Nelson, D.R., Chivas, A.R., Chappell, B.W., McCulloch, M.T.** (1988) Geochemical and isotopic systematics in carbonatites and implications for the evolution of ocean-island sources. *Geochim. Cosmochim. Acta*, vol.52, 1-17.
21. **Orlova, M.P., Ardontsev, S.N. and Shchadenkov, E.M.** (1986) Alkaline magmatism of the Aldan Shield and its specific mineralogical features. In: *Geology and geochemistry of the ore-bearing magmatic and metasomatic associations from the Maly BAM area* (Frumkin, I.M. Ed.). Yakutia Branch of the Siberian Division of the USSR Academy of Sciences, Yakutsk, 4-12.
22. **Orlova, M.P.** (1990) Mesozoic stage of magmatism. In: *Potassic alkaline magmatism of the Baikal-Stanovoy rift system* (Polyakov G.V. and Kepezinskas, V.V. Eds.) Nauka, Siberian Division of the USSR Academy of Sciences, Novosibirsk, 65-123.
23. **Plyusnin, G.S., Kolyago, Ye.K., Pakhol'chenko, Yu.A., Almychkova, T.N. and Sandimirova, G.P.** (1990) Rubidium-strontium age and genesis of the Kiya alkalic pluton, Enisei Ridge. *Doklady Earth Sci. Sec., Amer. Geol. Inst.*, vol.305, 207-210.
24. **Rub, M.G. and Levitsky, V.V.** (1962) Petrological-geochemical features of the Koksharovka massif of ultrabasic-alkaline rocks with post magmatic products. *Alkaline rocks of Siberia*. Publishing House of the USSR Academy of Sciences, Moscow, 99-124.
25. Sharma, T. and Clayton, R.N. (1965) Measurement of O^{18}/O^{16} ratios of total oxygen of carbonates. *Geochim. Cosmochim. Acta*, vol.29, 1347-1353.
26. **Smirnov, F.L., Entin, A.R., Ugr'umov, A.N. and Burnaikin, A.I.** (1975) Precambrian apatite mineralization at the fault zones of the central part of the Aldan Shield. *Phosphorite of Yakutia*. Yakutsk, 53-74.
27. **Sveshnikova, E.V., Semenov, E.I. and Homykov, A.P.** (1976) The Transangarsky alkaline massif, its rocks and minerals. Nauka, Moscow. 80pp.
28. **Taylor, S.R. and Gorton, M.P.** (1977) Geochemical application of spark source mass spectrography-. Element sensitivity, precision and accuracy. *Geochim.Cosmochim.Acta*, vol.41, 1375-1380.
29. **Zalishchak, B.L.** (1969) Koksharovskiy massif of ultramafic and alkaline rocks (South Primorye). Nauka, Moscow, 116pp.

Lamproites: a review of magmatic inclusions in minerals

V.V. Sharygin

*Institute of Mineralogy and Petrography, SB RAS, Koptyuga Pr. 3, 630090 Novosibirsk, Russia.
sharygin@uiggm.nsc.ru*

In this paper diverse petrographic types of world lamproites are reviewed and discussed in context of magmatic inclusions in minerals. According to high- and low-temperature thermometry of fluid and silicate melt inclusions, olivine lamproites began to crystallize under $T \gg 1100^\circ\text{C}$ and $P=4-6$ kb with formation of olivine phenocrysts. In leucite and sanidine lamproites phenocrysts appeared at $T > 1200^\circ\text{C}$ and groundmass minerals – at $T=950-1100^\circ\text{C}$. Study of inclusion glasses in minerals has shown that there is a common compositional trend in olivine and leucite lamproites from different occurrences (W.Kimberley, Leucite Hills, etc.). Initial melt evolution during their crystallization had an agpaitic trend and was towards gradual depletion in Al_2O_3 , CaO , MgO , P_2O_5 and enrichment in SiO_2 , FeO_T , BaO , TiO_2 , ZrO_2 , alkalis. This resulted in the formation of K-rich Al-undersaturated or Al-free silicates and K-Ba-titanates on the late stages of rock crystallization. According to cryometric, microprobe and Raman studies, volatile components such as F, Cl, S, CO_2 , N_2 , and H_2O played a significant role in the evolution of primary lamproitic magmas. In some cases, sulfide melt may be immiscibly separated from silicate melt at early stage of lamproite magma evolution. Moreover, carbonate melt and aqueous-saline fluid (or melt) may be separated from silicate liquid during the latest stages of lamproite crystallization. Lamproitic rocks from some localities of SE Spain (verite, fortunite) contain only inclusion glasses different in composition to those in lamproites from other localities. They are not agpaitic and have shoshonite-dacitic affinity.

In general, the evolution of lamproitic magma during crystallization differs strongly from that of other potassic liquids (in particular, shoshonite and K-basaltoid) in its peralkaline trend. Melt evolution during crystallization of these potassic rocks had a strong miassic trend and was directed towards a gradual increase of SiO_2 , Al_2O_3 , alkalis and depletion in FeO_T , MgO , CaO , TiO_2 and P_2O_5 .

Silicate melt inclusions in lamproite minerals contain daughter phases. In general, the majority of them are similar in composition to the groundmass minerals of the rocks, whereas chemistry of kalsilite is very specific. This mineral from lamproites is poor in Al_2O_3 and rich in MgO (up to 4.2 wt.%), Fe_2O_3 (up to 8 wt.%) and SiO_2 (up to 43.4 wt.%), and to be magnesioferrikalsilite. Chemistry of sulfide blebs in early lamproite minerals and conditions of the appearance of Al-spinel in lamproites are also considered.

INTRODUCTION

Thermobarogeochemical investigations of diverse igneous rocks provide insight into the physicochemical conditions of rock crystallization in each particular case [Roedder, 1984; Sobolev, 1996]. Especially it is very important for such unique rocks as lamproites. The origin of these perpotassic rocks has attracted the attention of many scientists due to their diamond potential and exotic mineralogy and geochemistry.

Magmatic inclusions in lamproite minerals may divide into silicate melt, fluid, sulfide and crystal species, including their combinations. They have been studied in lamproites from famous occurrences such as the West Kimberley province (Western Australia), Leucite Hills (Wyoming, USA), Smoky Butte (Montana, USA), Prairie Creek (Arkansas, USA) and the Murcia-Almeria province (SE Spain). In general, this paper represents a brief review of magmatic inclusion study of lamproites carried out by the author and others researchers during last 15 years [Bogatikov et al., 1991; Logvinova, Sobolev, 1995; Mitchell, 1991; Ryabchikov et al., 1986; Salvioli-Mariani, Toscani, 2001; Salvioli-Mariani, Venturelli, 1996; Salvioli-Mariani et al., 1991; Sharygin, 1991; Sharygin, 1997; Sharygin, 1998; Sharygin, Bazarova, 1991; Sharygin, Pospelova, 1998; Sharygin, Vladykin, 1994; Sharygin, et al., 1998; Sobolev et al. 1985; Sobolev et al., 1989; Sobolev et al., 1975; Solovova et al., 1989; Solovova et al., 1988].

ANALYTICAL METHODS

The various analytical techniques have applied by the author during magmatic inclusion study. Double-polished rock sections of about 50-100 μm in thickness were used for optical microscopy in transmitted and reflected light. The JEOL JSM-35 scanning electron microscope (SEM) and electron microprobe CAMEBAX at the United Institute of Geology, Geophysics and Mineralogy, Novosibirsk were used to identify crystalline phases of magmatic inclusions. A high temperature (<1600°C) heating stage with silicon carbide heating strip [Mikhailov, Shatsky, 1975] and Vernadsky heating stage calibrated at the melting points of Ag, Cu, Au, Mn, Si and $\text{K}_2\text{Cr}_2\text{O}_7$ was used for microthermometric investigations. The accuracy of temperature determination is around 10-15°C.

The chemical composition of crystalline phases and glasses of silicate melt inclusions was determined with the CAMEBAX electron microprobe at the United Institute of Geology, Geophysics and Mineralogy, Novosibirsk. Diopside (Ca, Mg, Si), orthoclase (K, Al), albite (Na), TiO_2 , almandine (Fe), spessartine (Mn), zircon (Zr), F- and Cl-bearing apatites (P, F, Cl), Sr- and Ba-rich glasses, CaSO_4 (S) were used as standards. Counting time = 10 sec, accelerating voltage = 20 kV, current =

20-40 nA. The spot microprobe analyses was carried out with a focused (2-3 μm) beam due to small sizes of the inclusions. It should be noted that the glassy nature of the analyzed inclusions placed some limitations on the reliability of Si, Al and alkalis analyses. K and Na may be volatilized and lost during analysis of glasses, leading to overestimation of Si and Al contents (especially, for miassic compositions). In some cases (when inclusions are large) to minimize alkali loss during analysis was undertaken by defocusing the electron beam. Devitrified silicate melt inclusions were specially prepared for microprobe analyses. They were initially heated to temperatures close to homogenization temperatures by the heating stage and then rapidly quenched.

Raman spectra were obtained using a RAMANOR U-1000 (JOBIN YVON) at the United Institute of Geology, Geophysics and Mineralogy, Novosibirsk to determine fluid composition in fluid inclusions and in gas bubbles of silicate melt inclusions.

DESCRIPTION OF MAGMATIC INCLUSIONS IN MINERALS

West Kimberley province, Western Australia

Olivine lamproites, Ellendale-7, -9, -11 pipes

Magmatic inclusions have been identified only in olivine-2 and in a thin (about 100 μm) marginal zone of olivine-1. Sometimes they form a solid framework within the olivine-1 grains and are linked with groundmass. Isolated silicate-melt and fluid inclusions are scarce. Their size varies from 5 to 20 μm , sometimes up to 50 μm . The phase composition of individual melt inclusions is glass + high-density fluid + daughter/trapped crystals, represented by phlogopite, orthopyroxene, kalsilite and others minerals (Fig. 1). Polycrystal inclusions, consisting of chromite + orthopyroxene, or combinations of these with some glass or fluid, are most common. All the above inclusions (silicate melt, fluid, combined) are considered as primary in origin [Bogatikov et al., 1991; Sobolev et al. 1985; Sobolev et al., 1989]. However, it is possible that some of them may be secondary [Sharygin, 1991]. Similar melt inclusions were also observed in olivine-2 from olivine lamproite of Prairie Creek [Solovova et al., 1989].

Distinct secondary fluid and melt (glass + low-density fluid) inclusions also occur in olivine of the Ellendale-11 rocks and are generally confined to healed microfractures in the periphery of the host olivine.

Phlogopite-leucite lamproites, 81 Mile Vent

Primary melt inclusions have been identified in phlogopite and apatite microphenocrysts. Their phase composition is glass + gas, diopside mainly occurs in phlogopite-hosted inclusions as daughter phase. The sizes vary from 1 to 20 μm . Melt, fluid-melt and fluid inclusions sometimes coexist in apatite [Sharygin, 1991]. Primary and secondary melt inclusions (2-20 μm) have been observed in microphenocrystal diopside only. Primary ones consist mainly of devitrified glass

Phlogopite-diopside-leucite lamproites, Walgidee Hill massif

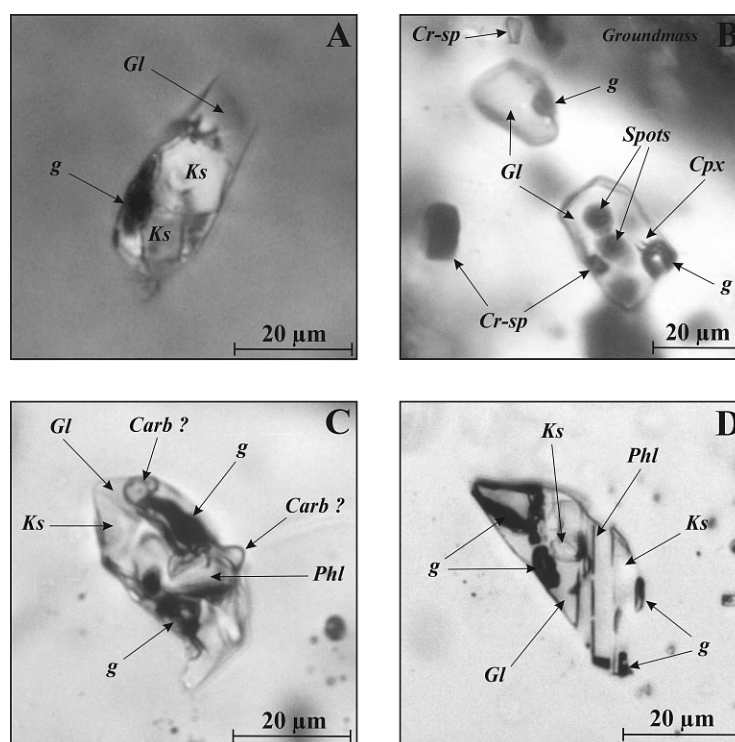


Fig. 1. Digital microphotographs of silicate melt inclusions in minerals of olivine lamproites from the Ellendale field (W.Kimberley, W.Australia).

A – in olivine-1 of the E-11 pipe, polarized light; **B** – in olivine-2 of the E-11 pipe, ordinary light; **C** – in olivine-1 of the E-9 pipe, ordinary light; **D** – in olivine-2 of the E-9 pipe, ordinary light. See [Jaques et al., 1986; Mitchell, Bergman, 1991] for location and description of pipes.

Note for photographs. **Gl** – glass, **g** – gas bubble, **Ks** – Mg-Fe-kalsilite, **Phl** – phlogopite, **Carb ?** – carbonate, **Arm** – armalcolite, **Cpx** – clinopyroxene, **Ap** – apatite, **Prd** – priderite, **Sulf** – sulfides, **Ilm ?** – ilmenite (pseudobrookite), **Lc** – leucite, **Cr-sp** – Cr-spinel, **Spots** – spots after microprobe beam.

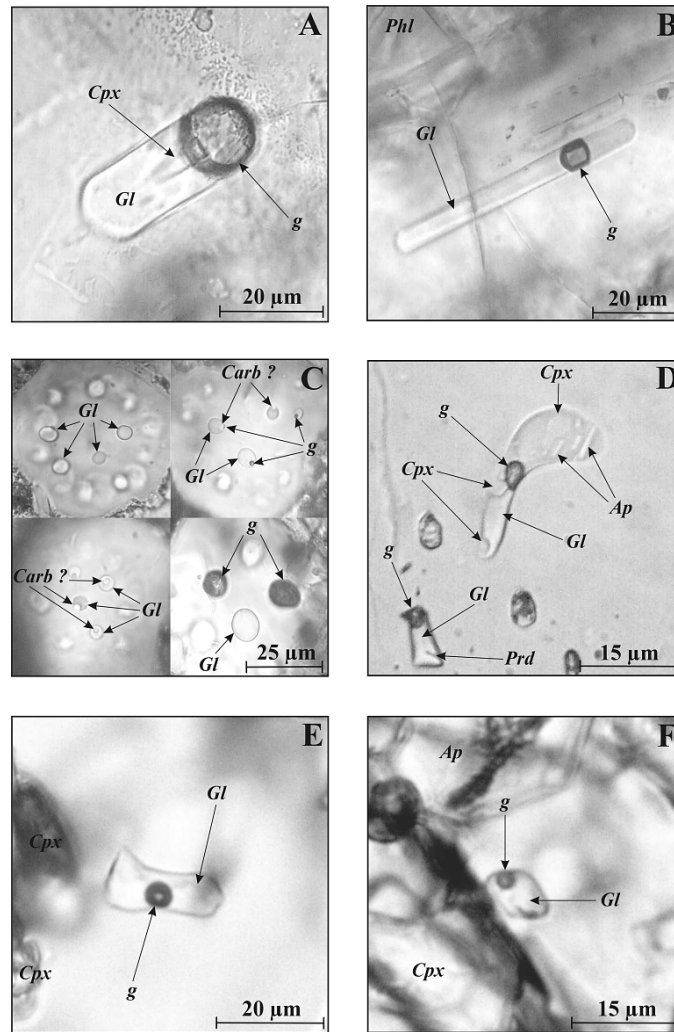


Fig. 2. Digital microphotographs of silicate melt inclusions in minerals of lamproites from Leucite Hills (Wyoming, USA).

A – in phlogopite of wyomingite, Steamboat Mountain, sample LH14-11, ordinary light; **B** – in apatite of wyomingite, Steamboat Mountain, sample LH14-11, ordinary light; **C** – different types of inclusions in leucite of wyomingite, sample LH15-2, Spring Butte, ordinary light; **D** – in the outer zone of olivine-1 of olivine orendite, sample LH10-2, North Table Mountain, ordinary light; **E** – in sanidine of olivine orendite, sample LH10-2, North Table Mountain, ordinary light; **F** – in K-richterite of olivine orendite, sample LH10-2, North Table Mountain, ordinary light.

See [Mitchell, Bergman, 1991] for location of the lamproite outcrops of Leucite Hills.

and gas. Phlogopite is a common daughter phase in these inclusions, whereas other minerals are scarce. Secondary inclusions are glass + gas and form chains through the host mineral [Sharygin, Vladykin, 1994].

Among other leucite lamproites of the W.Kimberley province, melt inclusions were also studied in minerals of olivine-leucite lamproite from Mt.Cedric and in

olivine-leucite hyalolamproite from Oscar Plug [Mitchell, 1991; Sobolev et al., 1989].

Leucite Hills, Wyoming, USA

Wyomingite (phlogopite-diopside-leucite lamproite)

Primary melt and fluid inclusions have been found in phenocrysts and microphenocrysts of the major rock-forming minerals in wyomingite from different outcrops (Emmons Mesa, Steamboat Mountain, Spring Butte, Zirkel Mesa): phlogopite, diopside, apatite and leucite [Mitchell, 1991; Sharygin, 1997, Sharygin, Bazarova, 1991; Sobolev et al. 1985]. Their sizes vary from 1-5 to 50-70 μm . The phase composition of the melt inclusions also varies from glass to glass + gas \pm daughter/trapped crystals (Fig. 2). Minerals found in the rock groundmass represent mainly the daughter phases in the melt inclusions. The most evolved melt inclusions in phlogopite phenocrysts contain Cr-rich olivine, barite, apatite and kalsilite as daughter/trapped phases [Sharygin, 1997; Sharygin, Bazarova, 1991]. Coexisting melt and fluid inclusions are typical of phlogopite phenocrysts and microphenocrystal leucites, where they usually decorate growth zones of the host minerals. Two-phase (greenish glass + gas) inclusions are rare in leucite. Melt inclusions where gas bubble is partially or completely filled by carbonate (or barite) are most common (Fig. 2C). The presence of carbonate/barite in a gas bubble is also common in melt and fluid-melt inclusions hosted by phlogopite and apatite. *Mitchell* [Mitchell, 1991] has observed chalcopyrite and barite as daughter phases of leucite-hosted inclusions in the Zirkel Mesa rocks.

Olivine orendite (phlogopite-olivine-sanidine-leucite lamproite)

Melt inclusions (primary in origin) were observed only in the peripheral zones of poikilitic crystals of sanidine and K-richterite in rocks from North Table Mountain (Fig. 2E-F). Their phase composition is greenish glass + gas, the size is 5-15 μm . Coexisted fluid and silicate melt inclusions were found in phenocrysts (xenocrysts?) of olivine. They form trails in the outer zones of olivine. Phase composition of silicate melt inclusions is glass + g \pm daughter crystals represented by diopside, apatite, priderite (Fig. 2D). The central zones of olivine sometimes contain Cr-spinel and sulfide blebs (MSS + chalcopyrite) [Sharygin, Pospelova, 1998].

Smoky Butte, Montana, USA

Two main rock varieties of this occurrence were studied: olivine-armalcolite-

phlogopite-leucite hyalolamproites and armalcolite-phlogopite-diopside-sanidine lamproite [Sharygin, 1998; Sharygin, Pospelova, 1998; Sharygin, et al., 1998]. Primary silicate melt inclusions were generally identified within olivine-2 (*Mg number* – 0.88-0.85, NiO - 0.2-0.4 wt.%, small grains) and the outer zones of

Glassy lamproites

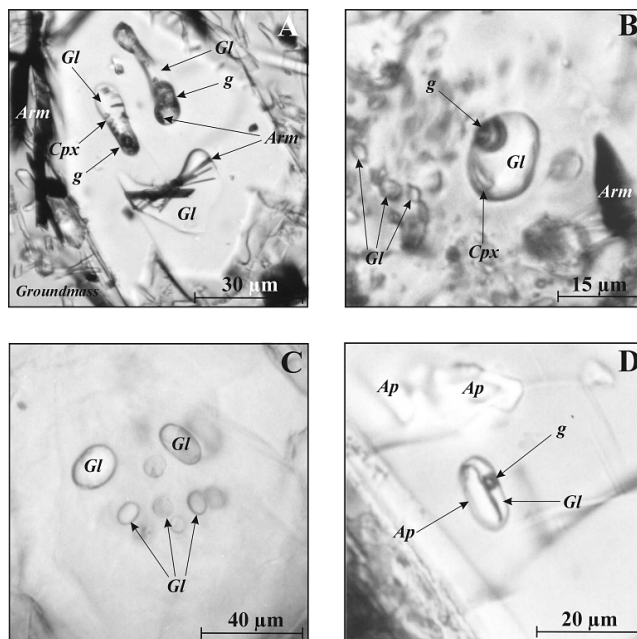


Fig. 3. Digital microphotographs of silicate melt inclusions in minerals of lamproites from Smoky Butte (Montana, USA).

A – in olivine-2 of glassy lamproite, sample SB-55, ordinary light; **B** – in the outer zone of phlogopite of sanidine-bearing lamproite, sample SB-65, ordinary light; **C** – inherited inclusions in analcite of glassy lamproite, sample SB-47, ordinary light; **D** – in clinopyroxene of sanidine-bearing lamproite, sample SB-60, ordinary light. See [Mitchell, Bergman, 1991; Mitchell et al., 1987; Sharygin et al., 1998] for location and description of samples.

olivine-1 (*Mg number* – 0.92-0.89, NiO - 0.5-0.8 wt.%, size -1-5 mm). Inclusion sizes vary from 10 to 50 μm . The phase composition is glass + gas + daughter crystals. The common crystalline phases found are armalcolite and apatite, while diopside and priderite occur rarely (Fig. 3a). In some silicate melt inclusions hosted by olivine, the gas bubble is completely filled by calcite. In addition to melt inclusions, single minute crystals of Cr-spinel and sulfides (Ni-rich sulfides + chalcopyrite) are rarely observed in olivine-1 [Sharygin, 1998; Sharygin, Pospelova, 1998].

Analcite microphenocrysts also contain melt inclusions. This mineral is not a primary magmatic mineral and has pseudomorphed leucite in the Smoky Butte

rocks [Gulliver et al., 1998]. Fresh leucite was only preserved as crystal inclusions in pyroxene. Thus, silicate-melt inclusions in analcite are inherited from leucite. They are concentrically aligned and similar to leucite-hosted inclusions in the Leucite Hills and Oscar Plug rocks [Mitchell, 1991; Sobolev et al., 1975]. Melt inclusions in the Smoky Butte analcite are chiefly monophase (green or yellow brown glass), sometimes with armalcolite and diopside as trapped minerals (Fig. 3C).

Sanidine-bearing lamproites

Silicate-melt inclusions are observed in groundmass diopside and apatite, and also in the peripheral zones of phlogopite phenocrysts (Fig. 3B, D). They are primary in origin and their phase composition is glass + gas, the sizes are 10-20 μm . Crystalline phases are rare and are mainly sanidine. Single crystals of apatite, armalcolite and leucite occur in diopside and phlogopite grains.

Murcia-Almeria province, SE Spain

Silicate melt inclusions have been found in the minerals from some lamproites from SE Spain (verite, fortunite, jumillite, cancalite and olivine-bearing lamproite of Puebla de Mula) [Bogatikov et al., 1991; Salvioli-Mariani, Venturelli, 1996; Sharygin, 1997; Solovova et al., 1989; Wagner, Velde, 1986].

Lamproites of Jumilla and Cancarix

In jumillites primary silicate melt inclusions were found in olivine-1, 2, apatite and clinopyroxene [Salvioli-Mariani, Venturelli, 1996; Sharygin, 1997; Wagner, Velde, 1986]. Their phase composition is glass + gas + daughter/trapped crystals represented by olivine, leucite, Cr-spinel, sanidine, ilmenite (pseudobrookite), apatite (Fig. 4A-B). Single crystals of Cr-spinel are sometimes associated with melt inclusions in olivine and clinopyroxene [Salvioli-Mariani, Venturelli, 1996].

In cancalites silicate melt inclusions were observed in essential minerals (olivine, phlogopite, sanidine, clinopyroxene, apatite, K-richterite and pseudobrookite) [Salvioli-Mariani, Venturelli, 1996]. Their phase composition is glass + gas \pm daughter/trapped crystals (Fig. 4.C-D). The sizes are up to 50-70 μm . Phlogopite, diopside, sanidine and other minerals typical of the rock groundmass occur within silicate-melt inclusions as crystalline phases. Such exotic minerals as dalyite and britholite were also found as daughter phases in sanidine-hosted inclusions from the Cancarix rocks [Salvioli-Mariani, Venturelli, 1996]. These minerals also occur as late-crystallizing phases in groundmass of the rocks of

Cancarix [Contini et al., 1993].

Lamproites of Vera, Fortuna and Puebla de Mula

Silicate melt inclusions were found mainly in phenocrystal olivine, orthopyroxene and phlogopite from these rocks [Bogatikov et al., 1991; Sharygin, 1997; Solovova et al., 1988]. Other minerals of these rocks rarely contain melt

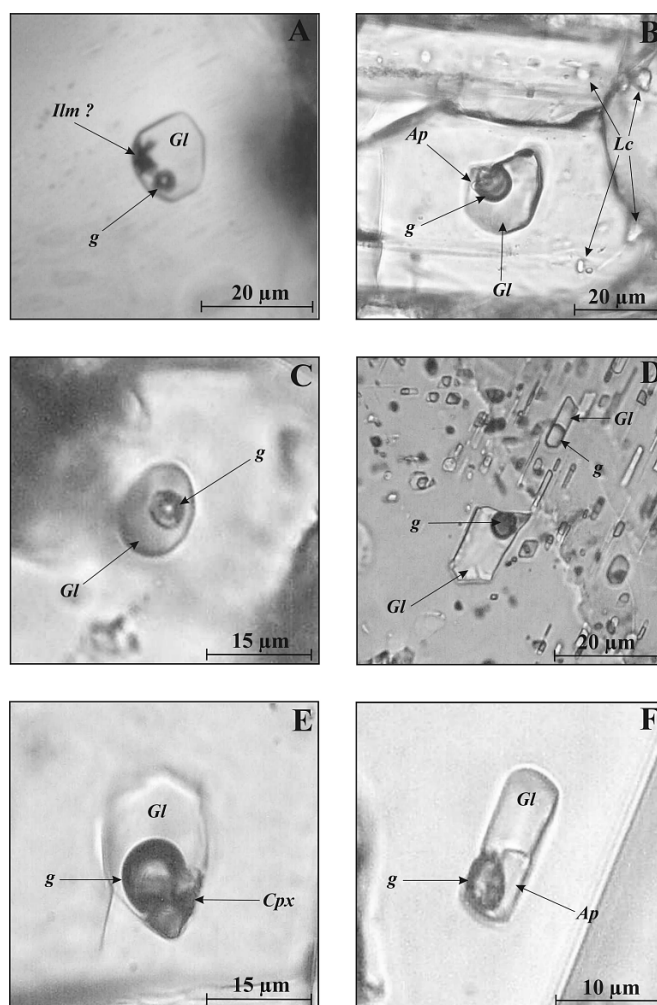


Fig. 4. Digital microphotographs of silicate melt inclusions in minerals of lamproites from Jumilla and Cancarix (SE Spain).

A – in apatite of jumillite, Jumilla, sample SP058, ordinary light; **B** – in the central zone of clinopyroxene of jumillite, Jumilla, sample SP469, ordinary light; **C** – in olivine-2 of cancalite,

Cancarix, sample SP725, ordinary light; **D** – in the outer zone of phlogopite of cancalite, Cancarix, sample SP725, ordinary light; **E** – in sanidine of cancalite, Cancarix, sample SP725,

ordinary light; **F** – in K-richterite of cancalite, Cancarix, sample SP725, ordinary light. See [Mitchell, Bergman, 1991; Salvioli-Mariani, Venturelli, 1996; Venturelli et al., 1984] for description of samples.

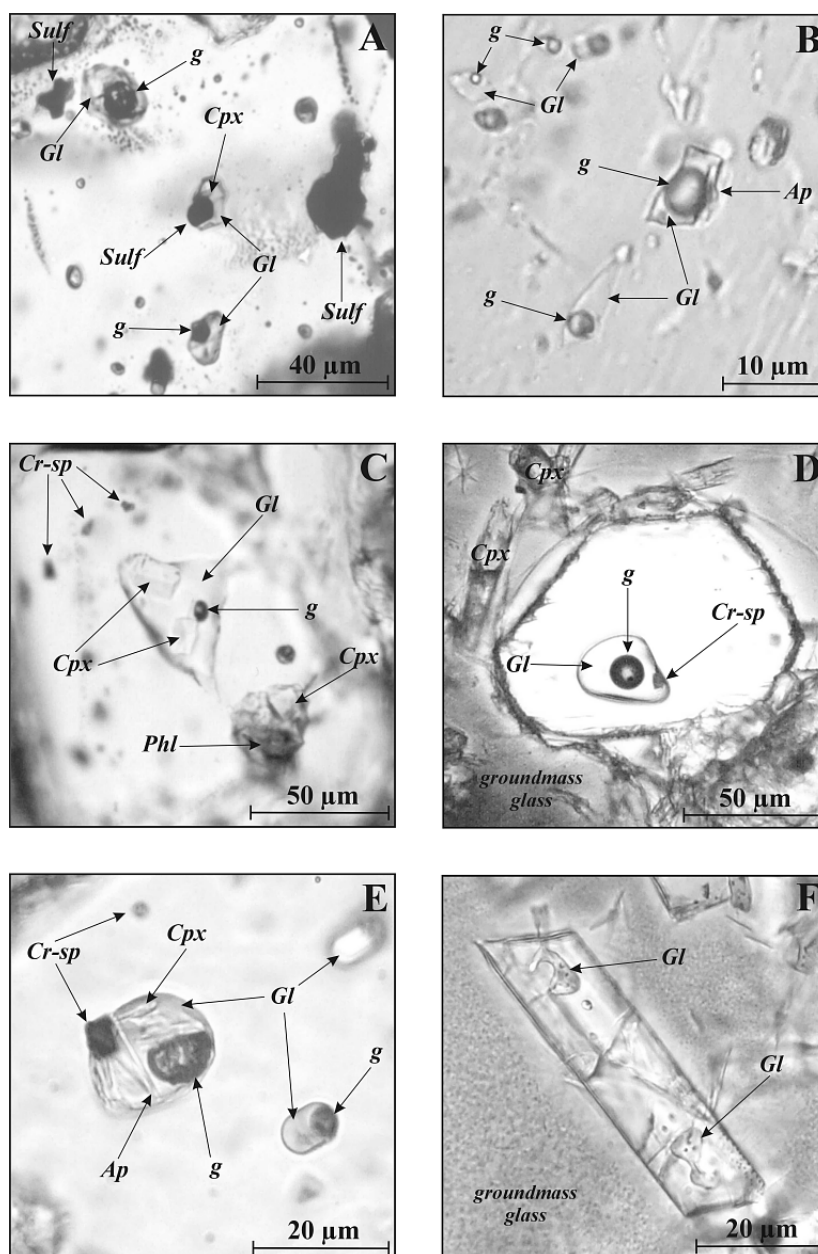


Fig. 5. Digital microphotographs of silicate melt inclusions in minerals of lamproites from Fortuna, Puebla de Mula and Vera (SE Spain).

A – in orthopyroxene of fortunite, Fortuna, sample SP049, ordinary light; **B** – in phlogopite of fortunite, Fortuna, sample SP049, ordinary light; **C** – in olivine-2 of olivine-sanidine lamproite, Puebla de Mula, sample SP081, ordinary light; **D** – in olivine-2 of verite, Vera, sample SP516, ordinary light; **E** - in olivine-2 of verite, Vera, sample SP516, ordinary light; **F** - in clinopyroxene of verite, Vera, sample SP516, ordinary light. See [Mitchell, Bergman, 1991; Venturelli et al., 1984] for description of samples.

inclusions. Magmatic calcite containing silicate-melt inclusions has been noted in verites [Solovova et al., 1988]. The phase composition of the melt inclusions varies

from glass to glass + gas \pm daughter/trapped crystals (Fig. 5). Minerals found in the rock groundmass represent mainly the daughter phases in the melt inclusions. In olivines of Vera and Puebla de Mula silicate melt inclusions usually associated with Cr-spinel crystals (Fig.5 C-E). Melt inclusions in orthopyroxene- and phlogopite-hosted inclusions from Fortuna sometimes contain Ni-rich sulfide inclusions or are associated with sulfide blebs (Fig. 5A). In addition Al-spinel occurs as single crystals in the Fortuna phlogopite. Such Al-spinel crystals occasionally contain melt inclusions (glass + gas). Gas bubble in some mineral-hosted inclusions from Vera and Fortuna may be heterogeneous and consist of liquid H₂O [Bogatikov et al., 1991; Solovova et al., 1988].

THERMOMETRY OF INCLUSIONS

Table 1 presents homogenization temperatures for silicate-melt inclusions in minerals of lamproites. Primary inclusions in olivine-2 of the Ellendale olivine lamproite homogenize at 950-1100°C [Bogatikov et al., 1991; Sharygin, 1991; Sharygin, 1991; Sobolev et al. 1985; Sobolev et al., 1989]. Homogenization temperatures of primary (?) melt inclusions hosted by olivine phenocrysts in olivine lamproites from Prairie Creek are 1050-1100°C [Solovova et al., 1989]. Primary inclusions in leucite lamproite minerals from Western Australia and Leucite Hills are homogenized at 1130-1250°C [Salvioli-Mariani et al., 1991; Sharygin, 1997; Sharygin, Bazarova, 1991]. Melt inclusions in lamproites of Smoky Butte and SE Spain are homogenized in broad range: at 1200-1350 (early minerals) and at 800-1150 (late minerals) [Sharygin, Bazarova, 1991; Sharygin, 1997; Sharygin, et al., 1998; Solovova et al., 1988]. Some inclusions in olivine-1 from the E-11 olivine lamproite [Bogatikov et al., 1991] and in phlogopite from wyomingite [Bogatikov et al., 1991; Sobolev et al., 1975] show too high homogenization temperatures that seem to be due to possible leakage during heating experiments. It should be noted that, in some cases, the temperature of primary inclusion homogenization might be considered as minimum trapping temperature of the inclusion and approximate minimum temperature of host mineral formation.

Freezing studies of olivine-hosted CO₂ inclusions coexisting with melt ones may be used to interpret the PT constraints of crystallization of lamproites from W.Kimberley and Prairie Creek. Minimum PT conditions are estimated as follows: 950-1100°C and >5-6 kb for the W.Australian olivine lamproite [Sobolev et al., 1989]; >1050°C and >4 kb for the Prairie Creek olivine lamproite [Solovova et al., 1989]. Oxygen fugacity during olivine-2 crystallization in olivine lamproites was close to the FMQ buffer [Bogatikov et al., 1991; Solovova et al., 1989].

The presence of the H₂O-liquid in gas bubbles of silicate melt inclusions in phlogopite in Ellendale lamproites [De Albuquerque Sgarbi, Gomes Valenca, *Table 1. Homogenization temperatures (T_{hom}) of silicate melt inclusions in lamproite minerals.*

Locality	Rock	Host	Melt inclusion		Reference
			origin	T_{hom} , °C	
W.Kimberley W.Australia	Ol lamproite p. E-11	Ol-1	primary	1170-1210	[5]
		Ol-2	primary	950-1050	[32, 42, 43]
		Ol-2	secondary	950-1010	[34]
	Ol lamproite, p. E-7, -9	Ol-2	primary	995-1100	[43]
	Phl-Lc lamproite 81 Mile Vent	Phl	primary	1130-1200	[32]
		Ap	primary	1170	
	Lc-Di-Ol lamproite Mt.Cedric	Ol-2	primary	1095-1100	[43]
		Di	primary	1025-1045	
	Phl-Di-Lc lamproite, p. E-26	Ap	primary	1070-1090	[5]
Phl-Di-Lc lamproite Walgidee Hill	Di	primary	1190-1220	[39]	
	Di	secondary	1140-1150		
Prairie Creek Arkansas, USA	Ol lamproite	Ol-2	primary	1050-1100	[45]
Leucite Hills Wyoming USA	wyomingite Emmons Mesa	Phl	primary	1240-1280	[36,44]
		Phl	secondary	1040-1100	
		Ap	primary	>1150	
		Lc	primary	1150-1250	
	wyomingite Steamboat Mountain	Di	primary	1220-1270	this work
		Phl	primary	1080-1220	
		Ap	primary	1170-1190	
	Ol orendite North Table Mountain	Lc	primary	1135-1150	
		Ol-1	secondary	1010-1100	
		Phl	primary	1190-1220	
Di		primary	1180-1210		
San	primary	990-1050			
Smoky Butte Montana USA	Ol-Arm-Phl-Lc hyalolamproite	Ol-2	primary	>1250	[40]
		Ap	primary	1220-1230	
	Arm-Phl-Di-San lamproite	Phl	primary	1085-1210	
		Di	primary	1160-1205	
Murcia-Almeria SE Spain	verite, Vera	Ol	primary	>>1200	[5, 46]
	jumillite Jumilla	Ol-1	primary	>1200	[30]
		Ol-2	primary	1200	
		Ap	primary	1170	
		Di	primary	1100-1150	
		San	primary	830-1055	
	cancalite Cancarix	Ol	primary	>1200	
		Di	primary	1170-1195	
		Ap	primary	1020-1200	
		San	primary	1070-1200	
	Ol-Phl-San-Di lamproite Puebla de Mula	Richt	primary	990-1150	
		Ol	primary	1350-1355	[34]
	fortunite Fortuna	Di	primary	1150-1215	
Opx		primary	1350-1365	this work	
Al-Sp		primary	1210-1240		
Gaussberg Antarctica	gaussbergite	Phl	primary	1185-1190	
		Ol	primary	>1250	[29]
		Di	primary	1100-1260	
		Lc	primary	1150-1280	

1993], as well as in olivine and calcite from Spanish verite [Contini et al., 1993] has been demonstrated by freezing/heating investigations.

CHEMISTRY OF MELT INCLUSION GLASSES

It should be noted that the composition of inclusion glasses (initial, residual and artificially chilled) may be interpreted as the composition of melt remaining after crystallization of their host minerals [Roedder, 1984], while glasses of homogenized inclusions in the earliest minerals are very close in chemistry to initial magma [Sobolev, 1996].

According to electron microprobe analysis, the inclusion glasses hosted by olivine phenocrysts of the E-11 olivine lamproites differ in composition from the host rock with regards to their MgO, TiO₂, BaO, ZrO₂, and alkalis contents and correspond to olivine-leucite and leucite lamproites with exception of SiO₂ and Na₂O (Table 2, Fig. 6). The residual glasses in the most evolved inclusions are more enriched in TiO₂ (up to 11.5 wt.%), BaO (up to 6 wt.%), ZrO₂ (up to 0.75 wt.%) and depleted in Al₂O₃ (down to 0.6 wt.%) and have a very high agpaitic index (31.0). Glasses in homogenized melt inclusions in the E-11 olivine-2 also drastically differ from the host olivine lamproite in having higher contents of TiO₂, alkalis, F and lower amounts of MgO [Sobolev et al. 1985]. The same characteristics of inclusion compositions are also typical of glasses in olivine lamproites from other occurrences in the Ellendale field and Prairie Creek [Sobolev et al., 1989; Solovova et al., 1989]. However, glasses of some unheated inclusion glasses drastically differ in composition from the above data. They have higher contents of SiO₂ (up to 64 wt.%), Al₂O₃ (7.8 wt.%) and lower concentrations of BaO (<1 wt.%), Na₂O (down to 1.2 wt.%), FeO (down to 3 wt.%) and TiO₂ (<1 wt.%). Possibly, these glasses represent the most evolved melt after crystallization of priderite.

In leucite lamproite (phlogopite-leucite lamproite of 81 Mile Vent, phlogopite-diopside-leucite lamproite of the Walgidee Hill, wyomingite and olivine orendite of the Leucite Hills volcanic field), the primary inclusion glasses trapped by the earliest phenocrysts (phlogopite, apatite, clinopyroxene) are similar in composition to the rocks investigated. Glasses in late minerals (leucite, diopside, sanidine) are richer in SiO₂, BaO, TiO₂, ZrO₂, FeO_T, Cl, alkalis and poor in Al₂O₃, CaO, MgO (Table 3, Fig. 6) and correspond to groundmass glasses of leucite and olivine-leucite lamproite [Gunter et al., 1990; Mitchell, 1991; Prider, 1982; Sharygin, Bazarova, 1991]. Like olivine lamproite, the most evolved silicate melt

Таб. 2. Химический состав (мас. %) пород и стекол включений в минералах лампроитов Западных Кимберли (Зап. Австралия).

Порода	Мин. хозяин	Фазовый состав включений	n	SiO ₂	TiO ₂	ZrO ₂	Al ₂ O ₃	FeO	MnO	MgO	CaO	Na ₂ O	K ₂ O	BaO	SrO	P ₂ O ₅	F	Cl	SO ₃	Сумма	Na+K/Al
O1 лампроит тр.Э-11		порода	1	42,50	2,39	0,09	3,50	7,77	0,12	25,70	4,77	0,53	2,21	1,36	0,11	1,35	0,45	0,01	0,03	98,92	0,94
	Ol-1	Gl+g	1	46,45	6,07	-	4,16	9,96	-	3,89	3,03	4,23	13,53	2,53	0,11	0,68	-	-	-	94,56	5,15
	Ol-1	Gl+Phl+g	1	43,03	4,76	-	1,30	8,81	-	9,82	3,83	4,42	15,30	3,51	0,06	1,51	-	-	-	94,56	15,46
	Ol-2	Gl+Ks+ore+g	1	43,71	10,54	-	1,11	6,64	0,11	4,05	5,89	3,52	9,90	4,53	0,13	1,09	-	-	-	91,20	14,64
	Ol-2	Gl+Ks+Ap+ore+g	1	43,79	11,45	0,74	0,63	8,00	0,10	4,12	4,86	4,23	11,08	5,97	0,36	0,90	1,01	0,43	-	97,67	31,00
	Ol-2	Gl+Di+g	2	64,31	0,54	0,03	7,83	3,05	-	5,01	3,42	1,20	12,26	0,71	-	0,12	0,61	0,11	0,09	99,29	1,95
	Ol-2	Gl+Cpx+g	1	46,13	6,09	0,51	4,04	10,19	-	6,16	1,94	3,20	10,97	4,41	0,45	2,58	0,90	-	-	97,57	4,33
	Ol-2	Gl+Opx+Richt+c p+g	1	62,06	1,57	0,18	10,11	3,61	-	4,12	0,24	0,18	2,61	0,50	0,18	1,45	0,02	-	-	86,83	0,30
	Ol-2	Gl+cp+g (T _{ном} =950°C)	1	44,70	6,20	0,41	4,50	8,90	-	8,00	4,21	2,41	10,50	3,25	0,43	2,13	1,43	-	-	97,09	3,41
	Ol-2	Gl _d (T _{ном} =1045- 995°C)	3	44,33	5,65	0,35	5,55	7,22	-	8,74	5,38	2,68	11,41	3,34	0,23	1,86	1,08	-	-	97,82	3,05
Phl-Lc лампроит эгерло 81 мили (тр.Э-5)		порода	1	52,15	6,15	0,25	6,58	5,56	0,08	8,35	2,51	0,39	9,66	1,21	0,21	1,47	0,51	0,01	0,10	97,57	1,68
	Phl	Gl+g	1	54,03	3,25	-	5,11	5,12	-	8,20	0,44	1,01	13,29	1,09	0,03	0,68	-	-	-	92,25	3,14
	Phl	Gl+cp+g	3	56,02	3,53	-	4,40	4,24	-	6,69	2,66	0,87	11,09	1,35	0,27	2,58	-	-	-	93,58	3,07
	Ap	Gl+g	5	55,95	6,83	-	3,78	5,81	-	6,52	2,31	0,67	11,66	1,54	0,17	2,10	-	-	-	97,40	3,65
	Ap	Gl+cp+g	1	54,45	5,05	-	3,14	11,37	-	9,36	1,03	0,08	9,93	0,94	0,00	0,61	-	-	-	95,96	3,57
Di-O1-Lc лампроит Маунт Седрик		порода	1	48,95	4,33	-	6,89	5,85	0,10	15,12	4,50	0,75	6,41	-	-	0,67	0,23	-	-	97,32	1,18
	Ol-2	Gl+Phl+g (T _{ном} =1100°C)	1	54,37	7,01	0,24	9,08	5,44	-	6,58	2,65	0,64	8,80	1,08	0,23	1,48	0,22	-	-	97,82	1,16
	Di	Gl _d (T _{ном} =1045°C)	1	52,11	9,54	0,28	3,55	7,81	-	7,03	4,65	0,53	10,06	2,01	0,32	2,17	0,33	-	-	100,39	3,31
	Di	Gl _d (T _{ном} =1045°C)	1	49,50	4,78	0,14	7,75	6,47	0,10	9,20	7,93	0,28	7,46	1,01	0,15	0,98	0,65	0,02	0,06	100,02	1,10
Phl-Di-Lc лампроит Волжиди Хилл	Di	Gl _d +g (T _{ном} =1190°C)	2	46,14	7,51	0,20	7,46	8,21	0,11	6,42	5,00	0,69	9,96	1,40	0,05	1,24	-	-	0,32	94,71	1,60
	Di	Gl _d +Phl+g (T _{ном} =1200°C)	3	45,49	7,30	0,17	7,40	7,83	0,10	6,41	5,70	0,89	10,64	1,47	0,00	1,22	-	-	0,46	95,08	1,75
	Di	Gl+g (вторичное)	1	56,39	8,06	0,21	7,71	9,38	0,13	1,17	0,57	1,10	12,02	1,19	0,00	0,12	-	-	0,08	98,13	1,91
	Di	Gl+g (вторичное)	1	60,94	6,34	-	5,45	8,05	-	2,51	0,95	0,82	9,75	1,16	0,04	0,53	-	-	-	96,54	2,19
O1-Lc гнатолампр. Оскар Плаз		порода	1	51,39	4,77	0,16	8,55	6,08	0,07	6,30	3,15	0,25	7,62	2,36	0,13	0,98	-	-	-	99,69	1,04
	Lc	Gl+g	3	51,33	8,10	-	1,03	7,57	-	8,83	3,77	1,63	11,07	3,27	-	-	-	-	-	96,60	14,40

Note. Electron microprobe analysis for inclusion glasses, total iron as FeO. Gl_d - fine-devitrified glass, Opx - orthopyroxene, Di - diopside, ore - ore mineral, Richt - K-richite, cp - non-identified transparent phase, others - see Fig. 1. Data on rock compositions from [Jaques et al., 1986; Prider, 1982; Sharygin, Vladykin, 1994; Sobolev et al., 1989]. Totals of rocks include LOI (wt.%): 6.04 - for the E-11 pipe; 4.29 - for the E-9 pipe; 2.38 - for 81 Mile Vent; 3.63 - for Mt. Cedric; 3.63 - for Walgidee Hill; 8.11 - for Oscar Plug. Data on inclusion glasses for p. E -11 (part), p. E -9, Mt. Cedric and Oscar Plug are quoted from [Mitchell, 1991; Ryabchikov et al., 1986; Sobolev et al. 1985; Sobolev et al., 1989]. Author's data are from [Sharygin, 1991; Sharygin, 1997; Sharygin, Vladykin, 1994].

inclusions are also enriched in TiO_2 , BaO , ZrO_2 , and are strongly agpaitic. Natural compositional analogues are found for some of the most-evolved inclusion glasses. For example, secondary inclusion glasses hosted by diopside in the Walgidee Hill phlogopite-diopside-leucite lamproite [Sharygin, 1997; Sharygin, Vladykin, 1994] correspond approximately to veined pegmatoid lamproites of this massif [Jaques et al., 1986]. The same compositional features were also found for inclusion glasses from other olivine-leucite and leucite lamproite from W.Kimberley and Leucite Hills [Mitchell, Bergman, 1991; Sobolev et al., 1989]. Unfortunately, distinct melt evolution during rock crystallization has been traced only for wyomingites (Emmons Mesa, Leucite Hills) in which silicate melt inclusions in four minerals were formed in the following sequence: apatite, phlogopite => leucite, diopside [Sharygin, Bazarova, 1991]. Melt evolution during wyomingite crystallization involved depletion of Al_2O_3 , MgO , CaO , P_2O_5 and the enrichment in SiO_2 , alkalis, FeO_T , TiO_2 , BaO , and ZrO_2 (Table 3, Fig. 6). The origin of liquids depleted in alumina and enriched in mafic components (except CaO) may be related to the crystallization of leucite. In general, the compositions of diopside-hosted glasses are similar to those of the groundmass glass of wyomingite. The actual residual liquid led to crystallization of priderite, K-richterite, barite and wadeite during the late stage [Carmichael, 1967]. Mitchell [Mitchell, 1991] has observed leucite-hosted inclusions with two coexisting silicate glasses differing in composition (low and high K-glasses, Zirkel Mesa) and described them as example of silicate-silicate liquid immiscibility. Inclusion glasses in sanidine of olivine orendite (Leucite Hills) correspond in chemistry to glasses of leucite-hosted inclusions from wyomingite. It should be noted that orendites and wyomingite are very similar in composition and their difference in moda is a result of various PT-conditions of initial primary magma [Mitchell, 1991; Barton, Hamilton, 1982; Gunter et al., 1990; Kuehner et al., 1981].

The primary inclusion glasses hosted by minerals from the Smoky Butte lamproites drastically differ in composition from the host rocks with respect to their SiO_2 , TiO_2 , MgO , Al_2O_3 , CaO , and P_2O_5 contents (Table 4, Fig. 7). They are similar to groundmass glass of the Smoky Butte rocks except that the latter typically has low alkali contents [Mitchell, Bergman, 1991; Mitchell et al., 1987; Sharygin, et al., 1998]. In general, their compositions approach those of glasses in minerals of the W.Kimberley and Leucite Hills leucite lamproites. However, some differences exist. Unlike glasses from W.Australia and the Leucite Hills, inclusion glasses at Smoky Butte contain higher amounts of Al_2O_3 (11-12.5 wt.%) and lower

abundances of Na_2O (<1 wt.%), FeO_T (<3 wt.%), MgO (<2 wt.%), TiO_2 (2-3 wt.%), and have an agpaitic index close to 1 (Table 2-4, Fig. 6-7). The low TiO_2 and BaO contents may be explained by early crystallization of armalcolite and priderite in the Smoky Butte rocks [Gulliver et al., 1998]. The presence of Fe-Ni-sulfides and armalcolite is an evidence of reduced conditions during early evolution of the Smoky Butte initial magma.

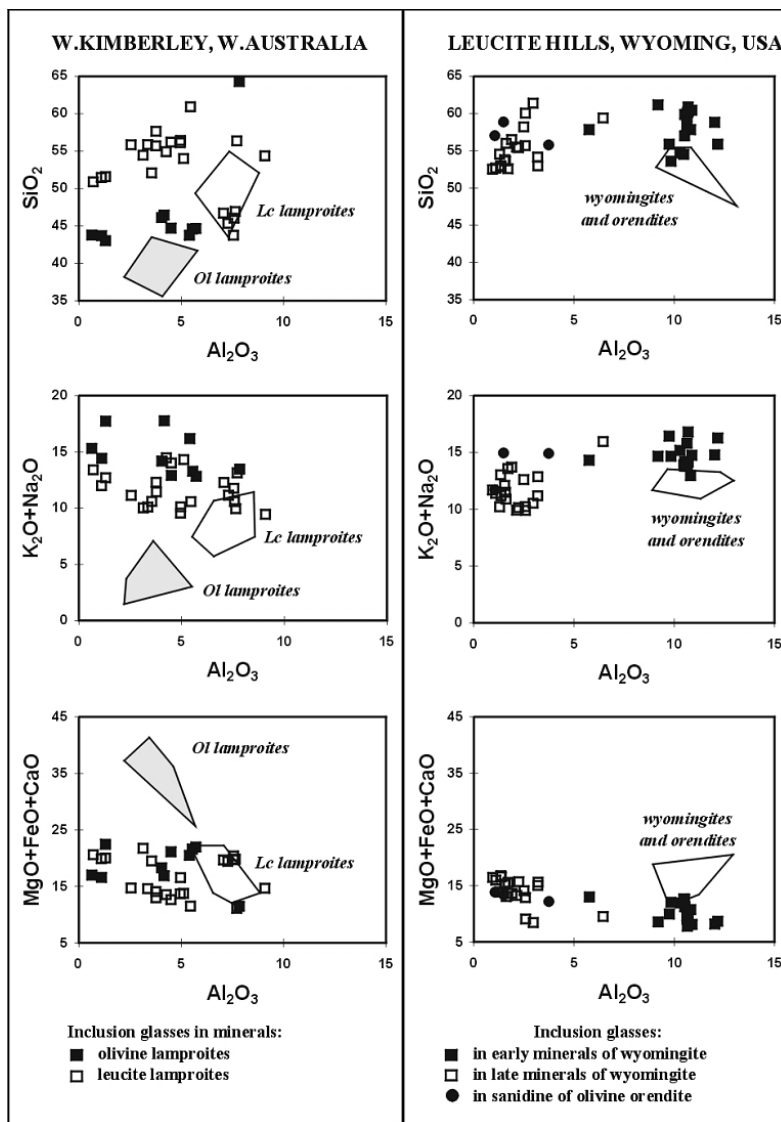


Fig. 6. Variation diagrams of Al_2O_3 versus SiO_2 , $\text{K}_2\text{O}+\text{Na}_2\text{O}$ and $\text{MgO}+\text{FeO}+\text{CaO}$ (in wt.%) for inclusion glasses in minerals and lamproites of W.Kimberley (W.Australia) and Leucite Hills (USA).

Fields are rock compositions. Data on rocks are from [Carmichael, 1967; Gunter et al., 1990; Jaques et al., 1986; Kuehner et al., 1981; Sobolev et al., 1975]. Some data on inclusion glasses are quoted from [Mitchell, 1991; Sobolev et al. 1985; Sobolev et al., 1989].

Таблица 3. Химический состав (мас.%) пород и стекол включений в минералах лампроитов Лейцит Хиллс (США).

Порода, Проявление	Мин. хозяин	Фазовый состав включений	n	SiO ₂	TiO ₂	ZrO ₂	Al ₂ O ₃	FeO	MnO	MgO	CaO	Na ₂ O	K ₂ O	BaO	SrO	P ₂ O ₅	F	Cl	SO ₃	Сумма	Na+K/Al
Вайомингит Emmons Mesa		порода	1	48,94	1,76	-	12,44	7,55	0,10	5,84	4,77	2,17	11,01	0,81	0,38	0,47	0,71	0,05	0,44	99,76	1,25
		Phl	5	56,68	0,72	-	10,62	5,10	0,14	5,93	0,04	3,40	11,38	0,71	0,10	0,38	0,05	0,12	0,10	95,47	1,69
		Phl	1	57,85	0,47	-	10,82	5,46	-	5,11	0,17	2,20	10,76	1,04	0,13	0,42	0,03	-	-	94,46	1,42
		Phl	1	55,89	1,41	-	12,17	4,19	-	4,41	0,06	3,93	12,34	0,61	0,12	0,68	0,28	-	-	96,09	1,62
		Ap	5	53,59	2,89	-	9,84	4,91	-	4,44	2,68	2,46	12,20	0,55	0,20	0,24	-	-	-	94,00	1,77
		Ap	1	54,52	3,40	-	10,47	4,54	-	5,89	2,22	2,54	11,37	0,57	0,18	0,10	0,20	-	-	96,00	1,57
		Ap	1	57,86	4,12	-	5,76	6,20	-	4,35	2,42	2,69	11,62	1,39	0,11	0,76	0,22	-	-	97,50	2,93
		Lc	10	53,29	7,53	-	1,73	7,15	-	7,37	1,11	3,61	8,26	3,75	0,12	1,81	-	-	-	95,73	8,59
		Lc	1	55,42	7,32	-	2,24	6,92	-	7,53	1,23	2,34	7,79	3,71	-	-	0,46	0,24	-	95,20	5,50
		Di	3	60,50	7,92	-	2,71	6,42	0,12	1,55	0,94	1,63	8,48	1,56	0,09	0,85	-	-	-	92,77	4,46
основная масса (стекло)	Di	1	59,40	4,39	-	6,45	7,35	-	1,55	0,62	4,39	11,47	1,15	0,00	0,05	-	-	-	-	96,82	3,09
		3	62,24	7,49	1,25	2,43	7,88	-	1,88	0,62	1,48	6,39	2,01	0,08	0,55	0,00	0,21	0,10	0,10	92,58	3,83
		6	51,12	2,11	0,26	11,28	5,43	0,08	6,48	4,87	1,56	10,95	0,78	0,28	1,32	0,58	0,02	0,44	100,6	1,27	
Вайомингит Steamboat Mountain		порода	1	60,88	0,51	0,30	10,69	3,22	-	3,66	1,20	3,57	13,22	0,66	0,16	0,21	-	0,04	0,11	98,43	1,89
	Phl	1	61,16	0,04	0,40	9,19	3,98	-	3,99	0,58	2,50	12,16	0,82	0,05	0,07	-	0,06	0,22	95,22	1,89	
	Ap	6	59,65	2,67	0,27	10,67	3,41	-	3,95	1,82	1,80	12,67	0,58	0,14	0,04	-	0,07	0,18	97,92	1,56	
Вайомингит Spring Butte		порода	1	51,57	2,42	0,17	10,10	4,20	0,08	7,78	5,03	1,31	11,32	0,73	0,26	1,61	-	-	-	99,62	1,25
	Lc	3	55,74	7,07	0,79	2,11	6,87	-	5,38	0,81	2,70	7,64	2,58	0,09	0,80	-	0,45	0,00	93,03	5,95	
Вайомингит Zirkel Mesa		порода	1	51,03	2,67	0,17	9,81	3,95	-	7,24	5,37	1,03	10,61	0,78	0,32	1,71	0,69	0,02	1,00	100,3	1,21
	Lc	2	57,35	7,05	-	2,20	6,15	-	6,95	0,75	4,10	9,05	5,05	-	-	-	-	-	-	98,65	7,36
Ой орендит North Table Mountain		порода	3	53,89	2,38	0,26	9,86	4,07	0,08	9,06	3,74	1,21	11,04	0,40	0,24	1,31	0,69	0,03	-	99,90	1,41
	San	1	55,79	7,52	-	3,74	5,68	-	5,44	1,04	2,72	12,19	1,61	0,26	-	0,12	0,21	-	-	96,32	4,83
	San	1	58,87	7,25	-	1,49	6,09	-	6,13	1,12	2,65	12,30	1,60	0,24	-	0,25	0,20	-	-	98,19	11,60
	San	1	57,04	7,68	-	1,06	6,87	-	6,29	0,69	1,98	9,73	2,08	-	-	0,11	0,25	-	-	93,78	12,27

Примечание. Bar - барит, San - санидин, другие обозначения смотри Рис.1 и Таблица 2. Данные по породам взяты из работ [6, 15, 19, 44]. Суммы пород включают п.п. (мас.%): 1.97 - Emmons Mesa; 2.67 - Steamboat Mountain; 2.79 - Spring Butte; 3.43 - Zirkel Mesa; 1.64 - North Table Mountain. Данные по стеклам включений из лампроитов Zirkel взяты из работы [22]. Данные автора из работ [34, 36].

Таблица 4. Химический состав (мас.%) пород и стекол включений в минералах лампроитов Смоки Бьютт (США).

Порода, Проявление	Мин. хозяин	Фазовый состав включений	n	SiO ₂	TiO ₂	ZrO ₂	Al ₂ O ₃	FeO	MnO	MgO	CaO	Na ₂ O	K ₂ O	BaO	StO	P ₂ O ₅	F	Cl	SO ₃	Сумма	Na+K/Al	
Ol-Arm-Phl-Lc гяло-лампроит	порода		6	51,78	5,37	0,24	8,60	5,03	0,07	8,17	5,10	2,06	5,26	0,77	0,33	2,05	0,50	-	0,04	100,1	1,05	
		Ol	Gl+Arm+Di+g	1	64,58	2,74	0,36	11,68	2,82	-	1,40	1,00	1,31	10,14	1,29	0,35	0,00	-	0,06	0,07	97,80	1,13
		Ol	Gl+Arm+g	1	65,43	3,03	-	13,15	2,45	0,00	1,51	0,73	1,07	11,12	0,74	0,00	-	0,39	0,08	0,08	99,78	1,05
		Ol	Gl+Arm+g	1	63,86	3,23	-	11,40	2,87	0,02	1,72	0,77	1,04	10,44	1,89	0,07	-	0,34	0,06	0,07	97,78	1,13
		Ol	Gl+Arm+g	1	63,55	3,61	0,28	12,64	2,52	-	1,80	0,49	0,93	10,63	1,64	0,09	0,01	-	0,08	0,07	98,34	1,03
		Ol	Gl+Arm+cp+g	1	64,30	2,38	0,22	12,52	2,77	-	1,93	1,20	0,82	10,11	1,36	0,15	0,31	-	0,05	0,06	98,18	0,98
		Ol	Gl+Arm+g	1	65,53	2,48	0,39	13,17	2,83	-	1,78	0,08	0,79	10,51	0,79	0,00	0,58	-	0,05	0,10	99,08	0,96
		Ol	Gl+Arm+g	1	63,41	2,80	0,33	12,08	3,83	-	1,69	0,14	1,01	10,60	1,16	0,00	0,32	-	0,05	0,09	97,51	1,08
		Ap	Gl+g	1	63,40	2,72	0,22	12,51	2,63	-	1,90	1,35	0,14	9,35	0,71	0,12	0,00	-	0,01	0,00	95,06	0,82
		Anc	Gl	1	67,52	3,25	0,48	7,00	3,54	-	2,26	0,86	0,20	0,86	1,46	0,18	0,16	-	0,05	0,04	87,86	0,17
		Anc	Gl	1	65,59	2,15	0,30	12,83	2,81	-	1,62	0,39	0,78	0,66	1,42	0,10	0,15	-	0,04	0,04	88,88	0,16
			основная масса (стекло)	1	65,28	4,26	-	11,12	3,83	0,03	2,25	0,84	0,83	1,37	1,58	0,19	-	0,47	0,06	0,07	92,18	0,26
			основная масса (стекло)	1	65,87	3,65	0,45	9,62	4,07	-	1,82	0,44	0,52	1,58	1,60	0,14	0,18	-	0,04	0,06	90,04	0,27
	Arm-Phl-Di-San лампроит	порода		6	51,60	5,57	0,22	9,74	5,27	0,05	6,74	4,40	0,80	8,70	0,69	0,32	2,11	0,53	-	0,06	99,98	1,10
		Phl	Gl+San+g	1	70,07	3,34	0,47	9,96	2,37	0,01	0,93	0,13	0,99	8,85	1,20	0,14	0,00	0,11	0,08	-	98,65	1,12
		Phl	Gl+g	1	67,50	3,31	0,40	11,38	1,57	-	0,82	0,46	0,51	10,49	1,01	-	0,00	-	-	-	97,45	1,08
		Phl	Gl+g	1	66,60	4,63	0,46	9,82	1,81	-	1,74	0,96	0,76	9,31	1,07	-	0,00	-	-	-	97,16	1,15
		Phl	Gl+cp+g	1	65,74	4,04	0,52	10,95	3,08	-	0,72	0,06	0,80	11,08	1,27	-	0,00	-	-	-	98,26	1,21
		Di	Gl+g	1	65,66	4,20	0,39	11,10	3,16	-	0,53	0,49	0,77	7,97	1,17	0,29	0,12	-	0,05	0,11	96,01	0,89
		Di	Gl+g	1	59,75	3,80	0,39	13,25	3,43	-	0,94	0,74	0,17	10,57	0,25	0,05	0,00	-	0,03	0,00	93,37	0,88
		Di	Gl+cp+g	1	60,33	0,89	0,82	12,49	3,05	-	4,12	0,58	0,16	12,04	0,04	-	0,05	-	-	-	94,57	1,05
		Arm	Gl+g	1	63,44	6,45	0,43	11,86	2,76	-	2,02	0,95	1,11	7,75	0,95	-	0,00	-	-	-	97,72	0,86
		Ap	Gl+g	1	63,03	3,00	0,39	11,40	3,17	-	1,55	0,52	0,17	12,36	1,00	0,03	0,03	-	0,02	0,01	96,68	1,20
		Ap	Gl+g	1	61,25	3,84	0,40	11,46	3,79	-	1,85	0,78	0,25	10,31	0,96	0,08	0,00	-	0,02	0,00	94,99	1,00
		Ap	Gl+Phl+San+g	1	69,91	5,11	-	8,38	3,96	0,12	0,92	0,82	1,05	6,63	1,02	-	0,00	0,04	0,13	-	98,09	1,06

Примечание. Anc - анализ. Данные по породам взяты из работ [25, 40]. Суммы пород включают п.п.п (мас.%): 4,86 - оливиновые гялолампроиты; 3,18 - санидиновые лампроиты. Данные по стеклам включений взяты из работы [40].

Таблица 5. Химический состав (мас.%) пород и стекол включений в минералах лампроитов ЮВ Испании.

Порода, Проявление	Мин. хозяин	Фазовый состав включений	n	SiO ₂	TiO ₂	ZrO ₂	Al ₂ O ₃	FeO	MnO	MgO	CaO	Na ₂ O	K ₂ O	BaO	SrO	P ₂ O ₅	F	Cl	LREE TR ₂ O ₃	Сумма	Na+ K/Al	
Верит <i>Vesca</i>		порода	1	66,50	1,45	0,08	9,82	3,22	0,03	2,68	2,25	1,11	7,34	0,15	0,05	0,54	-	-	0,07	99,82	1,01	
	Ol-2	Gl+cr+g	1	62,42	2,28	0,20	16,44	2,00	-	1,66	2,41	0,37	6,40	0,14	0,00	0,00	-	-	-	94,32	0,46	
	Ol-2	Gl+cr+g	1	60,66	2,93	0,18	16,56	2,16	0,02	1,63	3,31	0,57	7,06	0,17	0,00	0,00	0,76	0,21	0,09	96,31	0,52	
	Ol-2	Gl+g	1	63,13	2,82	0,20	16,52	2,53	-	1,37	1,94	0,49	7,65	0,16	0,00	0,00	-	-	-	96,81	0,55	
	Ol-2	Gl+g	1	60,60	2,78	0,20	16,46	2,09	0,01	1,57	3,73	0,63	7,72	0,13	0,00	0,00	0,44	0,22	0,10	96,68	0,57	
	Ol-2	Gl+cr+g	1	64,86	2,40	-	16,56	1,83	-	1,02	2,30	0,52	7,23	0,52	0,00	-	0,63	0,17	-	98,04	0,52	
Ol-Phl-San лампроит <i>Puebla de Mula</i>		порода	1	57,80	1,52	0,07	12,10	5,71	0,06	3,24	3,54	1,66	8,34	0,29	0,11	1,34	-	-	0,05	99,83	0,97	
	Ol-2	Gl+Di+g	1	69,41	1,19	0,05	11,74	3,53	-	2,90	1,03	0,22	6,70	0,10	0,00	0,01	-	-	-	96,88	0,64	
	Ol-2	Gl+g	1	69,94	2,00	0,24	10,88	2,88	0,02	1,76	0,22	0,96	5,83	0,08	0,00	0,07	0,13	0,41	0,08	95,50	0,73	
	Ol-2	Gl+g	1	70,43	2,40	0,27	11,27	2,07	0,01	1,78	0,22	1,16	6,87	0,07	0,00	0,12	0,06	0,37	0,08	97,18	0,83	
	Ol-2	Gl+Phl+Di+g	1	70,36	1,99	0,29	10,75	2,25	0,02	1,62	0,20	0,91	5,86	0,04	0,00	0,09	0,05	0,35	0,08	94,86	0,74	
	Ol-2	Gl+cr+g	1	62,97	1,36	0,26	14,09	4,56	0,03	2,49	0,39	0,49	10,61	0,14	0,00	0,07	0,36	0,27	0,14	98,23	0,88	
	Ol-2	Gl+cr+g	1	68,87	1,69	0,29	12,02	2,18	-	1,62	0,16	0,84	5,72	0,05	-	0,09	-	-	-	93,53	0,64	
	Phl	Gl+cr+g	1	65,80	0,10	0,24	10,39	4,49	-	3,56	2,23	1,63	8,05	0,12	-	0,00	-	-	-	96,61	1,08	
		порода		2	57,45	1,46	0,08	11,90	5,27	0,07	9,21	2,90	1,25	6,84	0,17	0,06	0,77	-	-	0,05	99,55	0,79
	Opх	Gl+cr+g	4	66,79	0,72	0,08	17,26	0,52	0,01	0,31	1,95	1,11	6,15	0,00	0,00	0,11	0,00	0,19	0,08	95,28	0,49	
Фортунит <i>Fortuna</i>	Opх	Gl+Di+Ap+g	1	66,41	0,30	0,11	18,79	0,50	-	0,28	1,81	1,28	6,82	0,00	0,00	0,11	-	-	-	96,41	0,51	
	Opх	Gl+Phl+Ap+g	1	67,08	0,53	0,07	16,83	1,23	-	1,17	1,96	1,63	6,59	0,02	0,00	0,62	-	-	-	97,73	0,58	
	Opх	Gl+cr+g	1	69,76	0,68	-	16,90	0,62	-	0,20	1,38	0,71	5,59	0,12	0,00	-	0,00	0,18	-	96,14	0,42	
	Opх	Gl+Di+Ap+g	1	68,18	0,23	-	16,76	0,40	-	0,11	3,41	0,67	5,12	0,01	0,00	-	0,00	0,23	-	95,12	0,39	
	Phl	Gl+g	1	65,38	0,22	-	18,11	0,33	-	1,73	1,57	1,32	7,77	0,07	0,00	-	0,07	0,09	-	96,66	0,58	
		порода		17	49,34	1,31	0,09	8,67	5,83	0,08	15,10	6,54	2,25	4,60	0,30	0,14	1,67	-	-	0,14	99,95	1,00
Хумиллит <i>Jumilla</i>	Ol-2	Gl+Di+Ap+ore+g	2	57,58	2,31	0,21	15,29	4,14	0,04	1,75	0,07	3,27	11,53	0,38	0,00	0,01	0,29	0,24	0,07	97,18	1,17	
	Ol-2	Gl+Phl+ore+g	1	58,26	0,00	-	8,50	6,33	-	4,25	0,74	5,41	11,26	0,09	0,00	-	0,10	0,44	-	95,38	2,49	
	Ol-2	Gl+Di+ore+g	1	62,50	2,10	-	10,41	4,63	-	2,68	0,74	3,41	8,76	0,98	0,00	-	0,17	0,62	-	96,98	1,45	
	Ap	Gl+g	3	59,45	3,39	0,58	9,17	6,51	0,04	2,72	0,61	2,34	7,42	0,00	0,00	0,58	0,17	0,74	0,13	93,85	1,30	

Примечание. Данные по породам взяты из работ [49, 50]. Суммы пород включают п.п. (мас.%): 4.53-вериты; 4.00 – лампроиты Пуэбла де Мула; 2.07 – фортуниты; 3.89 – хумиллиты. В таблице присутствуют новые данные автора и данные из работы [34], в таблицу не включены данные по стеклам включений из работ [5, 30, 46].

The inclusion glasses in minerals from Spanish lamproites also differ from their host rocks. They are rich in SiO_2 , Al_2O_3 , alkalis, ZrO_2 , Cl and poor in MgO, CaO, and P_2O_5 (Table 5, Fig. 8), and generally similar to groundmass glasses in the rock studied [Contini et al., 1993; Venturelli et al., 1984; Venturelli et al., 1991]. Previous studies of some melt inclusions from Spain, indicated the presence of F [1988].

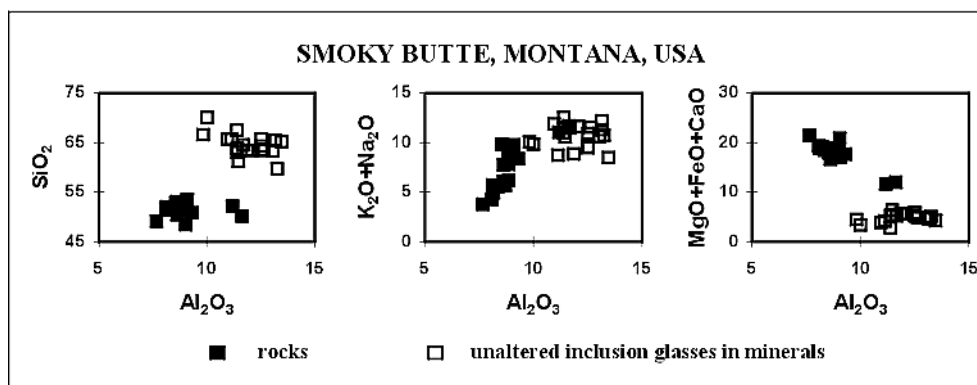


Fig. 7. Variation diagrams of Al_2O_3 versus SiO_2 , $\text{K}_2\text{O}+\text{Na}_2\text{O}$ and $\text{MgO}+\text{FeO}+\text{CaO}$ (in wt.%) for inclusion glasses in minerals and lamproites of Smoky Butte (USA).

Data on rocks and inclusion glasses are from [Mitchell et al., 1987; Jaques et al., 1986; Sharygin, et al., 1998].

(up to 0.9 wt.%) and Cl (up to 0.4 wt.%) [Bogatikov et al., 1991; Salvioli-Mariani, Venturelli, 1996]. Their agpaitic index varies from 0.4-0.6 (verites, fortunites) to 0.65-1.1 (olivine-bearing rocks of Puebla de Mula) and 1.2-16 (jumillites, cancalites). On the whole, among investigated Spanish lamproites, only rocks from Jumilla, Cancarix and Puebla de Mula are approximately similar to leucite lamproite from W.Kimberley and the Leucite Hills in the bulk composition of melt inclusion glasses [Salvioli-Mariani, Venturelli, 1996; Sharygin, 1997; Wagner, Velde, 1986]. Nevertheless, glasses in Spanish rocks differ from those of W. Kimberley and the Leucite Hills with respect to their high SiO_2 and low BaO contents and are similar to those from Smoky Butte. In general, inclusion glasses from some Spanish lamproite varieties (especially, verite and fortunite) display shoshonitic affinity and closely correspond in major element composition to dacites widespread in the Murcia-Almeria province [Venturelli et al., 1984; Venturelli et al., 1991].

RAMAN SPECTROSCOPY OF THE FLUID PHASE IN MELT INCLUSIONS

Raman investigations may reveal semi-quantatively the presence of following volatiles in inclusion bubbles: CO_2 , N_2 , H_2S , CH_4 and heavy hydrocarbons. Unfortunately, the determination of H_2O is precluded. Raman data on the fluid

phase of silicate-melt inclusions in olivine-2 (Smoky Butte glassy lamproite SB-11, see [Mitchell et al., 1987]; and verite) indicated the presence of only CO₂ and N₂. The gas bubble in an olivine-hosted inclusion at Smoky Butte consists of 26.6 mole % CO₂ and 73.4 mole % N₂, while that of an olivine-hosted inclusion in verite contains 51.7 mole % CO₂ and 48.3 mole % N₂. Some inclusions in verite olivine also contain about of 10 mole % H₂O-liquid in gas bubble [Solovova et al.,

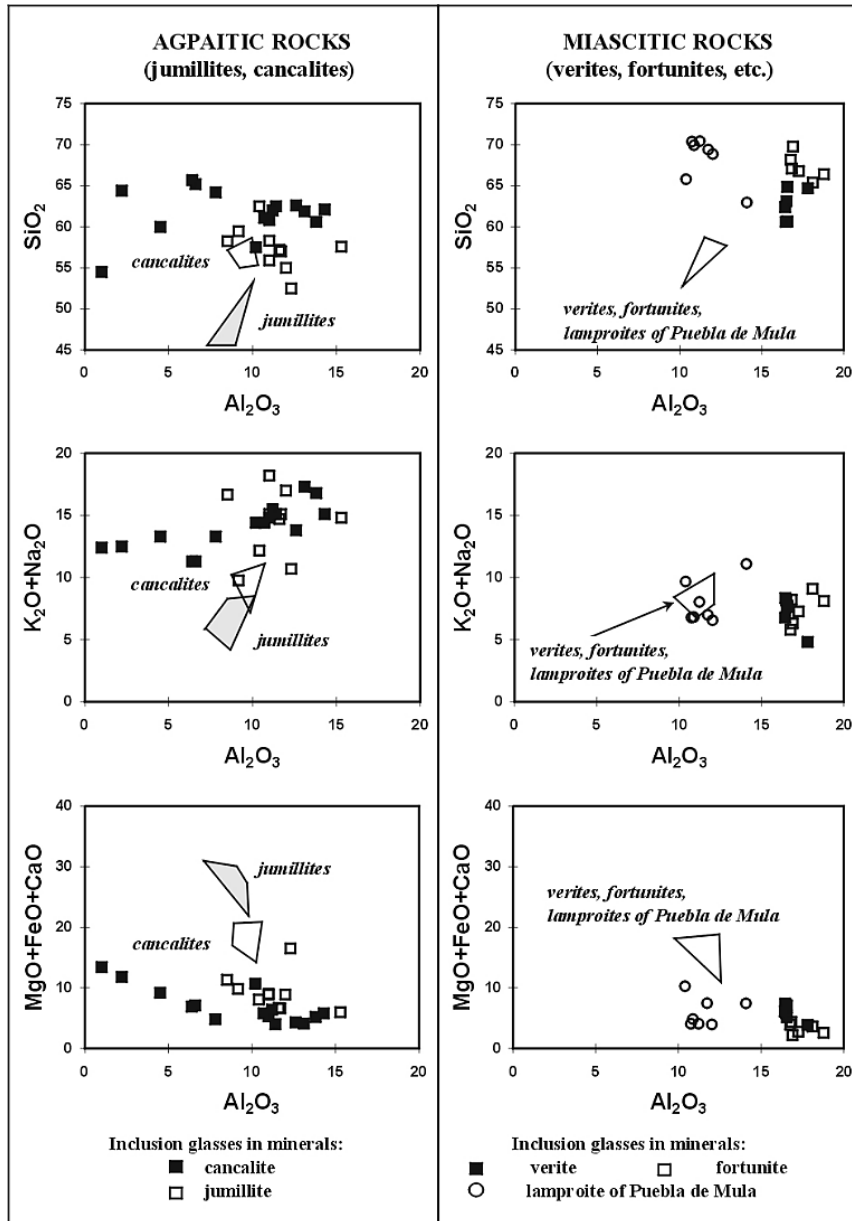


Fig. 8. Variation diagrams of Al₂O₃ versus SiO₂, K₂O+Na₂O and MgO+FeO+CaO (in wt.%) for inclusion glasses in minerals and lamproites of SE Spain. Fields are rock compositions.

Data on rocks are from [Contini et al., 1993; Venturelli et al., 1984; Venturelli et al., 1991]. Some data on inclusion glasses are quoted from [Bogatikov et al., 1991; Salvioli-Mariani, Venturelli, 1996; Sharygin, 1997; Sharygin, 1997].

Previously, the presence of N₂ in both glass and the gas bubble has been found in an olivine-hosted inclusion from the E-11 olivine lamproite [Ryabchikov et al., 1986]. The maximum contents of N₂ in the gas bubble of this inclusion are estimated to be 20 mole %. Cryometric and Raman investigations of primary fluid and combined inclusions in olivine-2 of the E-11 olivine lamproite have shown that fluids are CO₂-rich (>85 mole %) and H₂O-poor (<10 mole %). The minor components of the fluid have been accurately analyzed only by the Raman method. They are (in mole %): N₂ - up to 3.5, CO - up to 2.5, CH₄ - <0.2, H₂ - <0.4, H₂S - <0.3, NH₃ - <0.4, NO - <2.0, HF - <1.0 [Carmichael, 1967]. Raman study of a fluid inclusion (possibly, secondary in origin) in olivine-2 of the E-9 olivine lamproite indicates that fluid contains 83.8 mole % CO₂ and 16.2 mole % N₂ [Sharygin, 1997]. Preliminary cryometric study of silicate melt inclusions in orthopyroxene of fortunite shows the presence of low-density CO₂ in gas bubble.

COMPOSITION OF DAUGHTER PHASES OF MELT INCLUSIONS AND SINGLE CRYSTALS IN LAMPROITE MINERALS

In addition to glasses, crystalline phases in the inclusions and single crystal inclusions in phenocrysts have been studied (Table 6). In general, the majority of them (phlogopite, diopside, Cr-spinel, K-richterite, etc.) are similar in composition to the groundmass minerals of the rocks investigated. Coexisting enstatite, phlogopite and olivine in some inclusions seem to indicate high pressures (P>10 kb) during the earliest stage of lamproite crystallization, according to melting experiments undertaken on natural samples [Arima, Edgar, 1983; Barton, Hamilton, 1979; Barton, Hamilton, 1982; Edgar et al., 1992; Edgar, Mitchell, 1997; Foley, 1989; Foley, 1990; Gulliver et al., 1998; Mitchell, 1995]. Garnet, mantle indicator mineral, was not found in any of the melt inclusions. This mineral is observed only as single crystal inclusions in chromite macrocrysts (>0.5 mm) from the Ellendale-4 and Prairie Creek olivine lamproites [Logvinova, Sobolev, 1995]. The presence of such phases as kalsilite, Al-spinel and sulfide in lamproite minerals is very interesting.

Kalsilite

Kalsilite as a daughter phase (up to 10-15 μm) in the inclusions has been identified in olivine phenocrysts in the E-11 and E-7 olivine lamproites, in olivine-2 of the Prairie Creek olivine lamproites and in phlogopite phenocrysts in Leucite Hills wyomingites (Fig. 1) [Sharygin, 1991; Sharygin, 1997; Sharygin, Vladykin, 1994; Sobolev et al. 1985; Sobolev et al., 1989; Solovova et al., 1989].

Unfortunately, the alone composition does not permit an unambiguous identification of the mineral as kalsilite or kaliophilite. The minute size of the phase and location within the inclusions preclude X-ray diffraction studies. However, thermometric study of the Prairie Creek lamproites shows that this mineral has low melting temperature (about 660°C) and seems to be kalsilite. The origin of this mineral in lamproites is very enigmatic, as, according to *Mitchell and Bergman* [Mitchell, Bergman, 1991], kalsilite is considered as a “prohibited

Table 6.

Daughter/trapped phases of silicate melt inclusions in lamproite minerals.

Locality	Rock	Host	Daughter/trapped phases of inclusions	Reference
W.Kimberley W.Australia	Ol lamproite <i>pipes E-11, -9, -7</i>	Ol-1,2	Opx, Di, Richt, Phl, Ks, Ap, Per, Ilm, Cr-Sp, Fluor, Carb?	[32, 34, 42, 43]
	Phl-Lc lamproite <i>81 Mile Vent</i>	Phl	Di, Ap	[32]
	Phl-Di-Lc lamproite <i>Walgidee Hill</i>	Di	Phl, Prd, San?, Ks?	[39]
	Lc-Di-Ol lamproite <i>Mt.Cedric</i>	Ol-2	Phl	[43]
	Ol-Lc hyalolamproite <i>Oscar Plug</i>	Lc	Ap, Sulf	[22]
Leucite Hills Wyoming, USA	wyomingite <i>Emmons Mesa, Spring Butte</i>	Phl	Ol, Ks, Ap, Di, Bar, Cr-Sp, Lc, San, Carb?	[34, 36, 39]
		Ap	Bar, Prd, ore, Carb, Sulf	
	<i>Steamboat Mountain Zirkel Mesa</i>	Di	San, Lc	[22]
		Lc	Bar, Carb?, Sulf	
	Ol orendite <i>North Table Mountain</i>	Ol-1,2	Ap, Di, Prd, Cr-Sp, Sulf	[38]
San		Ap, Di	this work	
Prairie Creek Arkansas, USA	Ol lamproite	Ol-2	Di, Per, Richt, Sph, Ks, Carb?	[45]
Murcia-Almeria SE Spain	jumillite <i>Jumilla</i>	Ol	Di, Phl, Ap, Lc, San, Cr-Sp	[30, 31, 34, 52] this work
		Ap	Ol, Phl, Ilm?	
		Phl	San, Lc, Anc, Ap, Cr-Sp	
		Di	Ap, Lc, Phl, San, Cr-Sp	
	verite <i>Vera</i> fortunite <i>Fortuna</i>	Ol-2	Phl, San, Ap, Cr-Sp, Carb	[46] this work
		Opx	Di, Phl, Ap, Sulf	[38] this work
		Phl	Di, Ap, Sulf, Al-Sp	
	Ol-Phl-San-Di lamproite <i>Puebla de Mula</i>	Ol-2	Di, Ap, Phl, Lc?, Cr-Sp	
	cancalite <i>Cancarix</i>	Ol	Di, Ap, San, Lc, Phl	[30]
		Ap	Richt, San	
Di		Lc, San		
San		Richt, Phl, Ap, Dal, Brit		
Smoky Butte Montana, USA	Ol-Arm-Phl-lc hyalolamproite	Ol-1,2	Arm, Ap, Di, Prd, Carb, Cr-Sp, Sulf	[35, 38, 40]
		Anc	Arm, Di	
	Arm-Phl-Di-San lamproite	Phl	Di, San, Arm, Ap, Carb	
		Ap	Di, San, Lc, Phl	
		Di	Arm, San, Ap, Lc, Carb	

Note. Fluor - fluorite, Dal - dalyite, Brit - britholite, Sph - sphene, Per - perovskite. Carbonates are localized in gas bubble.

mineral” for lamproites. However, in contrast to kalsilites from kamafugites and other potassic rocks [Allan, Carmichael, 1984; Cundari, Ferguson, 1991; De Albuquerque Sgarbi, Gomes Valenca, 1993; Kostyuk et al., 1990], the mineral from lamproites is poorer in Al_2O_3 and richer in MgO (up to 4.2 wt.%), Fe_2O_3 (up to 8 wt.%) and SiO_2 (up to 43.4 wt.%), and thus a magnesioferrikalsilite (Table 7). Its unusual composition may be explained as a consequence of two possible substitutions: $\text{Al}^{3+} \rightleftharpoons \text{Fe}^{3+}$ and $2\text{Al}^{3+} \rightleftharpoons \text{Mg}^{2+} + \text{Si}^{4+}$ (Fig. 9). The appearance of this mineral seems to reflect the undersaturation of initial lamproitic magma in Al_2O_3 and SiO_2 [Sharygin, 1997] or reaction of olivine with relatively Si-rich

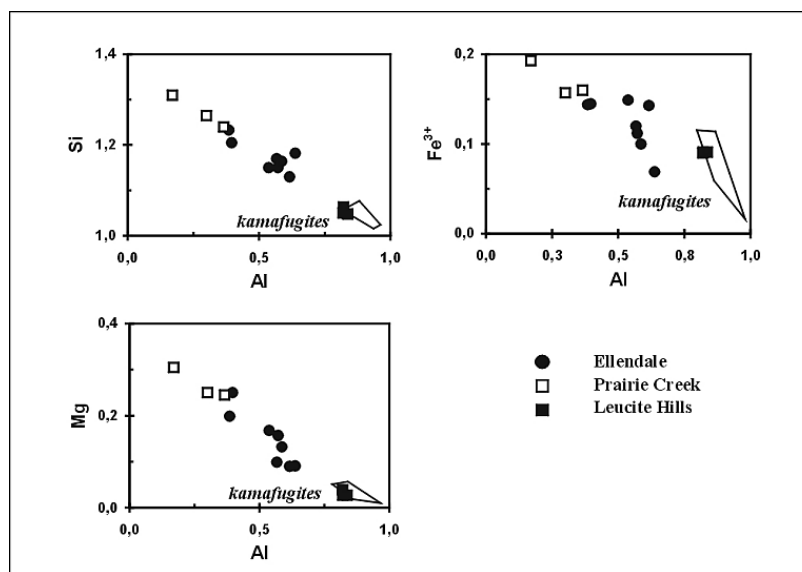


Fig. 9. Compositional variations for kalsilites (in a.f.u. at $O=4$) from lamproites compared with kalsilites from kamafugitic rocks.

Data are quoted from [Allan, Carmichael, 1984; Cundari, Ferguson, 1991; De Albuquerque Sgarbi, Gomes Valenca, 1993; Salvioli-Mariani et al., 1991; Sharygin, Vladykin, 1994; Sharygin, et al., 1998; Sobolev et al., 1989; Solovova et al., 1989].

magma [Mitchell, Bergman, 1991]. According to the experiments of *Wendlandt and Egger* [Wendlandt, Egger, 1980a; Wendlandt, Egger, 1980b], the coexistence of kalsilite with olivine, enstatite, phlogopite, liquid and gas within inclusion (in particular, in olivine lamproites of E-11 pipe) possibly evidences of high PT conditions (25-34 kb, 1160-1425°C) for the formation of the earliest phenocrysts in some lamproites. However, kalsilite was not observed in the products of high PT-experiments on natural lamproites [Arima, Edgar, 1983; Barton, Hamilton, 1979; Barton, Hamilton, 1982; Edgar et al., 1992; Edgar, Mitchell, 1997; Gulliver et al., 1998; Mitchell, 1995] and instead of it diverse potassic phases (K-Mg fluoride, K-Ti silicates, K-Ba phosphate) appear.

Al-spinel

Aluminous spinel (pleonaste-hercynite) was found as single crystals in leucite phenocrysts of the W.Kimberley leucite lamproite [Jaques, Foley, 1985], in phlogopite of wyomingite from Leucite Hills [Wagner, Velde, 1987], in phlogopite of some Spanish lamproites (Vera, Fortuna, Barqueros) [Wagner, Velde, 1987] and the Smoky Butte lamproites [Sharygin, et al., 1998]. The presence of this mineral is uncommon of such peralkaline rocks as lamproites. At present there are several points of view explaining the appearance of Al-spinel in lamproitic rocks:

Individual resorbed pleonaste grains in association with salite in wyomingites

*Table 7.**Kalsilite from silicate melt inclusions in lamproite minerals.*

Locality	Ellendale field, W.Kimberley						Prairie Creek	Leucite Hills Emmons Mesa				
	p. E-11			p.E-7								
Rock	Ol lamproite						Ol lamp.	Ol lamproite	wyomingite			
Host	Olivine-2						Ol-2	Olivine-2	Phlogopite			
SiO ₂	43,40	43,02	43,45	41,63	45,40	44,93	42,70	46,64	45,59	40,02	40,82	40,63
TiO ₂	0,43	0,39	0,50	0,37	0,62	0,59	0,43	0,61	0,50	0,22	0,17	0,19
Al ₂ O ₃	17,83	18,08	18,57	19,32	12,00	12,50	16,93	9,43	11,40	27,11	26,74	26,88
Fe ₂ O ₃	5,92	5,62	5,56	7,81	7,03	7,15	7,44	7,66	7,76	4,72	4,57	4,68
MgO	2,47	3,95	3,29	2,19	4,91	6,28	4,19	6,17	6,06	0,70	0,70	0,99
CaO	0,04	0,05	0,04	0,03	0,03	0,02	0,01	0,00	0,00	0,02	0,02	0,01
Na ₂ O	0,54	0,40	0,08	0,07	0,51	0,59	0,06	0,83	0,78	1,97	2,26	4,87
K ₂ O	28,70	28,61	28,45	28,33	28,75	28,07	28,41	27,91	25,31	25,32	24,83	22,01
BaO	0,29	0,18	0,06	0,10	0,36	0,37	0,05	0,20	0,40	0,10	0,06	0,11
Total	99,62	100,30	100,00	99,85	99,81	100,50	100,22	99,45	97,80	100,2	100,17	100,37
Referen ce	[32, 34, 39]	this work		[34]	[45]		[34]	this work				

from Leucite Hills are supposed to be fragments of desintergrated xenoliths of granulites or ultramafic rocks [Kuehner et al., 1981].

Single crystals of Al-spinel in leucite of leucite lamproites from W.Australia (Oscar Plug, Ellendale-7) and in leucite from some products of PT-experiments with gausbergites from Antarctica are interpreted as exsolution inclusions formed due to a considerable excess of Al, Mg and Fe in initially nonstoichiometric leucite [Jaques, Foley, 1985]. Single crystals of pleonaste in mica phenocrysts from wyomingites of Leucite Hills, some lamproites of SE Spain and Smoky Butte might be regarded as decay products of biotite xenocrysts (or unstable phlogopite enriched in Al) with decreasing pressure and constant (or increasing) oxygen fugacity [Contini et al., 1993; Sharygin, et al., 1998; Venturelli et al., 1984; Wagner, Velde, 1987].

Crystallites of Al-spinel in phlogopite of fortunite from SE Spain are one of the early phases crystallized from melt. This is confirmed by the presence of melt

inclusions with homogenization temperature 1210-1240°C (Table 1) in them and high-alumina miassic composition of inclusion glasses in early fortunite minerals [Sharygin, et al., 1998].

Sulfide inclusions

The presence of small amounts of sulfides is typical of lamproites. They were recognized in the groundmass of different lamproite types: in the Smoky Butte hyalolamproites - pyrite and pyrrhotite, in the Ellendale-11 olivine lamproite - chalcopyrite, in the SE Spain jumillite - galenite [Sharygin, et al., 1998]. Pentlandite and pyrrhotite occur with talc in olivine pseudomorphs from the groundmass of the AK1 olivine-phlogopite lamproite [Jaques et al., 1986]. However, taking into account the influence of alteration processes on the above rocks, the nature of these sulfides may be considered as secondary. Chalcopyrite has been previously identified as daughter phase in silicate-melt inclusions in leucite from the Leucite Hills wyomingite and the Oscar Plug olivine-leucite lamproite [Mitchell, 1991]. This is strong evidence about magmatic nature of chalcopyrite in lamproites. Polyphase sulfide inclusions were found in the earliest phenocrysts of lamproites during fluid inclusion study. They are observed in lamproites of Smoky Butte, Fortuna and Leucite Hills [Sharygin, 1997; Sharygin, Pospelova, 1998; Sharygin, et al., 1998].

In olivine hyalolamproite from Smoky Butte (Montana, USA) sulfides rarely occur as rounded globules (1-30 µm) in olivine-1 phenocrysts only (Mg# - 0.87-0.92, 0.5-0.8 wt.% NiO, size -1-5 mm). Sometimes they are associated with primary melt inclusions ($T_{\text{hom}} > 1250^{\circ}\text{C}$). The blebs are represented by following mineral associations: pentlandite + chalcopyrite; monosulfide solid solution (MSS) + chalcopyrite; violarite. Chalcopyrite in the essential amounts (up to 20 vol.%) occurs only in the largest (up to 20-30 µm) globules, while in small blebs it forms thin outer rim.

In fortunites of SE Spain sulfides are observed as both single globules (up to 20 µm) and isolations in primary silicate-melt inclusions hosted by orthopyroxene and phlogopite phenocrysts. Enstatite-hosted sulfide globules are represented by following assemblages: pentlandite + heazlewoodite, pentlandite, heazlewoodite, pentlandite + godlevskite, pentlandite + pyrrhotite. Small octahedral crystals of Fe-oxide occasionally occur in some sulfide globules. Homogenization temperature of silicate-melt inclusions coexisted with sulfide blebs in enstatite occurred at 1350°C.

In olivine orendite of North Table Mountain (Leucite Hills, USA) sulfides are found as globules (1-20 µm) in phenocrystal (xenocrystal) olivine only. They form rare trails in the host olivine and are associated with secondary fluid inclusions,

sometimes with secondary silicate-melt inclusions ($T_{\text{hom}}=1010-1100^{\circ}\text{C}$). The large sulfide blebs consist of MSS or MSS + chalcopyrite. Sometimes oriented inclusions of pentlandite may be observed in MSS.

Table 8. Phase and chemical composition of sulfide inclusions in lamproite minerals.

Phase composition of inclusions	Phase	n	Fe wt. %	Ni	Co	Cu	S	Total	Fe at. %	Ni	Co	Cu	S	Me/S	Ni/Fe
<i>In olivine-1 of Ol-Arm-Phl-Lc hyalolamproite, Smoky Butte, Montana, USA</i>															
Pn+Cp	Pn	2	28,79	37,37	0,17	0,46	33,30	100,1	23,42	28,92	0,13	0,33	47,19	1,12	0,55
Pn+Cp	Pn	2	28,43	37,57	0,17	0,68	33,19	100,1	23,16	29,12	0,13	0,49	47,10	1,12	0,56
Mss+Cp	Mss	1	4,36	56,32	0,00	3,42	35,49	99,59	3,55	43,64	0,00	2,45	50,36	0,99	0,92
Pn+Cp	Pn	2	26,55	39,70	0,10	0,09	33,43	99,87	21,63	30,77	0,08	0,06	47,45	1,11	0,59
Pn+Cp	Pn	1	26,76	39,75	0,20	0,10	33,13	99,94	21,83	30,85	0,15	0,07	47,09	1,12	0,59
Viol	Viol	2	11,07	45,47	0,13	1,60	41,50	99,77	8,64	33,75	0,10	1,10	56,41	0,77	0,80
Mss+Cp	Mss	2	3,20	58,27	0,00	2,69	35,81	99,97	2,59	44,93	0,00	1,92	50,56	0,98	0,95
Mss+Cp	Mss	2	5,52	53,03	0,00	5,51	35,79	99,85	4,48	40,96	0,00	3,93	50,62	0,98	0,90
Mss+Cp	Mss	2	5,93	55,03	0,00	3,68	35,46	100,1	4,81	42,46	0,00	2,62	50,11	1,00	0,90
Mss+Cp	Cp	1	30,37	0,14	0,00	34,28	34,91	99,70	25,01	0,11	0,00	24,81	50,07	1,00	0,00
Pn+Cp	Pn	2	29,11	37,35	0,17	0,17	33,31	100,1	23,67	28,89	0,13	0,12	47,18	1,12	0,55
	Cp	1	30,50	0,21	0,00	34,30	34,92	99,93	25,07	0,16	0,00	24,77	49,99	1,00	0,01
	ISM		29,32	31,78	0,14	5,29	33,55	100,1	23,88	24,62	0,11	3,79	47,60	1,10	0,51
Pn+Cp	Pn	2	27,30	39,21	0,11	0,19	33,18	99,99	22,26	30,41	0,08	0,14	47,12	1,12	0,58
	Cp	1	30,67	0,21	0,00	34,19	34,90	99,97	25,20	0,16	0,00	24,69	49,95	1,00	0,01
	ISM		27,81	33,36	0,09	5,29	33,44	99,99	22,69	25,90	0,07	3,79	47,54	1,10	0,53
<i>In olivine-1 of Ol orendite, North Table Mountain, Leucite Hills, Wyoming, USA</i>															
Mss+Pn	Mss	6	34,73	25,59	0,61	0,00	38,72	99,65	27,33	19,15	0,45	0,00	53,07	0,88	0,41
	Mss+Pn	1	33,43	27,40	0,56	0,04	38,61	100,1	26,26	20,47	0,42	0,03	52,83	0,89	0,44
Mss+Cp	Mss	1	33,34	27,40	0,47	0,15	38,69	100,1	26,17	20,46	0,35	0,10	52,91	0,89	0,44
	Cp	1	31,24	0,64	0,07	32,91	34,91	99,77	25,68	0,50	0,05	23,78	49,99	1,00	0,02
	ISM		33,03	23,39	0,41	5,06	38,12	100,1	26,10	17,58	0,31	3,52	52,49	0,91	0,40
Mss+Cp	Mss+Cp	1	33,18	19,93	0,37	8,04	38,32	99,84	26,27	15,01	0,28	5,59	52,85	0,89	0,36
<i>In orthopyroxene of fortunite, Fortuna, SE Spain</i>															
Pn+Cp	Pn+Cp	1	28,36	30,99	0,09	7,25	33,23	99,92	23,21	24,13	0,07	5,21	47,38	1,11	0,51
Pn+Gd*	Pn	1	18,43	48,15	0,06	0,11	33,20	99,95	15,08	37,48	0,05	0,08	47,32	1,11	0,71
	Gd	1	10,33	57,29	0,00	0,22	32,12	99,96	8,54	45,05	0,00	0,16	46,25	1,16	0,84
	ISM		16,00	50,89	0,04	0,14	32,88	99,95	13,13	39,73	0,03	0,10	47,00	1,13	0,75
Pn+Gd*	Gd	1	4,44	62,85	0,00	0,05	32,62	99,96	3,67	49,37	0,00	0,04	46,93	1,13	0,93
Pn+Hzss	Pn	2	25,76	40,72	0,27	0,06	33,20	100,1	21,01	31,58	0,21	0,04	47,16	1,12	0,60
	Hzss	2	8,54	62,36	0,00	0,26	28,65	99,81	7,24	50,27	0,00	0,19	42,30	1,36	0,87
	ISM		18,87	49,38	0,16	0,14	31,38	99,93	15,63	38,89	0,13	0,10	45,26	1,21	0,71
Pn	Pn	1	27,28	38,91	0,23	0,06	33,40	99,88	22,23	30,15	0,18	0,04	47,40	1,11	0,58
Pn	Pn	1	25,18	40,52	0,12	0,50	33,51	99,83	20,53	31,43	0,09	0,36	47,59	1,10	0,60
Pn+Hzss	Pn	4	28,59	37,96	0,07	0,02	33,28	99,92	23,29	29,42	0,05	0,01	47,23	1,12	0,56
	Hzss	1	12,51	57,37	0,07	0,09	29,77	99,81	10,51	45,83	0,06	0,07	43,55	1,30	0,81
Pn+Po	Pn	2	36,40	29,76	0,35	0,04	33,35	99,90	29,55	22,98	0,27	0,03	47,17	1,12	0,44
	Po	1	62,22	1,11	0,00	0,02	36,56	99,91	49,00	0,83	0,00	0,01	50,15	0,99	0,02
	ISM		38,98	26,90	0,32	0,04	33,67	99,90	31,55	20,71	0,24	0,03	47,47	1,11	0,40
Pn+Po	Po	1	60,91	0,28	0,00	0,01	38,78	99,98	47,31	0,21	0,00	0,01	52,47	0,91	0,00
Hzss	Hzss	1	17,56	51,15	0,08	0,25	30,90	99,94	14,59	40,43	0,06	0,18	44,73	1,24	0,73
Pn+Hzss	Pn+Hzss	1	20,23	45,84	0,16	0,14	33,46	99,83	16,53	35,63	0,12	0,10	47,62	1,10	0,68
Pn+Hzss	Pn	1	29,78	36,64	0,25	0,02	33,25	99,95	24,25	28,38	0,19	0,02	47,16	1,12	0,54
Po+Pn	Po	1	57,62	3,97	0,00	0,28	37,92	99,79	45,12	2,96	0,00	0,19	51,73	0,93	0,06
Pn+Fe-ox	Pn	2	28,14	38,17	0,20	0,01	33,35	99,87	22,93	29,58	0,15	0,01	47,33	1,11	0,56

Note. Pn - pentlandite ($Fe_xNi_{1-x})_{9-3y}S_8$, Cp - chalcopyrite $CuFeS_2$, Mss - monosulfide solid solution ($Fe_xNi_{1-x})_{1-y}S$, Viol - violarite ($Fe_xNi_{1-x})Ni_2S_4$, Gd - godlevskite ($Fe_xNi_{1-x})_9S_8$ or godlevskite solid solution ($Fe_xNi_{1-x})_{7-3y}S_6$, Hzss - heazlewoodite solid solution ($Fe_xNi_{1-x})_{3-3y}S_2$, Po - pyrrhotite $Fe_{1-x}S$, Fe-ox - cubic Fe-oxide (wüstite or magnetite), ISM - calculated initial sulfide melt, n - number of analyses. * - sulfide isolation in silicate melt inclusion (Pn+Gd or Pn+Hzss).

The main distinctive feature of sulfide inclusions in lamproites studied is extremely high content of Ni (Table 8). In the Smoky Butte rocks the MSS contain up to 50-63 wt.% of Ni. No MSS with that composition are found anywhere. The MSS from Smoky Butte is characterized by Me/S ratio equal to 0.98-1.00 and seems to be a member of the hexapyrrhotite solid solutions $(Fe,Ni)_{1-x}S$. The

Leucite Hills MSS (Ni - 27.4 wt.%) has composition intermediate between $(Fe,Ni)_9S_{10}$ - and $(Fe,Ni)_7S_8$ -types of solid solutions. Initial sulfide melt (ISM) calculated for some blebs from three localities shows the difference in composition. The Fortuna ISM has Me/S ratio equal to 1.1-1.2, the Smoky Butte ISM – Me/S=1.1, the Leucite Hills ISM – Me/S=0.9. Two last compositions are also rich in Cu (5 and 8 wt.%, respectively).

Homogenization temperatures of silicate-melt inclusions coexisted with sulfide globules in early lamproite minerals are an evidence about high trapping temperatures of sulfide melt and the existence of silicate - sulfide liquid immiscibility at high temperatures in lamproitic melt. Trapping temperatures of sulfide melt vary for different lamproite localities: $>1250^\circ C$ - Smoky Butte; $\sim 1350^\circ C$ - Fortuna; $\gg 1100^\circ C$ - Leucite Hills [38]. The abundance of Ni in the sulfide blebs probably should be related to mantle-derived source of lamproites.

DISCUSSION AND CONCLUSIONS

Regardless of the above-mentioned differences between diverse petrographic types of lamproites in the composition of inclusion glasses (Fig. 6-7, 10), a general trend is characteristic of both rock types from different occurrences of lamproitic magmatism (W.Kimberley, Leucite Hills, Smoky Butte, SE Spain). Initial melt evolution during crystallization had an agpaitic nature and initial melt was involved gradual depletion in Al_2O_3 , CaO, MgO, and P_2O_5 with enrichment in SiO_2 , FeO_T , BaO, TiO_2 , ZrO_2 , and alkalis. Volatiles, such as F (or HF), CO_2 , N_2 , and H_2O played significant role in primary lamproitic magmas. This evolutionary trend resulted in the formation of K-rich Al-undersaturated or Al-free silicates (Fe-rich K-feldspar, K-Ti-richichterite, scherbakovite, roedderite-chayesite and wadeite) and K-Ba-titanates (priderite, jeppeite) during the late stages of crystallization. Sulfide-silicate liquid immiscibility sometimes occurs in lamproitic melts at early stages of their crystallization. The presence of H_2O , salts (possibly chlorides), barite and calcite within some melt inclusions in lamproite minerals is evidence

that aqueous-saline (sulfate-carbonate-chloride) melt/or fluid might separate from silicate liquid during the latest stages of evolution. In some cases, this is expressed as late magmatic-hydrothermal activity. For example, apatite-hematite-carbonate assemblages occur as thin veins in jumillites [Salvioli-Mariani et al., 1991; Venturelli et al., 1991]. Late-crystallizing carbonates and barite are also typical of rocks from Prairie Creek, Smoky Butte and the Leucite Hills [Mitchell, Bergman, 1991; Sobolev et al., 1975; Wagner, Velde, 1986]. Some deviations in evolution of initial melt for lamproites of different localities possibly reflect processes which occurred with primitive lamproitic magma during its uplifting (contamination of mantle olivine, mixing in the mantle, contamination of the crustal material, mixing in the Earth crust).

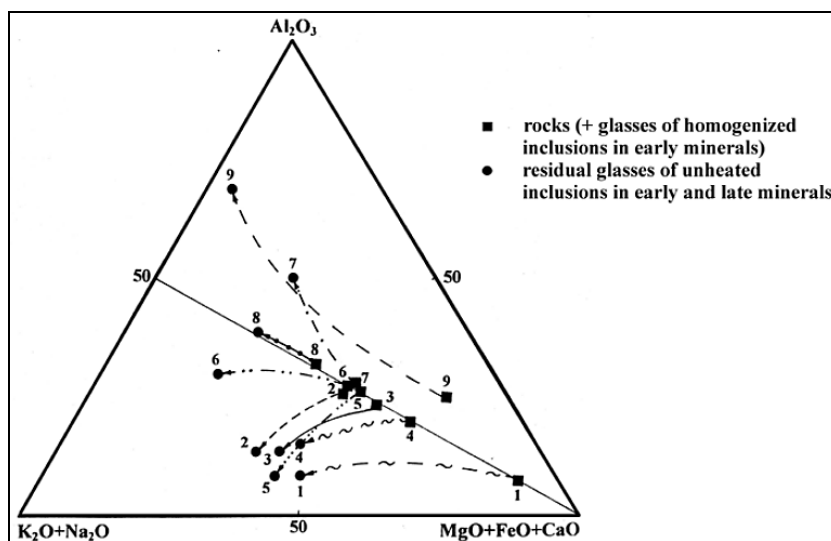


Fig. 10. Evolution of lamproites from different word localities (bulk rock → inclusion glasses in minerals) compared with evolution of K-basaltoids and shoshonites.

1 – olivine lamproites of W.Kimberley and Prairie Creek; 2 – leucite lamproites of W.Kimberley; 3 – wyomingites and orendites of Leucite Hills; 4 – jumillites of SE Spain; 5 – cancalites of SE Spain; 6 – lamproites of Smoky Butte; 7 – verites and fortunites of SE Spain; 8 – lamproites of Puebla de Mula, SE Spain; 9 – K-basaltoids and shoshonites. The line in triangle conventionally divides agpaite and miassic compositions (in wt.%).

Data on rocks and inclusion glasses are quoted from [Bogatikov et al., 1991; Carmichael, 1967; Contini et al., 1993; Gunter et al., 1990; Jaques et al., 1986; Kostyuk et al., 1990; Kuehner et al., 1981; Mitchell, 1991; Mitchell, Bergman, 1991; Mitchell et al., 1987; Salvioli-Mariani, Venturelli, 1996; Sharygin, 1991; Sharygin, 1993; Sharygin, 1997; Sharygin, Bazarova, 1991; Sharygin, Pospelova, 1994; Sharygin, Vladykin, 1994; Sharygin, et al., 1998; Sobolev et al. 1985; Sobolev et al., 1989; Sobolev et al., 1975; Solovova et al., 1989; Solovova et al., 1988; Vaggelli et al., 1993; Vaggelli et al., 1993; Venturelli et al., 1984; Venturelli et al.,

1991; Wagner, Velde, 1986;].

The majority of inclusions in some Spanish rocks (especially, in verites and fortunites) are different in composition to inclusion glasses from other lamproites. They are rich in SiO₂, Al₂O₃, alkalis and depleted in BaO, TiO₂, with a low apgaitic index (<1). Such features may be explained as result of mixing between lamproitic and shoshonitic/dacitic magmas according to a hypothesis proposed by *Venturelli et al.* [Venturelli et al., 1984; Venturelli et al., 1991]. Alternatively, some Spanish rocks related to the lamproitic family seem actually to be members of the shoshonitic clan (generally, leucite-free varieties).

In summary, the chemistry of glasses and daughter phases from melt inclusions hosted by lamproite minerals and the evolution of their composition from the earliest to latest minerals might be used as an additional parameter for distinguishing lamproites from other potassic rocks (especially, K-basaltoids) which are similar to lamproites in chemical and modal composition (Fig. 10). Recent studies of magmatic inclusions in other alkaline rocks (shoshonites, K-basaltoids) demonstrate significant differences with respect to lamproites [Kostyuk et al., 1990; Sharygin, 1993; Sharygin, Pospelova, 1994; Vaggelli et al., 1993]. Melt evolution during crystallization of these rock types was directed towards a gradual increase of SiO₂, Al₂O₃, alkalis and depletion in mafic elements, showing strong miassic trend.

ACKNOWLEDGMENTS

The author thanks Prof. N.V. Sobolev of Institute of Mineralogy and Petrography, Novosibirsk, Russia, Prof. R.H.Mitchell of Lakehead University, Thunder Bay, Canada, Prof. G.Venturelli of Parma University, Italy and Dr. N.V. Vladykin of the Institute of Geochemistry, Irkutsk, Russia for donating of lamproite specimens. The author is also greatly indebted to Mrs. L.N.Pospelova for microprobe data.

This research is supported by Russian Foundation of Fundamental Investigations (grant 00-15-98541 School).

REFERENCES

1. Allan, J.F. and Carmichael, I.S.E. 1984. Lamprophyric lavas in the Colima graben, SW Mexico. *Contrib. Mineral. Petrol.*, 88, 203-216.
2. Arima, M. and Edgar, A.D. 1983. A high pressure experimental study on a magnesian-rich leucite lamproite from the West Kimberley area, Australia: petrogenetic implications. *Contrib. Mineral. Petrol.*, 84, 228-234.
3. Barton, M. and Hamilton, D.L. 1979. The melting relationships of a madupite from the Leucite Hills, Wyoming, to 30 kb. *Contrib. Mineral. Petrol.*, 69, 133-142.
4. Barton, M. and Hamilton, D.L. 1982. Water-undersaturated melting experiments bearing upon the origin of potassium-rich magmas. *Mineral. Mag.*, 45, 267-278.
5. Bogatikov, O.A., Ryabchikov, I.D., Kononova, V.A. et al., 1991. Lamproites. PH Nauka, Moscow, 301 pp.

6. *Carmichael, I.S.E.* 1967. The mineralogy and petrology of the volcanic rocks from Leucite Hills, Wyoming. *Contrib. Mineral. Petrol.*, 15, 24-66.
7. *Contini, S., Venturelli, G., Toscani, L., Capedri, S. and Barbieri, M.* 1993. Cr-Zr-armalcolite-bearing lamproites of Cancarix, SE Spain. *Mineral. Mag.*, 57, 203-216.
8. *Cundari, A. and Ferguson, A.K.* 1991. Petrogenetic relationships between melilitite and lamproite in the Roman Comagmatic Region: the lavas of S.Venanzo and Cupaello. *Contrib. Mineral. Petrol.*, 107, 343-357.
9. *De Albuquerque Sgarbi, P.B. and Gomes Valenca, J.* 1993. Kalsilite in Brazilian kamafugitic rocks. *Mineral. Mag.*, 57, 165-171.
10. *Edgar, A.D., Charbonneau, H.E. and Mitchell, R.H.* 1992. Phase relations of an armalcolite-phlogopite lamproite from Smoky Butte, Montana: Applications to lamproite genesis. *J. Petrol.*, 33, 505-520.
11. *Edgar, A.D. and Mitchell, R.H.*, 1997. Ultra high pressure-temperature melting experiments on an SiO₂-rich lamproite from Smoky Butte, Montana: derivation of siliceous lamproite magmas from enriched sources deep in the continental mantle. *J. Petrol.*, 38, 457-477.
12. *Foley, S.F.* 1989. Experimental constraints on phlogopite chemistry in lamproites: 1. The effect of water activity and oxygen fugacity. *Eur. J. Mineral.*, 1, 411-426.
13. *Foley, S.F.* 1990. Experimental constraints on phlogopite chemistry in lamproites: 2. Effect of pressure-temperature variations. *Eur. J. Mineral.*, 2, 327-341.
14. *Gulliver, C.E., Edgar, A.D. and Mitchell, R.H.* 1998. Stability and composition of K-Ti-silicates, K-Ba-phosphate and K-Mg-fluoride at 0.85-2.6 GPa: implications for the genesis of potassic alkaline magmas. *Can. Mineral.*, 36, 1339-1346.
15. *Gunter, W.D., Hoinkes, G., Ogden, P. and Pajari, G.E.* 1990. Origin of leucite-rich and sanidine-rich flow layers in the Leucite Hills volcanic field, Wyoming. *J. Geophys. Res.*, 95 (B10), 15911-15928.
16. *Jaques, A.L. and Foley, S.F.* 1985. The origin of Al-rich spinel inclusions in leucite from leucite lamproites of Western Australia. *Amer. Mineral.*, 70, 1143-1150.
17. *Jaques, A.L., Lewis, J.D. and Smith, C.B.* 1986. Kimberlites and Lamproites of Western Australia. *Geol. Surv. Western Austr.*, Bull.132, 430 pp.
18. *Kostyuk, V.P., Panina, L.I., Zhidkov, A.Ya., Orlova, M.P. and Bazarova, T.Yu.* 1990. Potassium alkaline magmatism of Baikal-Stanovoy rifting system. *PH Nauka, Novosibirsk*, 239pp.
19. *Kuehner, S.M., Edgar, A.D. and Arima M.* 1981. Petrogenesis of the ultrapotassic rocks from the Leucite Hills, Wyoming. *Amer. Mineral.*, 66, 663-677.
20. *Logvinova, A.M. and Sobolev, N.V.* 1995. Morphology and composition of mineral inclusions in chromite macrocrysts from kimberlites and lamproites. *Extended Abstracts Volume of 6th Inter. Kimberlite Conference, Novosibirsk, Russia*, 331-332.
21. *Mikhailov, M.Yu. and Shatsky, V.S.* 1975. Silite heater for high-temperature microthermal stage. *In V.S.Sobolev, ed., Mineralogy of endogenetic formation from inclusions in minerals. Trudy W.Siberian Branch of All-Union Mineral. Soc., Novosibirsk, v. 2*, 109-110.
22. *Mitchell, R.H.*, 1991. Coexisting glasses occurring as inclusions in leucite from lamproites: examples of silicate liquid immiscibility in ultrapotassic magmas. *Mineral. Mag.*, 55, 197-202.
23. *Mitchell, R.H.*, 1995. Melting experiments on a sanidine phlogopite lamproite at 4-7 GPa and their bearing on the sources of lamproitic magmas. *J. Petrol.*, 36, 1455-1474.
24. *Mitchell, R.H. and Bergman, S.C.* 1991. *Petrology of Lamproites*. Plenum Publication, New York, 447 pp.
25. *Mitchell, R.H., Platt, R.G. and Downey, M.* 1987. *Petrology of lamproites from Smoky Butte, Montana*. *J. Petrol.*, 28, 645-677.
26. *Prider, R.T.* 1982. A glassy lamproite from the West Kimberley area, Western Australia. *Mineral. Mag.*, 45, 279-282.
27. *Roedder, E.* 1984. Fluid inclusions. *In P.H.Ribbe, ed., Reviews in Mineralogy, v.12, Mineralogical Society of America*, 644 pp
28. *Ryabchikov, I.D., Solovova, I.P., Sobolev, N.V., Sobolev, A.V., Bogatikov O.A., Aleshin, V.G. and Vashchenko, A.N.* 1986. Nitrogen in lamproitic magmas. *Dokladi AN SSSR*, 288, 976-979.
29. *Salvioli-Mariani, E. and Toscani, L.* 2001. Silicate melt inclusions and phase chemistry in olivine-leucitites of

- Gaussberg. Abstracts of XVI ECROFI, Porto 2001, Portugal, Memória, no. 7, 391-392.
30. *Salvioli-Mariani, E. and Venturelli, G. 1996.* Temperature of crystallization and evolution of the Jumilla and Cancarix lamproites (SE Spain) as suggested by melt and solid inclusions in minerals. *Eur. J. Mineral.*, vol.8, no.5, 1027-1039.
 31. *Salvioli-Mariani, E., Venturelli, G., Toscani, L. and Barbieri, M. 1991.* The Jumilla lamproites, SE Spain: Late magmatic hydrothermal activity (preliminary results). Abstracts of XI ECROFI, Firenze, Italy, *Plinius*, 5, 191-192.
 32. *Sharygin, V.V. 1991.* Chemical composition of melt inclusions in lamproite minerals, Ellendale field, Western Australia. *Soviet Geology and Geophysics*, 32 (11), 54-61.
 33. *Sharygin, V.V. 1993.* Melt evolution during crystallization of hauyne phonolites of East Eifel, W.Germany. *Russian Geology and Geophysics*, 34 (6), 84-95.
 34. *Sharygin, V.V. 1997.* Evolution of lamproites suggested by melt inclusions in minerals. *Russian Geology and Geophysics*, 38 (1), 142-153.
 35. *Sharygin, V.V. 1998.* Melt inclusions and chromite in lamproites from Smoky Butte, Montana. Extended Abstracts of 7th Inter. Kimberlite Conference, Cape Town, SAR, 785-787.
 36. *Sharygin, V.V. and Bazarova, T.Yu. 1991.* Melt evolution features during crystallization of wyomingite, Leucite Hills, USA. *Soviet Geology and Geophysics*, 32 (6), 51-57.
 37. *Sharygin, V.V. and Pospelova, L.N. 1994.* Melt evolution during crystallization of fergusonite-porphyrines, Eastern Pamir. *Russian Geology and Geophysics*, 35 (1), 93-99.
 38. *Sharygin, V.V. and Pospelova, L.N. 1998.* Sulfide inclusions in early lamproite minerals. Extended Abstracts of 7th Inter. Kimberlite Conference, Cape Town, SAR, 794-796.
 39. *Sharygin, V.V. and Vladykin, N.V. 1994.* Physicochemical conditions of lamproites from the Walgidee Hill massif, Western Australia. *Russian Geology and Geophysics*, 35 (4), 59-66.
 40. *Sharygin, V.V., Panina, L.I. and Vladykin, N.V. 1998.* Silicate-melt inclusions in minerals of lamproites from Smoky Butte (Montana, USA). *Russian Geology and Geophysics*, 39 (1), 35-51.
 41. *Sobolev, A.V. 1996.* Melt inclusions in minerals as source of principal petrogenetic information. *Petrologiya*, 4 (3), 228-239.
 42. *Sobolev, A.V., Sobolev N.V., Smith, C.B. et al. 1985.* New data on petrology of olivine lamproites of Western Australia from the results of the investigations of magmatic inclusions in olivines. *Doklady AN SSSR*, 284, 196-201.
 43. *Sobolev, A.V., Sobolev N.V., Smith, C.B. and Dubessy, J. 1989.* Fluid and melt composition in lamproites and kimberlites based on study of inclusions in olivine. *Geol. Soc. Austr. Spec. Publication*, 14, 220-240.
 44. *Sobolev, V.S., Bazarova, T.Yu. and Yagi, K. 1975.* Crystallization temperature of wyomingite from Leucite Hills. *Contrib. Mineral. Petrol.*, 49, 301-308.
 45. *Solovova, I.P., Girmis A.V., Kogarko, L.N. et al. 1989.* Geochemical peculiarities of the Prairie Creek lamproites based on data of study of microinclusions in olivines. *Geokhimiya*, 10, 1449-1459.
 46. *Solovova, I.P., Kogarko, L.N., Ryabchikov, I.D., Naumov, V.B., Girmis, A.V., Kononkova, N.N. and Venturelli, G. 1988.* Spanish high potassium magmas and evidence of their generation depth (as inferred from thermobarogeochemical data). *Doklady AN SSSR*, 303, 182-185.
 47. *Vaggelli, G., Belkin, H.E. and Francalanci, L. 1993.* Silicate-melt inclusions in the mineral phases of the Stromboli volcanic rocks: a contribution to the understanding of magmatic processes. *Acta Vulcanol.*, 3, 115-125.
 48. *Vaggelli, G., De Vivo, B. and Trigila, R. 1993.* Silicate-melt inclusions in recent Vesuvius lavas (1631-1944): II. Analytical chemistry. *J. Volcanol. Geotherm. Res.*, 58, 367-378.
 49. *Venturelli, G., Capedri, S., Di Batistini, G., Crawford, A., Kogarko, L.N. and Celestini, S. 1984.* The ultrapotassic rocks from southeastern Spain. *Lithos*, 17, 37-54.
 50. *Venturelli, G., Capedri, S., Barbieri, M., Toscani, L., Salvioli Mariani, E. and Zerbi, M. 1991.* The Jumilla lamproite revisited: a petrological oddity. *Eur. J. Mineral.*, 3, 123-145.
 51. *Venturelli, G., Toscani, L., Salvioli-Mariani, E. and Capedri, S. 1991.* Mixing between lamproitic and dacitic components in Miocene volcanic rocks of SE Spain. *Mineral. Mag.*, 56, 282-285.
 52. *Wagner, C. and Velde, D. 1986.* The mineralogy of K-richrichterite-bearing lamproite. *Amer. Mineral.*, 71, 17-37.
 53. *Wagner, C. and Velde, D. 1986.* Davanite, $K_2TiSi_6O_{15}$, in the Smoky Butte (Montana) lamproites. *Amer.*

Mineral., 71, 1473-1475.

54. Wagner, C. and Velde, D. 1987. Aluminous spinels in lamproites: occurrence and probable significance. Amer. Mineral., 72, 689-696.
55. Wendlandt, R.F. and Egger, D.H. 1980. The origin of potassic magmas: 1. Melting relations in the systems KAlSiO_4 - Mg_2SiO_4 - SiO_2 and KAlSiO_4 - MgO - SiO_2 - CO_2 to 30 kilobars. Amer. J. Sci., 280, 385-420.
56. Wendlandt, R.F. and Egger, D.H. 1980. The origin of potassic magmas: 2. Stability of phlogopite in natural spinel lherzolite and in system KAlSiO_4 - MgO - SiO_2 - H_2O - CO_2 at high pressures and temperatures. Amer. J. Sci., 280, 421-458.

THE CLASSIFICATION OF MELILITITE CLAN

R.H. Mitchell

*Department of Geology, Lakehead University, Thunder Bay,
Ontario, Canada P7B 5E1*

INTRODUCTION

The melilitite clan includes melilite-bearing rocks formed by the crystallization of melilititic parental magmas under plutonic, hypabyssal and extrusive conditions. The clan does not include kamafugites or melilite-bearing rocks associated with kalsilite-bearing potassic alkaline complexes. Representative examples of the clan are described below in the sequence: melilitites and related melilite nephelinites; melilitolite complexes; melnoites; followed by a brief exposition of current petrogenetic hypotheses proposed for primary melilitite magmas.

MELILITITES

The extrusive facies of the melilitite clan includes melilitites *sensu stricto*, i.e. rocks composed primarily of melilite plus clinopyroxene, and melilite-bearing nephelinites. There is a complete modal and compositional gradation between melilitites, melilite nephelinites and nephelinites, although this does not necessarily imply any simple petrogenetic relationships between the magmas forming these rock types. Increasing amounts of modal melilite are reflected by increasing calcium orthosilicate (larnite) in the CIPW normative composition.

Mineralogy

Melilitites typically consist of phenocrysts of olivine, melilite and clinopyroxene set in groundmass which may contain clinopyroxene, spinel, perovskite, melilite, nepheline, apatite, monticellite and phlogopite. In many examples melilite does not occur as phenocryst and its presence is restricted to the groundmass. Velde and Yoder (1976) have noted that melilite occurs as phenocrysts only when $(\text{Na}_2\text{O} + \text{K}_2\text{O}) > 7.25$ wt.%. Detailed discussion of the composition and paragenesis of the constituent minerals of melilitites is beyond the scope of this paper and comments are provided below for only the major phases.

Olivines in the majority of melilitites exhibit a characteristic skeletal morphology (Fig. 1), and are commonly termed "hopper olivines", with reference to olivines of similar morphology formed experimentally under conditions of rapid crystal growth [Moore and Erlank 1979, Donaldson 1976]. The olivines are forsterite-rich ($\text{mg} = 0.8 - 0.9$) and may comprise a mixed population of low and high pressure phenocrysts plus mantle-derived xenocrysts [Moore 1988, Moore

and Erlank 1979].

Melilite occurs as slender laths which commonly exhibit a median parting. The laths may contain very small optically distinct domains of melilite, termed “peg structures” (Fig. 2), set orthogonal to the parting. The origins of the structures are not well understood and are attributed to sub-solidus decomposition and/or inversion [Yoder 1973]. Melilites may be recognized optically by their common,

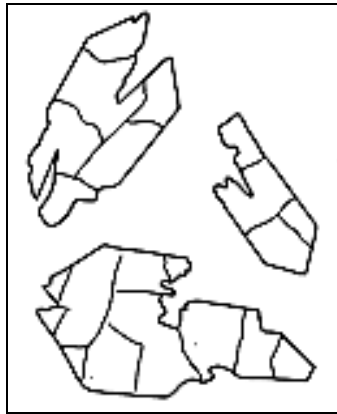


Fig. 1. Camera lucida drawings of skeletal or hopper olivine [Moore and Erlank 1979].

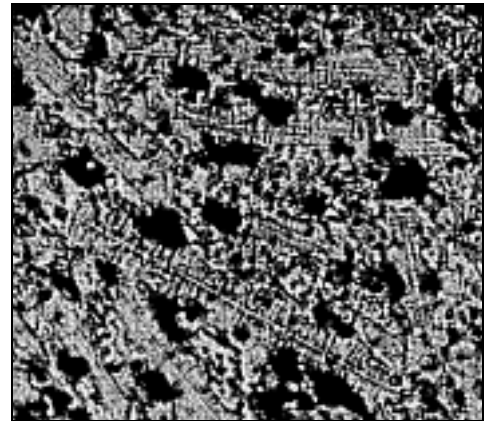


Fig. 2. Peg-structured melilite lath [Yoder 1973]. Field of view is about 200 microns.

but not characteristic, anomalous blue interference colours. Figure 3 shows that most igneous melilites are essentially members of a solid solution between Dkermanite ($\text{Ca}_2\text{MgSi}_2\text{O}_7$) and soda melilite ($\text{CaNaAlSi}_2\text{O}_7$) and that gehlenite ($\text{Ca}_2\text{Al}_2\text{SiO}_7$) contents are typically very low. Melilites are unstable at low temperatures ($<500^\circ\text{C}$) in the presence of water. Consequently, deuteritic fluids commonly cause melilite to be altered to, and/or pseudomorphed by, wollastonite,

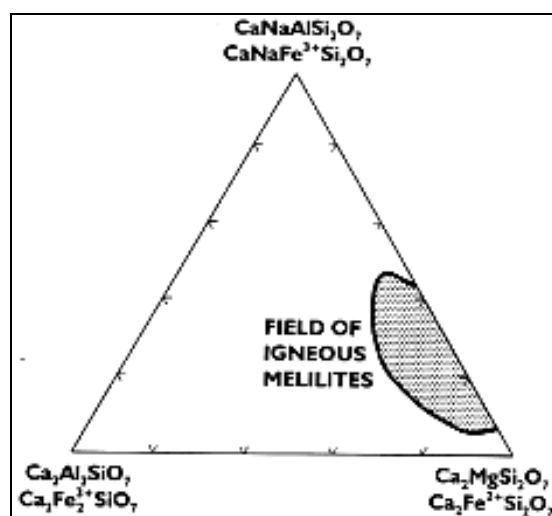


Fig. 3. Compositional range (mol.%) of melilite in igneous rocks [after Yoder 1973, Dawson et al. 1985].

monticellite, calcite, xonotlite [$\text{Ca}_6\text{Si}_6\text{O}_{17}(\text{OH})_2$], cebollite [$\text{Ca}_5\text{Al}_2\text{Si}_3\text{O}_{12}(\text{OH})_4$], vesuvianite, diopside, and hydrogrossular. The characteristic tabular morphology of many melilitites is due to the dominant development of the {001} faces and is commonly preserved during replacement.

Clinopyroxenes are typically titanian aluminian diopsides with very low Na_2O (<1 wt.%), but substantial TiO_2 (1-5 wt.%) and Al_2O_3 (1-10 wt.%) contents. They are essentially members of the solid solution series $\text{CaMgSi}_2\text{O}_6$ (diopside) - $\text{CaTiAl}_2\text{O}_6$ (titan-pyroxene) - $\text{CaAl}(\text{Al},\text{Si})_2\text{O}_6$ (Calcium Tscher-maks's pyroxene).

Composition

Table 1 presents representative bulk compositions of melilitites and shows that they are sodic silica undersaturated (<40% SiO_2) rocks characterised by low alumina and high CaO and MgO contents. Melilitites have high concentrations of Sr, Ba, Nb, Zr and REE relative to common basaltic rocks. REE distribution patterns (Fig. 4) demonstrate that the rocks are strongly enriched in the light REE and that Eu anomalies are not present. A characteristic feature of most melilitites and melilite nephelinites is enrichment in Ni and Cr coupled with **mg** numbers [$(X_{\text{Mg}} / (X_{\text{Mg}} + X_{\text{Fe}})) \cdot 100$] from 65-75; the bulk compositions of such rocks are commonly considered to be representative of their parental primary mantle-derived magmas [Frey *et al.* 1978, see below].

Table 1.

Representative compositions of melilitites.

Wt%	1	2	3	4	5	6	7	8
SiO₂	34.40	36.62	36.74	39.05	38.31	39.97	35.52	38.84
TiO₂	4.92	4.25	2.28	2.41	3.54	1.74	2.78	3.34
Al₂O₃	6.24	7.51	8.02	9.14	10.18	11.15	11.01	9.80
Fe₂O₃	16.78	14.09	10.87	11.30	4.28	4.70	9.82	16.10
FeO	-	-	-	-	7.72	6.11	7.13	-
MnO	0.24	0.20	0.20	0.19	0.19	0.19	0.25	0.21
MgO	15.77	16.74	18.91	18.19	15.20	14.15	11.46	14.31
CaO	14.39	12.83	16.36	13.74	13.16	15.64	12.17	12.32
Na₂O	1.91	3.16	1.94	2.31	2.63	3.00	4.84	2.28
K₂O	2.03	2.07	0.68	1.21	0.96	1.32	1.72	1.08
P₂O₅	1.76	0.91	0.86	0.70	0.75	0.87	1.05	0.65
CO₂	-	-	-	-	-	-	0.26	-
H₂O+	0.12	1.24	-	-	2.20	-	0.58	-
LOI	1.45	0.26	2.40	1.20	-	0.30	-	-
Total	100.01	99.88	99.26	99.44	99.19	99.14	98.59	98.93
Ni	232	425	563	545	379	273	230	357
mg#	0.70	0.75	0.78	0.76	0.70	0.73	0.72	0.78

Note. 1, 2, Garies and Gamoep, respectively [Rogers *et al.* 1992]; 3, 4, Urach and Hegau, respectively [Wilson *et al.* 1995]; 5, Balcones [Barker *et al.* 1987]; 6, Freemans Cove [Mitchell and Platt 1984]; 7, Honolulu [Clague and Frey 1982]; 8, Koloa [Maalte *et al.* 1992].

OCCURRENCE OF MELILITITES

Melilitites are typically found in intra-plate tectonic settings. They may be associated with either rift structures or lineaments, and are not exclusively confined to continental settings. Melilitites may be grouped into:

1. Melilitites occurring as minor members of volcanic suites dominated by either basalts or nephelinites. Examples include: Hawaiian Islands [Maalre *et al.* 1992, Clague and Frey 1982]; Canary Islands [Hoernle and Schmincke 1993]; Ahaggar massif, Algeria [Dautria *et al.* 1992], south eastern Australia-Tasmania

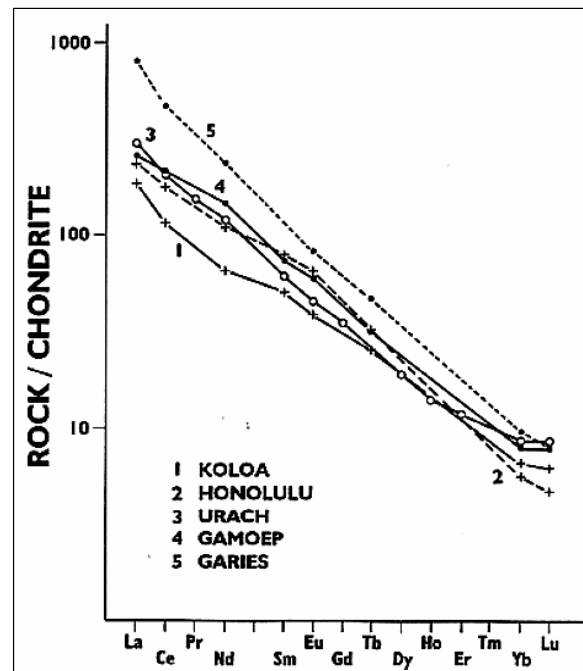


Fig. 4. Representative chondrite normalised REE distribution patterns for diverse melilitites.

*Data sources: 1, Koloa [Clague and Dalrymple 1988]; 2, Honolulu [Clague and Frey 1982]; 3, Urach [Wilson *et al.* 1995]; 4 - 5, Gamoep and Garies, respectively [Rogers *et al.* 1992].*

[Frey *et al.* 1978]; Freemans Cove, Canada [Mitchell and Platt 1984]; Gregory Rift, Kenya-Tanzania [Williams 1970, Dawson *et al.* 1985]; Rhine Graben [Wimmenauer 1974]. Suites occurring in a continental setting are commonly associated with phonolites.

2. Petrological provinces in which melilitites are the sole or volumetrically-dominant extrusive and/or subvolcanic rock type. Examples include: Balcones province, Texas [Spencer 1969] Namaqualand, South Africa [Moore and Verwoerd 1985]; Sutherland area, South Africa [De Wet 1975]; Eshowe, South Africa [Colgan *et al.* 1989]; the Urach and Hegau volcanic districts, Germany [Brey 1978]; Plou...nice, Czech Republic [Ulrych *et al.* 1988]; Missouri River Breaks [Hearn 1968]; Hudson Bay Lowlands [Janse *et al.* 1989]; the Terskii Coast of the Kandalaksha graben [Kalinkin *et al.* 1993]; Maimecha-Kotui province,

Siberia [Egorov 1970, Kogarko *et al.* 1995]; north-eastern Anabar province [Kovalskii *et al.* 1969], Malaita, Solomon Islands [Nixon *et al.* 1980]. This group of melilitites, with the exception of some oceanic Hawaiian examples, typically have lower silica contents than those associated with basaltic volcanism *sensu lato* (Table 1). Diatremes are common in these volcanic fields.

Representative examples of each group are described below, in order to illustrate some aspects of the petrological variation found within and between melilitite-bearing provinces.

Although there are some similarities, the overall differences are so significant that it is considered premature to conclude that a common petrogenetic scheme can be applied to all occurrences.

KOLOA AND HONOLULU VOLCANIC SERIES

Hawaiian volcanoes are characterized by three stages of activity: an initial shield building stage, represented by the rapid eruption of voluminous tholeiitic basalts; eruption of post-shield alkali basalts comprising less than 1% of the

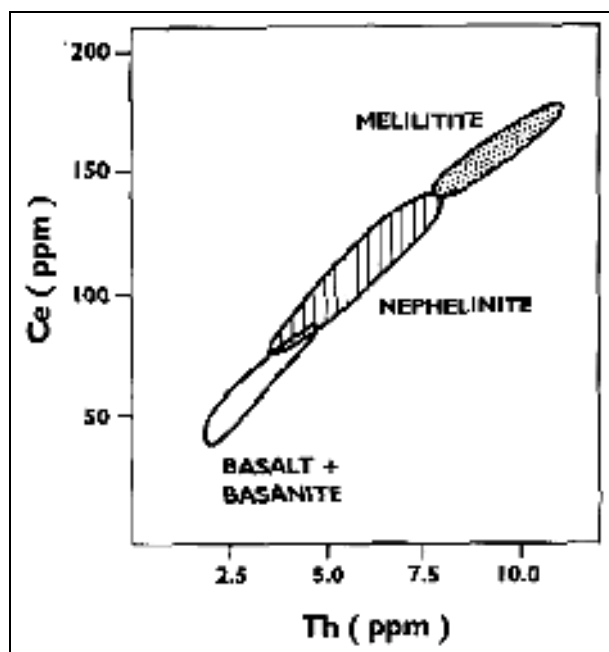


Fig. 5. Ce versus Th abundances of Honolulu Volcanic Series [after Clague and Frey 1982].

volume of the volcanoes; and after a period of quiescence, small amounts of very undersaturated magmas erupted as lavas and tuffs from short lived vents scattered along the flanks of the shield. Termed the “post-erosional series”, these latter magmas are exemplified by the basanites, olivine nephelinites and olivine melilitites of the Koloa (Kauai) and Honolulu (Oahu) Volcanic Series [Clague and Dalrymple 1988, Clague and Frey 1982].

The melilitites form small flows and pyroclastic deposits, the style of

volcanism being sub-aerial Hawaiian. Curiously, the nephelinites and melilitites have apparently not been subjected to detailed modern mineralogical studies, although some data for nephelinites are given by Mansker *et al.* (1979) and Wilkinson and Stolz (1983). The latter show that olivine melilite nephelinite from Moiliili (Oahu) contains phenocrysts of olivine set in a fine grained microphenocrystal groundmass of clinopyroxene, nepheline, titanomagnetite, melilite, olivine, sodalite and apatite. Clague and Dalrymple (1988) note that the rocks are mainly aphyric and holocrystalline. Compared to other melilitite provinces, the major characteristics of the Hawaiian melilite-bearing suites are the very small amounts of undersaturated rocks relative to those of associated basaltic rocks and the absence of diatremes, hypabyssal carbonate-rich rocks and phonolites. With regard to the latter, Wilkinson and Stolz (1983) have demonstrated that Hawaiian olivine melilite nephelinite cannot differentiate to phonolitic residua.

Geochemical studies of the Honolulu and Koloa volcanic suites [Clague and Frey 1982, Clague and Dalrymple 1988, Maalre *et al.* 1992] have demonstrated that most rocks have major element compositions indicating derivation from mantle-derived primary magmas, i.e. **mg**-numbers >65 and Ni > 200-250 ppm (Table 1). Incompatible trace element abundances show systematic variations with rock type, thus La/Yb ratios increase in the sequence; tholeiite (4), alkali basalt (12), nephelinite (18), melilitite (33), with increasing light REE abundances being directly correlated with increasing P and Th contents. Linear correlations exist between the abundances of highly incompatible elements such as Nb and P or Ce and Th (Fig. 5). These data are interpreted to indicate that the melilitites cannot be formed by the extensive fractional crystallization of a basaltic or nephelinite parental magma. Rather, Clague and Frey (1978) have concluded that the rocks represent the products a partial melting sequence, and suggest on the basis of trace element modelling that as the degree of melting of the mantle source *decreases*, the melts produced become richer in Ca, Ti, P, Th, REE and poorer in Si and Al. On the basis of Th abundances, Clague and Frey (1982) have concluded in the case of the Honolulu Volcanic Series the degree of melting of the source ranges from 2% for the nephelinite melilitite to 11% for alkali basalt and basanite. Sr, Nd and Pb isotopic compositions of the rocks indicate that they were formed from upper mantle-derived magmas (Fig. 6). Although the isotopic variation is not large, within the Kauai lavas, there is a trend of increasing $^{143}\text{Nd}/^{144}\text{Nd}$ and decreasing $^{87}\text{Sr}/^{86}\text{Sr}$ with decreasing SiO_2 content [Clague and Dalrymple 1988]. The post-erosional lavas are enriched in radiogenic ^{143}Nd and depleted in radiogenic ^{87}Sr relative to Hawaiian tholeiites. These differences, coupled with significant intra-formation and inter-island differences in isotopic compositions, indicate that mixing of material from several distinct sources must have been involved in establishing the isotopic signature of any given sample. Opinions differ as to the nature of these sources and the extent of mixing. Because of the association of the Hawaiian Islands with a mantle plume or hot spot, Clague and Frey (1982), Chen

and Frey (1985), and Clague and Dalrymple (1988) have favoured mixing between large volume melts of a plume-type source with small amounts of incipient melts of a heterogeneous MORB source. In contrast, Maalre *et al.* (1992) claim that MORB sources are not involved in the generation of the magmas and that all are derived from a zoned plume, whereas Stille *et al.* (1983) claim derivation from a highly depleted MORB-like source.. While discussion of these diverse hypotheses is beyond the scope of this paper, it is significant that all geochemical and isotopic studies have concluded that Hawaiian melilitites are undifferentiated low degree partial melts of a mantle source material.

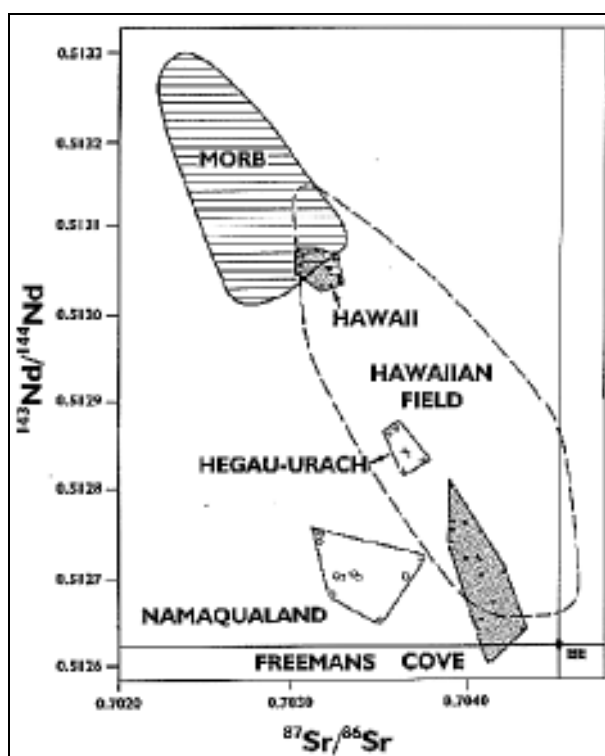


Fig. 6. Sr and Nd isotopic composition of some melilitites and related rocks.

Hawaiian post-erosional volcanics of the Koloa and Honolulu series [Maalre *et al.* 1992, Feigenson 1984, Stille *et al.* 1983]; Freemans Cove suite [Mitchell and Platt, unpub], Garies and Gamoep melilitites [Rogers *et al.* 1992]; Hegau-Urach melilitites [Wilson *et al.* 1995]. Fields for MORB and all Hawaiian lavas from Chen and Frey (1985). BE = Bulk Earth.

FREEMANS COVE SUITE

The Tertiary (46 Ma) Freemans Cove volcanic suite of Bathurst Island (Canada) consists of 5 agglomeratic vents, approximately 75 dikes and small plugs together with several sills [Mitchell and Platt 1983, 1984]. Lava flows are absent at the present level of erosion although lava fragments, bombs and scoria are common as clasts within the agglomerates. Stratovolcanoes, subaerial pyroclastic deposits, diatremes and carbonate-rich rocks are absent. The province consists primarily of olivine nephelinites and basanites with minor amounts of olivine melilite nephelinite, basalt (tholeiitic and alkaline) and phonolite.

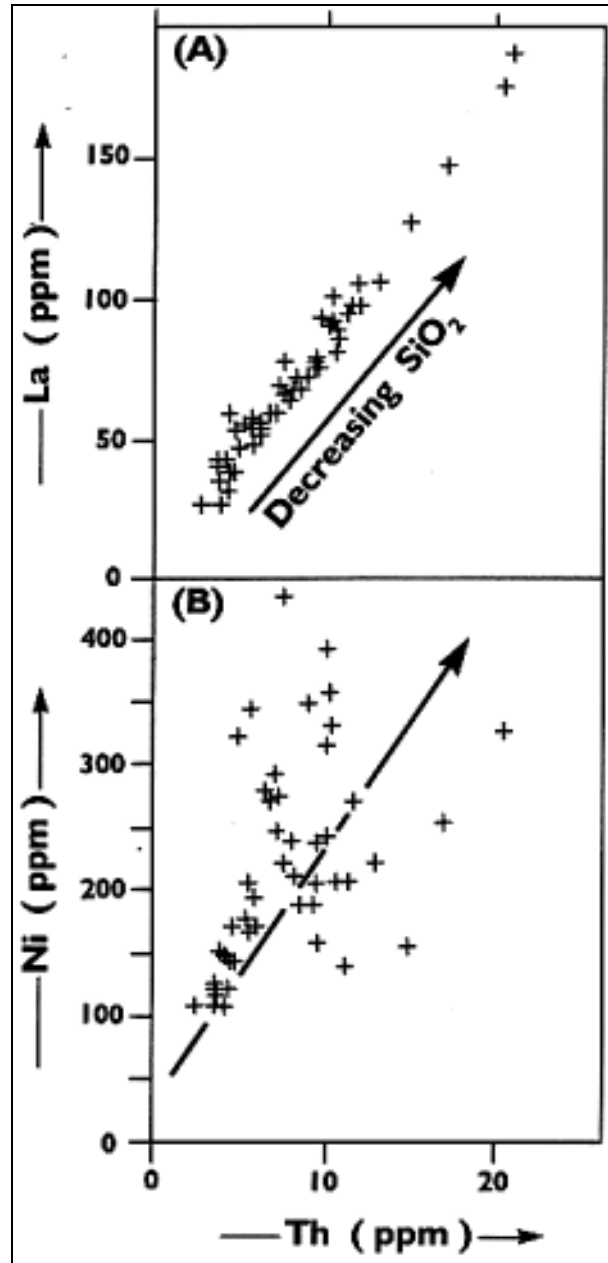


Fig. 7. Trace element abundance variation in the Freemans Cove Volcanic Suite.
 (A) La versus Th (B) Ni versus Th (All data Mitchell and Platt, unpub.).

The nephelinites contain phenocrysts of forsteritic olivine and Ti-Al diopside set in a groundmass of Ti-Al diopside, spinel, nepheline, apatite, Ti-Ba-rich phlogopite, zeolite and glass. Melilite occurs as colourless laths in melilite bearing examples. Nephelinites form two groups based on the presence or absence of normative larnite; melilite-bearing types (Table 1) are associated with the latter.

The melilite nephelinites, nephelinites and basanites have **mg** numbers and Ni contents characteristic of mantle-derived primary magmas and cannot be related to each other or the basaltic rocks by fractional crystallization processes. REE

contents, La/Yb ratios and incompatible trace element abundances increase in the sequence basalt, basanite, nephelinite, larnite normative nephelinite, melilite nephelinite. Incompatible elements exhibit systematic correlations (Fig.7A) similar to those observed for the Honolulu [Clague and Frey 1982] or S.E. Australian

[Frey *et al.* 1978] volcanic suites. Fig. 7B shows that rocks with high Ni contents also have high Th contents, a geochemical signature that is inconsistent with Th-enrichment by fractional crystallization. On the basis of these data, Mitchell and Platt (1984) have suggested that the suite formed from a series of primary magmas derived by the sequential partial melting of a common upper mantle source. The basalts may represent extensive partial melts of this source but have undergone some fractionation and/or crystal accumulation during emplacement. REE distribution patterns lack Eu anomalies indicating that the nephelinites and phonolites cannot be differentiates of the basanites, although the phonolites may be derived by high pressure fractionation of primary nephelinitic magmas.

Sr and Nd isotopic studies [Mitchell and Platt, unpub., Fig. 6) indicate that Freemans Cove magmas were derived from mantle that has experienced long term depletion of LREE and Rb relative to bulk Earth. However, their sources are not as depleted as those of the Hawaiian post -erosional volcanics. The data may be interpreted to suggest that the Freemans Cove magmas record a local asthenospheric signature or represent mixing between a Hawaiian-type or MORB-type source and a lithospheric mantle component.

The paucity of associated basaltic magmatism and presence of phonolites are notable differences between this and the Hawaiian Province; implying significant differences in the partial melting regimes and style of magma emplacement between the two provinces. Consequently, petrogenetic models advanced for Hawaiian undersaturated volcanism are unlikely to be relevant to this province.

The Freemans Cove suite is an example of intraplate magmatism associated with continental rifting [Mitchell and Platt 1983]. There is no compelling geological evidence, e.g. contemporaneous flood basalts, to indicate that magmatism was directly related to the melting of a mantle plume, Although extensive, possibly plume-related tholeiitic magmatism occurred earlier (58 Ma) in the Baffin Bay area it is considered that this was too remote from Bathurst Island (>500 miles) to have been involved in the genesis of the Freemans Cove suite. Mitchell and Platt (1984) have suggested that Freemans Cove magmatism was initiated by decompressional melting of a metasomatized lithospheric mantle source in response to tectonic uplift. However, this scheme is difficult to reconcile with the Sr and Nd isotopic data regarding the nature of the source.

BALCONES PROVINCE

The 67-86 Ma rocks of the Balcones Province occur as over 200 volcanic centres in a 400 km-long belt stretching from south west of Uvalde to northeast of Austin, Texas [Spencer 1969, Barker *et al* 1967]. The centres lie parallel to the

northern limit of the Ouachita fold belt. The rocks present include hypabyssal intrusive, extrusive and pyroclastic units. Stratovolcanoes and diatremes do not appear to be present, although submarine hydrovolcanic activity occurred at some of the vents. Most of the Balcones volcanoes are currently buried beneath younger coastal plain sediments.

The province is dominated by melilite olivine nephelinites. Rock types in order of increasing abundance are nepheline basanite, phonolite, alkali basalt, olivine nephelinite and melilite olivine nephelinite. Details of the petrography of the rocks are given by Spencer (1969). The majority of the melilite olivine nephelinites contain phenocrysts of olivine and titanite set in a groundmass of titanite, melilite, nepheline, spinel, apatite and perovskite. The basaltic rocks are found primarily in the Austin area, whereas the expression of the activity in the Uvalde area is bimodal phonolite-melilite olivine nephelinite volcanism.

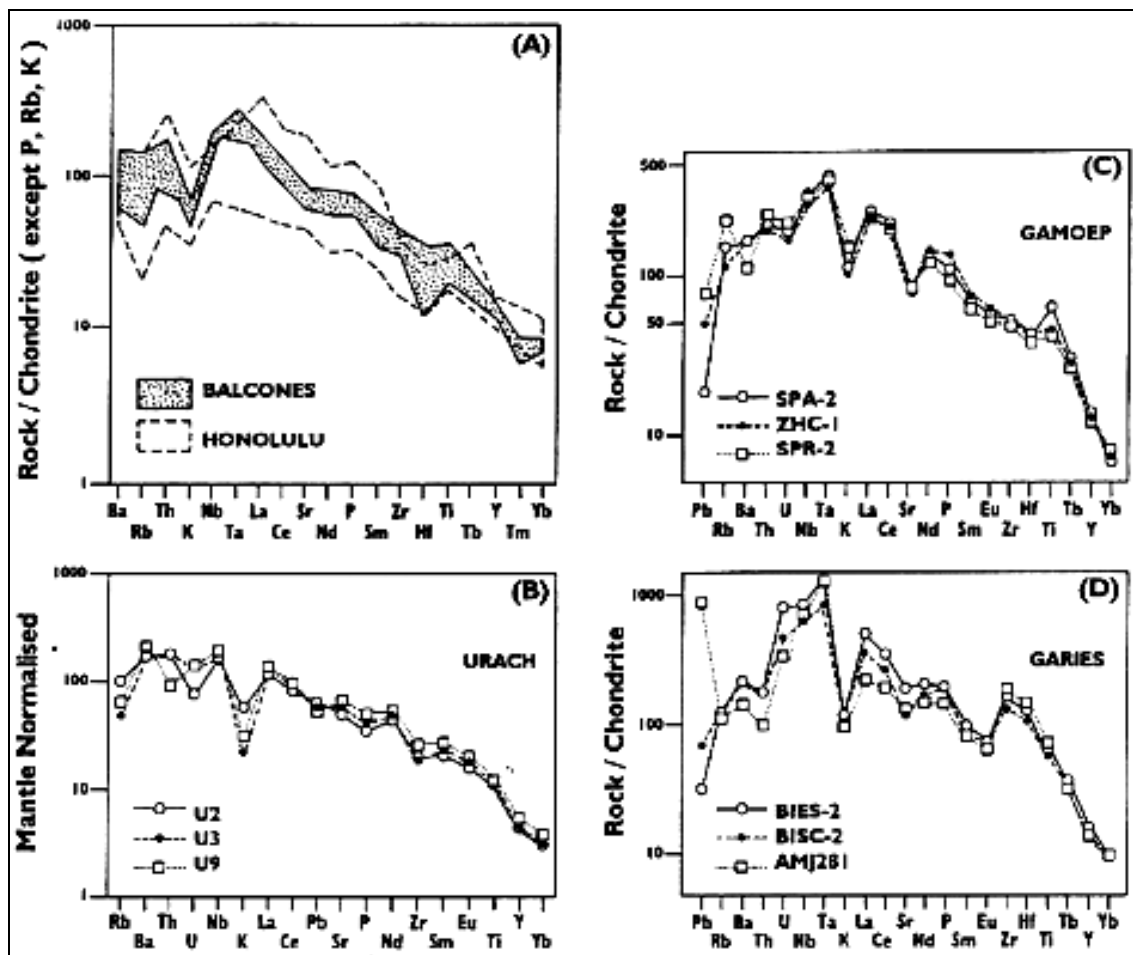


Fig. 8. Mantle or chondrite normalised incompatible trace element distribution diagrams (A) Balcones [Wittke and Mack 1993] and Honolulu [Clague and Frey 1982]; (B) Urach [Wilson et al. 1995]; (C) and (D) Gamoep and Garies [Rogers et al. 1992]. Note the significant K anomaly present in all examples and the Sr anomaly present only in the Namaqualand suite.

The melilite olivine nephelinites, olivine nephelinites and basanites have

major element compositions and Ni contents (Table 1) suggesting that they are unmodified primary partial melts of the upper mantle. Incompatible trace element abundances and LREE enrichment increase in a trend consistent with decreasing degrees of partial melting of the source from basalt to melilite olivine nephelinite [Barker *et al.* 1987, Wittke and Mack 1993]. Even though erupted in a continental environment, the nephelinites are considered by Wittke and Mack (1993) to display no signs of a lithospheric or subduction trace element or isotopic signature, as Figure 8 shows that the trace element signature is identical to that of the Honolulu Volcanics and Ti-Nb-Ta anomalies are absent. Sr and Nd isotopic studies suggest that the parental magmas were derived from sources with time integrated LREE depletion, and Wittke and Mack (1993) propose derivation of the magmas by variable degrees of partial melting of an asthenospheric garnet lherzolite source that was slightly less depleted than the source of N-type MORB and comparable to that of oceanic island basalts (OIB). Pb isotopic studies [Wittke and Mack 1993] demonstrate clearly that interaction of the magmas with the crust was negligible.

The Balcones province is obviously very different in character to the Hawaiian post-erosional series and although considered to be mantle-derived there is no direct geological evidence for the participation of a mantle plume in the genesis of the rocks. The province is similar in some respects to the Freemans Cove suite but differs in that melilite-bearing rocks are dominant. If derived from a similar source this difference must reflect a different melting regime.

HEGAU - URACH VOLCANIC FIELDS

The basalt-free Hegau and Urach volcanic fields [Keller *et al.* 1990, Wimmenauer 1974, Engelhardt and Weiskirchner 1963] which may be regarded as transitional to phonolite- and basalt-free melilitite provinces (Namaqualand, Hudson Bay Lowlands, Terskii Coast), consist of very Si-poor melilitites (Table 1), associated with minor amounts of phonolite. Activity resulted in the formation of both intrusive and extrusive (lavas and pyroclastics) rocks and, particularly in the Urach region, is characterized by diatreme formation (see below).

Detailed modern mineralogical studies have not been undertaken and investigations have been concerned primarily with volcanology and/or geochemistry of the rocks [Cloos 1941, Brey 1978, Wilson *et al.* 1995]. In common with other melilitite occurrences, the rocks are characterised by high **mg**-numbers and Ni contents together with enrichment in incompatible elements, especially Ba (100-150 ppm), Nb (100-140 ppm) and LREE (150-175 ppm Ce). Trace element signatures have significant K anomalies (Fig. 8), suggesting the presence of a residual potassic phase such as phlogopite in their sources. Sr and Nd isotopic compositions (Fig. 6) indicate derivation from depleted mantle sources. Compared to the Freemans Cove provinces the magmas are derived either from more depleted mantle and/or contain smaller amounts of OIB-type or lithospheric sources mixed with MORB-type source material.

NAMAQUALAND

The Namaqualand province [Moore and Verwoerd 1985] represents the extreme of the melilitite-bearing provinces in that it consists entirely of extremely silica-poor melilitites. Although, previous publications [Moore and Erlank 1979, Taljaard 1937] state that kimberlites occur in the province, it is now evident that the most of these rocks are altered or inadequately characterized melilitites [Mitchell 1986, 1995].

The province consists entirely of pipe-like intrusions and sediment-filled diatremes (see below), and is divisible into two fields; the northern older (59-77 Ma) Gamoep cluster and the younger (54-56 Ma) smaller Garies cluster, located 80 km to the southwest [Moore and Verwoerd 1985]. Although the Gamoep melilitites have enhanced MgO contents (Table 1) due to olivine accumulation, both they and the Garies melilitites appear to have formed from primary undifferentiated magmas derived from depleted mantle. Their sources appear to be depleted in Rb relative to those defining the main mantle array of Sr and Nd isotopic compositions upon which the majority of other melilitites lie (Fig.6). Melilitites in each cluster are distinct in their major and trace element characteristics [Rogers *et al.* 1992; fig. 9]. These differences do not result from differentiation processes and Rogers *et al.* (1992) suggest that the Garies cluster melilitites are derived by smaller degrees of partial melting of the same source as those of the Gamoep cluster. If Nb/Y ratios are indicative of the relative degrees of partial melting involved in the genesis of melilitites, it would appear that the Garies melilitites, with Nb/Y ratios typically greater than 7, represent the least degree of partial melt extracted from the mantle sources of all melilitite provinces.

MELILITITE PRIMARY MAGMAS

From the above data, it is apparent that undifferentiated primary melilitite magmas are commonly erupted either as components of a partial melting sequence or as discrete episodes of melilitite magmatism. In all instances small degrees of partial melting of a mantle source that has undergone long term depletion in Sm and Rb relative to bulk Earth are required by the isotopic and trace element data. Isotopic characteristics may reflect those of discrete asthenospheric mantle sources or mixing between material derived from MORB- and OIB-type sources with or without lithospheric contamination. There is no unique primary melilitite magma composition, rather there exists a range of compositions which, in general, become poorer in incompatible trace elements, CaO and MgO and richer in SiO₂ as the extent of partial melting of the source increases (Figs. 9 and 10). The compositions listed in Table 1 represent the spectrum of primary melilitite magmas which might be expected to undergo differentiation in hypabyssal and plutonic environments. This variation may explain the wide variety of rock types observed in diverse melilitolite complexes.

LOW PRESSURE DIFFERENTIATION

It is significant that low pressure (1-2 kb) differentiates are typically absent from melilitite provinces. Where differentiation has occurred (Balcones, Hegau-Urach) it has apparently taken place at relatively high pressures (5 kb?), with kaersutite fractionation leading to the generation of some types of phonolite, but

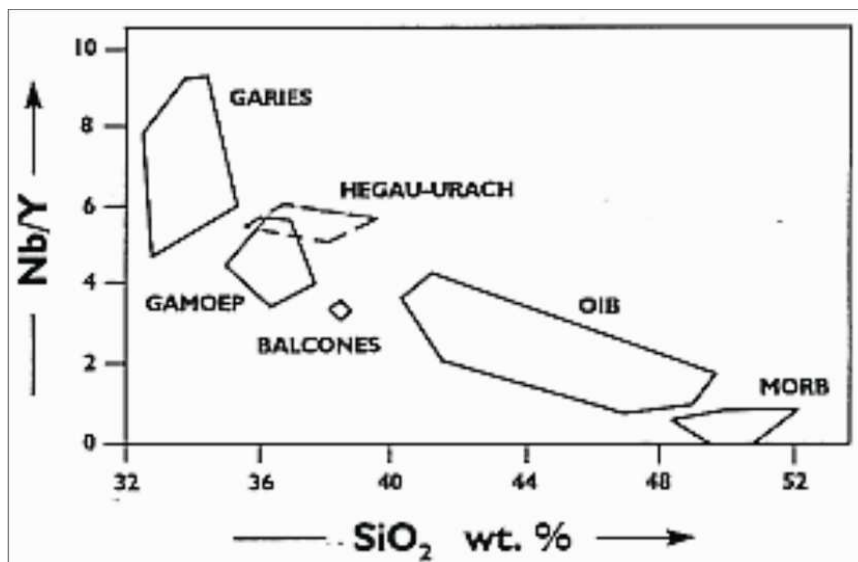


Fig. 9. *Nb/Y versus SiO₂ for Namaqualand [Rogers et al.1992], Hegau-Urach [Wilson et al. 1995], Balcones [Barker et al. 1987] melilitites.*

Data for oceanic island (OIB) and mid-oceanic ridge (MORB) basalts from Rogers et al. 1992].

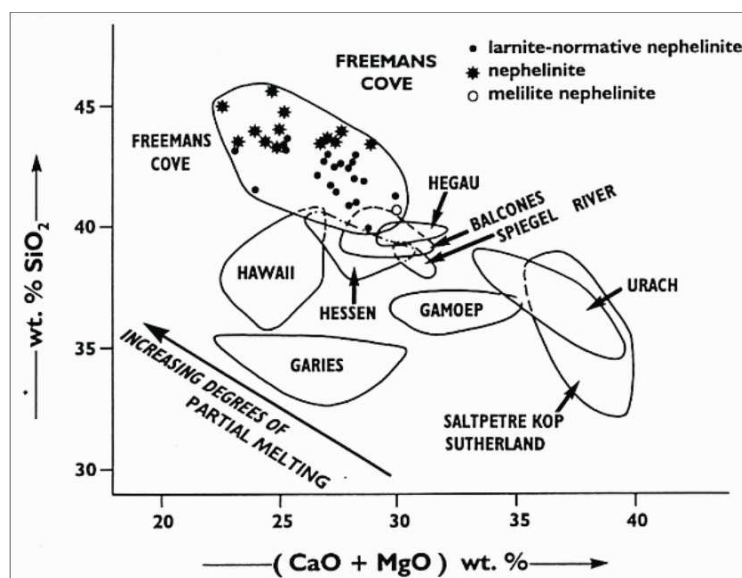


Fig.10. *(CaO + MgO) versus SiO₂ for melilitites and melilite nephelinites [after Brey 1978 and Mitchell and Platt (1984), with additional data for Hawaii from Maalte et al. (1992), Wilkinson and Stolz (1983) and Clague and Frey (1982). Data for Garies and Gamoep from Rogers et al (1992).*

without the formation of magmas of intermediate compositions [Barker *et al.* 1987]. The formation of large stratovolcanoes or long-lived, continuously replenished, fractionating magma chambers does not seem to be typical of melilitite volcanism, although both are characteristic features of nephelinitic volcanism. These differences may be related to the small volume of melilititic magmas coupled with their rapid emplacement as volatile-rich magmas. The reasons for the absence of low pressure intermediate and evolved lavas of the clan remain as yet poorly understood.

Experimental studies of the low pressure crystallization paths of natural olivine melilitites of the Urach or Namaqualand type have apparently not yet been undertaken. With regard to melilite nephelinites and olivine nephelinites, considerable experimental work has been undertaken on synthetic systems [Onuma and Yagi 1967; Platt and Edgar 1972; Gupta *et al.* 1973; Onuma and Yamamoto 1976, Yoder 1979; Pan and Longhi 1990] but very little information is available on the low pressure crystallization paths of natural samples [Gee and Sack 1988, Wilkinson and Stolz 1983]. The study of Gee and Sack (1988) although of importance in establishing some critical phase relationships between olivine, melilite and liquid, is not directly relevant to sodic melilitites, as the study investigated a strongly potassic rock composition.

Peterson (1989) has summarized the experimental studies, applied them to nephelinitic volcanism and suggested that two differentiation trends (Fig. 11) may be possible in sodic undersaturated liquids: (1) olivine nephelinite to nephelinite; (2) olivine melilite nephelinite (or melilitite) ! melilite nephelinite ! wollastonite nephelinite ! combeite nephelinite. The first trend is considered to be exemplified by Shombole and other mildly peralkaline nephelinite volcanoes in the Gregory Rift. The second trend is exceedingly rare and is exemplified by the strongly peralkaline lavas of Oldoinyo Lengai. Although both trends may lead to phonolitic residua, Wilkinson and Stolz (1983) have shown that low pressure fractionation of Hawaiian olivine melilite nephelinite leads to the formation of very small amounts of residual melilite-bearing nephelinite but not phonolites.

The relevance of these studies to melilitite provinces is debatable. There is no doubt that the east African nephelinite differentiation trends suggested by Peterson (1989) are realistic, but it is questionable whether volumetric relationships actually have permitted trend 2 to occur, as olivine melilitites are volumetrically insignificant compared to the nephelinites. Their limited abundance is in accord with them being very small partial melts. Thus, perhaps of greater significance is the possibility that each batch of the spectrum of primary melts generated by sequential partial fusion would have the opportunity to differentiate. Hence, the rare olivine melilitites need not necessarily be the antecedents of the nephelinites, and petrological relationships in the Gregory Rift may be more complex than the hypotheses of Peterson (1989), Peterson and Kjarsgaard (1995) and Kjarsgaard *et al.* (1995) suggest.

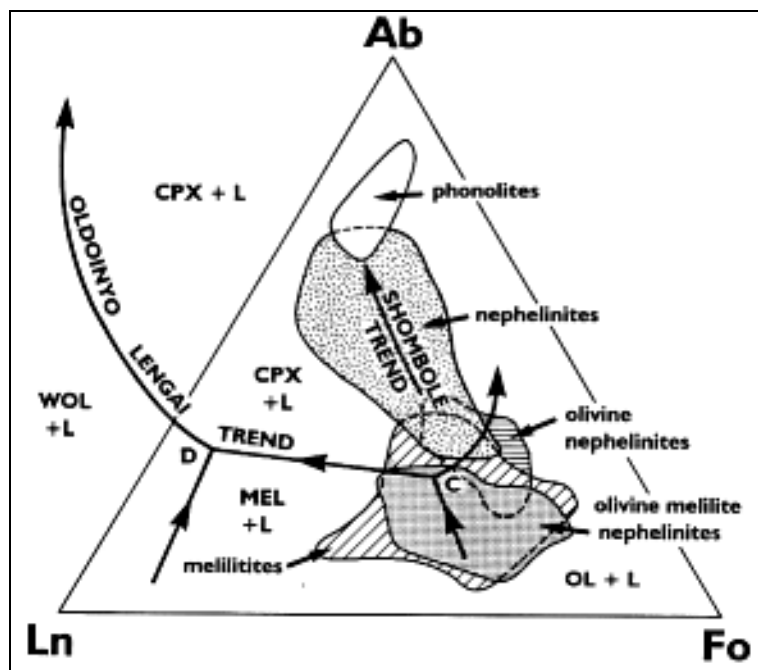


Fig. 11. Projection of the compositions of alkaline ultramafic lavas onto the plane Ab-Ln-Fo in the quaternary system Ne-Ab-Ln-Fo, together with the cotectics, liquidus phases and nephelinite crystallization trends postulated by Peterson (1989).

Point C is a distributary reaction point, involving olivine or melilite, which determines the crystallization trend followed. D is reaction point on the Oldoinyo Lengai trend at which melilite reacts with liquid to form wollastonite. All liquidus phases may co-exist with nepheline. WOL = wollastonite; CPX = clinopyroxene; Ol = olivine; MEL = melilite; L = liquid. [after Peterson 1989].

The formation of a sequence of partial melts does permit melilitites and nephelinites to co-exist within a province, although the geochemical data indicate that consanguineous olivine nephelinites cannot be differentiates of melilitites (or basanites) and *vice versa*. Differences between provinces such as the Gregory Rift and Namaqualand may simply reflect the cessation of the partial melting process in sources of the latter before nephelinites were produced. In this instance tectonic reasons must be sought to explain the discontinuation of melting. However, other possibilities such as derivation of the provinces from different sources and depths cannot as yet be excluded. Regardless, significant volumes of melilititic magma must have been involved in the formation of the Hegau-Urach and Namaqualand provinces and their failure to undergo low pressure differentiation along Peterson's (1989) trend 2 remains inexplicable.

DIATREME FACIES MELILITITE

Whereas phreatomagmatic vents are typical of the melilitites associated with basalts and nephelinites (Balcones, Freemans Cove, Hawaii), the formation of diatremes appears to be a characteristic style of magmatism associated only with more silica-poor melilititic magmas (Hegau, Urach, Eshowe, Namaqualand, Avon, etc). The Urach melilitite field may be regarded as the type locality for diatremes,

the initial detailed descriptions of their structures being given by Cloos (1941). As the volcanology of most melilitite provinces has been insufficiently investigated, it is not known if diatreme formation is a style of emplacement that is intrinsic to these magma types, or is merely a local phenomenon..

Diatremes are sub-volcanic intrusions whose origins are not well-understood. To reflect the association of diatremes with a variety of magma types, Mitchell (1986, p.74) has defined diatremes as “cone shaped, downward tapering, inclined or vertical structural units (intrusions), composed wholly or partly of angular, or rounded, clasts of cognate or xenolithic origin, with or without a matrix. Xenolithic clasts maybe derived from the walls or roof of the body. They are commonly well mixed and some xenoliths have apparently sunk within the diatreme”. Diatremes are volcanic features associated with volatile-rich magmatism commonly of an ultrabasic composition. Note that the term “diatreme” is not synonymous with “volcanic vent” and that the rocks comprising diatremes are not described as agglomerates. According to modern textural-genetic classifications [Clement and Skinner 1985, Mitchell 1995], rocks occurring in diatremes are described as diverse volcanoclastic rocks belong to the diatreme facies of the particular magma type involved in diatreme formation, e.g. volcanoclastic melilitite breccia, autolithic volcanoclastic kimberlite breccia.

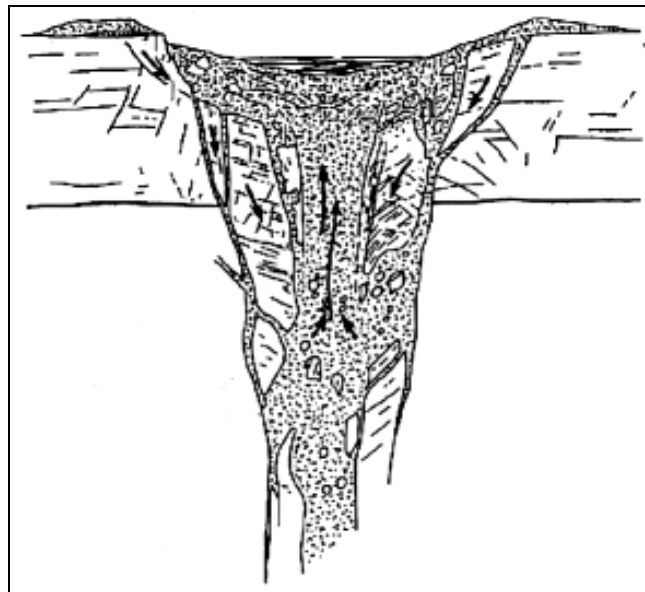


Fig. 12. Cross-section of the Jussi diatreme, Urach volcanic field [after Cloos 1941].

6] have demonstrated that there are such significant differences in the structure and contents of diatremes associated with kimberlites and melilitites that they are unlikely to have formed by similar processes. Diatremes which are similar in structure to melilitite diatremes are also formed in association with the phreatomagmatic eruption of some volatile-rich alkali basaltic magmas [Lorenz 1975, 1984], however it is as yet unknown whether melilitite diatremes were formed by the same processes.

Fig. 12 presents a cross-section through a typical melilitite diatreme from the Urach volcanic field. In this field diatremes range in diameter from a few tens of metres up to 1.2 km.

Significant characteristics of the diatremes in this and other melilitite provinces are: (1) the presence of pyroclastic and resedimented volcani-clastic rocks (epiclastic) in bowl-shaped depressions (crater facies rocks) at the top of the diatreme; (2) characteristic presence of autoliths and pelletal lapilli (see below); (3) permeation of highly mobile (fluidized?) tuffaceous/pyroclastic material into fractures and around displaced blocks of country rock; (4) marginal subsidence and downward transport of earlier erupted pyroclastics and detached country rock blocks; (5) late stage intrusion of hypabyssal rocks into the central conduit of the diatreme, with in some instances lava lake formation in the subsiding crater; (6) occurrence in thick sequences of highly porous and permeable sedimentary rocks.; (7) association with hydraulically active fault zones and lineaments. Detailed descriptions of melilititic diatremes may be found in Cloos (1941), Hearn (1968), Lorenz (1975, 1984), Clement (1982) and Mitchell (1986).

Pelletal lapilli are characteristic components of diatreme facies rocks. These consist of discrete spherical-to-elliptical, lapilli-sized (2-64mm) clasts consisting of fine grained igneous material. The lapilli commonly contain at their centres, a single relatively large euhedral crystal or crystal fragment. This core or kernel consists typically of olivine (fresh or pseudomorphed) and less commonly of phlogopite or other minerals. Country rock clasts very rarely form the cores of lapilli and juxtaposed country rock clasts are typically devoid of igneous mantles.

The mantles consist of fine grained melilitite or aln'ite. Microphenocrysts of melilitite and olivine are commonly tangentially orientated around the kernel of the lapillus and a poor-to-well developed concentric structure may be evident. Pelletal lapilli are *not* equivalent to accretionary lapilli found in subaerial pyroclastic deposits. The origins of pelletal lapilli remain the subject of considerable debate. Currently, they are believed to represent magma droplets formed by the explosive fragmentation or frothing of magma due to the rapid expulsion of dissolved volatiles [Clement 1982] or interaction of magma with groundwater [Lorenz 1979, Mitchell 1986].

Discussion of the genesis of diatremes is beyond the scope of this work but detailed information on this topic may be found in: Lorenz (1975, 1979, 1984); Clement (1982); Clement and Reid (1989); and Mitchell (1986, 1995). Hypotheses fall into two major groups; emplacement by either fluidized intrusion (volatile escape) with no or minor hydrovolcanic components or hydrovolcanic processes (phreatomagmatism and fluid-coolant interactions) dominate and fluidization is not significant. Hydrovolcanic processes seem applicable to most alkali basaltic and many melilititic diatremes but are not entirely satisfactory for kimberlitic diatremes. Fig. 13 illustrates the formation of a diatreme according to the hydrovolcanic model of Lorenz (1975, 1984).

The association of diatremes with CO₂-rich melilititic, orangeitic and

kimberlitic magmatism cannot be co-incidental. Mitchell and Bergman (1991) have suggested that this is a consequence of the lower solubility of CO₂ in these, relative to H₂O-rich, magmas [Brey and Green 1976]. Consequently, they may degas violently by fluidization-like processes at greater depths than basaltic or lamproitic magmas. The latter may not degass until they enter the shallow hydrovolcanic regime.

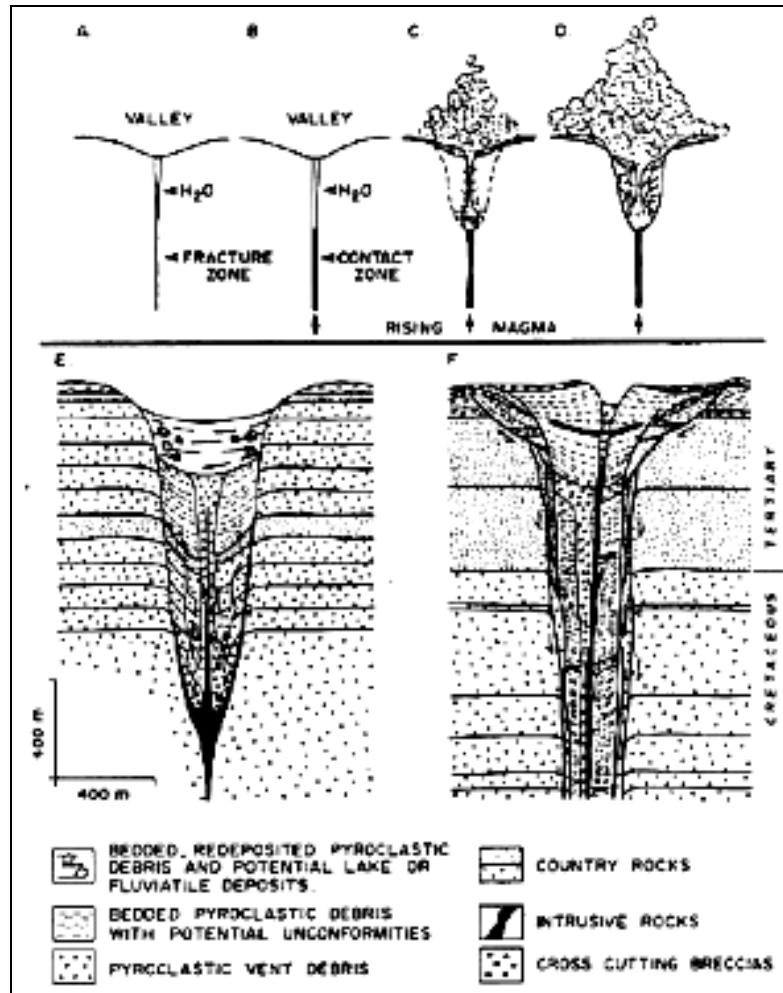


Fig. 13. A to E., Stages in the development of a hydrovolcanic diatreme as envisioned by Lorenz (1975, 1984); F., Vertical cross-section of the Black Butte diatreme, Montana [after Hearn 1968]. Note the central conduits of diatremes E and F are filled with hypabyssal magmatic material.

MELILITOLITES

The plutonic facies of the melilitite clan includes a wide variety of rocks composed principally of melilite, olivine, phlogopite, clinopyroxene and perovskite, and to lesser degree nepheline and primary calcite. Some phlogopite-rich rocks, e.g. okaite, uncomphgrite, phlogopite pyroxenite may be regarded as examples of the plutonic lamprophyre facies of the melilitite clan. With decreasing grain size there is complete transition to hypabyssal rocks, sometimes termed

micromelilitolites, and with increasing modal phlogopite to melnoites (see below). Melilitolites are known primarily from plutonic alkaline complexes and less commonly as xenoliths within volcanic rocks. The latter are apparently derived from cumulates formed in sub-volcanic magma chambers, e.g. blocks of afrikandite in pyroclastic rocks at Kerimasi (Tanzania).

OCCURRENCE

Alkaline complexes containing melilitolites are typically composed primarily of ultramafic alkaline rocks, principally the ijolite suite, and commonly associated with carbonatites. Although nepheline syenites may occur in some of these complexes, they are of relatively small volume compared to the ultramafic rocks. The paucity of nepheline syenite is one feature which serves to distinguish melilitolite-bearing complexes from ijolite-nepheline syenite carbonatite complexes associated with the nephelinite clan, e.g. Napak (Kenya), Fen (Norway), Magnet Cove (USA), Grrndal-Ika (Greenland), Nizhnesayanskii (Russia).

Two regions are characterized by the extensive development of melilitolite-bearing complexes: the Kola-Kandalaksha and Maimecha-Kotui regions of Russia. In other parts of the world they are found as isolated intrusions in alkaline rock provinces dominated by nepheline syenite-carbonatite complexes e.g., Gardiner in East Greenland, Oka in the Monteregian Hills province (Canada) or associated with alkaline ultramafic complexes lacking melilitolites but which are otherwise of similar petrological character, e.g. Tapira in the Goias-Minas Gerais (Brazil) pyroxenite-carbonatite province. Their apparent absence in the latter varieties may be merely related to the local extent of erosion and melilitolites may be present at depth. Melilitolite complexes have been insufficiently investigated to determine if there are real petrological differences between those found in the different associations. Most melilitolite complexes have not been subjected to modern mineralogical studies and published descriptions concentrate primarily upon their petrography. Exceptions include Iron Hill [Nash 1972] and the Gardiner complex [Nielsen 1980].

Melilitolite-bearing and associated complexes typically contain rocks enriched in magnetite, perovskite, apatite and phlogopite and hence are major economic sources of Ti, Nb, Fe, REE, mica and phosphate. The complexes are not agpaitic and the typomorphic Zr- and Nb bearing silicates and titanosilicates of such rocks e.g. eudialyte, lovozerite, lorenzenite, shcherbakovite etc., are not present. Instead Zr is typically sequestered in zircon, zirconolite ($\text{CaZrTi}_2\text{O}_7$), zirkelite $[(\text{Ca},\text{Ti},\text{Zr})_3\text{O}_5]$, calzirtite ($\text{Ca}_2\text{Ti}_2\text{Zr}_5\text{O}_{16}$) etc., and Ti and Nb in perovskite and pyrochlore. Economically significant Zr mineralization is not present.

KOLA-KANDALAKSHA REGION

Fig. 14 depicts the Kola-Kandalaksha region which includes the melilitolite-

bearing complexes of Turiy, Afrikander, Kovdor, Salmagorskii, and Kontozerskii. Others complexes in which melilitolites are not apparently present at the current level of exposure but which are otherwise petrologically similar include; Seiblyavr, Ozernaya Varaka, Lesnaya Varaka, Sallanlatvi, Vuoriyarvi. These complexes are on average slightly older (364-405 Ma) than the Lovozero (361 Ma) and Khibina (365 Ma) agpaitic complexes [Kogarko *et al.* 1995]. A 470-480 Ma swarm of melilitite-bearing lamprophyric and carbonatite dikes occurs along the shores of Kandalaksha Gulf [Bulakh and Ivanikov 1984]. Also found on the Terski Coast are numerous diatremes of melilitite and ultramafic rocks which are contemporaneous with the Turiy complex [Kalinkin *et al.* 1993].

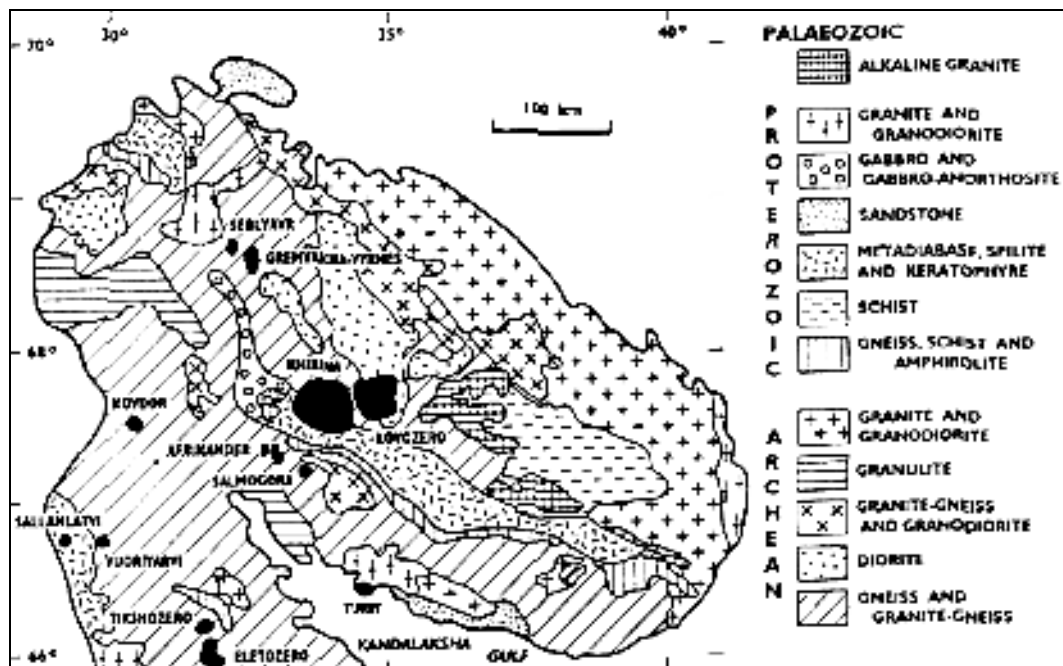


Fig. 14. Simplified geological map of the Kola Peninsula, Russia [after Zaitsev and Bell 1995 and Kukharenko *et al.* 1965] showing the locations of alkaline complexes (black).

Descriptions of the melilitolite-bearing complexes of the region may be found in Kukharenko *et al.* (1965) or Kogarko *et al.* (1995). Three groups of rock appear to be present in most examples: an early suite of ultramafic rocks (olivinites, pyroxenites); followed by members of the ijolite suite; and finally intrusion of carbonatites. Melilitolites appear to be typically associated with the initial ultramafic suite e.g. melilite olivinites and afrikandites at Afrikander, but may occur as intrusions emplaced subsequent to the ijolite suite e.g. okaites and turjaites at Turiy. However, interpretations of the petrology of the complexes must not be accepted uncritically given that these may be influenced by the metasomatic hypotheses favoured by many Russian petrologists.

The Afrikander complex is a small (7 km² area), poorly-exposed intrusion, which consists primarily of many textural and modal varieties of mela-ijolite and

nepheline pyroxenite [Kukharenko *et al* 1965]. The central portion of the intrusion is composed of olivinites, melilite olivinites and diopside- amphibole-bearing calcite carbonatites together with numerous veins of ijolite pegmatite and perovskite-titanite-titanomagnetite. The olivinites form megaxenoliths amongst coarse-grained pyroxenites. The main constituents are olivine, perovskite and magnetite. The rocks are commonly modally-layered; some layers contain very little silicate and are essentially magnetite-perovskite rocks. Melilite olivinites occur as thin layers adjacent to layers of fine grained olivinite. Melilite is present

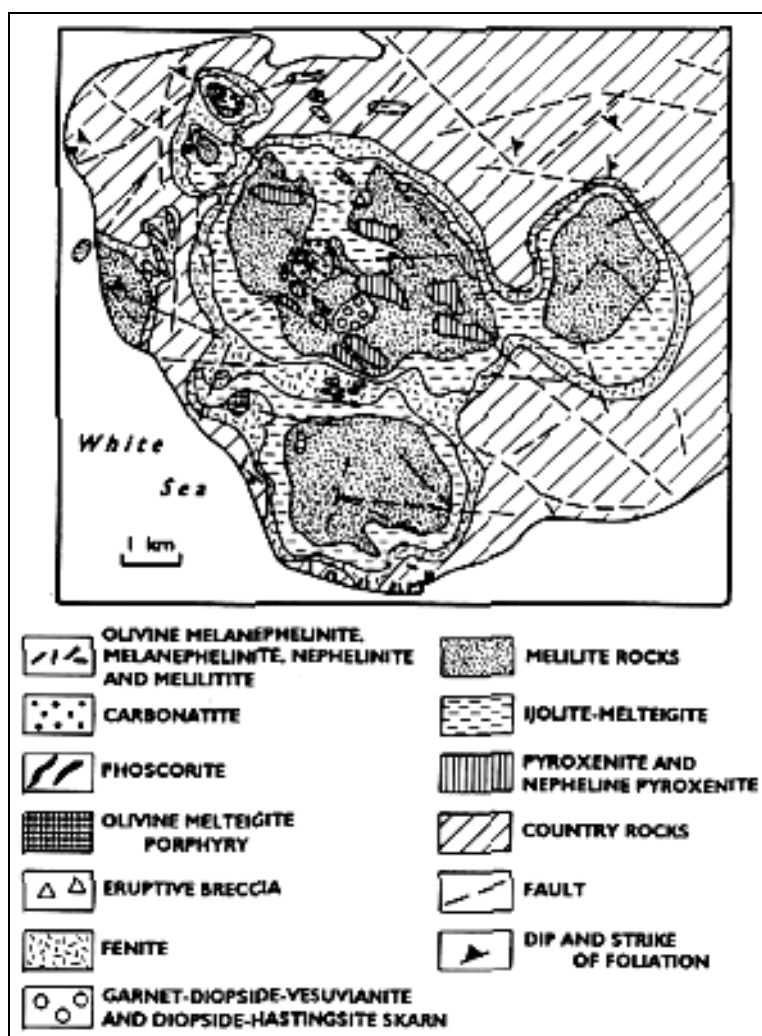


Fig. 15. Simplified geological map of the Turiy melilitolite complex, Terski Coast of Kandalaksha Gulf, Russia [after Bulakh and Uvanikov 1984 and Kogarko *et al.* 1995].

either as isolated plates and prisms whose long axes are orientated parallel to layering giving the rock a trachytic texture, or as clusters and segregations (up to 25 cm) composed essentially of melilite in melilite-free host. Also present are monticellite, phlogopite and calcite. Modal variations lead to rocks composed of melilite, perovskite and titanomagnetite i.e. afrikandite. The melilite crystals contain inclusions of olivine and perovskite and are commonly altered to celadonite,

wollasto-nite and calcite. Melilite is not found in the associated coarse grained olivinites.

The Turiy complex consists of three large intrusions [Central (28 km²), Southern (13 km²) and Kuznavolskii (15 km²)], several smaller ones (Letnegorsk, Gornoozersk) together with pre-, syn- and post-intrusive dike swarms (Fig. 15). The intrusions are composed of, in order of intrusion: olivinite and clinopyroxenite; members of the ijolite suite; melilitolites; ijolites; phoscorites (phlogopite-magnetite-apatite-forsterite rocks) and carbonatites. Figure 16 illustrates the structure of the Central intrusion as envisaged by Bulakh and Ivanikov (1984). Detailed modern mineralogical studies of the melilitolites have not been published, although some data are given by Ronenson *et al.* (1981).

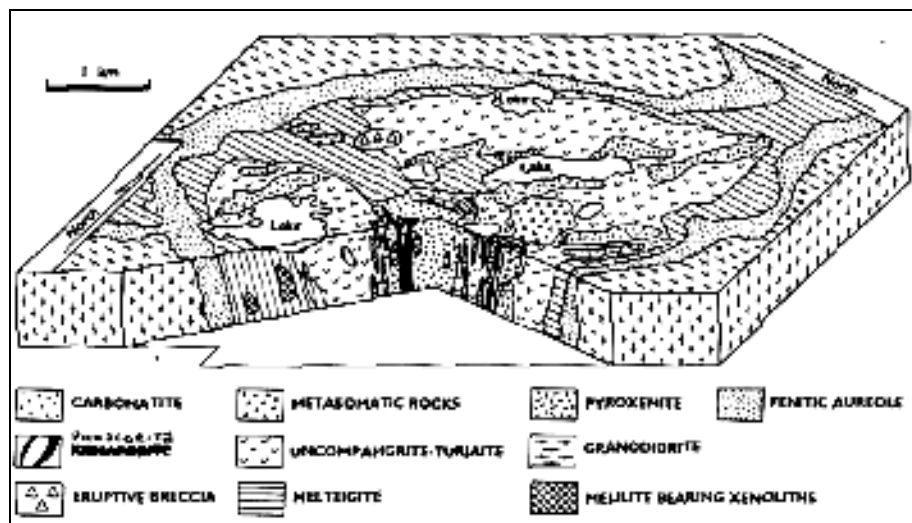


Fig. 16. Interpretation of the structure of the Central intrusion of the Turiy complex [after Bulakh and Ivanikov 1984].

The principal minerals of the melilitolites are melilite, nepheline, clinopyroxene and phlogopite with minor and/or accessory perovskite, apatite and magnetite. Subsidiary reactions have typically led to the formation of Ti-rich andradite and schorlomite. Although the modes vary widely the rocks, in contrast to those at Afrikander, typically exhibit a hypidiomorphic granular texture. Clinopyroxene and melilites have compositions similar to those found in melilitites. Nephelines have typical Morozewicz-Buerger plutonic nepheline compositions and are identical to those in associated ijolites.

GARDINER INTRUSION

The 50 Ma Gardiner intrusion is a 5km diameter ring-shaped ultramafic complex exposed as a nunatak at the head of Kangerdlugssuaq Fjord, East Greenland. Nielson (1980, 1981, 1994) has proposed that the rocks of the complex were intruded in four stages, as follows: (1) an ultramafic cumulate series of dunites and pyroxenites; (2) a suite of dikes and sills of shonkinite plus sodalite

and nepheline syenites; (3) a ring dike of melilitolites and related mela-ijolites, syenite and carbonatite; (4) a series of alkali pyroxenite, nepheline syenites, and leuco-ijolite dikes. Emplacement of the complex was preceded by the tholeiitic magmatism associated with continental break-up and formation of the North Atlantic, followed by intrusion of a regional dike swarm of olivine melanephelinites.

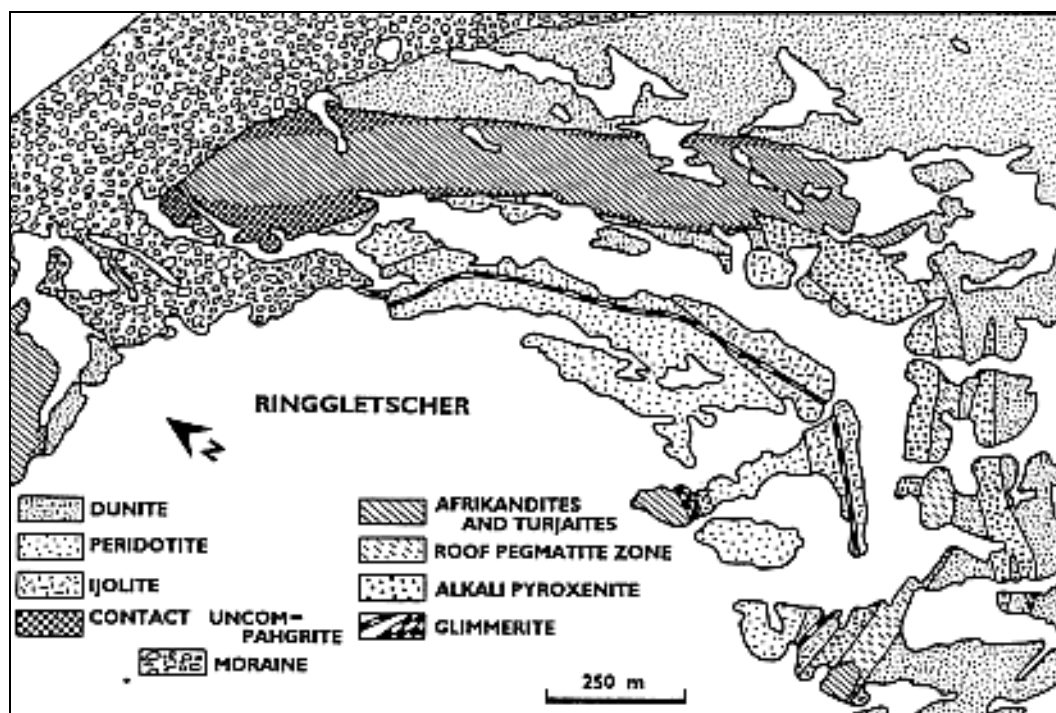


Fig. 17. Geological map of the melilitolite ring dike and related rocks in the north-east central part of the Gardiner complex, East Greenland [after Nielson 1980].

Figures 17 and 18 illustrates the geological relationships between the melilitolites and the earlier-formed ultramafic rocks. The melilitolite ring dike has chilled and sharp intrusive contacts with the dunites and ijolites, thus demonstrating an unquestionable magmatic origin. The interior of the dike is composed of an afrikandite consisting of euhedral perovskite, magnetite and apatite enclosed in large poikilitic plates of melilite. Clinopyroxene is rare and is resorbed where enclosed in melilite but fresh when included in other minerals. The clinopyroxene content of the rocks increases towards the contact with dunites and they are modally transitional into uncompahgrites. In the latter large resorbed prisms of diopside occur in a matrix of apatite, magnetite, perovskite, melilite and phlogopite. The dike also exhibits vertical zonation (Fig. 18), and with increasing phlogopite, nepheline and pyroxene contents, afrikandites grade upwards into phlogopite afrikandites, turjaites, and mela-ijolites. The latter, in the upper part of the body are transitional into diverse carbonatitic rocks. Most of the melilitolites have re-equilibrated/reacted at subsolidus temperatures.

Despite the wide modal variation and evidence for differentiation there is little variation in the composition of most of the minerals present [Nielson 1980]. Pyroxenes exhibit the most variation and are zoned in the range $\text{Ae}_2\text{Di}_{93-81}\text{Hd}_{7-11}$, although there is no systematic variation with location within the dike. Only pyroxenes in the roof melilites ($\text{Ae}_{1-14}\text{Di}_{86-66}\text{Hd}_{13-17}$) and sodalite syenite pegmatites ($\text{Ae}_{17}\text{Di}_{66}\text{Hd}_{17}$) are relatively-enriched in aegirine. Melilites show a

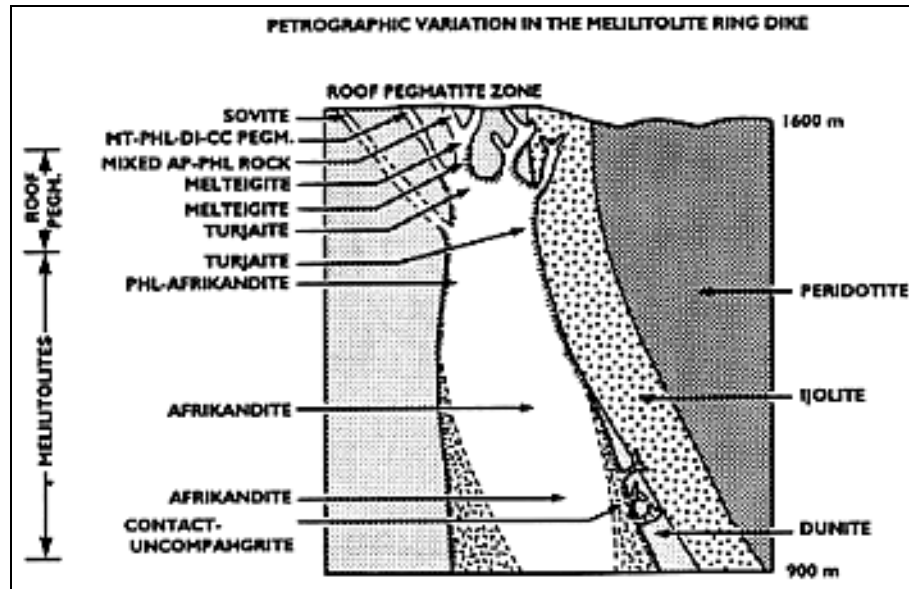


Fig. 18. Vertical cross-section of the melilitolite ring dike, Gardiner complex, East Greenland [after Nielson 1980].

small but systematic increase in Na_2O content with elevation and typically consist of about 60% akermanite, 10% Fe-akermanite and 30% soda-melilite.

Nielson (1980) has suggested that the observed petrological variation results from progressive solidification of the parental magma inward from the contacts and upwards towards the roof. Fractional crystallization leads to the concentration of incompatible elements and eventual crystallization of nepheline, phlogopite and calcite in the upper parts of the dike. The crystallization sequence and reaction relationship of diopside with liquid to form melilite (Fig. 19) are in accord with experimental studies of Onuma and Yagi (1967). Carbonatites are believed to separate by liquid immiscibility during the final stages of crystallization, the conjugate silicate liquid forming the mela-ijolites.

Nielson (1980,1994) considers that the parental magma to the melilitolite complex is represented in the regional dike swarms and is a larnite-normative olivine mela-nephelinite. Figures 20 and 21 illustrate the emplacement model and petrogenetic scheme for the complex respectively, as envisioned by Nielson (1994). In this scheme the ultramafic cumulate series represent crystallization of mela-nephelinite under volatile undersaturated conditions in an open magma chamber beneath the volcanic edifice.

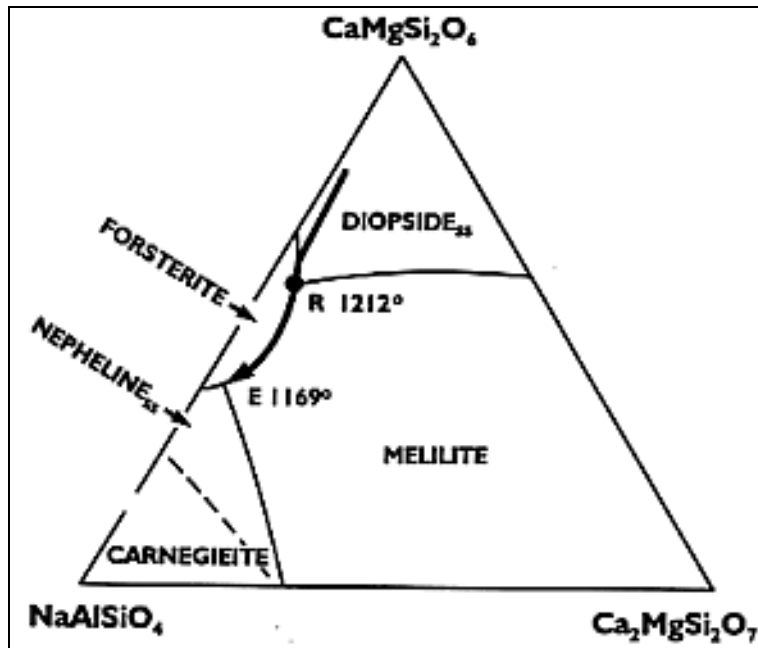


Fig. 19. The inferred liquid trend of the Gardiner melilitolite ring in the system nepheline - ekermanite - diopside [after Nielson 1980 and Onuma & Yagi 1967].

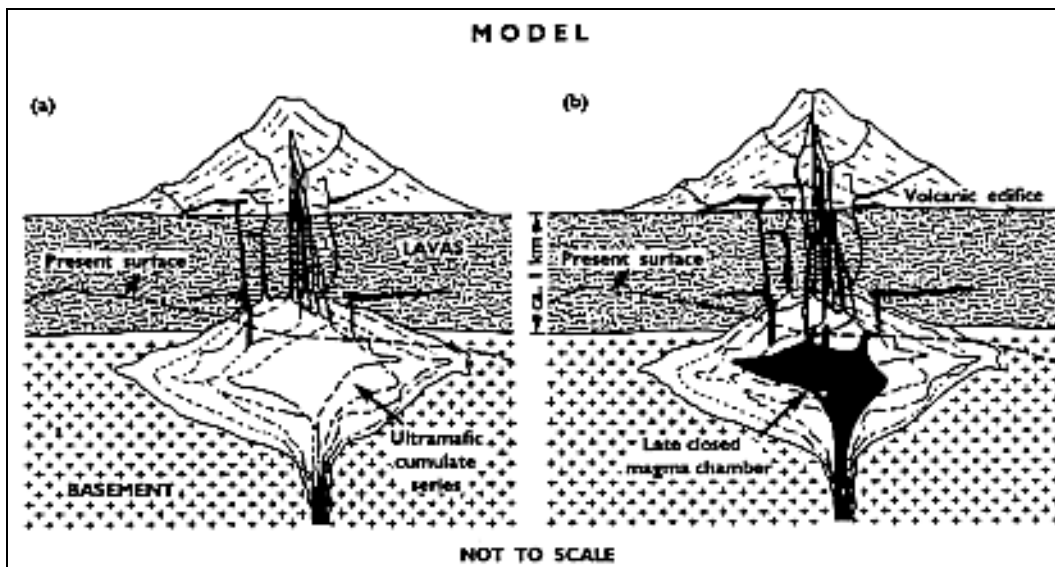


Fig. 20. Model for the evolution of the Gardiner complex [after Nielson 1994].

A. Ultramafic cumulates form in an open magma chamber, located at the Tertiary tholeiitic plateau lava - basement interface, beneath a mela-nephelinite stratovolcano. B. The magma chamber is filled and intruded by a final batch of mela-nephelinite magma which crystallizes under closed system plutonic conditions. In this model the bulk of the plutonic rocks formed in the magma chamber are not exposed and the melilitolite ring is regarded as an upper level apothesis of these rocks.

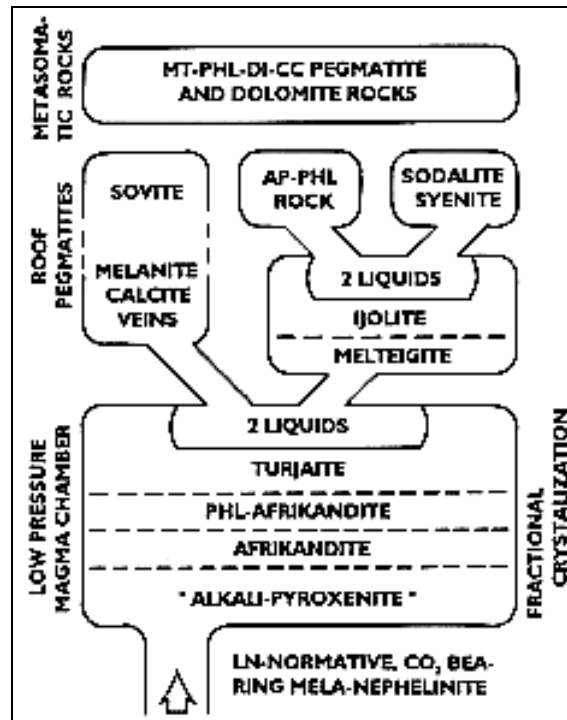


Fig. 21. Petrogenetic model for the evolution of the melilitolite ring dike, Gardiner complex [after Nielson 1980].

During the waning stages of activity, the last pulses of magma are believed to be trapped within the complex and thus evolve under closed system vapour saturated conditions. The fractionation trend towards melilititic compositions is induced by the crystallization of phlogopite and kaersutite. Nielson's (1984) hypothesis is important in that it seeks to integrate all melilite-bearing rocks in one model and suggests that melilitolite complexes such as Afrikaner and Turiy are exhumed magma chambers forming the roots of nephelinite volcanoes. Although the scheme seems appropriate for the Gardiner complex it is not applicable to melilititic provinces lacking associated nephelinite magmatism and melilitolite plutonism e.g. Namaqualand.

HYPABYSSAL MELILITES AND MELNOITES

Melilite is common in phlogopite-bearing hypabyssal rocks which are commonly termed lamprophyres (*sensu lato*), or ultramafic lamprophyres [*sensu* Rock 1986]. These rocks consist of widely varying amounts of diopside, phlogopite, melilite, olivine, monticellite, calcite and nepheline as essential minerals. They are commonly modally gradational into otherwise similar melilite-free rocks such as aillikite. Accessory minerals include Ti-chromite-magnetite, perovskite and apatite. As a consequence of their modal diversity these rocks have been given an inordinately large number of type locality names which have until recently prevented recognition of their consanguinity. Mitchell (1994) has suggested that the rocks represent the lamprophyric facies of the melilitite clan and

that they may all be described using compound mineralogical names as varieties of *melnoite*. The rocks commonly co-exist with phlogopite-poor or phlogopite-free micro-melilitolitic rocks and/or hypabyssal melilitites emphasising their genetic relationships to the melilitite clan. They appear to represent melilititic magmas which have crystallized under volatile-rich conditions.

Melnoites are commonly found as dikes or cone sheets associated with alkaline complexes e.g. Alnö, Sweden [von Eckermann 1948], and more rarely as isolated swarms e.g. McKellar Harbour, Ontario [Platt and Mitchell 1982] or dikes and diatremes (Avon area) in E.Missouri, S.Illinois and W.Kentucky belonging to the Waubougikou melnoite province [Lewis and Mitchell, unpub.], although the latter may be related to the un-exposed Omaha Pool or Hicks Dome complexes. Important and/or well characterized examples of melnoite suites are: Ploučni...e River region, Czech Republic [Ulrych *et al.* 1988], Coral Rapids, Hudson Bay Lowlands province, Canada [Edgar *et al.* 1994], Aln' complex [von Eckermann 1948], Como-Ile Cadieux, Quebec [Gold and Marchand 1969]; Kandalaksha Graben [Bulakh and Ivanikov 1984]; Blue Hills Complex, Namibia [Kurszlaukis *et al.* 1995, Janse 1971]. Other examples are tabulated in Rock (1991).

PLOUČNICE RIVER REGION OSEČNÁ COMPLEX

The upper region of the Ploučnice (or Polzen) River, northern Bohemia (Czech Republic) is characterized by the presence of many melnoitic hypabyssal intrusions and is the type locality of polzenites (*sensu lato*). Hypabyssal rocks in the Osečná area which are known to be associated with a subsurface intrusion are collectively termed the Osečná complex [Ulrych *et al.* 1988]. Fig. 22 indicates that the Osečná intrusion forms a lopolith-like body from which cone sheets of micromelilitolite emanate to the surface. The hidden part of the intrusion varies from 23-66m in thickness over an area of about 12.5 km². A series of earlier cone sheets of polzenite and minor micromelilitolite together with radial dikes of tephrite and basanite are centred upon the intrusion, although the focus of the former lies at greater depth. The complex provides an excellent illustration of the spatial relationships that exist between the different facies of the melilitite clan and of the modal variation that may be developed within a suite of consan-guineous rocks.

The Osečná intrusion is composed principally of nepheline olivine melilitolites (kug-dites) and metaso-matic derivatives formed during subsolidus recrystallization and reaction. The latter result in the replacement of melilitite by Zr-Ti-bearing andradite together with many secondary calc-silicate minerals and formation of phlogopite. Completely-altered rocks are olivine garnet phlogopites. In the centre of the complex and the feeder channel there occur rocks composed of calcite, clinopyroxene and decomposed nepheline and melilitite, representing gradations between ijolite, turjaite and carbonatite.

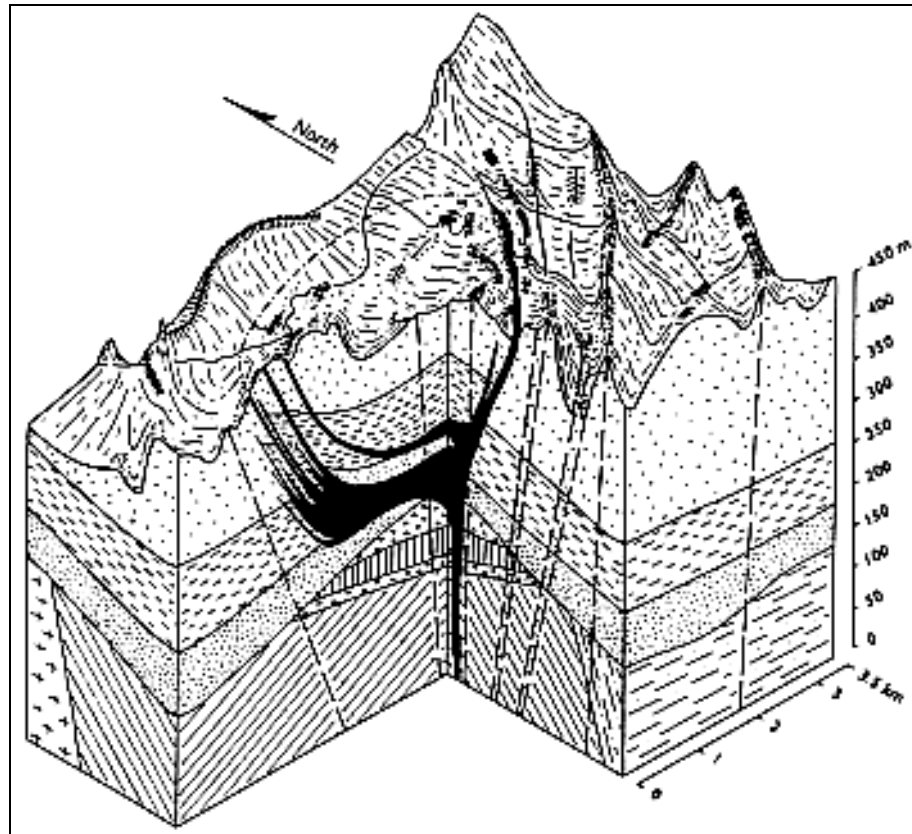


Fig. 22. Interpretation of the geology of the Osečná complex [after Ulrych *et al.* 1988].

The rocks forming the marginal parts of the intrusion and its associated cone sheets are micromelilitites (vesecites). These consist of olivine phenocrysts with monticellite rims set in a groundmass of melilite, nepheline, phlogopite, spinel, perovskite and calcite. The rocks differ from the coarser grained melilitolites in that they contain more monticellite and less phlogopite.

The earlier deeper focus cone sheets consist of clinopyroxene-bearing melnoites. Phenocrysts of olivine, phlogopite and clinopyroxene are set in a groundmass of melilite, nepheline, sodalite, hauyne, perovskite, spinel and apatite. Modes vary widely and there appears to be complete gradation between clinopyroxene-poor (modlibovites) and clinopyroxene-rich varieties (luhites).

Ulrych *et al.* (1986, 1988, 1990, 1994) have provided extensive data on the mineralogy and geochemistry of the complex. In common with the Gardiner intrusion many of the major minerals exhibit very little compositional variation and do not delineate the evolutionary sequence. However, geochemical data and field relationships suggest that the clinopyroxene-bearing melnoites represent a less evolved fraction of the magma than the melilitolite intrusion. Ulrych *et al.* (1988) suggest that the complex represents the upper parts of an evolving volcanic system. The Osečná complex has some similarities with the Gardiner complex in that the earliest melilite-bearing rocks also contain clinopyroxene and the latest are melajolites and carbonatitic rocks. Consequently, Ulrych *et al.* (1988) favour a similar

mela-nephelinite parental magma. If this model is correct a cumulate complex of dunites and clinopyroxenites possibly intruded by late melilitolites may be postulated to exist at depths.

The Osečná complex provides a bridge between the volcanic and plutonic facies of the melilitite clan and suggests a plausible relationship between hypabyssal melnoites and associated alkaline plutonic complexes. The complex illustrates well the relative roles of fractional crystallization, cooling rate and subsolidus reactions in the development of a modally diverse suite of rocks from a common parental magma. The great differences in the modes of melnoite suites associated with diverse alkaline complexes are thus merely a consequence of the vagaries of the crystallization histories of different batches of parental magma.

ORIGINS OF MELILITITE MAGMA

Initial hypotheses for the origin of melilitites suggested that they could be formed by the fractional crystallization of alkaline olivine basalts [O'Hara and Biggar 1969]. However, subsequent geochemical and experimental studies have rendered this hypothesis untenable. The role of volatiles in the generation of extremely undersaturated rocks was initially suggested by Bultitude and Green (1968) who claimed that Hawaiian-type melilitites could be formed by extremely small degrees of partial melting under hydrous conditions at depths of 60-70km, whereas continental-types lacking associated basalts were formed at 80-100 km depth. Generally increasing depth and lesser degrees of partial melting were considered to lead to increasing degrees of silica undersaturation.

Because of the common association of melilite-bearing rocks with carbonatites and the recognition of carbonation reactions in the mantle at high pressures, it was considered that the presence of carbon dioxide must play a significant role in the generation of extremely undersaturated magmas [Brey *et al.* 1978]. This hypothesis was subsequently confirmed by the experimental studies summarized below. The experimental work has followed two approaches to the problem of magma genesis. In one termed the inverse approach, the experimental principle followed is that a primary magma composition will have a unique point on its liquidus at which multiple saturation with minerals present in the source assemblage occurs. The pressure at which this occurs corresponds to the pressure at which the magma formed from this source. The studies involve determining the near-liquidus phase relationships of actual rocks whose bulk composition is considered to be representative of primary magmas.

The second approach termed the forward approach takes the mineral assemblage of potential sources and determines the composition of the liquids produced upon partial melting at known pressures and temperatures. Simplified compositions, usually Fe-free, relative to those of postulated natural mantle sources are commonly used as starting material in this type of work. Detailed discussion of the experimental studies that have been undertaken is beyond the scope of this work and only the major conclusions are presented.

NEAR-LIQUIDUS EXPERIMENTAL STUDIES

Many melilitites have bulk compositions which indicate that they might be unmodified primary mantle-derived melts, although they are poor in carbon dioxide due to volatile loss during eruption. To compensate for this deficiency, CO₂ is typically added to the compositions investigated by Brey and Green (1976, 1977), Brey (1978) and Brey and Ryabchikov (1994). These experimental studies demonstrate that the liquidus phases present are sensitive to the relative abundance of CO₂ and H₂O. Thus, the study of a melilitite plus H₂O and CO₂ by Brey and Green (1977) has shown that when CO₂ is dominant the liquidus phases at 30kb are garnet, orthopyroxene and clinopyroxene, whereas when H₂O is dominant, olivine or olivine plus clinopyroxene are the liquidus phases.

Brey (1978) has summarized and interpreted the experimental data to suggest that melilitites are derived from lherzolitic sources which include a carbonate phase, as at these pressures it is considered that any CO₂ present in the natural melt must have been derived from a carbonate mineral in the source. Studies by Wyllie and Huang (1976), among others, have shown that dolomite is the stable carbonate phase in carbonated lherzolite from about 25 to 35kb pressure. Hence, Brey (1978) suggest melilitites represent limited partial melts of dolomite garnet lherzolite. The dolomite is believed to be consumed during partial melting and therefore does not appear as a liquidus phase in the near-liquidus experiments. Brey (1978) concludes that increasing (CaO+MgO)/SiO₂ ratios of melilitites reflect increasing amounts of CO₂ in the source region, decreasing degrees of partial melting and increasing depth of origin. Melilitites associated with basaltic rocks from Tasmania are considered to be derived by 5% melting of pyrolite at 27kb/1160°C with 7-8 wt.% H₂O and 6-7 wt.% CO₂. In contrast, Namaqualand-type melilitites are considered to originate at higher pressures (30-35kb) from sources with higher CO₂ contents (> 13.5 wt.%).

Brey's (1978) work indicates that the formation of melilitite magmas takes place over a range of pressures and that their bulk composition is not controlled by an invariant point, or melting cusp, on the dolomite lherzolite solidus. These conclusions explain the observed range in composition of primary melilitites (Table 1, Fig.10) by showing them to be a series of melts related to a common source but derived by melting at differing depths under diverse volatile compositions.

NEAR-SOLIDUS PARTIAL MELTING EXPERIMENTAL STUDIES

Figure 23 summarizes postulated phase relationships in the system peridotite-CO₂ and shows that at relatively low pressures, dolomite is the stable mantle carbonate. Partial melting of dolomite garnet lherzolite along the solidus between the invariant points I₀ and I₆, should lead to the formation of a range of melilititic magmas [Brey 1978]. At higher pressures magnesite becomes the stable carbonate

mineral and liquids should be richer in Mg and more Si undersaturated than melilitites. The actual pressures and temperatures of these invariants points and solidi for realistic mantle compositions are as yet not well constrained. Figure 24 illustrates phase relationships for the system CaO-MgO-Al₂O₃-SiO₂-CO₂ from 2 - 12 GPa as determined by Canil and Scarfe (1990). Near-solidus partial melts in this system are extensive (23-39 wt.%). Determination of their composition is difficult, but those in equilibrium with dolomite at 3 GPa are interpreted to be melilititic in composition, whereas those in equilibrium with magnesite at 5-7 GPa are similar to kimberlites (Canil and Scarfe).

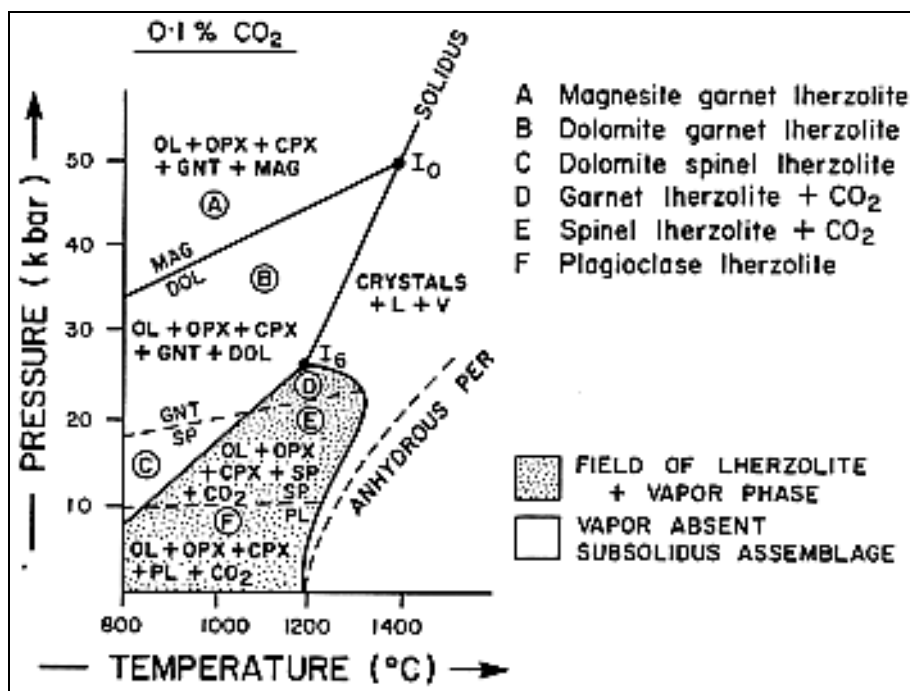


Fig. 23. Postulated phase relationships in the system peridotite - CO₂ (0.1%) based on experimental data and deductions from the system CaO-MgO-SiO₂-CO₂ [Wyllie and Huang 1976].

Note the carbonation reaction terminating at the invariant point I_6 on the peridotite solidus divides the diagram into vapour absent and vapour-bearing assemblages, as all CO₂ is consumed in the carbonation reaction. The subsolidus reaction of orthopyroxene and dolomite to give diopside plus magnesite defines a univariant line which terminates at the solidus at the invariant point I_0 . At pressures above I_0 , magnesite is stable at the solidus and partial melts are poorer in Si and have lower Ca/Mg ratios than liquids formed at lower pressures which are in equilibrium with dolomite. Solidus for anhydrous peridotite (PER) is shown as a dashed line [after Mitchell 1986].

A corollary to Canil and Scarfe's (1990) study is that it might be possible to generate a continuous spectrum of partial melts from carbonated upper mantle ranging in composition from kimberlite to melilitite. Geological evidence indicates that this rarely occurs as melilititic and kimberlitic magmatism are neither consanguineous nor contemporaneous [Mitchell 1986, 1995]. However, the hypothesis may explain the geographical association of kimberlite and melilitites

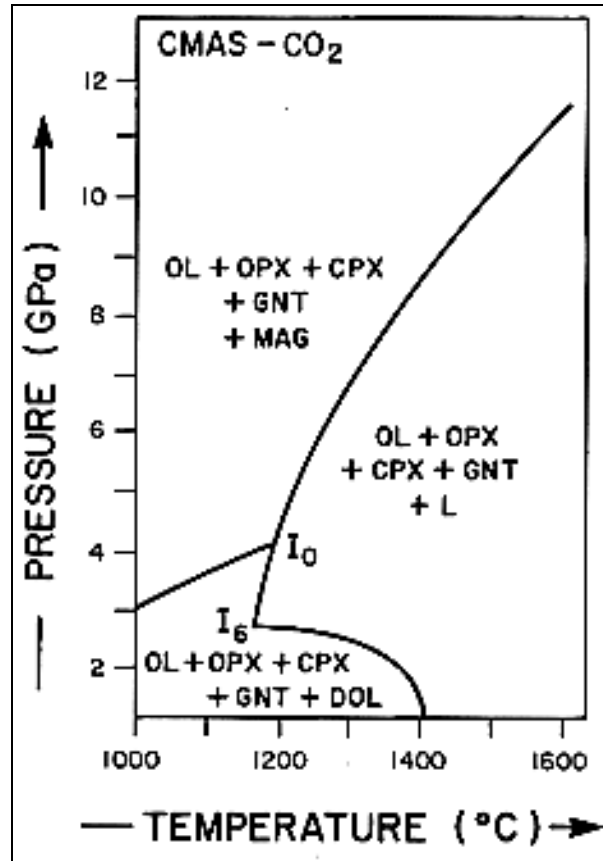


Fig. 24. Experimentally determined phase relationships up to 12 GPa pressure in the system $\text{CaO} - \text{MgO} - \text{Al}_2\text{O}_3 - \text{SiO}_2 - \text{CO}_2$ (after Canil & Scarfe 1990).

as observed in Namibia and the Anabar shield (Russia). The possibility of forming melilitites at depths below 120 km (>4 GPa) might explain the rare presence of diamond in some examples [Mitchell 1995] and the postulated occurrence of melilitite in some kimberlites [Scott Smith 1989]. Magmas forming these rocks may originate near the invariant point I_0 on the carbonated lherzolite solidus (Fig. 23). Speculations regarding the tectonic controls on magma generation which typically cause discrete kimberlitic or melilititic magmatism and not a continuum are beyond the scope of this work.

CONCLUSIONS

Melilititic magmas form a continuum of primary magma composition resulting from the partial melting of dolomitic garnet lherzolite over a pressure range of at least 2.7 - 4 GPa (80-120 km) under CO_2 -rich conditions. Increased degrees of partial melting at relatively low pressures leads to a partial melting sequence involving less undersaturated nephelinites, basanites and even alkali basalts (Hawaii, S.E. Australia). Partial melting at higher pressures is apparently restricted to the formation of low silica melilitites (Namaqualand). Low pressure differentiation of melilitite magmas occurs only rarely and the magma is erupted as

degassed undifferentiated lava. The restriction of diatremes to melilititic and kimberlitic magmas may be related to the low solubility of CO₂ in these melts. Volatiles may be retained in hypabyssal and plutonic environments resulting in the formation of melilitolites, melnoites and associated carbonatites, together with extensive sub-solidus re-equilibration and reaction.

ACKNOWLEDGEMENTS

This research is supported by the Natural Sciences and Engineering Research Council of Canada and Lakehead University. Dan Barker and Garth Platt are thanked for constructive reviews of the initial version of this work.

REFERENCES

1. BARKER, D.S., MITCHELL, R.H., McKAY, D. (1987): Late Cretaceous nephelinite to phonolite magmatism in the Balcones province, Texas. *In* Mantle Metasomatism and Alkaline Magmatism (E.M. Morris and J.D. Pasteris, eds.), *Geol. Soc. Amer. Spec. Paper*, 215, 293-304.
2. BREY, G. (1978): Origin of olivine melilitites - chemical and experimental constraints. *J. Volcanol. and Geothermal Res.* 3, 61-88.
3. BREY, G., GREEN, D.H. (1976): Solubility of CO₂ in olivine melilitite at high pressures and role of CO₂ in the Earth's upper mantle. *Contrib. Mineral. Petrol.* 55, 217-230.
4. BREY, G., GREEN, D.H. (1977): Systematic study of liquidus phase relationships in olivine melilitite + H₂O + CO₂ at high pressures and petrogenesis of an olivine melilitite magma. *Contrib. Mineral. Petrol.* 61, 141-162.
5. BREY, G., RYABCHIKOV, I.D. (1994): Carbon dioxide in strongly silica undersaturated melts and origin of kimberlite magma. *N. Jahrb. Mineral. Mh.* 1994, 449-463.
6. BULAKH, A.G., IVANIKOV, V.V. (1984): Проблемы минералогии и петрологии карбонатитов (*Problems of the Mineralogy and Petrology of Carbonatites*). Leningrad State University Press.
7. BULTITUDE, R.J., GREEN, D.H. (1968): Experimental study at high pressures on the origin of olivine nephelinite and olivine melilitite nephelinite. *Earth Planet. Sci Letts.* 3, 325-337.
8. CANIL, D., SCARFE, C.M. (1990): Phase relations in peridotite + CO₂ systems to 12 GPa: Implications for the origin of kimberlite and carbonate stability in the Earth's upper mantle. *J. Geophys. Res.* 95, B15805-B15816.
9. CHEN, C., FREY, F.A. (1985): Trace element and isotopic geochemistry of lavas from Haleakala volcano, East Maui, Hawaii: Implications for the origin of Hawaiian basalts. *J. Geophys. Res.* 90, B7743-B8768.
10. CLAGUE, D.A., DALRYMPLE, G..B. (1988): Age and petrology of the alkalic postshield and rejuvenated lava from Kauai, Hawaii. *Contrib. Mineral. Petrol.* 99, 202-218.
11. CLAGUE, D.A., FREY, F.A. (1982): Petrology and geochemistry of the Honolulu Volcanics, Oahu: Implications of the oceanic mantle beneath Hawaii. *J. Petrol.* 23, 447-504.
12. CLEMENT, C.R. (1982): A comparative geological study of some major kimberlite pipes in the Northern Cape and Orange Free State. Ph.D. Thesis (2 vols.) Univ. Cape Town.
13. CLEMENT, C.R., REID, A.M. (1989): The origin of kimberlite pipes: an interpretation based on a synthesis of geological features displayed by southern African occurrences. *In* Kimberlites and Related Rocks (J.Ross, ed.), *Proc. 4th. Internat. Kimberlite Conf. Geol. Soc. Australia Spec. Pub.* 14,1, 632-646.

14. CLEMENT, C.R., SKINNER, E.M.W. (1985): A textural genetic classification of kimberlites. *Trans. Geol. Soc. S. Africa*, 88, 403-409.
15. CLOOS, H. (1941): Bau und Tatigkeit von Tuffschloten. Untersuchungen an den Schwabischen Vulkanen. *Geol. Rundsch.* 32, 709-800.
16. COLGAN, E.A., CLARK, T.C., BRISTOW, J.W., ALLSOPP, H.L (1989): Geological setting, petrography and petrogenesis of olivine melilitites of the Natal Coast. In *Kimberlites and Related Rocks* (J. Ross, ed.), *Proc. 4th Internat. Kimberlite Conf. Geol. Soc. Australia Spec. Pub.* 14, 1, 417-435
17. DAUTRIA, J.M., DUPUY, C., TAKHERIST, D., DOSTAL, J. (1992): Carbonate metasomatism in the lithospheric mantle: peridotitic xenoliths from the melilititic district of the Sahara basin. *Contrib. Mineral. Petrol.* 111, 37-52.
18. DAWSON, J.B., SMITH, J.V., JONES, A.P. (1985): A comparative study of bulk rock and mineral chemistry of olivine melilitites and associated rocks from East and South Africa. *N.Jahrb. Mineral. Abh.* 152, 143-175.
19. DE WET, J.J. (1975): Carbonatite and related rocks at Saltpetre Kop, Sutherland, Cape Province. *Univ. Stellenbosch Ann. Ser.A1, Geol.* 1, 193-632.
20. DONALDSON, C.H. (1976): An experimental investigation of olivine morphology. *Contrib. Mineral. Petrol.* 57, 187-213.
21. EDGAR, A.D., PIZZOLATO, L.A., BUTLER, G.M. (1994): Petrology of the ultramafic lamprophyre and associated rocks at Coral Rapids, Abitibi River, Ontario. *Can. J. Earth. Sci.* 31, 1325-1334.
22. EGOROV, L.S. (1970): Carbonatites and ultrabasic-alkaline rocks of the Maimecha-Kotui region, N.Siberia. *Lithos* 3, 341-359.
23. ENGELHARDT, W., WEISKIRCHNER, W. (1963): Einfhhrung zu den exkursionen der Deutschen Mineralogischen Gesellschaft zu den Vulkanschloten der Schw@bischen Alb und vin den Hegau. *Fortschr. Mineral.* 40, 5-28.
24. FEIGENSON, M.D. (1984): Geochemistry of Kauai volcanics and a mixing model for the origin of Hawaiian alkali basalts. *Contrib. Mineral. Petrol.* 87, 109-119.
25. FREY, F.A., GREEN, D.H., ROY, S.D. (1978): Integrated models and basalt petrogenesis:
26. A study of quartz tholeiites to olivine melilitites from southeastern Australia utilizing geochemical and experimental petrological data. *J. Petrol.* 19, 463-513.
27. GEE, L.L., SACK, R. O. (1988): Experimental petrology of melilite nephelinites. *J. Petrol.* 29, 1233-1255.
28. GOLD, D.P., MARCHAND, M. (1969): The diatreme breccia pipes and dikes and the related aln'ite, kimberlite and carbonatite intrusions occurring in the Montreal and Oka areas, P.Q. In *Geology of the Montereian Hills* (G. Pouliot, ed.) *Geol. Assoc. Can. - Mineral. Assoc. Can. Guidebook*, 5-42.
29. GUPTA, A.K., VENKATESWARAN, G.P., LIDIAC, E.G., EDGAR, A.D. (1973): The system diopside-nepheline-Dkermanite-leucite and its bearing on the genesis of alkali-rich mafic and ultramafic rocks. *J. Geol.* 81, 209-218.
30. HEARN, B.C. (1968): Diatremes with kimberlitic affinities in North Central Montana. *Science* 159, 622-625.
31. HOERNLE, K., SCHMINCKE, H.U. (1993): The petrology of tholeiites through melilite nephelinites on Gran Canaria, Canary Islands: crystal fractionation, accumulation and depths of melting. *J.Petrol.* 34, 573-597.
32. JANSE, A.J.A. (1971): Monticellite-bearing porphyritic peridotite from Gross Brukkaros, S.W.A. *Trans. Geol. S. Africa*, 74, 45-56
33. JANSE, A.J.A., DOWNIE, I.F., REED, L.E., SINCLAIR, I.G.L. (1989): Alkaline intrusions in the Hudson Bay Lowlands, Canada. In *Kimberlites and Related Rocks* (J.Ross, ed.) *Proc. 4th Internat. Kimberlite Conf. Geol. Soc. Australia Spec. Pub.* 14, 2, 1192-1203.

34. KALINKIN, M.M., ARZAMASTSEV, A.A., POLYAKOV, I.V. (1993): Kimberlites and related rocks of the Kola region. *Petrology* 1, 205-214.
35. KELLER, J., BREY, G., LORENZ, V. and SACHS, P. (1990): IAVCEI 1990 Preconference excursion 2A: Volcanism and petrology of the Upper Rhine graben (Urach-Hegau-Kaiserstuhl). IAVCEI.
36. KHUKHARENKO, A.A., ORLOVA, M.P., BULAKH, A.G., BAGDASAROV, E.A., RIMSKAYA-KORSAKOVA, O.M., NEPHEDOV, E.I., ILINSKII, G.A., ERGEEV, A.S., ABAKUMOVA, N.B. (1965): Каледонский комплекс ультраосновных щелочных пород и карбонатитов Кольского полуострова и Северной Карелии (*The Caledonian Complex of Ultrabasic, Alkaline Rocks and Carbonatites of the Kola Peninsula and Northern Karelia*). Nedra, Moscow.
37. KJARSGAARD, B.A., HAMILTON, D.L., PETERSON, T.D. (1995): Peralkaline nephelinite-carbonatite liquid immiscibility: Comparison of phase compositions in experiments and natural lavas. *In Carbonatite Volcanism* (K. Bell and J. Keller, eds.) Springer-Verlag, Berlin, 163-190.
38. KOGARKO, L.N, KONONOVA, V.A., ORLOVA, M.P., WOOLLEY A.R. (1995): *Alkaline Rocks and Carbonatites of the World Part 2: Former USSR*. Chapman and Hall, London.
39. KOVALSKII, V.V., NIKISHOV, K.N., EGOROV, O.S. (1969): Кимберлиты и карбонатиты Восточного и Юго-Восточного склонов Анабарской антиклизы (*Kimberlite and Carbonatite Occurrences in the Eastern and South-eastern Parts of the Anabar Anticline*). Nauka, Moscow.
40. KURSZLAUKIS, S., FRANZ, L., BREY, G., SMITH, C.B. (1995): Geochemistry and evolution of the ultrabasic Blue Hills Intrusive complex (Namibia). *Ext. Abstrs. 6th Internat. Kimberlite Conf. Novosibirsk*, 308-310.
41. LORENZ, V. (1975): Formation of phreatomagmatic maar-diatreme volcanoes and its relevance to kimberlite diatremes. *Phys. Chem. Earth*, 9, 17-27.
42. LORENZ, V. (1979): Phreatomagmatic origin of the olivine melilitite diatremes in the Swabian Alb, Germany. *In Kimberlites, Diatremes and Diamonds* (F.R. Boyd and H.O.A. Meyer, eds.). *Proc. 2nd. Internat. Kimberlite Conf. Amer. Geophys. Union, Washington, D.C.* 1, 354-363.
43. LORENZ, V. (1984): Explosive volcanism in the West Eifel volcanic field, Germany. *In Kimberlites and Related Rocks* (J. Kornprobst, ed.). *Proc. 3rd Internat. Kimberlite Conf. Elsevier, New York*, 1, 299-307.
44. MAALQE, S., JAMES, D., SMEDLEY, P., PETERSEN, S., GARMANN, L.B. (1992): The Koloa volcanic suite of Kauai, Hawaii. *J. Petrol.* 33, 761-784.
45. MANSKER, W.L., EWING, R.C., KEIL, K. (1979): Barian titanian biotites in nephelinites from Oahu, Hawaii. *Am. Mineral.* 64, 156-159.
46. MITCHELL, R.H. (1986): *Kimberlites: Mineralogy, Geochemistry and Petrology*. Plenum Press, New York.
47. MITCHELL, R.H. (1994): The lamprophyre facies. *Mineral. Petrol.* 51, 137-146.
48. MITCHELL, R.H. (1995): *Kimberlites, Orangeites and Related Rocks*. Plenum Press, New York.
49. MITCHELL, R.H., PLATT, R.G. (1983): Primitive nephelinitic volcanism associated with rifting and uplift in the Canadian Arctic. *Nature*, 303, 609-612.
50. MITCHELL, R.H., PLATT, R.G. (1984): The Freemans Cove volcanic suite: field relations, petrochemistry and tectonic setting of nephelinite-basanite volcanism associated with rifting in the Canadian Arctic Archipelago. *Can. J. Earth Sci.* 21 428-436.
51. MOORE, A.E. (1988): Olivine: A monitor of magma evolutionary paths in kimberlites and olivine melilitites. *Contrib. Mineral. Petrol.* 99, 238-248.

52. MOORE, A.E., ERLANK, A.J. (1979): Unusual olivine zoning-evidence for complex physico-chemical changes during the evolution of olivine melilitite and kimberlite magmas. *Contrib. Mineral. Petrol.* 70, 391-405
53. MOORE, A.E., VERWOERD, W.J. (1985): The olivine melilitite-"kimberlite"-carbonatite suite of Namaqualand and Bushmanland, South Africa. *Trans. Geol. Soc. S. Africa*, 88, 281-294.
54. NASH, W.P. (1972): Mineralogy and petrology of the Iron Hill carbonatite complex, Colorado. *Geol. Soc. Amer. Bull.* 83, 1361-1382.
55. NIELSON, T.F.D. (1980): The petrology of a melilitolite, melteigite, carbonatite and syenite ring dike system in the Gardiner complex, East Greenland. *Lithos*, 13, 181-197.
56. NIELSON, T.F.D. (1981): The ultramafic cumulate series, Gardiner complex, East Greenland: Cumulates in a shallow level magma chamber of a nephelinitic volcano. *Contrib. Mineral. Petrol.* 76, 60-72.
57. NIELSON, T.F.D. (1994): Alkaline dike swarms of the Gardiner complex and the origin of ultramafic alkaline complexes. *Geochem. Internat.* 31, 37-56.
58. NIXON, P.H., MITCHELL, R.H., ROGERS, N.W. (1980): Petrogenesis of aln'itic rocks from Malaita, Solomon Islands, Melanesia. *Mineral. Mag.* 43, 587-596.
59. O'HARA, M.J., BIGGAR, G.M. (1969): Diopside + spinel equilibria, anorthite and forsterite reaction relationships in silica-poor liquids in the system CaO - MgO - Al₂O₃ - SiO₂ at atmospheric pressure and their bearing on the genesis of melilitites and nephelinites. *Amer. J. Sci.* 267A, 364-390.
60. ONUMA, K., YAGI, K. (1967): The system diopside-Dkermanite-nepheline. *Amer. Mineral.* 52, 227-243.
61. ONUMA, K., YAMAMOTO, M. (1976): Crystallization in the silica-undersaturated portion of the system diopside-nepheline-Dkermanite-silica and its bearing on the formation of melilitites and nephelinites. *J. Fac. Sci. Hokkaido Univ. Ser. IV*, 17, 347-355.
62. PAN, V., LONGHI, J. (1990): The system Mg₂SiO₄ - Ca₂SiO₄ - CaAl₂O₄ - NaAlSiO₄ - SiO₂ : One atmosphere liquidus equilibria of analogs of alkaline mafic lavas. *Contrib. Mineral. Petrol.* 105, 569-584.
63. PETERSON, T.D. (1989): Peralkaline nephelinites II. Low pressure fractionation and the hypersodic lavas of Oldoinyo L'engai. *Contrib. Mineral. Petrol.* 102, 236-346.
64. PETERSON, T.D., KJARSGAARD, B.A. (1995): What are the parental magmas at Oldoinyo Lengai? In *Carbonatite Volcanism* (K. Bell and J. Keller, eds.) Springer-Verlag, Berlin, 148-162.
65. PLATT, R.G., EDGAR, A.D. (1972): The system nepheline-diopside-sanidine and its significance to the genesis of melilite- and olivine-bearing alkaline rocks. *J. Geol.* 80, 224-236.
66. PLATT, R.G., MITCHELL, R.H. (1982): The Marathon dikes: Ultrabasic lamprophyres from the vicinity of McKellar Harbour, N.W. Ontario. *Amer. Mineral.* 67, 907-916.
67. ROCK, N.M.S. (1986): The nature and origin of lamprophyres: Aln'ites and allied rocks (ultramafic lamprophyres). *J. Petrol.* 27, 193-227.
68. ROCK, N.M.S. (1991): *Lamprophyres*. Blackie and Son, Edinburgh.
69. ROGERS, N.W., HAWKESWORTH, C.J., PALACZ, Z.A. (1992): Phlogopite and the generation of olivine melilitites from Namaqualand, South Africa and implications for element fractionation processes in the upper mantle. *Lithos*, 28, 347-365.
70. RONENSON, B.M., AFANASYEV, B.V., LEVIN, V.Y. (1981): Turjaite parageneses of Tur'ya Peninsula. *Internat. Geol. Rev.* 23, 535-543.
71. SCOTT SMITH, B.H. (1989): Lamproites and kimberlites in India. *N. Jahrb. Mineral. Abh.* 161, 193-225.
72. SPENCER, A.B. (1969): Alkalic igneous rocks of the Balcones province, Texas. *J. Petrol.* 10, 272-306.
73. STILLE, P., UNRUH, D.M., TATSUMOTO, M. (1983): Pb, Sr, Nd and Hf isotopic

- evidence of multiple sources for Oahu, Hawaii basalts. *Nature*, 304, 25-29.
74. TALJAARD, M.S. (1937): South African melilite basalts and their relations. *Trans. Geol. Soc. S. Africa*, 39, 281-316.
 75. ULRYCH, J., PIVEC, E., RUTŠEK, J. (1986): Spinel zonation in melilite rocks of the Ploučnice River region, Czechoslovakia. *N. Jahrb. Mineral. Abh.*, 155, 129-146,
 76. ULRYCH, J., POVONDRA, P., RUTŠEK, J. and PIVEC, E. (1988): Melilitic and melilite-bearing subvolcanic rocks from the Ploučnice River region, Czechoslovakia. *Acta Universitatis Carolinae Geologica*, 1988, 195-231.
 77. ULRYCH, J., PIVEC, E., RUTŠEK, J. and POVONDRA, P. (1990): Olivines - monticellites and clinopyroxenes in melilitic rocks, Ploučnice River region, Czechoslovakia, *Acta Universitatis Carolinae Geologica*, 1990, 141-164.
 78. ULRYCH, J., POVONDRA, P., PIVEC, E., RUTŠEK, SITEK, J. (1994): Compositional evolution in metasomatic garnet in melilitic rocks of the Osečná complex, Bohemia. *Canad. Mineral.* 32, 637-647.
 80. VELDE, D., YODER, H.S. (1976): The chemical composition of melilite-bearing eruptive rocks. *Carnegie Instit. Washington Yearbook*, 75, 754-580.
 81. VON ECKERMANN, H. (1948): The alkaline district of Aln' Island. *Sveriges Geol. Unders'kning Ser. Ca. No. 36*.
 82. WILKINSON, J.F.G., STOLZ, A.J. (1983): Low pressure fractionation of strongly undersaturated alkaline ultrabasic magma: The olivine-melilite-nephelinite at Moiliili, Oahu, Hawaii. *Contrib. Mineral. Petrol.* 83, 363-374.
 83. WILLIAMS, L.A.J. (1970): The volcanics of the Gregory Rift Valley, East Africa. *Bull. Volcan.* XXXIV, 439-465.
 84. WILSON, M., ROSENBAUM, J.M., DUNWORTH, E.A. (1995): Melilitites: Partial melts of the thermal boundary layer? *Contrib. Mineral. Petrol.* 119, 181-196.
 85. WIMMENAUER, W. (1974): The alkaline rock provinces of central Europe and France. *In The Alkaline Rocks* (H.Srrensen, ed.), J. Wiley and Sons, London, 238-271.
 87. WITTKE, J.H., MACK, L.E. (1993): OIB-like mantle source for continental alkaline rocks of the Balcones Province, Texas: Trace element and isotopic evidence. *J.Geol.* 101, 333-344.
 88. WYLLIE, P.J., HUANG, W.L. (1976): Carbonation and melting reactions in the system CaO - MgO - SiO₂ - CO₂ at mantle pressures with geophysical and petrological applications. *Contrib. Mineral.Petrol.* 54, 79-207.
 89. YODER, H.S. (1973): Melilite stability and paragenesis. *Fortschr. Mineral.* 50, 140-173.
 90. YODER, H.S. (1979): Melilite-bearing rocks and related lamprophyres. *In The Evolution of The Igneous Rocks* (H.S. Yoder, ed.), Princeton Univ. Press, New Jersey, 391-411.
 91. ZAITSEV, A., BELL, K. (1995): Sr and Nd isotope data of apatite, calcite and dolomites as indicators of sources, and the relationships of phoscorites and carbonatites from the Kovdor massif, Kola Peninsula, Russia. *Contrib. Mineral. Petrol.* 121, 324-335.

Early Paleozoic Kimberlite-Melnoite Magmatism of the Pri-Polar Urals And the Geodynamic Formation Model

I.L. Mahotkin¹, Yu.A. Podkuiko², D.Z. Zhuravlev³

¹ *De Beers Moscow Office, Russia, 125047, Moscow.*

² *GUP «Sosvappromgeologia», Russia, Tiumen oblast, v. Saranpaul*

³ *IGEM RAS, Russia, 109017, Moscow*

Khartess ultramafic intrusions comprise four rock types: kimberlites, melnoitic kimberlites, melnoites and allicites. Sm-Nd data show Upper Cambrian age of the Khartess intrusions. Origin of Khartess kimberlites and related rocks is a result of the rifting process affected on highly depleted lithospheric mantle of the Central Uralian zone of the Pri Polar Urals which was part of Barents platform block. Depletion degree of Ural lithospheric mantle increased towards the shallow level. The most dip horizons of the Ural lithospheric mantle were slightly enriched in LREE at the Mid-Upper Riphean age.

INTRODUCTION

The kimberlite magmatism of the Pri-Polar Urals, which are known as Khartess kimberlite complex, is situated to the Riphean structures of the Uralian mobile belt [Lukjanova, Belskiy, 1987]. The age and the origin of this complex are still under discussion. If compared to the typical kimberlites of the ancient platforms, Khartess complex rocks are depleted in to rare element [Mahotkin, Podkuiko, 1998]. K-Ar isotope data, indicating that these rocks were formed between the Upper Perm and Triassic [Mahotkin et al., 1997], does not agree with the geological information on their Early Paleozoic age.

In order to confirm the age and origin of the Pri-Polar Urals kimberlite magmatism authors carried out isotope-geochemical studies (K-Ar; Rb-Sr; Sm-Nd) of the seven rock samples from the Khartess complex and of the four samples of potassic lamprophyres and basalts from the Sertynja River, which supposedly could have been formed in a single tectonic-magmatic stage together with kimberlite.

GEOLOGICAL LOCATION

The Khartess kimberlite complex is located in the upper reaches of the Khartess River. This complex consists of six dykes submeridionally stretched and sizing from 1 to 2 km. All the bodies are localised to a narrow, 10 km in size submeridional tectonic structure, composed by the Upper Riphean sandstones and siltstones (Fig. 1). This submeridional structure is limited by thrusts from the East and from the West. Alongside the eastern fault the Upper Riphean sediments are overlapped by a tectonic plate, composed by Lower Mid-Ordovician terrigenous-

carbonate sediments of the Levminskaya zone. No kimberlite outcrops are registered within the Ordovician rock field.

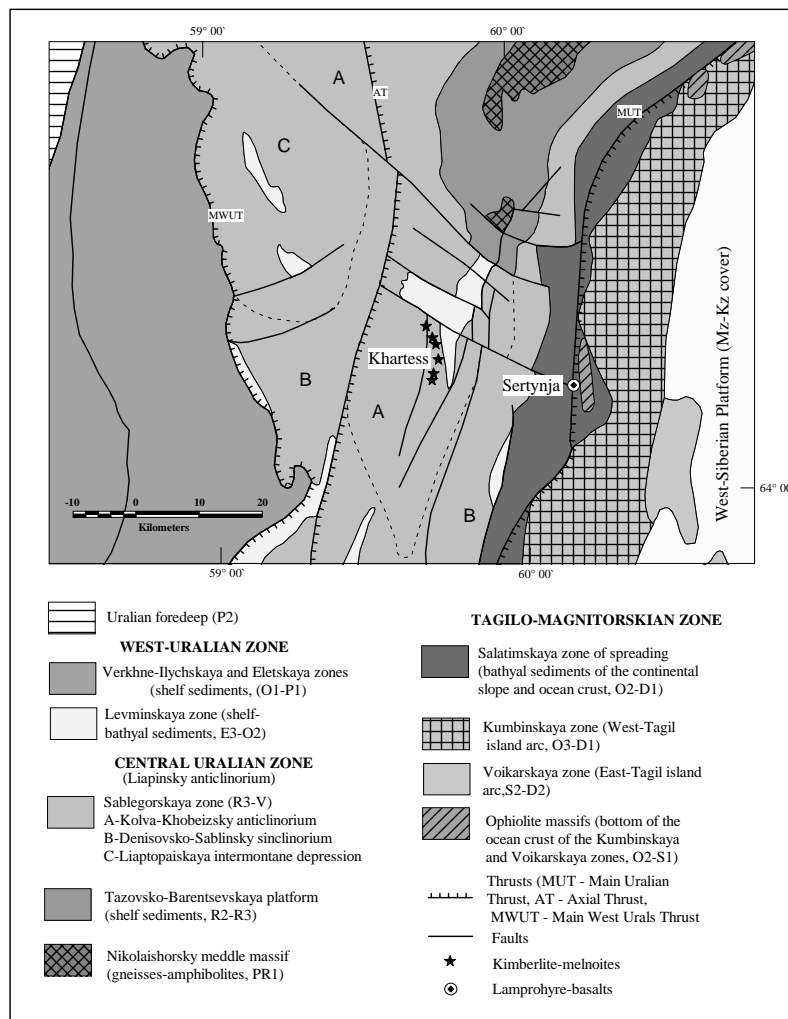


Fig. 1. Geological position of Khartess kimberlite complex, subpolar Ural

In the regional tectonic structure, the Khartess kimberlite complex is situated to axial southern zone of the Lyapinsky anticlinorium which is present of intersection of the submeridional Central Uralian zone (Paleozoic structure of the Urals mobile belt) and the Pre-Uralian (Late Proterozoic) basement structures of the north-western stretch. With regards to the Pre-Uralian structures, the Khartess kimberlite complex is situated to the southern ending of the Kolvo-Khobeizsky Anticlinorium zone (Fig. 1). The core of this anticlinorium zone is exposed to the north from the kimberlite area and is composed of Middle-Riphean terrigenous-carbonate platform sediments and the Lowe-Proterozoic gneisses and amphibolites of the so-called Nikolaishorsky middle massif.

Lamprophyres and basalts of the Sertynja River comprise small dykes, which intrude into Salatimskaya zone of spreading of paleocontinental slope. These bodies are localised to the east of the Khartess kimberlite complex and coincide with the Main Ural Thrust.

PETROGRAPHY

Among the dykes of the Khartess kimberlite complex the authors have studied three bodies, discriminating by their mineral and chemical composition presented in Table 1. In the first body the groundmass of the porphyritic rocks is completely replaced by rod-like aggregate of the sodium amphibole and talc with slight trace of chlorite (samples K-2-5, K-2-6). There is a high possibility that the amphibole of this groundmass could have been formed after the primary melilitites, which is indicated by the sodium alkalinity of the rocks ($K_2O/Na_2O = 0.23$), medium contents of $SiO_2 \sim 46$ wt % and $CaO \sim 8$ wt % (Table). These rocks are identified as melnoites. This term was introduced by Skinner [Scott Smith, 1995] to define paleotypic and cainotypic olivine melilitic subvolcanic rocks, which are close by its mineral assemblages to kimberlites, but slightly differs from them by texture, mineralogy and chemistry, mainly K/Na ratio (Fig. 2).

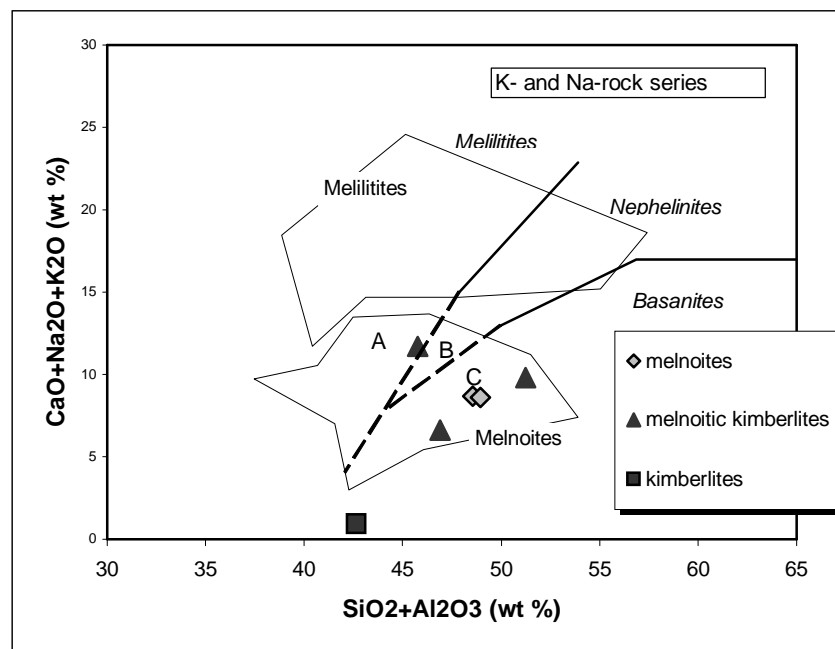


Fig. 2. The $CaO + Na_2O + K_2O - SiO_2 + Al_2O_3$ diagram for K- and Na-rock series.

The diagram shows the fields of melnoites, melilitites and solid boundary lines, discriminating the areas of melilitites, nephelinites and basanites (after Le Bas, 1989).

The distinct porphyritic rocks of the second body have the freshest appearance (Fig. 3). The groundmass of these rocks is composed by the fine-grained rosette-like aggregate of chlorite-serpentine or antigorite-serpentine (*sample K-3-5*). The visible phlogopite is absent in the groundmass, however its structure and the high potassium ratio ($K_2O/Na_2O = 3$) indicate the original presence of phlogopite. Generally the rocks are characterised by the low contents of $SiO_2 \sim 39$ wt %, $CaO \sim 0,57$ wt % and very high contents of $MgO \sim 34$ wt %. The rocks of this body have got all the texture-petrographic features of kimberlites and were classified as segregation serpentine kimberlites of hypabyssal facies. The

Khartes kimberlites as well as other kimberlites are typical olivine macrocrystic accumulated rock type (Fig. 4) and their chemistry is similar to kimberlites (Fig.5).

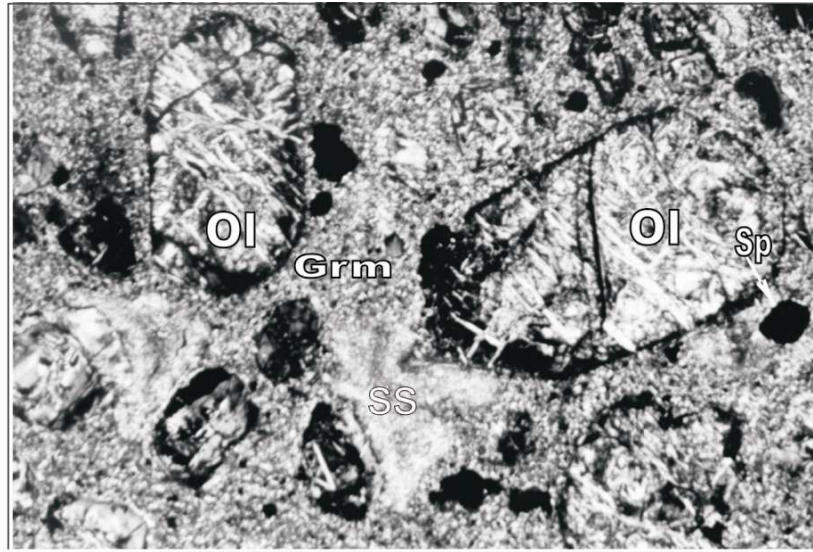


Fig. 3. Thin section photograph of sample K-3-5 in cross-polarized light.

Field of view =6 mm Segregationary serpentine kimberlites: Ol-Olivine, Sp-spinel, and SS-serpentine segregation in ground-mass-Grm

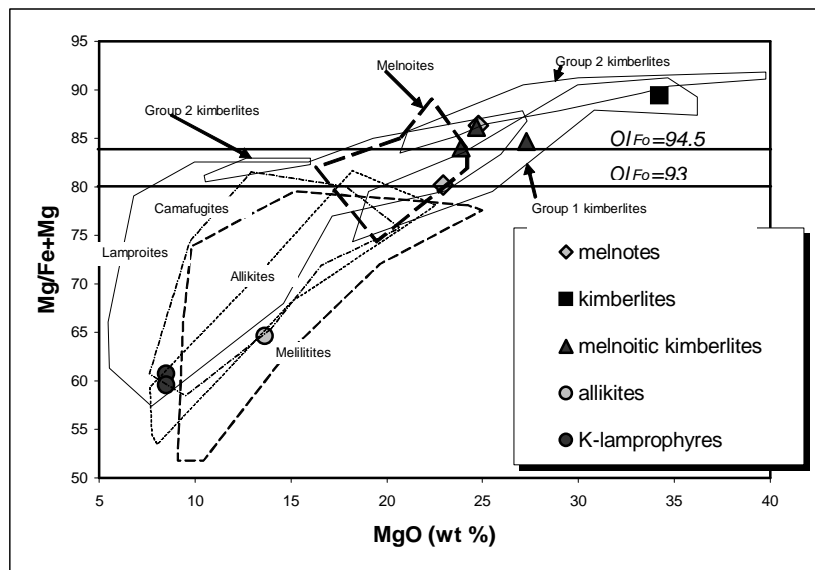


Fig. 4. Plot of $Mg/(Mg+Fe)$ vs MgO for magmatic rocks.

The plot shows the fields of Group 1 kimberlites, Group 2 kimberlites, lampro-ites, melnoites, meli-litites, camafugites and allikites. The horizontal solid lines show mg-number of melt which is equili-brium with olivine composition Fo 94.5 and Fo93 under $Kd=0.3$.

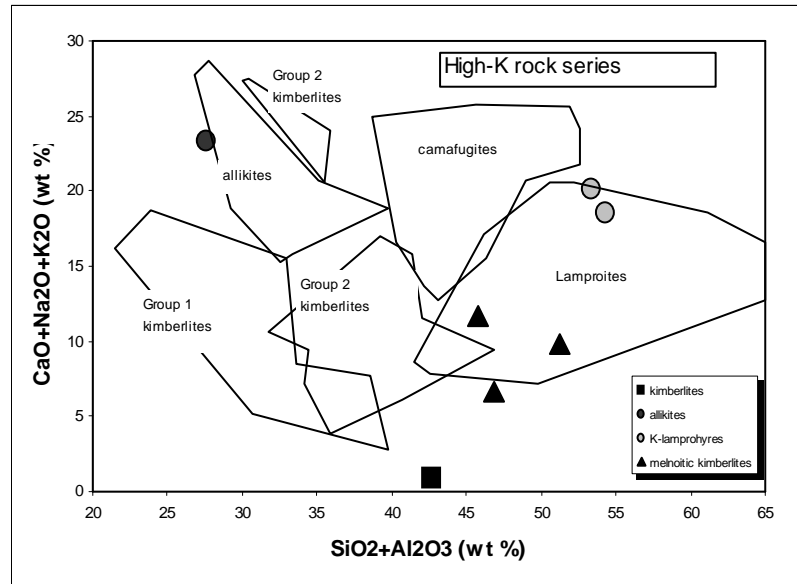


Fig. 5. The $CaO + Na_2O + K_2O - SiO_2 + Al_2O_3$ diagram.

The diagram (Fig. 6 b) shows the fields of Group 1 kimberlites, Group 2 kimberlites, lamproites, camafugites and allikites

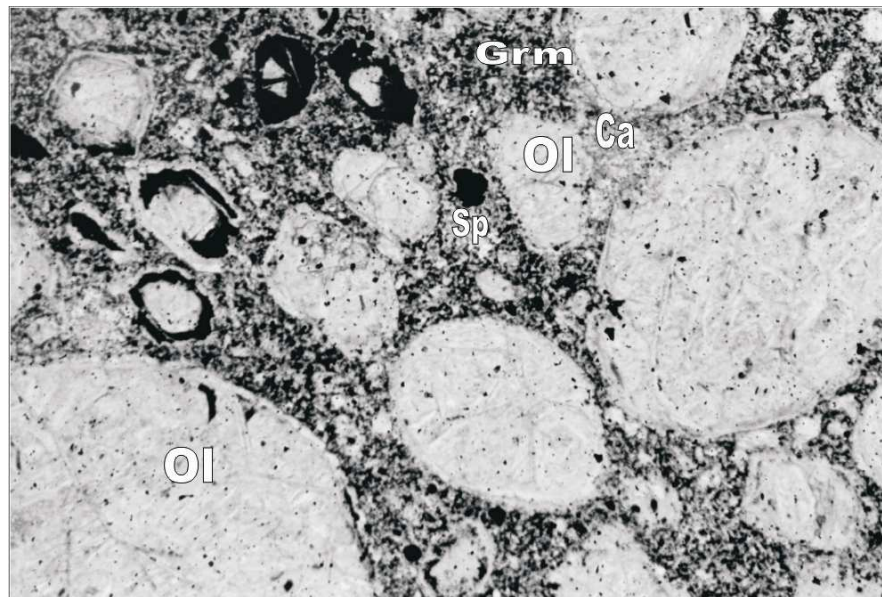


Fig. 6. Thin section photograph of sample 1002-13 in plane polarized light.

Field of view = 6 mm. Macrocrystic amphibole melnoitic kimberlites: Ol-Olivine, Sp-spinel and Ca- calcite in amphibole bearing groundmass-Grm

The third kimberlite body is located on the contact line with the western fault, separating two tectonic plates of the Upper Riphean rock. This body represents the serpentine tectonic melange zone, filled by numerous boudines (0,1-1,3 m in cross-section) of relatively poor metamorphosed olivine rich porphyritic ultramafic rock (Fig. 6). The groundmass of this rock is composed by medium-granular fibrous-rod-like aggregate of talc and amphibole with traces of phlogopite, chlorite and

calcite (*samples 1400-24, 1400-34, 1400-37*). This rock type is classified as melnoitic kimberlites (Fig. 6A part from porphyritic rocks, the boudines also comprise small bodies of equigranular ultramafic rock, enriched by carbonate, phlogopite, apatite and ore minerals, which classified as allikites (*sample 1400-9*).

Lamprophyres from the Sertynja River (*samples K-108-5,5 u K-108-1,4*) are represented by vaguely porphyritic rocks with small phenocrysts of fresh clinopiroxene and groundmass of phlogopite-amphibole composition.

Basalts from the Sertynja River are represented by lava and tuff breccias of porphyritic clinopiroxene-plagioclase tholeitic basalts (*sample 4254-4, 4255-4*).

Trace elements (exclude Cr, Ni determined by AA) are analysed by ISP-MS and major elements are analysed by wet chemical analyses in IGEM, Russian Academy of Science, Moscow.

AGE AND ISOTOPIC COMPOSITION

The K-Ar data of the Khartess melnoitic kimberlite (*samples 1400-24, 1400-37, 1400-9*) vary in the wide range of the values 244-261 Ma, which are interpreted by the authors as the age of the last stage of metamorphism.

The K-Ar data of lamprophyres and basalts of the Sertynja River resulted in the two narrow ranges – respectively 315-317 +/-5 Ma (Bashkirsko-Serpukhovsky epoch of Middle Carboniferous) and 338-348 +/-14 Ma (Visean epoch of the Early Carboniferous).

For Rb-Sr isotope system the regression line, calculated on the basis of four samples of melnoitic kimberlite (*samples 1400-24, 1400-34, 1400-37, 1400-9*), results in $T=257 \pm 5$ (2 δ) Ma. This line has a low value MSWD=2.4, that allows interpret this line as isochrone. This isochrone is probably formed as a result of isotopic homogenises at the final stage of Uralian rock metamorphism. The regression line of Sm-Nd isotope system, calculated on the basis of the same four samples of melnoitic kimberlite, results in the age: $T=506 \pm 184$ (2 δ) Ma and the low value MSWD=2.9. This line can therefore be interpreted as isochrone, corresponding to the Upper Cambrian age of the kimberlite origin. The high error of the age value is related to the small range of varieties $^{147}\text{Sm}/^{144}\text{Nd}$ in the analysed rocks.

MANTLE SOURCES

All the analysed samples of the Khartess kimberlitic rocks, lamprophyres and basalts of the Sertynja River are characterised by a high positive value of ϵ_{Nd} , being respectively ~ 3.7-4.06; 8.4-8.5; 6.7-6.8, which indicates the depleted type of their mantle sources. The model age with respect to the depleted mantle for melnoites is 1.3 Ba and for melnoitic kimberlite and kimberlite it varies in the

Table 1.

Samples	K-2-5	K-2-6	K-3-5	1400-24	1400-34	1400-37	1400-9	K-108-5.5	K-108-1.4	4254-4	4255-4
SiO₂ wt, %	46.35	46.65	39.15	43.50	41.00	46.20	21.75	37.75	37.75	55.90	50.45
TiO₂	0.20	0.55	0.15	0.12	0.20	0.27	2.55	1.50	1.60	0.30	0.35
Al₂O₃	2.20	2.30	3.50	3.40	4.75	5.05	5.80	15.65	16.60	11.35	17.50
Fe₂O₃	8.45	5.55	6.68	7.21	6.23	5.56	10.31	1.91	1.40	2.80	3.14
FeO	3.91	2.95	2.20	3.52	3.57	3.04	5.88	9.43	10.43	5.00	6.45
MnO	0.13	0.17	0.17	0.13	0.19	0.16	0.17	0.21	0.21	0.15	0.17
MgO	22.96	24.80	34.24	27.28	23.88	24.70	13.65	8.50	8.50	8.70	5.01
CaO	7.96	7.98	0.57	5.70	9.69	7.12	18.80	15.23	14.36	8.05	7.56
Na₂O	0.58	0.50	0.09	0.25	0.60	0.55	0.15	0.36	0.27	1.57	2.67
K₂O	0.14	0.11	0.28	0.66	1.40	2.15	4.39	4.56	3.99	0.05	1.14
P₂O₅	0.03	0.05	0.21	0.24	0.20	0.07	0.68	0.13	0.04	0.12	0.03
H₂O⁻	0.43	0.72	1.21	0.42	0.20	0.23	0.13	0.54	0.35	0.37	0.29
H₂O⁺	3.35	3.57	10.65	6.70	4.81	4.21	2.14	3.81	4.42	4.44	4.71
CO₂	2.42	3.45	0.31	0.45	2.62	0.31	13.75	0.36	0.24	1.32	0.16
Total	99.11	99.35	99.41	99.58	99.34	99.62	100.15	99.94	100.16	100.12	99.63
mg#	80.2	86.3	89.4	84.7	84.0	86.1	64.6	60.7	59.6	70.1	52.2
K₂O/Na₂O	0.24	0.22	3.11	2.64	2.33	3.91	29.27	12.67	14.78	0.03	0.43
Cr, ppm	2160	1990	2670	2710	2250	2140	390	218	203	422	75
Ni	1786	1190	2142	1548	1667	1428	172	72	74	115	50
Co	61.9	67.6	93.6	73.2	68.6	66.0	51.5	58.4	53.7	42.4	33.7
V	66.9	84.5	85.3	83.8	91.2	115.4	191.6	433.3	376.7	179.2	218.0
Sc	14.7	18.0	39.3	32.8	43.9	52.9	51.5	86.0	79.6	54.5	58.5
Cs	0.25	0.26	1.10	3.15	0.98	2.22	3.35	48.96	52.47	0.18	0.28
Rb	1.7	2.3	14.0	18.3	31.9	56.4	131.7	114.5	86.6	1.1	10.7
Li	14.1	13.5	9.3	12.1	15.5	11.7	13.1	617.1	572.3	12.3	11.4
Sr	238	223	67	183	298	93	6544	94	180	17	231
Ba	24	17	50	37	119	161	926	121	124	7	70
Y	3.5	2.1	4.8	6.0	10.1	5.7	51.8	40.7	38.0	9.9	12.0
Zr	4.8	4.0	10.4	14.9	12.4	21.8	197.6	100.6	96.9	24.4	29.5
Nb	2.17	0.97	1.23	0.95	1.87	1.99	41.33	5.05	4.13	0.73	0.76
Hf	0.145	0.130	0.262	0.489	0.510	0.795	5.236	2.689	3.201	0.826	1.001
Ta	0.077	0.101	0.139	0.045	0.162	0.068	2.820	0.341	0.273	0.033	0.061
La	3.006	1.403	5.217	5.492	11.465	4.696	41.064	3.897	3.921	1.241	1.541
Ce	5.303	2.916	9.591	11.245	15.696	10.014	89.909	11.344	11.645	2.909	3.750
Pr	0.598	0.394	1.257	1.300	1.745	1.244	11.271	1.818	1.990	0.559	0.580
Nd	2.656	1.700	5.563	5.911	8.269	5.903	47.393	10.730	10.503	2.755	2.814
Sm	0.937	0.434	1.231	1.581	1.876	1.639	10.029	3.702	3.648	1.173	1.123
Eu	0.222	0.167	0.369	0.443	0.618	0.456	4.455	1.354	1.301	0.305	0.473
Tb	0.110	0.061	0.163	0.247	0.318	0.224	1.563	0.941	0.919	0.244	0.268
Gd	0.704	0.456	1.075	1.501	1.963	1.195	9.385	4.766	4.703	1.141	1.303
Dy	0.673	0.527	0.991	1.070	1.922	0.985	8.196	5.715	5.924	1.477	1.664
Ho	0.138	0.073	0.179	0.211	0.433	0.243	1.748	1.246	1.193	0.349	0.392
Er	0.378	0.284	0.485	0.646	1.172	0.473	4.907	3.462	3.619	1.087	1.152
Tm	0.039	0.017	0.074	0.078	0.152	0.087	0.726	0.478	0.510	0.139	0.136
Yb	0.380	0.212	0.358	0.544	1.315	0.509	4.695	3.281	3.586	1.186	1.170
Lu	0.037	0.043	0.029	0.102	0.182	0.086	0.684	0.593	0.494	0.179	0.181
Pb	8.01	3.41	7.62	4.82	3.55	0.84	19.86	0.29	1.16	1.85	4.63
Th	0.22	0.29	0.84	1.00	1.51	1.10	3.61	0.18	0.21	0.25	0.26
Samples	K-2-5	K-2-6	K-3-5	1400-24	1400-34	1400-37	1400-9	K-108-5.5	K-108-1.4	4254-4	4255-4

End of Table 1.

Samples	K-2-5	K-2-6	K-3-5	1400-24	1400-34	1400-37	1400-9	K-108-5.5	K-108-1.4	4254-4	4255-4
U	0.75	0.25	0.92	0.24	0.84	0.32	1.15	0.12	0.15	0.08	0.14
Cu	31.1	7.4	33.3	34.0	100.8	48.2	144.6	47.6	50.4	51.6	59.7
Zn	34.8	36.2	70.9	48.4	83.9	74.1	50.7	93.1	91.4	50.8	100.8
Ga	1.9	2.2	5.8	5.1	7.1	8.2	6.6	10.5	14.1	12.9	15.7
Be	1.5	1.7	1.2	1.5	2.5	1.5	0.9	0.7	0.4	0.3	0.3
Mo	0.09	0.01	0.24	0.22	0.56	0.29	0.41	0.50	0.63	0.36	0.52
W	1.40	1.19	0.91	0.22	0.28	0.18	0.35	0.20	0.29	0.34	0.17
(La/Yb)	5.25	4.40	9.68	6.71	5.79	6.13	5.81	0.79	0.73	0.69	0.87
Ni/Co	28.8	17.6	22.9	21.1	24.3	21.7	3.3	1.2	1.4	2.7	1.5
Sampl es	K-2-5	K-2-6	K-3-5	1400-24	1400-34	1400-37	1400-9	K-108-5.5	K-108-1.4	4254-4	4255-4

range of 1.1-0.94 Ba. The model age with respect to the depleted mantle for lamprophyres and basalts of the Sertynja River produces even more ancient results, corresponding to the Early Proterozoic and even the Archaean. Such ancient model age means that their mantle source was either ancient Archaean-Early Proterozoic depleted lithosphere mantle or the degree of depletion of the Uralian mantle, exceeded the values applied in the standard model of the depleted mantle. All the three groups of the Khartess kimberlitic rocks are enriched in LREE. The rate of their enrichment grows in the following order: melnoite, melnoitic kimberlite, kimberlite $(La/Yb)_N=4.4-5.2$; $5.8-6.7$ and 9.7 (Fig. 7). However, even in the kimberlite sample the LREE content does not reach the values, typical for kimberlite of ancient platforms. The fact that most of the Khartess kimberlitic rocks are characterised by low values of HREE: $(Yb)_N=1.3-3.2$, means that they were formed as a result of melting of the mantle, composed by garnet peridotites.

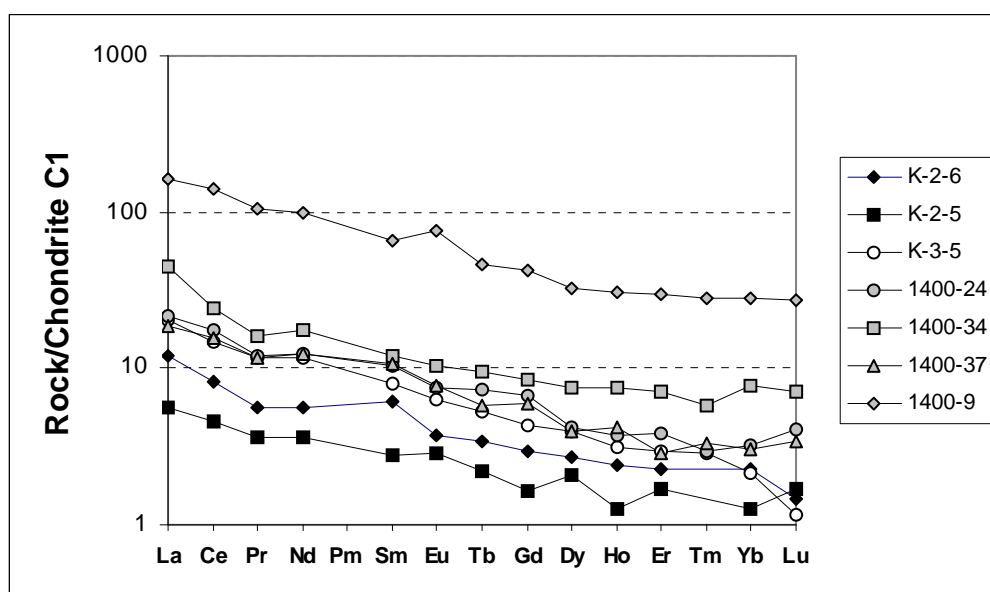


Fig. 7. REE patterns of Khartess rocks.

All the three types of the Khartess kimberlitic rocks have distinct differences in the patterns of rare-earth elements (REE) and in the spider-diagrams of trace elements. These differences indicate several geochemical mantle types within their common mantle region. The biggest difference is registered between melnoitic kimberlites and melnoites. Their spider-diagrams are different in the absence of Ta-Nb and Ti minimum for melnoites. Inter-element variations of the high field strong elements (HFSE) in melnoite are similar to those of within-plate basalts of ocean islands (OIB source), and by the ratio of certain elements the melnoites are similar to the enriched tholeiitic basalts of the Mid-Ocean Ridges (E-MORB source). The melnoites also possess the typical features of continental basalts, if the HFSE variations are considered together with the LREE variations. Melnoitic kimberlites have geochemical features, which occur both in MORB source and in the island-arc tholeiitic basalts (IATB-source). The kimberlites have intermediate geochemical characteristics of the source types: OIB, MORB and IATB.

Unlike the Khartess kimberlitic rocks, the lamprophyres and basalts of the Sertynja River are poor in LREE ($(La/Yb)_N = 0.7-0.88$), which means that they were generated from the strongly depleted mantle. The high contents of HREE in lamprophyres and basalts, being respectively $(Yb)_N = 7$ and ~ 20 , may be explained by their origin at shallow level of the Upper mantle, composed by spinel peridotites.

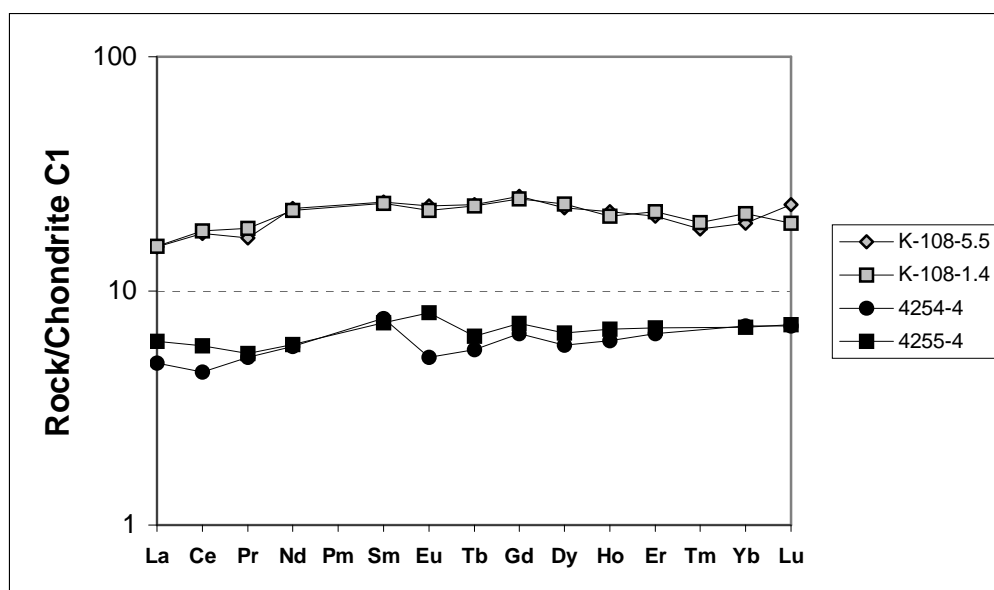


Fig. 8. REE patterns of Sertynja rocks.

Inter-element variations of Ti-Zr, Zr/Y-Zr, Ti-V, Th-Hf/3-Ta, La-Y-Nb, FeO-MgO-Al₂O₃, Ti/Y-Nb/Y, Zr/4-2Nb-Y, K₂O/Yb-Ta/Yb indicate that the basalts from the Sertynja River have the features of both the IATB-source, and the MORB-source. The lamprophyres of the Sertynja River are characterised by the geochemical features, typical of the most depleted N-MORB-source and partly – of the IATB-source. Since the lamprophyres and basalts of the Sertynja River were

formed within the continental environment, the presence of the MORB component in their mantle sources proves not so much the oceanic condition of their origin, but rather the highly depleted composition of their mantle sources. This geochemical result pretty well agrees with the results of their isotopic data. It is likely that the involvement of this ancient highly depleted lithosphere mantle in the collision processes during the Early-Middle Paleozoic resulted in the occurrence of IATB-source components in the mantle region. Judging by the plot $K_2O/Yb-Ta/Yb$, the proximity of the mantle sources of lamprophyres and basalts of the Sertynja to the IATB-source could have resulted from enrichment of the primarily depleted mantle by the fluid components.

GEODYNAMIC REGIME AND THE STRUCTURE OF LITHOSPHERE

Basing on the obtained isotope and geochemical data, one can draw a conclusion that the lithosphere mantle of the Central Uralian zone of the Pri Polar Urals was characterised highly depleted composition, and it was stratified by the depletion degree. The depletion degree increased towards the shallow level, where it even seemed to exceed the values applied in the standard model of depleted mantle. The dipper horizons of this lithospheric depleted mantle were slightly enriched in LREE at the Mid-Upper Riphean, that is likely related to the Riphean rifting within the Lower Proterozoic Barents platform.

The distinct correlation between the fine geochemical features of the Khartess melnoites, melnoitic kimberlites, kimberlites and their Nd model age indicates that the variety of their isotope composition was mostly likely formed as a result of the time integrated process in the ancient lithospheric mantle of the Pri Polar Urals. While probability of mixing of the young (Upper Cambrian) isotope-homogeneous plum-related component with this lithospheric mantle was limited. Thus the obtained results mostly correspond to origin the Khartess kimberlite complex by rifting, during which the lithospheric plate starts breaking and becomes thinner under the influence of external horizontal stretch tension, and not under the influence of the deep mantle plum rising towards its base [Mahotkin et al., 1997]. The mantle melts are formed at the bottom of this lithospheric plate as a result of adiabatic decompression of the depleted lithosphere substance.

The Upper Cambrian age of the Khartess kimberlite complex precisely corresponds to the beginning of the rifting stage in evolution of the Paleozoic Uralian mobile belt, when the Upper Cambrian and Lower Ordovician submeridional graben-shaped depressions were formed within the continental crust of Central Uralian zone (Fig. 1). This initial rifting stage ends by formation of the ocean crust of the Lower-Mid Ordovician age in the east of Urals [Savelieva, Nesbitt, 1996].

Certain similarity between the rift-related kimberlite-melnoite magmatism of the Pri Polar Urals and the supposedly Cambrian magmatism of the Blagodat mountain in the Northern Urals, comprising carbonatites and kimberlite-like

(melnoite) rocks, probable indicates a much expanded activity of the alkaline-ultramafic rift-related magmatism within the continental margin of the Uralian mobile belt.

REFERENCES

1. Lukjanova L.I., Belskiy A.V. Kimberlite magmatism of the Pri Polar Urals. *Sovetskaya Geologia*. 1987. № 1. P. 92-102.
2. Mahotkin I.L., Podkuiko Yu.A. Kimberlites of the Pri Polar Urals as a new geochemical type of kimberlitic rocks, depleted in the rare elements. *DAN RAN*. 1998. V. 362. № 2. P. 245-251.
3. Mahotkin I.L., Zhuravlev D.Z., Lebedev I.A., Arakelyants M.M. Age and origin of the mantle sources of kimberlites and potassic lamprophyres of the Pri Polar Urals. Abstracts of the VI Urals petrographic Symposium. 1997. Yekaterinburg. P. 97-99.
4. Mahotkin I.L., Zhuravlev D.Z., Sablukov S.M., Zherdev P.Yu, Thompson R.N., Gibson S.A. Plum-lithosphere interaction As a geodynamic formation model of the Arkhangelsk diamond-bearing Province. *DAN RAN*. 1997. V. 353. № 2. P. 228-232.
5. Savelieva G. N., Nesbitt R. W. A synthesis of the stratigraphic and tectonic setting of the Uralian ophiolites. *Journal of the Geological Society*. London. 1996, vol. 153, pp. 525-537.
6. Scott Smith B.H. Petrology and diamonds. *Explor. Mining. Geol.* 1995. Vol. 4, No.2, pp. 127-140.

Early Paleozoic Kimberlite-Melnoite Magmatism of the Pri-Polar Urals And the Geodynamic Formation Model

I.L. Mahotkin¹, Yu.A. Podkuiko², D.Z. Zhuravlev³

¹ *De Beers Moscow Office, Russia, 125047, Moscow.*

² *GUP «Sosvapromgeologia», Russia, Tiumen oblast, v. Saranpaul*

³ *IGEM RAS, Russia, 109017, Moscow*

INTRODUCTION

Kimberlite-like rocks (lamproites, kimberlites, monchequites) from the Aldan shield (Amga River basin) contain disintegrated mantle inclusions: pyropes, Cr-diopsides, orthopyroxenes, Cr-spinels, phlogopites, Cr-bearing pargasites, etc. The concentrates from the Gornaya and Ogonek pipes and the Aldanskaya dyke were used for the reconstruction of lithospheric mantle keel structure. The experience of pyroxene-based TP reconstruction seems to be very useful and is more simple than pyrope thermobarometry, which needs very accurate analytic data. The chemistry of mantle xenocrysts suggests that they were captured from quite different rock types. The determination of TRE elements determined with LAM ICP method in the Analytic Center in the UIGGM SD RAS allows a calculation of peridotite modal abundances and melting parameters. The composition of host alkaline lamprophyric (lamproitic) rocks obtained by the same method on a finegrained matrix reveals typical features of primitive mantle melts.

LOCATION AND GEOLOGY

The dykes and pipes of kimberlite-like rocks discovered in the upper reaches of the Chompolo (Fig.1) river by the Amakinskaya expedition [Shilina, Zeitling, 1959] are located within the Yamalakhsky gorst. The diatremes were referred to the T-P stage due to the discovery of pyropes and Cr-diopsides in Early Jurassic sandstones and conglomerates. Oval pipes 60-110 m across, and submeridional dykes 360-800 m long and up to 40m thick are composed of gray breccias containing various mantle nodules and crust debris (Fig. 2).

MICROXENOCRYSTS

Xenocrysts do not exceed 2-3 mm in sizes. Pink and purple garnets usually prevail over orange varieties rarely found in intergrowths with augites. Dark garnets are intergrown with kaersutite, mica and K-Fsp (sanidine). The debris of granulite associations are abundant increasing quartz content up to 10-20%. In the

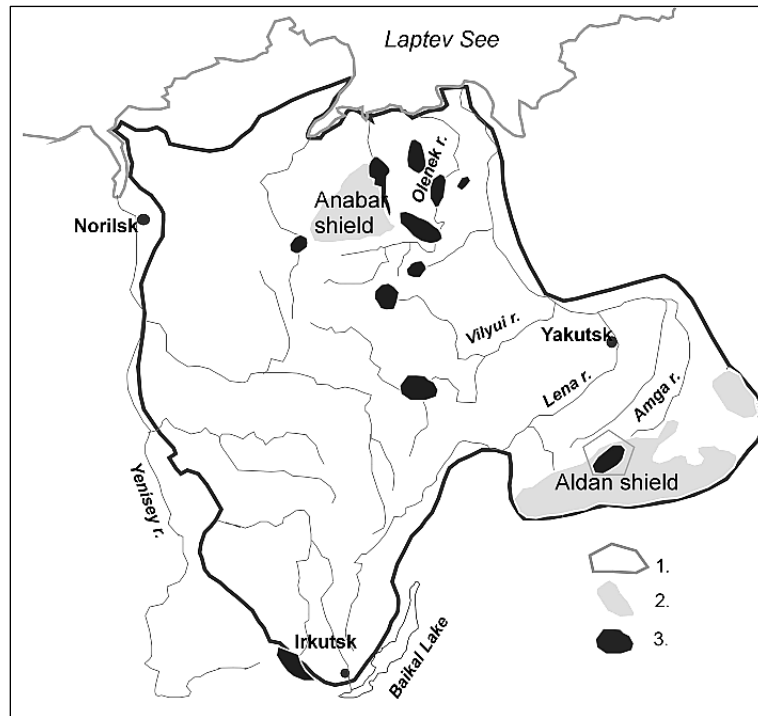


Fig. 1. Scheme of the kimberlite location on the Siberian platform.

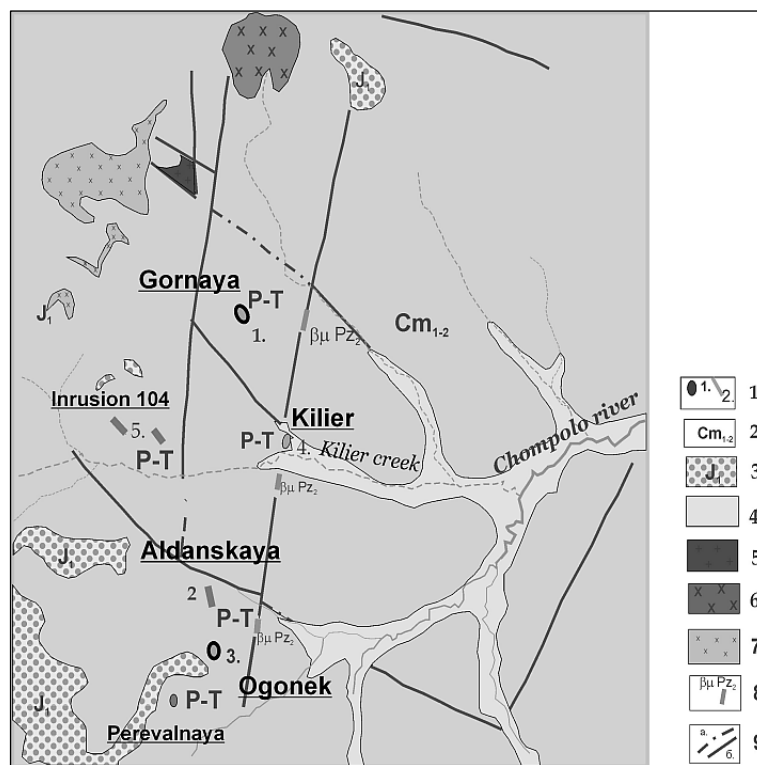


Fig. 2. Scheme of Chompolo field.

Ogonek pipe pyropes are usually surrounded by bright emerald-colored Cr-fucksite. Fine Cr diopsides grains rarely occur in deformed Cr – pyro-pes. Emerald clinopyroxenes rarely include spinel and phlogopites and exclusive tube-like fluid inclusions. Yellow or light- brown orthopyroxene are cleavaged. Sulfide globules are met in more dark varieties. Two-pyroxene or garnet-spinel intergrowths and

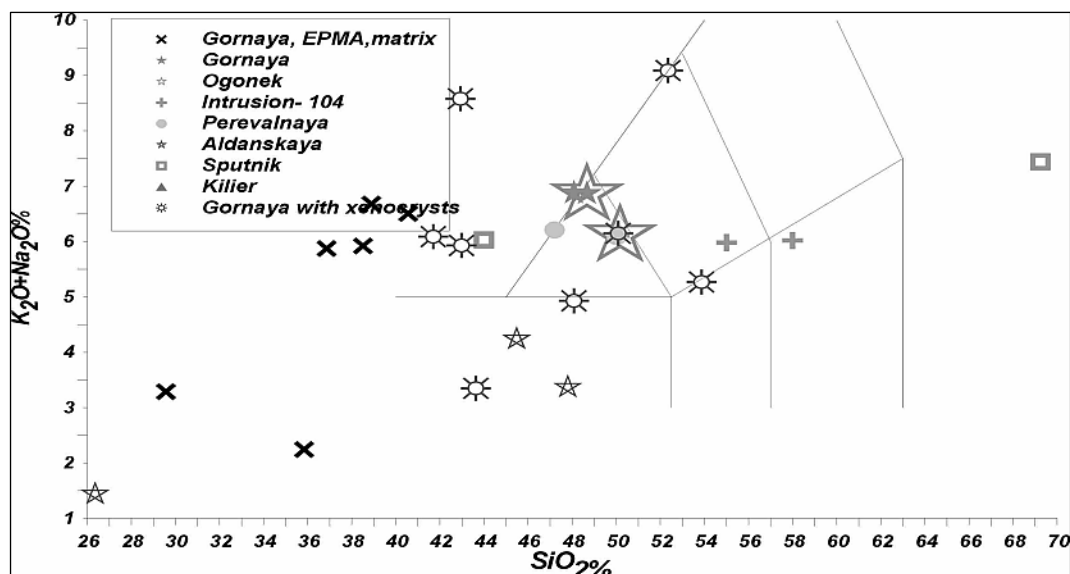


Fig. 3. Bulk rock composition of the volcanics in Chompolo field.

small pieces of fine-grained lherzolites or phlogopite porphyroclasts with Cr-diopside and olivine are sparse.

Clinopyroxene compiles ~ 30% of total xenocryst population, orthopyroxene – 5-10, pargasite amphibole is rare, but black hornblende is typical Cr-spinels and chromites 0.5-3mm in diameter form octahedrons; finegrained inclusions are found in the deformed garnet.

METHODS OF EXAMINATION

Deep-seated xenocrysts were selected from rocks after their crushing by standard electromagnetic and density separation, mounted and analyzed with EPMA CamebaxMicro in the Analytic center of UIGGM: pyropes and other garnets- 210; Cr-diopsides -170; orthopyroxenes –85; Cr-spinels – 80; olivines-7; amphiboles –62; micas –30. The selected minerals were analyzed by LAM –ICP using “Finigan- Element “ apparatus with “Finigan UV LaserProbe”, 266 nm and scanning technique.

COMPOSITION OF ROCK AND PHENOCRYSTS

The rocks constituting diatremes highly vary in chemistry. This is common in the kimberlitic fields, where lamproites, kimberlites, alnoites, and carbonatites occur together [Carlson et al., 1996; Jaques, 1998 etc.]. The variations in TAS and other diagrams are partly explained by abundant compositionally variable xenocrysts. Quartz and K-feldspars from gneisses shift the figurative points of host volcanics in the diagram to the field of subalkaline rocks [Kornilova, 1997], but originally they should be located in the kimberlitic and lamproitic fields. EPMA analyses of the matrix with a widen beam reveal 2-5% K₂O that is found

also in melt inclusions in kimberlite megacrysts [Franz et al., 1999]. The amount of LOI, due to the presence of carbonate in matrix, varies and negatively correlates

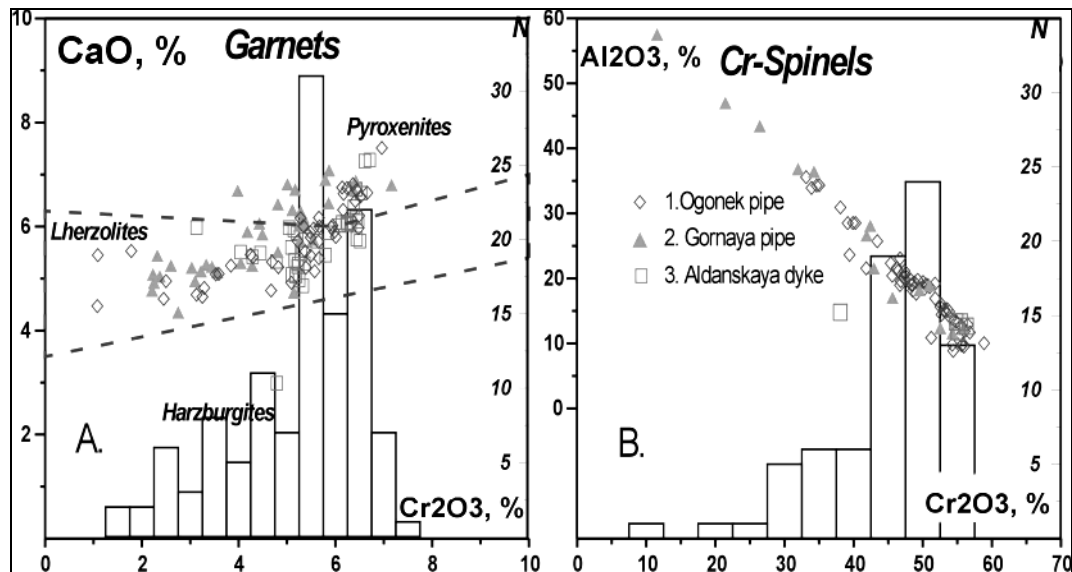


Fig. 4. Cr- Ca diagram for garnets from Chompolo field.

with K₂O. The dissolution of serpentinite debris can partly explain the local MgO enrichment (Fig.3).

Montichellite and perovskite occur together with olivine (fe#~15%), low-T° Ti- bearing diopside or salite and Ti- phlogopite in less abundant in the debris parts. The rare occurrence of alkali K- amphiboles, undersaturated K- silicates, and titanites is not typical of lamproites, though the amorphous masses with high TiO₂ and K₂O concentrations have been found. Originally, those rocks refer to the kimberlite- lamproite type, like those from Altoparonaiba Brazil [Carlson et al., 1996]. Typical monchiquites usually associate with the rocks of a shallower origin: Ne- sienites, nephelinites, camptonites [Wagner et al, 1996] with Sp –lherzolites as mantle inclusions.

MINERAL CHEMISTRY

Purple and violet garnets in the Cr₂O₃-CaO diagram form a trend subparallel to Cr₂O₃ axis but starting from 4% for the Gornaya pipe and from 5% for the Ogonek and Aldanskaya dyke. This trend shifts to a higher CaO content, as it was found for peridotitic pyropes from the Jericho pipe (Canada) [Kopylova et al., 1999] and Finnish pipes [Peltonen et al, 2000] (Fig.4).

Mg- rich clinopyroxenes are in fields with higher *mg*' then common peridotitic varieties, but lower then in Cr- diopsides from Archangelsk kimberlites (Sablukov et al., 2000) (Fig.5). Compositions with Cr₂O₃ >3%, Na₂O ~ 3,25%, Al₂O₃ ~3.5% typical for the Goranya pipe have been found only in harzburgites from Nicos kimberlites (Somerset Island) [Schmidberger, Francis, 1999] and Finland pipes [Kukkonen, Peltonen, 1998; Peltonen et al., 2000], where they

correspond to ~40 kbar. The most wide spread varieties ($1.5 < \text{FeO} < 2\%$, $\text{Cr}_2\text{O}_3 \sim 2-1\%$, $\text{Na}_2\text{O} \sim 2-1.5$, $\text{Al}_2\text{O}_3 \sim 2.5-1.5$, $mg' = 95-93$) are characteristic for the lherzolites

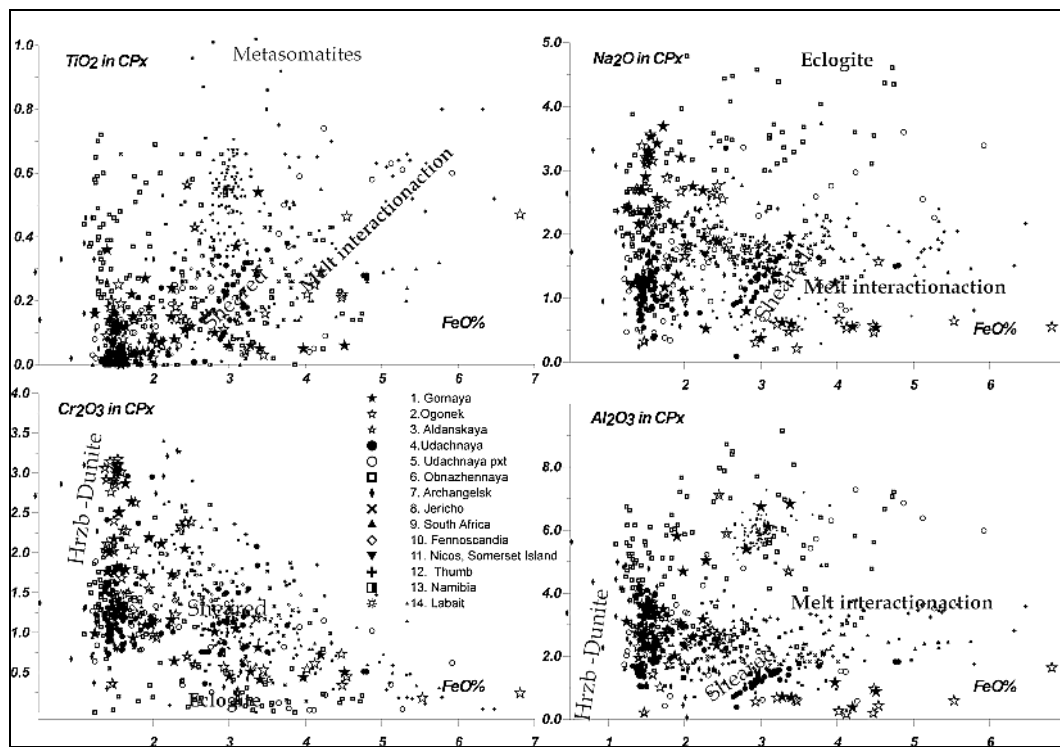


Fig. 5. Variations of CPx compositions (stars) from Chompolo comparing with those from other xenolith in World kimberlites.

captured from the moderate depths of 30-40 kbar [Boyd et al., 1997; Nixon, Boyd, 1973]. More ferriferous compositions with high Na_2O and low Cr_2O_3 are characteristic of pyroxenites from the Obnazhennaya pipe [Ovchinnikov, 1990], where they and eclogites refer to 35-40 kbar. Our studied Cr-diopsides definitely differ from those found in alkali basalt xenoliths, and in Proterozoic Sp-(Ga) peridotite massifs at the folded margin of the Siberian platform [Gornova, Petrova, 1999]. The pyroxenes with relatively low Cr (~0.5) often are richer in Fe than those commonly found in kimberlitic xenoliths. Their unsimilarity with HT deformed peridotites from the bottom of the craton keel [Nixon, Boyd, 1973; Boyd et al, 1997; Pokhilenko, 1993] has been supported by high scattering.

They differ also from H-Ti clinopyroxenes from Tansanian metasomatized mantle [Lee, Rudnick., 2000]. Fe-Ti augites probably came from low crust cumulates. (Fig.5, 6).

Orthopyroxenes from the Gornaya pipe of Mg-, Cr- rich type differ from most enstatites from the kimberlite xenoliths and the neighboring Ogonek pipe ($mg' \sim 93$, $\text{Cr}_2\text{O}_3 \sim 0.9-0.4$) They are specified by wide variations of FeO (to 10%) and high Cr content. They also differ from the trends of the melt interaction of Thumb [Ehrenberg, 1982; Smith, 1986], and from Labait metasomatites [Lee, Rudnick, 2000]. The increase of FeO, Al_2O_3 , TiO_2 and CaO suggests the heating and

fertilization. But they do not reach the contents of the fertile Vitim mantle [Ashchepkov et al., 1986] and other localities from younger platforms. Olivines with high MgO and CaO concentrations evidence for a depleted but hot mantle or may refer to the carbonatite melt influence.

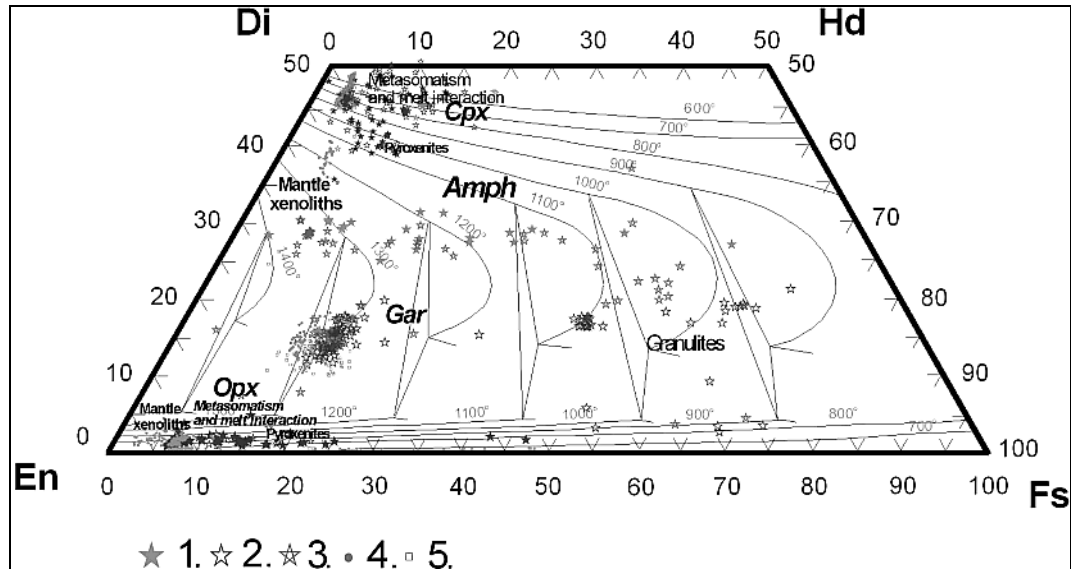


Fig. 6. CMF pyroxene triangle with the solidus lines after Lindsley (1983) for minerals from Aldan kimberlite-like pipes (stars) comparing with Udachnaya (circles) and Obnajennaya [Ovchinnikov, 1990] (squares).

Cr-spinels from Aldan pipes show a common mantle trend - 56-11 % Cr₂O₃. The Cr-richest inclusions have been found in garnets with 6-7% Cr₂O₃. The admixture of magnetite mineral in most Cr-rich varieties means the interaction with magma at a deep level of capturing. The histograms of Cr₂O₃ for both, garnets and Cr-spinels, are close, thus proving the dependence on pressure. (Fig.4)

We have analysed Cr-bearing amphiboles, in particular, Ti-pargasite and pargasitic hornblende. Fe-Ti-rich but Cr-poor amphiboles are from the lower crust. Richterite probably resulted from metasomatic processes. Phlogopite from peridotite has a common composition referring to the Sp or Sp-Gar transition [Arai, 1984]. In the Ogonek pipe fuchsite intergrown with Cr-pyropes is common. In these pipes typical kimberlite megacrysts, such as Py-Alm garnets and ilmenites, are absent, that is more typical of lamproites.

GEOCHEMISTRY OF DEEP-SEATED XENOCRYSTS

Garnet and clinopyroxene grains from the Ogonek pipe were analyzed in the Analytic center of UIGGM with LAM ICP MS using Finigan Element apparatus with "UV LaserProbe", 266 frequency.

The obtained TRE spectra show the features typical of the minerals from peridotitic keel of cratons. Garnets have a convex (U shaped) HREE patterns like those found for peridotites from the diamond facies [Pokhilenko, 2000] (Fig.7).

The U-patterns of Tyradak and Tychan garnets [Griffin et al, 1997] show that they could exist in a more wide pressure interval.

Cr-diopsides display high La/Yb ratios and the humps shifted to the LREE part. This is the sign of a low-degree melting with a high garnet proportion. They

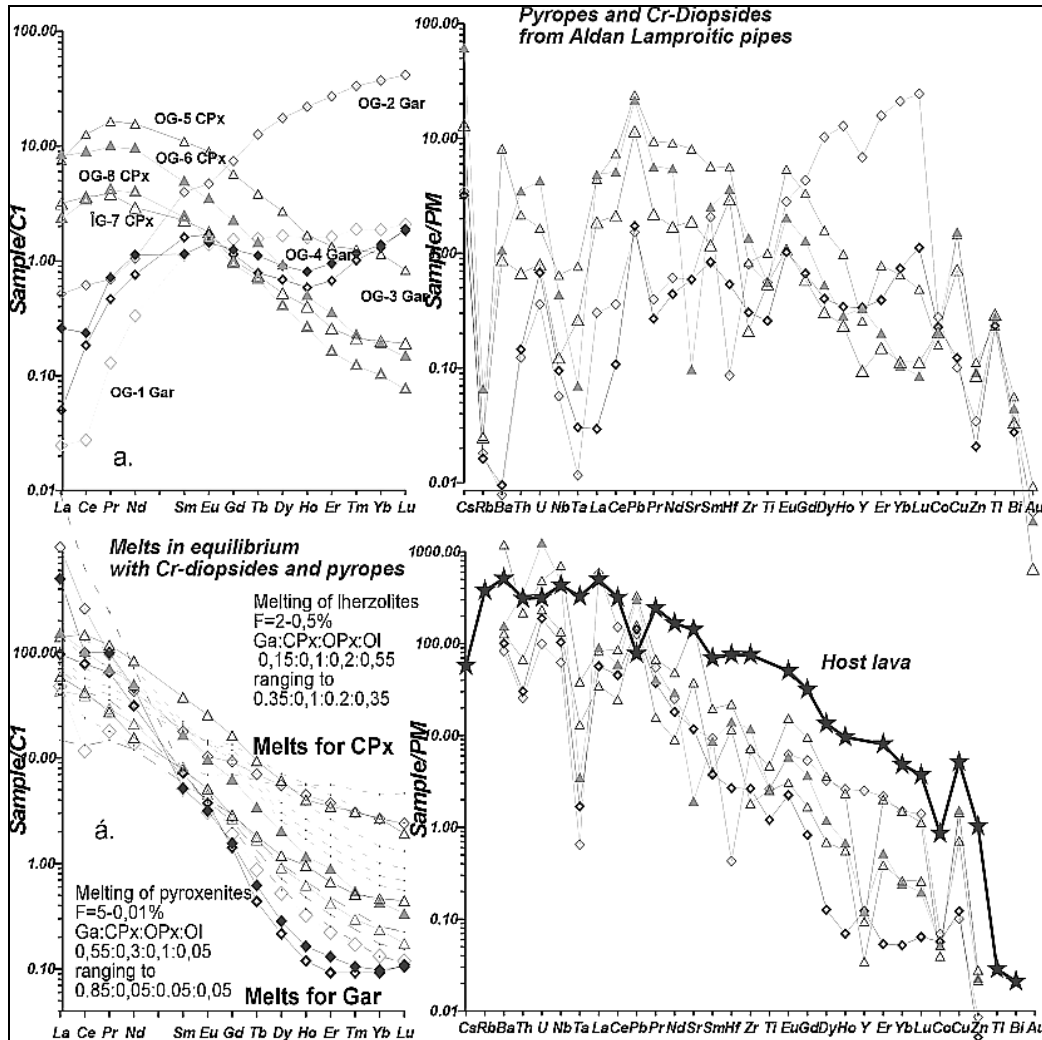


Fig. 7. TRE composition of mantle xenocrysts from Aldan kimberlites.

differ from the rounded patterns for primitive Gar-Sp lherzolites from rift zones (Vitim, Transbaikal etc.) and those crystallized from OIB-type magmas, having both high La/Nd_n, Gd/Yb_n ratios. Deep HFSE minimums evidence for their origin from the same mantle column as the analyzed garnets (Fig.7).

Vice versa, the host kimberlite-like rocks from the Gornaya pipe have the signs of primary mantle magmas with OIB-like patterns with a ~700 elevation relative to C1, that is higher then for the majority of alkali- basaltic, lamproitic and kimberlitic melts. Their TRE spectra are similar to Brazilian rocks from Altoaranaiba [Carlson et al., 1996], kimberlitic pipes of Finlandia [Kukkonen, Peltonen, 1999; Peltonen et al., 2000] and others, and definitely differ from the

analyzed Siberian and North China kimberlites having more evident HFSE dips and lower HREE contents [Nowell et al., 1998]. (Fig.8)

THERMOBAROMETRY

The lack of mineral intergrowths does not allow the use of tradition methods of Ga-Opx and other polymineral thermobarometry. We used orthopyroxene

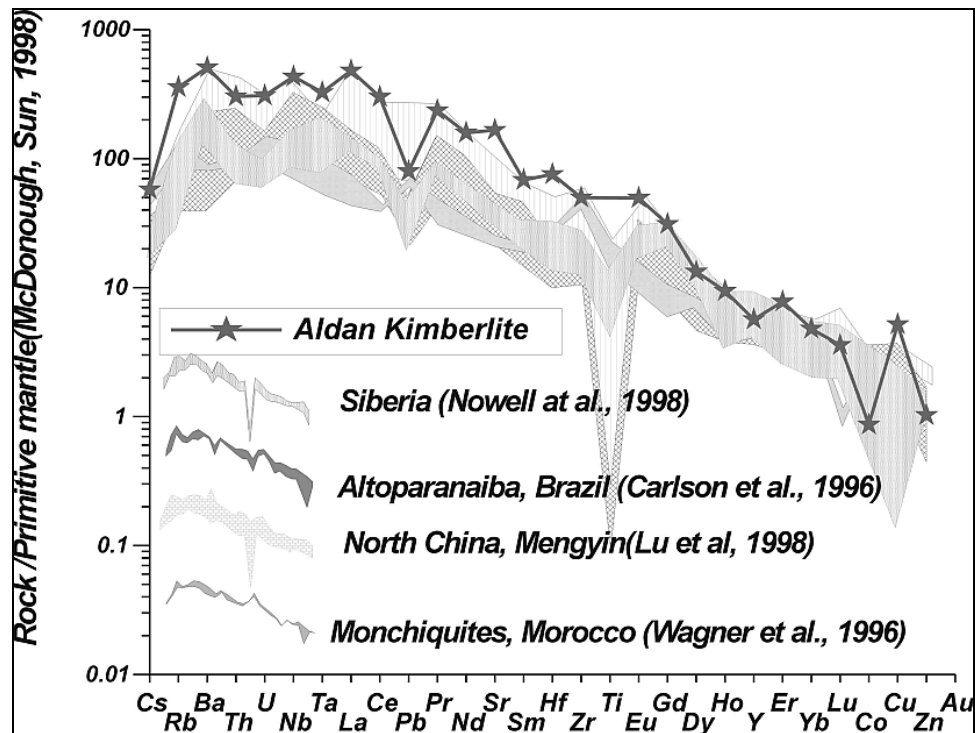


Fig. 8. TRE contents of rocks comparing with other kimberlites.

[Brey- Kohler, 1991- McGregor, 1974] and recent clinopyroxenes thermobarometry [Nimis et al., 2000] For 1000 mineral associations from different pipes including the data from the PHD theses by S.M.Kuligin (1995) and Yu.I. Ovchinnikov (1990) for the Udachnaya and Obnazhennaya pipes we tested the correlation between the methods using the same mineral phases for the calculation: Opx and Cpx, respectively. McGregor's (1974) barometer overestimates the HP part compared to the barometers of Nickel- Green (1985), Brey-Kohler (1990), Harley (1984). This method gives better estimates than the Cpx barometer after Nimis- Taylor (2000) overestimating the pressure values for deformed peridotites. A new Cpx barometer after Ashchepkov (2000) reveals a better correlation with Opx methods. The clinopyroxene thermometer by Nimis & Taylor (2000) have an excellent correlation with most two- pyroxene methods including that by Brey- Kohler (2000) and lower with Opx-thermometry.

TP plots for four cratons (Fig.9) are to compare the reproducibility of the geotherms based on ortho- and clinopyroxenes and to find out the general features of the lithospheric mantle. The pyroxene geotherms for Aldan split on the hot

branch close to the SEA geotherm [Cull et al., 1991], and the cold one is close to the Nicos pipe, and Somerset island. The Cpx-based geotherm corresponds mainly to a 35mw/m^2 heat flow or is lower. It starts near 40kbar and, though several plotted points increases to 60 kbar, close to sheared peridotites. The use of the new barometer by Ashchepkov (2001) even increases their number. The number of hot LP points is much lower compared with those received with orthopyroxene methods. The latter gives a colder branch 45mw/m^2 that is typical of the marginal and rifted zones in craton areas. The scattered hot field in the upper part corresponds to 30-20 kbar. It should be noted that according to Opx thermobarometry the heated upper parts have been also reconstructed for the Udachnaya pipe [Malygina, Pokhilenko, 2000].

Checking the pyroxene equilibrium in a pyroxene triangle [Lindsley,1983] and in other diagrams shows that they came from different assemblages, thus explaining the disagreement in thermobarometric estimates. The amount of the hot course-grained harzburgites relative to depleted lherzolites in the upper part of the mantle column should be higher in the lower part, where cold garnet-bearing clinopyroxenites prevail. Since orthopyroxenes in hydrous kimberlite magmas are easily substituted by serpentine, the orthopyroxene geotherm seems to be less representative.

Garnet geothermobarometry gives the same interval of 42-20 kbar for the mantle column beneath Aldan pipes [Ryan et al., 1996]. The obtained amphibole PT field gives the heated conditions in the crust (9-2 kbar, 500-800oC), which agree with the HT character of granulites.

In combined PT diagrams the deepest and coldest geotherms have been determined for the central parts of large ancient cratons: Slave, Siberian, Fennoscandian, and Amasonian. They have a deep hot excited branch, a 55-30 kbar conductive branch and a $P < 30\text{kbar}$ branch with a steep adiabatic slope of the geotherm. The latter either consists of individual layers, like in the Udachaya (reinterpretation of the data after Boyd et al. (1997) or was determined by the cessation of exchange reaction due to the decreasing temperatures (Fig.6).

PT estimates for South Africa xenoliths from Early and Late Proterozoic kimberlites of the Kaapvaal, Kongo and Zimbabwe cratons correspond to a hotter $40\text{-}45\text{mw/m}^2$ geotherm. A few of young pipes from the Namibia (Gibeon) and Tanzania cratons (Olmani) reveal higher PT conditions. This is a general tendency for the xenoliths from young kimberlites including the Mesozoic pipes from Somerset (Canada) [Schmidberger, Francis, 2000], Mesozoic kimberlites from Siberia [Pokhilenko et al, 2000], and Cenozoic ones from Thumb (Colorado) [Ehrenberg, 1982], and Labait (Tanzania) [Lee, Rudnick, 2000]. The Aldan Mesozoic mantle is the hottest from all the localities.

DISCUSSION AND INTERPRETATION

The reconstruction of the structure and composition of the mantle section beneath kimberlite pipes according to petrographic features [Nixon, Boyd, 1973;

Kopylova et al., 1999; Franz et al., 1996; Schmidberger, Francis, 1999] and garnet mineral geochemistry [Griffin et al., 1996, 1999] have been widely used. TP - dependences of ortho- and clinopyroxene compositions show that the Aldan craton,

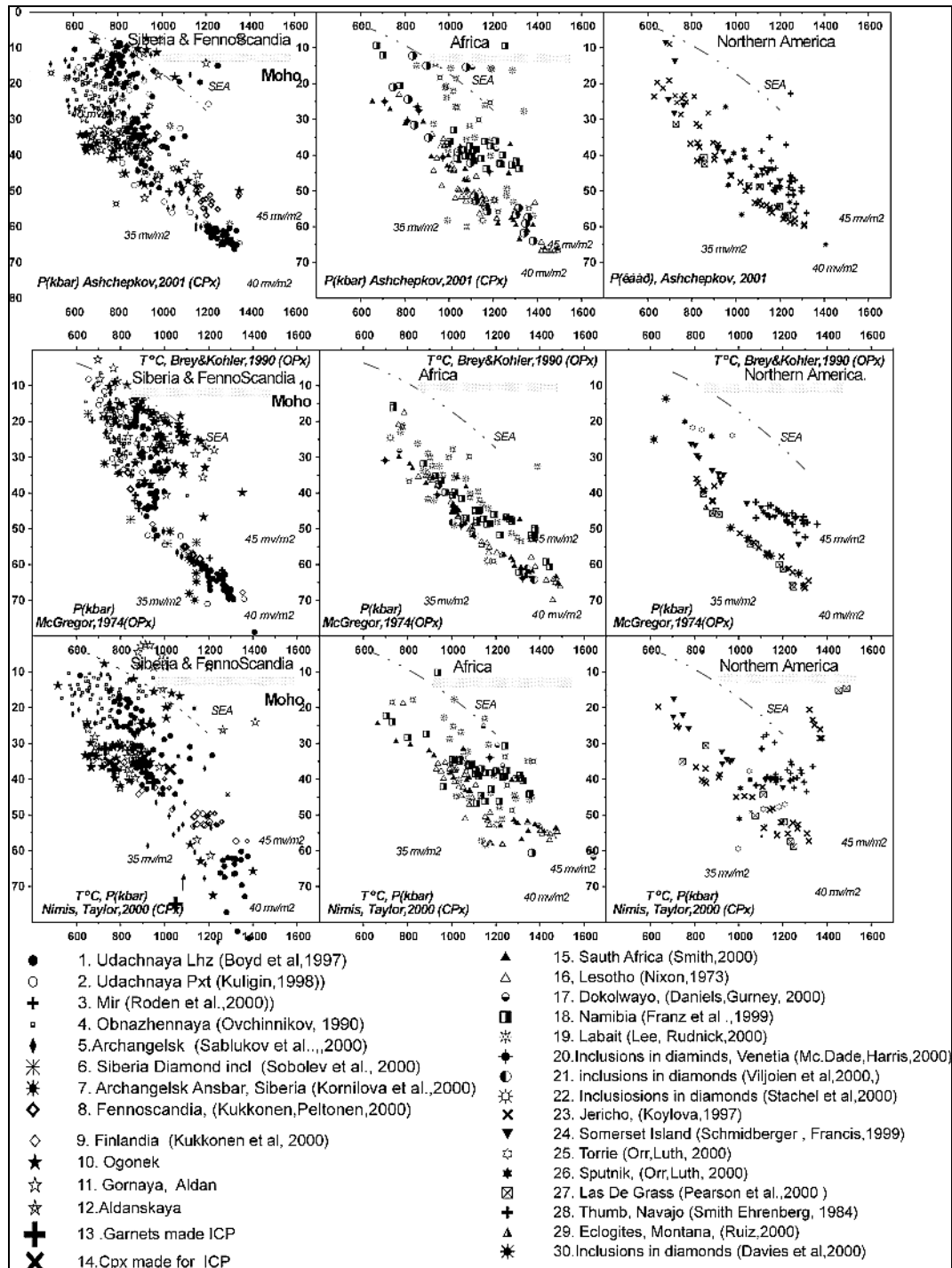


Fig. 9. TP diagram for pyroxenes from Amga comparing with other localities.

like the others, have a layered mantle structure. Most Mg- pyroxenes from the 40-32 kbar interval have the composition determined by the degree of melting and

depletion. At the lower temperatures the Tchernak mineral in clinopyroxene rises, (Ca, Al, Ti), but Cr and Na decrease with T° and P. In the 40-30 interval Fe# gently falls and then again rises. This is characteristic also for the mantle beneath young platforms [Ashchepkov et al., 1997]. Some Fe# rich clinopyroxenes at 60 kbar could have been captured from sheared peridotites, similar to those from South Africa [Nixon, Boyd, 1973], and Siberia [Boyd et al., 1997; Pokhilenko et al., 1976; 1993]. Although they have close concentrations, Aldan clinopyroxene has lower Na and Ti contents and do not demonstrate any rise of these components with pressure and temperature as is typical of sheared varieties. The high TP values could be due to the uncertainties in thermobarometry. Nimis and Taylor (2000) method overestimates HP conditions. Fe-rich compositions at $P > 40$ kbar [Ashchepkov, 2001] allow a suggestion about the presence of melt lenses at the moment of eruption.

TP-dependent variations are less evident for orthopyroxenes. The decrease of Cr and the rise of Ti, Al, Fe with pressure are shifted to $\sim 7-8$ kbars downward comparing with Nimis-Taylor estimates (see Fe in fig.10) due to the disagreement of barometric methods. The agreement between McGregor's (1974) and new Jd-Cpx barometer by Ashchepkov (2001) is better. According to garnet composition we can also suggest a two- or more layered model for the Aldan mantle. The rise of Ca- Cr in pyrope correlates with the behavior of Cr in clinopyroxene.

Major and TRE chemistry of garnet and clinopyroxene allows a suggestion that the interval of 18-35 kbar is composed of moderately depleted and primitive garnet lherzolites and, possibly, harzburgites. The upper spinel facies part (12-22 kbar) consists of depleted lherzolites and highly ferriferous (to 8-10% FeO in Opx) Opx- rich peridotites, their Fe# rising fast. The 20-30 kbar interval corresponds to the minimum on the peridotite volatile-rich solidus. These are common depths of the asthenosphere beneath continents and the field of basaltic magma generation. The content of Fe and Ti in pyroxenes is close to that of HT peridotites (to 1200°C) from the Obnazhennaya [Ovchinnikov, 1990] and Udachnaya pipes [Boyd et al., 1997; Malygina, Pokhilenko, 2000].

The interval of 35-45 kbar, where uvarovite rises in garnet, seems to be essentially pyroxenitic and could result from the interaction of moderately depleted peridotites with low Fe-Ti, Ca-rich protokimberlitic or carbonatitic melts [Boyd et al., 1997]. But the mineral chemistry of peridotites usually correlates with chemical and modal composition of rocks and is close to harzburgite xenoliths from the Nicos pipe. The geochemistry of coexisting melts shows that Ga/Cpx ratio in melting assemblages was 0.8-0.55. This also suggests garnet harzburgite or garnet websterite (garnetites) assemblage. As the pressure decreases, Fe- slightly decreases, possibly due to the melt influence from beneath, and then Fe# rises 'upward' suggesting an interaction with differentiating rising melts. This situation is common for the mantle in many basaltic localities in Vitim, Sludyanka [Ashchepkov, 1991], and in the Shkotov plateau (unpublished), but there the hottest Fe- rich associations occur in the basement of the mantle column.

Phlogopite intergrowths and rare fluid inclusions evidence for metasomatic processes for the Ga- Sp transition and above it. Garnet-fuchsinite intergrowths suggest a deep-seated metasomatism or garnet reactions with H₂O – K₂O rich (lamproitic) melts.

Omphacite suggests the presence of subducted eclogites in the mantle keel structure. Some orange garnets can also belong to the eclogite paragenesis. The lower crust is composed of basic and acid granulites and Gar- Cpx-Amph- Fs- Bi cumulates.

THE PROCESSES OF MELTING AND REGENERATION

Low HREE content in garnets is difficult to explain by the melting in low-T conditions, where garnet has a maximum [van Achterbergh, 1998]. This could be due to the chromatographic effects in rocks with a high modal proportion of garnet influencing the percolating matter by high HREE values in KD in this part. In the multi-component spidergrams garnets are essentially depleted in HFSE and differ from pyropes from the western part of the Siberian platform [Griffin et al., 1996, 1999] and other regions. This can be explained by the depleted character of source mantle peridotites, like it is typical for subduction wedges. They could be washed out by the melts precipitating oxides and accessory minerals, such as zircon, rutile, and apatite, that is typical for carbonatites. Ce minimums, in addition, evidence for zircon or apatite crystallization.

The parental melts for garnet reconstructed with KD refer to a lower melting degree than those for clinopyroxene. The calculated Ga/Cpx ratios for the rocks they came from are essentially higher than those for clinopyroxenes. The former are close to garnetites – garnet wehrlites with a large Gar proportion or to garnet harzburgites, the latter - to lherzolites or websterites.

All the REE spectra for the parental melts for garnet and clinopyroxene form a fan-like curve family, which is likely controlled by the modal proportion of garnet. In general, the higher is Cr content, the higher is Gd/Yb_n ratio and LREE content, and the lower are the melting degree and HREE. All this add up to the increase of Ca in garnet and the absence of cold orthopyroxenes with those features suggests an essentially Ga- Cpx layer with an increasing proportion of garnet with pressure in the 35-45 interval of the mantle column. Ce-minimums in garnet likely correspond to the co- precipitation of zircon or apatite and hardly be related to the subducted sediments.

One of the analyzed HT low-Na clinopyroxenes has a common rounded enriched REE pattern typical for primitive lherzolites. A high elevation of TRE spectra up to 700 relative to the PM of host rocks suggests an input of highly enriched material, because no melting and fractionating models can produce such patterns from the primitive mantle. The melting source should be 5-8 higher in the REE level. The process of the diapiric upwelling of enriched perovskite material [Kaminsky, 2001] from the Earth's interior is more probable than the input of LREE via a melt-fluid influx [Bogatikov et al., 1999].

THE REASONS FOR THE LAYERING IN THE ALDAN MANTLE

The layering is a common feature of the lithospheric keel of cratons [Griffin et al., 1996, 1999; O'Reilly et al., 2001; Nixon, Boyd, 1973; Boyd et al., 1997, Kopylova et al., 1998; Kukkonen, Peltonen, 2000; etc.). It forms mainly in the early stages of mantle evolution in Archaean and Proterozoic times and smaller amounts were frozen to it later at 500 Ma mainly due to the subduction processes. They are getting younger downward. [Pearson et al., 1999; O'Reilly et al., 2001]. The irregular character of the sequences evidences for the twining, metasomatism, remelting and melt percolation processes locally in the lithospheric keel. According to experimental data and thermometric formulas, koringite minal in garnet increases with pressure and grossular rises with temperature. Uvarovite minal has a larger cell dimension and the trends of its growth in the Cr_2O_3 -CaO diagram corresponds to the changes in the system and the modal compositions, but the rise in this case does not mean an evident pressure increase. Nearly isobaric character of the pyrope–uvarovite substitution trend is supported by mineral thermobarometry.

Combined Cr_2O_3 - CaO diagram for pyropes from kimberlites [Huggerty, 1994] have no essential brakes reflecting a general regularity of garnet isomorphism with pressure in a nearly constant system. The inflection of trends in the Cr_2O_3 –CaO diagram often corresponds to 40 kbar according to Cr-pyrope thermobarometry [Ryan et al., 1997]. At this depth and below, the subducted eclogites became common in the lithospheric keel of the craton. In the case of Aldan no signs of subduction sequences, except for one omphacite, and no signs of serious depletion characteristic for the mantle subduction wedges, i.e. no subcalcic garnets and Mg- olivines. Nevertheless, the changes of the garnet trend indicate that the 40 kbar (130-140km) boundary has a lithologic nature and may mark the stop of a rising melt.

The increase of uvarovite suggests the enrichment of the system in CaO and, possibly, the processes of werhlitization [Boyd et al., 1997] under the influence of Ca-rich (carbonatite) melts. The inversion of Fe# with increasing of pressure implies the interaction with asthenospheric (?) melts, which come from the interior.

Widening of the garnet lherzolites field in Cr_2O_3 -CaO in the low-pressure part at 20-30 kbar is related to the motley composition of the melts due to the processes of regeneration in the minimum on the peridotitic solidus with volatiles, where the concentration of various melts is possible even at normal geothermal gradients. This feature is typical of the Siberian (Paleozoic) mantle subjected to the influence of plume melts.

COMMON STRUCTURAL FEATURES OF MANTLE SECTIONS AND POSSIBLE EVOLUTION OF THE MANTLE KEEL BENEATH THE SIBERIAN PLATFORM

The thermobarometry evidences that marginal and rifted regions within the cratons are often essentially and irregularly heated usually up to 50mv/m^2 [Lee, Rudnick, 2000, Schmidtberger, Francis, 1998; Franz et al., 2000; Smith, 1999]. This is due to the combination of different factors. As a rule the rifts at the peripheral parts of continents are related to plume magmatism or/and to the extension in the back areas of subduction zones. Tomographic models show that vertical cold zones often occur together with gently subducting slabs. The sinking of large lithospheric masses or delamination of eclogites and dense garnet cumulates is followed by rise of fluid flows and convection resulting in the melting and generation of the so-called “baby plums”, common for Europe and other regions. High heat flows are also typical of the suture zones within ancient cratons, which serve as traps for deep rising melts. The typical rift heat flow values of $85\text{-}90\text{mv/m}^2$, however, have been found only in the Aldan region. Even the Cenozoic lavas from the East-Africa rift do not carry such a heated material from relatively deep levels of the lithospheric keel of craton. In this case it is possible to suggest the influence of a greater source of the heat flow, e.g. the Siberian P-T plum. The plum has not produced flood basalts in this region, but the influence of those plums is spreading over vast territories usually.

Eclogite bodies in mantle sections are found at a 40kbar level and deeper, while the depleted coarse-grained Ga-harzburgites at 50 kbar [Pokhilenko et al., 1993]. After the creation of a moderately depleted lherzolitic core beneath the continents the further growth of the lithospheric keel is related to subduction processes followed by the freezing of peridotite wedges together with underlying eclogites and sometimes the twining of subduction wedges. Subduction is usually accompanied by fluid flows, the fusion at the front induces the percolation of SiO_2 -rich melts [Kelemen, 1996; Boyd et al., 1997]. If a thermal, dense or lithological boundary existed, it could stop the ascending of melts and cause the creation of pyroxenite-rich horizons. It should be noted that the Obnazhennaya pipe of Mesozoic age has a large portion of pyroxenites in the lower part of the section, that are deeper changed by the eclogites, locally of a typical subduction type.

The mantle sections beneath the kimberlites from the periphery of the craton, including Aldan, often start a 40-45 kbar depth [Pokhilenko, Sobolev, 2000; Ovchinnikov, 1990]. The plume activity can be accompanied by the remelting of pyroxenites, submelting of peridotites and abrupt decrease of peridotite viscosity resulting in the delamination of dense pyroxenite-rich eclogite blocks from the basement of the craton or/and intrusion of deep melts to the 40 kbar boundary.

The middle part of the section at 40-30 kbar has no essential Fe-enrichment judging on clinopyroxenes but it was hardly influenced by the Fe-rich melts according to Opx thus the melt-rock interaction results in the Fe-harzburgite creation in relatively shallow mantle.

The major peridotite mineral – olivine - has a large module of thermal expansion, more than ultramafic melts, and its density essentially depends on the temperature. At relatively low geothermal gradients olivine floats at the pressure lower than 65 kbar [Agee, 1998]. This corresponds to the conditions of the lithospheric keel basement. Furthermore, the continental geotherm crosses the volatile-rich peridotite solidus, determining the position of the asthenospheric roof beneath the cratons.

The available analyzed material does not allow a determination of the presence of diamond facie material in Aldan diatremes, though some thermobarometric estimates evidence about such a possibility.

CONCLUSIONS

1. Aldan pipes are represented by the contaminated varieties of kimberlites and lamproites, possibly mixed.
2. The level of xenolith capture corresponds to the pressures of 40-35 kbar.
3. The mantle column beneath Aldan pipes has a layered structure.
4. The irregular heating of the mantle column is characteristic of the marginal parts of the cratons and modern rifted regions and, possibly, is caused by the intrusion of plum melts.
5. The lithospheric craton keel is permeable for the melts located in the upper part within the minimum of the peridotite solidus.

The work was supported by RBRF grants no. 99-05-65688, 00-05-65288.

REFERENCES

1. Agee C. B. Crystal-liquid density inversions in terrestrial and lunar magmas. //Physics of the Earth and Planetary Interiors. 1998. V.107. pp. 63–74
2. Arai S. Pressure- temperature dependent compositional relations of phlogopitic micas in upper mantle peridotites.//Contrib. Miner.Petrol. 1984, v. 87, pp.260-264.
3. Ashchepkov I.V. Jd barometer for mantle peridotites and eclogites and thermal conditions of the lithospheric keels of cratons and their surroundings. //GSA November 5 - 8, 2001 Annual Meeting.
4. Boyd, F.R., Pokhilenko, N.P., Pearson, D.G., Mertzman, S.A., Sobolev, N.V., Finger, L.W., 1997. Composition of the Siberian cratonic mantle: evidence from Udachnaya peridotites xenoliths.//Contrib. Mineral. Petrol. 128, pp. 228–246.
5. Brey G.P., Kohler T., 1990 Geothermobarometry in four phase lherzolites II: new thermobarometers and practical assessment of using thermobarometers.//J.Petrol., 31: pp. 1353-1378.
6. Carlson R. W., Esperança S., Svisero D. P. Chemical and Os isotopic study of Cretaceous potassic rocks from Southern Brazil.//Contrib. Mineral. Petrol., 125 (1996) 4, pp. 393-405
7. Cull J.P., O'Reilly S. Y., Griffin W.L. Xenolith geotherms and crustal models in Eastern Australia. //Tectonophysics, 1991, 192, N 3-4, pp. 359-366.
8. Ehrenberg S.N., Petrogenesis of garnet lherzolite and megacrystalline nodules from the Thumb, Navajo volcanic field.// J.Petrol., 1982, v.23/4, pp. 507-547.

9. Franz L., Brey G.P., Okrusch M. 1996. Steady state geotherm, thermal disturbances, and tectonic development of the lower lithosphere underneath the Gibeon Kimberlite Province, Namibia. // *Contrib. Mineral. and Petrol.* 1996. Vol. 126. N 1-2. pp. 181-198.
10. Gornova M.A. & Petrova Z.I. - Mantle peridotites of granulite-gneiss complex as fragments of archaic (?) ophiolites in the Baikal region (Russia) - 24 - 2 - 223
11. Griffin W.L., Ryan C.G., Kaminsky F.V., O'Reilly S.Y., Natapov L.M., Win T.T., Kinny P.D., Jaques A.L. Kimberlite and lamproite diamond pipes // *AGSO J. Austral. Geol. and Geophys.* 1998. Vol. 17. N 4. pp. 153-162.
12. Kaminsky F.V., Zakharchenko O.D., Davis R., Griffin W.L., Khachatryan-Blinova G.K., Shiryayev A.A. Super diamonds from Jina, Mato Grosso, state Brazil.// *Contrib. Mineral. Petrol.* 2001. vol. 140, pp. 734-753.
13. Kopylova M.G.; Russell J.K.; Cookenboo H. Petrology of peridotite and pyroxenite xenoliths from the Jericho kimberlite: Implications for the thermal state of the mantle beneath the Slave craton, northern Canada// *J. Petrol.* 1999. Vol. 40. N 1. pp. 79-104
14. Kornilova V.P. Petrography and mineralogy of the calc- alkaline laprophyres and eruptive breccias from Chompolo area. *Fatherland (Russian) geology.* 1997, N9, pp. 6-9.
15. Kukkonen I.T., Peltonen P. Xenolith-controlled geotherm for the central Fennoscandian Shield: implications for lithosphere–asthenosphere relations *Tectonophysics* 304. 1999. pp. 301–315.
16. Kuligin S.S., Pokhilenko N.P. Mineralogy of xenoliths of garnet pyroxenites from kimberlite pipes of Siberian platform. *Extended Abstracts 7IKC.* Cape Town. pp. 480- 482.
17. Lee C.-T., Rudnick R. L. Compositionally Stratified Cratonic Lithosphere Petrology and Geochemistry of Peridotite Xenoliths from the Labait Volcano, Tanzania/ *Proceedings of the VII international Kimberlite Conference.* P.H. Nixon volume. 2000. Red Roof Design cc. Cape Town, South Africa, pp.503-521
18. MacGregor, I.D., 1974. The system MgO–Al₂O₃–SiO₂: solubility of Al₂O₃ in enstatite for spinel and garnet–spinel compositions.// *Am. Mineral.* 59, pp. 110–119.
19. Nimis P., Taylor W. Single clinopyroxene thermobarometry for garnet peridotites. Part I. Calibration and testing of a Cr-in-Cpx barometer and an enstatite-in-Cpx thermometer. *Contrib Mineral Petrol* 139 (2000) 5, pp. 541-554
20. Nixon, P.H., Boyd, F.R., 1973. Petrogenesis of the granular and sheared ultrabasic nodule suite in kimberlite. In: Nixon, P.H. Ed., *Lesotho Kimberlites.* Cape and Transvaal, Cape Town, pp. 48–56.
21. Nowell G.V., Kempton P.D., Pearson D.G. trace element and isotope geochemistry of Siberian Kimberlites. *Extended Abstracts 7IKC.* Cape Town. pp. 631- 633.
22. O'Reilly S.Y., William L.Griffin, Poudjom Djomani Y.H., Morgan P. 2001 Are Lithosphere Forever Tracking Changes in Subcontinental Lithospheric Mantle Through Time. *GSA Today* V.11, N4. pp. 4-9.
23. Pearson D.G. The age of continental roots. *Lithos* 48 1999. pp. 171–194.
24. Peltonen P., Huhma H., Tyni M., Shimizu N. Garnet peridotite xenoliths from kimberlites of Finland: nature of continental mantle at an Archaean craton – Proterozoic mobile belt transition. *Proceedings of the VII international Kimberlite Conference.* The P.H. Nixon volume. 2000 . pp. 664-676.
25. Pokhilenko N.P., Pearson D.G., Boyd F.R., Sobolev N.V. Megacrystalline dunites: sources of Siberian diamonds // *Carnegie Inst. Wash. Yearb.*, 1991, 90, pp. 11-18
26. Ryan, C.G., Griffin, W.L., Pearson, N., 1996. Garnet Geotherms: a technique for derivation of P–T data from Cr-pyrope garnets. *J. Geophys. Res.* 101, pp. 5611–5625.
27. Sablukov S.M., Sablukova L.I., Shavyrina M.V. 2000. Mantle xenoliths from the kimberlite deposits of the Zymny Bereg Archangelsk diomondiferrous province. // *Petrology.* N8., v.5 pp. 518-548.

28. Schmidberger S. S., Francis D. 2001. Constraints on the Trace Element Composition of the Archean Mantle Root beneath Somerset Island, Arctic Canada *J. Petrology* 2001 42: pp. 1095-1117.
29. Shilina G.N., Zeitlin S.M. About the first finding of the kimberlites on Aldan shield.//*Soviet geology*. 1959, N10. pp.132-136.
30. Sobolev, N.V., 1974. Deep-Seated Inclusions in Kimberlites and the Problem of the Composition of the Upper Mantle (in Russian). Nauka Press, Novosibirsk, 264 pp. [English Translation (1977), ed. by F.R.Boyd,American Geophysical Union, Washington,DC,279 pp.
31. Van Achterbergh E., Griffin W.L., Shee S.R., Wayatyt B.A., Sharma A.L. Natural trace element distribution coefficients for garnet clinopyroxene and orthopyroxene: variations with temperature and pressure. *Extended Abstracts 7IKC*. Cape Town., pp. 934- 936.
32. Wagner C., Deloule E., Mokhtari A. 1996. Richterite-bearing peridotites and MARID-type inclusions in lavas from North Eastern Morocco: mineralogy and D/H isotopic studies. *Contrib. Mineral. Petrol.* (1996) 124: pp. 406–421.

Noble gas (He, Ar) isotope evidence for sources of Devonian alkaline magmatism and ore formation related within the Kola province (NW Russia)

V.A. Nivin, S.V. Ikorsky, I.L. Kamensky

Geological Institute, Kola Science Centre RAS, 14, Fersman Str., Apatity 184209, Russia

INTRODUCTION

About 20 intrusive alkaline-ultramafic, carbonatite-bearing for the most part, complexes (CAUC) and the giant nepheline-syenite with foidolites Khibina and Lovozero plutons were formed within the Kola segment of the Fennoscandian shield as a result of the Devonian pulse of alkaline magmatism. Their geology, petrology, mineralogy and metallogeny have predominantly been studied in detail and described in a plenty of publications, including the recent survey (e.g., Kogarko et al., 1995). Isotope-geochemical (Sr, Nd) characteristics of these intrusions indicate mantle origin of the parent melts (mostly from the depleted source) and rather low or lack of crustal contamination [Kramm and Kogarko, 1994; Beard et al., 1996]. Saturation of these rock suits with volatile components is favorable for the study of noble gas isotopes which are accepted as geochemical tracers of many geological processes. In a lot of instances a data set on He and Ar isotope compositions and their abundances in rocks and minerals allows to identify sources and to evaluate mixture proportions of fluids in the course of generation and evolution of magmatic melts and ore forming systems, to judge degassing pattern, the extent to which country rocks are assimilated, influence and participation of near-surface processes in the formation of different sequences. As for the Kola alkaline province the outlook for such approach is supported by a number of previous studies [Tolstikhin et al., 1985; Nivin et al., 1988, 1993; Mitrofanov et al., 1995; Marty et al., 1998; Tolstikhin et al., 1999a, 1999b]. According to those researches, in particular, helium isotope ratios being close to those in deep lower mantle plumes were first found in the Paleozoic magmatic suits as well as highest for terrestrial rocks concentrations of primordial ^3He were measured.

The new evidence from abundances of He and Ar isotopes in nepheline-syenite massifs and ore-bearing phoscorite-carbonatite series of CAUC is presented in this study along with earlier obtained data.

SAMPLES AND METHODS

Noble gas isotope concentrations and ratios have been explored in the rocks and, to a lesser extent, minerals from 9 CAUC, including Kovdor, Seblyavr, Vouriyarvi, Salmagorskii, Turiy Peninsula, Lesnaya Varaka, Ozernaya Varaka, Kontozerskii and Sallanlatvi massifs as well as the Khibina and Lovozero nepheline-syenite plutons and related with them, respectively, apatite and rare-metal deposits.

Methods of He and Ar measurements have been repeatedly described earlier [e.g., Marty et al., 1998; Tolstikhin et al., 1999b]. Here it is significant to mention that the rare gas extraction from rock and mineral samples was carried out by two procedures: melting in high vacuum electrical furnace and milling in pumped out glass ampoules. In the first case the total gas was extracted from all sample volume, in the second case – mainly from fluid inclusions (FI) in minerals. Below subscripts “tot” and “fi” are used to symbolize these gas types. A comparison between whole-rock (mineral) abundances of helium and argon isotopes and those to be expected from concentrations of parent elements (U, Th, Li, K), rock age and assumptions for closed system, allows us to estimate the trapped gas constituent. In FI of many minerals the isotopic ratio of trapped gases can be retained over a long time being close to the initial ratio and with lesser admixture of radiogenic component as compared to gases in crystalline matrix.

Interpreting the results obtained we used the following recent estimates of isotope ratios in the Earth's reservoirs: $^3\text{He}/^4\text{He}$ (it is the most informative indicator of deep fluid sources) in crust $\sim 2 \cdot 10^{-8}$, in upper mantle $\sim 1.1 \cdot 10^{-5}$, in lower mantle $\sim 1.1 \cdot 10^{-5}$; $^{40}\text{Ar}/^{36}\text{Ar}$ in atmosphere – 395.5, in upper mantle $\sim 40,000$, in lower mantle $\sim 5.000\text{-}6.000$ [Tolstikhin and Marty, 1998].

RESULTS AND DISCUSSION

The ranges and averages of He and Ar isotope concentrations and ratios in rock series of all CAUC studied and in all rocks of these typical complexes as well the Khibina and Lovozero massifs are tabulated in Table 1.

Helium concentrations and $^3\text{He}/^4\text{He}$ ratio in the rocks under examination vary in ranges of several magnitudes. On the whole, CAUC ultramafic rocks are distinguished from other rock series by the highest helium mean concentrations and isotope ratios, carbonatites and phoscorites are characterized by the widest scatter and the Seblyavr complex is noteworthy for maximum values of these parameters both total and in fluid inclusions.

Variations in abundances of Ar isotopes, especially in FI, are far lesser, though $^{40}\text{Ar}/^{36}\text{Ar}$ ratio in carbonatite series ranges from air-like one to 50,000.

The nepheline-syenite massifs are characterized by reduced $^3\text{He}/^4\text{He}$ ratios and the more radioactive Lovozero rocks are also distinguished by the highest ^4He and enhanced ^{40}Ar bulk concentrations and minimal values of $^{40}\text{Ar}/^{36}\text{Ar}$ ratios in FI

Таблица 1.
Вариации и средние значения концентраций и отношений изотопов благородных газов в породах щелочно-ультраосновных с карбонатами и нефелин-сиенитовых комплексов Кольской провинции

Породы, массив	Пределы колебаний (над чертой) и средние значения (под чертой) изотопно-газовых параметров (в скобках - количество образцов)										
	В породе (в целом)					Во флюидных включениях					
	^4He см ³ /г, x 10 ⁻⁶	$^3\text{He}/^4\text{He}$ x 10 ⁻⁸	^{40}Ar см ³ /г, x 10 ⁻⁶	$^{40}\text{Ar}/^{36}\text{Ar}$	^4He см ³ /г, x 10 ⁻⁶	$^3\text{He}/^4\text{He}$ x 10 ⁻⁸	^{40}Ar см ³ /г, x 10 ⁻⁶	$^{40}\text{Ar}/^{36}\text{Ar}$	^4He см ³ /г, x 10 ⁻⁶	$^3\text{He}/^4\text{He}$ x 10 ⁻⁸	^{40}Ar см ³ /г, x 10 ⁻⁶
Щелочно-ультраосновные комплексы											
Ультраосновные ¹⁾	11,9 - 1010 249,9 (15)	20,5 - 1560 519,5 (15)	1,8 - 37,2 9,8 (21)	394 - 7327 2229 (21)	0,17 - 64 7,8 (58)	39,2 - 3299 1079,8 (58)	0,1 - 7,4 1,8 (34)	345 - 3000 1446 (34)			
Щелочные ¹⁾	16 - 135 58,7 (4)	22,9 - 622 262,7 (4)	13,5 - 59,1 32,2 (4)	4451 - 20707 9348 (4)	0,3 - 56 11 (29)	69,5 - 1965 534,1 (29)	3,2 - 5,9 4,8 (3)	636 - 2268 1397 (3)			
Карбонатиты и фоскориты ¹⁾	2 - 1554 123 (73)	1 - 1140 194,7 (73)	0,5 - 157 21,8 (66)	310 - 50000 3564 (66)	0,04 - 374 21,6 (98)	1 - 2557 544,1 (98)	0,2 - 16,7 3,9 (28)	296 - 3743 1411 (28)			
Ковдор ²⁾	7,4 - 341 67,7 (16)	19,7 - 1084 312,8 (16)	3,5 - 157 32,6 (22)	632 - 50000 6712 (22)	0,17 - 374 23,5 (29)	62 - 1956 820,1 (29)	0,5 - 4,3 1,7 (5)	1509 - 2985 2225 (5)			
Себьявр ²⁾	11,6 - 1010 222,7 (15)	19,4 - 1560 464,8 (15)	0,9 - 37,1 10,4 (21)	383 - 4934 1593 (21)	0,37 - 21,8 5,4 (29)	81,2 - 3299 1352,2 (29)	0,4 - 4,4 2,1 (15)	435 - 2185 1145 (15)			
Вуориярви ²⁾	23 - 489 304 (4)	2,1 - 79 35,4 (4)	12,2 - 29,3 20,6 (4)	1078 - 3774 1995 (4)	0,47 - 174 26,1 (25)	6,8 - 2086 567 (25)	2,6 - 3,4 3 (3)	1493 - 1754 1611 (3)			
Щелочные массивы											
Хибинский ²⁾	2,3 - 485 127 (53)	0,7 - 43,5 11,6 (53)	1,5 - 191,3 40,9 (53)	392 - 40600 8170 (53)	0,03 - 226 17,3 (106)	0,8 - 182 44,7 (106)	1,9 - 9,6 4 (4)	866 - 1840 1516 (4)			
Ловозерский ²⁾	23 - 28000 1777 (27)	0,5 - 22,9 6,2 (27)	12,1 - 150 62,6 (27)	601 - 18110 7119 (27)	0,5 - 632 49,5 (46)	0,4 - 117,5 12,7 (46)	0,8 - 3,5 2,2 (3)	394 - 590 492 (3)			

Примечание. 1) из всех изученных массивов; 2) все типы пород. Использованы собственные анализы авторов, выполненные в Геологическом институте КНЦ РАН в 1985-2001 г.г.

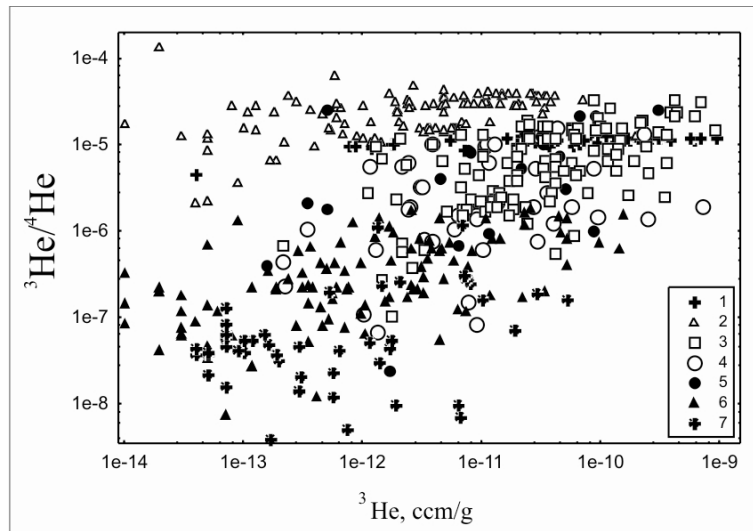


Fig. 1. Comparison of helium isotope abundances in basalts (compiled by Tolstikhin et al., 1999) and in fluid inclusions of Kola intrusions.

Rock samples: 1 – MORB, 2 – OIB, 3 – ultramafic and alkaline from CAUC, 4 – carbonatites, 5 – phoscorites, 6 – Khibina, 7 – Lovozero.

A comparison between measured and calculated abundances of helium isotopes in the rocks, high (higher than and similar to those in MORB and some OIB of “hot spots”, respectively) $^3\text{He}/^4\text{He}$ ratios in FI of some samples (Fig. 1) strongly suggest the presence of enriched in ^3He , lower mantle plume component in the trapped fluid. Also, Figure 1 illustrates the widest range of helium isotope characteristics of phoscorites and carbonatites as well a united trend in points of samples from all examined massifs on the $^3\text{He} - ^3\text{He}/^4\text{He}$ coordinates.

The positive correlations between ratio of $\text{U}+0.24\text{Th}$ (this value is proportional to radiogenic ^4He production) to ^3He and $^4\text{He}/^3\text{He}$ ratio indicate significant contribution of radiogenic helium to the gas extracted by melting (Fig. 2). The alignment of the most samples below evolution line evidences a helium loss, usual for rocks of any origin. By means of a similar, but on a linear scale, plot, the initial $^4\text{He}/^3\text{He}$ ratio making up 30,000 and corresponding to the lowest ratios measured in FI has been estimated for Kola CAUC [Tolstikhin et al., 1999b].

The better direct relation of ^3He and ^4He in fluid inclusions (Fig. 3) than in the whole rocks, the closer connection between ^3He and $^3\text{He}/^4\text{He}$, $^3\text{He}_{\text{fi}}$ and $^3\text{He}_{\text{tot}}$ (Fig. 4) as compared with ^4He and $^3\text{He}/^4\text{He}$, $^4\text{He}_{\text{fi}}$ and $^4\text{He}_{\text{tot}}$ suggest different nature of measured helium isotopes, the best retention, especially in FI, of trapped helium with reference to radiogenic one produced in situ, a predominant loss of the latter, its essential impact on helium isotope composition in crystalline matrix and much lesser influence on that in FI.

The distinct pattern of the relationship between $(^3\text{He}/^4\text{He})_{\text{fi}}$ and $^3\text{He}_{\text{fi}}/^3\text{He}_{\text{tot}}$ has been revealed for different rock groups. These ratios, being not correlative in

CAUC ultramafic rocks, show a weak positive correlation in phoscorite-carbonatite series and closer coupling in Khibina and Lovozero rocks. Such

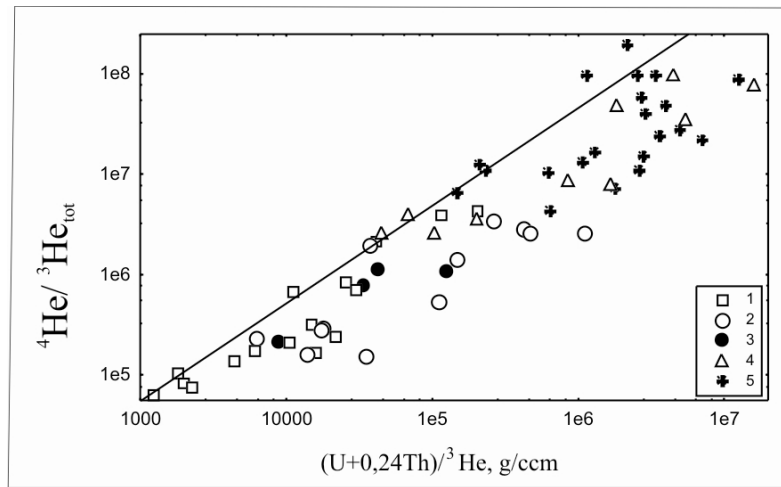


Fig. 2. Relationships between whole-rock abundances of parent and daughter species in U-Th-He system.

Sloping straight line – reference 370 Ma evolution line. Rock samples: 1 – CAUC ultramafic and alkaline, 2 – carbonatites, 3 – phoscorites, 4 – Khibina, 5 – Lovozero.

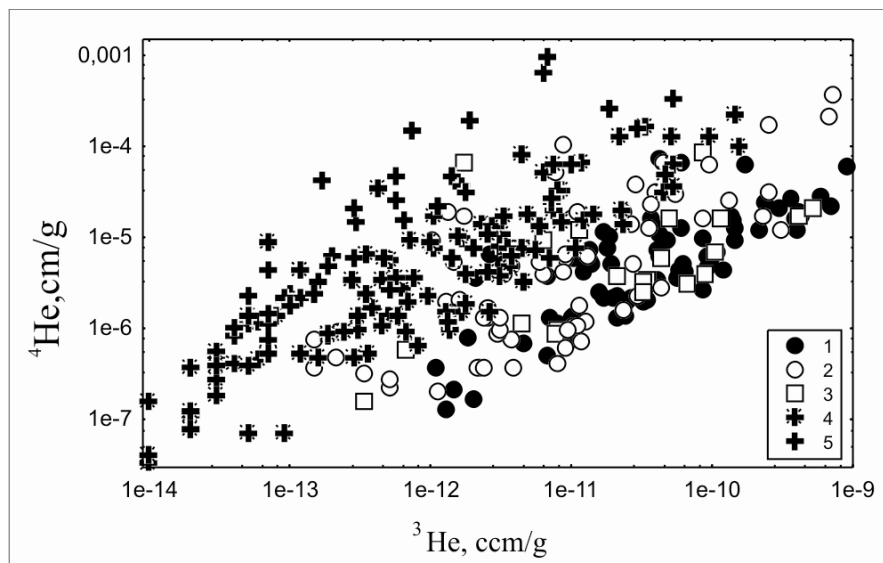


Fig. 3. Relationships of helium isotopes in fluid inclusions.

Rock samples: ultramafic (1), carbonatites (2) and phoscorite (3) of CAUC; the Khibina (4) and Lovozero (5) massifs.

discrepancies could be derived from dissimilar proportions of primary and secondary fluid inclusions. And really, in ultramafic rocks the fluid phase is usually trapped in primary melt inclusions, both primary and secondary FI are observed in phoscorites and carbonatites and the preponderance of gas inclusions in the Khibina and Lovozero minerals have been formed at postmagmatic stages of pluton evolution and are secondary [Ikorsky et al., 1992; Sokolov, 1994; Veksler et al., 1998].

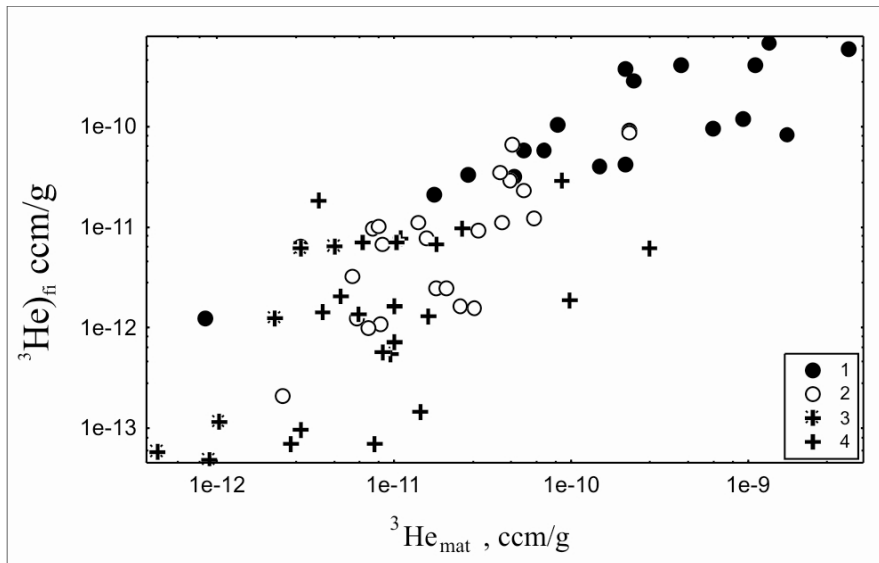


Fig. 4. Relation of ^3He abundances in mineral crystalline matrix (subscript “mat”) and fluid inclusions.

Rocks: CAUC ultramafic (1), carbonatites and phoscorites (2); the Khibina (3) and Lovozero (4) massifs.

The sensitivity of $^3\text{He}/^4\text{He}$ ratio to the conditions of mineral formation is particularly manifested in carbonatite series. Under broad variations of this parameter in carbonatites of different formation stages, the lowest ratios are revealed in samples with clear signs of postmagmatic alterations (recrystallization, metasomatic substitution, relatively low-temperature mineralization). Conversely, the rocks touched upon postmagmatic processes to the least degree are characterized by enhanced $^3\text{He}/^4\text{He}$ values. Forsterite- and pyroxene-calcite carbonatites of the second stage as well dolomite and calcite-dolomite carbonatites of the fourth stage are distinguished with high average helium isotope ratios and, according to geological and petrological data, with a wider set of magmatic crystallization traces.

In the most rock samples of nepheline-syenite massifs ^4He losses (from 5 to 90 %) are comparable with these in CAUC (Fig. 5). But in the former case ratios of measured and calculated ^3He concentrations are less by a factor of several magnitudes that can imply an essential degassing of mantle melts before magmatic crystallization of Khibina and Lovozero nepheline syenites and foidolites.

In FI of Khibina rocks the regular increase in $^3\text{He}/^4\text{He}$ ratio is revealed from massive khibinites forming the peripheral arch of the massif to trachytoid khibinites and then to foyaites of its central part. The apatite-bearing ijolite-urtite complex, rischorrites including, like CAUC phoscorite-carbonatite series, is characterized by the widest (among Khibina rocks) range of rare gas isotope abundances. Apatite ores in themselves along with Khibina carbonatites are

distinguished by enhanced helium concentrations and low $^3\text{He}/^4\text{He}$ ratios. Though sometimes the latter have relatively high values in pyroxene from the ores.

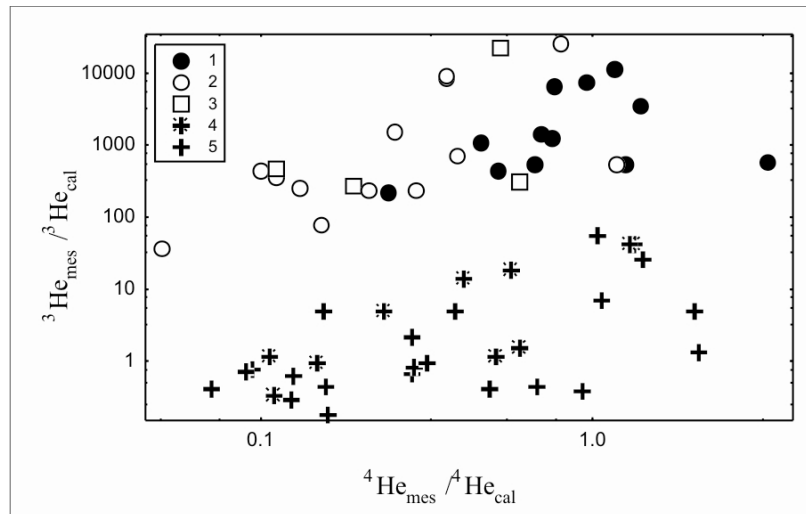


Fig. 5. Comparison of measured (*mes*) and calculated (*cal*) abundances of ^4He and ^3He .

Rocks: ultramafic (1), carbonatites (2) and phoscorites (3) of CAUC; Khibina (4) and Lovozero (5).

Helium extracted by melting from the most Lovozero rocks is predominantly radiogenic one. Only some samples of foyaite, juvite and poikilitic nepheline syenite, mainly from low part of the layered complex, show enhanced (up to $23 \cdot 10^{-8}$) $^3\text{He}/^4\text{He}$ ratio. In FI of poikilitic syenites, augite porphyrites from volcanic complex and fenites from exocontact of the pluton this ratio may amount to as much as 10^{-6} and over. Ore (loparite) malignite, urtite and lujavrite of layered complex and juvite of eudyalite complex are notable for the highest helium concentrations and minimal $^3\text{He}/^4\text{He}$ values both in the whole rocks and FI. Nevertheless, in the most radioactive malignite sample there was found the fivefold excess of the measured ^3He quantity relative to calculated one that is considerably more than likely an error of computation.

Low potassium concentrations in CAUC carbonatites and phoscorites are favor using of $^{40}\text{Ar} - ^{36}\text{Ar}$ system to identify the atmogenic component of fluid. Isotope composition of argon trapped in FI, as compared with total one, is to far lesser degree undergone changes at the expense of radiogenic $^{40}\text{Ar}^*$ addition produced in situ. This is supported by a positive correlation of $^{40}\text{Ar}_{\text{fi}}$ and $^{36}\text{Ar}_{\text{fi}}$ (Fig. 6) and absence of relationship between $^{40}\text{Ar}_{\text{tot}}$ and $^{36}\text{Ar}_{\text{tot}}$ in CAUC. Not many argon determinations in FI of nepheline syenites show still a closer correlation of Ar isotopes.

In K-Ar evolution diagram (Fig. 7) the most points of carbonatites and phoscorites lie above the isochrone thus implying considerable excess of radiogenic argon. $^{40}\text{Ar}/^{36}\text{Ar}$ ratio in trapped gas could be about 1000. And indeed, by means of similar graphs on the linear coordinates for separate massifs this initial ratio has been estimated as 900-1200 in the rocks of CAUC carbonatite series and close to atmogenic one in Khibina and Lovozero rocks.

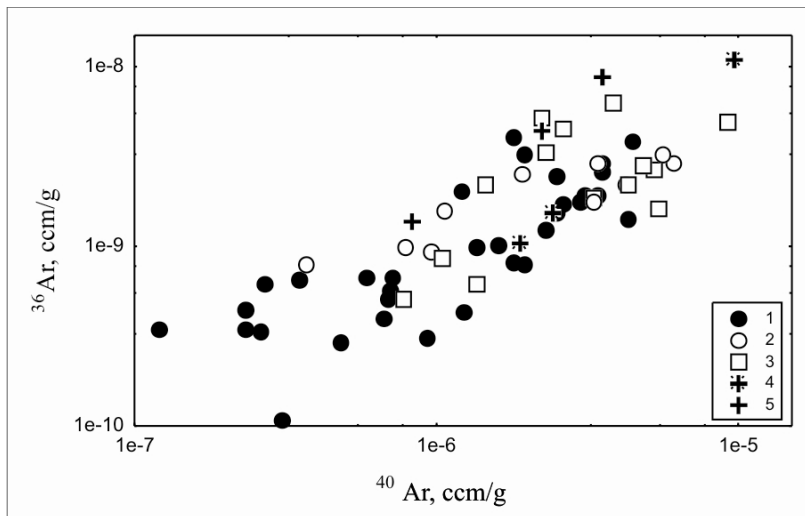


Fig. 6. Correlation of argon isotopes in fluid inclusions.

Rocks: ultramafic (1), carbonatites (2) and phoscorites (3) of CAUC; Khibina (4) and Lovozero (5).

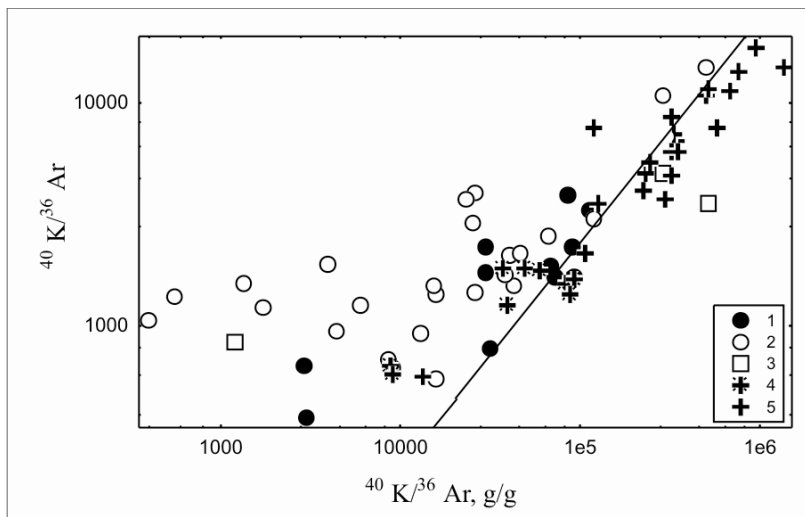


Fig. 7. K-Ar evolution diagram. Sloping straight line – reference 370 Ma evolution line.

Rocks: ultramafic (1), carbonatites (2) and phoscorites (3) of CAUC; Khibina (4) and Lovozero (5).

The relationship pattern of parent elements (U, Th, K) and daughter radiogenic He and Ar isotopes (Fig. 8) confirms a preferred loss of radiogenic helium since figurative points of the most samples are situated below concordia.

The outlined regular reinforcement of correlation between ${}^3\text{He}$ and ${}^4\text{He}/{}^{40}\text{Ar}^*$ in gases extracted by milling from ultramafic rocks to carbonatites and phoscorite and then to nepheline syenites (Fig. 9) can be one more point in favor of different nature of fluid inclusions in these rock series. Moreover, clear narrowing in range of radiogenic He and Ar isotope ratio is observed here with increase in ${}^3\text{He}$ concentration that is with decrease of its loss. Proximity of isotope characteristics

of the Kola alkaline intrusions and OIB suggests also their similar sources. Basing on interpretation of isotope-geochemical data, different authors assume both

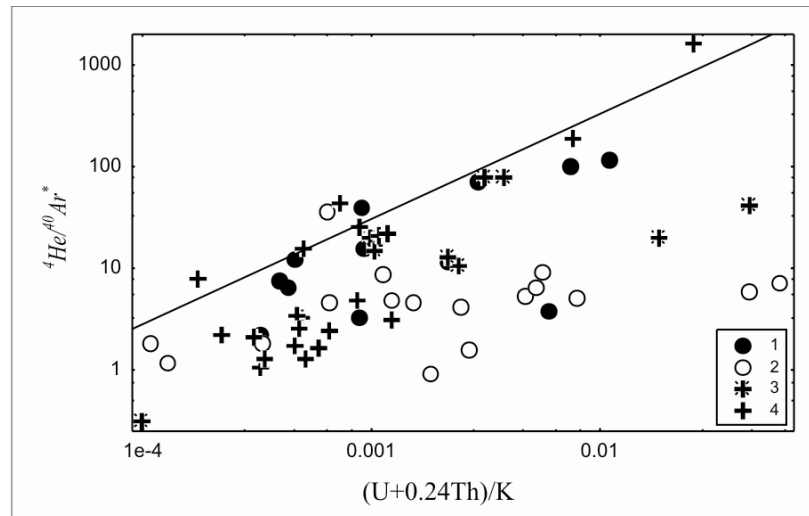


Fig. 8. Relationships between parent element (U, Th, K) and daughter isotope ($^4\text{He}/^{40}\text{Ar}^*$) ratios. Rocks: ultramafic (1), carbonatites and phoscorites (2) of CAUC; Khibina (3) and Lovozero (4).

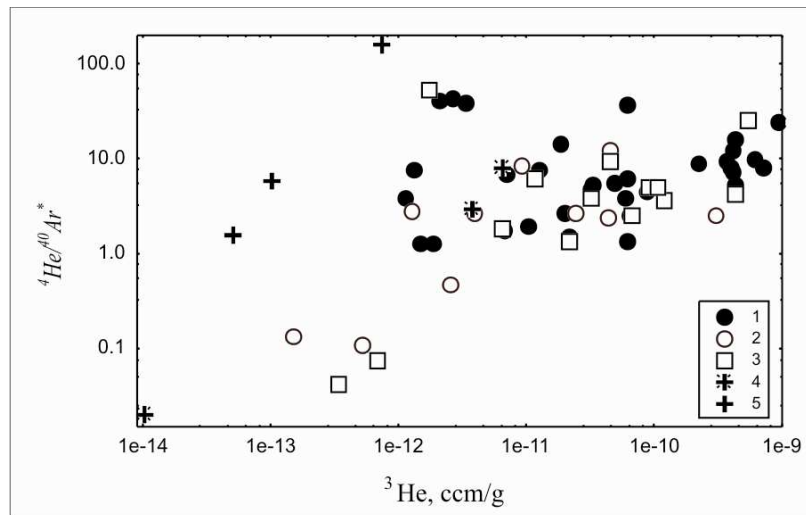


Fig. 9. Relationships of ^3He abundance and $^4\text{He}/^{40}\text{Ar}^*$ ratio in fluid inclusions. Rocks: ultramafic (1), carbonatites (2) and phoscorites (3) of CAUC; Khibina (4) and Lovozero (5).

lithospheric and asthenospheric sources for basalt melts. The models of generation and evolution of parent melts for continental alkaline and carbonatite complexes provide the metasomatized enriched lithospheric source in the most cases [e.g., Wyllie et al., 1990; Kogarko et al., 1994]. Noble gas isotope characteristics obtained are consistent with both such suppositions and the more common lithospheric model combined isotopic, geochronological and geophysical data [Mckenzie and O’Nions, 1995]. The latter model is envisaged the existence of two layers in subcontinental lithosphere. The composition of one layer is close to MORB source and the other overlying layer is depleted relatively to MORB. Both

were changed by means of supplying (10-30 % by volume) of metasomatic melt appearing 0.3-0.5 % fusion from asthenospheric mantle. Since subcontinental lithosphere is a long living conservative reservoir, the period between beginning of the metasomatic processes and emplacement of parent alkaline magmas in the crust can be rather long. Basing on Rb-Sr system, for the Kola Devonian complexes such time gap is estimated as 50-350 Ma. This, taking into account age of alkaline magmatism, review of the Earth's degassing modern models and U-Th systematics, allows us to exclude the upper mantle from potential sources of primordial noble gases in alkaline and carbonatite rocks [Tolstikhin et al., 1999b]. The lower mantle, perhaps its stagnant and less degassing regions, is suggested to be such source.

On the basis of computer-simulation derived evaluations of noble gas contents in the main Earth's reservoirs [Tolstikhin and Marty, 1998] their contributions to parent melts of the Kola CAUC are estimated. The matter mass proportions of the less degassing lower mantle reservoir, upper mantle and meteoric water saturated with atmogenic gases make up 2 %, 97.95 % and 0.05 %, respectively [Tolstikhin et al., 1999b]. The foregoing comparison of CAUC and nepheline-syenite intrusions in gas isotope characteristics suggests that in general these estimations can also be extended to the Khibina and Lovozero plutons having regard to their distinct conditions of magmatic crystallization (first of all, of smaller depths) and character of postmagmatic alterations. While, the greater participation of the crustal essentially water fluid with dissolved atmogenic gas components is suggested in formation of the nepheline-syenite massifs especially at the late stages of their evolution.

CONCLUDING REMARKS

Present-day isotope composition of noble gases in the rocks of Paleozoic alkaline and ultramafic-alkaline with carbonatites complexes of the Kola province as well of large mineral deposits related is controlled by (a) degassing extent of parent melts, (b) quantity of trapped isotopes and their retention depending on shifting properties of enclosing minerals, (c) duration, intensity and character of postmagmatic processes, (d) partial contamination with crustal fluid and atmogenic components, (e) concentration of radioactive elements, production, migration and loss of radiogenic isotopes. In its turn, intensification of degassing is determined by composition, rate of ascent and crystallization conditions of the melts, including depth of a magmatic chamber and degree of system openness with respect to fluid.

Noble gas isotope characteristics of the concerned complexes strongly suggest that origin of their primary melts was initiated with a deep mantle plume. The lower mantle constituent is surely established in the plume. These are consistent with the models based on other geochemical and geophysical evidence and envisaging, as dominant, previously metasomatised lithospheric source of parent melts.

Gas-geochemical features of phoscorites and carbonatites reflect their later formation relatively to associated ultramafic and alkaline rocks. Magnetite ores in CAUC formed mainly by magmatic crystallization and subsequently underwent partial and uneven postmagmatic changes caused broad variations in their mineral composition.

Agpaitic melts formed the Khibina and Lovozero nepheline-syenite plutons proved to be the most degasified that was likely determined by their high alkalinity, lesser depth and longer, because of huge magmatic chambers, crystallization. Prolonged cooling, high contents of alkalis and accumulation of chemically active fluids in melt stipulated intensive postmagmatic, mainly autometasomatic, processes. Hypabyssal conditions promoted contamination of magmatic fluids with atmogenic components predominantly at late stages of massif formation.

Not fundamental, on the whole, distinctions in gas isotope factors of ore-bearing complexes, ore mineralization of different types and their host rocks can indicate commonness of the sources and origin as well as some discrepancy in formation conditions and postmagmatic transformations.

The authors thank Dr. I. Tolstikhin for helpful discussion, constructional suggestions and remarks promoted improvement of work.

This study was supported by Russian Foundation for Basic Research, grant 00-05-64174.

REFERENCES

1. Beard A. D., Downes H., Vetrin V., Kempton P.D., Maluski H. (1996) Petrogenesis of Devonian lamprophyre and carbonatite minor intrusions, Kandalaksha Gulf (Kola Peninsula, Russia). *Lithos* 39, 93-119.
2. Ikorsky S.V., Nivin V.A. and Pripachkin V.A. (1992). Gas geochemistry of endogenic formations (monograph). St.- Petersburg, Nauka, 176 p. (in Russian).
3. Kogarko, L.N., Kononova, V.A., Orlova, M.P., Woolley, A.R. (1995). *Alkaline Rocks and Carbonatites of the World, Part 2: Former USSR*. Chapman & Hall, London, 230 p.
4. Kramm U., Kogarko L. N. (1994) Nd and Sr isotope signatures of the Khibina and Lovozero agpaitic centres, Kola Alkaline Province. Russia. *Lithos* 32, 225-242.
5. Marty B., Tolstikhin I., Kamensky I., Nivin V., Balaganskaya E., Zimmermann J.-L. (1998). Plume-derived rare gases in 380 Ma carbonatites from the Kola region (Russia) and the argon isotopic composition in the deep mantle. *Earth and Planetary Science Letters*, Vol.164, No.1-2, pp. 179-192.
6. McKenzie D. and O'Nions R.K. (1995). *The source regions of ocean Island basalts*. Oxford Univ. Press. 133-159.
7. Mitrofanov F. P., Ikorsky S. V., and Kamensky I. L. (1995) He isotopes in Paleozoic alkaline intrusions of Kola Peninsula and Northern Karelija. *Dokl. Russian Acad. Sci.* 345, 243-246 (in Russian).

8. Nivin V.A., Kamenskiy I.L., Tolstikhin I.N.(1988).Helium and argon isotope compositions in rocks of the ore horizons of the Lovozero massif. *Geochemistry International*, 25/8, pp. 27-32.
9. Nivin V.A., Kamensky I.L. and Tolstikhin I.N. (1993) Helium and argon isotope abundances in rocks of Lovozero alkaline masssif. - *Isotopenpraxis*, Vol.28, pp. 281-287.
10. Sokolov S.V. (1994). Alkaline carbonatite complexes and carbonatite formation conditions. *Geochemistry International* 31(6), 46-54.
11. Tolstikhin I. N., Kamensky I. L., Sharkov I. V., Dudkin O.B., Pripachkin V. A. (1985) Isotopes of light noble gases in carbonatites of the Kola Peninsula. Kola Sci. Center, Russian Acad Sci. 42 p. (in Russian).
12. Tolstikhin I.N., Marty B. (1998). The evolution of terrestrial volatiles: a view from helium, neon, argon and nitrogen isotope modeling. *Chemical Geology*, Vol.147, pp. 27-52.
13. Tolstikhin I.N., Kamensky I.L., Nivin V.A., Vetrin V.R., Balaganskaya E.G., Ikorsky S.V., Gannibal M.A., Kirnarsky Yu.M., Marty B., Weiss D., Verhulst A., Demaiffe D. (1999a). Low mantle plume component in 370 Ma old Kola ultrabasic-alkaline-carbonatite complexes: Evidences from rare gas isotopes and related trace elements. *Russian Journal of Earth Sciences, English Translation*, Vol. 1, No. 2 (Print version of the online electronic journal <http://eos.wdcb.rssi.ru/rjes/>), pp. 179-222.
14. Tolstikhin I.N., Kamensky I.L., Marty B., Nivin V.A., Vetrin V.R., Balaganskaya E.G., Ikorsky S.V., Gannibal M.A., Kirnarsky Yu.M., Weiss D., Verhulst A., and Demaiffe D. (1999b). Low mantle plume component in Devonian Kola ultrabasic-alkaline-carbonatite complexes: Evidences from rare gas isotopes and related parent elements. Reprint. Apatity-Nancy-Bruxelles, 97 p (in English and Russian).
15. Veksler I.V., Nielsen T.F.D. and Sokolov S.V. (1998) Mineralogy of crystallized melt inclusions from Gardiner and Kovdor ultramafic alkaline complexes: Implications for carbonatite genesis. *J. Petrology*, Vol. 39, No. 11&12, pp. 2015-2031.
16. Wyllie P. J., Baker M. B., and White B. (1990) Experimental boundaries for the origin and evolution of carbonatites. *Lithos* 26, 3-19.

Evolution of South Indian enriched lithospheric mantle: Evidence from the Yelagiri and Sevattur alkaline plutons in Tamil Nadu, South India

**T. Miyazaki¹, H. Kagami¹, V. Ram Mohan², K. Shuto³
and T. Morikiyo⁴**

¹ *Graduate School of Science and Technology, Niigata University, Niigata 950-2181, Japan*

² *Department of Geology, University of Madras, Chennai 600 025, India*

³ *Department of Geology, Faculty of Science, Niigata University, Niigata 950-2181, Japan*

⁴ *Department of Geology, Faculty of Science, Shinshu University, Matsumoto 390-8621, Japan*

Alkaline magmatism in the northern part of south Indian granulite terrain is important to understand the crustal formation on the southern periphery of the Dharwar craton. In Proterozoic, the Yelagiri and Sevattur alkaline complexes intrude into the country rocks comprising epidote hornblende gneiss. The initial Sr and Nd isotope ratios of the Sevattur carbonatites suggest their derivation from an alkaline metal and LREE enriched mantle source. However, the syenites of the Yelagiri and Sevattur plutons have distinctly different isotopic characteristics from the Sevattur carbonatites, represented by their low initial Nd isotope ratios. Combined geochemical and isotopic characteristics of the Yelagiri and Sevattur syenites indicate that the syenitic magmas were derived from highly differentiated mantle-derived alkali basaltic magmas. The Yelagiri and Sevattur syenites are characterized by pronounced enrichment in LIL and large negative Nb anomaly, indicating subduction related signature of their source mantle. The geochemical and isotopic signatures of other mantle-derived intrusive rocks with different ages from ca. 2.5 Ga to ca. 0.75 Ga also indicate the existence of subduction related enriched mantle. Therefore, it is considered that this enriched mantle was formed by the subduction-related geological processes, which probably occurred at a convergent margin along the southern and/or southeastern edge of the Dharwar craton, and survived, as sub-continental lithospheric mantle, from early Proterozoic until at least 750 to 800 Ma ago.

INTRODUCTION

More than 40 alkaline plutons occur in eastern and southern Peninsular India [Ratnakar & Leelanandam, 1989; Rajesh & Santosh, 1996]. These plutons intrude the South Indian high-grade granulite terrains as well as the Eastern Ghats granulite belt. Some of the alkaline plutons are accompanied with carbonatites and form carbonatite complexes. In the northern part of the South Indian granulite terrain in the Vellore and Dharmapuri districts of Tamil Nadu, which lies just south of the amphibolite faces - granulite faces transition zone, a number of alkaline plutons comprising saturated syenite, pyroxenite and carbonatite have been reported [Udas & Krishnamurthy, 1970; Borodin et al., 1971; Krishnamurthy, 1977; Subramanian et al., 1978; Viladkar & Subramanian, 1995; Miyazaki et al., 1999; etc.]. These complexes are located along a major NE-SW trending lineament

[Grady, 1971] in a gneissic terrain. This region is important to understand the crustal formation on the periphery of the Dharwar craton.

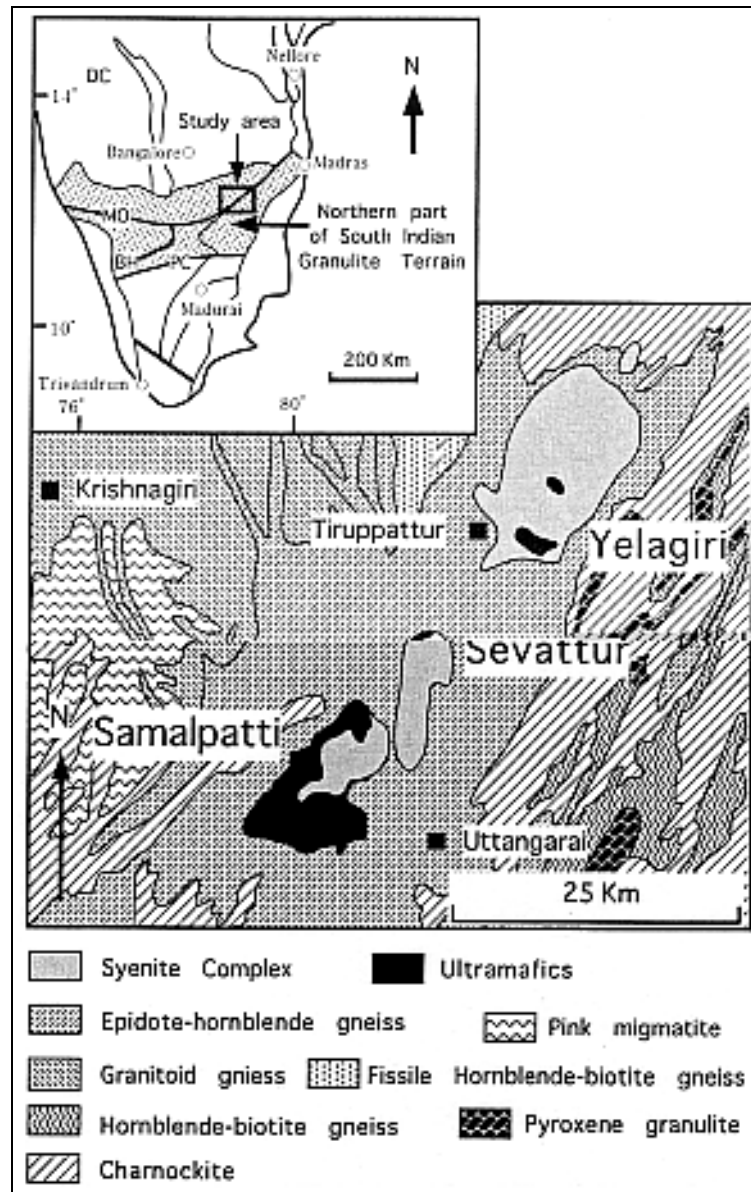


Fig. 1. Simplified geological map of northern Tamil Nadu area [modified from Geological Survey of India, 1995].

The Yelagiri pluton is located at the northern most part, Sevattur pluton is in the middle and Samalpatti pluton is situated further southwest (Fig. 1). The Sevattur and Samalpatti are associated with carbonatite and form alkali-carbonatite complexes. The age of the alkaline magmatism reported from Yelagiri, Sevattur and Samalpatti include a Rb-Sr whole rock isochron age of 757 ± 32 Ma [Miyazaki et al., 2000] for the Yelagiri syenites, a K-Ar age of 700 ± 30 Ma for phlogopite from the Samalpatti carbonatites [Moralev et al., 1975], Rb-Sr whole rock isochron

ages of 767 \pm 8 Ma [Kumar et al., 1998] and 756 \pm 11Ma [Miyazaki et al., 2000] for the Sevattur syenites, Rb-Sr whole rock-mineral isochron ages of 771 \pm 18 Ma and 773 \pm 18 Ma for the Sevattur carbonatites and pyroxenites respectively [Kumar & Gopalan, 1991] and a whole rock lead/lead age of 801 \pm 11 Ma for the Sevattur carbonatites [Schleicher et al., 1997]. These age data of these plutons indicate late Proterozoic alkaline magmatic activity in the region.

Sr and Nd isotope data from carbonatites have now been shown to be effective in monitoring the nature of the subcontinental mantle [e.g. Bell & Blenkinsop, 1989], even though the relationships between carbonatites and their associated silicate rocks are complex and still not be completely understood [Bell et al., 1998]. Mainly in last decade, comprehensive isotopic studies of carbonatites and their associated silicate rocks reveal that there are several alkaline-carbonatite complexes with wide isotopic variation in the associated silicate rocks, which requires the involvement of other mantle components and/or continental crust or is result of isotopic heterogeneity of mantle source [e.g. Bell & Peterson, 1991; Simonetti & Bell, 1994; Bell, 1998; Harmer & Gittins, 1998; Harmer, 1999]. Although several alkaline plutons in Tamil Nadu are not associated with carbonatite, comprehensive Sr and Nd isotopic investigation of alkali-carbonatite complexes provides important information about petrogenesis and source characteristics not only alkaline-carbonatite complexes but also non-carbonatite associated alkaline plutons.

The existence of alkali metal and LREE enriched subcontinental upper mantle are recognized under this region [e.g., Kumar & Gopalan, 1991; Wickham et al., 1994; Reddy et al., 1995; Kumar et al., 1998; Schleicher et al., 1998; Miyazaki et al., 2000]. Kumar et al. [1998] insisted that this enriched mantle had existed as sub-continental lithospheric mantle under this region and had been a closed-system since about 2.5-2.6 Ga. Radhakrishna & Joseph [1998] also revealed that tholeiite dyke swarms (1.6 and 1.8 Ga) in this region were derived from enriched lithospheric mantle. However, several problems about the Yelagiri and Sevattur syenites, such as petrogenesis, source characteristics and relation to enriched lithospheric mantle, are not clearly elucidated. In this paper, detail petrogenetic studies about the Yelagiri and Sevattur plutons in Tamil Nadu, were described.

YELAGIRI AND SEVATTUR PLUTONS

The Yelagiri and Sevattur plutons (Fig. 1) intrude along NE-SW fault system and into the Archaean epidote-hornblende gneisses, which constitute the country rocks of the region. These gneisses are highly sheared, and these gneisses rarely contain relic patches of charnockite indicating that they are retrogressive in origin. Peucat et al. [1989, 1993] reported whole rock Rb-Sr and Sm-Nd isochron ages of 2463 \pm 65 and 2455 \pm 121 Ma and U-Pb and $^{207}\text{Pb}/^{206}\text{Pb}$ single zircon ages of 2550-2530 \pm 5 Ma for the Krishnagiri gneisses, which are tonalitic-trondhjemitic,

granitic gneisses and charnockites neighboring the Yelagiri, Sevattur and Samalpatti plutons.

The Yelagiri pluton is an elliptical body of about 20X12 km² elongated in NE-SW direction. The Yelagiri pluton is almost entirely composed of syenite with pyroxenite and biotite pyroxenite. Pyroxenites occur as mafic patches or bands in syenite or xenolithic blocks with sharp contacts in the syenite. Although geological information on the Yelagiri pluton is not sufficient, almost no constituent rocks of this pluton show strong deformation and metamorphism such as observed in the country rocks. Hence, this pluton is considered to keep the initial signature of intrusive pluton.

The Sevattur pluton, located 10 km southwest of Yelagiri pluton, has an oval sharp elongated in N-S direction and measures about 12X5 km². Syenite also forms the major lithounit in the Sevattur pluton, and syenite is rimmed on the north by carbonatite and subsequently by pyroxenite. The carbonatite occurs as arcuate bodies boarding a large syenite stock. Similarly arcuate outcrops of pyroxenite occur outward of the carbonatite. The carbonatite body, which is about 3km in length with a maximum width of 200m in the central part, is mostly dolomitic carbonatite with dykelets of sövite and lesser ankeritic carbonatite. The carbonatite incorporates a number of xenoliths of basement gneisses, syenite and pyroxenite [Udas & Krishnamurthy, 1970; Borodin et al., 1971; Krishnamurthy, 1977; Viladkar & Subramanian, 1995; Kumar et al., 1998]. Pyroxenite also occurs as xenolithic blocks in syenite and carbonatite. The detailed mineralogy of the Sevattur carbonatite and associated rocks has been described by Viladkar & Subramanian [1995]. Entirely, there is no evidence that the Sevattur pluton suffered strong deformation and metamorphism. Hence, this pluton is also considered to keep the initial signature of intrusive pluton.

According to the geochemical characteristics described in Miyazaki et al. [2000], the Sevattur syenites may show magmatic evolution, which are mainly controlled by fractional crystallization. On the other hand, some open system behaviors (ex. magma mixing, crustal contamination, etc.) are considered to have influenced on mineralogical and geochemical characteristics of the Yelagiri syenites.

Nd-Sr ISOTOPES

Initial Sr and Nd isotope ratios and epsilon values were calculated (Fig. 2). The Yelagiri syenites show a range of epsilon Sr (T=760Ma) from 21.0 to 26.3 and of epsilon Nd (T=760Ma) from -11.4 to -8.1. While Sevattur syenites exhibit a range of epsilon Nd(T) from -9.9 to -9.4 within the range of the Yelagiri syenites. The epsilon Sr(T) of the Sevattur syenites is lower ranging between 10.0 to 12.4. Pyroxenites and high silica rocks of the Sevattur pluton have similar or closer Sr and Nd isotope characteristics to the Sevattur syenites, whereas epsilon Sr (T) values of the Yelagiri pyroxenites are shifted to higher epsilon Sr (T) values. This epsilon Sr (T) diversity of the Yelagiri pyroxenites are considered to be the result

of secondary alteration, since negative correlation between Sr concentration and epsilon Sr (T) value and deformed textures of phlogopites are observed. Carbonatites from the Sevattur show epsilon Sr (T) range from 21.0 to 24.3, as in the case of the Yelagiri syenites. However, epsilon Nd (T) range of the Sevattur carbonatites (epsilon Nd (T)= -6.6 to -4.4) is somewhat higher than the ranges of syenites of both plutons.

The oxygen and carbon isotopic compositions of calcites and dolomites from the Sevattur carbonatite samples show very little variation, with average values of $\delta^{18}\text{O} = +7.1$ and $\delta^{13}\text{C} = -5.2$ from calcites and $\delta^{18}\text{O} = +7.3$ and $\delta^{13}\text{C} = -4.8$ from dolomites [Miyazaki et al., 2000]. All carbonatite samples analyzed plot within the field for 'primary igneous carbonatites' [Keller & Hoefs, 1995]. The $\delta^{18}\text{O}$ and $\delta^{13}\text{C}$ data of the Sevattur carbonatites indicate that they originated from mantle-derived melts. Because of the very high concentrations of Sr and Nd in carbonatite magmas, their low melting temperatures and probable rapid transport through the crust, crustal contamination for these elements is minimum in comparison to most other mantle-derived magma types [Bell & Blenkinsop, 1989]. Thus the initial Sr and Nd isotope ratios for the carbonatites are likely to be representative of their mantle source. The Sevattur carbonatites have high initial $^{87}\text{Sr}/^{86}\text{Sr}$ ratios and low initial $^{143}\text{Nd}/^{144}\text{Nd}$ ratios relative to the bulk earth and

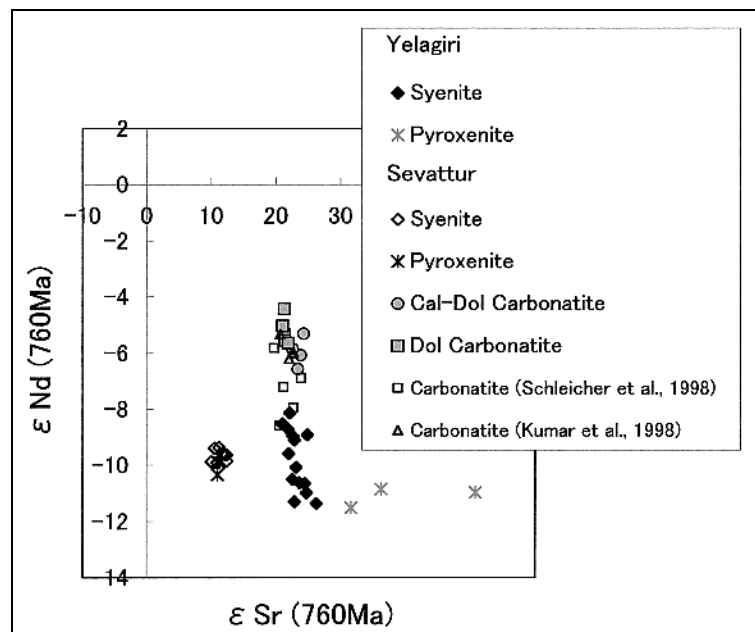


Fig.2. Epsilon Sr (T) vs. epsilon Nd (T) diagram for Yelagiri and Sevattur rocks.

CHUR (Fig. 2). Thus, these isotope ratios imply an alkali metal and LREE enriched mantle as the source of the Sevattur and Samalpatti carbonatites. Several authors also described the existence of enriched subcontinental mantle source in this region [e.g., Kumar & Gopalan, 1991; Wickham et al., 1994; Reddy et al. 1995; Kumar et al., 1998; Schleicher et al., 1998; Miyazaki et al., 2000]. However,

syenites and pyroxenites of the Sevattur pluton show low initial epsilon Sr and epsilon Nd values compared to the values of Sevattur carbonatites (Fig. 2). The Yelagiri syenites also show low initial epsilon Nd values compared to the values of Sevattur carbonatites, even though initial epsilon Sr values are similar to the values of Sevattur carbonatites. It is noticeable that silicate rocks of both plutons have low initial epsilon Nd values compared to the values of the Sevattur carbonatites. These isotopic diversities between carbonatites and silicate rocks may be caused by differences in their source or different influences from other materials. Isotopic differences of silicate rocks are also observed between the Yelagiri and Sevattur plutons. Their contemporary activity, close spatial relationship and generally similar petrographical and geochemical characteristics lead us to expect genetic relationship between the Yelagiri and Sevattur syenites. However, initial epsilon Sr values of silicate rocks are significantly different between the Yelagiri and Sevattur plutons (Fig. 2).

RELATIONSHIP BETWEEN CARBONATITES AND SILICATE ROCKS

In this section, currently popular models for the petrogenetic association between carbonatites and associated alkaline silicate rocks are assessed in the light of the geochemical and isotopic data for the carbonatite, syenite and pyroxenite at the Sevattur and Yelagiri. Although almost geochemical and isotopic data of carbonatites support the idea that carbonatite magma is derived from mantle materials, there are several models for the genesis of carbonatites.

Models for the genesis of carbonatites are now in very controversial. Mainly, following two possibility are considered: (1) Carbonatite melt is derived as an immiscible liquid that separates from a fractionated silicate magma of nephelinitic composition, the composition of the immiscible carbonatite liquid being directly related to the composition of the parental silicate magma [Le Bas, 1977, 1981, 1987; Kjarsgaard & Hamilton, 1989]; (2) Carbonatite magmas may be derived directly through low degrees of melting of carbonated mantle peridotite [Wallace & Green, 1988; Thibault et al., 1992; Dalton & Wood, 1993; Sweeney, 1994; Harmer, 1999].

If differentiation took place in a closed system then the silicate and carbonate would be expected to have similar isotopic signatures. The sharp contrast in isotopic composition between the carbonate and silicate components of the Sevattur and Yelagiri is difficult to reconcile with liquid immiscibility (Fig. 2). Although, still more evaluations are needed, carbonatite magma of the Sevattur pluton may be derived by directly melting of carbonated mantle peridotite.

PETROGENESIS OF THE YELAGIRI AND SEVATTUR SYENITES

A number of models have been proposed for the origin of syenites, which show large geochemical diversity and occur in a variety of tectonic settings [e.g.,

Ewart, 1982; Harris et al., 1983; Nielson, 1987; Fletcher & Beddoe-Stephens, 1987; Smith et al., 1988]. It is likely that the bulk of continental syenites were derived by crystal fractionation of mantle-derived alkali basaltic magma with/without interaction with pre-existing continental crust [Ewart, 1982; Downes, 1987; Fitton, 1987; Nielson, 1987; Fletcher & Beddoe-Stephens, 1987; etc.]. Other presumable model for the generation of syenitic and more evolved felsic magmas include partial melting of amphibolites with alkali basalt composition at the base of the lower crust [Smith et al., 1988].

To elucidate models, initial epsilon Sr and epsilon Nd values (calculated at 760 Ma) of granulite gneisses of neighboring Krishnagiri area [Peucat et al., 1989] are compared with those of the Sevattur and Yelagiri plutons. These gneisses are tonalitic, granitic and chanokitic gneisses with paleopressures from 5 to 6 kb [Peucat et al., 1989]. These crustal rocks have initial epsilon Sr (760 Ma) values from -20 to 211 and initial epsilon Nd (760 Ma) values from -31 to -18. The range of initial epsilon Sr values is very wide and includes the values for the Sevattur and Yelagiri plutons. On the other hand, the initial epsilon Nd values are low compared with the Yelagiri and Sevattur syenites. This fact suggests that the sources of these syenites are not crustal rocks distributed around the Yelagiri and Sevattur plutons. More high-grade crustal rocks are believed to occur in the deeper part of the crust. These high-grade crustal rocks are supposed to be high pressure charnockites such as exposed in the Nilgiris Hills, Shevaroy and Biligirirangan Hills and Harur Hills [Peucat et al., 1989]. The highest pressures are recorded in the Shevaroy and Biligirirangan Hills (7.5-8 kb), and along the northern slope of the Nilgiris Hills (9kb) [Janardhan et al., 1982; Raith et al., 1983]. These high-pressure charnockites have initial epsilon Sr (760Ma) values from -24 to 88. Although only two high-pressure charnockite data of Biligirirangan Hills are available, their initial epsilon Nd (760Ma) values range from -32 to -26. These initial epsilon Sr and epsilon Nd values are similar to the Krishnagiri chanokitic and tonalitic gneisses. Therefore, these high-pressure charnockites are excluded from the candidates of the sources of the Yelagiri and Sevattur syenites.

Therefore, it is understood that the Yelagiri and Sevattur syenites were derived by crystal fractionation of mantle-derived alkali basaltic magma. Considering the low Cr and Ni concentrations and low Mg# of the Yelagiri and Sevattur syenites, the origins of the Yelagiri and Sevattur syenite magmas were highly differentiated alkali basaltic magmas, which might be differentiated by crystal fractionation within a lower-crustal magma chamber before emplacement of separate batches of syenitic magma into middle to upper crustal levels.

CAUSE OF ISOTOPIC VARIATIONS

A number of Sr and Nd isotopic studies of other carbonatite complexes in the world revealed that carbonatite and associated silicate rocks generally have similar initial Sr and Nd isotope ratios, indicating their derivation from common or isotopically similar mantle source, even though diversity of their petrogenesis.

However, recent comprehensive isotopic studies of carbonatites and their associated silicate rocks show that there are several alkaline-carbonatite complexes with wide isotopic variation in the associated silicate rocks, which require the involvement of other components, such as continental crust, or indicate isotopic heterogeneity of mantle components [e.g. Bell & Peterson, 1991; Simonetti & Bell, 1994; Bell, 1998; Harmer & Gittins, 1998; Harmer, 1999].

As described above, silicate rocks of the Yelagiri and Sevattur plutons show low initial epsilon Nd values (low initial Nd isotope ratios) compared to the values of carbonatites representing the values of the enriched mantle. If the involvement of crustal components caused these isotopic varieties, crustal involvement probably occurred (1) during intrusion and differentiation of syenitic magma or (2) within a lower-crustal magma chamber, in which homogenizing also occurred, before emplacement of separate batches of syenitic magma into middle to upper crustal levels.

In the first case, AFC or binary mixing process involving mantle deriving magma and crustal materials are considered to be operated during intrusion and differentiation. If AFC or binary mixing process involving mantle derived magma and crustal materials is effectively operated, the trend decreasing initial $^{143}\text{Nd}/^{144}\text{Nd}$ ratio with increasing SiO_2 is expected to be observed. However, the Yelagiri and Sevattur syenites do not show such trend supporting AFC or binary mixing process. The Sevattur syenites have relatively constant initial $^{143}\text{Nd}/^{144}\text{Nd}$ ratios, whereas the Yelagiri syenites show “opposite” trend increasing initial $^{143}\text{Nd}/^{144}\text{Nd}$ ratio with increasing SiO_2 [Miyazaki et al., 2000]. Other chemical parameters (e.g., Mg#, $\text{Na}_2\text{O}+\text{K}_2\text{O}$, Nb, Zr) of the Yelagiri syenites also show similar trends increasing initial $^{143}\text{Nd}/^{144}\text{Nd}$ ratio with increasing evolution [Miyazaki, 2000]. According to relationships between initial $^{143}\text{Nd}/^{144}\text{Nd}$ ratios and SiO_2 of the Yelagiri and Sevattur syenites, AFC or binary mixing involving mantle derived magma and crustal materials is not probable process in the Yelagiri and Sevattur syenites. Therefore, the Sr and Nd isotopic characteristics of the Yelagiri and Sevattur silicate rocks are not result of isotopic change caused by crustal materials during intrusion and differentiation.

In the second case, crustal involvement and homogenizing are occurred within a lower-crustal magma chamber before emplacement. Precise estimation of crustal involvement with Sr and Nd isotopes are difficult, because of insufficient information (such as Sr and Nd concentrations) of alkali basaltic magma derived from mantle. However, average Sr and Nd concentrations of metamorphic rocks around the Yelagiri and Sevattur plutons are considerably lower than those of the Yelagiri and Sevattur syenites, which are about 500 ppm and 20 ppm, respectively, and similar to the average concentrations of the lower continental crust reported by Weaver & Tarney [1984]. Therefore, Sr and Nd isotopic influences of crustal material are considered to be little, even though considerable amount of crustal material are injected into the alkali basaltic magma. This fact probably indicates that the second case is also not probable to explain the isotopic variations of the

Yelagiri and Sevattur plutons. Therefore, the cause of the isotopic varieties of the Yelagiri and Sevattur plutons are considered to be the heterogeneity of enriched lithospheric mantle.

Contribution from a substantial body of experimental and mantle xenoliths studies [e.g. Green & Wallace, 1988; Yaxley et al., 1991; Dautria et al., 1992; Hauri et al., 1993; Ionov et al., 1993; Rudnick et al., 1993; Yaxley & Green, 1996] revealed the existence of the reaction zone at depth about 2 GPa, in which mantle derived primary carbonate melt progressively metasomatise mantle lherzolite to wehrlite with the expulsion of CO₂ [Harmer & Gittins, 1998; Harmer, 1999]. Haggerty [1989] referred to this zone as a 'metasome'. As argued by Meen [1987], Haggerty [1989] and Meen et al. [1989], the depth interval of the thermal maximum, or 'ledge', in the solidus for peridotite-CO₂ will be a zone where long-lived enrichments are most likely to be preserved. If these enriched phases are preserved, the 'metasome' level in the mantle will develop anomalous isotopic signatures with the passage of geological time. Harmer [1999] proposed, then, that the contrasting isotopic characteristics of the silicate and carbonatite components at Spitskop are caused by the involvement of this 'metasome'.

The contrasting isotopic characteristics of the silicate and carbonatite components at Yelagiri and Sevattur are also explicated by this idea. The alkali basaltic magma, generating the Yelagiri and Sevattur silicate rocks, are considered to have been derived from isotopically anomalous lithospheric mantle (metasome) generated by trace element enrichment trapped at peridotite-CO₂ 'ledge' during an earlier episode, whereas the carbonatites are considered to have been derived from more deeper region, as described in previous section.

NATURE OF MANTLE SOURCE

Alkaline magmas can be generated in almost all tectonic settings, with their tectonic affinities being clearly reflected in their geochemical signatures [Zhao et al., 1995]. For example, alkaline suites formed in subduction-related regimes, or those derived from a source which has been previously modified by subduction processes, usually show a distinctive negative Nb anomaly on trace-element distribution spiderdiagrams [e.g., Rogers et al., 1985; Nelson & McCulloch, 1989], whereas those from continental rift zones or oceanic island settings display no or slightly positive Nb anomalies [e.g., McDonough et al., 1985; Menzies, 1987]. In addition, the subduction-related alkaline rocks usually have more evolved isotopic compositions [Rogers et al., 1985; Nelson & McCulloch, 1989], characterized by high initial Sr isotope ratios and low initial Nd isotope ratios, similar to subduction-related calc-alkaline or tholeiitic basalts. In contrast, uncontaminated rift- or hotspot-related alkaline rocks normally show essentially primitive isotopic signatures, typified by low initial Sr isotope ratios and high initial Nd isotope ratios, similar to ocean island basalts [McDonough et al., 1985; Clague, 1987; Menzies, 1987]. Such geochemical and isotopic distinctions are usually attributed to their different mantle sources.

The syenites of the Yelagiri and Sevattur plutons show remarkably similar spiderdiagram patterns characterized by pronounced negative Nb anomalies (Fig. 4), and evolved isotopic compositions (Fig. 2). As described previously, the characteristics were not imposed by crustal effects on the magmas, but were derived from the mantle sources. Therefore, their parental magmas are probably related to subduction-modified lithospheric mantle sources. The subduction-related alkaline magmas are considered to have been derived from metasomatised mantle wedges above the deepest part of the subduction zone [Wyllie & Sekine, 1982; Baker, 1987], or the subcontinental lithospheric mantle, which has been previously modified by subduction processes [e.g., Liégeois & Black, 1987; Nelson & McCulloch, 1989]. The choice of the two alternative models depends on the tectonic setting of the Yelagiri and Sevattur syenites. Scarcity of geological evidence for subduction activity at the time of syenite intrusions, and following isotopic and geochemical evidences support the second idea.

EVOLUTION OF THE ENRICHED LITHOSPHERIC MANTLE

Kumar et al. [1998] revealed that the Hogenakal (carbonatite and pyroxenite) and Pikkili (nepheline-syenite) plutons, which are located southwest of the Yelagiri and Sevattur plutons, have Rb-Sr and Sm-Nd isochron ages of about 2.4 Ga and their initial Sr and Nd isotope ratios are very close to the bulk earth and CHUR. As has been noted by many authors [Bell & Blenkinsop, 1987, 1989; Woolley, 1989 and references therein] the geographic localization of carbonatite magmatism over long periods, which has been observed at several localities, implies lithospheric control, and probably tapping of the same source. Although widely different in ages, the Hogenakal and Sevattur carbonatite complexes are less than 75 km apart. Hence, Kumar et al. [1998] showed that their Sr and Nd isotopic compositions consisted with evolution in isolated lithospheric mantle that had been enriched in LIL elements not long before generation of the Hogenakal magmas. The evolution lines for both Sr and Nd isotopes intersect bulk earth and CHUR evolution near 2.5-2.6 Ga (Fig. 3).

Kumar et al. [1998] also showed that mantle-derived rocks, such as the 2.51-2.52 Ga Closepet batholith (southern part) [Jayananda et al., 1995], and the 2.0 Ga Agali-Coimbatore dyke swarm [Radhakrishna et al., 1995], overlap or close to the evolution lines defined by the Hogenakal and Sevattur carbonatites. The Sr and Nd isotopes of the Samalpatti carbonatites [Schleicher et al., 1998; Miyazaki 2000] and the Sr isotopes of the Salem alkaline rocks [Reddy et al., 1995] also overlap with the evolution line (Fig. 3). These facts strongly support the idea that the isolated enriched mantle has existed as sub-continental lithospheric mantle under the northern part of South Indian granulite terrain and has been a closed-system since about 2.5-2.6 Ga [Kumar et al., 1998].

The long lived existence of this isolated enriched lithospheric mantle are also indicated by the trace element characteristics of the Yelagiri and Sevattur syenites and mantle derived dykes from Agali-Coimbatore [Radhakrishna et al.,

1995], Tiruvannamalai and Dharmapuri [Radhakrishna & Joseph, 1998], these dykes also situate in the northern part of South Indian granulite terrain. The Tiruvannamalai and Dharmapuri dykes are iron-rich tholeiites and have K-Ar ages of 1650Ma and 1800Ma [Radhakrishna et al., 1999]. Fig. 4 shows primordial mantle [Sun & McDonough, 1989] normalized trace-element distribution

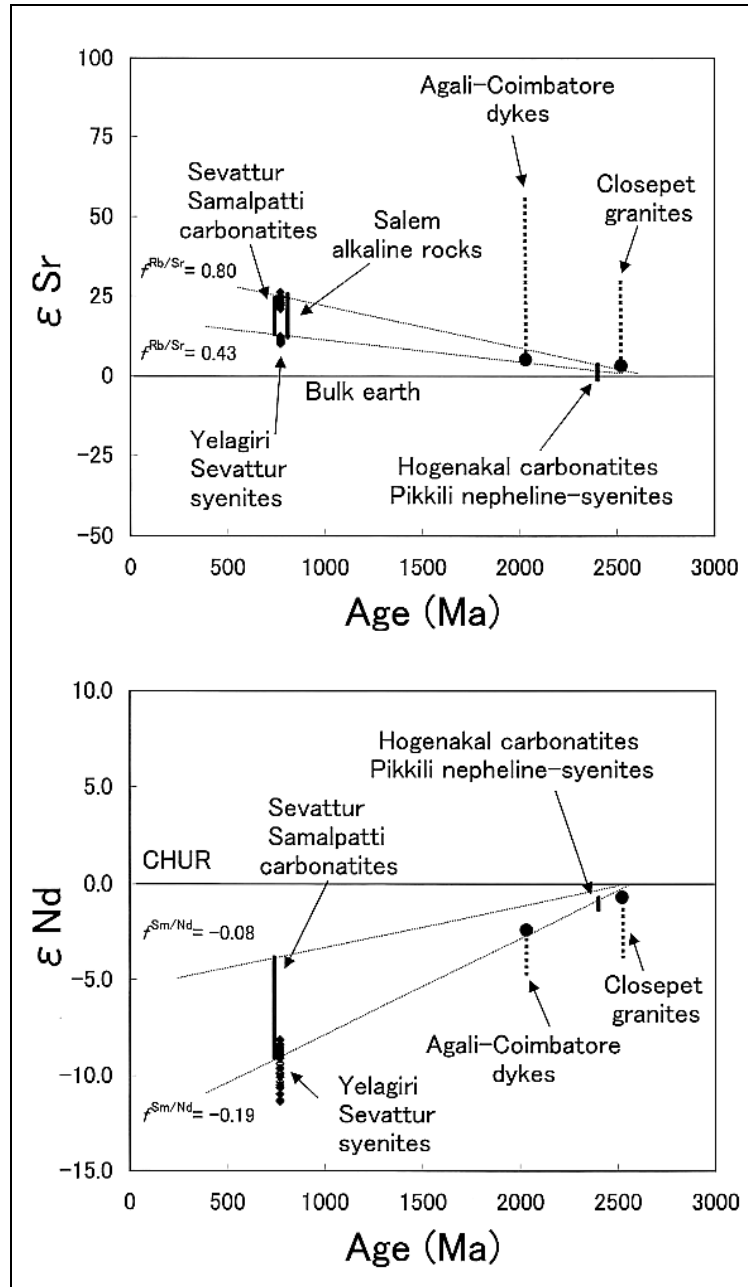


Fig.3. Evolution diagrams showing neodymium and strontium isotopic evolution over time in terms of epsilon parameters. Modified from Kumar et al. [1998].

spiderdiagrams of the Yelagiri and Sevattur syenites and tholeiite dykes from Agali-Coimbatore, Tiruvannamalai and Dharmapuri. Trace element distribution patterns of these tholeiite dykes show similar enrichment in LIL, deficiency in HFS

elements and negative Nb anomaly to the Yelagiri and Sevattur syenites, indicating that the parental magmas of these tholeiite dykes are also related to subduction-modified lithospheric mantle sources. According to the isotopic and geochemical evidences described above, this enriched lithospheric mantle was

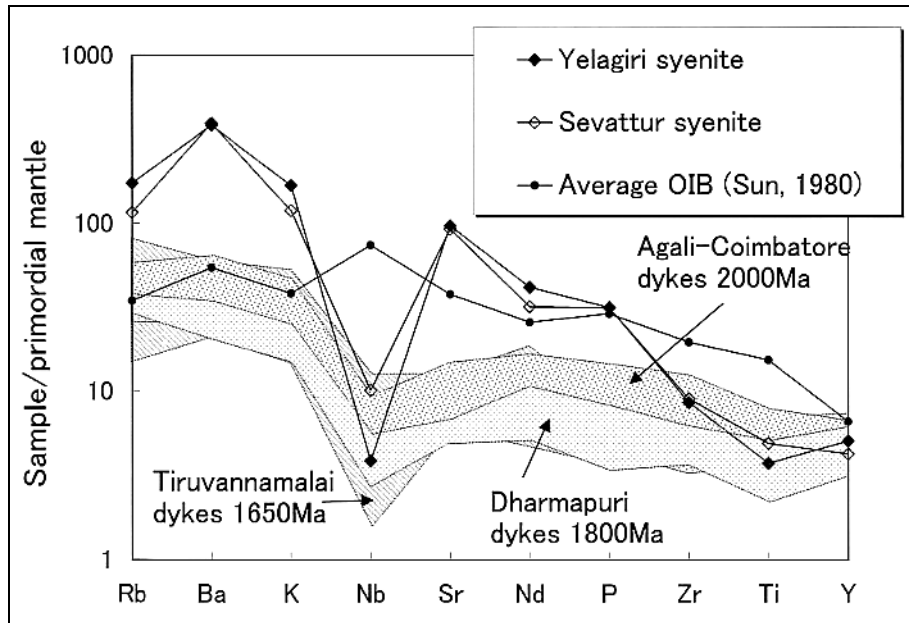


Fig.4. Primordial mantle normalized multi-element patterns of the Yelagiri and Sevattur syenites in comparison with Proterozoic dike suites.

formed by the subduction-related geological processes along the southern and/or southeastern edge of the Dharwar craton and survived convective disruption in the mantle, as sub-continental lithospheric mantle, from early Proterozoic until at least 760 Ma ago.

ACKNOWLEDGMENT

This work was partly supported by the Grant in Aid of Fukada Geological Institute. I greatly acknowledge to Prof. M. Yoshida, Osaka City University, for his encouragement and providing research facilities. I sincerely express my gratitude to the late Prof. K. C. Rajasekaran, University of Madras, for his guidance, encouragement and great support to perform field survey.

REFERENCES

1. Baker, B. H. [1987] Outline of the petrology of the Kenya rift alkaline province. In: Fitton, J. G. & Upton, B. G. J. (Eds) *Alkaline Igneous Rocks*. Geol. Soc. London, *Special Publication* 30, 293-311.
2. Bell, K. [1998] Radiogenic isotope constraints on relationships between carbonatites and associated silicate rocks - a brief review. *J. Petrol.* 39, 1987-1996.
3. Bell, K. & Blenkinsop, J. [1987] Archaean depleted mantle: Evidence from neodymium and strontium initial isotopic ratios of carbonatites. *Geochim. Cosmochim. Acta* 51, 291-298.

4. Bell, K. & Blenkinsop, J. [1989] Neodymium and strontium isotope geochemistry of carbonatites. In: Bell, K. (Ed.) *Carbonatites-Genesis and Evolution*. Unwin Hyman, London, 278-300.
5. Bell, K. & Peterson, T. [1991] Nd and Sr isotope systematics of Shombole volcano, East Africa, and the links between nephelinites, phonolites, and carbonatites. *Geology* 19, 582-585.
6. Bell, K., Kjarsgaard, B. A. & Simonetti, A. [1998] Carbonatites – into the twenty-first century. *J. Petrol.* 39, 1839-1845.
7. Borodin, L.S., Gopal, V., Moralev, V.M., & Subramanian, V. [1971] Precambrian carbonatites of Tamil Nadu, South India. *J. Geol. Soc. India* 12, 101-112.
8. Clague, D. A. [1987] Hawaiian alkaline volcanism. In: Fitton, J. G. & Upton, B. G. J. (Eds) *Alkaline Igneous Rocks. Geol. Soc. London, Special Publication* 30, 227-252..
9. Dalton, J. A. & Wood, B. J. [1993] The compositions of primary carbonate melts and their evolution through wallrock reaction in the mantle. *Earth Planet. Sci. Lett.* 119, 511-525.
10. Dautria, J. M., Dupuy, C., Takherist, D. & Dostal, J. [1992] Carbonate metasomatism in the lithospheric mantle: the peridotitic xenoliths from a melilititic district of the Sahara Basin. *Contrib. Mineral. Petrol.* 111, 37-52.
11. Downes, H. [1987] Tertiary and Quaternary volcanism in the Massif Central, France. In: Fitton, J. G. & Upton, B. G. J. (Eds) *Alkaline Igneous Rocks. Geol. Soc. London, Special Publication* 30, 517-530.
12. Ewart, A. [1982] Petrogenesis of the Tertiary anorogenic volcanic series of Southern Queensland, Australia, in the light of trace element geochemistry and O, Sr and Pb isotopes. *J. Petrol.* 23, 344-382.
13. Fitton, J. G. [1987] The Cameroon line, West Africa: a comparison between oceanic and continental alkaline volcanism. In: Fitton, J. G. & Upton, B. G. J. (Eds) *Alkaline Igneous Rocks. Geol. Soc. London, Special Publication* 30, 273-291.
14. Fletcher, C. J. N. & Beddoe-Stephens [1987] The petrology, chemistry and crystallization history of the Velasco alkaline province, eastern Bolivia. In: Fitton, J. G. & Upton, B. G. J. (Eds) *Alkaline Igneous Rocks. Geol. Soc. London, Special Publication* 30, 403-413.
15. Geological Survey of India [1995] Geological and Mineral map of Tamil Nadu and Pondicherry, Scale 1: 500,000. *Geological Survey of India*.
16. Grady, J.C. [1971] Deep main faults in South India. *J. Geol. Soc. India* 12, 56-62.
17. Green, D. H. & Wallace, M. E. [1988] Mantle metasomatism by ephemeral carbonatite melts. *Nature* 336, 459-462.
18. Haggerty, S. E. [1989] Mantle metasomes and the kinship between carbonatites and kimberlites. In: Bell, K. (Ed.) *Carbonatites-Genesis and Evolution*. Unwin Hyman, London, 546-560.
19. Harmer, R. E. [1999] The petrogenetic association of carbonatite and alkaline magmatism: constraints from the Spitskop complex, South Africa. *J. Petrol.* 40, 525-548.
20. Harmer, R. E. & Gittins, J. [1998] The case for primary, mantle-derived carbonatite magma. *J. Petrol.* 39, 1895-1903.
21. Harris, N. B. W., Duyverman, H. J. & Almond, D. C. [1983] The trace element and isotope geochemistry of the Sabaloka Igneous Complex, Sudan. *J. Geol. Soc. London* 140, 245-256.
22. Hauri, E. H., Shimizu, N., Dieu, J. J. & Hart, S. R. [1993] Evidence for hotspot-related carbonatite metasomatism in the oceanic upper mantle. *Nature* 365, 221-227.
23. Ionov, D. A., Dupuy, C., O'Reilly, S. Y., Kopylova, M. G. & Genshaft, Y. S. [1993] Carbonated peridotite xenoliths from Spitsbergen: implications for trace element signature of mantle carbonate metasomatism. *Earth Planet. Sci. Lett.* 119, 283-297.
24. Janardhan, A. S., Newton, R. C. & Hansen, E. C. [1982] The transformation of amphibolite facies gneiss to charnockite in southern Karnataka and northern Tamil Nadu, India. *Contrib.*

Mineral. Petrol. 79, 130-149.

25. Jayananda, M., Martin, H., Peucat, J. -J. & Mahabaleswar, B. [1995] Late Archaean crust-mantle interactions: geochemistry of LREE-enriched mantle derived magmas. Example of the Closepet batholith, southern India. *Contrib. Mineral. Petrol.* 119, 314-329.
26. Keller, J. & Hoefs, J. [1995] Stable isotope characteristics of recent natrocarbonatites from Oldoinyo Lengai. In: Bell, K. & Keller, J. (Eds) *Carbonatite Volcanism: Oldoinyo Lengai and Petrogenesis of Natrocarbonatites*. IAVCEL Proceeding of Volcanology. IAVCEL, 113-123.
27. Kjarsgaard, B. A. & Hamilton, D. L. [1989] The genesis of carbonatites by immiscibility. In: Bell, K. (Ed.) *Carbonatites-Genesis and Evolution*. Unwin Hyman, London, pp. 388-404.
28. Krishnamurthy, P. [1977] On some geochemical aspects of Sevattur carbonatite complex, North Arcot district, Tamil Nadu. *J. Geol. Soc. India* 18, 265-274.
29. Kumar, A. & Gopalan, K. [1991] Precise Rb-Sr age and enriched mantle source of the Sevattur carbonatites, Tamil Nadu, South India. *Curr. Sci.* 60, 653-655.
30. Kumar, A., Charan, S.N., Gopalan, K. & Macdougall, J.D. [1998] A long-lived enriched mantle source for two Proterozoic carbonatite complexes from Tamil Nadu, southern India. *Geochim. Cosmochim. Acta* 62, 515-523.
31. Le Bas, M. J. [1977] *Carbonatite-Nephelinite Volcanism*. London: John Wiley, 347 pp.
32. Le Bas, M. J. [1981] Carbonatite magmas. *Mineral. Mag.* 44, 133-140.
33. Le Bas, M. J. [1987] Nephelinites and carbonatites. In: Fitton, J. G. & Upton, B. G. J. (Eds) *Alkaline Igneous Rocks. Geol. Soc. London, Special Publication* 30, 53-84.
34. Liégeois, J. P. & Black, R. [1987] Alkaline magmatism subsequent to collision in the Pan-African belt of the Adrar des Iforas (Mali). In: Fitton, J. G. & Upton, B. G. J. (Eds) *Alkaline Igneous Rocks. Geol. Soc. London, Special Publication* 30, 381-401.
35. McDonough, W. F., McCulloch, M. T. & Sun, S. -S. [1985] Isotopic and geochemical systematics in Tertiary-Recent basalts from southeastern Australia and implications for the evolution of the sub-continental lithosphere. *Geochim. Cosmochim. Acta* 49, 2051-2067.
36. Meen, J. K. [1987] Mantle metasomatism and carbonatites: an experimental study of a complex relationship. In: Morris, E. M. & Pasteris, J. D. (Eds) *Mantle Metasomatism and Alkaline Magmatism. Geol. Soc. Am. Spec. Paper* 215, 91-100.
37. Meen, J. K., Ayers, J. C. & Fregeau, E. J. [1989] A model of mantle metasomatism by carbonated alkaline melts: trace element and isotopic compositions of mantle source regions of carbonatites and other continental igneous rocks. In: Bell, K. (Ed.) *Carbonatites-Genesis and Evolution*. Unwin Hyman, London, 464-499.
38. Menzies, M. [1987] Alkaline rocks and their inclusions: a window on the Earth's interior. In: Fitton, J. G. & Upton, B. G. J. (Eds) *Alkaline Igneous Rocks. Geol. Soc. London, Special Publication* 30, 15-27.
39. Miyazaki, T. [2000] Isotope geochemical study of the Yelagiri and Sevattur alkaline plutons from Tamil Nadu, South India: their petrogenesis and existence of enriched lithospheric mantle. *Ph.D. Thesis, Niigata Univ.* 202 pp.
40. Miyazaki, T., Rajesh, H. M., Ram Mohan, V., Rajasekaran, K. C., Kalaiselvan, A., Rao, A. T. & Srinivasa Rao, K. [1999] Field study of alkaline plutons in Tamil Nadu and Andhra Pradesh, South India, 1997-1998. *J. Geosci. Osaka City Univ.* 42, 205-214.
41. Miyazaki, T., Kagami, H., Shuto, K., Morikiyo, T., Ram Mohan, V. & Rajasekaran, K. C. [2000] Rb-Sr geochronology, Nd-Sr isotopes and whole rock geochemistry of Yelagiri and Sevattur syenites, Tamil Nadu, South India. *Gondwana Res.* 3, 39-53.
42. Moralev, V.M., Voronovski, S.N. & Borodin, L.S. [1975] New findings about the age of carbonatites and syenites from Southern India. *USSR Acad. Sci.* 222, 46-48.
43. Nelson, D. R. & McCulloch, M. T. [1989] Enriched mantle components and mantle recycling of sediments. In: Ross, J. (Ed) *Kimberlites and Related Rocks, Vol. 1, Their*

- Composition, Occurrence, Origin and Emplacement, Geol. Soc. Aust. Spec. Publ.* 14, 560-570.
44. Nielsen, T. F. D. [1987] Tertiary alkaline magmatism in East Greenland: a review. In: Fitton, J. G. & Upton, B. G. J. (Eds) *Alkaline Igneous Rocks. Geol. Soc. London, Special Publication* 30, 489-515.
 45. Peucat, J.-J., Vidal, P., Bernard-Griffiths, J. & Condie, K.C. [1989] Sr, Nd and Pb isotopic systematics in the Archean low- to high-grade transition zone of southern India: syn-accretion versus post-accretion granulites. *J. Geol.* 97, 537-550.
 46. Peucat, J. -J., Mahabaleswar, B. & Jayananda, M. [1993] Age of younger tonalitic magmatism and granulitic metamorphism in the South Indian transition zone (Krishnagiri area); comparison with older Peninsular gneisses from the Gorur-Hassan area. *J. Metamorphic Geol.* 11, 879-888.
 47. Radhakrishna, T. & Joseph, M. [1998] Geochemistry and petrogenesis of the Proterozoic dykes in Tamil nadu, southern India: another example of the Archean lithospheric mantle source. *Geol. Rundsch.* 87, 268-282.
 48. Radhakrishna, T., Pearson, D. G. & Mathai, J. [1995] Evolution of Archean Southern Indian lithospheric mantle: a geochemical study of Proterozoic Agali-Coimbatore dykes. *Contib. Mineral. Petrol.* 121, 351-363.
 49. Radhakrishna, T., Maluski, H., Mitchell J. G. & Joseph, M. [1999] $^{40}\text{Ar}/^{39}\text{Ar}$ and K/Ar geochronology of the dykes from the south Indian granulite terrain. *Tectonophysics* 304, 109-129.
 50. Raith, M., Raase, P. & Ackermann, D. [1983] Regional geothermobarometry in the granulite facies terrane of south India. *Royal Soc. (Edinburgh) Earth Sci. Trans.* 73, 221-244.
 51. Rajesh, H.M., & Santosh, M. [1996] Alkaline magmatism in Peninsular India. *Gondwana Research Group Mem.* 3, 91-115.
 52. Ratnakar, J., & Leelanandam, C. [1989] Petrology of the alkaline plutons from the eastern and southern Peninsular India. *Mem. Geol. Soc. India* 15, 145-176.
 53. Reddy, B.M., Janardhan, A.S. & Peucat, J.J. [1995] Geochemistry, age and origin of alkaline and ultramafic rocks of Salem, Tamil Nadu, South India. *J. Geol. Soc. India* 45, 251-262.
 54. Rogers, N. W., Hawkesworth, C. J., Parker, R. J. & Marsh, J. S. [1985] The geochemistry of potassic lavas from Vulsini, central Italy and implications for mantle enrichment processes beneath the Roman region. *Contrib. Mineral. Petrol.* 90, 244-257.
 55. Rudnick, R. L., McDonough, W. F. & Chappell, B. W. [1993] Carbonatite metasomatism in the northern Tanzanian mantle – petrographic and geochemical characteristics. *Earth Planet. Sci. Lett.* 114, 463-475.
 56. Schleicher, H., Todt, W., Viladkar, S.G. & Schmidt, F. [1997] Pb/Pb age determinations on Newania and Sevattur carbonatites of India: evidence for multi-stage histories. *Chem. Geol.* 140, 261-273.
 57. Schleicher, H., Kramm, U., Pernicka, E., Schidlowski, M., Schmidt, F., Subramanian, V., Todt, W. & Viladkar, S.G. [1998] Enriched subcontinental upper mantle beneath southern India: evidence from Pb, Nd, Sr and C-O isotopic studies on Tamil Nadu carbonatites. *J. Petrol.* 39, 1765-1785.
 58. Simonetti, A. & Bell, K. [1994] Isotopic and geochemical investigation of the Chilwa island carbonatite complex, Malawi: evidence for a depleted mantle source region, liquid immiscibility, and open-system behavior. *J. Petrol.* 35, 1597-1621.
 59. Smith, I. E. M., White, A. J. R., Chappell, B. W. & Eggleton, R. A. [1988] Fractionation in a zoned monzonite pluton: Mount Dromedary, southeastern Australia. *Geol. Mag.* 125, 273-284.
 60. Subramanian, V., Viladkar, S.G., & Upendran, R. [1978] Carbonatite alkaline complex of

- Samalpatti, Dharampuri district, Tamil Nadu. *J. Geol. Soc. India* 19, 206-216.
61. Sun, S. -S. & McDonough, W. F. [1989] Chemical and isotopic systematics of oceanic basalts: implications for mantle composition and processes. In: Saunders, A. D. & Norry, M. J. (Eds) *Magmatism in the Ocean Basins. Geol. Soc. Spec. Publ.* 42, 313-345.
 62. Sweeney, R. J. [1994] Carbonatite melt compositions in the earth's mantle. *Earth Planet. Sci. Lett.* 128, 259-270.
 63. Thibault, Y., Edgar, A. D. & Lloyd, F. E. [1992] Experimental investigation of melts from a carbonated phlogopite lherzolite: implications for metasomatism in the continental lithosphere. *Amer. Mineral.* 77, 784-794.
 64. Udas, G.R., & Krishnamurthy, P. [1970] Carbonatites of Sevattur and Jogipatti, Madras State, India. *Proc. Indian National Sci. Acad.* 36, 331-343.
 65. Veksler, I. V., Petibon, C., Jenner, G. A., Dorfman, A. M. & Dingwell, D. B. [1998] Trace element partitioning in immiscible silicate-carbonate liquid systems: an initial experimental study using a centrifuge autoclave. *J. Petrol.* 39, 2095-2104.
 66. Viladkar, S.G., & Subramanian, V. [1995] Mineralogy and geochemistry of the carbonatites of the Sevattur and Samalpatti complexes, Tamil Nadu. *J. Geol. Soc. India* 45, 505-517.
 67. Wallace, M. E. & Green, D. H. [1988] An experimental determination of primary carbonatite magma composition. *Nature* 335, 343-346.
 68. Weaver, B. & Tarney, J. [1984] Empirical approach to estimating the composition of the continental crust. *Nature* 310, 557-575.
 69. Wickham, S.M., Janardhan, A.S. & Stern, R.J. [1994] Regional carbonate alteration of the crust by mantle-derived magmatic fluids, Tamil Nadu, South India. *J. Geol.* 102, 379-398.
 70. Woolley, A. R. [1989] The spatial and temporal distribution of carbonatites. In: Bell, K. (Ed.) *Carbonatites-Genesis and Evolution*. Unwin Hyman, London, 15-37.
 71. Wyllie, P. J. & Sekine, T. [1982] The formation of mantle phlogopite in subduction zone hybridization. *Contrib. Mineral. Petrol.* 79, 375-380.
 72. Yaxley, G. M. & Green, D. H. [1996] Experimental reconstruction of sodic dolomite carbonatite melts from metasomatised lithosphere. *Contrib. Mineral. Petrol.* 124, 359-369.
 73. Yaxley, G. M., Crawford, A. J. & Green, D. H. [1991] Evidence for carbonatite metasomatism in spinel peridotite xenoliths from Western Victoria, Australia. *Earth Planet. Sci. Lett.* 107, 305-317.
 74. Zhao, J. -X., Shiraishi, K., Ellis, D. J. & Sheraton, J. W. [1995] Geochemical and isotopic studies of syenites from the Yamato Mountains, East Antarctica: Implications for the origin of syenitic magmas. *Geochim. Cosmochim. Acta* 59, 1363-1382.

Cenozoic flood basalt volcanism, mantle xenoliths and melting regions in the lithospheric mantle of the Baikal rift and other regions of Central Asia.

I.V. Ashchepkov¹, S.V. Travin¹, L. Andre², O.S. Khmelnikova¹

¹ *United Institute of Geology geophysics and Mineralogy, Novosibirsk, Russia*

² *Royal Museum of Central Africa, Tervuren, Belgium*

INTRODUCTION

Cenozoic volcanic fields and plateaus in Eastern Siberia (and Central Asia) form the chains which tracing the permeable zones coinciding with the boundaries of lithospheric plates and microcontinents. Two double chains - island arc and a continental margin conform with the Pacific ocean boundaries and subduction zones, the others refers to Paleozoic and Mesozoic suture zones or have another nature. Cenozoic plateaus are similar to the chain of European "baby" plums strengthened from Azorean islands – to Pannonia [Hofmann, 1997] and located in back side of subduction zone.

Miocene - Pleistocene Cenozoic plateaus of 20-0.5 ma ages are located at a distance of about 500-600 km on the triple junctions of convective cells (Fig.1). Early Cenozoic fields of 40-70 ma ages are more widespread and scattered. They reveal motley melt composition due to the differentiation and the interaction with the lower crust and relics of the postsubduction lithospheric mantle subsided reduced later. The level of their last stop corresponds to spinel facies or to Moho boundary. Late Cenozoic plum basalts form the more compact flood plateaus. They came from garnet facies having the signs of the interactions of deep mater with the pyroxenite- peridotite fertile mantle in the Gar-Sp transition and upper lithospheric mantle. The melts interaction with metasomatized mantle is recorded by the enrichment in HFSE components and more hydrous composition. Hydrous melts usually appear in starting and final stages of plum activity, probably transporing the mater from beneath 400 boundary -wadsleyite layer.

Volcanoes are grouping in the area of basaltic plateau [Rasskazov,1996] forming the similar to the shield volcanoes with the individual chemistry due to the evolution of plume mater level of the magmagenation and preceding mantle history in each block. Hot stream mater is migrating in plateau in circle (like for Vitim) or 8– type (in case of location on the fractures) trajectory Udokan [Rasskazov et al., 1998] [Dobretsov, Kirdyashkin, 1994]. The opening of magma transferring fractures is controlled by dynamic pressure of the hot stream. In geoblocks with the unfractured crust it create the uprisers. Tthere

the lack of heat transferring results in the anomalous heating and high mantle plasticity that allows the a rise up of fast mantle diapirs elevating to $N \times 10$ km in < 10 ma. They contain relics and symplectites after garnet in shallow part of spinel facies.

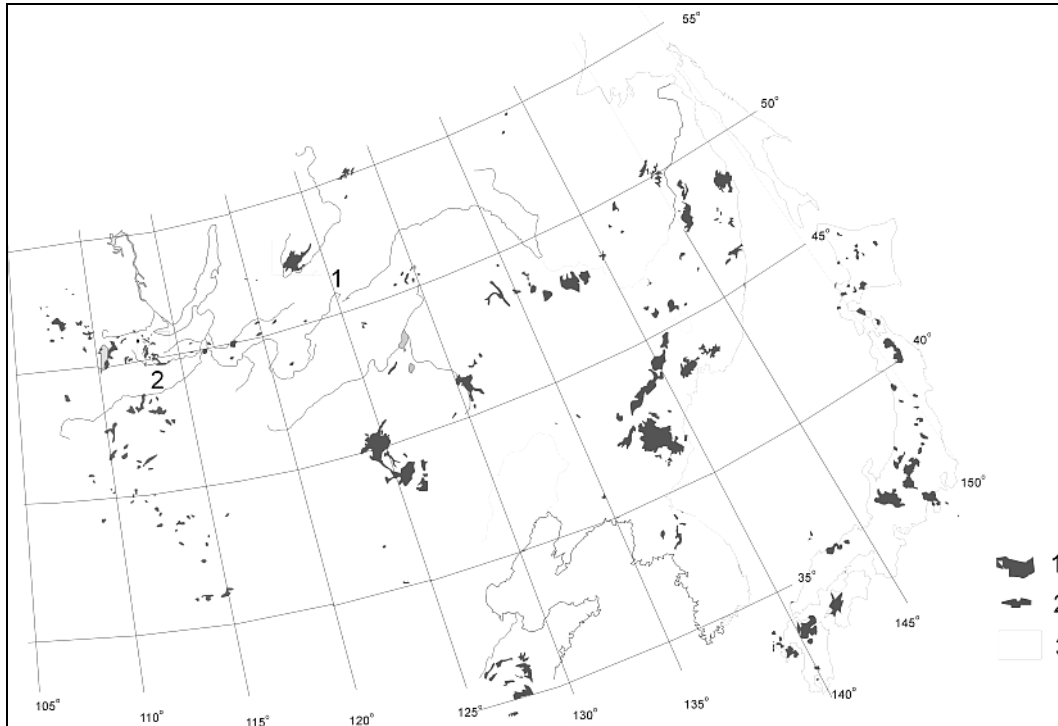


Fig.1. Scheme of the Cenozoic basalt field distribution on the structure of the Central Asia.

Fractured basement of the depression allow to melts easily flow to the surface. There the heating of the mantle may be even lower due to rapid melt escape.

STAGES

The stages, general features of basaltic volcanism and the construction of the mantle columns are similar for the several plateaus. Prerifting stage in Vitim is followed by the formation of metasomatic assemblages and the asthenosheric layer due to volatile inflow from possibly distant magmatic source.

In the 1st stage the melts are characterized by high K/Na ratios like picrite basalts in Vitim melaleutites in Udakan, melahawaiites etc. and were generated at a depth of 35-45kbar (Fig.2.). Intrusion of water-bearing melts and inflow of volatiles in 1st stage in Vitim (18ma) were followed by the appearance of metasomatic layers in the roofs and creation of the anatexic melt system in 20-25 kbar interval. They develops after the melting of earlier metasomatics and create a branched vein system due to the migration of low viscous melts.

In the 2nd stage the appearance of main portion of plume melts (16-12ma) was characterized by the generation of Mg- basanites in 30-20 kbar interval. The next 3-rd stage was characterized by the rising of the melt generation region to the garnet-spinel transition (25-15 kbar) and remelting of the pyroxenite

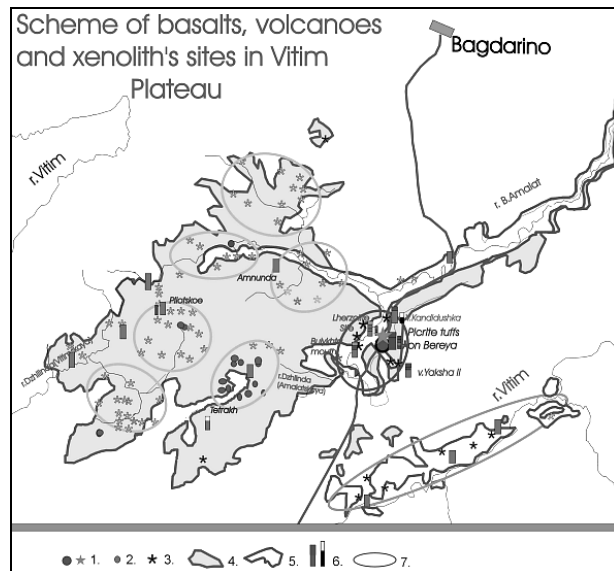


Fig.2. Scheme of Vitim basalt plateau.

1. Picrite basalts tuff.
2. Barried volcanoes.,
3. Cinder cone volcanoes,
4. Miocen basalts.,
5. Pleistocene Quaternary basalts.
6. Xenoliths garnet and spinel and cumulates (white).
7. Groups the similar volcanoes.

layers and upper vein system, fracturing, flowing up the m elts and fast creation of the lava plateau (9-6ma). After the escape of the main melt portion from the magmatic system splits into several layers. In this stage the series of cinder cone volcanoes appeared in NW part of the plateau. Post erosion valley basalts (2-1.5 ma) produced at the depth 20-25 kbar seems to be record the episode of tectonic-induced plume activation. The latest hydrous melts appeared in the tale of the Vitim ‘baby’ plume were followed by the creation of modern cinder cones (1.-0.5 ma) and melting at a 20-27 kbar interval.

THERMOBAROMETRY

TP trajectories for the basalts [calculated after Albarede et al., 1992] display two branches for water – bearing and dry melts. The first one corresponds to TP gradients of the hot areas in the tomographic models beneath the lava plateaus [Sobolev et al., 1997] while lherzolitic SEA type geotherms are characteristic for the cold areas (Fig.2). Melt generation areas fluctuate according to the ages being lower in the initial and last stage.

The heating conditions in the mantle recorded by mantle xenoliths are essentially different for each individual stages.

Relatively gentle 1-st stage Miocene geotherm received by a common thermobarometry (T^02P_x -PGaOpx) for Vitim plateau changes to more hot in the

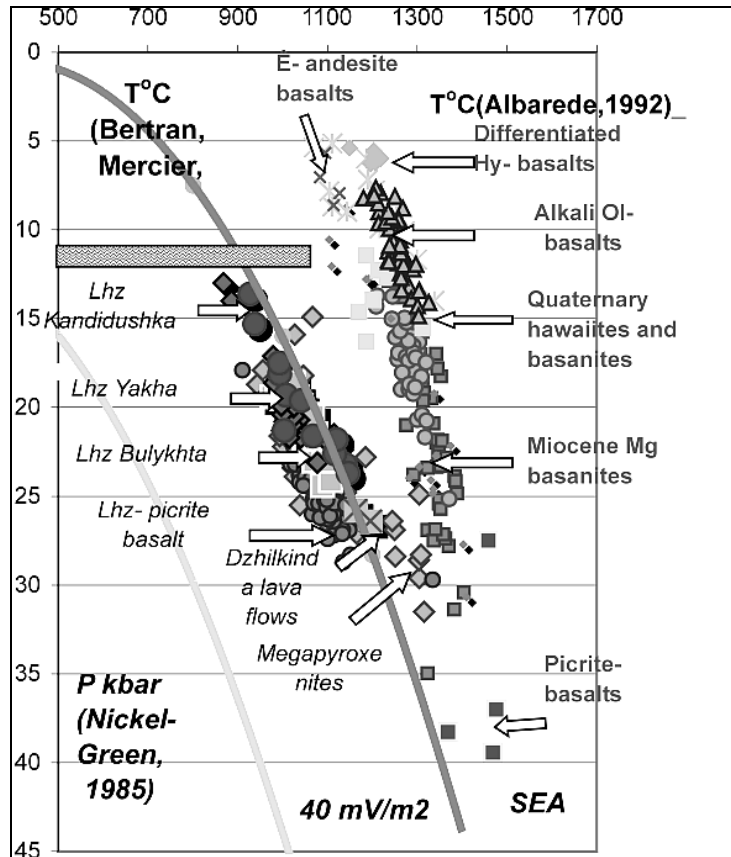


Fig 3. TP estimates for basalts and xenoliths from Vitim, Khamar- Daban and Dzhdida.

Pleistocene. Each volcano of that stage carries xenoliths reveal slightly different thermal gradients and TP intervals.

Black giant grained pyroxenites create the hot branch intermediate between basaltic and lherzolitic one and a few deformed lherzolites are close to them in PT conditions (Fig.3).

Black hybrid more fine-grained pyroxenites from the smaller veins corresponds to more low temperature conditions. Fe- Cr websterites and wehrlites are slightly hotter than common anatectic websterites that are close in TP conditions to lherzolites. Shallow cumulates reveal the colder conditions due to the exchange with the crust and the less heated spinel facie lherzolites.

Orthopyroxene thermobarometry (T^0 Brey-Kohler90-P Perkins-Newton) suggests a complex construction of mantle columns. The obtained TP trajectories are due to the mantle upwelling and melt intrusion and percolation at the different levels. The upper part starts from 14 kbar and remains relatively stable reflecting lower T lithospheric conditions. In the lower part of mantle section the geotherms continuously rise from stage to stage reflecting a diapiric rise of primitive lherzolite mater from the garnet facie level and melt percolation (Fig.4).

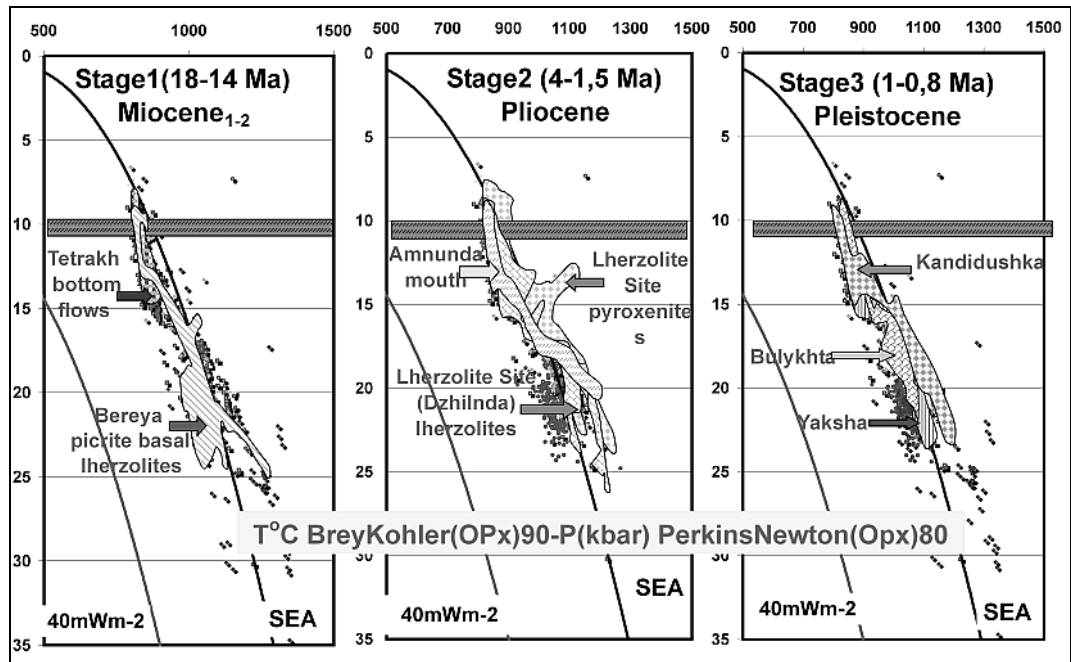


Fig 4. OPX Thermobarometry for 3 stage of mantle evolution beneath Vitim plateau.

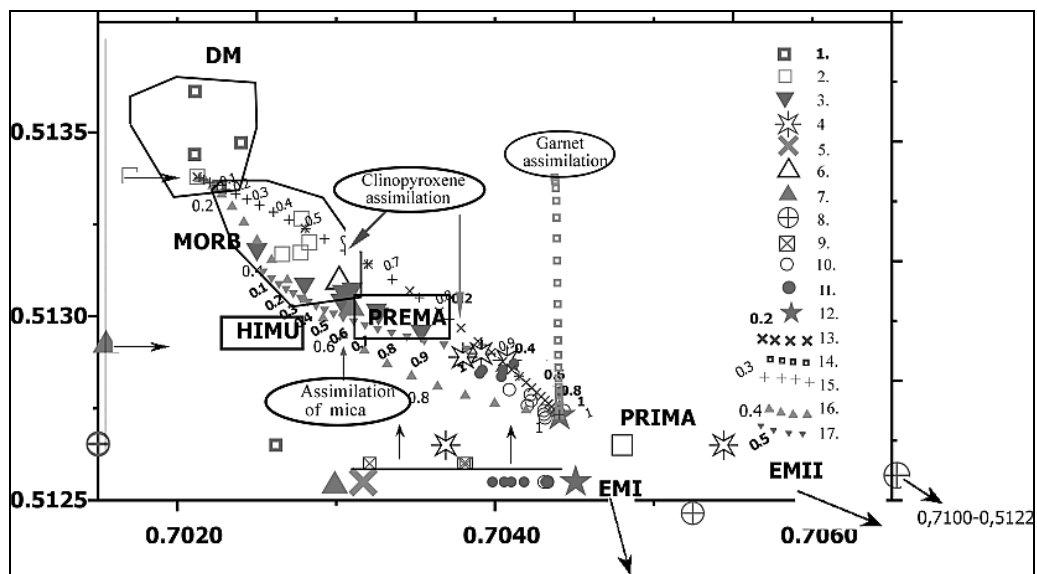


Fig 5. Sr-Nd isotopic diagram for mantle peridotites and basalts from Vitim Sr-Nd isotopic features of Vitim pyroxenites compared with the composition of lherzolitic [Ionov, Jagoutz, 1988] and basaltic [Litasov et al, 2000] ones.

Minerals from: 1. Garnet lherzolites; 2. Spinel lherzolites 3. Amph- Phl bearing veins and pyroxenites in lherzolites; 4. Black megapyroxenites; 5. High temperature green pyroxenite; 6. Gray transitional websterite; 7. Cr-diopside websterite; 8. Low pressure cumulates; 9. Spinel lherzolites from the Pleistocene Kandidushka volcano. 10. Post erosion Plio-Pleistocene lavas from valley flows and scoria cones; 11. Miocene lava plateau flow; 12 Picrite basalts. Mixing lines: 13.- Binary mixing between picrite basalts and Cpx from garnet lherzolite 14. – AFC of picrite basalts with lherzolite garnet; 15 AFC of picrite basalts with the pyroxene; 16. AFC of picrite basalts with mica; 17 AFC of melt parental for megapyroxenites and Cpx from garnet lherzolite.

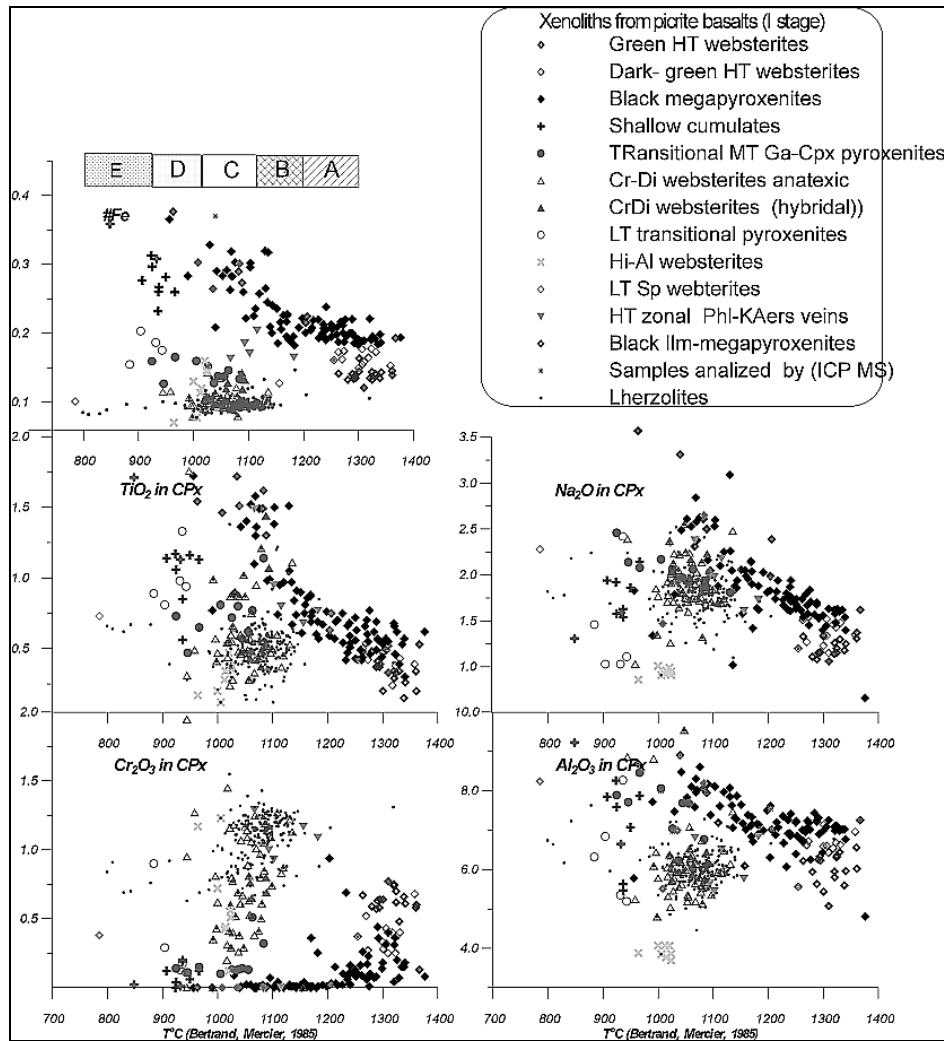


Fig. 6. Diagram T-CPx variations for the picrite-basalt stage (1) in Vitim.

ISOTOPIC FEATURES

Mantle column under the Vitim plateau is isotopically stratified. The lower part of Gar-facie corresponds to deep common convective DMM reservoir while the Sp-facie peridotites have typical MORB features (Fig.5). Basalts from the plum head and tail are close to Bulk Earth while Miocene basalts have upto 90% admixture of the Iherzolite material. Megapyroxenites are more contaminated. Anatexic websterites have the features showing the melting of Phl bearing websterite or fluid admixture. The Iherzolites from Quaternary basalts are much more enriched (radiogenic in Sr) suggesting the reaction with basaltic melts.

CONSTRUCTION OF MANTLE COLUMNS

In every stage construction of mantle column is changing. In Vitim plateau (5) and Hamar Daban (4) several different stages were recognized.

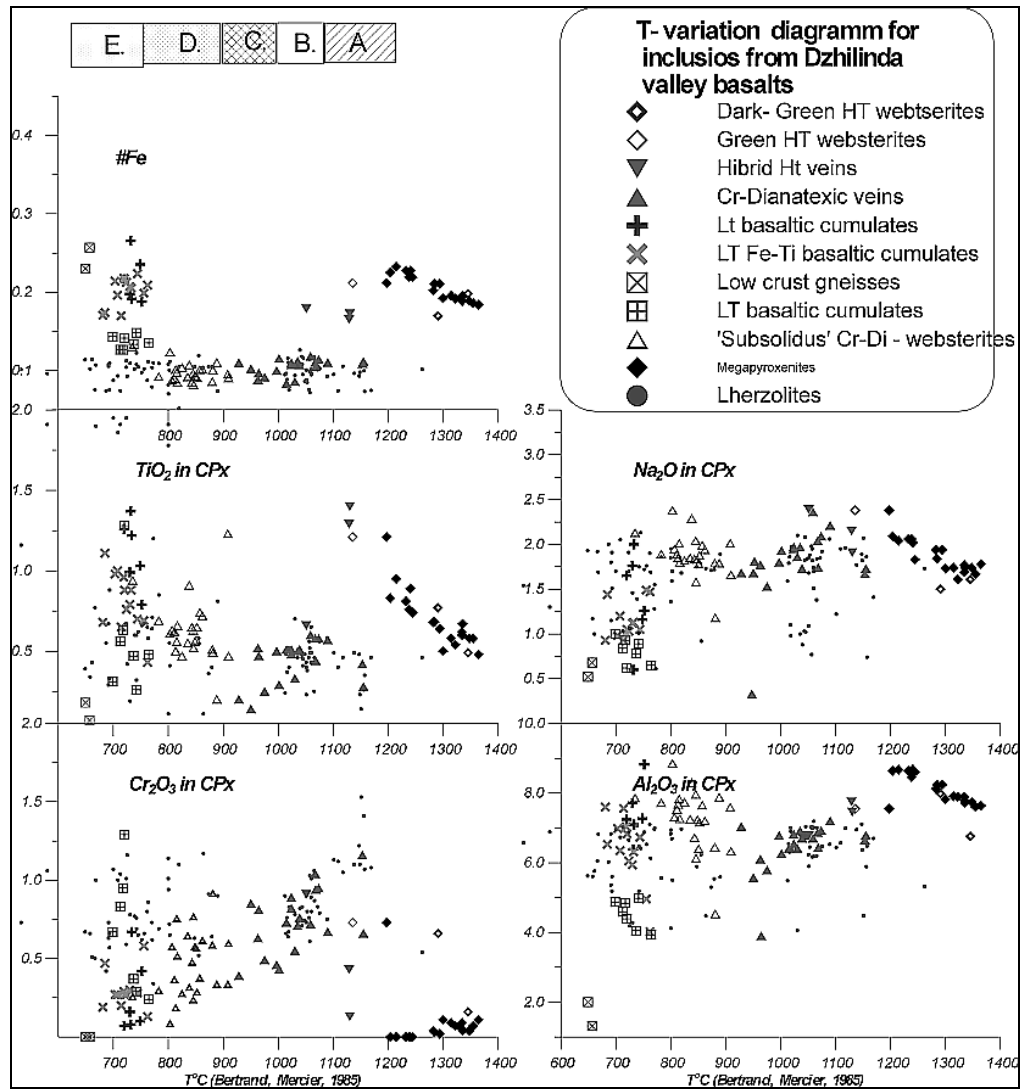


Fig. 7. Diagram T- CPx variations for stage (4) of valley basalts in Vitim.

In the pre-rifting stage beneath in Bereya block in Vitim three TP interval of metasomatic associations corresponds to the temperature peaks of megacrystalline pyroxenites that probably represents the intermediate magmatic chambers of basaltic melts. A) 1050-1150°C and 26-22 kbars with the relatively hot zonal Phl-Kaers veins at the basement of the sampled mantle column; B) 1000-950 a scattered essentially phlogopitic pockets and veinlets in the top of garnet facie at 20-17kbar ;C) in spinel facie at 15-12 kbar, 800-900°C it is represented by pargasitic intergranular veinlets. Cr-diopside websterites are distributed in whole sampled interval being more abundant near the Gar-Sp transition. Fe-Cr diopside veins are more characteristics for the bottom but also are present in the top also is present at the top where Fe- content in the lherzolites gradually rises. The structure of the lherzolites in mantle section regularly changes from highly – and through the moderately deformed, to equal grained with the signs of percolation and then to coarse grained mosaic (Fig.6).

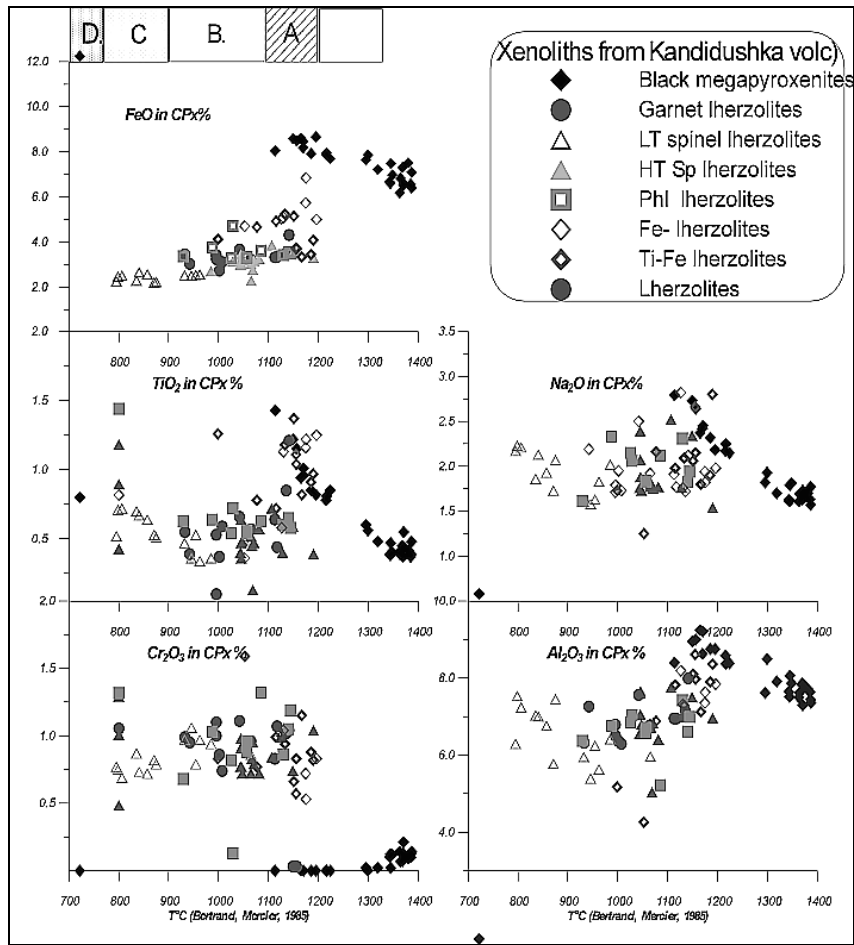


Fig.8. Diagram T- CPx variations for stage (5) of Pleistocene cinder cones Vitim.

At the bottom of the lava plateau the 2nd stage shallow mantle Sp-lherzolite xenoliths of Al- type and hybrid HT pyroxenites corresponds to 12-15 kbar interval. The 3rd stage xenoliths found in the top of the flood basalt lava plateau are Al- lherzolites and websterites with similar mineralogy and more rare deep xenoliths with asthenospheric signatures.

4- th stage of post-erosion valley flow basalts carry the xenoliths that reveal a sharp layering (Fig.7) in mantle column. Two lenses of pseudogarnet lherzolites at the bottom are separated from typical spinel lherzolites by the horizon of Cr-websterites. Spinel lherzolites form the central part are characterized by low oxidation state and include pyroxenite lenses with the signs of interaction with melts came from garnet facie. The lherzolites at the upper horizon are splitting into three branches and at least three types of pyroxenites with varying chemistry are found here, the most differentiated varieties are located beneath the basement of the crust.

In 5stage in Pleistocene time mantle column also had three major units but with more gentle transition. The lower part is represented HT Fe- lherzolites and harzburgites, more shallow part is composed from fertile Sp and Gar lherzolites with partly decomposed garnet and phlogopite veinlets. Rare groups of Fe -

lherzolites appear also in two upper units. Second unit is characterized by the spinel lherzolites of primitive type with the kink bands and equilibrated structures. Garnet lherzolites with the relics of garnets and or garnet bearing- veinlets are characteristic for this unit. Al- type fine- grained and moderately depleted coarse-grained lherzolites are located in the third upper unit (Fig.8).

In Khamar Daban the prerifting stage xenoliths – bearing basalts have not been found but the other stages are similar. Primitive and moderately depleted lherzolites (Hubutui flow- 18ma; basement beneath the Tumu-sun volcano (20ma). HT Fe-lherzolites from Slyudyanka (16 ma) corresponds to the first stage in the basement of lava plateau. Abundant cumulates and Al- type lherzolites were found in the flows near the top of lava plateau. Volcanoes on the top of basaltic lava plateau carry mainly Al type xenoliths (7-9 ma). Posterosion lava flow of Margasan river valley (8 –2 ma) carry the samples characterizing a layered mantle section. The Bartoy volcanoes (15-0.5ma) in southern slope of Khamar Daban carry the xenoliths typical of highly metasomatized and stratified mantle.

Structurally the mantle section is uniform in the large areas not less than 50 km in diameter in the stage of lava plateau creation at the NW part of Vitim plateau. The area of the basaltic volcanism with same mantle structure is shortening in Pliocene time to 35-40 km migrating to the SE. Pleistocene volcanism is restricted by 20 km “garnet” ring locating at the same area where the volcanism started.

THE WAY OF MELT MOVEMENT

Relative rarity of the hot Fe- peridotites with $T > 1200^{\circ}$ evidences that basaltic melts could have pass through the separated system of channels. Only in the early stages of the generation of a basaltic plateau several hybrid HT pyroxenites may pretend on media of the magma conducting and accumulating and HT Fe lherzolites may represent contact zones of such a systems. A relative abundance of veined and metasomatic rocks is high in initial and finishing stage because low viscous hydrous melts pass directly through the mantle column. The melt migration in is followed and results in the penetration of tremendous amount of volatiles in the interval 17-27 kbar. There the migration of the intergranular melts may be nearly continuous during the stage of cration of the lava plateau and brings to the homogenization of the region of percolation and enrichment of upper parts of the mantle diapirs in the pyroxenites material. At the starting and in the post-erosion mantle stage the fields of magma generation was more restricted locating near the intermediate magmatic chambers.

Judging on the extra high temperatures of the basaltic melts pass in pulsing regime step by step intruding the upper levels. In each stage the new melt portions appeared from beneath. They come in to the equilibrium with the surrounding mantle remelting pyroxenites and metasomatics. The amount of the

melts was much more in the more permeable areas such as Vereya block in Vitim.

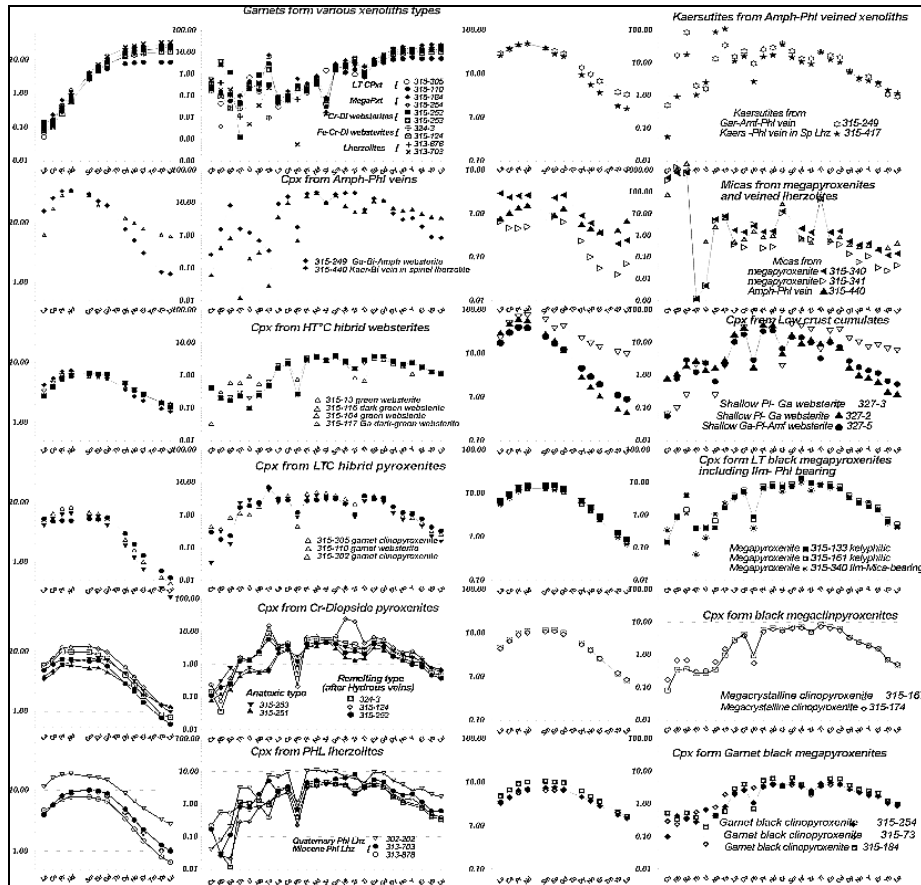


Fig.9. TRE multicomponent diagrams and REE patterns for the minerals from xenoliths from Picrite-basalts.

GEOCHEMISTRY OF MANTLE ROCKS AND THEIR PARENTAL MELTS

Geochemical characteristics of the black pyroxenite group are very close to the erupted basalts but are characterized by more fractionated spectrums of the TRE elements. Calculations shows that starting from the most primitive garnet megapyroxenites the degree of fractionation is about 45%. Hybrid HT pyroxenites have flattened patterns due to the contamination in wall rock peridotites. Transitional MT pyroxenites have a very high inclination of the HREE and sometimes mirror like- TRE patterns due to the dissolution of the walls of the channels of percolation. Fe Cr –diopside veins with the HFSE maximums were formed due to the melting of the metasomatics, their variable slopes of the TRE patterns can be explained by varying compositions of the melting assemblages (Fig.9).

Lherzolite TRE patterns for the first pre-rifting stage reveal spectrums typical for garnet or spinel facies with the common modal abundances and rare chromatographic effects [Ashchepkov, Salters, 1998] of melt percolation.

In post-erosion valley basalts TRE patterns of the lherzolites in the top of mantle column are typical for spinel lherzolites but suggest different degree of depletion and practical lack of percolating chromatographic effects also. Rare samples in the central part of the section display the mixed trace element signatures of basaltic melt and lherzolic material. They are close to the patterns characteristics of the garnet decomposition with slightly humpered trace element diagrams.

RESULTS OF THE MELT PERCOLATION AND ERUPTION ON THE BASALTS

Intensive uplift of lava plateaus to 1 km or more due to the dynamic support of the plum is followed by the cutting of the relief. At the post erosion stage the escape of the magmatic reservoir results to the crushing of the arch system and valley basalt creation filling the canyons. The last stage of the lava plateau developing was characterized by the formation of cinder volcanic apparatus and relatively small tongues of basaltic flows.

This model of the developing of mantle and basalt plateaus differ from the typical models of the decompression melting. Melts rise from the interior as a great drops coming periodically [Humphreys et al., 2000]. They stop and concentrate near the dense boundaries and phase transitions in the deep and shallow mantle at 660, 400, 250, 100, 60 km. The interaction with the solid peridotite mater take place in each level due to heating, submelting and remelting of wall rocks and the products of their own passage.

Stream of the fluid flow which comes before the main portion of basaltic magma is responsible for the melting and scattered metasomatism. Not long before the coming of the hydrous melts in the initial and last stage the intergranular melt pockets appear in the upper asthenospheric level. Plum heard hydrous melts assimilate the melt pockets and preceding metasomatics. At the main stage of basaltic plateau the prevailing mechanism is reactional interaction with the peridotite mantle column and the assimilation of different pyroxenites and possibly the intergranular melts. At the finishing stage the intrusion of tail of plume melts produce polybaric magmatic chambers and melt passage the intergranular space in their roofs according to the AFC process.

REFERENCES

1. Albarede F. 1992. How deep do common basaltic magmas form and differentiate. *Journal of Geophysic Research* v.97, pp. 10997-11009.
2. Ashchepkov I.V. ,Andre L.,Malkovets V.G.,Litasov Yu.D.,Travin A.V. The Stages of the Melt Percolation in the Mantle Beneath Vitim (TransBaikal). *Journal of Conference Abstract* V4, N1, P. 362
3. Ashchepkov I.V. Andre L. Cr-Diopside Veins in Vitim Mantle. Origin and evolution.

- Journal of Conference Abstract V4, N1, Pp.358-359
4. Ashchepkov I.V.1991. Deep seated xenoliths of Baikal rift zone. Novosibirsk. 1991, 160 p (in Russian).
 5. DePaolo D. 1981. Trace elements and isotopic effects of combined wallrock assimilation and fractional crystallization. //Earth. Plan. Sci. Lett. v.53, pp.198-202.
 6. Dobretsov N.L, Kirdyashkin A.G. 1994. Deep seated geodynamics. Novosibirsk – 299p. (in Russian).
 7. Hofmann A.W., Mantle geochemistry: the message from oceanic volcanism. 1997. Nature v.385, pp. 219-229.
 8. Humphreys E. D., Dueker K.G, Schutt D.L., Smith R.B.2000. Beneath Yellowstone: Evaluating Plume and Nonplume Models Using Teleseismic Images of the Upper Mantle. GSA Today. v.10:123 pp.1-7.
 9. Ionov D. A., Jagoutz E., 1989. Sr and Nd isotopic composition in minerals of garnet and spinel peridotite xenoliths from the Vitim Highland: first data for mantle inclusions in the USSR. Trans. (Dokl.) USSR Acad. Sci., Earth Sci. Sect. v. 301, p 232-236.
 10. Ionov, D.A., Hofmann, A.W., 1995. Nb– Ta-rich mantle amphiboles and micas: implications for subduction-related metasomatic trace element fractionations. Earth and Planetary Science Letters 131, 341– 356.
 11. Litasov, Yu.D. 1997. Petrology of mantle xenolith and basalts from Baikal rift//PHD thesis. Hokkaido University. Japan.
 12. O'Reilly S.Y., Griffin W.L. 1985 A xenolith derived geotherm for southeastern Australia and its geological implications. Tectonophysics. 111, 41-63.
 13. Rasskazov S.V., Ivanov A .V., Brandt I.S., Brandt S.B..Migration of the Late Cenozoic volcanism of the Udokan field within the structure of Baikalian and Baikal- Olekma-Stanovaya system. Trans.E.Sc. RASc. 1998, v.360, n3 pp.378-382? in Russian.
 14. Rasskazov, S.V., Ivanov, A.V., Brandt, S.B., 1996. Development of volcanism with rifting relaxation, detail study of Late Cenozoic Bereya area, Vitim volcanic field. Proc. Geol. Symp. IEC SB RAS, Irkutsk, Russia, pp. 56–58, in Russian .
 15. Sobolev S.V., Zeyen H., Stoll G., Werling F., Alherr R., Fuchs K. 1996. Upper mantle temperatures from teleseismic tomography of French Massif Central including effects of composition, mineral reactions, anharmonicity, anelasticity and partial melt Earth. Plan. Sci. Lett. v.139, pp.147-163.

Geochemistry of the rare lithophile elements, Zr, Hf, Nb, Ta, Th, U, and variations in their ratios during fractionation of alkali-basalt series in oceanic islands

A. M. Asavin

*Vernadskiy Institute of Geochemistry and Analytical Chemistry,
Russian Academy of Sciences, Moscow*

INTRODUCTION

The very low distribution coefficients in equilibrium of mineral-melt type for many lithophile elements allow us to take their values as close to zero, which simplifies describing fractionation; during magmatic differentiation, partial melting of mantle substrate, and other geochemical processes. It is also now assumed that Zr/Hf, Zr, Nb, Th/U, and Ta/Th remain virtually constant during the formation of magmatic series and correspond to the primary values in the magmatic sources. Most researchers use both of these assumptions as bases for subsequent geochemical constructions. Here we attempt to discuss the reality of those assumptions from new data on distribution of lithophile elements in minerals and rocks from the volcanic series oceanic islands as in our investigation and in literature sources. Also we construct models the behaviour of this group of elements during crystallisation differentiation in alkali-basalt magma

PATTERNS IN RARE-ELEMENT DISTRIBUTION IN MINERAL-MELT EQUILIBRIA

The compositions of the volcanites (ankaramites, alkali basalts, trachytes, and so on) reflect the stages of evolution in the primary magma (initial, middle, and final), and we were able to trace the variations in the distribution coefficients of the rare elements during in-situ differentiation. The degree of differentiation was determined from the magnesium index $Mg/(Mg + Fe)$. The least differentiated magmas in the alkali-basalt series in these islands correspond in composition to ankaramites, ankaramite-basalts, and alkali olivine basalts. In the final stages of differentiation, nepheline-feldspar eutectic melts of phonolite and trachyte compositions arise, while trachybasalts and trachyandesites are formed in the middle stages [Barsukov et al., 1981]. These are virtually unaltered volcanics containing large numbers of phenocrysts and having a fine-grained groundmass.

These volcanic series were produced by extensive fractional crystallization in the magma reservoirs. To characterize the evolution of an alkali magma in a magma chamber, we early constructed a quantitative model for the fractionation [Barsukov et al., 1981] and determined the ratios between the settling crystalline phases and the residual liquids. The model was tested by using the distributions for the rare-earth elements [Kogarko et al.,

1984] and the iron group elements [Kogarko et al., 1985], and the same research was continued via the geochemistry of Zr, Hf, Nb, Ta, Th, and U [Kogarko et al., 1995]. Rare-element distribution coefficients in mineral-melt equilibrium are mainly responsible parameter of these models. As we show in review of coefficient distribution for lithophile group elements [Asavin, 1995] olivine, plagioclase, feldspar are of low value of coefficients, and K decreases to 0.01. In the other hand the highest concentrations of Zr, Hf, Th, and U occur in the pyroxenes and kaersutites, whereas Nb and Ta concentrate appreciably in the magnetites. The are mean value of the coefficients distribution mineral-liquid for severals stages of evolution alkaline magma show in table 1.

These observations agree with published data [Asavin, 1995; Dostal et al., 1983], but our studies reveal new patterns for the clinopyroxenes. In all the specimens, K_{Zr} for augite is less than that for Hf on average by a factor of two. K_{Zr} in the pyroxenes is about twice that for niobium. The differences between K_{Hf} and K_{Ta} are even larger. This means that there may be major changes in Zr/Hf, Zr/Nb, and Hf/Ta during alkali magma evolution (rise in Zr/Hf and fall in Zr/Nb during fractionation), which is linked to removal of pyroxene.

The low values of the combined distribution coefficients for these elements govern their accumulation during evolution of the alkali magmas in these ocean islands. This is evident from the concentrations of the rare elements in the groundmass and in the rocks. The contents of all these elements in the groundmass clearly increase [Asavin, 1995].

PATTERNS IN RARE-ELEMENT DISTRIBUTION IN VOLCANIC SERIES FROM OCEAN ISLANDS

Let us now consider the, Zr/Hf, Nb/Ta, and Th/U concentration ratios. These ratios are taken as constant in the literature and are used as geochemical indicators [Garg, 1981; Pearce, Norry, 1979; Ryerson, Watson, 1987]. Our above data on the distribution coefficients show that there are possible variations in these ratios. Figure 1-2 shows histograms for Zr/Nb Zr/Hf, Nb/Ta, and Th/U in the Gran Canaria, St. Helena, Tristan da Cunha, and other island series, and also published evidence for other regions where alkali volcanism occurs.

Zr/Nb

Histograms of Zr/Nb ratio exposed on fig 1. There are histograms from different islands have closely forms. They are asymmetric, with maximum on lower value (between 3-6) and wide slope of curve with high value (10-12). It is interesting, that the southern series has maximum on histograms less than in northern parts of Atlantic. Correlation between geographical locality and Zr/Nb ratio we could not explain on this investigation. Other phenomenon is rise value of Zr/Nb ratio in most volcanic series. As show data of pyroxene and magnetite coefficients distribution, fractionation must decrees one.

Table 1.

Mean value for Rare-Element distribution coefficients mineral-liquid
[Asavin et al., 1995; Asavin, 1995].

Mineral	Type of melts	Zr	Hf	Nb	Ta	Th	U
Magnetite	Ankaramite	0.47	0.53	0.41	0.14	0.036	0.016
	Alkaline basalt	0.185	0.263	0.48	0.27	0.216	0.168
	Trachibasalt	1.02	0.464	0.264		0.234	0.315
	Trachianandesite	0.184	0.241	0.179		0.242	0.143
	Phonolite	0.63	0.43		0.79	0.44	0.75
Olivine	Ankaramite	0.013	0.052	0.0064		0.021	0.034
	Alkaline basalt	0.016	0.014	0.0086	0.031	0.016	0.017
Chromediopside	Ankaramite		0.23		0.074		
Augite	Ankaramite	0.453	0.827	0.165	0.12	0.064	0.034
	Alkaline basalt	0.364	0.76	0.026		0.026	0.008
	Trachite	0.261	0.946	0.055		0.075	0.062
	Trachianandesite	0.38	0.746	0.117	0.017	0.187	0.048
	Ordanshit	0.95	0.57	0.58		0.41	0.29
Amphibole	12879		0.84		0.05		
Plagioclase	Ankaramite basalt		<0.07		<0.05		
	Alkaline basalt	0.023	0.089	0.008		0.084	0.043
	Ordanshit	0.019	0.114	0.033		0.044	0.018
Hauine	Phonolite	0.012	0.019	0.0158		0.07	0.061

Nb/Ta

The peak in the histogram for our series is close to 15 (Fig. 2). Estimates by others [Jochum et al., 1989; Claque, Frey, 1980] give a similar figure. Some phonolites and trachytes give values that differ appreciably: 9 and 20. Variations from 10 to 32 have been found also in alkali volcanites on Tenerife and in the Kenya rift [Wolff, 1987; Baker et al., 1977]. A likely factor governing changes in this ratio in the trachytes and phonolites is the crystallisation of sphene, which segregates in the final stages and according to Green's experimental data is due to K_{Ta} being higher than K_{Nb} [Green, Pearson, 1987]. Sphene crystallisation should cause Nb/Ta to rise appreciably. Figure 3

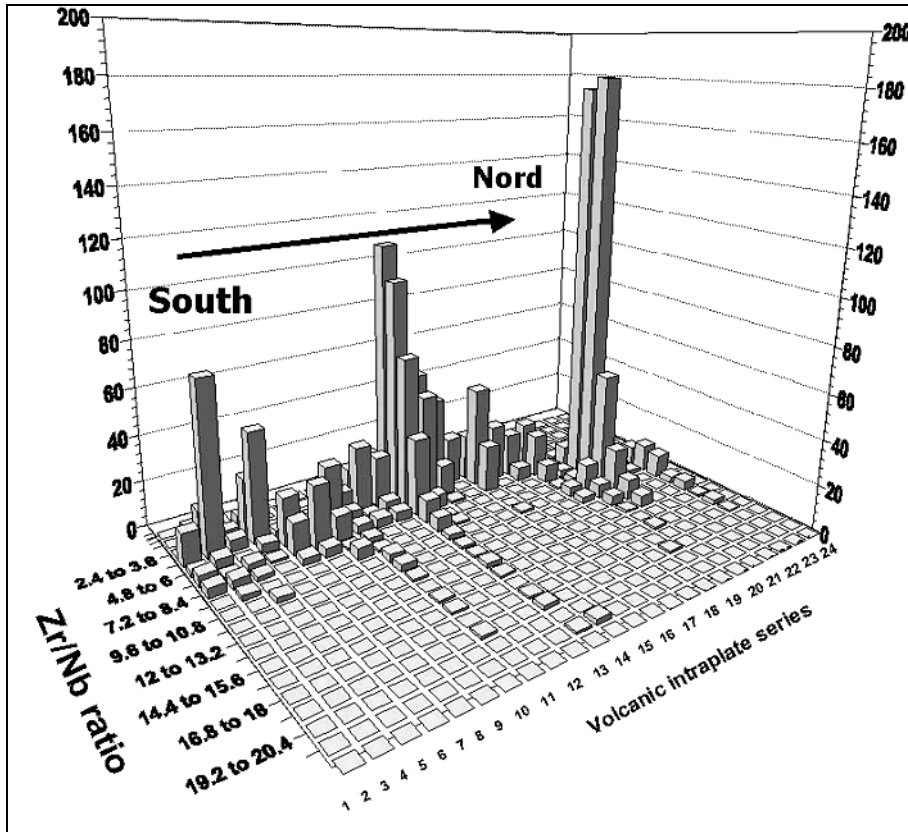


Fig. 1. Zr/Nb histograms for ocean island volcanites Atlantic ocean.
Legend for volcanic series see in Table2.

Table 2. Legend for fig. 1 Volcanic series of the Atlantic islands

N series on fig.1	Latitude	Longitude	Name of locality
1	-1.26	5.37	Pagu Isl.
2	-15.95	-5.70	San Helena Isl.
3	-3.85	-32.42	Fernando de Noronha Isl.
4	-37.32	-12.73	Tristan da Cunha Isl.
5	-40.32	-9.92	Goph Isl.
6	-54.43	3.42	Bove Isl.
7	-7.93	-14.37	Ascension Isl.
8	1.62	7.45	Principe Isl.
9	15.25	-23.17	Cape Verde arch.
10	16.50	-24.30	
11	28.75	-19.00	Canary arch.
12	29.22	-13.46	
13	33.07	-16.33	Madeira isl.
14	36.97	-25.12	Azores arch.
15	38.00	-25.00	
16	38.67	-28.05	
17	39.00	-27.00	

End of Table 2.

N series on fig.1	Latitude	Longitude	Name of locality
18	64.02	-19.65	Iceland isl.
19	64.42	-14.53	
20	65.02	-14.30	
21	65.07	-16.83	
22	65.26	-14.27	
23	65.88	-16.84	
24	71.00	-8.50	Jan Main isl.

also shows that Nb/Ta has a wider range in some island series. For example, our data from the 17th voyage of the R/V *Academician Boris Petrov* show that about half of the specimens had Nb/Ta > 15 for series from Brazilian islands (Fernando da Noronha and Trindade).

Th/U

The mean value for these series is 4.2. Substantial deviations from it occur only in some phonolites and trachytes, which give 10-13, while there is a slight rise (up to 5 or more) in it during fractionation. Th/U in the groundmass is usually higher than that in the whole rock, possibly because of the mobility of uranium during water-rock interaction in the late stages of mineral formation. Figure 2 shows that a similar pattern occurs in volcanites from other ocean islands. There are always specimens with elevated values of this ratio. Interest attaches to our preliminary data on Th/U in the Galapagos Island basalts (data from the 9th voyage of the R/V *Academician Boris Petrov*), for which we find very low values.

Zr/Hf

There are considerable fluctuations in this. Two peaks occur in Fig. 2. The first (Zr/Hf = 35-40) is close to the values characterising most volcanic series [Garg, 1981, Jochum et al., 1989]. This peak is clearly exposed on series Kergelen and Azores group. The second peak is 60-70 Zr/Hf ratio. There is rare situation on the volcanic series. There is value 35 for tholeiitic series sea mounts for example [Claque, Frey, 1980] There are the same high value Zr/Hf observed from series Fernando de Noronha and Trindade islands. As whole there are wide variation observed as rule in high alkaline series. As we show the correlation between Zr/Hf ratio and the type of the rock is about null. There are alkaline basalts, ankaramites (isl. Gran Canaria, Tristan da Cunha), most part of ankaramites of Gran Canaria, trachyte and phonolites has high Zr/Hf ratio. We don't know what the type of process define variable of this ratio, but it is not the crystallisation differentiation of alkaline magma. According to the model, Zr/Hf should increase in the St Helena series from 44 in the alkali basalts to 53 in the phonolites, while in the Tristan da Cunha series, it should increase from 55 in the alkali olivine basalts to 64 in the trachyte. These models do not explain the existence

of similar rare-element contents in certain primitive magmas and their derivatives, since with low K_{comb} differentiation must necessarily produce appreciable increases in the rare-element contents in the residual melts. There is thus a conflict: on the one hand, the model gives a good description of the evolution of the petrogenetic elements in ocean-island alkali magmas

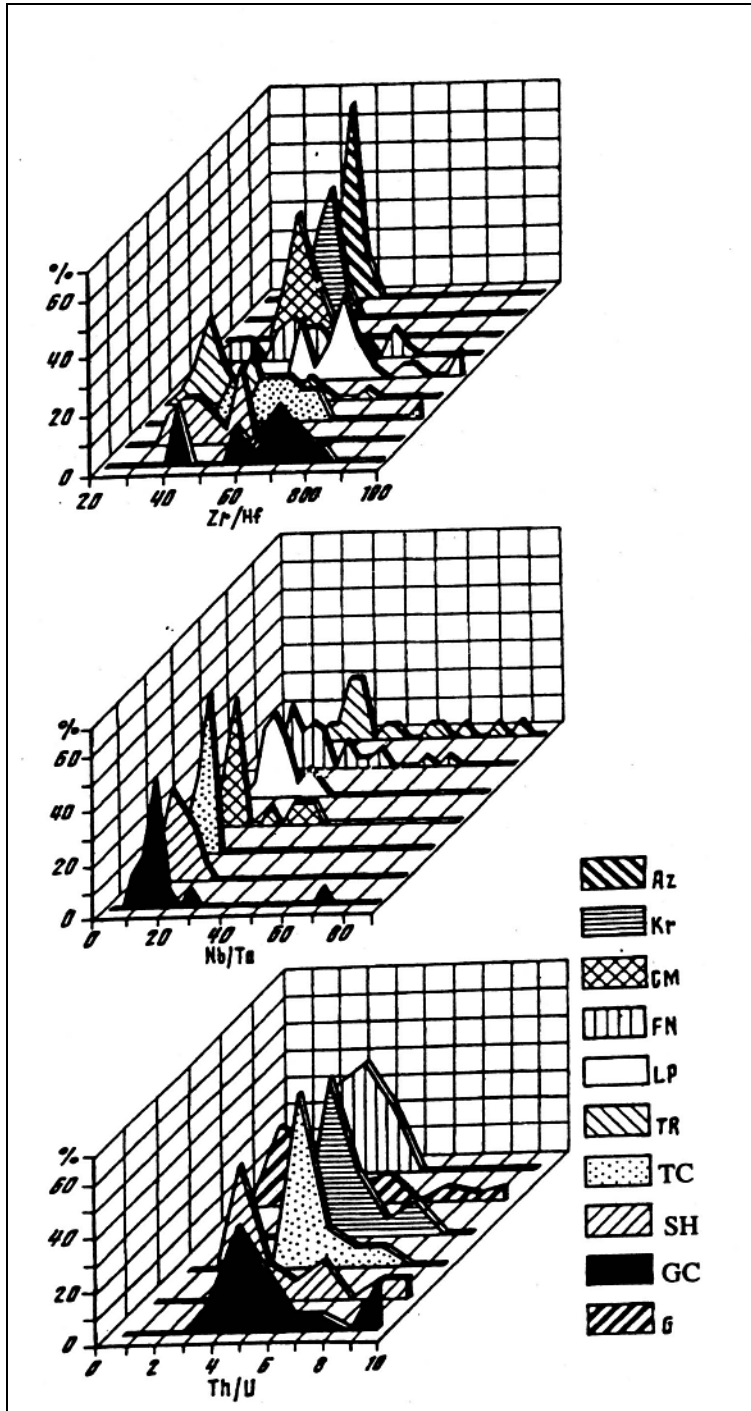


Fig. 2. Zr/Hf, Nb/Ta, and Th/U histograms for volcanites in series: GC Gran Canaria, SH St Helena, TC Tristan da Cunha, TR Trindade, LP La Palma, FN Fernando da Noronha, M Mao (Cape Verde archipelago) [Fumes, Stillman, 1987], Kr Kerguelen [Giret, 1983], Az Azores archipelago [White et al., 1979], G Galapagos archipelago.

and the distributions of various rare elements, while on the other, the model cannot explain the distributions of Zr, Hf, Nb, Ta, Th, and U. To eliminate this conflict, we suggest fractionation accompanied by replenishment, and assume that the primary magma for the alkali basalt series was not a single one but consisted of a set of batches similar in major-element composition but differing in contents of the rare lithophile elements. These batches during crystallization differentiation evolved along similar paths (because the fractionation conditions were similar and there were similarities in the major element contents in the primary magmas), but the differences in concentration of the rare elements in these magmas are responsible for differences in the degree of their accumulation during differentiation. The reasons for the differences in rare-element composition in the primary batches of alkali magma remain unclear. One may consider mantle metasomatism, whose effects are being actively researched at present together with changes in the degree of mantle partial melting, realization of fractional melting, and mixing of instantaneous partial melts.

ACKNOWLEDGMENTS

The study was supported by the Ministry of Mineral Sources and Technology, project N. 12P-(00)MO.

REFERENCES

1. Ramendik, G. I., O. I. Kryuchkova, D. A. Tyurin, and S. M. Gronskeya, 1988. *Zh. Anal. Khim.*, 43, No. 7, 1177.
2. Knipovich, Yu. N. and Yu. V. Morachevskiy (editors), 1956. *Analiz Mineral'nogo syr'ya [Mineral Raw Material Analysis]*, Nauka, Leningrad.
3. Barsukov, V. L., L. N. Kogarko, A. I. Polyakov, et al., 1981. *Geokhimiya*, No. 12, 1816.
4. Kogarko, L. N., A. M. Asavin, V. L. Barsukov, G. M. Kolesov, et al., 1984. *Geokhimiya*, No. 5, 639.
5. Kogarko, L. N., V. L. Barsukov, A. M. Asavin, A. I. Polyakov, et al., 1985. *Geokhimiya*, No. 8, 1124.
6. A. M. Asavin, L. N. Kogarko, V. A. Karpushina, G. M. Kolesov, O. I. Kryuchkova, and D. A. Tyurin. 1995 *Geochemistry International* 32, No. 4 p26.
7. A. M. Asavin. 1995 *Geochemistry International* 32 No. 5 p115
8. Dostal, J., C. Dupuy, J. P. Carron, et al., 1983. *Geochim. et Cosmochim. Acta*, 47, No. 3, 525.
9. Baxter, A. N., 1976. *Bull. Geol. Soc. Amer.*, 87, 1028.
10. Brandle, J. L. and Cerguera, 1975. *Estud. Geol.*, 31, No. 3-4, 375.
11. Weaver, B. L., D. A. Wood, J. Turney, and J. L. Jorner, 1987. *Alkaline Igneous Rocks*, Pergamon Press, London, p. 253.
12. Garg, A. N., 1981. *Chem. Geol.*, 34, No. 3/4, 235.
13. Pearce, J. A. and M. J. Norry, 1979. *Contribs. Mineral, and Petrol.*, 69, 33.
14. Ryerson, E. S. and E. B. Watson, 1987. *Earth Planet. Sci. Lett.*, 86, No. 2-4, 225.
15. Jochum, K. P., W. F. McDonough, H. Palme, and B. Spette, 1989. *Nature*, 340, No. 6234, 548.
16. Claque, D. A. and F. A. Frey, 1980. *DSDP*, v. 55, p. 559.

17. Wolff, J. A., 1987. *Lithos*, 20, No. 3, 207.
18. Baker, B. H., G. G. Goles, and W. P. Leeman, 1977. *Contribs. Mineral, and Petrol.*, 64, 303.
19. Green, T. H. and N. S. Pearson, 1987. *Geochim. et Cosmochim. Acta*, 51, No. 1, 55.
20. Michell, R. H., 1985. *Trans. Geolog. Soc. S. Afr.*, 88, 379.
21. Bogatikov, O. A., V. A. Kononova, I. L. Makhotkin, et al., 1987. *Vulkanologiya i Seysmologiya*, No. 1, 15.
22. Zielinski, R. A., 1975. *Geochim. et Cosmochim. Acta*, 39, 713.
23. Imslund, P., J. G. Larsen, T. Preztrik, and E. Sigmond, 1977. *Lithos*, 10, 213.
24. Bishop, A. C., A. R. Wooldey, and V. K. Din, 1973. *Contribs. Mineral, and Petrol.*, 39, No. 4, 309.
25. Fumes, H. and C. J. Stillman, 1987. *J. Geol. Soc. London*, 144, 227.
26. White, W. E., M. D. Tapia, and J. G. Schilling, 1979. *Contribs. Mineral, and Petrol.*, 69, 201.
27. Giret, A., 1983. *Le Plutonisme Oceanique Intraplaque: Exemple des lies Kergulen*. CNFRA, No. 54, 209.

Formation of Precambrian lithosphere mantle - geochemical analysis of coarse-grained peridotites from kimberlites, Siberian craton

M.A. Gornova ¹, L.V. Solovjeva ², O.M. Glazunov ¹, O.Yu. Belozerova ¹

¹ *Institute of geochemistry, SB RAS, 664033, Irkutsk, Favorsky str. 1 «a»*

² *Institute of the Earth's crust, SB RAS, 664033, Irkutsk, Lermontov 128*

ABSTRACT

The fresh coarse-grained spinel and garnet lherzolites from deep-seated xenoliths and kimberlites (Udachnaya and Obnazhennaya pipes) were studied by ICP-MS for a wide scope of elements. The studied xenoliths mainly involve usual peridotites, depleted by the clinopyroxene and garnet. Two garnet lherzolites with high Gnt and Cpx contents from the Udachnaya and Obnazhennaya pipes are cumulative in terms of the petrographic features. The comparison of lines rare element distributions on the spider diagrams with different degree of compatibility in lherzolites indicated that the most incompatible elements (to Gd) were subjected to the significant enrichment in xenoliths. The melting parameters for coarse-grained peridotites were restored using HREE level and shape. The correspondence of the petrochemical composition of rocks to these melting conditions was checked by the comparison with the petrochemical compositions of restites calculated from Walter [1999]. Three groups of restites were revealed. They were shown to form under the polybaric fractional melting in different ranges of pressure and degrees of melting. Both komatiite and basalt melts can be complementary to them. The former restites, were most likely subjected to vertical movements and subsolidus transformations.

INTRODUCTION

As opposed to the younger continental lithosphere, the geochemical features of the Precambrian lithosphere mantle of the cratons haven't been studied [Mc Donough, 1990]. The rare element contents are given mainly using the rare element characteristics of minerals, mainly garnet and clinopyroxene [Shimizu et al., 1997]. The isotope-geochemical data, based on studies of deep xenoliths from the kimberlites of the South Africa and Siberia [Walker et al., 1989; Pearson et al., 1995 a, b, c] are sufficient. However, the analysis of the concentrations of rare elements and their relative distribution in bulk samples from the craton lithosphere mantle, can contribute much to the model, describing its origin. The cratonic lithosphere mantle itself determines the geochemical and isotope-geochemical character of such intraplate potash magmas as lamproites and kimberlites [Flasher et al., 1985].

The gap in the geochemical data on rocks is related to the fact that the material of the deep xenoliths in kimberlites undergoes significant changes when they uplift to the surface and on the post-pipe stage. In addition, the traces of

different-stage mantle metasomatism, which shifts the primary ratios of rare elements, inheriting from the protolith, are found in the substance of deep xenoliths from kimberlites. [Kramers et al., 1983; Hawkesworth et al., 1990, Solovjeva et al., 1997].

The present paper gives the results of petrochemical and geochemical studies of incompatible rare elements in relatively weakly changed xenoliths of the spinel and garnet lherzolites from Udachnaya and Obnazhennaya pipes, located on different parts of the Siberian Platform and belonging to different terranes [Rozen et al., 2000]. The Udachnaya pipe occurs in the Daldyn kimberlite field [Khar'kiv et al., 1998], situated in the central part of the platform.

The age of its intrusion was determined by SHRIMP method as Middle Devonian (≈ 360 Ma) [Kinny et al., 1997]. The Obnazhennaya pipe is included into the Kuoisk field, located on the western edge of the Olenok tectonic block, which is found in the northeast of the Siberian Platform. The age of kimberlites from the Kuoisk field was dated from perovskites (SHRIMP) as 128-170 Ma (Kinny et al., 1997). The coarse-grained spinel and garnet lherzolites and two kimberlites samples were analyzed for a wide scope of rare elements. All lherzolites, except for two, belong to the coarse-grained usual peridotites, depleted by garnet and clinopyroxene, in terms of the modal mineral composition and by the main basaltoid components in terms of the bulk composition [Dawson, 1980; Boyd, 1989; Boyed et al., 1997]. These rocks are considered to be the residue from the melting of komatiite melts [Boyd, 1989; Canil, 1992; Walter, 1998].

Two samples (namely garnet lherzolite 555/80 from the Udachnaya pipe and garnet lherzolite 74-831 from the Obnazhennaya pipe) are the rocks, enriched by garnet and clinopyroxene. The first one belongs to the cumulative series of garnet clinopyroxenites i.e. olivine websterites –lherzolites, which were intruded into the lithosphere mantle later than the metamorphic stage [Solovjeva et al., 1994]. The garnet lherzolite 74-831 from the Obnazhennaya pipe is the member of the differentiated pyroxenite-websterite-lherzolite series, which has gone through the common metamorphic reconstruction with the coarse-grained peridotites [Solovjeva et al., 1994]. As opposed to the lithosphere mantle near the Udachnaya pipe, which is marked by scarce metamorphic pyroxenite-websterite rocks, the pipes of the Kuoisk field contain much more rocks from the complicated pyroxenite series than usual coarse-grained peridotites.

This article tests the restite model, which was developed for the petrogenic elements. REE are known [Johnson, 1990] to be very sensitive and reliable indicators of the melting. The obtained new data on rare elements for 13 grained peridotite samples from the kimberlite pipes (Obnazhennaya and Udachnaya pipes) of the Siberian platform and the REE modeling of melting in the Primitive Mantle (PM) allowed the consideration of this model again.

SAMPLING, ANALYTICAL TECHNIQUES

Material was selected from the centre of xenoliths which have been crushed into small (1-5 mm) pieces on a steel anvil, and handpicked to exclude any kimberlite incrustations or alteration material. The weight of selected material was 5-15 g. The picked material was crushed again up to 1 mm; about a half portion of it was then quartered for mineral counting and selection of monomineral fractions. One portion of quartered material was washed in quartz-distilled water and dried, then it was manually crushed in an agate pestle under pure alcohol.

The modal composition was determined by grain numbers in two fractions of secondary quartering (i.e. in fractions of 1-0.5 mm and 0.5-0.3 mm), both numbering 2000-3000 grains and 300-600 grains respectively; the average of both determinations were taken as modal.

The freshly crushed fragments were separated from weathered incrustations, xenolith inclusions and limestone fragments, as well as from olivine xenocryst, garnet and ilmenite >1 mm, using the binocular, and then pounded with an agate pestle under pure alcohol.

The mineral analyses using the JEOL Superprobe 733 as well as the bulk samples of rare elements analyses by standard techniques using ICP-MS were carried out at the Institute of Geochemistry SB RAS.

PETROGRAPHY OF ROCKS AND CHEMICAL COMPOSITION OF MINERALS

The petrographic description of spinel and garnet lherzolites from the Udachnaya and Obnazhennaya pipes is given below. The detailed description of enriched garnet lherzolites of cumulative type from the Udachnaya pipe and garnet lherzolites from the complicated pyroxenite-websterite-lherzolite series from the Obnazhennaya pipe is presented in Solovjeva et al., 1994.

Spinel lherzolites

The rocks possess the granoblastic texture with unclear aligned current structure. The rock pattern consists of the carcass of large grains of olivine (-3-8 mm, in some cases to 10-12 mm) and orthopyroxene (3-5 mm). Some strongly deformed relict megacrysts are up to 15-25 mm). Small (0.5-3 mm, rarely to 5 mm) irregular spinel and clinopyroxene grains are found in the intergrain space between the olivine and orthopyroxene. A noticed aligned current structure results from the extended crystals of olivine, orthopyroxene and interstices. The spinel and clinopyroxene enrich the sites located close to relict large crystals of orthopyroxene and in cases the spinel grains are elongated as chains in terms of the schistosity. The spinel forms the simplectite intergrowths with the clinopyroxene, in cases with the orthopyroxene and olivine or the specific penetration consisting of fine fibers (\angle 0.1 mm) along the grain boundaries. The modal mineral

composition in four studied spinel lherzolites from the Udachnaya pipe varies within the intervals: 0.15-1.5% Sp, 0.5-3% Cpx; 19-53% Opx; 45-80% Ol.

Garnet lherzolites

The rocks possess the characteristic granoblastic textures and marked orientation of minerals. Small garnet and clinopyroxene grains occur in the intergrain space between the subidiomorphic olivine crystals (3-8 mm, in cases to 10 mm) and more xenomorphic orthopyroxene (3-5 mm, as well as rare deformed crystals of up to 10-25 mm). The garnet as if cements the orthopyroxene and olivine as curved impregnations, and forms the chains of small rounded grains along the contiguous system of oblique fissures and along the cleavage in large relict orthopyroxene grains. The latter sometimes contain the rare tabular intergrowths of clinopyroxene (< 0.05 mm). The finest (< 10-15 μ) parallel lamellae of clinopyroxene in the orthopyroxene and vice versa are observed on the microprobe. The main minerals in the investigated samples from the Udachnaya pipe vary in the following intervals: 2-19 % Gnt; 0.3-8% Cpx; 20-29 % Opx; 52-72 % Ol. As compared to the spinel lherzolites the concentration of the orthopyroxene significantly decreases, which is in some cases due to the reaction of the spinel-garnet transition : $Sp+Opx \rightarrow Gnt+Ol$.

Inhomogenities in the distribution of primary minerals in the spinel and garnet lherzolites are related to the findings of relict large crystal of the orthopyroxene with the recrystallized textures of spinel, clinopyroxene and garnet decomposition and a weak lamination found in each tenth sample. The lamination contains the parallel schistosity, discontinuous layers of 2-5 mm thick, composed mainly of $Sp+Cpx$ or $Gnt + Cpx$. The pseudolayering is associated with the destruction and recrystallization of large grains of the primary pyroxene with the structures of Sp, Cpx, Gnt decomposition. This indicates the compression conditions, leading to the decay of solid solutions of the primary mixed pyroxene and further recrystallization into the granoblastic pattern with the $Sp+Cpx$, $Gnt+Cpx$ pinching out into the intergrain space. The next episode of cooling occurs in clinopyroxene lamellas in orthopyroxene grains and vice versa after the granoblastic pattern is formed.

The peculiar feature of the grained spinel and garnet lherzolites from the Udachnaya pipe is rare but constant occurrence of plates of phlogopite, paragenic with main minerals and related textural-equilibrium mica of the earlier stage [from Solovjeva et al., 1997]. The phenomenon, which is poorly studied is the polychromous pattern of olivine, found at least in $\frac{1}{4}$ of grained spinel and garnet samples from the Udachnaya pipe. It represents a unique block-like zoning with coloring of central blocks and zones in large crystals as light brown and orange with the transition to greenish and colorless in the marginal parts. Solovjeva et al. [1998], who has described this phenomenon for the first time relate it to the

reduction of the oxidized iron in the olivine under the influence of reduced pre-kimberlite fluids.

The secondary alterations of xenoliths are connected with the post-pipe stage of kimberlite transformation and the later mantle metasomatism [Solovjeva et al., 1997]. The post-pipe alterations are different in investigated xenolith samples: the serpentine alteration with insignificant calcite and accessory mineral concentrations is observed in the samples 2/84; 345/87; 325/87; 343/87; 555/80 from the Udachnaya pipe as well as in samples from the Obnazhennaya pipe. Serpentine concentrations, occurring in the olivine and to lesser extent in the orthopyroxene varies from 5 to 25 %. The secondary mineralization is: calcite gouges (≤ 0.5 %) and dark brown gouges and spots (≤ 0.1 %) are found on grains of primary minerals in the xenoliths from the non-serpentinized kimberlite (Udachnaya pipe; 501a/80; 47/82; 48/82; 42/82; 45/82). The dark brown gouges contain minor contents of Al-Cr-spinel, troilite, magnesioferrite, perclase, determined by x-ray. The minerals associated with the late metasomatism involve the fine polymineral reaction borders on the primary minerals: fibrous orthopyroxene+ finely squamosed phlogopite+ Al-Cr spinel on the garnet; fibrous magnesia amphibole + secondary clinopyroxene + titanium spinel on the orthopyroxene. The grains of the primary clinopyroxene are partially destructed and faded on the margins and the cleavage; the spot-like ore mineral appears. The narrow (10-30 μ) borders of titanium-magnetite or high-titanium Cr-spinel are observed on the primary transparent spinel lherzolites. The total content of secondary products of this stage does not exceed 1%.

Samples. Udachnaya pipe.

47/82 – spinel lherzolite: 0.4 % Sp; 0.5 % Cpx; 18.9 % Opx; 80.2 % clear Ol.

48/82 – spinel lherzolite: 0.5 % Sp; 3 % Cpx; 3.8 % Opx; 58.5 % greenish Ol.

501a/80 – spinel lherzolite: 1.1 % Sp; 0.4 % Cpx; 53 % Opx; 45.5 % clear Ol.

345/87 – spinel lherzolite: 1.5 % Sp; 1.8 % Cpx; 50.3 % Opx; 46.4 % polychrome Ol, plate Phl I (2,5 mm).

42/82 – garnet lherzolite: 7 % Gnt; 2.5 % Cpx; 28.5 % Opx; 62 % Ol.

45/82 - garnet lherzolite: 1.8 % Gnt; 8.2 % Cpx; 28.4 % Opx; 61.6 % polychrome Ol.

325/82 – garnet lherzolite: 18.6 % Gnt; 1.9 % Cpx; 27.1 % Opx; 52.4 % polychrome Ol.

343/87 – garnet lherzolite: 10.7 % Gnt; 0.3 % Cpx; 20 % Opx; 69 % polychrome Ol, plate Phl I (3 mm), relic deformed big grain of Opx (10 mm) with Cpx plate.

2/84 – garnet lherzolite: 5 % Gnt; 2 % Cpx; 25 % Opx; 68 % green-pale; relic deformed grain of Opx (1.7 cm) with oriented chains small Gnt grains.

555/80 – garnet lherzolite: 17.5 % Gnt; 17.5 % Cpx; 30 % Opx; 35 % Ol; <1 % Phl I.

The rock texture converts from hypidiomorphic to granoblastic with feature of cumulative one.

303/87 – basaltoid kimberlite, 250 horizon. Dark green rock with large-porphyry texture: 10-15 % rounded Ol I phenocrysts (>1 mm), 20-30 % subidiomorphic Ol II phenocryst are set in a serpentinite-carbonate matrix.

Obnazhennaya pipe

74-807 – spinel lherzolite: 3 % Sp; 7 % Cpx; 20 % Opx; 70 % Ol.

74-190 – garnet lherzolite: 10 % Gnt; 5 % Cpx; 15 % Opx; 70 % Ol.

74-831 – garnet lherzolite: 25 % Gnt; 20 % Cpx; 20 % Opx; 35 % Ol.

74-185 – garnet lherzolite c metasomatic Phl I: 15 % Gnt; 7 % Cpx; 20 % Opx; 43 % Ol; 15 % Phl I.

74-334/2 – dark green-grey large-porphyry kimberlite. 30-40 % rounded green-pale Ol I (>1 mm) phenocryst, 20-30 % Ol II and 3-5 % small plate Phl are set in fine-grained serpentinite-carbonate matrix.

The primary minerals from four studied spinel lherzolites from the Udachnaya pipe lie in the range of compositions of this rock type, described earlier [Solovjeva et al., 1994; Boyd et al., 1997]. The olivine has the range $MgO/(MgO+FeO) = 0.924 - 0.931$ m.f. (mole fraction). Moreover, the olivine of one and the same color in one grain does not show marked difference in terms of the composition. The orthopyroxenes contains 1.5-3.2 % of Al_2O_3 ; 0.25-0.5% of CaO and show significant decrease of Al_2O_3 , Cr_2O_3 , CaO in narrow (20-50 μ) zones on the contact with the fine reaction zone. The clinopyroxene is marked by high $CaO/(CaO+MgO)$ ration (from 0.494 to 0.55 m.f. Inhomogeneous content of Cr and Al oxides is more typical of clinopyroxene as compared to other minerals, which is due to the late metasomatism. Al-spinel has the noticed variations in Cr_2O_3 and Al_2O_3 content (21.9-40% and 28.6-47.4%).

The primary minerals in the studied garnet lherzolite with low clinopyroxene and garnet concentrations correspond totally to minerals from the rocks of this type [Solovjeva et al., 1994, Boyd et al., 1997]. Main characteristics of minerals are Ol-0.915-0.928 $MgO/(MgO + FeO)$ m.f; Opx-0.3-1.4% Al_2O_3 ; Cpx -0.482-0.490 $CaO/(CaO + MgO)$ m.f; Gnt -3.0-7.8 Cr_2O_3 ; 4.6-6.1% CaO. Almost all minerals do not contain TiO_2 (<0.03%). T and P for studied garnet lherzolites are calculated using equations by Finnerty, Boyd [1984] and for the major part of samples they lie in the range from 775-880°C, that correspond to the data for these rocks, given from Boyd et al. [1997]. Large relic grains of the orthopyroxene are isochemical to smaller orthopyroxene from the granoblastic matrix. In the xenoliths with the polychromous olivine the latter do not show the noticeable changes in the composition depending on the color. Fine zones (20-50 μ) of a different composition are observed in the orthopyroxene and garnet close to the reaction borders. Moreover the contents of Cr, Al, Ca oxides markedly decrease in the marginal parts of grains. Cr_2O_3 and CaO concentrations change in the narrow

marginal zones of the garnet on the boundary with the kefilites both towards the increase and decrease.

The garnet lherzolites of the cumulative series from the Udachnaya pipe have higher iron and titanium concentrations in minerals as opposed to the usual type of garnet lherzolites from this pipe [Solovjeva et al., 1994]. The characteristics of the minerals from the garnet lherzolite of this series is: 555/80: Ol-0.908 MgO/(MgO+FeO) m.f.; Opx - 0.55 % Al₂O₃, 0.06 % TiO₂; Cpx - 0.479 CaO/(CaO+MgO) m.f., 0.25% TiO₂; Gnt -2.29% Cr₂O₃, 0.26 % TiO₂. T and P of the primary paragenesis according to the formulas of Finnerty, Boyd are equal to 859⁰C and 39 Kbars, correspondingly.

In terms of the chemical composition of minerals the spinel and garnet lherzolites, depleted in the garnet and clinopyroxene from the Obnazhennaya pipe are similar to rocks of this type from the Udachnaya pipe. The main difference is that the clinopyroxene contains more of TiO₂ and Al₂O₃ and the garnets are marked by higher TiO₂ content and lower Cr₂O₃ concentration when MgO/(MgO+ FeO) is comparable. The characteristics of the minerals in the analyzed samples is:

Spinel lherzolite 74-807: Ol -0.924 MgO/(MgO + FeO m.f.; Opx -2.25 % Al₂O₃, 0.06 % TiO₂; Cpx -0.03% TiO₂, 0.502 CaO/(CaO+MgO) m.f.; Sp-29.2% Cr₂O₃.

Garnet lherzolite 74-190:Ol-0.920 MgO/(MgO+FeO) m.f.; Opx -0.90% Al₂O₃, 0.07% TiO₂; Cpx -0.35% TiO₂, 0.496 CaO/(CaO+mgO) m.f.; Gnt -0.1 % TiO₂, 2.60 %Cr₂O₃. T and P are from Finnerty and Boyd formulas 558⁰C and 14 Kbars, correspondingly.

The garnet lherzolites with high garnet and clinopyroxene contents 74-831:0.924 MgO/(MgO+FeO) m.f.; Opx - 1.44 % of Al₂O₃, 0.07 TiO₂; Cpx - 0.20 % TiO₂, 0.512, CaO/(CaO + MgO) m.f.; Gnt - 0.10 5 TiO₂, 2.60% Cr₂O₃.

PETROCHEMISTRY AND GEOCHEMISTRY

The chemical and rare element compositions of coarse-grained spinel and garnet lherzolites are given in Table 1. The petrochemical features of rocks are given on Fig.1. The composition of the primitive mantle (PM) from [McDonough, Sun, 1995] is used for the comparison. Among the considered group of samples the garnet lherzolites 555/80 and 74/831 are characterized by the higher Al₂O₃, CaO and lower MgO, SiO₂ contents as opposed to the PM. It correlates with the proposed cumulative nature. All other samples show the different degree of the depletion as compared with PM. The range of compositional variations for these rocks overlaps both the more depleted coarse-grained peridotites from the kimberlites of the Kapvaal and Siberian cratons [Boyd et al., 1997] and less depleted peridotites of the «oceanic trend» [Takahashi, 1990]. It should be noted that the spinel and garnet lherzolites are not different in the chemical composition.

The rocks are marked by the MgO increase (Fig.1) and Al₂O₃ and CaO decrease. Such relations are common to the peridotite series from the xenoliths in basalts and

Table 1.

Major (wt%) and trace element (ppm) abundances of peridotite xenoliths and kimberlites from the Siberian craton.

NN	1	2	3	4	5	6	7	8
Sample	501a/80	48/82	47/82	345/87	74-807	325/87	42/82	45/82
SiO ₂	49.96	47.39	44.09	47.91	42.60	45.48	46.51	46.99
Al ₂ O ₃	1.26	1.52	0.38	2.18	3.87	4.34	1.69	1.02
Cr ₂ O ₃	0.78	0.41	0.27	0.69	0.96	0.87	0.41	0.25
ΣFeO	5.95	5.81	6.95	6.17	7.47	6.89	6.54	6.77
MnO	0.14	0.13	0.03	0.08	0.13	0.10	0.07	0.13
MgO	41.38	43.70	47.79	42.04	41.29	40.47	43.48	42.50
CaO	0.33	0.78	0.20	0.67	3.25	1.57	1.04	1.94
Na ₂ O	0.00	0.01	0.00	0.03	0.22	0.06	0.01	0.10
K ₂ O	0.00	0.00	0.00	0.00	0.17	0.00	0.00	0.00
NiO	0.19	0.25	0.29	0.23	-	0.22	0.25	0.30
Rb	7.72	10.14	7.8	8.81	2.58	13.1	10.96	11.28
Ba	41.9	68	96	52.6	77.1	70.4	72	32.86
Th	0.36	0.07	0.17	0.31	0.59	0.32	0.19	0.29
Nb	3.38	1.35	1.75	2.26	2.09	1.26	1.07	3.03
La	2.45	1.43	1.8	1.4	2.34	1.15	1.44	2.45
Ce	4.47	1.77	2.55	2.4	3.94	2.02	2.08	5.11
Pr	0.47	0.2	0.29	0.23	0.47	0.27	0.25	0.56
Sr	20.5	8	10	45.7	78.8	47.5	21	38
Nd	2.06	1.02	1.4	1.04	1.71	1.06	1.23	2.3
Hf	1.24	0.43	0.34	0.37	0.39	0.31	0.44	0.25
Sm	0.42	0.26	0.32	0.21	0.45	0.25	0.3	0.26
Zr	27	16	14	10.2	10.1	8.09	16	8.85
Eu	0.08	0.059	0.058	0.04	0.09	0.07	0.05	0.085
Ti	120	210	308	720	240	1020	214	
Gd	0.39	0.28	0.36	0.2	0.39	0.31	0.33	0.3
Tb	0.04	0.054	0.066	0.02	0.07	0.06	0.061	0.05
Dy	0.27	0.33	0.37	0.16	0.41	0.34	0.37	0.32
Y	1.68	2.42	2.83	0.92	2.67	2.74	2.7	2.33
Ho	0.07	0.074	0.083	0.04	0.09	0.08	0.083	0.08
Er	0.18	0.25	0.28	0.1	0.3	0.32	0.26	0.2
Tm	0.03	0.044	0.042	0.02	0.05	0.07	0.046	0.03
Yb	0.15	0.29	0.3	0.11	0.31	0.46	0.33	0.26
Lu	0.03	0.05	0.047	0.03	0.06	0.09	0.055	0.03

kimberlites and are considered as the verification of the formation as restites after a different degree of the partial melting. The analysis of experimental works [Walter, 1998; Walter, 1999] indicates that relative to the composition of the primitive mantle in restites the MgO content increases while Al₂O₃ and CaO concentrations decrease proportional to the melting degree. The concentration of Σ

FeO is related to the reverse correlation with the pressure, thus when the melting degree is the same it is less in restites, formed under higher pressure. For instance, for pressures ≈ 60 -70 Kbars and $F \approx 60\%$, ΣFeO concentration in restites amounts to approximately 6 wt %. In restites, formed under the pressure of 10-20 Kbars,

End of Table 1.

NN	9	10	11	12	13	14	15
Sample	2/84	74-190	555/80	74-831	74-185	303/87	74-334
SiO ₂	44.79	45.01	48.56	46.99	45.5		
Al ₂ O ₃	1.69	1.47	4.60	8.49	8.94		
Cr ₂ O ₃	0.57	0.28	0.71	1.58	-		
ΣFeO	6.68	7.85	6.78	5.77	7.13		
MnO	0.12	0.10	0.16	0.13	0.1		
MgO	45.34	44.05	34.15	29.85	28.99		
CaO	0.52	0.96	4.34	6.87	4.9		
Na ₂ O	0.02	0.13	0.47	0.22	1.24		
K ₂ O	0.01	0.10	0.00	0.00	2.92		
NiO	0.25	-	0.12	-	-		
Rb	8.75	2.26	22.8	10.3	55.9	58.96	32.03
Ba	41.12	26.7	152.5	87.7	934	940.06	330.59
Th	0.41	1.04	0.79	1.64	2.03	8.19	22.29
Nb	5.15	6.17	9.36	8.54	34.10	121.31	202.27
La	3.84	5.31	6.03	6.49	20.5	71.37	155.78
Ce	5.27	8.88	10.41	11.7	39.4	124.83	255.87
Pr	0.53	0.96	1.22	1.45	3.83	12.45	25.57
Sr	28	25.4	47.6	64.5	198	420.7	970.44
Nd	2.1	3.37	4.58	5.42	16.4	37.62	76.92
Hf	0.42	0.27	1.1	0.76	1.64	2.12	2.18
Sm	0.37	0.6	1.04	1.21	28	6.1	11.33
Zr	14.5	8.36	34.7	22.6	60	91.27	109.97
Eu	0.12	0.18	0.38	0.42	0.69	1.49	2.8
Ti		300	1740	2100	-	5948	2684
Gd	0.28	0.51	1.1	1.73	2.2	3.39	6.46
Tb	0.04	0.08	0.2	0.38	0.21	-	-
Dy	0.28	0.37	1.02	2.16	1.18	1.96	3.62
Y	1.74	2.09	6.26	14.2	5.9	9.99	19.88
Ho	0.06	0.07	0.2	0.51	0.23	0.29	0.57
Er	0.17	0.23	0.66	1.69	0.54	0.73	1.26
Tm	0.02	0.03	0.1	0.29	-	0.08	0.15
Yb	0.18	0.18	0.59	1.54	0.35	0.54	0.88
Lu	0.03	0.03	0.11	0.3	0.06	0.08	0.13

Note. 1-5 – coarse-grained spinel peridotites from Udachnaya (1-4) and Obnazhennaya (5) pipes; 6-10- coarse-grained garnet lherzolites from Udachnaya (6-9) and Obnazhennaya (10) pipes; 11- cumulative garnet lherzolites from Udachnaya pipe, 12- cumulative garnet lherzolites from Obnazhennaya pipe; 13- garnet lherzolite with Phl from Obnazhennaya pipe; 14- basaltoid kimberlite from Udachnaya pipe; 15- kimberlite from Obnazhennaya pipe. The whole rock values (1-4, 6-9, 12) are calculated from major element concentration of minerals and their modal compositions.

$\Sigma\text{FeO} \approx 7.5\text{-}8.5$ wt %, that is similar to the concentration in the primitive mantle. SiO_2 content in restites should not exceed the composition of PM. It decreases with the growth of the melting degree to ≈ 45 wt % ($F = 40\%$) under the polybaric fractional melting and to 41 wt % ($F = 40\%$) under the batch melting.

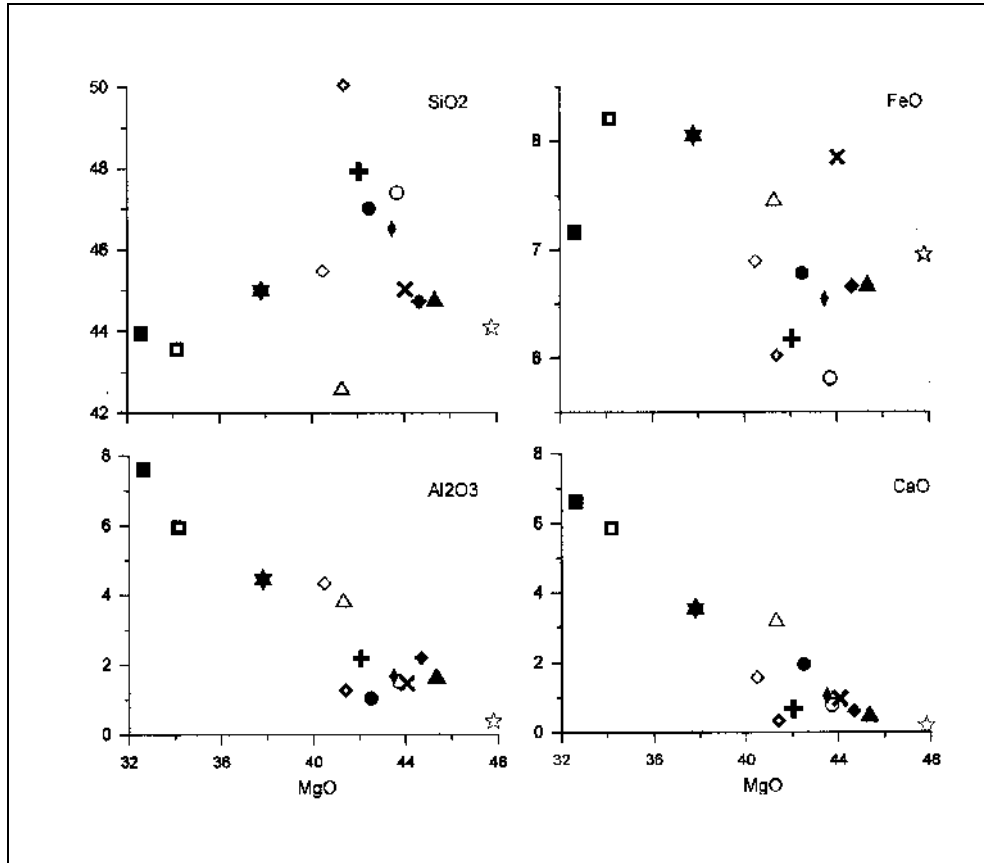


Fig. 1. Variation of chemical components against MgO (wt%) in peridotite xenoliths from the Siberian craton.

Udachnaya pipe: spinel peridotites (501/80 – open rhomb with heavy line, 48/82 – open circle, 47/82 – open star, 345/87 – right cross); garnet peridotites (325/87 – open rhomb, 42/82 – solid elongated rhomb, 45/82 – solid circle, 2/84 – solid triangle, 343/87 – solid rhomb, 555/80 – open square).

Obnazhennaya pipe: spinel peridotite (74/807 – open triangle), garnet peridotites (74/190 – oblique cross, 74/831 – solid square).

Composition primitive mantle taken from McDonough, Sun (1995) – solid star.

Among studied samples the garnet (325/86) and spinel (74/807) lherzolites are marked by the least melting degrees. ΣFeO concentration in rocks varies from 5.8 to 7.85 wt %. Thus, at least two groups of samples, formed under different pressure can be distinguished. The samples 74-190 and 74-807 have higher ΣFeO content (7.47-7.85 wt %), corresponding to the SiO_2 contents (43.6-45 wt %) from the melting model. They could originate under the pressure of 10-20 Kbars. The rest samples possess lower ΣFeO content and might be formed under higher pressure. An increased SiO_2 contents corresponding to the increased orthopyroxene

concentrations and negative correlation SiO_2 - ΣFeO are typical of samples 501a/80, 345/87, 45/82, 48/82, 42/82.

The rare element concentrations normalized to PM are plotted for the studied peridotites and kimberlites from both pipes (Fig.2). There is an increase of lherzolites lines parallel to kimberlite lines starting from Gd in the left part of the

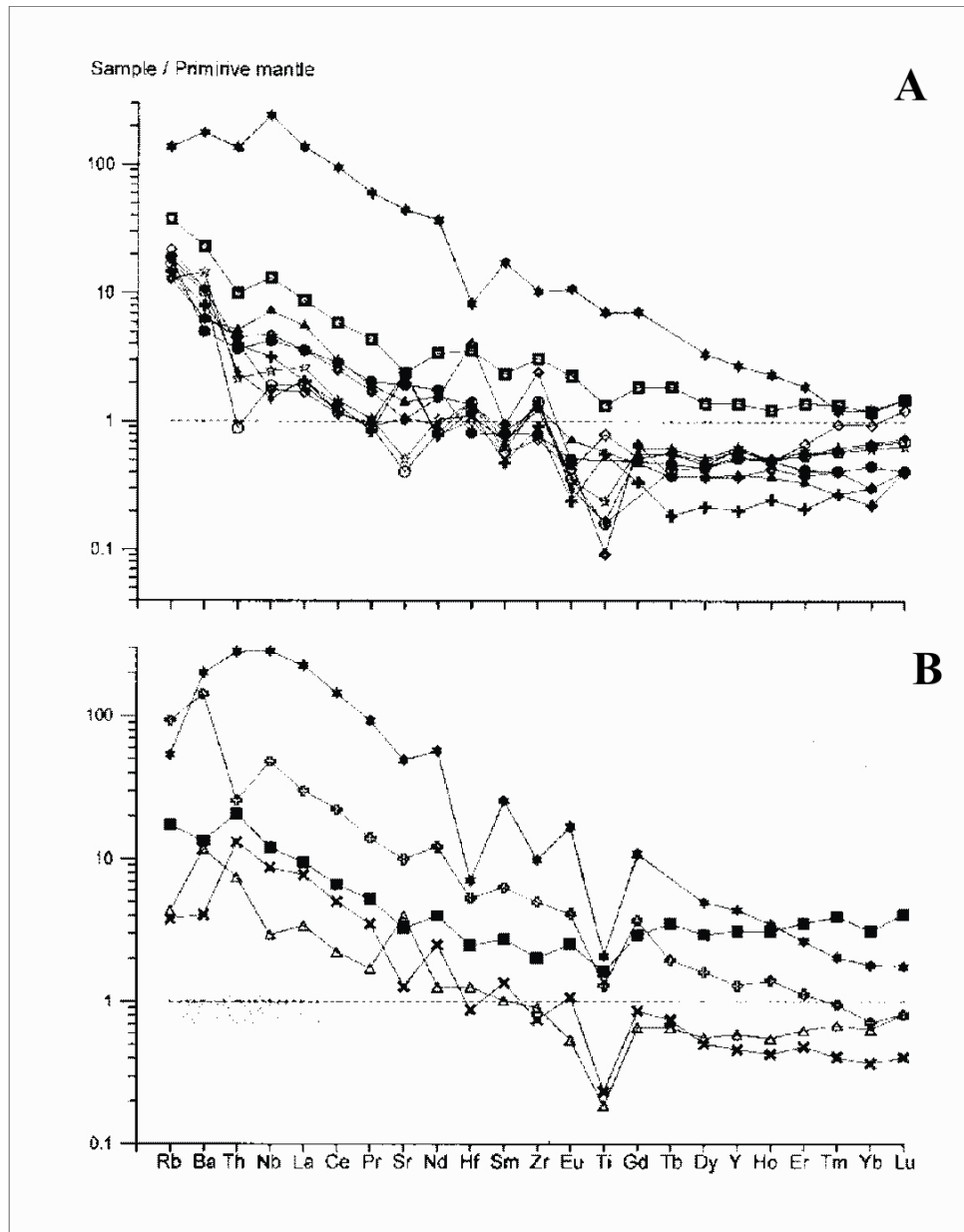


Fig. 2. Incompatible trace-element abundances in peridotites and kimberlites from Udachnaya (A) and Obnazhennaya (B) pipes, normalized to primitive mantle abundance (McDonough, Sun, 1995).

Symbols for peridotites are the same as in Fig. 1; kimberlites – solid stars; garnet peridotite 74-185 with Phl I– open cross.

plot. It most likely indicates the significant effect of the incompatible element supply on the peridotites. This supply is associated with the kimberlite origin in

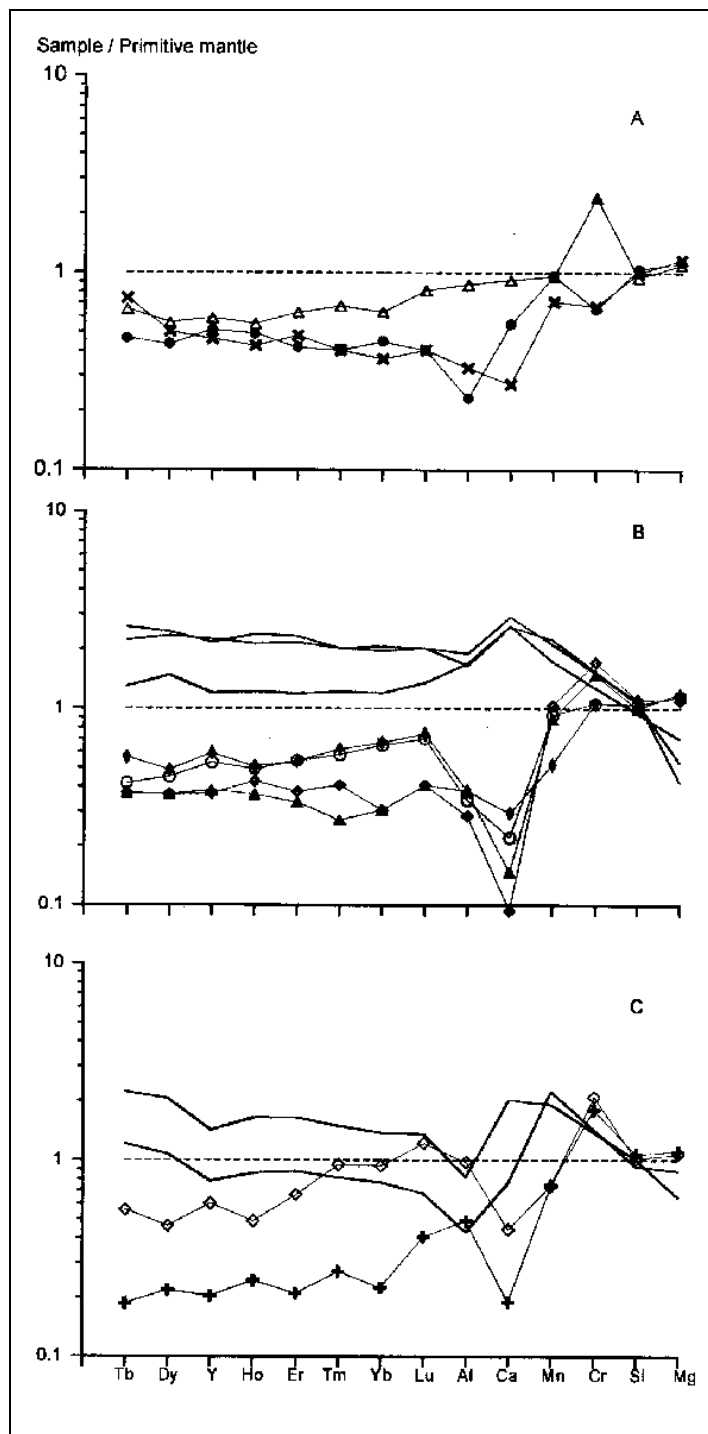


Fig. 3. Mantle-normalized diagrams for peridotite xenoliths from the Siberian craton.

Normalized values taken from McDonough, Sun (1995). Peridotite symbols are the same as in Fig. 1. Lines: 3B) komatiites from Tisdale Township, Abitibi greenstone belt, Canada [Xie et al., 1993]; 3C) komatiites from Boston Township, Abitibi greenstone belt, Canada [Xie et al., 1993].

particular late metasomatism. The line of the phlogopite garnet lherzolite from the Obnazhennaya pipe is markedly shifted upwards toward the kimberlite line (Fig. 2B). Some significant distinctions as curves, e.g. Zr, Hf peaks on the lherzolite lines and minima kimberlite lines from the Udachnaya pipe require further investigations. On the whole, the comparison with the kimberlites shows that the majority of samples are marked by the metasomatic supply of the most incompatible elements starting from Gd, thus only heavy rare earth elements and Y are used for further consideration. The samples 555/80 and 74/831 show higher concentrations of heavy rare earth elements as compared to the PM, that is related to the cumulative nature.

Fig. 3 gives the concentrations of petrogenic and heavy rare earth elements in the coarse-grained peridotites, normalized to the primitive mantle. The elements are given according to the increase of incompatible degree from the right to the left for the basalt-peridotite system [McDonough, Sun, 1995]. Si concentrations in restites and basalt melt are similar ($D_{Si} \approx 1$). The far is the element situated towards the left from Si, the less are the normalized concentrations in the restites. The far is the element located to the right from Si, the greater are the normalized contents in the restite. The restite, complementary to the basalt melt should have the smooth slope curve lower than the PM composition. The greater inclination indicates the great melting degrees.

Fig. 3A presents the spinel(74/807) and garnet (190/74, 45/82) lherzolites. The sample 74/807 is marked by the smooth slope curve from Mg to Dy (except for Cr). The samples 45/82 and 190/74 possess the greater inclination of the curve in the petrogenic part of elements, i.e. the greater melting degrees. Starting from Lu the inclination of curves is disturbed, that is probably related to the kimberlite impact. These samples could be formed under different degree of the primitive mantle melting in conditions of low pressures leading to the basalt origin.

Fig. 3B shows the spinel (48/82, 501/80) and garnet (42/82, 2/84) lherzolites. The slope of curves for these rocks is violated by the Ca, Al minima, moreover $Ca_N \ll Al_N$, that proves their impossible origin as restites resulting from the melting of the primitive mantle with the basalt generation. The melts, similar to Al-depleted komatiites Tisdale Township, Abitibi greenstone belt, Canada [Xie et al., 1993] can be complementary to such restites. They are marked by the following concentrations: MgO \approx 26-21 wt %, Al₂O₃ \sim 6.8-8 wt% and ratios CaO/Al₂O₃ \sim 1.2, (Gd / Yb)_N \sim 1.2-1.4. On this plot they demonstrate reverse to the considered samples curves with $Ca_N \gg Al_N$; $Al_N \geq Yb_N$, Lu_N ; $Tb_N > Yb_N$). The depletion increases in the rock series from 42/82, 48/82 to 2/84, 501a/80.

Fig. 3C represents the spinel (345/87) and garnet (325/87) lherzolites. A slope of curves for these rocks is violated by Ca minimum, while the normalized Al contents are higher than the normalized Yb concentrations. Al-depleted komatiites, similar to Boston Township komatiites, Abitibi greenstone belt Canada [Xie et al., 1993] are complementary to such restites. These melts have the following characteristics: MgO \sim 32-25 wt %, Al₂O₃ \approx 1.7-3.4 wt %; (Gd/Yb)_N \sim 2.7-3.0 and

have the reverse to restites curves with $Ca_N \gg Al_N$, $Al_N < Yb_N$, Lu_N and $Tb_N \gg Yb_N$. The spinel lherzolite 345/87 is more depleted than the garnet lherzolite 325/87.

$Lu_N/Ho_N \sim 2.2$. in peridotites from C group, while in B group peridotites it amounts to ≈ 1.4 , and in group A peridotites this ratio ≈ 1.3 .

REE concentrations in restites were calculated [Gornova et al., 2001] under the polybaric fractional melting and batch melting of the PM in the spinel and garnet stability fields and for different melting degrees (table 2, Fig. 4). The analysis of these calculations allow the following conclusions:

Table 2. Parameters used in melting models.

Model		P GPa	Melting reaction	Reference
Polybaric fractional melting (0.1GPa kbar-1.2 % melt) in the spinel stability field. PM = 0,52 Ol+ 0.27 Opx + 0.18 Cpx+ 0.03 Sp		2.6-1.9	0,08 Ol + 0,92 Cpx + 0,08 Sp = 0,08 Opx + 1L	Kinzler, 1997
		1.9-1.7	1,53 Cpx + 0,09 Sp = 0,15 Ol + 0,47 Opx + 1L	
		1.7-1	0,13 Opx + 0,89 Cpx+0,12 Sp = 0,13Ol +1L	
Initial polybaric fractional 5% melting in the garnet stability field followed by an additional polybaric fractional melting in the spinel stability field (0.1 GPa – 1% melt). PM = 0,6 OL+ 0,2 Opx + 0,1 Cpx + 0,1 Gr		3-2.5	0,08 Ol + 0,81 Cpx +0,3 Gr = 1L +0,19 Opx	Walter, 1998
		2.5	1 Ol+4,67 Gr+1L=3,7 Opx+1,9 Cpx+1,07 Sp	Walter et al., 1995
		2.5-1.5	As in the stability field of spinel	Kinzler, 1997
Polybaric fractional melting in the garnet stability field. PM = 0.54 Ol+ 0.3 Cpx+ 0.16 Gr		7-6	0,26 Ol + 0.5 Cpx + 0.24 Gr = 1L	Walter, 1998
		6-5	0,3 Ol + 0,44 Cpx + 0,26 Gr =1L	
		5-4	0,06 Ol + 2,25 Cpx + 1,21 Gr = 1L +2,52 Opx	
		4-2.6	0.04 Ol + 0.96 Opx = 1L	
Isobaric batch melting in the garnet stability field. PM = 0.54 Ol+ 0.31Cpx + 0.15 Gr	F= 0-31%	6	0.33 Ol + 0.4 Cpx + 0.27 Gr = L	Walter, 1998
	F= 31-41%		0.24 Ol + 1,74 Cpx + 0,4 Gr = 1L + 1,38 Opx	
	F= 41-51%		0.15 Ol + 0.51 Opx + 0.34 Gr = 1L	

Notes. PM – primitive mantle, Ol – olivine, Opx – orthopyroxene, Cpx – clinopyroxene, Sp – spinel, Gr- garnet, L - melt.

Equations for calculating residual bulk compositions taken from Shaw (1970):
 $C^S = C_0 \times (1 - PF/D_0)^{1/P} / (1 - F)$ (polybaric fractional melting);
 $C^S = C_0 \times [(1 - F)(1 + F/(D_0 - PF))]^{-1}$ (isobaric batch melting). C^S – residual solid, C_0 – composition solid, initial composition is PM [McDonough, Sun, 1995], D_0 – bulk distribution coefficient, P – bulk melt coefficient, F – degree of melting. C_0 , D_0 u P recalculates accordingly melting reaction. $D^{mineral/liquid}$ (La, Ce, Nd, Sm, Eu, Gd, Dy, Er, Yb) taken from Johnson (1998).

1) HREE concentrations decrease and Yb/Gd increases in restites with the growth of the melting degree.

2) If the initial pressure and melting degrees are similar, the REE contents in restites are lower and Yb/Gd is higher for the polybaric fractional melting as compared with the batch one.

3) For the polybaric fractional melting in the garnet stability fields if the melting degree is the same the greater is the initial pressure the higher are REE concentrations in restites and lower is Yb/Gd.

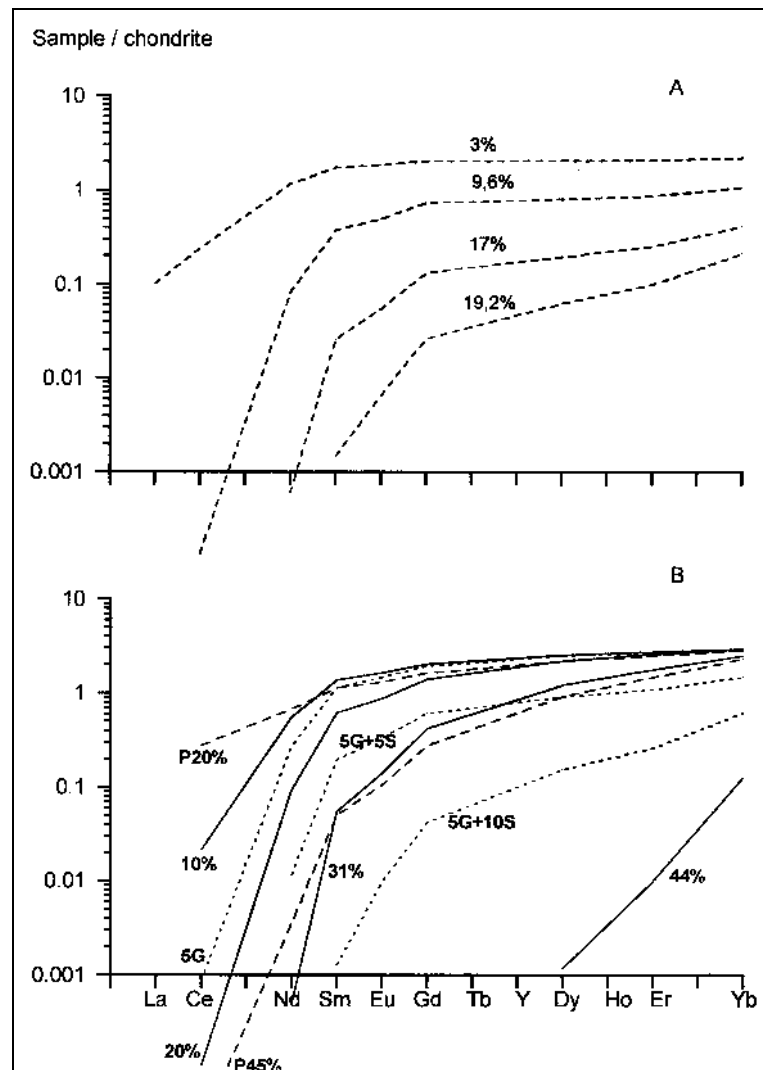


Fig. 4. Calculated composition of residues after melting of primitive mantle.

A) Dashed lines - polybaric fractional melting in the spinel stability field (2.6-1GPa). Degrees of melting are 3 %, 9.6 %, 17 % and 19,2 %.

B) Point lines - polybaric fractional melting (3-1.5GPa). 5G is 5 % melting in the garnet stability field; 5 G + 5 S is 5 % melting in the garnet field followed by 5 % melting in the spinel field; 5 G + 10 S is 5 % melting in the garnet field followed by 10 % melting in the spinel field. Dashed lines (P 20 % and P 45 %) - isobaric batch melting in the garnet stability field (6GPa). Degrees of melting are 20 % and 45 %.

Lines - polybaric fractional melting in the garnet stability field (7-2.6GPa). Degrees of melting are 10 %, 20 %, 31 % and 44 %.

4) REE concentration and Yb/Gd in restites allow the reliable identification of melting conditions (pressure, melting degree and mechanism of melting).

DISCUSSION AND CONCLUSIONS

The coarse-grained peridotite inclusions from the kimberlite pipes of the Siberian Platform indicate a wide range of concentrations of petrogenic and rare earth elements, which verifies the formation conditions. The melting parameters were restored using HREE level and shape. The correspondence of the petrochemical composition of rocks to these melting conditions was checked by the comparison with the petrochemical compositions of restites calculated from Walter [1999]. The above allowed the revealing of four groups with the corresponding rare element and petrochemical compositions.

Group 1. As opposed to the primitive mantle the samples of garnet lherzolites 555/80, 74/831 are enriched by Al_2O_3 , CaO, ΣFeO , REE, and cannot be restites. In terms of the chemical composition the sample 555/80 is similar to Al-non-depleted komatiite, while the sample 74/831 is similar to the komatiite basalts or recent tholeiites of island arcs.

Group 2 A (samples 74/807, 190/74, 45/82). The spinel and garnet peridotites could originate as a result of 5-9% polybaric fractional melting of the primitive mantle in the spinel stability field. The concentrations of petrogenic elements agree with the data on the melting conditions. The increase of the melting degree from 74/807 to 74/190 is confirmed by the increase of MgO and Al_2O_3 , CaO, HREE decrease. The garnet occurrence in samples 190/74 and 45/82 results from the subsolidus transformations.

Group 2 B (samples 48/82, 501a/80, 47/82, 42/82, 2/84). The spinel and garnet peridotites of this group could originate from the polybaric fractional melting in the garnet stability field in the interval from 50 to 30 kbars with the variations of the melting degrees ~ 15 - 20 %, which is in accordance with the petrochemical rock composition. The komatiites of Tisdale Township type are most likely complementary to these restites and could originate under the pressure of ~50 kbars and the melting degree of ~15-20% [Walter, 1998].

Group 2 C (garnet 325/87 and spinel 345/87 lherzolites). A steep inclination of HREE curves in these samples well agrees to the calculated curves for ~ 31 % and 35 % degrees of polybaric fractional melting of the PM in the ranges of 70-39 and 70-35 kbars, correspondingly. The petrochemical composition is similar to the restite compositions, calculated under these parameters of the melting. The complementary melts with petrochemical characteristics similar to Al-depleted Boston Township komatiites could originate under $P \sim 80\text{-}90$ kbars and the melting degree of 30-25 % [Walter, 1998]. The ideas on the origin of komatiites under relatively small pressure are based on these arguments [Walter, 1998, Nisbet, Walker, 1982]. There is another viewpoint, which is experimentally confirmed. This view [Wei et al., 1990] points out that the komatiites are formed under higher

pressure with the participation of high-baric phases (majoritic garnet, perovskite). Al-depleted komatiites could originate under high melting degrees from the PM sites, depleted by majoritic garnet, Al-enriched komatiites resulted from the sites of PM enriched in majoritic garnet. Thus, the peridotites of 2C groups can be considered in a different way. The sample 325/87 is similar to the composition of the PM enriched in majoritic garnet. Fig. 3 C represents the enrichment by Al, Sr, Yb and depletion by Ca, Mn, which agrees with the distribution coefficients for these elements [Ohtani et al., 1989] between the majoritic garnet and ultrabasic melt. A thorough analysis using the greater amount of rare elements is needed to consider the latter possibility.

The peridotites most likely underwent the multi-stage origin and the movements and subsolidus transformations could occur after the partial melting and removal of melts. It resulted in the occurrence of spinel peridotites among rocks, formed under high pressure in the garnet stability field. It also resulted in the occurrence of garnet peridotite in the group of rocks, formed in the spinel stability field. It complicates the use of the mineral composition for checking the restite hypothesis of coarse-grained peridotite origin. In terms of the proposed restite model the enrichment in SiO₂ and high concentrations of modal orthopyroxene can derive from later metamorphic sorting of minerals [Boyd et al., 1997] or metasomatic SiO₂ supply [Keleman et al., 1998; Kesson, Rigwood, 1989].

The performed investigations showed the perspectives of REE using to reconstruct the mechanisms of the Precambrian lithosphere origin. The coarse-grained peridotites of the Siberian craton are not the homogenous group. They include both the cumulative and restite ones. The latter could generate in a wide range of pressure and melting degrees. The complementary to them are both komatiite and basalt melts.

REFERENCES

1. Boyd F. R. Compositional distinction between oceanic and cratonic lithosphere // *Earth Planet. Sci. Letts*, 1989, v. 96, p. 15-26.
2. Boyd F. R., Pokhilenko N. P., Pearson D. G. et al. Composition of the siberian cratonic mantle: evidence from Udachnaya peridotite xenoliths// *Contrib. Mineral. Petrol.*, 1997, v. 128, p. 228-246.
3. Canil D. Orthopyroxene stability along the peridotite solidus and the origin of cratonic lithosphere beneath southern Africa// *Earth Planet. Sci. Letts.*, 1992, v. 111, p. 83-95.
4. Khar'kiv A.D., Zinchuk N.N., Kryuchkov A.I. *Bedrock deposits of world's diamonds / Nedra, Moscow, 1998, 555 pp. (in Russian).*
5. Dawson J. B. *Kimberlites and their xenoliths // Springer-Verlag, Berlin, Heidelberg, New York, 1980, 300 p.*
6. Finnerty A.A., Boyd F.R. Evaluation of thermobarometers for garnet peridotites // *Geochim. Cosmoch. Acta*, 1984, v.48, p. 15-27
7. Flaser .K. J., Hawkesworth C. J., Erlank A. J. et al. Sr, Nd and Pb isotope and minor element geochemistry of lamproites and kimberlites // *Earth Planet. Sci. Letts*, 1985, v. 76, p. 57-70.

8. Gornova M. A., Tsypukov M.Yu., Sandimirova G. P., Smirnova E. V. Melting of Precambrian mantle: geochemical analysis restite orogenic peridotites of periphery Siberian craton // *Doklady RAS*, 2001, v. 378, p. 383- 386.
9. Hawkesworth C. J., Kempton P. D., Rogers et al. Continental mantle and shallow level enrichment processes in the Earth's mantle // *Earth Planet. Sci. Letts.*, 1990, v. 96, p. 256-268.
10. Johnson K. T. M., Dick J. B. H., Shimizu N. Melting in the oceanic upper mantle: an ion microprobe study of diopsides in abyssal peridotites // *J. Geophys. Res.*, 1990, v. 95, № B 3, p. 2661-2678.
11. Johnson K. T. M. Experimental determination of partition coefficients for rare earth and high-field-strength elements between clinopyroxene, garnet, and basaltic melt at high pressures // *Contrib. Mineral. Petrol.*, 1998. – № 133. – P. 60-68.
12. Keleman P. B., Hart S. R., Bernstein S. Silica enrichment in the continental upper mantle via melt/rock reaction // *Earth Planet. Sci. Letts.*, 1998, v. 164, p. 387-406.
13. Kesson S. E., Ringwood A. E. Slabe-mantle interactions 2. The formation of diamonds // *Chemical Geology*, 1989, v. 78, p. 97-118.
14. Kinzler R.J. Melting of mantle peridotite at pressures approaching the spinel to garnet transition: application to mid-ocean ridge basalt petrogenesis // *J. Geophys. Res.*, 1997. – V.102, № B1. – P.853-874.
15. Kinny P. D., Griffin B. J., Heaman L. M. et al. SHRIMP U-Pb ages of perowskite from Yakutian kimberlites // *Russian Geology and Geophysics*, 1997, v. 1/38, p. 91-100.
16. Kramers J. D., Roddick J. C., Dawson J. B. Trace element and isotope studies on veined, metasomatic and “MARID” xenoliths from Bultfontein, South Africa // *Earth Planet. Sci. Letts.*, 1983, v. 65, p. 90-106.
17. McDonough W. F. Constrains on composition continental lithospheric mantle // *Earth Planet. Sci. Letts.*, 1990, v. 101, p. 1-18.
18. McDonough W. F., Sun S.-s. The composition of the Earth // *Chemical Geology*, 1995, v. 120, p. 223-253.
19. Nisbet E. G., Walker D. Komatiites and the structure of the Archean mantle // *Earth Planet. Sci. Letts.*, 1982, v. 60, p. 105-113.
20. Ohtani E., Kawabe I., Moriyama J., Nagata Y. Partitioning of elements between majorite garnet and melt and implications for petrogenesis of komatiite // *Contrib. Mineral. Petrol.*, 1989, v. 103, p. 263-269.
21. Pearson D. G., Shirey S. B., Carlson R. W. et al. Re-Os, Sm-Nd isotope evidence for thick Archaean lithospheric mantle beneath Siberian craton modified by multi-stage metasomatism // *Geochim. Cosmoch. Acta*, 1995a, v.59, p. 959-977.
22. Pearson D. G., Carlson R. W., Shirey S. B., Nixon P. H. Stabilisation of Archaean lithospheric mantle: a Re-Os, isotope study of peridotite xenoliths from the Kaapvaal craton // *Earth Planet. Sci. Letts.*, 1995b, v. 134, p. 341-357.
23. Pearson D. G., Snyder G. A., Shirey S. B. et al. Archaean Re-Os age for Siberian eclogites and constrains on Archaean tectonics // *Nature*, 1995c, v. 374, p. 711-713.
24. Rozen O. M., Журавлев D. Z., Cyhanov M. K. et al. Isotope -geochemical and age characteristics early proterozoic terranes, collision zones and related anorthozites on the Northeast of Siberian craton // *Russian Geology and Geophysics*, 2000, v. 41, № 2, p. 163-180.
25. Shaw D. M. Trace element fractionation during anatexis // *Geochim Cosmochim. Acta*, 1970, v. 34, p. 237-243.
26. Shimizu N., Pokhilenko N. P. , Boyd F. R., Pearson D. G. Geochemical characteristics of mantle xenoliths from Udachnaya kimberlite pipe // *Russian Geology and Geophysics*, 1997, v. 1/38, p. 194-205.

27. Solovjeva L. V., Egorov K. N., Markova M. E. et al. Mantle metasomatism and melting in mantle-derived xenoliths from the Udachnaya kimberlite: their possible relationship with diamond and kimberlite formation // *Russian Geology and Geophysics*, 1997, v. 1/38, p. 182-204.
28. Solovjeva L.V., Barankevich V.G., Bayukov O.A. et al. Polychrome olivines in coarse grained lherzolites from the Udachnaya pipe – possible indicators of reduced metasomatism // *Ext. Abstr., 7th Int. Kimb. Conf.*, Cape Town, 1998, p. 841-843.
29. Solovjeva L.V., Vladimirov B. M., Dneprovskaja JI. B. et al. Kimberlites and kimberlite-like rocks. Upper mantle beneath Siberian craton, Nauka, Novosibirsk, 1994, 256 pp. (in Russian).
30. Takahashi E. Speculations on the Archean mantle: Missing link between komatiite and depleted garnet peridotite // *J. Geophys. Res.*, 1990, v. 95, p. 15941-15954.
31. Walker R. J., Carlson R. W., Shirey S. R., Boyd F. R. Os, Sr, Nd and isotope systematics of southern African peridotite xenoliths: implications for the chemical evolution of subcontinental mantle // *Geochim. Cosmoch. Acta*, 1989, v. 53, p. 1583-1595.
32. Walter M. J., Sisson T. W., Presnall D. C. A mass proportion method for calculation melting reactions and application to melting of model upper mantle lherzolite // *Earth Planet. Sci. Lett.*, 1995, v. 135, p. 77-90.
33. Walter M. J. Melting of garnet peridotite and the origin of komatiite and depleted lithosphere // *J. Petrology*. 1998. V. 39. N 1. P. 29-60.
34. Walter M. J. Melting residues of fertile peridotite and the origin of cratonic lithosphere // *Mantle petrology: field observations and high pressure experimentation* (Ed.: Y. Fei, C. M. Bertka, B. O. Mysen). The Geochemical Society, Special publication N 6. 1999. P. 225-239.
35. Wei K., Tronnes R. G., Scarfe C. M. Phase relations of aluminum-undepleted and aluminum-depleted komatiites at pressures of 4-12 Gpa // *J. Geophys. Res.*, 1990, v. 95, p. 15817-15827.
36. Xie Q., Kerrich R., Fan J. HFSE / REE fractionations recorded in three komatiite-basalt sequences, Archean Abitibi greenstone belt: Implications for multiple plume sources and depths // *Geochim. Cosmoch. Acta*, 1993, v. 57, p. 4111-4118.

EVOLUTION OF THE CENTRAL ASIAN "HOT" FIELD IN THE PHANEROZOIC AND SOME PROBLEMS OF PLUME TECTONICS

M.I. Kuzmin¹, V.V. Yarmolyuk², V.I. Kovalenko², V.G. Ivanov¹

¹ *Institute of the Geochemistry SB RAS, Irkutsk, Russia*

² *Institute of Geology, Mineralogy and Ore Deposits, RAS, Moscow, Russia*

INTRODUCTION

In the science of geology the new paradigm called the deep-seated geodynamics has been recently put forward. It is aimed at evaluation of global processes with regard to interaction of the Earth's shell at different depths. The hot fields of the mantle have become the study objects for considering the deep-seated geodynamics. They were first distinguished in 1983 [Zonenshain, Kuzmin, 1983] based on delineating of the occurrences of intraplate magmatism on the Earth surface. The total of four fields not associated with lithosphere plate boundaries have been recognized. The two large fields (Pacific and African) have dimensions 10000-12000 km across and two minor fields (Central Asian and Tasmanian or Australian-Antarctic) which are 2000-3000 km across. The geoid-shaped anomalies are supplementary characteristics of these fields. Positive anomalies of the geoid about +80 m are confined to large fields (Pacific and African), while "small" fields are typified by negative anomalies from -20 to -80 m [Zonenshain, Kuzmin, 1994]. Large fields are recognized from the increased position of the asthenosphere mirror understood as hypsometric position of the spreading axes relative to the sea level. In the African field it achieves 500-1000 m above the sea level. In the African field it reaches 500-1000 m above the sea level (Ethiopian and Iceland rifts).

The intraplate magmatism is typified by associations of increased alkalinity, that is alkaline basalts, alkaline gabbroids, phonolites, trachytes-comendites, pantellerites and others. In some segments of mid-oceanic ridges crossed by hot fields, the oceanic basalts consist of E-MORB varieties. Their major difference from N-MORB basalts typical for the rest segments of rift zones of oceans is due to enrichment (by 2-3 times) in coherent elements contents, e.g. light lanthanoids. This indicates the relationship of the intraplate magmatism sources with the mantle different from depleted mantle which is the source of N-MORB basalts.

The assumptions were made both on the juvenile, low mantle source of such melts and on the recycled one in the subduction processes of lithosphere origin of the enriched mantle.

The geological, geochemical and paleomagnetic data are attracted for considering this subject. Based on such data the correlation was found between

inversions of the magnetic field of the Earth which were undoubtedly associated with the dynamics of the core, the volume of intraplate magmatism products. The resultant statement points to the low mantle origin of hot fields of the Earth mantle (Larsen, Zonenshain, Kuzmin). Having this in mind, the idea was offered on the two-layer mantle convection, and the upper mantle convection is responsible for the processes associated with plate tectonics, whereas the ascending of plumes occurs from the lower mantle, layer "D" (boundary between the core and mantle of the layer with high temperature (1000o) gradient) are due to the processes of intraplate magmatism [Zonenshain et al., Zonenshain, Kuzmin, 1994]. The experimental works by Dobretsov and Kirdyashkin (1994) showed the possibility of two-layer mantle convection.

The results of seismographic investigations were crucial in considering the problem on the deep-seated structure of the Earth. The studies by Dzevonsky (???), Japanese geophysicists [Fucao et al., 1994; Maruyama, 1994] assume existence in the mantle of high- and low-velocity zones which are traced from the bottom of lithosphere to the core. It appears that they were compared with the "cold" and "heated", accordingly or partially melted (low velocity) mantle. It is to be underlined that with such interpretation heated mantle is located under the African and Pacific hot fields, while the projections of cold (high-velocity) areas of the mantle correspond to the minor Central-Asian and Tasmanian fields.

Using interpretation of these data the Japanese geophysicists offered the following model of circulation of the mantle material in the Earth. In the cold Asian plume the cold subducted substance descends down the mantle of the Earth to "D" layer. The response of this layer to transport of cold ("heavy") substance causes squeezing of hot plumes in the other places which looking as a huge mushroom rise to the lower mantle splitting into a series of isolated plumes in the upper mantle and a chain of "hot spots" in the lithosphere.

Considering the history of Rhodinia splitting which resulted in formation of the Pacific and Paleo-Asian oceans and later (?) Uralian, Japetus and other oceans [Maruyama, 1994], they proposed the following model of Earth evolution. After splitting Siberia amalgamated with a series of continental blocks, including Northern and Southern China which formed Eurasia and caused subsiding of the cold lithosphere material in the Permian and Triassic continuing subsidence in subduction zones to the core-mantle boundary. The presence of such a "cold" crater had to lead to formation of sedimentary depression basins and absence of intraplate magmatism in contrast to the area of issue towards the hot plume surface.

However, analysis of P2-T1 geological events on the Eurasian continent, made by Dobretsov [Dobretsov, Kirdyashkin, 1993] shows that this stage is marked by origination of the Siberian platform traps. The early phase of alkaline magmatism of the Maimecha-Kotuy province is dated by the same age (253-255 Ma). This time or much earlier (Carboniferous) is related to formation of a wide spectrum of granitoid rocks on Altay, Trans-Baikal, Mongolia, Northern China.

Some of them may be due to the palingenesis processes under influence of hot mantle flows. It is evident that a widespread formation of magmatic rocks is referred by Dobretsov to the system of deep-seated low-mantle plumes. Their action on the asthenosphere caused uplifting of the larger part of the North Asia territory, while on the termination of this uplift originated practically closed system of sedimentary basins. A high magmatic activity retained over the territory in later stages of the geological history which is in contradiction with the conclusions of the Japanese geologists and requires clarification of the causes for this activity to take place in the region characterized by predominance of “cold” mantle in the basement.

In our study we decided to provide a simple explanation of hot and cold plumes from the viewpoint of presence and absence of intraplate magmatism. For this purpose we considered the products of intraplate magmatism of Central Asia which are available within the Siberian craton and its folded surroundings from Cambrian to Ordovician up to now.

INTRAPLATE MAGMATISM IN THE PHANEROZOIC HISTORY OF NORTH ASIA

The intraplate endogenous activity on the Asian resulted in the system of grabens, horsts, domal uplifts and occurrences of magmatic rocks of increased alkalinity, which are characterized by heightened contents of incoherent elements [Yarmolyuk et al., 2000].

In the Early- Mid-Paleozoic epoch the intraplate magmatic rocks started their development in the Altay-Sayan and Viluy areas (Tab. 1).

The Altay-Sayan area of intraplate magmatism covers the territory of Minusinsk basin, Tuva, Eastern and Western Sayan and North-Western Mongolia with the area 500x700 km. This is where geochronological investigations of rocks were carried out in a series of plutonic complexes and “dumb” volcanic associations. The results made us postpone the time of the area origination by nearly 100 Ma by the onset of Ordovician. The most common are the rocks of the Sangilensky complex with the age 460-450 Ma. Since that time and by the beginning of Devonian the intrusive activity was continuous and resulted in formation of massifs of ultrabasic alkaline rocks, nepheline syenites, alkaline and Li-F granites. The range of ages of these rocks detected by Rb-Sr and K-Ar methods vary between 450 and 400 Ma. The peak of intraplate activity in the region was in the Early Devonian. This was the time of scattered rifting which led to formation of numerous depressions and grabens scattered over the region, and it was accompanied by large-scale eruptions of lava of primarily basic composition, e.g. basalts, tephrites, trachybasalts, as well as phonolites, trachytes, trachyrhyolites and comendites. The eruptions were accompanied by intrusions of teshenites, alkaline granites and syenites. In the Middle Devonian magmatic

activity attenuated. The extent of magmatic activity in the Altay-Sayan area was significant. Thus, in the Minusinsk basin 50000 cubic meters of lava were erupted. So it can be inferred that that over 100000 cubic meters of igneous rocks were formed.

Table 1.

Epochs, provinces and areas of intraplate magmatism.

Epochs and stages of activity	Provinces and regions of intraplate activity (numbers in brackets indicate the dates of rocks, Ma)	
Early-Middle Paleozoic	Altay-Sayan	
Late Silurian– Early Devonian Ordovician-Silurian	Alkaline magmatism [490, 460, 450-410] – rift stage – [400-390] – alkaline magmatism [375]	Viluy – alkaline magmatism of domal uplift – rift stage – alkaline magmatism
Late Paleozoic - Early Mesozoic	Barguzin-Vitim [330 – 290]	Rift system of Central Asia, Late Paleozoic, including: – Gobi-Tien-Shan rift zone [310-285]
Late Carboniferous– Early Permian	Synnyrsky and Udino-Vitim rift zones, Angara-Vitim batholith	Gobi-Altay rift zone [275] – North Mongolian rift zone [265-250]
Mid-Permian	Siberian trappean [255-235]	– formation of zonal-symmetric Khangay magmatic area [255-250]
Late Permian- Early Triassic	West Siberian Rift system [235-218]	Early Mesozoic – formation of zonal-symmetric Khentey magmatic area [235-190]
Late Mesozoic Early Cenozoic Late Jurassic	Central-Asian intracontinental	
Early Cretaceous	– origination of the hot spots system: South-Khangay (SKh), East-Mongolian (EM), West-Zabaikalian (WZ), Central-Aldan (CA) [170-140] – formation of graben system (rifting) in SKh, EM, WZ areas with plateau-basalt eruptions [140-100] – suppressed eruptions in volcanic areas of SKh, WZ and CA [100-30]	
Late Cretaceous – Early Cenozoic		
Late Cenozoic	Central and East Asian intracontinental – rejuvenation of magmatism in SKh, WZ and CA areas; origination of the new rift system (Baikalian and Shansi) and hot spots (South Baikalian, Darigangsky, etc.) [<25]	

Viluy region is known for origination of a series of rift zones. The earliest magmatic events are dated as the Late Silurian. They proceeded on the background of growing uplift in the central part of the region and were characterized by high-alkaline composition of igneous rocks represented by trachytes, trachybasalts, trachytes, phonolites, as well as massifs of ultrabasic alkaline rocks with carbonatites lying on the eastern edge of the Siberian platform and Sette-Dabanu. The phase of the highest tectonic and magmatic activity covered the Middle and Late Devonian. It was followed by splitting of domal uplift of the triple system of grabens and accompanying splitting of plateau eruption of subalkaline and tholeiite basalts. The eruption were intermittent with sedimentation which resulted in formation in the grabens of many kilometers long sedimentary volcanogenic sequences. In time of formation of the area there were erupted voluminous magmatic products. Only in the Viluy belt of grabens their amount was estimated approximately to be 100000 cubic meters.

Late Paleozoic - Early Mesozoic epoch corresponds to the events occurring between 330 and 185 Ma. It was the time of most large-scale intraplate processes covering the entire territory of the Late Paleozoic North-Asian continent. It consists of the belt of subparallel rift zones filled with bimodal basalt-comendite and basalt-pantellerite associations and controlling distribution of numerous massifs of alkaline granites and syenites. The belt originated on the southern active continental margin and extended for over 3000 km with the width 600 km through the territory of Western Zabaikalia, Mongolia, North-Western China, including Tarim and Eastern Kazakhstan. The shift for about 600 km is observed between the rifting zones and the Siberian continent margin (310-290 Ma) far inside (260-250 Ma). Few stages are marked in this epoch.

The early stage includes origination of the Gobi-Tien-Shan rift zone over the the Siberian paleocontinent margin with Rb-Sm isochron dates 310-285 Ma, as well as formation over the territory of Zabaikalia of the Angara-Vitim granitoid batholith with the area 500x300 km. The latter is outlined by the belts of intrusions and massifs of alkaline-ultrabasic and basic rocks, alkaline granites and syenites referred to the Synnyrsky complex (300-285 Ma) in the north, in the south they are referred to the Saizhensky (320-390 Ma) and partly to Zazinsky one.

Permian-Early Triassic stage covers the time span 280-240 Ma and corresponds to the completing of formation of the structural framework of the Central Asian rift system. The moving zone of the rift formation inside the continent in the Late-Early Permian caused formation of the Gobi-Altay and in the Permian North-Mongolian rift zones, and along with them there emerged the Khangay granitoid batholith which formed similarly to the Angara-Vitim batholith under the influence of intraplate sources of heat. The age of batholith rocks, estimated after U-Pb dates of zircons to be 255-250 Ma.

Together with formation of the Central-Asian rift system in the end of the Permian-beginning of Triassic there occurred the most voluminous plateau-basalt eruptions with formation of the trappean province of the Siberian platform. Its

products covered the area over 1500000 square km. Formation of the trappean area evidently began in the its north-western part in the Maimecha-Kotuy and Norilsk regions where alkaline basaltoids and subalkaline differentiated basalts erupted within the time span 253-246 Ma.

The Early Mesozoic stage (T_{2-3} - J_1 ; 230-185 Ma) is characterized by the migration of the areas of preceding stage eastwards. It was the time when zonal symmetric magmatic area reminding the Permian area in structure, came into sight within the Central-Asian foldbelt. However, in contrast to the latter its core (Khentey batholith) was shifted towards east from the core of the Permian area (Khangay batholith) nearly by 800 km. The age of batholith with the total area over 50000 square km is evaluated to be Mid- Late Triassic based on geological data, as well as in accordance with the results of Rb-Sr dating of rocks of its major Kyrinsky (229 Ma) and Mesinsky (206 Ma) complexes.

In the Early Mesozoic the intraplate activity proceeded within the north-western framing of the Siberian platform. The West Siberian region was dominated by the rifting processes which split the Pre-Mesozoic foundation of the territory into a series of large rifts which fixed it. Grabens are filled with Triassic sequences composed of volcanic series (basalts, alkaline basaltoids, rhyolites) and clastic rocks. The largest Urengoy graben opened in the northern part as so-called paleo-ocean with newly formed oceanic crust in the basement. The time of its formation is defined within the interval 235-218 Ma.

By the period 190 Ma the intraplate activity decayed sharply thus indicating termination of the Late Paleozoic - Early Mesozoic epoch.

The Late Mesozoic - Early Cenozoic epoch covers about 150 Ma of the geological history of the region since Middle Jurassic (~ 170 Ma) and to the beginning of the Miocene (~25 Ma). Throughout this epoch the character of magmatic activity changed and the two stages in the magmatism development were recognized.

Late Jurassic - Early Cretaceous stage (170 - 100 Ma) corresponds to the time of formation of the East Mongolian, West-Zabaikalian, South-Khangay and Central Aldan volcanic areas. Their development was due to the rifting processes and were accompanied by sufficiently large-scale magmatic activity. Along with predominant plateau basalts in these areas originated volcanic associations with trachytes, trachyrhyolites, pantellerites, phonolites, tephrites. as well as small and rare massifs of nepheline and leucite syenites, alkaline syenites and granites, Li-F granites and ongonites, shonkinites and carbonatites. The peak of tectonic and magmatic activity occurred in the beginning of the Early Cretaceous (130-140 Ma).

Late Cretaceous - Early Cenozoic stage (100-25 Ma) is marked by suppressed but regular magmatic activity. In the West Zabaikalian, South-Khangay and East Mongolian areas there formed small lava fields and shield volcanoes. The composition of volcanic products was defined by the basic alkaline products, e.g. tephrites, basanites, nephelinites and subalkaline basalts.

The Late Cenozoic epoch (< 25 Ma) is related to the processes of the recent intraplate volcanic and tectonic activization which covered the territory of Central and East Asia. The magmatic activity corresponded to the continuation of the Late Mesozoic - Early Cenozoic magmatic history in the West Zabaikalian, South-Khangay and Central Aldan volcanic areas which incorporated extensive lava plateaus like Vitim, Central Khangay, and Udokan. At the same time, there originated a series of new volcanic areas like South-Baikalian and Darigangsky associated with origination of the new hot spot system. Their activity led to formation of numerous large lava fields scattered over the territory of Central and East Asia. The South Baikal volcanic area is characterized by the most prolonged and multi-stage magmatic history. The volcanic products of the epoch consist exclusively of the lavas of basic composition of increased alkalinity.

The materials provided point out that throughout Phanerozoic period the intraplate processes proceeded within the Siberian craton and its southern and western folded framing. They were located within separate areas typified by the following features of the geological history:

- (i) long-term development (tens of Ma) of intraplate activity in the region;
- (ii) Relatively constant position within the continent;
- (ii) Continuous magmatic activity with characteristics intraplate magmatic specialization;

As regards the volume of intraplate magmatic rocks of different ages, it should be marked that during entire Paleozoic and Mesozoic the intensity of magmatism actually did not vary (Fig. 3). An exception was interval 253-246 Ma - the time eruption of Siberian traps when for a short period over $1.5 \times 10^6 \text{ km}^3$ of magmatic rocks erupted [Zonenshain et al., 1991].

In the Late Cretaceous there was a sharp fall to 100 cubic kilometers in the intraplate magmatism volume. Insignificant extent in magmatic activity retained to the end of Oligocene, and only in the Late Cenozoic (< 25 Ma) the volume of erupted lavas achieved the level of magmatic productivity in the first half of the Late Mesozoic.

FEATURES OF COMPOSITION OF INTRAPLATE MAGMATISM PRODUCT IN CENTRAL ASIA

Figure 1 represents the spidergrams for Siberian platform traps [Almukhamedov et al., 1999] and Mesozoic basalts of Western Zabaikalia. The formations of the Siberian platform margins were contributed by involvement of the undepleted mantle of EM-II type. It is clear that traps are well correlated with the basalts of oceanic islands, while Mesozoic basalts of Western Zabaikalia against OIB basalts are enriched in Ba, K, La, Pb, Sr, Nd, P, Li and impoverished in Th, Nb, Ta, Hf and Mo. It should be noted that the Mesozoic granitoids of

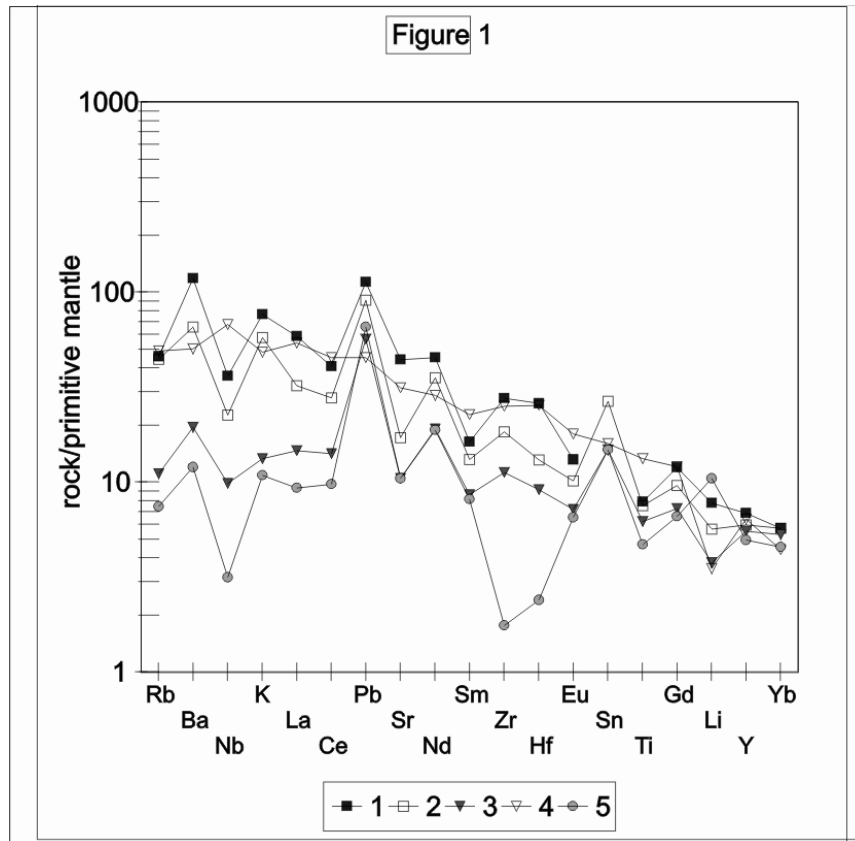


Fig. 1. 1 - Central Mongolian rift zone; 2 - subalkaline basalts of Siberian platform; 3 - tholeiites of Siberian platform; 4 - OIB; 5 - gabbroids of Angara-Vitim batholith

Zabaikalia making up the core of the Mesozoic zonal tectonic-magmatic area, have analogous anomalies of the composition as compared to the average composition of the Earth [Taylor, McLennan, 1988], depleted in Nb, Ta, Hf, and Mo and enriched in Ba, Li (Fig. 2). Similarity in the composition of basalts - the derivatives of the mantle sources and crustal granitoids are evidently the evidence of the effect of trans-magmatic fluids onto the crust, which stimulated the processes of anatexis along with the heat of melts.

To characterize the sources of magmatic melts which were involved in formation of intraplate magmatism we conducted systematic investigations of the isotope composition of Sr and Nd in the basites of different magmatic areas. All the results are yielded in Figure 3. It should be underlined that the data used characterize the rocks of basic composition. They formed from the mantle sources and thus represent the compositions of mantle plumes responsible for intraplate activity. The classification of magmatic mantle sources is given below after Hoffman [Hoffman, 1997].

The basic rocks of the Devonian associations of Northwestern Mongolia (Altay-Sayan area) are noticeably different from magmatic rocks of later epochs of magmatism. Their compositions correspond to the source of melts which was largely depleted relative to rare-earth elements ($\epsilon_{Nd} > 4$) and was characterized by wide variations of the values ϵ_{Sr} . Along with moderately depleted mantle of

PREMA (or OIB) type their formation was contributed by the Rb- and radiogenic Sr-enriched mantle of EM-II type.

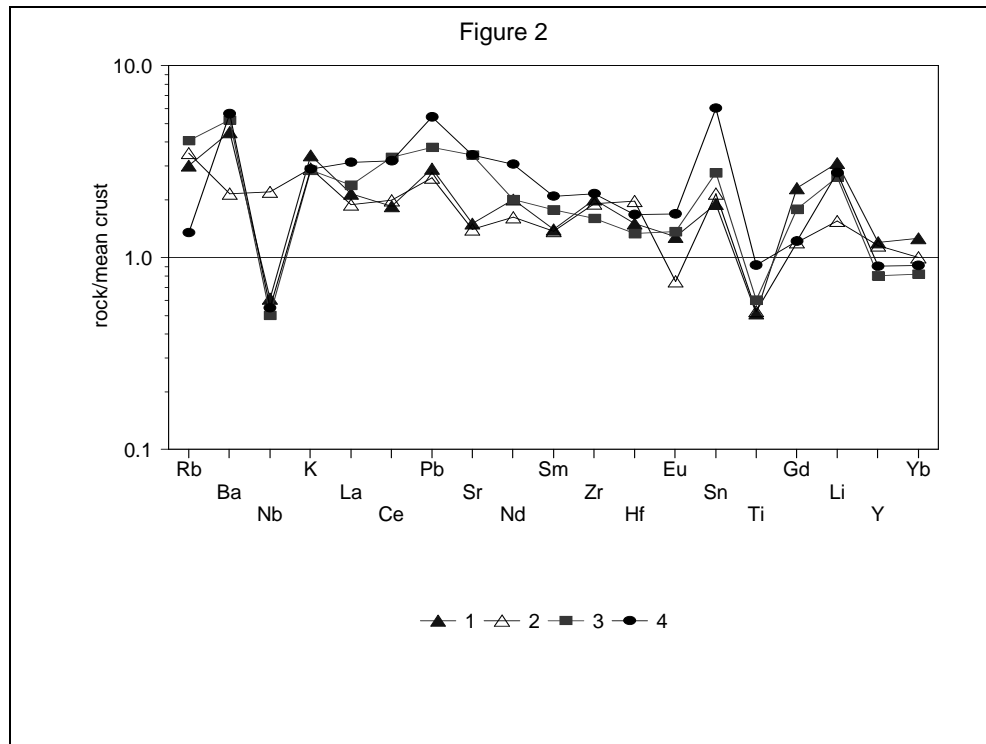


Fig. 2. 1 - granites of West Zabaikalia; 2 - upper crust; 3 - early phase of Angara-Vitim batholith; 4 - main phase of Angara-Vitim batholith

For magmatic associations which formed in the Late Paleozoic - Early Mesozoic and Late Mesozoic epochs of intraplate magmatism similar compositions of sources are established. These fields are located between the compositions of two types of mantle sources: radiogenic Sr enriched mantle (EM-II) and moderately depleted mantle (PREMA) which assumes their participation in rock formation. Participation of PREMA source was of secondary importance, for it did not lead to formation of rocks with corresponding isotope parameters and only defined elongation of the field of compositions of intraplate rocks in the appropriate direction.

In this respect it is interesting to compare the isotope composition of the Siberian platform traps, synplutonic basite intrusions which accompany formation of the Angara-Vitim batholith and basalts of the Late Paleozoic rift system in Central Asia. They all produce a compact field on the diagram (Fig. 3). The basalts of the Gobi-Tien Shan rift zone are somewhat distinguished on their background. They differ from basalts of other Late Paleozoic rift zones of Central Asia by more depleted compositions (ϵ_{Sr} to -15 and ϵ_{Nd} to +7). As was shown [Kovalenko et al., 1999] this specific feature was defined by a simultaneous participation in magma formation of different sources of melts, namely enriched material of the mantle plume and depleted mantle of non-subducted wedge.

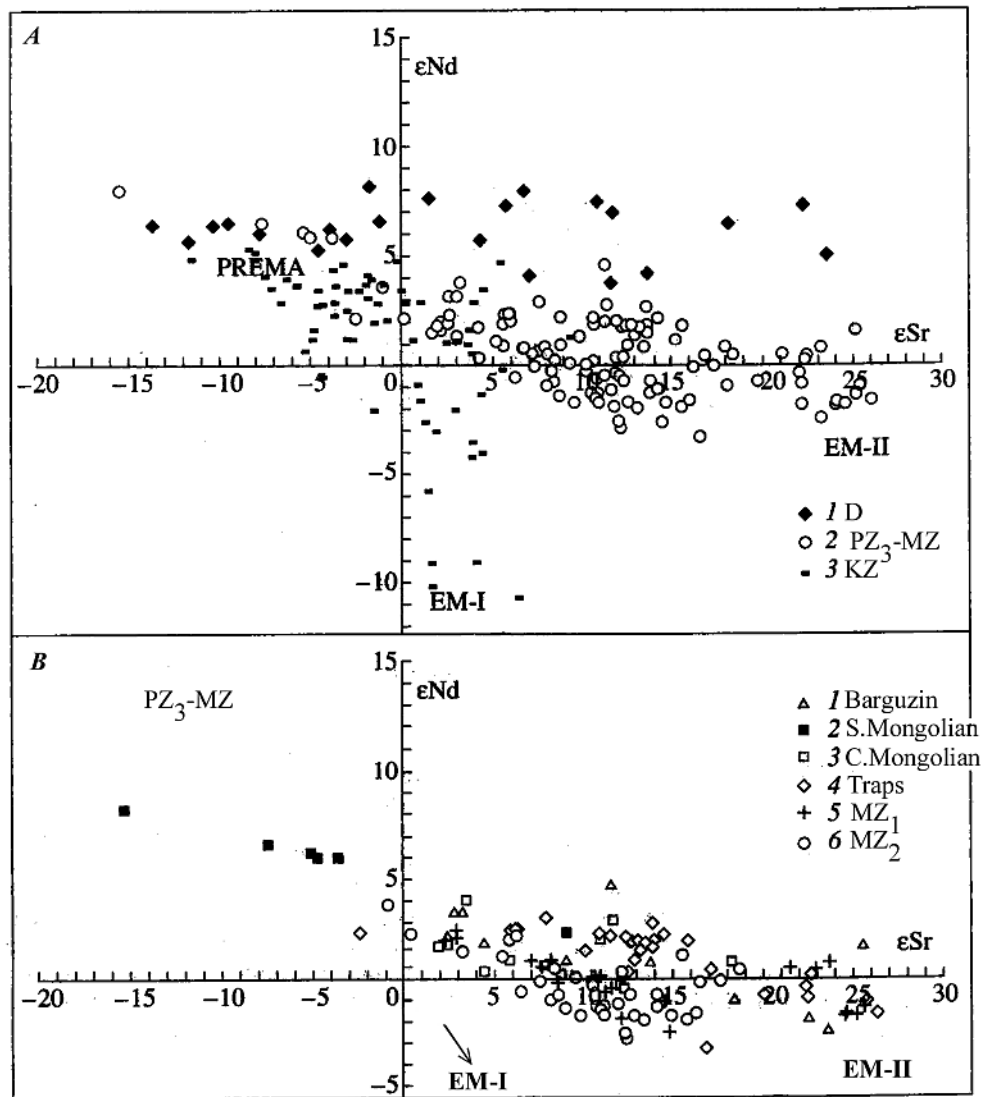


Fig. 3 See text.

In general the field of compositions of intraplate magmatic rocks most specific are Early- and Late Cenozoic basites (Fig. 3). They are typified by moderately depleted isotope compositions (ϵ_{Sr} to -10 and ϵ_{Nd} to +7), corresponding to the PREMA type mantle, as well as compositions enriched in Nd relative to Sm (ϵ_{Nd} to -10) at insignificant variations of the isotope composition with Sr. The latter are typical for the products of melting of the enriched mantle of EM-I type [Hoffman, 1997].

The differences in the isotope compositions of magmatic sources have the age trend. As evident from Fig. 4, in Central Asia predominant are the products in which the isotope composition of Nd is close to CHUR (EM-II type mantle after Nd-Sr isotope classification, Fig. 4). They are attributed to the epochs of the highest magmatic productivity and originate in the Devonian and become dominant from the beginning of the Late Paleozoic. In the end of the Mesozoic and Cenozoic the moderately depleted sources of magmatism (PREMA) predominated,

which coincided with a sharp decay in magmatism productivity [Yarmolyuk et al., 2000]. The sources of magmatism were found to have in the Late Cenozoic mantle of EM-I type, its appearance is in accord with rejuvenation of intraplate activity.

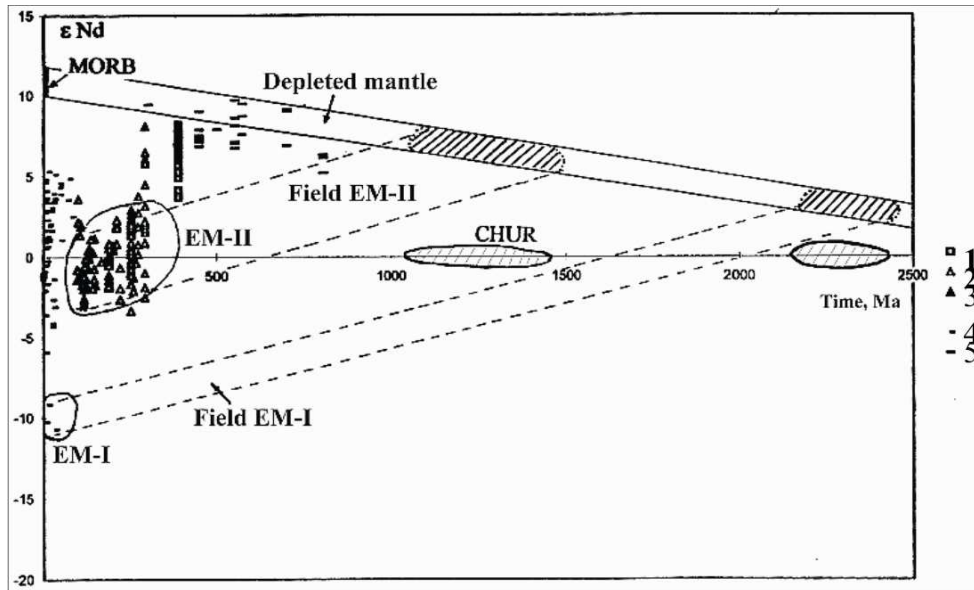


Fig.4. Isotope composition variations of Nd basites of magmatic associations in North Asia versus the age of their formation and model ages of their sources.

Magmatic associations: 1-4 intraplate: 1 - Middle Paleozoic, 2 - Late Paleozoic, Early and Late Mesozoic in genera, 3 - Late Carboniferous - Early Permian Gobi-Tien Shan rift zone formed with depleted mantle involved, 4 - Late Cretaceous - Early Cenozoic; 5 - ophiolite complexes.

Diagram 4 displays the isotope compositions of Nd ophiolite complexes of Central Asia, accordingly [Kovalenko et al., 1999]. The rocks of ophiolite complexes lie in the field of compositions of depleted mantle. It should also be noted that some compositions of these rocks indicate the evidence of contribution of the enriched mantle sources in their formation. This agrees well with geological data providing evidence on participation of oceanic island rocks in the structure of ophiolite complexes, e.g. Dzhida zone [Al'mukhamedov et al., 1996] and in variscides of South Mongolia. In particular, these data point to the presence of mantle plumes both under continental masses and in the oceanic basins surrounding continents.

DISCUSSION OF RESULTS

The geochemical investigations, with regard to the history of development of intraplate magmatism, are applied to construct the isotope-geochemical model of the mantle under the Central Asian field [Yarmolyuk et al., 2000].

Formation of intraplate magmatism of Central Asia was associated with the mantle source of PREMA, EM-I and EM-II type. Among them the leading role belonged to EM-II mantle mixed with the PREMA source. This mantle was involved in the intraplate magmatism of different magmatic areas of North Asia at

least since Late Paleozoic and to the Late Cretaceous, that is during 200 Ma. If basalts of the mid-oceanic ridges, which contributed to formation of ophiolites of all Phanerozoic foldbelts of Central Asia (to Early Mesozoic, included) are the products of the depleted upper mantle, the intraplate basalts correspond to the sources PREMA or EM-II related to deeper shells of the mantle.

In the history of intraplate magmatism of North Asia the change of the depleted mantle EM0II for moderately depleted mantle PREMA in the melt source coincided with a sharp drop of productivity of intraplate magmatism and cessation of tectonic activity. It appears that decay in activity is associated with the change of thermal state of the Earth interior and subsidence of isotherms into the mantle depth. The consequence should be subsidence of the level of mantle plume origination which enables to assume a deeper location of the PREMA type mantle relative to EM-II mantle. It should be kept in mind that PREMA type mantle is the source of the main bulk of basalts of oceanic islands and it is believed to be located in the low mantle.

The next change of the composition of intraplate magmatism sources coincided with the outburst of intraplate activity in the Late Cenozoic in Central and East Asia. It seems that this outburst had to be initiated by the thermal impulse in the basement of the mantle plume. It is supposed that the EM-I mantle was the carrier of this impulse. Its products first appeared in the composition of intraplate associations from that time. Thus, we assume its deeper occurrence relative to the other types of mantle sources.

EM-II and EM-I sources enriched in Sr and Nd may be linked with the crustal and lithosphere remains buried in subduction zones. If this is valid, the age of EM-II sources of the intraplate associations of North Asia is estimated to be 1,1 - 1,5 Ga lithosphere and that of EM-I source is 2,3 - 2.5 Ga (Fig. 4).

It may be assumed that EM-II source sits on the boundary of the upper/low mantle, while EM-I source descended to the boundary of the low mantle with core.

Consideration of the Phanerozoic history of the Siberian continent shows that practically all this time the continent contacted with the mantle plumes. That fact that plumes belong to the unified system undergoing common laws of development is underlined by the similarity of the source composition which participated in their formation. This system of plumes was referred to as the North-Asian superplume [Yarmolyuk et al., 2000]. Its dimensions may be judged from the area within which was the intraplate activity and which in the Paleozoic epochs of superplume development covered the area of North Asia. It is believed that superplume had the structure of gigantic mushroom, with its hat diminishing due to insufficient thermal influx causing dying off of separate plumes. The most active and long-living in this system was the Central Asian plume which was evidently located under the superplume basement. The reconstructions of Siberia movement in the Phanerozoic [Yarmolyuk et al., 2000] indicate that in the Paleozoic-Mesozoic time Siberia was in the zone of influence of the African-Atlantic field, in particular since the end of

Paleozoic- beginning of Mesozoic and its northern "Iceland" part. This somehow agrees with the conclusions of some authors on the possible relation of Siberian traps with the Iceland hot spot. However, in the Late Mesozoic the area of intraplate magmatism of Central Asia lost the link with "hot field or mantle superplume" and displaced to the zone of "cold" plume. It is evident that intraplate magmatism was associated with dynamics of development of "cold" plume. This should be considered in making up the potential models of intraplate magmatism in time.

The reconstructions made enable to propose the following model of evolution of the Central Asian hot field in the Phanerozoic [Yarmolyuk et al., 2000]. After splitting of Rhodinia and Siberian continent drift to the northwest in the Cambrian it fell in the field of influence of African-Atlantic hot field. It appears that since Cambrian the Siberian continent developed under the influence of Central Asian (at present African-Atlantic) of the hot superplume (Fig. 5). However in the history of the Siberian craton and its foldbelt there were evidently lithosphere movements with different depths of the bottom occurrence of moving lithosphere-mantle blocks. In some cases these blocks included mantle shells up to the layer stimulating the intraplate activity and thus covered practically entire upper mantle. This ensured preservation of the root system of mantle flows and permanent position of the areas covered by intraplate activity on the Earth surface. In changing the geographic position of the continent. Such displacements may be inferred for the Central Asian plume in the Middle and Late Paleozoic. In other cases the sliding surface located essentially higher and broke the column of mantle plume which caused cessation of intraplate development in some areas and origination in some others, in accordance with movement of the lithosphere block above the plume basement. Thus, this was the way how events developed in rotation of the continent above the Siberian plume. As a result, the link of the latter with the Barguzin-Vitim area was broken, and magmatic activity terminated, and new intraplate area originated with large-scale trappean eruptions on the site of stoppage of continental lithosphere under the mantle plume.

Further movement of continental masses relative to superplume evidently caused displacement along with lithosphere of deeper horizons of the mantle including the system of channels of intraplate activity and the sources of this activity and possibly covering the fragments of the upper parts of the low mantle. We assume that the cause of movement of such a powerful lithosphere-mantle packet was formation and development in the neighbouring area of the Earth of "cold" superplume which as if caught the fragments of the buried lithosphere from the adjacent areas of the mantle. Evidently, one of the most significant concentrations of such a lithosphere was in the mantle of the Asian continent, its crust formed with the subduction processes involved throughout Phanerozoic. As it appears, the flowing of buried lithosphere towards "cold" plume could lead to the movement of all shells containing lithosphere. As a result, the Asian continent

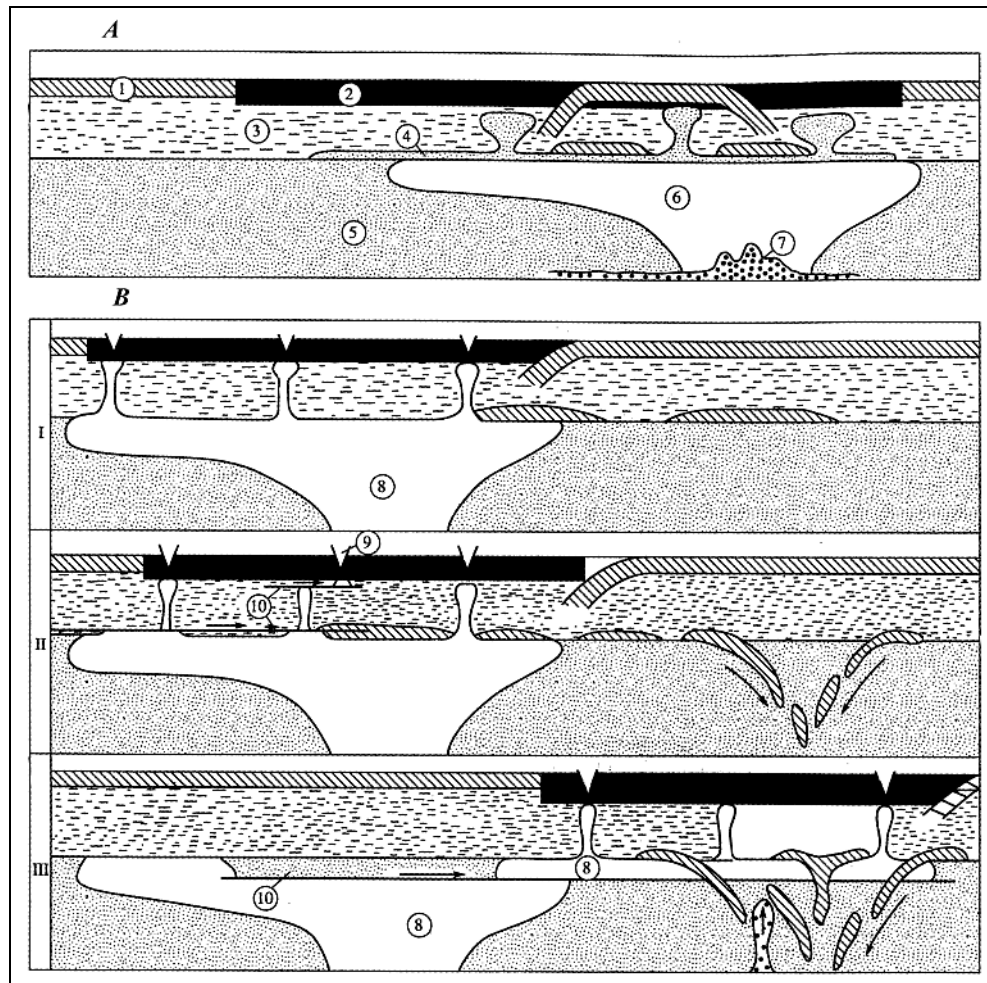


Fig. 5. The distribution of isotope sources of magmatism in the structure of the Asian superplume (A) and model of its evolution when it interacts with a “cold” superplume.

Numbers in circles: 1-2 – lithosphere: 1 – oceanic, 2 – continental; 3-8 – mantle: 3 – upper (depleted), 4 – enriches (EM-II type), 5 – lower, 6 – lower “hot” of PREMA type, 7 – enriched (EM-I type), 8 – “hot” mantle of the superplume on the whole, 9 – rifts and area of mantle hot spots, 10 – surfaces of deep stripping.

I – Pz₁₋₂, II – Mz₁, III – Mz₂-Kz

shifted and fixed its position above the “cold” superplume. The Central Asian province lost the association with its deep-seated low mantle roots, which brought to a gradual decay of intraplate activity. However, the relicts of “hot” mantle retained in the upper mantle of the region where they are fixed by the methods of deep-seated seismic sounding. The Late Cenozoic outburst of intraplate activity, like in the first variant was evidently due to the reaction of the core boundary and the lower mantle to the action from “cold” superplume.

The above reconstruction help to agree the notions on the existence of “hot” mantle under the Siberian continent throughout the larger part of the Phanerozoic with the data on its recent “cold” state.

The study was supported by the RFFR, grants 99-05-64209, 00-05-54623, 01-05-97250.

REFERENCES

1. Al'mukhamedov A.I., Gordienko I.V., Kuzmin M.I., Tomurtogoo O., Tomurhuu D., 1999, Dzhida zone as the fragment of the Paleo-Asian ocean. *Geotectonics*, # 4, p. 25-42.
2. Al'mukhamedov A.I., Medvedev A.Ya., Kirda N.P., 1999, Comparative analysis of geodynamics of the Permian-Triassic magmatism in East and West Siberia. *J.Geologia i Geofizika*, v. 40, # 11, p. 1575-1587.
3. Dobretsov N.L., Kirdyashkin A.G., 1993, Application of two-layer convection to structural features and geodynamics of the Earth. *J.Geologia i Geofizika*, № 1, p.3-26.
4. Dobretsov N.L., Kirdyashkin A.G., 1994, (1995) Deep-seated geodynamics . Siberian Branch Publ. 299 p.
5. Zonenshain L.P., Kuzmin M.I., 1983, Intraplate magmatism and its significance for nominal processes in the Earth mantle, *Geotectonics*, # 1, p. 28-45..
6. Zonenshain L.P., Kuzmin M.I., 1993, Deep-seated geodynamics, *J.Geologia i Geofizika*, № 4, p.3-12.
7. Kovalenko V.I., Yarmolyuk V.V., Kovach V.P. et al., 1999, Crust-forming processes and structure of the crust and mantle in formation of the Central-Asian foldbelt: Sm-Nd isotope data. *Geotectonics*, № 3, p.21-41.
8. Taylor S.P., McLennan S.M., *Continental crust, its composition and evolution*, Moscow: Mir Publ. . 380 p.
9. Yarmolyuk V.V., Kovalenko V.I., Kuzmin M.I., 2000, North-Asian superplume in the Phanerozoic: magmatism and deep-seated geodynamics, *Geotectonics*, № 5, p.3-29.
10. Dziewonski A.M., Woodhouse J.H. Three-dimensional Earth's structure and mantle convection – Abstr., 28th Int. Geol. Cong., 1989 Washington, v. 1, p. 427-428.
11. Fukao Y., Obayashi M., Inoue H., Nenfai M. Subducting slabs stagnant in the mantle transition zone // *J. Geophys. Res. B*. 1992. Vol. 97, N 4. P.4809-4822.
12. Hoffman A.W. Mantle geochemistry: the message from oceanic volcanism // *Nature*. 1997. V. 385. № 16. P.219-229.
13. Larson R.L., Olson P. Mantle plumes control magnetic reversal frequency // *Earth and Planet. Sci. Lett.* 1991. Vol. 107. P.437-447.
14. Maruyama S., Kumazawa M., Kawakami S. Towards a new paradigm in the Earth's dynamics // *J. Geol. Soc. Jap.* 1994. Vol. 100, N 1. P.1-3.
15. Zonenshain L.P., Kuzmin M.I., Bocharova N.Y. Hot-field tectonics // *Technophysics*. 1991. Vol. 199. № 2-4. P.165-192.

CARBONATITES OF INDIA: AN OVERVIEW

S.G. VILADKAR

Geology Department, St. Xavier's College, Mumbai 400 001, India, viladkar@bom2.vsnl.net.in

Carbonatite occurrences were unknown in India until 1963, when the first description of the Amba Dongar complex was published by Sukheswala and Udas (1963). Nevertheless, the intrusive nature of this carbonatite was first recognised by Sukheswala in 1960 when he visited Amba Dongar in connection with fluorite prospecting [Sukheswala, 1976]. No further fieldwork from the area was reported until 1963, when a note on the geology of Amba Dongar proper was published by Subramaniam and Parimoo (1963), who unfortunately failed to identify the carbonatites. At the same time, the work by Sukheswala and Udas (1963) appeared claiming the first discovery of carbonatite in India. The Geological Survey of India continued the mapping of Amba Dongar, and demarcated the zones of fluorite mineralization; estimating the fluorite deposits at approximately 11.6 million tons averaging 30 wt% CaF₂. This is the largest deposit of fluorite in India and one of the largest in the world. Later mapping by the students of the Geology department of St. Xavier's College, under the supervision of Professor Sukheswala established the presence of two more carbonatite-occurring areas proximal to Amba Dongar (Siriwasan and Panwad-Kawant), and thus the Chhota Udaipur area emerged as the largest carbonatite-alkalic province in the Deccan Trap terrain.

Subsequent to Amba Dongar discovery, many other carbonatite occurrences were reported from different parts of the Indian sub-continent. The Newania carbonatite, composed predominantly of magnesian rauhaugite and associated with a strong sodic fenite aureole, was recognised during investigation of associated radioactive minerals (pyrochlore) for the Department of Atomic Energy [Dar, 1964] and later confirmed by Deans (1967), and investigated in detail by Viladkar and Wimmenauer (1986) and Viladkar and Pawaskar (1989). Viladkar et al., (1993) and Viladkar (1998) reported highly uraniferous pyrochlore (20 to 22% U₃O₈), and hydrothermal veins rich in malachite and chalcopyrite.

During their examination of the vermiculite deposit associated with pyroxenite at Sevathur, in the north Arcot district of Tamil Nadu (also referred to as Koratti), V. Gopal and Joubin of U.N.D.P. (United Nations Development Program) reported carbonatite. This was later investigated by Borodin and the geologists of the State Geological Department [Borodin et al., 1971]. The discovery of carbonatite at Sevathur led to the discovery of several other carbonatites in the region, including the ones at Samalpatti and Pakkanadu. There are roughly 8 carbonatite occurrences related to the major NE-SW fault zone in

Tamil Nadu, and together form the largest carbonatite-alkalic province in South India.

Carbonatite discoveries at Sung Valley and Barmer came much later (1980's). Thus from 1963 onwards to this date about 30 carbonatite occurrences have been reported from different parts of India. Not all of these carbonatites form mappable units and some are volumetrically inconspicuous. Many of them occur as thin veins traversing host alkaline silicate rocks and in some cases their carbonatitic nature has yet to be established. It has already been stated [Sukheswala and Viladkar, 1978] that some of the so-called carbonatites, e.g. Hingoria [Udas and Krishnamurthy, 1968], Koteshwar, Chikti Mondri, and Netrang [Yellur, 1968] have not proved to be carbonatites. In this respect, the authors would like to point out that many of the carbonatite clusters shown in Woolley's (1989) distribution map of Indian carbonatites (around Amba Dongar, in Tamil Nadu, and along the Eastern Ghats) as well as some (especially around Amba Dongar) shown by Srivastava and Hall (1995) are misrepresented.

Of the total 31 carbonatite occurrences in India, only Amba Dongar, Newania, Sung Valley, and those located in Tamil Nadu will be discussed here as they have been investigated in somewhat greater details.

The distribution of Indian carbonatite-alkalic complexes is listed in Table 1. The majority of Indian carbonatites are emplaced in pre-Cambrian granite-gneiss terrains; Amba Dongar, Panwad-Kawant, and Siriwasan are exceptions since they intrude Bagh sandstones and Deccan basalts. The geochronological data is limited, however, available data shows that carbonatite-alkalic magmatism on the Indian sub-continent occurred over a large time interval, from pre-Cambrian to Eocene. The oldest carbonatite complex is Hogenakal (2000 Ma) [Natarajan et al., 1994], and the youngest is perhaps the Amba Dongar complex which seems to have emplaced during the late stages of Deccan volcanism either coinciding with or postdating the main phase of emplacement of Deccan Traps around 65 Ma [Courtilot et al., 1988] or 61.5 Ma [Deans et al., 1973]. In general, there are two distinct age groups; one associated with the Narmada-Son lineament with ages between 100 Ma and 65 Ma; the other group is defined by Proterozoic ages and occur along the Aravalli and Eastern Ghat rifts, and NE-SW trending major faults in Tamil Nadu. No true volcanic carbonatite has been reported thus far, however, recently Viladkar et al (2001) reported the presence of nephelinitic tuff and pyroclastics in western part of Amba Dongar complex.

CARBONATITE OCCURRENCES AND TECTONICS

Based on detailed geophysical and structural geology investigations, carbonatite-alkalic complexes of India are located in and are associated with six major tectonic rifts/lineaments. These include: 1- Eastern Ghat mobile belt; 2 - Narmada rift zone; 3 - Aravalli rift zone; 4 - Assam-Meghalaya plateau; 5 - Western Ghat faults; and 6 - Cuddapah-Godavari rifts.

The Amba Dongar carbonatite-alkalic complex is situated just 6 km north of the major Narmada fault zone [West, 1962; Choubey, 1971; Crawford, 1978; and Mishra, 1977]. It is interesting to note that aeromagnetic study of this lineament (Geological Survey of India), revealed the presence of seventeen plugs of ultrabasic rocks of various size, and some deep faults which may extend to a depth of 30 to 40 km [Krishnaswamy, 1982]. Westward extension of this lineament may explain the presence of carbonatite dikes in parts of Saurashtra [Mishra, 1981]. Further eastward, the Narmada lineament joins with another major rift - the Son lineament. Crawford (1978) also envisages eastward extension of the Narmada-Son lineament to the Assam-Meghalaya plateau, and possibly end at the eastern Himalayan syntaxial bend and westward into Madagascar with possible extension into southeastern Ethiopia [Crawford, 1978]. Of interest is the fact that the Sung Valley (Meghalaya) and Samchampi (Assam) carbonatite complexes seem to be situated along the eastward extension of the Narmada-Son lineament, however, this may be purely coincidental. The only carbonatite-kimberlite complex of India (Jungal Valley) is located within the Son-Valley rift. The Narmada-Son rift thus forms the largest lineament in central India, which has led some [Choubey, 1971; West, 1962] to believe that rifting has occurred over a considerable period of time from late Cretaceous to middle Tertiary.

The Assam-Meghalaya plateau was formed during the Mesozoic-Cenozoic collision between the Indian and Asian continents [Desikacher, 1974]. This plateau contains lineaments which trend E-W to ENE-WSW, and N-S to NE-SW, and according to Krishnamurthy (1988) the Sung Valley carbonatite is located at the intersection of these two lineaments.

The carbonatites from south India have been associated with the Nilgiri Rift [Udas et al., 1974], and it is [Udas et al., 1974] suggested that the block faulting movement occurred in several stages which resulted in NE-SW trending fault systems. Grady (1971) has shown six major faults trending between $N30^{\circ}E$ and $N40^{\circ}E$, and carbonatite complexes of Sevathur, Samalpatti, Jogipati, Reddipatti, Karapattu, Pallasurakkarai, and Pakkanadu are located along these fault zones. Few carbonatite occurrences have also been reported from the Eastern Ghat Mobile Belt. The kimberlitic rocks of Wajrakarur and Chelima are considered to be closely associated with this NE-SW trending graben, which cross cuts the Cuddapah basin in the east and crystalline complex in the west. Several other carbonatite-nepheline syenite complexes, Kunavaram, Medupalli and Arepalli, are also located along this major fault structure.

In northwestern India, the oldest rift, Aravalli, trends practically NE-SW, and Mishra (1982) showed the presence of two prominent lineaments striking NE-SW; major hydrothermal, base metal deposits of Rajasthan are located along these lineaments. Both the Mundwara and Newania carbonatite-alkaline complexes are situated within the Aravalli Rift zone and associated lineaments. Further to the west, the Sarnu-Dandali nephelinite-carbonatite complex is located proximal to

another lineament present on either side of the Luni Valley [Narayan Das et al., 1978].

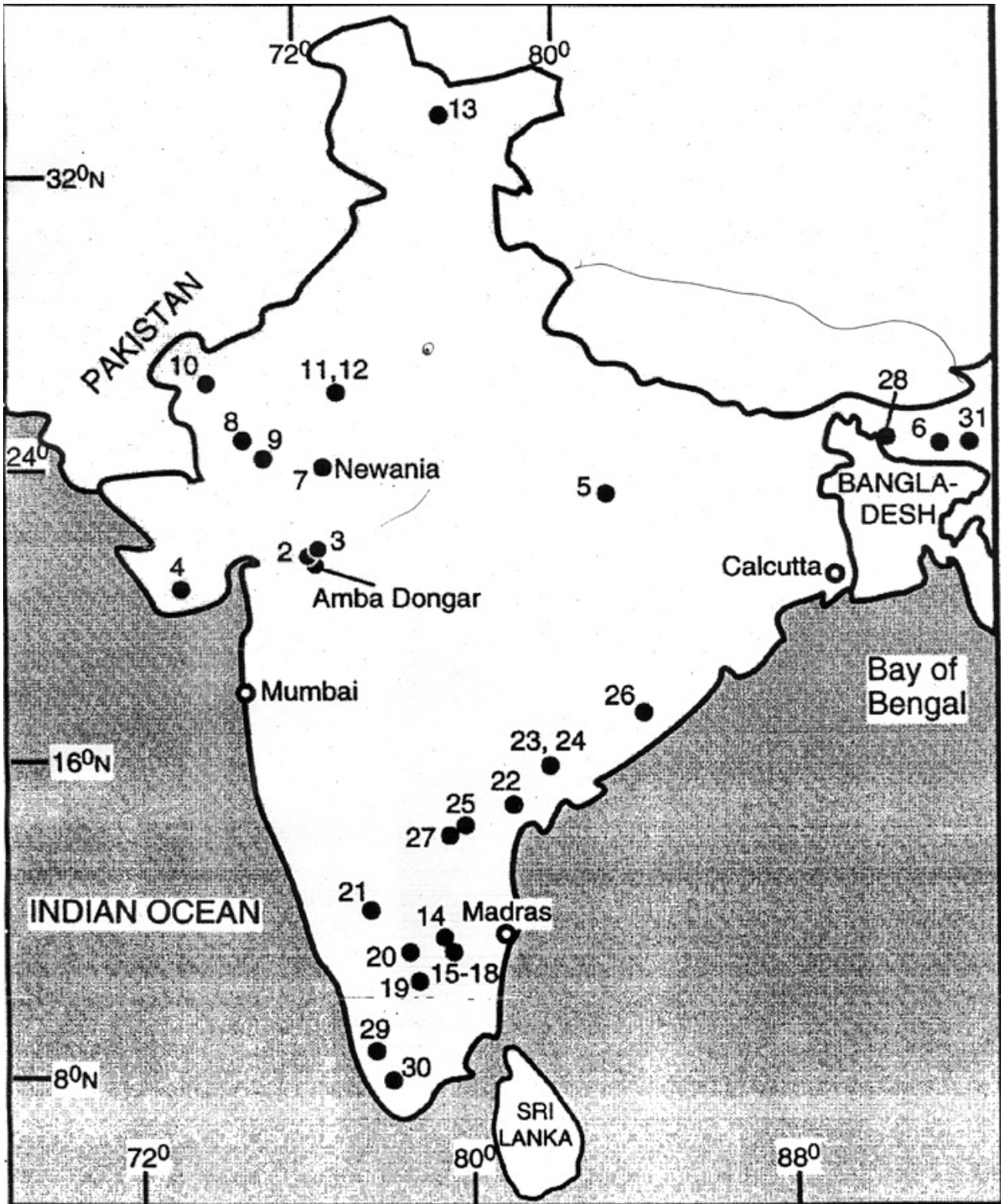


Table 1.

Distribution of carbonatite-alkalic complexes of India.

Name	Age (Ma)	Form, associated rocks	Economic minerals	References
1. Amba Dongar, Gujarat		Subvolcanic diatreme with ring-dike of sövite and plugs of ankeritic carbonatite	11.6 mt of fluorite	Sukheswala & Udas, 1963, 1964; Viladkar, 1981; Viladkar & Dulski, 1986; Viladkar & Wimmenauer, 1992
2. Panwad-Kawant, Gujarat		Dike complex of carbonatites and alkaline rocks		Sukheswala & Avasia, 1971
3. Siriwasan, Gujarat		11 km long sill of carbonatite in sandstone, dikes and plugs of alkaline rocks		Sukheswala & Borges, 1975; Sethna & Borges, 1981
4. Rajula, Gujarat		Carbonatite dikes associated with rhyolite and trachyte		Mishra, 1977
5. Mirzapur, Uttar Pradesh		Carbonatite associated with kimberlite	Diamond	Chattopadhyaya & Venkatraman, 1976
6. Wah Sung, Meghalaya	156	Sövite associated with pyroxenite, ijolite, nepheline syenite, syenite	Pyrochlore & Apatite	Sheik & Saraswat, 1977; Krishnamurthy, 1985; Krishna et al., 1991
7. Newania, Rajasthan	759	Rauhaugite later intruded by ankeritic carbonatite	Apatite	Phadke & Jhingran, 1968; Viladkar, 1980; Viladkar & Wimmenauer, 1986
8. Mundwara, Rajasthan	56.8	Sövite & beforosite dikes associated with pyroxenite, gabbro, theralite, nepheline syenite intrusives		Subramanyam & Rao, 1972; Udas et al., 1976; Le Bas & Srivastava, 1986
9. Kishengarh, Rajasthan		Sövite veins in nepheline syenite		Geological Survey News, 1973
10. Barmer, Rajasthan		Sövite dikes in nepheline phonolite		Narayandas et al., 1978; Viladkar & Martin, in press
11. Dhancholi, Harayana		Calcitic carbonatite with sheets and lenses of magnetite		Ramiengar & Vishwnathan, Geological Survey News, 1978
12. Khetri copper belt, Rajasthan		Sövite veins in gneiss		Basu & Narsayya, Geological Survey News, 1983
13. Puga Valley Ladakh, J & K				Geological Survey News, 1973
14. Sevathur, Tamil Nadu	720	Rauhaugite intruded by ankeritic carbonatite & associated with pyroxenite, syenite	Pyrochlore, Apatite, Vermiculite	Udas & Krishnamurthy, 1970; Borodin et al., 1971; Viladkar & Subramaniam, in press
15. Jokipatti, Tamil Nadu		Sövite associated with pyroxenite and syenite		Udas & Krishnamurthy, 1970; Borodin et al., 1971

16. Karapattu & Redipatti, Tamil Nadu		Beforsite lenses in gneiss		Borodin et al., 1971
17. Pallasullakkarai, Tamil Nadu		Beforsite lenses in pyroxenite	Monazite, Ilmenorutile	Borodin et al., 1971
18. Samalpatti, Tamil Nadu		Sövite, beforsite, and silico-carbonatite along contact between pyroxenite and syenite		Subramaniam et al., 1978
19. Pakkanadu, Tamil Nadu		Silico-carbonatite in gneiss	Monazite, Allanite	Borodin et al., 1971
20. Hogenakal, Tamil Nadu		Silico-carbonatite lenses in gneiss and associated pyroxenite, syenite		Srinivasan, 1973
21. Hogenakal, Karnataka	2000	Sövite and silico-carbonatite lenses in migmatite		Ramakrishnan et al., 1973
22. Vinayakpuram, Kunawaram, Andhra Pradesh		Silico-carbonatite lenses in nepheline syenite		Janardana Rao & Murthy, 1973
23. Medupalli, Andhra Pradesh		Silico-carbonatite lenses in nepheline syenite		Sharma et al., 1973
24. Arepalli, Andhra Pradesh		Silico-carbonatite lenses in nepheline syenite		Sharma et al., 1973
25. Elchuru, Andhra Pradesh		Silico-carbonatite lenses in nepheline syenite		Leelanandam et al., 1972
26. Bora, Visakhapatanam, Andhra Pradesh	1500	Sövite associated with pyroxenite and dunite		Geological Survey News, 1975
27. Chelima, Andhra Pradesh		Carbonatite associated with kimberlite	Diamond	Udas et al., 1976
28. Swangkre, Meghalaya		Carbonatite, ijolite, lamprophyre		Nambiar & Golani, 1985
29. Munnar, Kerala		Carbonatite, alkali granite-syenite		Santosh et al., 1987
30. Khambammettu, Tamil Nadu		Carbonatite veins		Balkrishnan et al., 1985
31. Samchampi, Assam		Carbonatite, ijolite, pyroxenite, syenite		Kumar et al., 1989

GEOLOGY OF COMPLEXES

AMBA DONGAR

In the sub-volcanic diatreme at Amba Dongar sövite forms a large ring-dike which collars an inner rim of carbonatite breccia. The ankeritic carbonatite, younger in the carbonatite sequence, invades sövite at several outcrops as thin dikes and plugs with varying sizes. Large number carbonatitic dikes are encountered within the ring complex. Majority of them are alvikites and occur in two distinct phases. Alvikites-I invade sandstone, basalt and breccia while alvikites-II intrude sövite and some fenite outcrops. Dolomitic carbonatite does not form a mappable unit and occurs only as thin lenses in sövite. Only one thin dike was, however, observed in the center of Amba Dongar village. Nephelinite plugs form a discontinuous chain of outcrops in the outer periphery of the complex at Mongra, Khandla, Kharvi (W and NW of Amba Dongar), Amba Dongar phalia and behind mines (N of Amba Dongar) and Kadipani village and Moti Chikli (NE and E of Amba Dongar).

The Amba Dongar carbonatite complex is underlain by pre-Cambrian Dharwar granitic basement gneisses, which are exposed 40 kms north of Amba Dongar (near the village of Chhota Udaipur). A few kilometers south of Chhota Udaipur, the Dharwar metamorphic basement is overlain by a basal conglomerate from the Cretaceous Bagh sedimentary sequence. The conglomerate, in turn, is overlain by gritty sandstone, and then fine-grained sandstone southwards. Near Panwad village (approximately 16 kms north of Amba Dongar), and further to the south, the Bagh beds are overlain by Deccan flood basalt flows (Eocene). The sequence repeats at several locations between Panwad and Kawant due to en-echelon faults [Sukheswala and Avasia, 1971]. All the sandstone outcrops, which occur at low elevations compared to the carbonatite exposures, show dips between 10°S to 15°S. As one approaches the Amba Dongar complex, the picture changes dramatically from Moti Chikli onwards. Elevations rise abruptly (doming), and reversal of dips are noted in the sandstone and overlying basalts, and this is attributable to forceful injection of the carbonatite-alkalic magma. The effects of doming are noted upto a 8 km periphery for the area surrounding Amba Dongar. Field observations help to establish following sequence of events in formation of ring structure [Viladkar, 1996]:

1. eruption of nephelinite and phonolite rocks in the outer zone,
2. emplacement of large plug (> 1.5 km diameter) of carbonatite breccia leading to initial doming of sandstone-basalt sequence,
3. the dome was then pierced by the forceful outburst of carbonatite magma which helped widening the vent and emplacement of sövite ring dike and alvikites, fenitization of surrounding Bagh sandstone in situ and blocks of sandstone in sövite magma, nephelinite blocks were phlogopitized,

4. carbonatite activity went on with emplacement of alvikite II (phlogopitization of sodic fenites) and then ankeritic carbonatite plugs within sövite and ended with hydrothermal mineralization,

5. the original core of carbonatite breccia was reduced to a concentric ring due to intrusive basalt from the same conduit forming new core of the ring structure.

NEWANIA

The carbonatite outcrop striking WNW with an average dip of about 40° towards SSE, swells in the central part and its width diminishes gradually at both ends. Rauhaugite intruded in three phases: 1. The earliest phase is coarse grained rauhaugite with more than 90% modal carbonate and accessory apatite, magnetite and pyrochlore. 2. Medium to fine grained type which tends to be porphyritic with apatite, magnetite and 3. Rauhaugite with sodic amphibole, phlogopite, zircon, apatite and magnetite.

The carbonatite outcrop shows presence of distorted bands and streaks of apatite all over the length of the outcrop but particularly abundant in the central part. The banding is also accentuated by the presence of magnetite, sodic amphibole and phlogopite.

The rauhaugite is intruded by ankeritic carbonatite which in the process has metasomatically replaced rauhaugite all along intrusive contact. The ankeritic melt must have been hydrous as in the replacement zones amphibole and phlogopite have been converted to chlorite. A few dikes of ankeritic carbonatite occur also in the fenite zone. The youngest phase of carbonatite (ankerite+siderite) seems to have intruded with sharp and at times chilled contact with host carbonatite. Such dikes are thinner but can be easily distinguished in the field as they are dark brown to almost black in colour.

Carbonates in carbonatites of Newania are most diverse such as calcite, dolomite, ankerite, siderite, magnesian siderite and Fe-magnesite [Viladkar, 1998]. Magnesite occurs as scattered spots in dolomite. In this respect Newania resembles Lueshe carbonatite, Zaire where magnesite had been reported earlier [Meyer and Bethune, 1958].

A zone of strong sodic fenitization had developed at the contact between carbonatite and country rock granite-gneiss. Farther away from the carbonatite contact the fenites become more leucocratic and finally grade into pure potassic type [Viladkar, 1980].

SUNG VALLEY

In the Sung Valley complex carbonatites and associated pyroxenite, ijolite and syenite intrude the Pre-Cambrian Shillong series which consists of quartzite and phyllite. Pyroxenites, which cover more than 75% of the complex, are cumulate rocks with high Mg, moderately high Cr and Ni and low Zr content. Highly weathered peridotite, with serpentine pseudomorphed after olivine,

encountered in the northern part of the pyroxenite body. Ijolite intrudes pyroxenite at several places forming a broken ring structure. In addition, a small plug and thin dikes are located within large outcrops of pyroxenite. Nepheline syenite dikes are comparatively minor and they intrude both ijolite and pyroxenite with sharp contact. Carbonatite dikes are found only in the southern part of the complex, where they intrude both, pyroxenite and ijolite. A large number of K-feldspar xenocrysts, books of phlogopite micas and blocks of silicate rocks are noticed in carbonatite outcrops.

Though the effects of fenitization are widespread in ijolite and pyroxenite, it is difficult to demarcate the zones of fenitization.

SEVATHUR AND SAMALPATTI

Sevathur carbonatite, composed predominantly of coarse grained rauhaugite forms a crescent shaped outcrop which is in contact with pyroxenite in the west and northwest and with Peninsular gneiss in the southwest and with trachytic syenite in the east. Number of xenoliths of basement gneiss, pyroxenite and syenite are seen in carbonatite outcrop. The ankeritic carbonatite intrudes rauhaugite with prominent reaction zone with replacement of rauhaugite by ankerite [Viladkar and Subramanian, 1995]. Besides dolomite-ankerite-calcite (in decreasing order of abundance), the carbonatite contain apatite, magnetite, phlogopite, Na-amphibole, zircon, baddeleyite, urano-pyrochlore, monazite and allanite.

The Samalpatti carbonatite-pyroxenite-syenite complex is situated 30 km southwest of Tirupattur.

EVOLUTION AND ORIGIN OF CARBONATITE COMPLEXES

AMBA DONGAR

Differentiation of the parental magma from sövite to ankeritic carbonatite produced an increase in Fe, Mn, Mg, Ba, and Th contents [Viladkar, 1981]. The differentiation model is supported by an increase in the contents of rare-earth-elements; total REE abundances and LREE increase in the order: sövite and alvikite < ankeritic carbonatite < ankeritic carbonatite containing barite, fluorite, monazite and quartz [Viladkar and Dulski, 1986]. Radiogenic isotope data from the different carbonatite phases, however, indicate that differentiation did not proceed in a closed magma system.

Nd, Pb, Sr, O and C isotope data from the Amba Dongar carbonatites [Simonetti et al., 1995] and associated fluorite (+sulfide) mineralization [Simonetti and Bell, 1995] indicate a complex formational history. Compared to the uniform Nd ($^{143}\text{Nd}/^{144}\text{Nd}$: 0.51248 to 0.51253), Pb (206/204: 19.05 to 19.19) and Sr ($^{87}\text{Sr}/^{86}\text{Sr}$: 0.70549 to 0.70628) values for the calciocarbonatites (sövite), those from the ferrocyanatites (ankeritic carbonatite) are slightly more variable. A carbon and oxygen isotope survey indicates that the magmatic differentiation series

sovite, alvikite, ankeritic carbonatite is beset with a distinct isotopic trend characterised by a moderate rise in $\delta^{13}\text{C}$ coupled with a sizeable increase in $\delta^{18}\text{O}$. From an average of $-4.6 \pm 0.4\%$ (PDB) for the least differentiated coarse grained sovite, $\delta^{13}\text{C}$ values slowly increase in the alvikite ($-3.7 \pm 0.6\%$) and ankeritic carbonatites ($-3.0 \pm 1.1\%$), whereas $\delta^{18}\text{O}$ rises from $10.3 \pm 1.7\%$ (SMOW) to $17.5 \pm 5.8\%$ over the same sequence, reaching extremes between 20 and 28% in the latest generation of ankeritic carbonatite. While an apparent correlation between $\delta^{13}\text{C}$ and $\delta^{18}\text{O}$ range of 7-13% conforms with the similar findings from other carbonatite complexes and probably reflex a Rayleigh fractionation process, the observed upsurge of $\delta^{18}\text{O}$ notable in the late phase ankeritic carbonatite is demonstrably related to a late phase low temperature hydrothermal activity involving large scale participation of $\delta^{18}\text{O}$ depleted groundwaters. As a whole the Amba Dongar complex the characteristic $^{13}\text{C}/^{12}\text{C}$ label of deep-seated (primordial) carbon, reflecting the carbon isotope composition of the subcontinental upper mantle below the Narmada rift zone of the Indian sub-continent [Viladkar and Schidlowski, 2000]. The Nd, Pb and Sr isotope ratios, and the "mantle-like" C and O isotope data for the calciocarbonatites indicate derivation from an enriched mantle source region, similar to that giving rise to the surrounding Deccan flood basalts. In contrast, the isotope data for the ferrocarnatites are attributed to low-temperature groundwater interaction related to the formation of the associated massive fluorite deposits. Sr isotope ratios for several varieties of Amba Dongar fluorites ($^{87}\text{Sr}/^{86}\text{Sr}$: 0.70910 to 0.71729) are extremely variable, and intermediate between those from the carbonatites and host Bagh sandstone (0.75359 to 0.78274). In contrast, the initial $^{143}\text{Nd}/^{144}\text{Nd}$ isotope values from most of the fluorites (0.51240 to 0.51247) are relatively uniform, quite different to those from the surrounding Bagh sandstones (0.51122 to 0.51149), but similar to those from the carbonatites. The isotope results from the fluorites are partly consistent with a model for fluorite deposition involving interaction between ground waters within the surrounding country rocks and an F-rich, carbonatite-derived fluid undergoing cooling

NEWANIA

The Newania carbonatite is unique amongst Indian carbonatites because of its highly magnesian composition (up to 19 wt% MgO) [Viladkar and Wimmenauer, 1986]. This feature is important because it is experimentally shown that [Wallace and Green, 1988] the small degree partial melts associated with a metasomatized, mantle peridotite at pressures of 21 to 30 kbar and temperatures 930 to 1080 °C, has composition of dolomitic (~14 wt% MgO) carbonatite magma that coexists with an amphibole lherzolite assemblage. In addition, phlogopite-carbonate peridotite will produce more magnesian melt compositions with increasing pressure which may be attributed to both a change in carbonatite mineralogy from

dolomite to magnesite at about 32 kb [Brey et al. 1983; Olafsson and Eggler 1983], and melts becoming more picritic [Wendlandt, 1984]. Complexes such as Sarfartoq (Greenland) and Newania (Rajasthan, India), however, do consist predominantly of dolomite-rich carbonatites (MgO levels > 14 wt%), and hence may be candidates for direct partial melts from the mantle.

Of the major elements, Ca, Mg and Fe show a fractionation trend from Mg-rich to Fe-rich carbonatites. Both Mn and P contents are higher in rauhaugite than in ankeritic carbonatite. A primitive mantle-normalized plot for trace elements shows an increase in the contents of all trace elements from rauhaugite to ankeritic carbonatite, which may be attributable to crystal fractionation. In the chondrite-normalized REE plot, pure, coarse-grained rauhaugite contains the lowest concentration of REEs, whereas the highest REE and LREE abundances are noted in the rauhaugite, which is rich in pyrochlore and zircon (some are highly Ce-enriched). Compared to the rauhaugite, the ankeritic carbonatite shows steeper negatively-sloped REE patterns and the highest La/Yb ratio again suggesting that they are later differentiates. On the basis of Sr, C and O isotopes rauhaugite appears to be unmodified mantle melt. Gruau et al., (1995) from their Sr, Nd studies suggest derivation of Newania dolomitic carbonatite from an old, LREE-enriched lithospheric mantle source.

The age of Newania carbonatite remains controversial. Deans and Powell (1968) dated the complex at 959 ± 24 Ma by K/Ar method on alkali amphibole. Gruau et al., (1995) confirmed this age on the basis of RBA/Sr and K/Ar data from carbonatite and fenite. However, their Sm-Nd and U-Pb results from carbonatites give an older age in the range of 1200 – 1400 Ma. These results led them to suggest that 1200-1400 Ma represents the age of magmatic emplacement of carbonatite while 900-950 Ma represents high temperature metamorphic event which has reset RBA-Sr and K-Ar systematics. Recently, Schleicher et al., (1997) obtained still higher Pb/Pb ages. Their results indicate a two stage evolution of the Newania carbonatite. Accordingly, 2230 Ma is the age of emplacement of rauhaugite while ankeritic carbonatite seems to have intruded much later at 1587 ± 51 Ma. The extreme long age hiatus between rauhaugite and ankeritic carbonatite is difficult to explain.

SUNG VALLEY

In Sung valley among all silicate rocks, the pyroxenite constitutes the bulk of the complex. Inclusions of pyroxenite are seen in ijolites while both pyroxenite and ijolite xenoliths are common in carbonatites. The order of emplacement as established from the field relations and confirmed from mineralogy and geochemistry is pyroxenite - ijolite - nepheline syenite and syenite - carbonatite. Pyroxenite are cumulate rocks with high MgO moderately high Cr and Ni and low Zr content. Incompatible elements show enrichment in ijolite while carbonatites are highly enriched in incompatible elements compared to primitive mantle values. REE abundances increase in the order pyroxenite < feldspathic pyroxenite < ijolite

< syenite < carbonatite. A carbonated nephelinitic magma is thought to be the primary magma for the suit of rocks of the complex, and crystallization of this magma under shallow plutonic conditions produced pyroxenite-ijolite-nepheline syenite- carbonatite series [Viladkar et al., 1994].

The origin of the Sung Valley carbonatite, may be related to the Rajmahal flood basaltic province (on account of almost similar age 134 Ma for carbonatite and 114 Ma of Rajmahal basalt) which was produced by the underlying Kerguelen plume at the time of intrusion. By analogy, the carbonatite complexes along the Narmada-Son lineament are also hosted and similar in age to the Deccan flood basalts, and therefore suggest that alkaline magmatism is genetically linked to basaltic volcanism. On the basis of similar Pb isotope data between the Amba Dongar carbonatite and present-day volcanics from the Island of Réunion, the present location of the "hot-spot" which produced the Deccan flood basaltic province 65 Ma ago, Simonetti et al. (1995) suggested a link between the mantle source region which produced the carbonatite magmatism and hot-spot activity (along with the associated flood basaltic province). On the basis of their recent Pb/Pb age data Veena et al., (1998) suggest that the Sung Valley carbonatite and associated silicate rocks may represent the earliest phase of magmatic activity that was precursor of Kerguelen mantle plume close break up of India from Australia and Antarctica.

SEVATHUR AND SAMALPATTI

The first radiometric age (720 ± 30 Ma) on Sevathur carbonatite by K/Ar method was obtained by Deans and Powell (1968) using biotite from pyroxenite adjacent to carbonatite exposure. Subsequently, Moralev et al., (1975) and Parthasarathy and Sankar Das (1976) using phlogopite (K/Ar) pyrochlore (Pb/Pb) gave two more age data of 600 and 845 Ma respectively. Almost at the same time Nagpaul and Mehta (1975) using zircon (fission track U/Pb) obtained age of 1330 ± 40 Ma for Sevathur carbonatites. Yet another age of 771 ± 18 Ma for carbonatite and 773 ± 13 Ma for pyroxenite was obtained by Anil Kumar and Gopalan (1991). Recently, however, Schleicher et al., (1997) reported much precise dating (on whole rock Pb/Pb isocron age) of 801 ± 11 Ma for Sevathur carbonatite.

These carbonatites show very low $^{143}\text{Nd}/^{144}\text{Nd}$ (0.5116 – 0.5122) and very high Sr isotopic ratios (0.7045-0.7054) [Schleicher et al., 1998]. On the basis of this data Schleicher et al., argue that the Tamil Nadu carbonatites may characterise an enriched upper mantle at 800 Ma. This enriched mantle component is either directly defined by the initial Sr and Nd ratios (moderately more enriched than present day EM1) or suggest an interaction of two mantle components within an isotopically heterogeneous mantle, one of them being even more enriched (sub-continental lithosphere).

REFERENCES

1. Kumar A., Gopalan, K. Precise Rb-Sr age and enriched mantle source of the Sevattthur carbonatites, Tamil Nadu, South India. *Current Science*, 1991, 60, pp. 653-655.
2. Basu S.K., Narsayya B.L. A probable zone of carbonatite and fenitic rock association in the eastern part of the Khetri copper belt, northeastern Rajasthan. *Geological Survey of India*, 1983, 113, pp. 7-15.
3. Borodin L.S., Gopal V., Moralev V.M., Subramanian V. Precambrian carbonatites of Tamil Nadu; South India. *Journal of Geological Society of India*, 1971, 12, pp. 101-112.
4. Brey G., Brice W.R., Ellis D.J., Green D.H., Harris K.L., Ryabchikov I.D. Pyroxene-carbonatite relations in the upper mantle. *Earth and Planetary Science Letters*, 1983, 62, pp. 63-74.
5. Chattopadhyay N., Hashimi S. The Sung Valley alkaline-ultramafic-carbonatite complex, East Khasi and Jaintia Hills district, Meghalaya. *Records Geological Survey of India*, 1984, 113, pp. 24-33.
6. Choubey V.D. Narmada-Son lineament, India. *Nature - Physical Science*, 1971, 232, pp. 38-40.
7. Courtillot V., Feraud G., Maluski H., Vandamme D., Moreau M.G., Besse J. Deccan flood basalts and the Cretaceous/Tertiary boundary. *Nature*, 1988, 333, pp. 843-846.
8. Crawford A.R. India, Ceylon and Pakistan: new age data and comparison with Australia. *Nature*, 1969, 223, pp. 380-384.
9. Crawford A.R. Narmada-Son lineament of India traced into Madagascar. *Journal Geological Society of India*, 1978, 19, pp. 144-153.
10. Dar K.K. Some geological data. *Atomic Energy Minerals in India*. *Journal Geological Society of India*, 1964, 5, pp. 112-120.
11. Deans T. A review of carbonatite investigations in India and Pakistan: A report on visit to India in January-February 1967. Unpublished report.
12. Deans T., Powell J.L. Trace elements and strontium isotopes in carbonatites, fluorites and limestones from India and Pakistan. *Nature*, 1968, 218, pp. 750-752.
13. Deans T., Sukheswala R. N., Sethna S. F., Viladkar S. G. Metasomatic feldspar rocks (potash fenites) associated with the fluorite deposits and carbonatites of Amba Dongar, Gujarat, India: *Institution of Mining and Metallurgy Transactions*, 1973, 82, pp.33-40.
14. Desikacher S.V. A review of the tectonic and geological history of eastern India in terms of plate tectonic theory. *Journal Geological Society of India*, 1974, 15, pp. 137-149.
15. Duncan R.A., Pyle D.G. Rapid eruption of the Deccan flood basalts at the Cretaceous/Tertiary boundary. *Nature*, 1988, 333, pp. 841-843.
16. Gopalan K, Macdougall J.D., Roy A.B., Murli A.V. Sm-Nd evidence for 3.3 Ga old rocks in Rajasthan, northwestern India. *Precambrian Res.* 1990, 48, pp. 287-297.
17. Grady J.C. Deep main faults in South India. *Journal Geological Society of India*, 1971, 12, pp. 56-62.
18. Gruau G., Petibon C., Viladkar S.G., Fourcade S., Bernard-Griffiths J., Mace J. Extreme isotopic signatures in carbonatites from Newania Rajasthan. *Terra Abstracts*, 1995, 7, p. 336.
19. Janardana R., Murthy I.S.N. On the occurrence of carbonatites in the Vinayakpuram Kunavaram syenite band, Khammam district, Andhra Pradesh. *Journal Geological Society of India*, 1973, 14, pp. 431-433.
20. Krishna V., Pandey B.K., Krishnamurthy P., Gupta J.N. Pb, Sr and Nd isotopic systematics of Sung Valley carbonatites, Meghalaya, India: Implications for contemporary sub-crustal upper mantle characterization. 5-th National Symposium on Mass Spectrometry, 1991, 19/1-19/4.

21. Krishnamurthy P. Carbonatites of India. *Exploration and Research for Atomic Minerals*, 1988, 1, pp. 81-115.
22. Krishnaswamy V.S. The Deccan volcanic episode, related tectonism and geothermal manifestations. *Memoir Geological Society of India*, 1981, 3, pp. 1-7.
23. Kumar D., Mamallan R., Saravanan B., Jain S.K., Krishnamurthy P. *Exploration Research Atomic Minerals*, 1989, 2, pp. 183-199.
24. Leelanandam C., Krishna S.G., Mallikarjuna R., Subramanyam K. Occurrence of carbonatites near Elchuru, Ongole district, Andhra Pradesh. *Current Science*, 1972, 41, 335-336.
25. Mishra D.C. Possible extension of Narmada-Son lineament towards Murray Ridge Arabian Sea and the Eastern Syntaxial bend of the Himalayas. *Earth Planetary Science Letters*, 1977, 36, pp. 301-308.
26. Mishra S.P. New genetic model for base metals in the Aravalli region, India. *Symposium on Metallogeny of the Precambrian*, I.G.C.P. Project 91, 1982, pp. 63-70.
27. Moralev V.M., Voronovski S.N., Borodin L.S. New findings about the age of carbonatites and syenites from southern Indian. *USSR Academy of Sciences*, 1975, 222
28. Meyer A., Bethune P. The Lueshe carbonatite (Kivu, Belgian Congo): *Int. Geol. Congr.* 21st, sess. Pt. 13, 1960, pp. 304-309.
29. Nagpaul K.K., Mehta P.P. Cooling history of south India as revealed by fission tracks studies. *American Journal of Science*, 1975, 275, pp. 753-762.
30. Nambiar A.R., Golani P.R. A new find of carbonatite from Meghalaya. *Current Science*, 1985, 54, pp. 281-282.
31. Narayan Das G.R., Bagchi A.K., Chaube D.N., Sharma C.V., Navaneetham K.V. Rare metal content, geology and tectonic setting of the alkaline complexes across the Trans Aravalli region, Rajasthan. *Recent Researches in Geology*, 1978, 7, pp. 201-217.
32. Natarajan M., Bhaskar R.B., Parthasarathy R., Kumar A., Gopalan K. 2.0 Ga old pyroxenite-carbonatite complex of Hogenakal, Tamil Nadu, South India. *Precambrian Research*, 1994, 65, pp. 167-181.
33. Olafsson M., Eggler D.H. Phase relations of amphibole, amphibole-carbonate, and phlogopite-carbonate peridotite: petrologic constraints on the asthenosphere. *Earth and Planetary Science Letters*, 1983, 64, pp. 305-315.
34. Phadke A.V., Jhingran A.G. On the carbonatites at Newania, Udaipur district, Rajasthan. *Journal of Geological Society of India*, 1968, 9, pp. 165-169.
35. Parthasarathy R., Sankardas M. Th, U and Pb contents of some Indian zircons and their ages. *Journal Geological Society of India*, 1976, 17, pp. 262-271.
36. Ramakrishnan M., Mallikarjuna C., Ballal N.R.R. Carbonatite dyke near Mysore State. *Journal Geological Society of India*, 1973, 14, pp. 200-201.
37. Raman P.K., Vishwanathan T.V. Carbonatite complex near Borra, Visakhapatnam district, Andhra Pradesh. *Journal Geological Society of India*, 1977, 18, pp. 605-616.
38. Ramiengar A.S., Ramakrishnan M., Vishwanatham M.N. Charnockite-gneiss-complex relationship in southern Karnataka. *Journal Geological Society of India*, 1978, 19, pp. 411-419.
39. Santosh M., Thampi P.K., Iyer, S.S., Vasconcellos M.B.A. Rare earth element geochemistry of the Munnar carbonatite, Central Kerala. *Journal Geological Society of India*, 1987, 29, pp. 335-343.
40. Schleicher H., Kramm U., Pernicka E., Schidlowski M., Schmidt F., Todt W., Viladkar, S.G. Enriched subcontinental upper mantle beneath southern India: evidence from Nd, Sr, Pb and C-O isotopic studies on Tamil Nadu carbonatites. *Sixth V.M. Goldschmidt Conference- Journal of Conference. Abstracts* 1, 1996, p. 542.

41. Schleicher H., Kramm U., Pernick E., Schidlowski M., Schmidt F., Subramian V., Todt W., Viladkar S.G. Enriched Subcontinental Upper mantle beneath South India: Evidence from Pb, Nd, Sr and C-O Isotopic Studies on Tamil Nadu carbonatites. *Jour. Petro.*, 1998, 39, pp. 1765-1785.
42. Schleicher H., Todt W., Viladkar S.G., Schmidt F. Pb/Pb age determinations on Newania and Sevathur carbonatites of India: evidence for multi-stage histories. *Chem. Geol.*, 1997, 140, pp. 261-273.
43. Sharma S.R., Devendranath T., Jayaram M.S. Carbonatites from nepheline syenite near Kunavaram district, Andhra Pradesh. *Journal Geological Society of India*, 1973, 12, p. 89
44. Sheik Y., Saraswat A.C. A preliminary note on the carbonatites in Wah Sung Valley of Jaintia Hills district, Meghalaya. *Current Science*, 1977, 46, pp. 703-704.
45. Simonetti A., Bell K., Viladkar S. G. Isotopic data from the Amba Dongar carbonatite complex, west-central India: evidence for an enriched mantle source. *Chemical Geology (Isotope Geoscience Section)*, 1995, 122, pp. 185-198.
46. Simonetti A., Bell K. Nd, Pb, and Sr isotope systematics of fluorite at the Amba Dongar carbonatite complex, India: evidence for hydrothermal and crustal fluid mixing. *Economic Geology*, 1995a, 90, pp. 2018-2027.
47. Srinivasan V. The carbonatite of Hogenakal, Tamil Nadu, South India. *Journal Geological Society of India*, 1977, 18, pp. 598-604.
48. Srivastava R.K., Hall R.P. Tectonic setting of Indian carbonatites. In: Srivastava, R.K. and Chandra, R. (eds) *Magmatism in relation to diverse tectonic settings*. Oxford & IBH Publishing, New Delhi, 1995.
49. Subramaniam A.P., Parimoo M.L. Fluorspar mineralization related to Deccan basalt volcanism at Ambadongar, Baroda district, India. *Nature*, 1963, 198, pp. 563-564.
50. Subramanyam N.P, Murali A.V., Rao G.V.U. Age of Mundwara igneous complex, Rajasthan. *Current Science*, 1972, 41, pp. 63-64.
51. Subramanyam N.P., Rao G.V.U. Carbonatite veins of Mundwara igneous complex, Rajasthan. *Journal Geological Society of India*, 1972, 13, pp. 388-391.
52. Subramaniam V., Viladkar S.G., Upendran R. Carbonatite alkalic complex of Samalpatti Dharampuri district, Tamil Nadu. *Geological Society of India*, 19, pp.206-216.
53. Sukheswala R.N. 1976. Carbonatite kimberlite complexes of India. IMA Volume, Bangalore, 1978, pp. 429-437.
54. Sukheswala R.N., Avasia R.K. Carbonatite-alkalic complex of Panwad-Kawant, Gujarat, and its bearing on the structural characteristics of the Area. *Bulletin Volcanologique*, 1971, 35-3, pp. 564-578.
55. Sukheswala R.N., Avasia R.K., Viladkar S.G. Deccan basalts associated with carbonatite volcanism, Chhota Udaipur, Baroda district, Gujarat, India. *Third Indo-Soviet Symposium on Earth Sciences, Archean Geochemistry and Comparative Study of Deccan Traps and Siberian Traps Abstract Volume*. 1978.
56. Sukheswala R.N., Borges S.M. The carbonatite-injected sandstones of Siriwasan, Chhota Udaipur, Gujarat. *Indian Journal of Earth Sciences*, 1975, 2, pp. 1-10.
57. Sukheswala R.N., Udas G.R. Note on the carbonatite of Ambadongar and its economic potentialities. *Science and Culture*, 1963, 29, pp. 563-568.
58. Sukheswala R.N., Viladkar S.G. The carbonatites of India. *Proceedings First International Symposium on Carbonatites, Brazil*, 1978, pp. 277-293.
59. Sukheswala R. N., Viladkar S. G. Fenitized sandstones in Amba Dongar carbonatites, Gujarat, India. *Journal Geological Society of India*, 1981, 22, pp. 368-374.
60. Udas G.R., Narayan Das G.R., Sharma C.V. Carbonatites of India in relation to structural setting. *Proc. of Intern. Seminar on Tectonics and Mettallogeny of SE Asia and Far East*. Geological Survey of India Miscellaneous Publication, 1974, 34, 77-92.

61. Udas G.R., Krishnamurthy P. An account of a rich fluorite deposit at Hingoria, Broach district, Gujarat state. *Current Science*, 1968, 37, pp. 77-78.
62. Udas G.R., Krishnamurthy P. Carbonatites of Sevathur and Jokipatti, Madras State, India. *Proceedings Indian National Science Academy*, 1970, 36, pp. 331-343.
63. Viladkar S.G. The fenitized aureole of the Newania carbonatite, Rajasthan. *Geological Magazine*, 1980, 117, pp. 285-292.
64. Viladkar S.G. The carbonatites of Amba Dongar, Gujarat, India. *Bulletin Geological Society of Finland*, 1981, 53, pp. 17-28.
65. Viladkar S.G. Alkaline rocks associated with the carbonatites of Amba Dongar, Gujarat, India. *Indian Mineralogist (Sukheswala Volume)*, 1985, pp. 130-135.
66. Viladkar S.G. Fenitization at the Ambadongar carbonatite alkaline complex, India. In: Gabriel, M. (ed.) *Proc. NEMIRAM Symposium, Czechoslovakia*, 1986, pp. 170-189.
67. Viladkar S.G., Wimmenauer W. Mineralogy and geochemistry of the Newania carbonatite-fenite complex, Rajasthan, India. *Neues Jahrbuch für Mineralogie Abhandlungen*, 1986, 156, pp. 1-21.
68. Viladkar S.G. Phlogopitization at Amba Dongar complex, Gujarat, India. *Neues Jahrbuch Mineralogie Abhandlungen*, 1991, 162, pp. 201-213.
69. Viladkar S. G., Dulski P. Rare earth element abundances in carbonatites, alkaline rocks and fenites of the Amba Dongar complex, Gujarat, India. *Neues Jahrbuch für Mineralogie Monatshefte H-1*, 1986, pp. 37-48.
70. Viladkar S.G., Kienast J.R., Fourcade S., Mineralogy of the Newania carbonatites, Rajasthan, India. *IAGOD Symposium Abstracts, Orleans, France*, 1993.
71. Viladkar S.G., Pawaskar, P.B. Rare earth element abundances in carbonatites and fenites of the Newania complex, Rajasthan, India. *Bulletin Geological Society of Finland*, 1989, 61, pp. 113-122.
72. Viladkar S.G., Schleicher H., Pawaskar P.B. Mineralogy and geochemistry of the Sung Valley carbonatite complex, Shillong, Meghalaya, India. *Neues Jahrbuch Mineralogie Monatshefte*, 1994, 11, pp. 499-517.
73. Viladkar S.G., Subramaniam V. Mineralogy and geochemistry of the carbonatites of the Sevathur and Samalpatti complexes, Tamil Nadu. *Journal Geological Society of India*, 1995, 45, pp. 505-517.
74. Viladkar S.G., Wimmenauer W. Mineralogy and geochemistry of the Newania carbonatite-fenite complex, Rajasthan, India. *Neues Jahrbuch für Mineralogie Abhandlungen*, 1986, 156, pp. 1-21.
75. Viladkar S. G., Wimmenauer W. Geochemical and petrological studies on the Amba Dongar carbonatites (Gujarat, India). *Chemical Erde*, 1992, 52, pp. 277-291.
76. Viladkar S. G. *Geology of the Carbonatite-alkalic diatreme of Amba Dongar, Gujarat*. Published by the GMDC Science and Research Centre, Ahmedabad, 1996.
77. Viladkar S.G. Carbonatite occurrences in Rajasthan, India. *Petrology*, 1998, vol. 6, N. 3, pp. 295-306.
78. Viladkar S.G., Schidlowski M. Carbon and Oxygen Isotope Geochemistry of the Amba Dongar Carbonatite Complex (Gujarat, India): *Gondwana Research*, 2000, 3, No.3, pp. 415-424.
79. Viladkar S.G., Ramesh R., Avasia R.K. Stratified Carbonatite and Nephelinite composition tuff of Amba Dongar carbonatite-alkalic complex, Gujarat. *Symp. on carbonatites and associated alkaline rocks and Field Workshop on the Carbonatites of Tamil Nadu. Abstract Volume*, 2001, p. 49.
80. Wallace M.E., Green D.H. An experimental determination of primary carbonatite magma composition. *Nature*, 1988, 335, pp. 343-346.

81. Wendlandt R.F. An experimental and theoretical analysis of partial melting in the system $KAlSiO_4$ -CaO-MgO-SiO₂-CO₂ and applications to the genesis of potassic magmas, carbonatites and kimberlites. Kornprobst, J. (ed.) Kimberlites I: Kimberlites and related rocks. Proc. of the Third Intern. Kimb. Conf. Elsevier, N.York, 1984. pp. 359-369.
82. West W.D. The line of the Narmada-Son Valley. *Current Science*, 1962, 31, p. 143.
83. Woolley A.R. The spatial and temporal distribution of carbonatites. In: Bell, K. (ed.), *Carbonatites: Genesis and evolution*. Unwin Hyman, London, 1989, pp. 15-37.
84. Yellur D.D. Carbonatite complexes as related to the structure of the Narmada valley. *Journal Geological Society of India*, 1968, 9, pp. 118-123.